

Evaluating Innovative Nutrient Management Options and Seasonal Groundwater Recharge Dynamics in an Agricultural Source Water Protection Area

by

Jacqueline M. Brook

A thesis
presented to the University of Waterloo
in fulfillment of the
thesis requirement for the degree of
Master of Science
in
Earth Sciences

Waterloo, Ontario, Canada, 2012

© Jacqueline M. Brook 2012

AUTHOR'S DECLARATION

I hereby declare that I am the sole author of this thesis. This is a true copy of the thesis, including any required final revisions, as accepted by my examiners.

I understand that my thesis may be made electronically available to the public.

Acknowledgements

I gratefully acknowledge the financial support of the following agencies: the Ontario Graduate Scholarship Program, the Canadian Water Network, the Ontario Ministry of the Environment Best in Science Program, and the Natural Science and Engineering Research Council of Canada. I would also like to thank the County of Oxford for allowing the use of the study site, and to the Upper Thames River Conservation Authority and Ontario Ministry of Agriculture, Food and Rural Affairs for providing technical help with the nitrogen management study.

I would first like to thank my thesis supervisor Dr. David Rudolph for his support, for the opportunity to carry out two very interesting field projects, financial and technical resources. I would also like to thank my committee members Dr. Brewster Conant Jr. for his assistance in the field as well as his reviews of earlier drafts of my thesis, and to Dr. Emil Frind for initially taking me on as a student and for his ongoing support by accepting to be on my committee. I am indebted Don King for including my work into the design of his nitrogen management project and providing the corn yield and shallow soil data, as well as David Start for his valuable insight into agricultural processes and the historical management of the Oxford County lands.

I owe a special thanks to Paul Johnson and Robert Ingleton for their hard work in the field collecting soil cores and installing equipment. Their collective knowledge and advice was invaluable to the work presented herein. I would like to acknowledge Paul for the design of the temperature probe casing used in this study; the one used was only one of his many ingenious designs. Thanks to Marcelo Sousa, who spent many cold days with me in the field during the spring melt, provided a great deal of guidance in the modeling of temperature, and has been a constant source of advice and encouragement since my first day on campus. I would also like to mention Cynthia Davis, Hagit Blumenthal, Jeff Melchin, Christina Micheli and Ashley Rudy for their help collecting field data and processing samples in the lab.

Finally I would like thank my husband Tyler, my parents Kevin and Leslie-Anne and my brother Travis for their unconditional support.

Abstract

This thesis presents two interrelated studies that consider nutrient management and seasonal changes in recharge on agricultural lands within the context of source water protection. The research focuses first on the management of the risk to groundwater quality through the implementation of various nutrient management practices and secondly considers the dynamic nature of the transport pathway to the groundwater system associated with seasonal changes in climate and hydrology. The combined results provide insight into several of the key factors influencing the protection of groundwater sources within the agricultural landscape.

Field work was completed between 2009 and 2010 on an agricultural field near the City of Woodstock, Ontario. The site is located within a source water protection area; the two-year travel time zone of the Thornton Well Field which represents the primary water supply for the City of Woodstock and which has experienced chronic increases in nitrate concentrations over the last few decades. The wells are completed in glacial overburden consisting of intermingling sand and gravel till aquifers which overly a limestone bedrock aquifer. Agricultural best or beneficial management practices (BMPs) field have been implemented and monitored since 2004. The BMPs were adopted in order to reduce nitrogen losses to the aquifer, and consisted of a reduction in nitrogen fertilizer application rates over a series of agricultural fields located near the well

The first study is a one year experiment designed to compare alternative nutrient management practices for corn. Combinations of fertilizer treatments with or without a legume cover crop (red clover) were assessed. The fertilizer treatments studied were: a polymer coated urea (slow-release fertilizer) applied at planting, a conventional urea applied at planting, side-dress treatment of a solution of urea and ammonium nitrate in water containing 28% nitrogen with two different application rates applied in the early summer, and a control. The legume cover crop was incorporated in the soil in the previous fall, and acts as a slow release fertilizer as nitrogen is made available to the following crop as the plants decompose. Treatments were compared based on crop yield, overall economic return, and the potential for nitrate leaching. The potential for nitrate leaching was evaluated with bi-weekly shallow soil core during the growing season, and deep soil cores taken before planting, after harvest and the following spring. The deep cores allowed changes in nitrate storage below the rooting zone to be assessed.

The results of this study highlight the importance of timing of fertilizer applications and rate of fertilizer applications. Treatments which provide a delay in the release or application of fertilizer, the polymer-coated urea, the calculator-rate side-dress and the clover cover crop, were found to be

advantageous. The polymer-coated urea treatments and side-dress treatments were found to reduce leaching compared to the conventional urea treatment. Treatments with the clover cover crops were not found to reduce crop yields or increase leaching potential, and lower fertilizer costs associated to this practice were found to have a positive economic effect. Plots treated with the high-rate side-dress fertilizer application lost more nitrate to the subsurface compared to the other treatment options, and an economic disadvantage was observed as yields did not compensate for higher fertilizer costs. The study highlights the advantages of the different treatments under study, which may be used to inform policy makers and farmers in the selection of economically and environmentally sustainable nutrient management BMP options.

Groundwater monitoring at the site over the years has identified interesting recharge dynamics, particularly in the vicinity of an ephemeral stream which develops annually during spring and winter melt events in a low lying area of the study site. It was hypothesized that rapid recharge could occur beneath the stream allowing for surface water to quickly reach groundwater, posing a threat to municipal water wells. The current framework of source water protection does not take into account the potential risk posed by this type recharge event. At this field site, rapid infiltration associated with this type of event may pose a risk to drinking water quality due to the proximity of the stream to the pumping wells and the nature of the aquifer.

The second study examines rapid groundwater recharge processes beneath the ephemeral stream during the course of a spring melt in 2010. The goals of the study were to quantify recharge at one location beneath the stream and to assess whether temperature variations above the water table can be used as a tracer to reasonably estimate recharge during a short live recharge event. A novel housing for the temperature sensors was designed in order to deploy and position them into gravelly materials within the vadose zone, which reduced the potential for the formation of preferential pathways and permitted the retrieval of the sensors at a later date. Field data were collected during the course of the spring melt period from a network of groundwater monitoring wells and subsurface temperature sensors. Spatial and temporal changes in groundwater geochemistry, hydraulic head and temperature were used to characterize recharge dynamics at the field site. Recharge beneath a segment of the ephemeral stream was quantified through the numerical analysis of the field data using Hydrus 1-D, a one-dimensional numerical model designed to simulate soil water flow and heat transport in variably saturated porous media. Site specific data were used to create the model domain, provide estimates of physical parameters, and to define initial and time variable boundary conditions. Model parameters were first calibrated by simulating periods where it was expected that soils would be gravity drained with minimal soil water flow, and then further refined by simulating the period when the ephemeral stream was present. A final

set of parameters was determined, and the initial gravity drained conditions were re-simulated. The model was able to reproduce field observations under different flow scenarios using the final set of parameters, suggesting that the conceptual model and final model domain representative of the actual field conditions. The successful simulation of the field data sets under the different flow scenarios also increases confidence in the uniqueness of the model results. The model estimated that 0.15 m of recharge occurred beneath the instrumented site during the period between March 9th and March 22nd of 2010 when the ephemeral stream was present. This represents approximately a third of the expected total annual recharge for this location. Regional changes in hydraulic head, groundwater temperature and groundwater chemistry provided additional insight into the dynamic nature of the recharge process during the spring melt period and further illustrated the spatial variability of the aquifers' response to the stream. The study found that the use of temperature as a tracer provided useful and quantifiable insight into recharge phenomena. The results of this study suggest that high rates of rapid recharge occur beneath the ephemeral stream, and are spatially variable. This type of focused infiltration that occurs during the spring melt may represent a risk to municipal water quality if the infiltrating waters are carrying contaminants.

Table of Contents

Author's Declaration.....	ii
Acknowledgements.....	iii
Abstract.....	iv
Table of Contents.....	vii
List of Tables	xii
List of Figures	xiii
Chapter 1 Issues in Source Water Protection in Agriculture	1
1.1 Source Water Protection	1
1.1.1 Agricultural Groundwater Contamination	1
1.1.2 Recharge	2
1.1.3 Current Studies.....	2
Chapter 2 The County of Oxford Lands - A Source Water Protection Area.....	4
2.1 Introduction.....	4
2.1.1 Study Site	4
2.1.2 Geology and Hydrogeology	5
2.1.3 Investigation of BMPs	5
2.1.4 Ephemeral Stream Channel.....	6
Chapter 3 Innovative nitrogen management strategies to reduce impacts to groundwater quality in source protection areas.....	13
3.1 Introduction.....	13
3.1.1 The Nitrogen Problem in Agriculture	13
3.1.2 Objectives	14
3.1.3 Study Approach.....	14
3.2 Background.....	15
3.2.1 The Life Cycle of Corn	16
3.2.2 Nitrogen Treatment Options	16
3.2.2.1 Comparing Biologically Fixed Nitrogen and Synthetic Fertilizers.....	16
3.2.2.2 Comparing Control-Release to Conventional Spring Applied Nitrogen Fertilizers	18
3.2.2.3 Comparing Side-Dressed to Conventional Spring Applied Nitrogen Fertilizers	20
3.3 Methodology and Approach.....	21

3.3.1	Innovative Nitrogen Study	21
3.3.1.1	Study Design	21
3.3.1.2	Fertilizer Application Treatments	22
3.3.1.3	Corn Calculator	22
3.3.2	Field Data Collection	23
3.3.2.1	Shallow Cores	23
3.3.2.2	Corn Grain Yield.....	23
3.3.2.3	Deep Cores of the Unsaturated Zone	23
3.3.2.4	Bromide Tracer and Moisture Content Measurements	24
3.3.3	Geologic Core Analysis	25
3.3.3.1	Moisture Content Analysis.....	25
3.3.3.2	Pore-water Anion Concentration.....	26
3.3.3.3	Cumulative Nitrate Mass	26
3.3.3.4	Depth Averaged Pore-Water Concentration	27
3.3.3.5	Movement of the Bromide Tracer.....	27
3.4	Results.....	31
3.4.1	Study Site Stratigraphy	31
3.4.2	Meteorological Data.....	31
3.4.3	Shallow Core Results	32
3.4.4	Corn Yields	33
3.4.5	Economic Return.....	33
3.4.6	Bromide Tracer	34
3.4.7	Deep Core Results.....	34
3.4.7.1	Deep Core Nitrate Profiles	35
3.4.7.2	Deep Core Cumulative Nitrate Mass and Depth Averaged Pore-Water Concentrations	38
3.5	Discussion	66
3.5.1	Comparing Biologically Fixed Nitrogen and Synthetic Fertilizers.....	66
3.5.2	Comparing Control-Release to Conventional Spring Applied Nitrogen Fertilizers	67
3.5.3	Comparing Side-Dressed to Spring Applied Nitrogen Fertilizers	68
3.6	Conclusions.....	69
3.7	Recommendations.....	72
Chapter 4	Estimating Recharge from an Ephemeral Stream during a Spring Melt.....	74
4.1	Introduction.....	74
4.1.1	Objectives and Approach.....	75

4.2	Background	77
4.2.1	Applications of Heat Transport for Recharge Estimation	77
4.2.2	Heat Transport through Porous Media	77
4.3	Methodology	78
4.3.1	Field Data collection	79
4.3.1.1	Bromide Tracer	79
4.3.1.2	Deep Core Collection	79
4.3.1.3	Calculating Recharge Using Surface applied Bromide Tracer	80
4.3.1.4	Moisture Content.....	81
4.3.1.5	Monitoring Wells and Groundwater Sampling	82
4.3.1.6	Temperature Probes	83
4.3.1.7	Surface Instrumentation	84
4.3.2	The HYDRUS-1D Model	84
4.3.2.1	Water Flow.....	84
4.3.2.2	Soil Hydraulic Properties for Unsaturated Flow	85
4.3.2.3	Heat Transport.....	86
4.3.2.4	Model Domain	88
4.3.2.5	Boundary Conditions	88
4.3.2.6	Initial Conditions.....	89
4.3.2.7	Model Calibration	89
4.3.2.7.1	Calibrating – Gravity Drained Case.....	90
4.3.2.7.2	Calibrating – Ephemeral Stream Present	91
	During	91
4.3.2.7.3	Sensitivity Analysis of Saturated Hydraulic Conductivity	91
4.4	Results.....	98
4.4.1	Soil Stratigraphy	98
4.4.2	Moisture Content.....	98
4.4.3	Ephemeral Stream Development.....	98
4.4.4	Monitoring Wells and Groundwater Sampling	99
4.4.4.1	Regional Hydraulic Head Fluctuations	99
4.4.4.2	Regional Groundwater Temperature Fluctuations	100
4.4.4.3	Groundwater Geochemistry	101
4.4.4.4	Well WO37	102
4.4.4.5	Soil Temperature.....	102
4.4.5	Recharge Estimate Using Bromide Tracer.....	104
4.4.6	Modeling Results	105

4.4.6.1	Model Calibration – Gravity Drained Soil Conditions	105
4.4.6.1.1	Hydraulic Parameters	106
4.4.6.1.2	Heat Parameters	107
4.4.6.2	Model Calibration – Ephemeral Stream Present	108
4.4.6.3	Sensitivity Analysis of Saturated Hydraulic Conductivity	109
4.5	Discussion	146
4.5.1	Field Monitoring	146
4.5.2	Model Estimates.....	146
4.5.3	Sources of Errors.....	148
4.5.4	Temperature Probe Installations	149
4.6	Conclusions.....	151
4.7	Recommendations.....	152
Chapter 5	Overall Conclusions.....	154
References.....		157
Appendix A	Time Line of Field Sampling Efforts and Equipment Installation	167
Appendix B	Shallow Core Nitrate Data	168
Appendix C	Soil Core Profiles	171
Appendix D	Soil Core Sampling Results – Chapter 3.....	194
Appendix E	Soil Nitrate Concentration Profiles	211
Appendix F	Cumulative Nitrate.....	221
Appendix G	Moisture Content – Chapter 3	229
Appendix H	Stratigraphic Core Logs – Chapter 4.....	232
Appendix I	Soil Core Sampling Results – Chapter 4.....	237
Appendix J	Monitoring Well Dimensions and Location.....	239
Appendix K	Monthly Groundwater Chemistry Monitoring Results	240
Appendix L	Moisture Content – Chapter 4.....	247
Appendix M	Simulated Moisture Content - Homogeneous Lower Layer	249
Appendix N	Input Parameters for Gravity Drained Model Calibration	254
Appendix O	Simulated and Observed Temperature Beginning on March 3 rd , 2010	256
Appendix P	Inputted Moisture Retention Parameters - Ephemeral Stream Present	258
Appendix Q	Sensitivity Analysis.....	259
Appendix R	Simulated and Observed Temperatures – Gravity Drained	296
Appendix S	Simulated and Observed Moisture Content - Fully Drained.....	301
Appendix T	Boundary Conditions - April 12 th to June 1 st , 2010.....	306

Appendix U	Boundary Conditions – August 24 th to October 1 st , 2010	309
Appendix V	Boundary Conditions - March 9 th to March 22 nd , 2010.....	312
Appendix W	Iteration Criteria for All Simulations.....	315

List of Tables

Table 3.3.1 Rates of fertilizer application.....	28
Table 3.4.1 Long term average daily temperatures and total precipitation for each month collected from Environment Canada's Meteorological Station at Woodstock (Environment Canada, 2011), and average daily temperature and total precipitation for between May 2009 and May 2010 collected from the meteorological station onsite.	42
Table 3.4.2 Cost estimates of all treatment inputs.	43
Table 3.4.3 Return per treatment from the most lucrative to the least for the year of 2009.	44
Table 3.4.4 Peak concentrations ($\text{mg NO}_3^{-1}\text{-N/kg soil}$) of each treatment the different sampling times, and percent change in peak concentration.	45
Table 4.3.1 Temperature probe depths.....	92
Table 4.4.1 Recharge rate and total recharge estimations for the period between March 3rd and May 6th, 2010.	113
Table 4.4.2 Final moisture retention parameters.....	114
Table 4.4.3 Recharge estimates from the sensitivity analysis and annotations of the fit of the temperature simulations the observed data.	115
Table 4.4.4 Moisture retention parameters for silt and clay soils.	116
Table 4.4.5 Moisture retention parameters for silty gravel and sand soils.....	117

List of Figures

Figure 2.1.1 Location of Study site within Southern Ontario. Contains data for the University of Waterloo (n.d.).....	8
Figure 2.1.2 Topography of land owned by the County of Oxford, and two year time of travel capture zone. Contains data from the Corporation of the County of Oxford (County of Oxford GIS, 2005).	9
Figure 2.1.3 Quaternary geology of the study site. Adapted from Bekeris (2007). Contains data from the Corporation of the County of Oxford (County of Oxford GIS, 2005).	10
Figure 2.1.4 Geologic cross-section (north-east to south-west) in the north-east edge of the site, in the vicinity ephemeral stream site. Adapted from Haslauer (2005). Contains data from the Corporation of the County of Oxford (County of Oxford GIS, 2005).	11
Figure 2.1.5 Geologic cross-section (north-west to south-east) in the north-east edge of the site, in the vicinity ephemeral stream site. Adapted from Haslauer (2005). Contains data from the Corporation of the County of Oxford (County of Oxford GIS, 2005)	12
Figure 3.3.1 Location of the fields in the upper and lower positions.....	29
Figure 3.3.2 Study design, and location of core extraction and bromide tracer application.	30
Figure 3.4.1 Stratigraphic cross-section of the no clover block. Constructed from composite cores.....	46
Figure 3.4.2 Stratigraphic cross-section of the clover block. Constructed from composite cores.....	47
Figure 3.4.3 Total monthly precipitation for the period between May 2009 and May 2010.	48
Figure 3.4.4 Average monthly temperature for the period between May 2009 and May 2010.	48
Figure 3.4.5 Soil nitrate concentration in the shallow cores taken during the growing season of 2009 in the no clover plots. Grey line indicates the timint of the application of the side-dress fertilizer.....	49
Figure 3.4.6 Soil nitrate concentration in the shallow cores taken during the growing season of 2009 in the clover block. Grey line indicates the timint of the application of the side-dress fertilizer.	50
Figure 3.4.7 Corn yields (kg/ha) from the 2009 growing season in the no clover and the clover plots.	51
Figure 3.4.8 Soil bromide concentration profiles the fall of 2009 and the spring 2010.	52
Figure 3.4.9 Soil nitrate concentration profiles for the control (a) no clover and (b) clover treatments in the spring of 2009 and the fall of 2009.	53
Figure 3.4.10 Soil nitrate concentration profiles for the control (a) no clover and (b) clover treatments in the fall 2009 and spring of 2010.	54
Figure 3.4.11 Soil nitrate concentration profiles for the calculator rate side-dress (a) no clover and (b) clover treatments in the spring of 2009 and the fall of 2009.	55
Figure 3.4.12 Soil nitrate concentration profiles for the calculator rate sidedress (a) no clover and (b) clover treatments in the fall 2009 and spring of 2010.....	56

Figure 3.4.13 Cumulative nitrate mass profiles for the control (a) no clover and (b) clover treatments in the spring 2009, fall 2009 and spring 2010.....	57
Figure 3.4.14 Representative cores of the total soil nitrate mass of each treatment and sample time in the no clover plots within and below the rooting zone. Percent change compared to the (previous core), as well as the [spring of 2009].	58
Figure 3.4.15 Representative cores of the total soil nitrate mass of each treatment and sample time in the clover plots within and below the rooting zone. Percent change compared to the (previous core), as well as the [spring of 2009].	59
Figure 3.4.16 Representative cores of the total soil nitrate mass of each treatment and sample time in the no clover plots within and below the rooting zone to the maximum point of vertical migration. Percent change compared to the (previous core).	60
Figure 3.4.17 Representative cores of the total soil nitrate mass of each treatment and sample time in the clover plots within and below the rooting zone to the maximum point of vertical migration. Percent change compared to the (previous core).	61
Figure 3.4.18 Representative cores of the depth-averaged pore-water concentration of each treatment and sample time in the no clover block within and below the rooting zone. Percent change compared to the (previous core), as well as the [spring of 2009].	62
Figure 3.4.19 Representative cores of the depth-averaged pore-water concentration of each treatment and sample time in the clover block within and below the rooting zone. Percent change compared to the (previous core), as well as the [spring of 2009].	63
Figure 3.4.20 Representative cores of the depth-averaged pore-water concentration of each treatment and sample time in the no clover plots within the rooting zone and below the rooting zone to the maximum point of vertical migration. Percent change compared to the (previous core).	64
Figure 3.4.21 Representative cores of the depth-averaged pore-water concentration of each treatment and sample time in the clover block within the rooting zone and below the rooting zone to the maximum point of vertical migration. Percent change compared to the (previous core).....	65
Figure 4.3.1 Map of monitoring wells sampled in the vicinity of the ephemeral stream, meteorological station, location of temperature probes, the bromide plot and neutron access tube.....	93
Figure 4.3.2 Field instrument installations in and near the ephemeral stream. WO37 and WO63 are monitoring wells. Soil temperature probes depths are: T1 (13 cm), T2 (26 cm), T3 (39 cm), T4 (53 cm), T5 (87 cm), T6 (121 cm) and T7 (156 cm).	94
Figure 4.3.3 Schematic of a temperature probe installation showing the protective casing and borehole construction.....	95

Figure 4.3.4 The Chung and Horton (1987) relationships between thermal conductivity and moisture content for Sand, Loam and Clay.....	96
Figure 4.3.5 Visual representation of the pressure and temperature boundary conditions. WO37 is a monitoring well. T1 is a soil temperature probe placed at a depth of 13 cm below the ground surface.....	97
Figure 4.4.1 A conceptual representation of the soil stratigraphy used for the model, and the soil layers used by the model.	118
Figure 4.4.2 Moisture content profiles for the month of March measured with neutron probe.....	119
Figure 4.4.3 Pictures of Station 1 during the spring melt. (a) Picture of temperature probes from Station 1 facing toward Curry Road March 6th 2010. (b) Picture of Station 1 and temperature probes from between Station 1 and WO62 on March 9th 2010 Arrows indicate flow direction.	120
Figure 4.4.4 Pictures of stream flowing from Curry Road looking south over the culvert during the spring melt. (a) Picture of stream taken in by Mike Christie on March 18th, 2010 (Koch, 2009). (b) Picture of stream taken on March 9th, 2010, the day when wells and temperature probes start to record changes in temperature. Arrows indicate flow direction.	121
Figure 4.4.5 Change in hydraulic head over time in each monitoring well relative to March 1st, 2010 at midnight.	122
Figure 4.4.6 Range (maximum minus minimum) of changes in hydraulic head recorded in monitoring wells over the month of March plotted against the northing of the well casing.	123
Figure 4.4.7 Maps of the change in groundwater head relative to midnight on the 1st of March, in the vicinity of the ephemeral stream during the month of March, 2010.....	124
Figure 4.4.8 Change in temperature over time in each monitoring well relative to March 1st, 2010 at midnight.	125
Figure 4.4.9 Range (maximum minus minimum) of temperature change recorded in monitoring wells (excluding WO40) over the month of March plotted against the elevation of the ground at the casing. .	126
Figure 4.4.10 Maps of change in groundwater temperature in Aquifer 3 relative to midnight on the 1st of March, in the vicinity of the ephemeral stream during the month of March, 2010.	127
Figure 4.4.11 Maps of change in groundwater temperature in Aquifer 3 on March 15 th , 2010 in the vicinity of the ephemeral stream.	128
Figure 4.4.12 Monthly monitoring in wells where a notable decreases in both nitrate and chloride concentration occurred after the melt event.	129
Figure 4.4.13 Water level (meters below ground surface) and temperature (°C) recorded between 2005 and 2010 in WO37. The date when the well was repaired (January 16th, 2010) is marked by a vertical grey line.	130

Figure 4.4.14 Pressure and temperature changes in WO37 in March, 2010. The periods highlighted in yellow are those where there is a steep decrease in groundwater temperature coinciding with a steep increase in water level.....	131
Figure 4.4.15 Air, soil and groundwater temperature (°C) between January and December of 2010. Soil temperature probes depths are: T1 (13 cm), T2 (26 cm), T3 (39 cm), T4 (53 cm), T5 (87 cm), T6 (121 cm) and T7 (156 cm).....	132
Figure 4.4.16 Air, surface water, soil and groundwater temperature (°C), surface water height (cm) and groundwater depth (mbgs) between March 1st and 22nd, 2010. Soil temperature probes depths are: T1 (13 cm), T2 (26 cm), T3 (39 cm), T4 (53 cm), T5 (87 cm), T6 (121 cm) and T7 (156 cm).	133
Figure 4.4.17 Soil bromide concentration and volumetric water content profiles in March 5th, 2010. ...	134
Figure 4.4.18 Soil bromide concentration and volumetric water content profiles in May 6th, 2010.	134
Figure 4.4.19 Simulated moisture content profiles every five days of simulation between midnight on April 12th and June 1st, 2010. The initial moisture content inputted into the model is shown on April 12th, 2010.	135
Figure 4.4.20 Simulated moisture content profiles every five days of simulation between midnight on August 24th and on October 31st, 2010. The initial moisture content inputted into the model is shown on August 24th.....	136
Figure 4.4.21 Simulated and observed temperature at different depths between April 12th and June 1st, 2010 for calibration in unsaturated conditions. Note that the observation node for T3 was placed 5 cm lower than indicated from field measurements.	137
Figure 4.4.22 Simulated and observed temperature at different depths between August 24th and October 31st, 2010 for calibration in unsaturated conditions. Note that the observation node for T3 was placed 5 cm lower than indicated from field measurements.	138
Figure 4.4.23 Scenario 1 - Simulated and observed temperature at different depths between March 9th and March 22nd, 2010, for calibration during partially saturated conditions. Note that the observation node for T3 was placed 5 cm lower than indicated from field measurements.	139
Figure 4.4.24 Scenario 2 - Simulated and observed temperature at different depths between March 9th and March 22nd, 2010, for calibration during partially saturated conditions. Note that the observation node for T3 was placed 5 cm lower than indicated from field measurements.	140
Figure 4.4.25 Cumulative infiltration (m) and the height of the water column at the surface for scenarios 1 and 2.....	141
Figure 4.4.26 Example of Sensitivity Analysis Results on Simulated Soil Temperature (see Figure Q.29).	142

Figure 4.4.27 Change of saturated hydraulic conductivity vs. simulated cumulative infiltration for scenarios 1 and 2.....	143
Figure 4.4.28 Simulated and observed temperature profiles between August 24th to October 31st, 2010 using the moisture retention parameters obtained from calibration when the ephemeral stream was present.....	144
Figure 4.4.29 Simulated and observed temperature profiles between August 24th to October 31st, 2010 using altered moisture retention parameters obtained from calibration when the ephemeral stream was present by increasing the hydraulic conductivity of the lower eight layers by two.	145

Chapter 1

Issues in Source Water Protection in Agriculture

1.1 Source Water Protection

Source water protection is regarded as the first barrier in a multi-barrier approach to providing safe drinking water. It is done on both local and regional scales and involves identifying risks posed to sources of potable water, both surface water and groundwater, and enacting a plan to mitigate those risks. This mitigation is accomplished through institutional arrangements for land use planning and water management through the voluntary adoption of Best or Beneficial Management Practices (BMPs). In Ontario, Canada many communities began to implement source water protection plans in the wake of the Walkerton tragedy in 2000 where the presence of E. coli bacteria in the municipal drinking water resulted in the death of seven people and impacted the health of thousands of other residents. In 2006, the Province of Ontario created legislation, the Clean Water Act, which requires communities in the province to develop source water protection plans for their municipal sources of drinking water.

Agricultural land use practices have been documented to have influenced groundwater quality on regional scales worldwide (Vitousek et al., 1997; Smil, 1999). The impacts of agricultural practices are classified both as point and non point source contaminant problems and the management of these impacts is a significant component of many source water protection plans in Ontario and elsewhere. To date there is a paucity of field-base evidence on how to most efficiently manage agricultural operations in order to limit environmental impacts and maintain financial viability. The research presented herein is focused on several aspects of agricultural land use practices within the context of source water protection for municipal groundwater supplies.

1.1.1 Agricultural Groundwater Contamination

Potential major groundwater contaminants from agriculture include nutrients (nitrates and phosphates), microbial pathogens and other agrichemicals (Goss et al. 1998). Of these, nitrate is the single most common groundwater contaminant (Freeze and Cherry, 1979). Increases in nitrogen fertilizer applications for crop production, particularly with synthetic fertilizers, have been correlated to increases in nitrate in drinking water supplies. Nitrate from excess fertilizer application is leached from the rooting zone of crops and transported by infiltrating water to groundwater systems or surface water bodies (Addiscott et al., 1991; Spalding and Exner, 1993; Vitousek et al., 1997; Smil, 1999; Burkart and Stoner, 2002). In order to protect water quality, BMPs that reduce nitrate losses from agricultural fields are sought. In the simplest terms, BMPs associated with nitrogen fertilizer application attempt to maximize the efficiency of

the rate and timing of applications in order to sustain a productive crop and minimize losses to the environment. Combined approaches, including strict nutrient management plans and crop rotation strategies, have shown promise in this regard (Clark et al. 1998; Clark et al. 1999; Kramer et al., 2002a; Gentile, 2008), but there is little performance data available to assess the effectiveness of these BMP strategies.

1.1.2 Recharge

The impact of nitrate losses to the environment is influenced by the rate and timing of groundwater recharge. Large amounts of recharge can dilute nitrate concentrations in groundwater, but also provide a vehicle for nitrate movement from the surface to groundwater aquifers. Recharge varies temporally due to seasonal changes in hydrology and spatially due to topography and stratigraphy. Typically recharge is greatest in areas of low topography with well drained soils during periods of high rainfall or during snow melts. Proper assessments of recharge are essential in order to estimate the impact of nitrate losses over larger areas.

1.1.3 Current Studies

Two interrelated projects were undertaken as part of this thesis to address agricultural land management issues from a source water protection perspective. The two projects were conducted on land owned by the County of Oxford, located south of City of Woodstock, Ontario. An introduction to the study site and the previous work completed at the site are presented in Chapter 2. The two projects are presented in Chapter 3 and Chapter 4 and include a presentation of the study problem and objectives, methodology, results, a discussion of the results and conclusions unique to each project. A summary of the findings of both projects are presented in Chapter 5.

The first project, presented in Chapter 3 employs data collected from cores of the unsaturated zone to quantify changes in nitrate mass storage beneath agricultural field locations where different nitrogen fertilizer management strategies were being evaluated. The different fertilizer strategies were designed to provide better synchrony between nutrient availability and crop demand during the growing season. The evolution in stored nitrate mass over time was used as a metric to assess the performance of the different techniques in limiting leaching of excess nitrate below the root zone. Other parameters such as crop yields, associated crop management costs, and changes in nitrate concentrations in shallow soils during the growing season, are examined to assess the effectiveness of each treatment with regards to losses of nitrate to the subsurface as well as economic benefit.

The second project, presented in Chapter 4, uses subsurface temperature profiles to assess recharge dynamics in the vicinity of an ephemeral stream which developed during the spring melt on the agricultural study site. Rapid and potentially significant rates of groundwater recharge are thought to be occurring in this area, which may influence the vulnerability of the municipal water wells associated with potential surface sources of contamination. Subsurface temperature monitoring was suggested because rapid groundwater temperature changes had been observed during previous investigations at the site and have been used as evidence of the possibility of rapid infiltration in the vicinity of the ephemeral stream.

The use of temperature fluctuations as a means to determine recharge rates is a tool that is growing in popularity, especially in applications determining exchanges between surface water and groundwater. The advantage of such a technique is that temperature is a naturally occurring tracer and is a robust parameter to monitor (Constantz, 2008). Thermistors were installed in the unsaturated zone below the site of an ephemeral stream which forms during the spring melt event. Transient data from the temperature probes were used to estimate infiltration into the soil during the melt event using a one-dimensional model. Such estimates, in turn, can provide insight into the potential risk to local municipal groundwater supplies from contaminants infiltrating during this type of extreme hydrologic event.

Chapter 2

The County of Oxford Lands - A Source Water Protection Area

2.1 Introduction

This chapter introduces the study site located on the County of Oxford lands, near the City of Woodstock. An overview of the geology, hydrogeology, changes in agricultural practices, and previous studies conducted at the site are outlined here. This information provides the context for the studies presented in this thesis.

2.1.1 Study Site

The study site is located in south-western Ontario, two kilometers south-west of the City of Woodstock (Figure 2.1.1). The study site is just west of the Thornton Well Field, which provides the majority of the drinking water to the City of Woodstock and the surrounding residents. Water distribution for the region is managed by the County of Oxford. In the mid 1990's nitrate concentration in several of the Thornton supply wells began to exceed the maximum allowable concentration (MAC) of 10 mg NO₃-N/L. As agriculture is the dominant land-use in the region, a trend of increasing nitrate concentrations in the supply wells since the 1970's was suggested to be a result of increased fertilizer use in the region over the last several decades (Padusenko, 2001). Oxford's current water management scheme involves controlling pumping rates of the different wells and blending water sources in order to maintain nitrate concentrations below the MAC in the distribution system.

In 2003, the County of Oxford purchased 111 hectares of land located within the two year time of travel capture zone of the Thornton Well Field (Figure 2.1.2). This land was purchased as part of a source water protection plan to mitigate the risk of nitrate contamination to the well field. The County decided to keep the land in cultivation rather than take it out of production, so it was leased back to local farmers with the restriction that best or beneficial management practices (BMPs) needed to be implemented to reduce nitrate leaching at the site. Notable changes to agriculture practices since the purchase of the land include: conversion from manure as the dominant source of nitrogen fertilizer to exclusive use of synthetic fertilizers, lower application rates of nitrogen fertilizer, conversion from crops requiring high nitrate fertilizer application rates to crops requiring lower rates (e.g., hard red winter wheat to soft red winter wheat), and finally some fields were converted from crops to continual grass (Bekeris, 2007). A typical three year rotation on the land consists of corn, soybean and winter wheat under-seeded with red

clover. Overall, these changes have resulted in a significant decrease of applied nitrogen to the site since 2003. Researchers at the University of Waterloo have been conducting a variety of research projects at the site since 1998 focused on the impact of agricultural land management activities on groundwater quality in the vicinity of the Thornton Well Field. This has included the long term monitoring of the implemented BMPs at the site since 2004.

2.1.2 Geology and Hydrogeology

Topography at the study site is gently rolling with the elevation ranging from 300 to 340 meters above sea level (masl) (Figure 2.1.2). The surficial geology at the site consists mainly of Zorra Till; a stiff, stony silt till (Cowan, 1975). A glaciofluvial outwash channel is present in a low-lying area on the eastern side of the study site (Figure 2.1.3). The glacial overburden sediment range between approximately 30 m and 80 m in thickness and are composed of intermingled deposits of glacial till, and sand and gravel. The bedrock geology in the region consists of a Silurian dolostone and shale, as well as a Devonian limestone (Cowan, 1975)

Hydrogeological investigations of the site were conducted by Padusenko (2001) and Haslauer (2005). A conceptual model of the site presented by Haslauer (2005) identifies five main aquifer units (Figure 2.1.4 and Figure 2.1.5). Four of these are sand and gravel aquifers located within overburden system inter-layered with four till aquitards and the fifth aquifer is a bed rock aquifer. Aquifer 3, 4, and 5 are water supply aquifers, Aquifer 1 is unsaturated over most of the site, with occasional perched zones. Aquifer 2 is unsaturated over most of the site; however, saturated conditions are encountered where the glacial outwash channel is part of Aquifer 2 (Figure 2.1.3). In this area, there is evidence of a direct hydraulic connection between the ground surface and Aquifer 2, as well as some hydraulic connection between Aquifer 2 and Aquifer 3 (Figure 2.1.5) (Haslauer (2005). Under the field site, groundwater flows towards the well field in a radial manner. The depth to the water table varies over the site depending on topography; in low lying locations groundwater may be 2 meters below ground surface, but at higher elevations the water table is tens of meters below the ground surface (Haslauer, 2005).

2.1.3 Investigation of BMPs

Movement of solutes in unsaturated conditions can be very slow and it may take several years before the changes to land management practices can be observed in the groundwater. In order to assess the impact of the BMPs, Bekeris (2007) used a novel technique involving the coring of the unsaturated zone in order to monitor changes in stored nitrate over time. The investigation took place between January 2005 and May 2006.

Eight topographically different locations were selected for detailed investigation; these were referred to as recharge stations (or stations). At each station a potassium bromide tracer was applied to a three meter by three meter plot, and a neutron access tube was installed. Neutron access tubes consisted of PVC pipes inserted into the ground, in order to allow passage of a neutron probe, which is used to estimate moisture content of the surrounding soil. The movement of the bromide tracer, as tracked through the chemical analysis of soil samples derived from subsequent coring campaigns, allowed for estimation of recharge at each station and provided a proxy for the movement of nitrate. Temporal monitoring of the soil nitrate concentration contained in the soil cores collected within the unsaturated zone at each of the stations allowed for a comparison of stored nitrate mass prior and after the implementation of BMPs. The BMP under investigation was an overall decrease of nitrogen fertilizer applications. Between May of 2007 to October of 2008, Koch (2009) expanded this work to include another seven stations, and attempted to interpolate changes in nitrate storage over the entire area owned by the County of Oxford where the BMP activity was implemented.

Several different land management practices were employed at the site in order to reduce the overall nitrate loading to the groundwater system. Investigations comparing the different alternative nutrient management practices are needed to assess their relative effectiveness in reducing nitrate loading at the site while maintaining productive agriculture. To this end, Chapter 3 presents a one year study comparing different nitrogen management strategies applied at the field site, where the movement of nitrate was monitored in and below the rooting zone to assess the leaching potential.

2.1.4 Ephemeral Stream Channel

Most years an ephemeral stream develops in a low lying area on the north-east corner of the site as a result of a mid-winter and/or spring melt. The stream flows in a southeast direction across the study site draining water from outside of the two year time of travel zone, and in some years may flow to within close proximity of the Thornton municipal water supply wells. Below the flow path of the ephemeral stream, there is geologic evidence that suggests there may be a direct hydraulic connection between the ground surface and the main groundwater production unit (Aquifer 3), due to the absence of Aquitards 1 and 2 and discontinuity of Aquitard 3 (Figure 2.1.5) (Haslauer, 2005). In addition, the water table is quite high in this area; fluctuating between two and three meters below ground surface during the year. Both Haslauer (2005) and Koch (2009) noted that there are conditions for rapid infiltration in this area, as indicated by a variable hydraulic head and groundwater temperature response to the spring melt observed in monitoring wells.

In order to assess the correlation between extreme hydrologic events such as melt events and the occurrence of microbiological species in both the surface water and ground water. Between the fall of 2007 and mid-2009, Christie (n.d.) sampled groundwater, tile outfall, and ephemeral surface water for nitrate and chloride as well as three water quality indicator bacteria: *Escherichia coli*, total coliforms (TC), and aerobic endospores (AE) between the fall of 2007 and mid-2009. Samples were taken regularly on a monthly basis, and sampling frequency increased during extreme hydrologic events. A total of 450 microbial samples were taken between November 2007 and May of 2009. It was found that water sampled from tile outfall and ephemeral stream surface water contained the highest concentrations of TC and AE, and groundwater concentrations of TC and AE were highest immediately after melt events. Isolated peaks in TC and AE were observed four month later in municipal wells and monitoring wells nearby, possibly indicating a time-lag in the arrival of the spring infiltration. This study was the motivation for the current study, as a more detailed quantification of recharge dynamics associated with this type of surface runoff phenomenon is critical for assessing the vulnerability of the production aquifer in this region to surface sources of contamination. Chapter 4 presents a novel approach of assessing recharge at the site using temperature as a tracer.

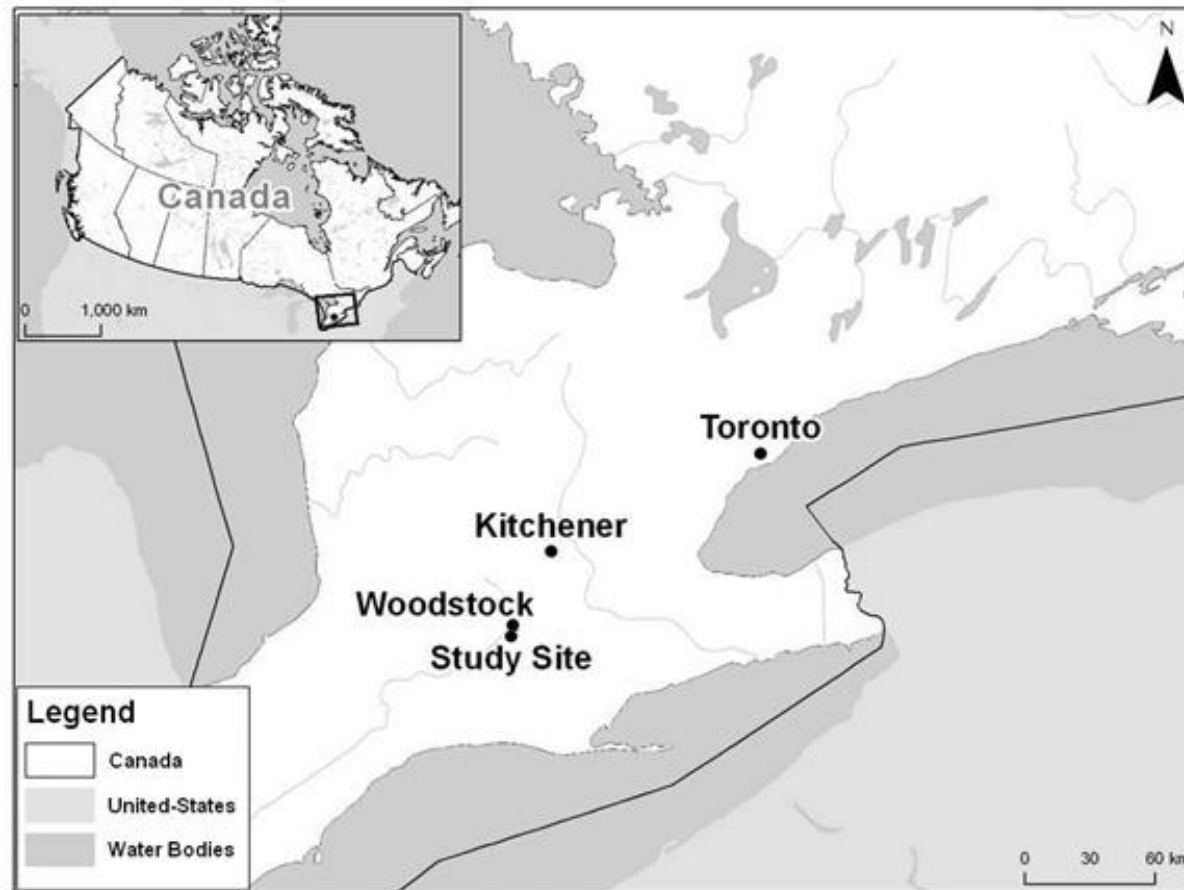


Figure 2.1.1 Location of Study site within Southern Ontario. Contains data for the University of Waterloo (n.d.)

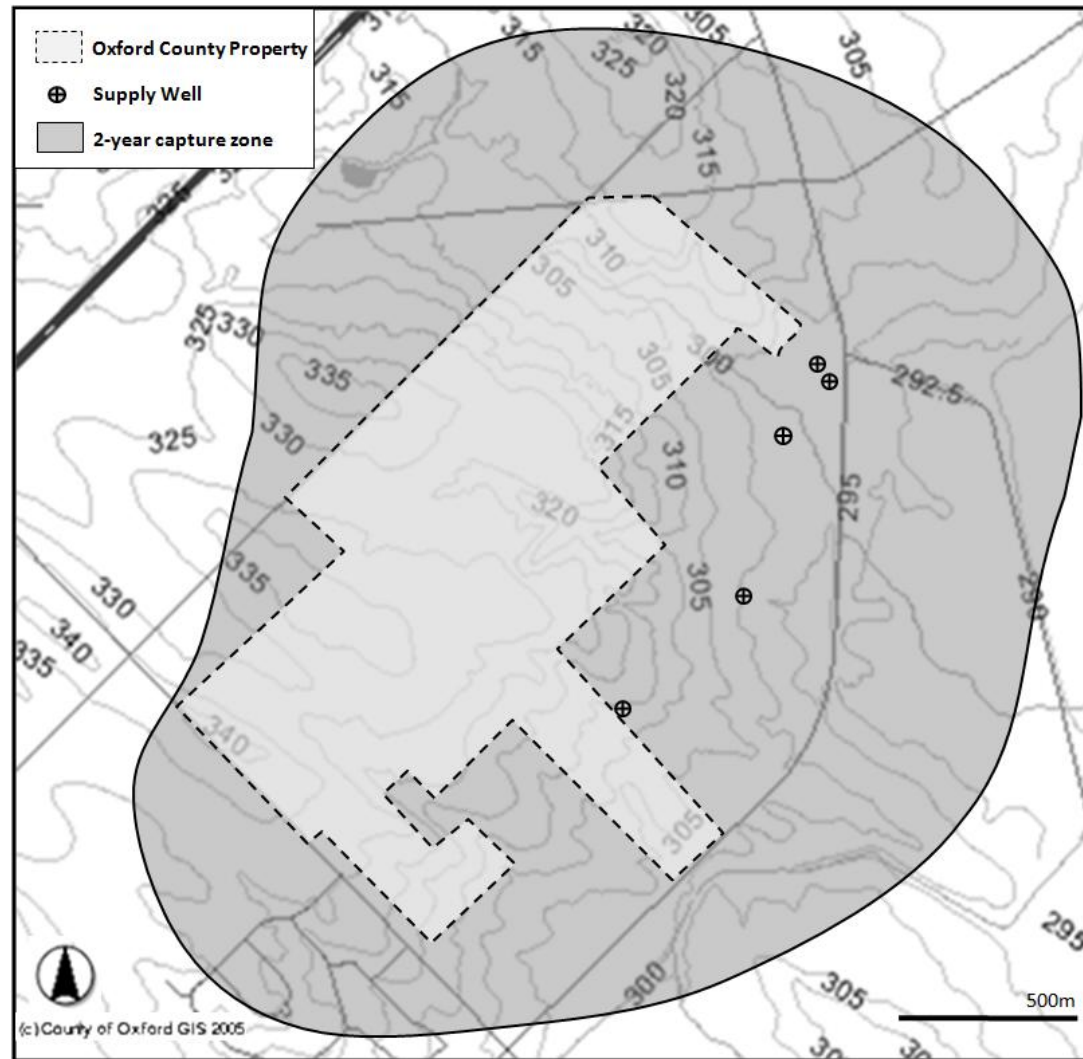


Figure 2.1.2 Topography of land owned by the County of Oxford, and two year time of travel capture zone. Contains data from the Corporation of the County of Oxford (County of Oxford GIS. 2005).

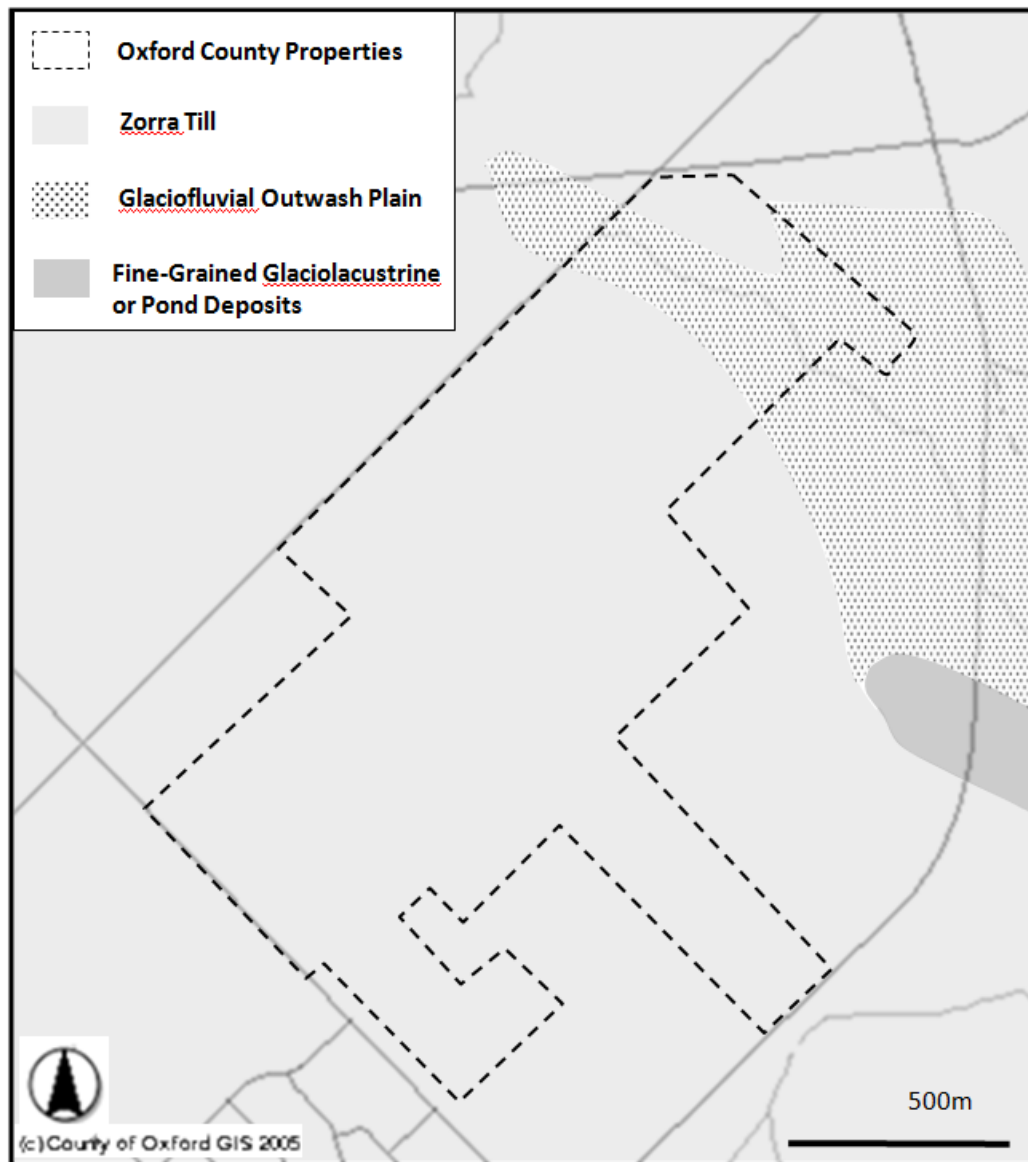


Figure 2.1.3 Quaternary geology of the study site. Adapted from Bekeris (2007). Contains data from the Corporation of the County of Oxford (County of Oxford GIS, 2005).

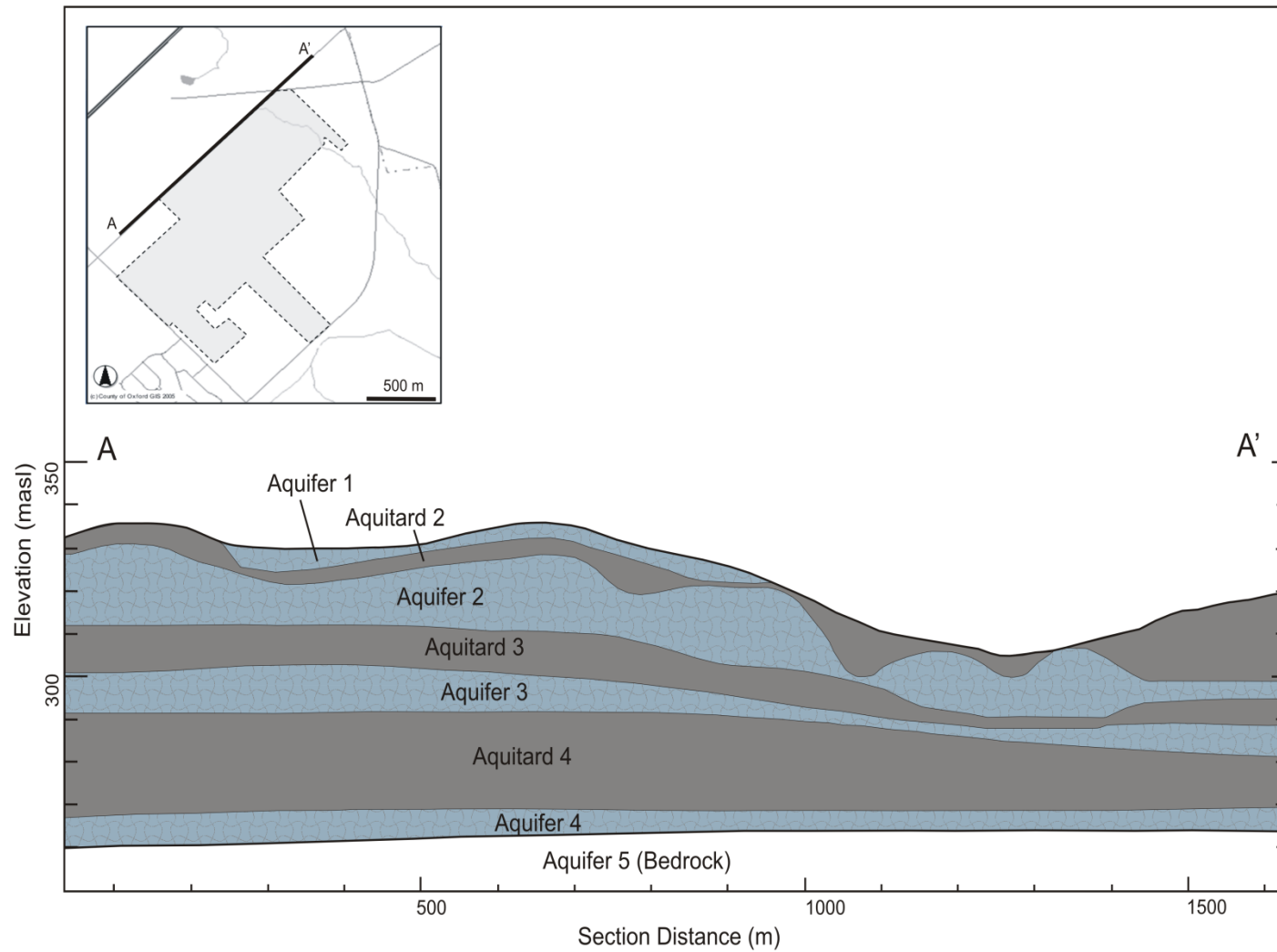


Figure 2.1.4 Geologic cross-section (north-east to south-west) in the north-east edge of the site, in the vicinity ephemeral stream site. Adapted from Haslauer (2005). Contains data from the Corporation of the County of Oxford (County of Oxford GIS, 2005).

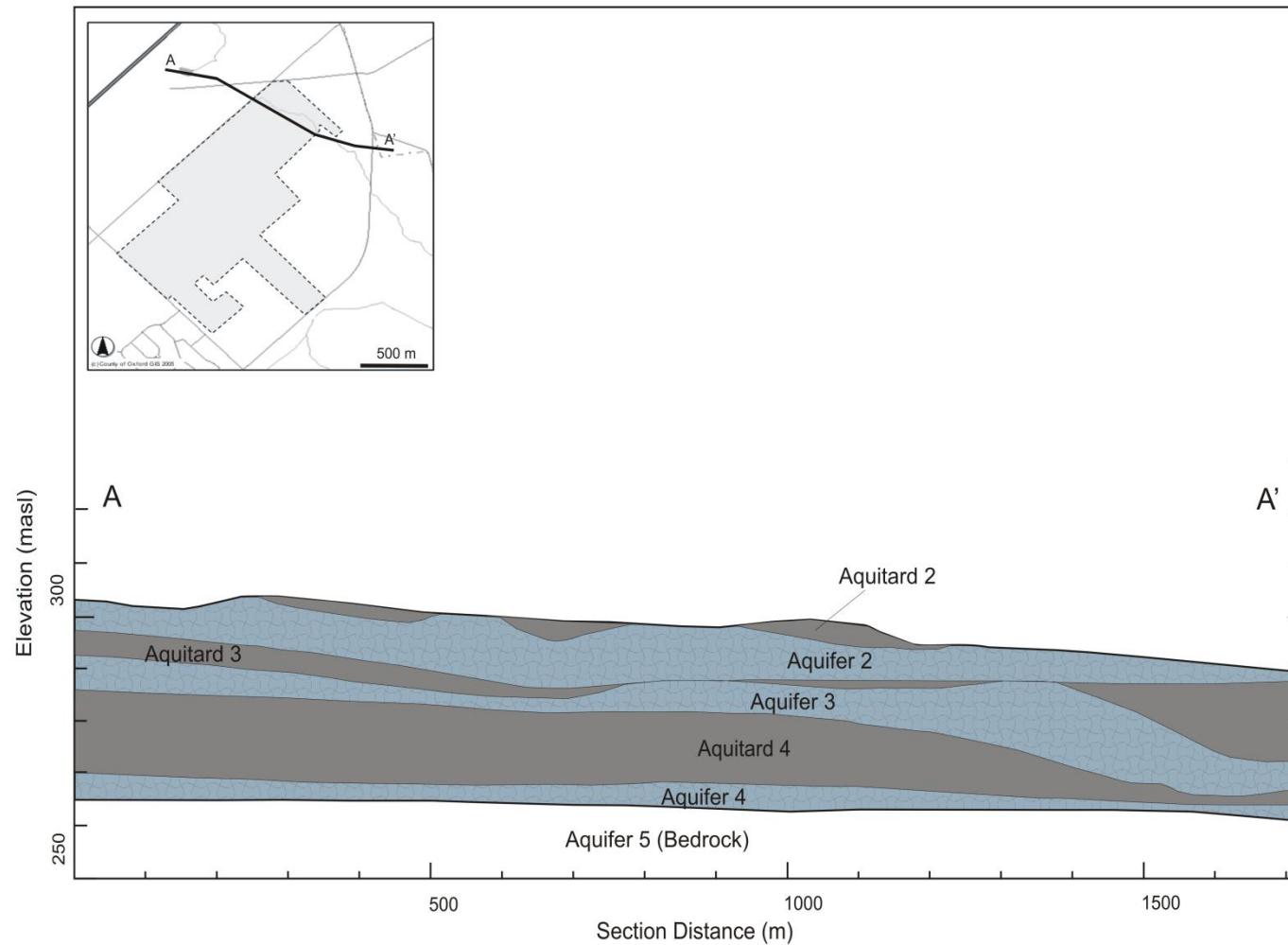


Figure 2.1.5 Geologic cross-section (north-west to south-east) in the north-east edge of the site, in the vicinity ephemeral stream site. Adapted from Haslauer (2005). Contains data from the Corporation of the County of Oxford (County of Oxford GIS, 2005)

Chapter 3

Innovative nitrogen management strategies to reduce impacts to groundwater quality in source protection areas

3.1 Introduction

This section introduces the problem of nitrogen in agriculture, presents the objectives of this study and outlines the study approach.

3.1.1 The Nitrogen Problem in Agriculture

The terrestrial nitrogen cycle has been significantly altered since the preindustrial era, effectively more than doubling the mass of fixed nitrogen in biological systems (Vitousek et al., 1997; Smil, 1999). Crop production is the largest source of anthropogenically fixed nitrogen, and over half of all anthropogenically fixed nitrogen inputs to terrestrial ecosystems can be attributed to synthetic fertilizers (Smil, 1999; Vitousek et al., 1997). Among other technological advances in agriculture, the use of synthetic fertilizers has allowed farmers to keep up with ever increasing food demands as the world's population increases. In fact Smil (2001) estimated that in the mid 1990's 40% of the world's nitrogen in dietary protein was derived from synthetic fertilizers, and estimates that by 2050 this will have increased to 60%. Increasing food demand due to human population growth ensures that the use of synthetic nitrogen fertilizers will continue at high rates for decades to come (Vitousek et al., 1997; Smil, 2001; Crews and Peoples, 2004).

Increases in nitrogen application, particularly from synthetic fertilizers, has been correlated to increases in nitrate in drinking water supplies, as nitrate is leached from the rooting zone of crops and transported by infiltrating water to groundwater systems and surface water bodies (Addiscott et al., 1991; Spalding and Exner, 1993; Burkart and Stoner, 2002). As synthetic fertilizers are relatively inexpensive, the application of excess fertilizer is often regarded as insurance against yield losses (Vitousek et al. 1997; Crews and Peoples, 2005). However, a relatively high percentage of applied fertilizer is typically lost to the environment, either in gaseous form or in solution (Vitousek et al., 1997; Smil, 1999). This waste is an economic loss to farmers, and is a global issue as nitrate is the single most common groundwater contaminant (Freeze and Cherry, 1979). Many management practices that increase crop use efficiency of nitrogen are recognized, and improvements are being sought. Farmers and researchers now face a challenge of balancing increases in food supply while minimizing the risk to the environment.

The study presented herein is unique in its approach. A comprehensive comparison of various combined nitrogen BMPs for inputs to agricultural lands is presented from both an agronomic and

environmental perspective. Treatments that have relatively better agronomic returns and reduce nitrate losses to the subsurface are sought. From an agronomic perspective, treatments are compared with regard to their corn yield and economic returns. From an environmental perspective, treatments are compared with regard to the change of nitrate concentrations in the subsurface with time.

3.1.2 Objectives

The primary goal of this study is to investigate the benefits of different combined nitrogen management and cropping practices in reducing the leaching potential of nitrate under corn within a source water protection area. This study compares different fertilizer applications in two scenarios: with and without the use of green manures. The objectives of this study are to:

- Evaluate the leaching potential of combining synthetic fertilizers with a green manure versus treatments with only synthetic fertilizers.
- Compare the leaching potential of the different fertilizer treatments.
- Evaluate the economic implications of the alternative nutrient management practices
- Recommend treatments that reduce nitrate leaching while maintaining crop yields.

3.1.3 Study Approach

Field studies are needed to give better recommendations of nutrient management techniques that will reduce nitrate leaching while maintaining acceptable yields. The following study tracks the change of nitrate storage near the surface during the growing season, as well as changes in nitrate storage at depth after planting, after harvest and after one year. A bromide tracer was applied at the site to evaluate the furthest extent of vertical migration of the nitrogen treatments, as well as to estimate recharge near the site. Corn yields were measured, and an economic analysis of the different treatments was conducted. Meteorological parameters such as precipitation were also monitored on-site.

Section 3.2 provides a background of the different nutrient management techniques in this study. Section 3.3 describes study design and the methods used to evaluate the different techniques. Section 3.4 presents the results and Section 3.5 provides an interpretation of the results. Section 3.6 presents the conclusions of this study and Section 3.7 makes recommendations relative to the study objectives.

3.2 Background

Imperfect timing between nitrogen supplied from fertilizers relative to nitrogen demand by crops decreases the nitrogen use efficiency of crops, and causes nitrogen excess in the environment (Crews and Peoples, 2005). Better synchrony between supply and crop demand is needed to maximize agronomic output while reducing losses of nitrogen to the environment (Cassman et al., 2002). Leaching losses occur when there is a build-up of mineral nitrogen in the soil, which is transported through the subsurface by infiltrating water during periods of groundwater recharge, contaminating groundwater aquifers (Addiscott, 1991). During the growing season, the period of greatest risk of leaching loss is generally after fertilizer application when the concentration of mineral nitrogen is far higher than the ability of the crop to utilize it. Leaching losses after harvest may also be relatively high (Crews and People, 2005).

Various methods to achieve better synchrony have been devised; some entail applying fertilizers later in the growing season when crop demand for nitrogen peaks, others involve using fertilizer sources that gradually release nutrients. The latter includes both synthetic fertilizers, which delay the release of nutrients, as well as employing organic sources of nitrogen such as legume cover crops, which release nitrogen as plant matter decomposes. The treatments under review in this study encompass different combinations of these approaches. This study investigates the advantages of three beneficial management practices: the use of biologically fixed nitrogen, polymer-coated nitrogen fertilizer, and side-dress applications of nitrogen fertilizer.

Biologically fixed nitrogen is a traditional source of nitrogen in agriculture, the use of which decreased with the adoption of synthetic fertilizers. (Power and Scheppers, 1989; Dinnes et al., 2002). Concerns of the environmental impacts of excess nitrogen and the rising cost of synthetic fertilizers have created a growing interest in reintegrating biologically fixed nitrogen as a nitrogen supply (Dinnes et al., 2002; Kramer et al 2002a; Crews and Peoples, 2004). The most common source of biologically fixed nitrogen is from legumes. The practice of green manuring utilizes this organic source of nitrogen, which is made available to subsequent crops through the gradual decomposition of legume plant material.

Controlled-release fertilizers, such as polymer-coated nitrogen fertilizers, also supply crops with nutrients gradually over the growing season. The advantage of such a product is that it may reduce leaching losses and provide better synchrony with crops, as nutrients are released in a controlled manner by diffusion through the polymer coating.

Side-dressing is a practice where the bulk of nitrogen fertilizer is applied after the crop has been established. Typically the recommended rate of fertilizer application is less than a spring application of fertilizer. Such a practice may also help reduce leaching and increase nutrient use efficiency as early season losses can be avoided.

3.2.1 The Life Cycle of Corn

From planting to harvesting corn crops are marked by several life stages. Hanway (1963) delineated stages of growth based on the different identifying characteristics of the corn plant. Some important stages of growth will be outlined here. After planting, the first stage of corn development is emergence, the time lag between planting and this stage depends on soil moisture conditions and temperature. Typically emergence will occur 8 to 10 days after planting. Early stages of corn growth are delineated by the number of leaves. The next important stage in the physiological development of corn plants is marked by the appearance of tassels; these are the male flowers of the corn plant which produce pollen. Tassels appear at the top of the corn stalk around the time when the 16th leaf is visible. This is followed by emergence of silks, the female flowers of the corn plant, and the shedding of pollen. At this point, vegetative growth has stopped as future energy will be supplied to the growth within the ears. Physiological maturity of the corn plant generally occurs 2 months after silking.

Nitrogen uptake by corn crops has been shown to vary during the life cycle. Typically uptake is highest during a stage of rapid growth early in the season, with the maximum accumulation of nitrogen occurring near silking (Sayre, 1948; Hay et al., 1953; Hanway, 1962; Ruselle et al., 1983). During this period a single corn plant can accumulate as much as 170 mg plant⁻¹ day⁻¹ of nitrogen (Ruselle et al., 1983). Nitrogen fertilizer use efficiency can be improved by delaying the application of nitrogen fertilizer until after the crops are well established (Nelson, 1956; Welch et al., 1971). However, if the delay is too long, this may cause decreases in yields and poor nutrient use efficiency of the applied fertilizer (Nelson, 1956; Pumphrey and Harris, 1956; Jung et al., 1972).

3.2.2 Nitrogen Treatment Options

3.2.2.1 *Comparing Biologically Fixed Nitrogen and Synthetic Fertilizers*

The use of legumes as a source of nitrogen for crops has been promoted as an alternative to conventional agricultural systems that use synthetic fertilizers. Relatively few studies have directly compared nitrate leaching under crops supplied with biologically fixed nitrogen to those supplied with synthetic fertilizers only. Some studies have suggested that there is less leaching under fields using legumes as the main source of nitrogen compared to conventional systems using synthetic fertilizers (Owens et al. 1994; Drinkwater et al. 1998). Sinclair and Cassman (1999) warns that such results should be considered with

caution as the conventional agricultural practices used are not necessarily representative of beneficial management practices that help reduce nitrogen leaching. Studies comparing leaching losses of nitrogen under fields supplied with either synthetic fertilizers or legume fertilizers over different rotations note that there are seasonal differences in leaching losses under both, but found that these systems were relatively similar overall (Groffman et al., 1987; Stopes et al., 2002).

Loss of nitrate to the subsurface is dependent on how much of the applied fertilizer is available to plants for uptake and how much is retained in the soil. This can be examined using the isotope dilution method to compare the distribution of a N-15 isotope tracer in systems supplied with either biologically fixed nitrogen or synthetic nitrogen fertilizer. Studies using this method suggest that crops recover a higher percentage of the synthetic nitrogen fertilizer, whereas a higher proportion of nitrogen applied in the form of legumes was retained in the soil (Harris et al. 1994; Janzen et al., 1990; Varco et al., 1993; Kramer et al. 2002a; Kramer et al. 2002b; Ladd and Amato, 1986; Muriuki et al., 2007). The total recovery (soil and plants) of the tracer is generally higher in treatments receiving organic sources of nitrogen. Although some authors do not find the difference in total recovery between treatments to be significant (Harris et al., 1994; Kramer, 2002b; Ladd and Amato, 1986), others have found there to be a marked difference between treatments (Janzen et al., 1990).

The differences in the distribution of the tracer nitrogen between field soils receiving either synthetic nitrogen fertilizer or legume nitrogen are due to the form of nitrogen present from each source during the growing season. Synthetic fertilizers are present in mineral forms that are more readily taken up by plants early in the growing season (Janzen et al, 1990; Harris et al., 1994). Studies suggest that the efficiency of use of the applied nitrogen by the crop is not affected by the mineral form of nitrogen applied when comparing different types of synthetic fertilizer treatments (Ladd and Amato, 1986; Reddy and Reddy; 1993).

Smaller recovery of tracer nitrogen from organic sources in crops may be because the tracer remains in un-decomposed organic matter (Janzen et al, 1990; Harris et al., 1994). It has been suggested that this lower recovery may be due to substitution within the nitrogen pool, where recently applied nitrogen is immobilized by soil microbes and unlabeled soil nitrogen is mobilized (Varco et al., 1993). Studies conducted over two consecutive crops found that the trend of higher concentrations of stored nitrogen in the soil from legume treatments was maintained from one crop to the next (Ladd and Amato, 1986; Harris et al., 1994).

Agricultural treatments using organic sources of nitrogen have been found to accumulate nitrogen and carbon in the soil over time, whereas long term agricultural treatments using synthetic fertilizers tend to decrease reserves over time (Clark et al., 1998; Tilman, 1998; Kramer et al., 2002b). In this way, the integration of legumes in a cropping system has been suggested to contribute to the long term fertility of soil (Azam et al 1985; Janzen et al., 1990; Clark et al., 1998; Kramer et al., 2002b; Muriuki et al., 2007). The decomposition of organic matter and the mineralization of nitrogen are mediated by microbes, which use organic matter as a source of carbon for respiration and growth. Mineral nitrogen released from legume plant material or present from an application of synthetic fertilizer may be assimilated by soil microbes, effectively immobilizing the nitrogen, a process limited by the amount of carbon (Crews and Peoples, 2005). Therefore, soils with higher amounts of organic matter may retain higher concentrations of nitrogen, which are immobilized by a large microbial population. The release of mineral nitrogen in a legume cropping system differs from one using synthetic fertilizers; legumes provide a delayed sustained release of mineral nitrogen, whereas conventional synthetic fertilizers contribute a large flush of mineral nitrogen when it is applied (Groffman et al, 1987; Stute and Posner, 1995; Kramer et al, 2002a; Crews and Peoples, 2005). The rate of uptake of legume derived nitrogen by crops is constant throughout the growing season, whereas uptake of synthetic nitrogen fertilizer tends to peak early in the season and decrease with time (Kramer et al., 2002a). It has been suggested that better synchronization of nitrogen supply and peak demand may be achieved with a combination of both sources, where synthetic fertilizers provides nitrogen earlier in the season accompanied by a sustained release of nitrogen from legume fertilizer (Kramer et al., 2002a). Combining these sources may also have the beneficial effect of immobilizing a portion of mineral nitrogen applied to the soil early in the growing season, which may be released in full or in part later on, resulting in possible reduced nitrogen losses during the growing season (Kramer et al., 2002a; Crews and Peoples, 2005; Gentile, 2008). The adoption of low-input systems which employ legume cover crops and reduced synthetic nitrogen fertilizers may also have an economic advantage due to the reduced cost of inputs. A study by Clark et al. (1999) comparing a low-input system utilizing a combination of both legumes and synthetic fertilizers to an organic system and conventional system found that the low-input system had higher yields and net returns.

3.2.2.2 Comparing Control-Release to Conventional Spring Applied Nitrogen Fertilizers

There are two basic types of controlled or slow release products: low solubility fertilizers and coated water-soluble fertilizers (Blaylock et al., 2005). Although there is no official differentiation between the terms controlled-release and slow-release, coated fertilizers are typically referred to as control-release fertilizers (CRF), and low solubility fertilizers are typically referred to as slow-release fertilizers (SRF) (Trenkel, 1997). Laboratory experiments comparing CRFs and SRFs to conventional soluble fertilizers

have found the formers to significantly reduce relative leaching of nitrogen (Alva, 1992; Wang and Alva, 1996; Paramasivam and Alva, 1997). A study by Mikkelsen et al. (1994) comparing six different types of fertilizers, three CRFs and three SRFs, for the production of ornamental container grown crops found that, in general, coated fertilizers out performed non-coated fertilizers in reducing nitrogen leaching losses and increasing yields.

The most common coated fertilizers are sulfur- and polymer-coated products. These products release fertilizer through somewhat different mechanisms: sulfur-coated fertilizer is released through the degradation of the coating, which is biologically mediated, as well as a through diffusion of the somewhat porous coating, whereas with polymer-coated fertilizer the semi-permeable polymer coating allows water to be absorbed which dissolves the encapsulated fertilizer releasing it through diffusion (Trenkel, 1997; Blaylock et al., 2005). Sulfur-coated products are much less expensive to produce than polymer-coated products; however, some argue that the polymer-coated products may be more promising as they can be designed to release nutrients in a more controlled manner (Trenkel, 1997; Blaylock et al., 2005).

The release of nutrients from polymer-coated fertilizers is controlled by polymer chemistry, coating thickness, the presence of soil moisture, and soil temperature (Trenkel, 1997; Blaylock et al., 2005; Du et al., 2006). The nutrient release pattern of polymer-coated fertilizers has been described as having three stages: a lag stage, a linear release stage, and a decay stage (Du et al., 2006). The advantage of this release pattern compared to conventional fertilizers is that it limits the amount of nutrients present in the soil when crop nutrient demand is low in the early growing season when the risk of nutrient loss is high, and releases nutrients gradually during crop growth which may result in better nitrogen use efficiency.

Until recently, the application of such fertilizers has been limited to high value applications such as fruits and vegetables, turf grass management, and ornamentals crops (Hauck, 1985; Mikkelsen et al., 1994; Blaylock et al., 2005, Shaviv, 2005). However, as the prices decrease, there is a growing interest in these types of fertilizers for widespread crop production (Blaylock et al., 2005). Studies have observed similar or higher yields for potato (Waddell et al., 1999, Zvomuya et al., 2003; LeMonte et al., 2009; Hyatt et al., 2010; Wilson et al., 2010), corn (Blaylock et al., 2004, Moore, 2008; Nelson et al., 2009; Noellsch et al., 2009), and wheat (Haderlein et al., 2001) using polymer-coated nitrogen fertilizers applied compared to similar applications of conventional fertilizers. Polymer-coated nitrogen fertilizers have been observed to have higher nitrogen use efficiencies in corn production (Noellsch et al., 2009), and they have been observed to reduce leaching under a variety of different crops (Zvomuya et al., 2003; Nelson et al., 2009; Wilson et al., 2010). Although, these products are touted as green fertilizers reducing leaching, some studies have found nitrogen concentrations in the form of nitrate and ammonium to persist

at higher levels than conventional fertilizers at the end of the growing season (Paramasivam and Alva, 1997; Moore, 2008). This may result in greater losses following harvest if another crop does not immediately follow. Still, these products hold a lot of promise in areas particularly prone to leaching losses, such as well drained soils which receive large amounts of spring rains (Zvomuya et al., 2003)

3.2.2.3 Comparing Side-Dressed to Conventional Spring Applied Nitrogen Fertilizers

Side-dressing is a practice where the bulk of nitrogen fertilizer is applied after the crop has been established. The advantages of delaying the bulk of the application of nitrogen fertilizer until a corn crop is well established, has been acknowledged since the 1920s (Jung et al., 1972). When compared to conventional spring applications of nitrogen fertilizers for the production of corn, side-dress fertilizers have been found to have similar or higher yields (Pumphrey and Harris, 1956; Welch et al., 1971), as well as higher nitrogen use efficiencies (Welch et al., 1971). Improved nitrogen use efficiency and yields may be due to better synchrony between nutrient supply and the time of high crop demand. In years favorable to the production of corn at the lowest application rate, Pumphrey and Harris (1956) noted an increase in nitrogen use efficiency as the application of nitrogen fertilizer was delayed until the corn plants were 6-12 inches tall. A study by Jung et al. (1972) found that maximum rate of nitrogen uptake and maximum yields were obtained when nitrogen fertilizer was applied between the 5th and 8th weeks after planting. Authors noted that in the 7th week in the first year of trials that corn was 25 cm high. In Ontario it is recommended that side-dress application be applied before the corn is 30 cm high (OMAFRA, 2011a). This corresponds approximately to the 6 leaf stage (OMAFRA, 2011b). The timing of nutrient application is important when applying a side-dress of fertilizers, as studies have shown that nutrient use efficiencies and yields may decrease if the delay is too long (Nelson, 1956; Pumphrey and Harris, 1956; Jung et al., 1972).

3.3 Methodology and Approach

The field, laboratory and computational methods used to compare the different nutrient application treatments in this project are summarized in this section. Soil nitrate concentrations near the surface were monitored during the growing season with shallow soil sampling, and pore-water nitrate concentrations in the deeper unsaturated zone were estimated using deep core data. This information was used to compare nitrate leaching potential of the different treatments. Corn yields were monitored, and the costs of different treatments were estimated in order to compare the agronomic and economic benefits of the different treatments.

A chemical tracer (bromide) was applied in a section of the field, and the vertical migration of the tracer was used to determine the depth in the unsaturated zone affected by the treatments at a given time. The average pore-water nitrate concentration and nitrate mass for segments of interest was calculated by dividing the cumulative nitrate mass at points of observation by the length of the segment. The changes in nitrate storage were used as evidence to compare relative nitrate leaching potential between the selected treatments. Details of the different methods employed throughout the study are provided below.

3.3.1 Innovative Nitrogen Study

A 2-year research project, beginning in the spring of 2009, was implemented on a section of the Oxford land in order to study a series of different nitrogen management practices. The project was designed and conducted by researchers from the Soil Resources Group (SRG) in Guelph, Ontario and the author worked in direct collaboration with Mr. Don King of SRG throughout the course of the work. The location of the plots is presented in Figure 3.3.1. Only the results of the first year of study are presented here; from May 2009 to May 2010.

3.3.1.1 Study Design

The study employs a randomized block design of three replicates containing five plots separated by a buffer, each plot represents one treatment. Plots were approximately 18 m by 6 m (60 ft by 20 ft). A schematic of the study design is presented in Figure 3.3.2. The randomized blocks are replicated on two adjacent fields: one had a previous crop of winter wheat, and the other had a previous crop of winter wheat under-seeded to red clover. This design was replicated in two topographic positions: an upper and lower position. Because deep cores were only collected at the lower position, only the results from this position are discussed here.

3.3.1.2 *Fertilizer Application Treatments*

Five different fertilizer treatments were compared on two fields; one with a previous crop of winter wheat under-seeded with red clover and the other with a previous crop of only winter wheat. The treatments included:

- A control with only a starter nitrogen applied in the spring
 - A conventional urea fertilizer applied in the spring
 - A polymer-coated urea fertilizer applied in the spring
- A side-dress application of a solution of urea and ammonium nitrate in water containing 28% nitrogen (UAN 28) was applied in the early summer with “calculator rate”
- A side-dress application of UAN 28 with a high rate applied in the early summer.
 - All five treatments received a starter nitrogen application.

The rates of nitrogen application on the plots with a previous crop of winter wheat, hereafter named the “no clover” plots, as well as the fields with a previous crop of winter wheat under-seeded to red clover, hereafter named the “clover” plots, are summarized in Table 3.3.1. Rates differed between treatments, as well as between fields with different previous crops. The calculator rate side-dress treatments are recommended at a lower rate than the applications applied in the spring, for example, because it is applied later in the growing period when there is a lower risk of fertilizer losses due to run off or leaching. With the exception of the control and the high rate side-dress application, all rates were calculated using the Ontario Ministry of Agriculture, Food and Rural Affairs (OMAFRA) corn nitrogen calculator (the use of the tool will be described in Section 3.3.1.3). The high rate side-dress application was comparable to historical rates of nitrogen application in Ontario (David Start, pers. comm.). The red clover is a green manure in this study, it was incorporated into the soil the previous fall, and treatments which had a previous crop of winter wheat under-seeded with clover were given a nitrogen credit by the OMAFRA’s corn calculator. This resulted lower recommended application rates of synthetic fertilizer, as some will be supplied by the decomposition of the red clover. A timeline of seeding and application of fertilizer is presented in Appendix A.

3.3.1.3 *Corn Calculator*

In order to assist corn farmers in determining nutrient requirements for the specific conditions on their farm a user-friendly computer-based program was developed by OMAFRA (GOCorn.net, n.d.). The Corn Nitrogen Calculator allows farmers to estimate the application rate of nitrogen fertilizer needed for crops in order to have economical returns. The calculator takes into account economic information (the expected price of corn as well as the price of fertilizer); agronomic information (the fertilizer type, the

time of fertilizer application either pre-plant or side-dress, the expected yield, the previous crop, the rate of applied starter nitrogen and the rate of manure application); and environmental information (approximate heat units, the region of Ontario, and the soil type). This information is used to estimate recommended nutrient applications rates. For example, recommended fertilizer applications are usually lower for a side-dress application than a pre-plant application, and the fields previously planted with a clover cover crop are recommended a lower rate than those previously planted with a cereal crop.

3.3.2 Field Data Collection

A time line of field sampling efforts and equipment installation is presented in Appendix A. Note that initial study design included the use of suction lysimeters inserted one meter below the surface of the ground in order to assess leaching loss from the different treatments based on the analysis of pore water samples. Due to the local field conditions, it was not possible to extract enough soil water for chemical analysis and the lysimeter sampling program was abandoned.

3.3.2.1 *Shallow Cores*

Shallow soil samples were taken by hand, using soil sampling tubes (2.5 cm; 1 inch outer diameter (OD)), from each plot on a biweekly basis during the growing season (May to September). These were collected collaboratively between, the University of Waterloo, the Soil Resource Group (SRG), and the Upper Thames Conservation Authority. Soil samples were an amalgam of five to seven 30 cm (12 inch) long samples taken between corn rows in the middle of each plot, down the length of the plot, and then mixed in a bucket. The mixed samples were then sent to Agri-Food Analysis in Guelph, Ontario by SRG and analyzed for soil nitrogen concentration using KCl extraction and a spectrophotometer. These samples were taken in order to determine the change in nitrate storage near surface during the growing season.

3.3.2.2 *Corn Grain Yield*

Corn was harvested by hand on November 11th, 2009, in each field from 8 m long sections in two central corn rows. This was a collaborative effort between the University of Waterloo, SRG, OMAFRA and the Upper Thames Conservation Authority. Personnel from OMAFRA weighted the total mass of each row, and took a subsample for moisture. The yield was normalized to a standard moisture content of 15.5%¹. The yield of each row within a plot was averaged in order to represent the average corn yield of the plot.

3.3.2.3 *Deep Cores of the Unsaturated Zone*

A core approximately 4.5 m in depth was collected under each treatment in May of 2009, December of 2009, and again in May of 2010. The purpose of these cores was to determine stratigraphy as well as

¹ This is the standard moisture content by weight used to determine a bushel of corn, which is a unit of measurement for dry commodities often used in agriculture.

monitor the change in stored nitrate with depth at three specific times: the beginning of the growing season, after harvest and after one winter season. The May 2009 geologic cores were taken 3 m into replicate 1 from the field between a two central corn rows. Only one replicate was cored from each treatment due to budgetary and time constraints. Subsequent cores from each treatment were taken approximately 50 cm away from the previous coring location in the same corn row.

Core extraction was accomplished using the Geoprobe® direct push method using 5.7 cm (2.25 in.) outer-diameter core barrels. The boreholes were immediately filled with bentonite chips. The three top cores were collected taken in 50 cm long sections to maximize the amount of soil recovered in the soft top soil. The subsequent 2 cores were taken in 1.5 m (5ft) long sections. Analysis of the core was done at the University of Waterloo as described in section 3.3.3.

3.3.2.4 Bromide Tracer and Moisture Content Measurements

A solution of 6 kg of potassium bromide (KBr) and 18L of deionized water was applied to a 3 m by 3 m area located between the two treatment plots on June 16th, 2009 (Figure 3.3.2). The area was divided in four and the solution was applied to one quadrant at a time using watering cans. The resulting aqueous solution concentration was 2.24×10^5 ppm bromide and the surface concentration was 0.45 kg Br/m². The distribution of nitrate within the core depth can be divided into two parts: soil influenced by the application of nitrogen fertilizers and soil that is not. The movement of this tracer was used as a proxy for nitrate migration through the soil. The depth to the centre of mass of the tracer (see Section 3.3.3.5) as well as the depth of the furthest point of tracer migration (the last sample interval where the tracer is detected), are used to provided an estimate of the depth to which the various nutrient management alternatives would have influenced the soil nitrate concentration during the experiment.

A 2 inch inside diameter (ID) PVC neutron access tube was installed at the centre of the area where the bromide was applied in order to permit occasional monitoring of the soil water content, which could be used for estimates of recharge. The access tube was inserted in a 6.8 m deep borehole. This core was logged for stratigraphy and water content. Two subsequent cores were taken within the area where the tracer was applied in December 2009 and May 2010. These cores were logged for stratigraphy, water content and bromide concentration in order to determine the vertical migration of the tracer with time as described below. Moisture content measurements were taken using a model 503 DR Hydroprobe Neutron Moisture Probe (CPN International Inc.). Measurements were taken monthly; however, there are gaps in the data as the access tube needed to be buried to allow the passage of heavy machinery. Note that although moisture content measurements were taken at the site, these were not used in the assessment of the treatments. However for completeness, these data are presented in Appendix G.

3.3.3 Geologic Core Analysis

The deep continuous cores taken from the treatment plots and near the neutron access tube were analyzed in the laboratory at the University of Waterloo. The stratigraphy of each core was logged using the Unified Soil Classification System (ASTM, 2006). Cores taken from the treatments were sub-sampled and analyzed for water content along with soil nitrate and chloride concentrations as described below.

The deep coring method used to estimate nitrate mass stored in the unsaturated zone has been previously used by others at the study site (Hauslauer, 2005; Bekeris, 2007; Koch, 2009). First, each core was cut into two lengthwise, one half of the core was used for water content measurements, and the mirroring half was used to analyze nitrate, bromide and chloride concentration. Samples were taken in approximately 5 cm segments at approximately 10 cm intervals.

3.3.3.1 Moisture Content Analysis

Samples for moisture measurement were weighed, oven-dried at 110°C for 24 hours and then reweighed. Information extracted consisted of gravimetric water content, volumetric water content, and bulk density.

The gravimetric water content is the ratio of the mass of the water to the mass of the soil particles in the sample (Fetter, 2001; Haslauer, 2005).

$$\theta_g = \frac{W_m - W_d}{W_d} = \frac{W_w}{W_s} \quad (3.4.1)$$

where

- θ_g is the gravimetric water content (dimensionless ratio)
- W_m is the mass of the moist soil sample (g)
- W_d is the mass of the dry soil sample (g)
- W_w is the mass of the water (g)
- W_s is the mass of the soil particles (g)

The volumetric water content is the ratio of the volume of water to the volume of the sample (Bekeris, 2007; Fetter, 2001).

$$\theta_v = \frac{\left(\frac{W_w}{\rho_w}\right)}{A \cdot L} = \frac{V_w}{V} \quad (3.4.2)$$

where

- θ_v is the volumetric water content (dimensionless ratio)

- ρ_w is the density of water at 20°C (g/cm³)
 A is the area of the cross section of a half core (cm²)
 L is the is the length of the sample segment (cm)
 V_w is the volume of water in the sample (cm³)
 V is the volume of the sample (cm³)

The dry bulk density of soil is determined using the mass of the soil particles divided by the volume of the sample (Fetter, 2001; Freeze and Cherry, 1979).

$$\rho_b = \frac{W_m}{V} \quad (3.4.3)$$

where

- ρ_b is the bulk density of the soil (g/cm³)

3.3.3.2 Pore-water Anion Concentration

The samples selected for anion analysis were allowed to air dry for 48 hours. The soil was then ground with a mortar and pestle and sifted through a 2 mm sieve. A 5 g subsample was combined with 50 ml of deionized water and shaken over night. The solution was then centrifuged and the supernatant fluid was decanted and stored in a freezer prior to analysis. It should be noted that this process results in a ten times dilution factor between the soil concentration and the resulting supernatant fluid. Samples were then analyzed at the University of Waterloo for nitrate, chloride and bromide with a Dionex, ICS 3000 ion chromatograph equipped with a IonPac AS 4 x 250 mm analytical column.

Assuming there is no adsorption to soil particles the aqueous concentration of anions in the pore-water is calculated as the soil concentration multiplied by the density of water and divided by the gravimetric water content (Bekeris, 2007; Cole, 2008).

$$C_{aq} = \frac{C_{soil}}{\theta_g} \rho_w \quad (3.4.4)$$

where

- C_{aq} is pore-water concentration of a given sample (mg/L_{pore-water})
 C_{soil} is soil concentration (mg/kg_{soil})

3.3.3.3 Cumulative Nitrate Mass

Cumulative stored soil nitrate mass was calculated for each treatment using the following equation (Bekeris, 2007).

$$M_{\text{cum},j} = \sum_{i=1}^j C_{\text{soil},i} \cdot l_i \cdot \rho_{\text{b,ave}} \quad (3.4.5)$$

where

- $M_{\text{cum},j}$ is the cumulative mass at sampling point j (g/m^2)
- $C_{\text{soil},i}$ is the soil concentration of a given soil sample ($\text{mg}/\text{kg}_{\text{soil}}$)
- l_i is the length of the interval represented by the sample (m)
- $\rho_{\text{b,ave}}$ is the average bulk density of all the cores (g/cm^3)

In most cases the length represented by the sample is the depth of the sample minus the depth of the previous sample. In areas where the gaps between these two sample points is large, the cumulative concentration of the sample at point i is an average of the concentrations at sample point $i-1$ and sample point i , each sharing half the length between the two sample points.

3.3.3.4 Depth Averaged Pore-Water Concentration

The depth averaged pore-water nitrate concentration of a segment of interest was calculated using the following equation.

$$C_{\text{avg}} = \frac{\sum_{i=1}^j C_{\text{aq},i} \cdot l_i}{\sum_{i=1}^j l_i} \quad (3.4.6)$$

where

- C_{avg} is the depth-weighted pore-water nitrate concentration of the segment of interest between point j and k ($\text{mg}/\text{L}_{\text{pore-water}}$)

3.3.3.5 Movement of the Bromide Tracer

The migration rate of a surface applied tracer like bromide can be used to estimate groundwater recharge rates. It can also be used as a proxy to estimate the depth of influence of each treatment. The centre of mass was used as a reference point for the change in nitrate storage from one sampling period to the next. The depth of the centre of mass of the tracer may be calculated using the following equation (Bekeris, 2007).

$$z_{\text{centre}} = \frac{\sum_{i=1}^n C_{\text{soil},i} \cdot l_i \cdot z_i}{\sum_{i=1}^n C_{\text{soil},i} \cdot l_i} \quad (2.4.8)$$

where

- z_{centre} is the depth of the centre of mass of the tracer (m)
- z_i is the depth of the core sample (m)

Table 3.3.1 Rates of fertilizer application.

Treatment	No Clover: kgN/Ha (lbN/ac.)	Clover: kgN/Ha (lbN/ac.)
Control	6 (5)	6 (5)
Preplant Polymer Coated Urea	155 (138)	85 (76)
Preplant Conventional Urea	155 (138)	85 (76)
Calculator Rate Side Dress Application of UAN 28%	140 (125)	77 (69)
High Rate Side Dress Application of UAN 28%	194 (170)	194 (170)

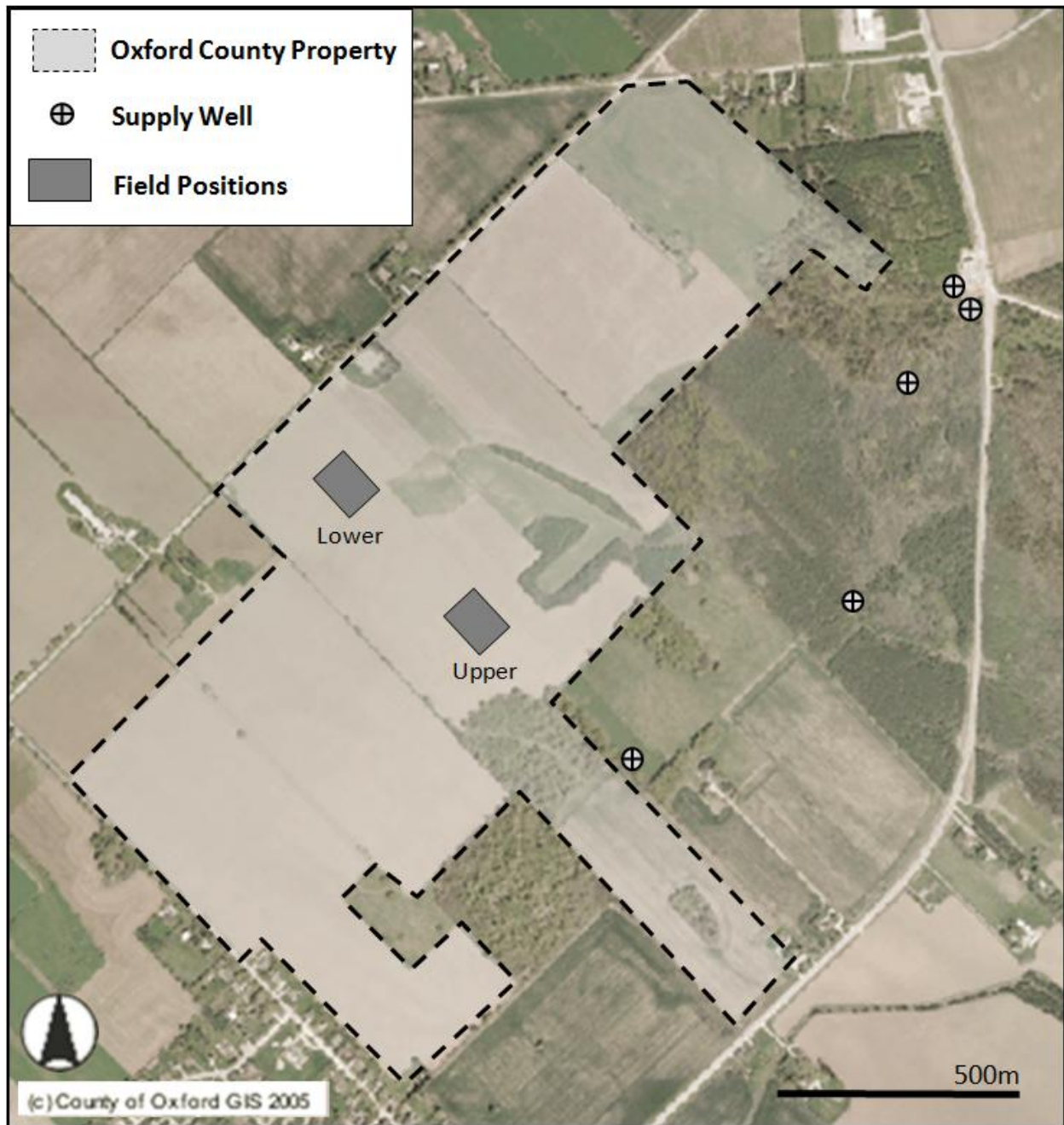
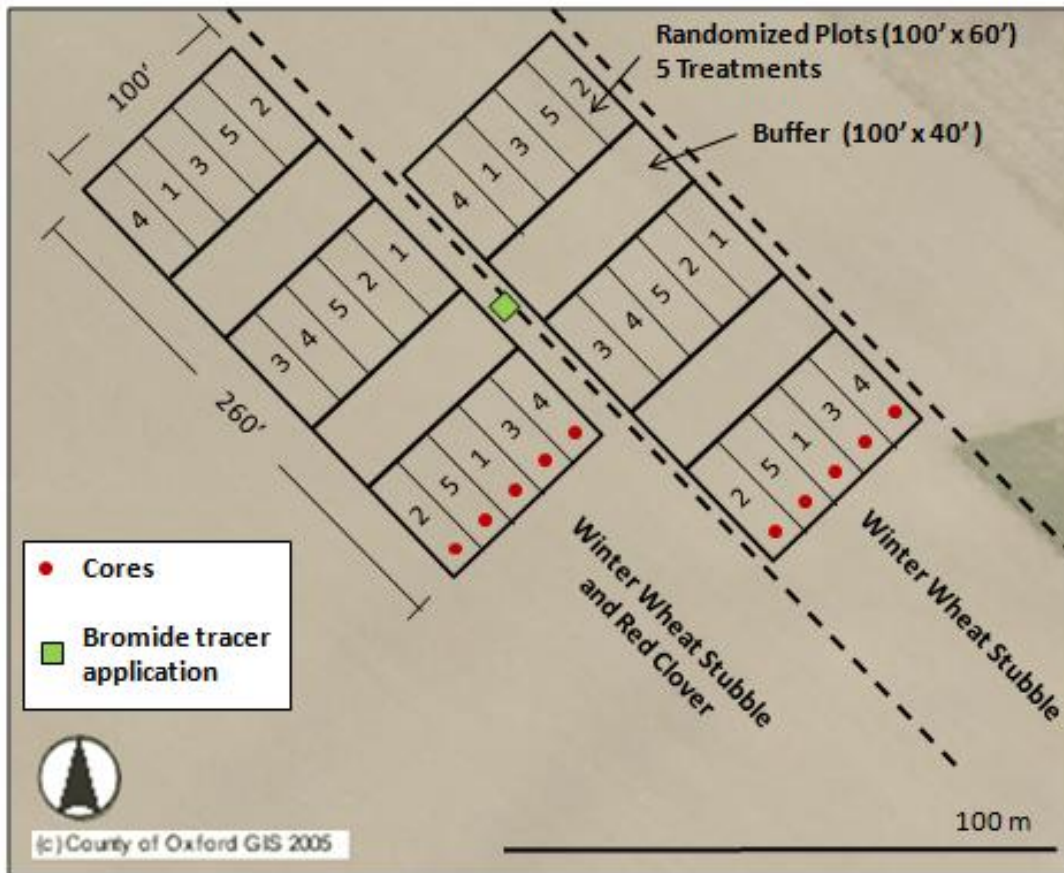


Figure 3.3.1 Location of the fields in the upper and lower positions
Contains data from the Corporation of the County of Oxford (County of Oxford GIS, 2005).



- 1 – Polymer Coated Urea
- 2 – Conventional Urea
- 3 – Calculator Rate Side-Dress
- 4 – High Rate Side-Dress
- 5 – Control

Figure 3.3.2 Study design, and location of core extraction and bromide tracer application. Contains data from the Corporation of the County of Oxford (County of Oxford GIS, 2005).

3.4 Results

This section summarizes the results of the field and laboratory activities used to compare the different nutrient application treatments under study.

3.4.1 Study Site Stratigraphy

As more than one core was taken from each location, the stratigraphic core logs were amalgamated in order to create a representative geologic core of each location. This was especially useful as very few cores had full recovery; that is to say, the length of core brought to the surface often did not exactly equal the depth of coring. Cross sections of the soil layers under the clover cover crop and the no clover cover crop treatments were constructed using the representative geologic cores; these are presented in Figure 3.4.1 and Figure 3.4.2. The individual cores are also presented in Appendix C.

The stratigraphy at the site consists of a clayey-silt topsoil (0.2 to 0.5 m thick) which overlies a layer of silty clay that grades to clayey silt (0.8 to 2 m thick). This is underlain by well graded sands in most of the plots. The south-eastern corner of the clover block is underlain by sand and gravel deposits, which are inter-layered with thin layers of fine sand and silt. A sequence of fine sands and silty sands occurs in almost all the plots at depths between 3.4 m and 4.4 m below ground surface.

3.4.2 Meteorological Data

Crops in this study were rain fed. The total precipitation for each month and the average monthly temperature between May 2009 and May 2010 is presented graphically Figure 3.4.3 and Figure 3.4.4. These data indicate that total precipitation is relatively higher during the growing season (between May and October), than during the winter. Although there is more precipitation during this period, the average temperature is also higher. This resulted in the soils being dry and hard during the summer months and wetter in the fall and early spring. The absence of crops during these periods, coupled with wetter conditions make the risk of nitrate leaching higher in the spring and fall than in the summer when crops are taking up nitrogen and transpiring moisture from the soil.

Table 3.4.1 shows the long term average daily temperature and total precipitation for each month from the Environment Canada's meteorological station located in Woodstock, as well as the average daily temperature and total precipitation recorded at the meteorological station on site between May 2009 and May 2010. In comparison to the long term average, the growing season in 2009 (May to October) received more precipitation. The average daily temperatures collected on site for almost every month during the growing season were lower in 2009 compared to the long term average; however, these are

generally within one standard deviation of the long term average. As corn typically does better during hot and wet growing seasons, overall crop production in 2009 was not limited due to the weather.

3.4.3 Shallow Core Results

The average shallow core nitrate concentrations during the growing season for each treatment were compiled by Don King of SRG. Figure 3.4.5 presents the results in the no clover field and Figure 3.4.6 presents the results of the clover field. The raw data are presented in Appendix B. As seen in the raw data, there is considerable variability between replicates during some sampling periods which affects the average concentration presented in the graphs. Still some broad trends may be deciphered.

The most notable trend, present in both the no clover and clover treatments, is the delay in the release of nitrate until the second sampling effort in plots containing the polymer-coated urea. These data should be compared to the conventional urea treatment as both treatments were applied at planting. Even though these nitrogen fertilizer treatments were applied at the same rate and time, there is a higher concentration of nitrate (~15-30 mg NO₃/kg soil) in the first sample under the conventional urea treatment compared to the polymer-coated urea treatment. This illustrates the slow release characteristics of the polymer-coated urea.

In the no clover plots, the conventional and polymer-coated urea treatments maintain higher concentrations of nitrate in the soil during the growing season compared to the control. During the early half of the growing season (May to August), the side-dress treatments have similar nitrate concentrations, which are lower than the spring applied treatments. In the fall, the concentration of nitrate in all treatments decreased and converged, with the exception of the high rate side-dress treatment, which is higher. The high rate side-dress treatment maintained a similar nitrate concentration throughout the growing season and the fall concentrations are higher than all other treatments.

In contrast, the treatments in the clover field behave more similarly to each other (with the exception of the high rate side-dress treatment) than was observed where no clover cover crop was present. Initially (May 2009) the concentration of the control, the polymer-coated urea and both side-dress treatments are slightly higher and the conventional urea treatment is lower compared to what was observed in the no clover cover field. The slight increase in nitrate concentration in the soil under most treatments demonstrates that the clover is likely providing nitrogen to the system. However, the fact that the concentrations are lower in conventional urea treatment indicates that this contribution does not result in as large a release of nitrogen in the spring as using only synthetic fertilizers (without slow release properties). With the exception of the high rate side-dress, all treatments then converge very tightly and

progressively decreased in the early fall. Similar to the no clover plot, the high rate side-dress treatment maintains a relatively high concentration of nitrate in the soil throughout the fall.

Note that the concentration of the high rate side-dress treatment on clover in August and September is quite variable. The reason for this is unknown, although the apparent reduction in late August may have been the result of denitrification occurring either in situ, as sampling was generally planned shortly after a rain event as the soils would be less hard and easier to sample, or after sampling as samples were not immediately chilled after collection.

3.4.4 Corn Yields

Figure 3.4.7 presents the average corn yields from each treatment during the 2009 growing season in units of kg/ha. Paired t-tests were conducted by Don King to compare treatments. Yields were statistically similar across all treatments between no clover and clover plots, with the exception of the control treatments, where the clover plot had significantly larger yields. In the no clover plot, all four of the non-control treatments had yields that were statistically similar to each other and statistically different compared to the control, which had lower yields. In the clover plot, yields were similar between the control and the polymer-coated urea treatment, while all other treatments were statistically different from the control, having higher yields. Of the non-control treatments, the only ones that differ statistically are in the clover plots where the polymer-coated urea is significantly lower than the calculator rate side-dress treatment.

3.4.5 Economic Return

The costs associated to the different treatments are summarized in Table 3.4.2. The average profit for the no clover plot and clover plots is calculated using the equations noted below, which were provided by Don King. Other costs, include those that all treatments have in common, include the price of corn seed, herbicides, pesticides and labour costs. These costs were not estimated.

No Clover

$$\begin{aligned} \text{Profit } (\$/\text{ha}) &= \text{Price Corn } (\$/\text{kg}) \times \text{Yield } (\text{kg}/\text{ha}) \\ &- \text{Fertilizer Price } (\$/\text{kgN}) \times \text{Rate of Application } (\text{kgN}/\text{ha}) - \text{Other Costs } (\$/\text{ha}) \end{aligned}$$

Clover

$$\begin{aligned} \text{Profit } (\$/\text{ha}) &= \text{Price Corn } (\$/\text{kg}) \times \text{Yield } (\text{kg}/\text{ha}) - \text{Price of Applying Clover } (\$/\text{ac}) \\ &- \text{Fertilizer Price } (\$/\text{kgN}) \times \text{Rate of Application } (\text{kgN}/\text{ha}) - \text{Other Costs } (\$/\text{ac}) \end{aligned}$$

Table 3.4.3 presents a list of treatments from highest return to lowest return. The treatment with the highest return was the conventional urea on clover, the treatment with the lowest return was the control treatment with no clover. With the exception of high rate side-dress, a financial advantage was seen for treatments in the clover plots compared to those in the no clover plots. This difference is likely due to the lower cost of applying clover for equivalent rate of nitrogen fertilizer. Using the OMAFRA calculator as a guide and the prices outlined in Table 3.4.2, the calculator rate side-dress treatment saved \$67.40/ha, the conventional urea saved \$81.75/ha, and the polymer-coated urea treatment saved \$100.65/ha. The high rate side-dress treatments did not do well due to the higher cost of fertilizer without added benefit in terms of yield, as the nitrogen supplied probably surpassed the nitrogen demand. The returns of the the polymer-coated urea treatments are in the middle of the pack relative to the other treatments, the mediocre returns are probably a result of its higher cost (13% higher than conventional urea). The calculator rate side-dress treatment on clover had the second highest returns; however, the same treatment with no clover had the 7th highest return of all 10 treatments.

3.4.6 Bromide Tracer

Analysis of core samples collected at the bromide application area showed that in the fall of 2009 the peak concentration occurs at 0.28 meter point below the surface and in the spring of 2010, it occurs 0.59 meters below the ground surface. Figure 3.4.8 shows the bromide concentrations profiles in the fall of 2009 and the spring of 2010. Table D.1 in Appendix D contains the concentrations of bromide in the cores in the fall of 2009 and the spring of 2010. Centre of mass was determined to be located 0.37 meter below ground surface in the fall and 0.76 meter below ground surface in the spring of 2010. The furthest migration of bromide in the fall of 2009 is 1.83 meters, and 3.36 meters in the spring of 2010. These points will be used as points of reference in order to compare depth of leaching impacts between the different treatments.

3.4.7 Deep Core Results

A summary of the deep soil core profiles (soil nitrate concentration, gravimetric water content, pore-water nitrate, and bulk density) is presented in Appendix C. Raw data is presented in Appendix D. Note that, although samples were tested for chloride, this information has not been interpreted; however, it was useful in determining anomalies caused by “pushdown”. Pushdown occurs when soil from the surface has fallen into the cored hole and is subsequently sampled; this only occurs at the top of a section of core. Because chloride concentrations are much higher at the surface than at depth, a high concentration of chloride at the top of a section of core is most likely due to push down. All samples suspected of consisting of pushdown were discarded when creating profiles, and are highlighted in the presentation of raw data.

The high rate side-dress was not cored in the spring of 2009. Initially, it was determined that the rate of nitrogen application of this treatment would be based on a pre-side-dress soil nitrate test. However, as the results indicated that the needed application would be very low, close to the control, it was decided that a high rate application would show more contrasting results. As this was not part of the original design of the project, the high rate side-dress treatment was not cored in the spring of 2009, but it was later included in the deep soil core analysis in the fall of 2009 and the spring of 2010.

As all the cores were taken from the same general area, they exhibit similar trends with relation to nitrate concentration, moisture content, and dry bulk density. Soil nitrate concentrations are highest near the surface and are quite low at depth, at all sampling times in all treatments cored; there is no trend of nitrate storage relative to any particular soil layer. Gravimetric water content is typically highest near the surface and decreases gradually with depth, this is intuitive as the soils near the surface are finer and would; therefore, have higher moisture retention capacity. In some cases, water retention is higher in some layers, this typically occurs in cores extracted in the spring. Although these peaks do not occur in all the cores extracted at this time, they are typically in similar conditions; that is within fine soil underlain by a coarser soil. Higher water contents commonly occur in the silty clay layer overlying sand between one and two meters below ground surface, and in the fine sand and silty sand layers mentioned in section 3.4.1. In some cores, the moisture at the very surface is quite low, such as the fall 2009 core taken from the high rate side-dress treatment without clover. This is likely due to the influence of evapotranspiration.

Pore-water nitrate concentration is the quotient of soil nitrate concentration and gravimetric water content; therefore, samples with low water content are often characterized by high pore-water concentrations. As a consequences, although the pore-water nitrate concentration generally follows the same trend as soil nitrate concentration, there are some pore-water nitrate peaks in areas where soil nitrate concentration had none due to low water contents. Lastly bulk density was relatively consistent with depth, and there is no strong trend from one core to the next relating bulk density to any particular soil layer.

3.4.7.1 Deep Core Nitrate Profiles

Figure 3.4.9 and Figure 3.4.10 present soil nitrate concentration ($\text{mg NO}_3^{-1}\text{-N/kg soil}$) profiles comparing the nitrate content of the three sampling campaigns of the control treatments. The control treatment is shown because it does not exhibit any odd behavior and is a baseline against which other treatments are compared. The remainder of the profiles is presented in Appendix E. In order to ease comparison, there is a figure illustrating the profiles of each treatment in the spring of 2009 and the fall of 2009 and one comparing profiles in the fall of 2009 and the spring of 2010 for each treatment.

In the analysis of deep core data from the spring of 2009, some parts of the time line are important to highlight. The spring 2009 cores were collected from the field site on May 25th and 26th. The corn was planted on May 5th, 2009. The conventional urea and the polymer-coated urea treatments were applied on May 5th, 2009, and both side-dress treatments, were applied on June 16th, 2009. This means that the conventional urea and polymer-coated urea treatments were the only treatments that had received an application of nitrogen fertilizer, in addition to the starter nitrogen, when the spring 2009 cores were collected. Considering that the previous nutrient application history is similar across all plots, the nitrate profiles beneath the three other treatments should be relatively similar within their respective plots at this time.

The nitrate distribution in the spring 2009 cores all share a similar profile shape: there are higher concentrations of nitrate in the near surface (top 1 meter), and then less storage of nitrate with depth, with the peak concentration observed in the first sample. This is the case in all but one treatment, the clover calculator side-dress treatment (Figure 3.4.11 and Figure 3.4.12). Here, the peak was located at the second sampling point.

The peak concentrations for each treatment are presented in Table 3.4.4. In the no clover plot, the calculator side-dress treatment and the control have relatively low peak concentrations (17.7 mg NO₃⁻¹-N/kg soil and 31.7 mg NO₃⁻¹-N/kg soil, respectively). At this time, both of these treatments act as controls as neither has received an application of fertilizer. The polymer-coated urea profile is relatively similar to these applications, having a peak concentration of 16.1 mg NO₃⁻¹-N/kg soil. In contrast, the conventional urea application has a high peak soil nitrate concentration of 41.2 mg NO₃⁻¹-N/kg soil and relatively high concentrations near the surface to approximately half a meter below the ground surface.

The peak concentrations in the clover plot are quite comparable to their mirrored treatments in the no clover plot, with the exception of the calculator side-dress treatment. The maximum concentrations under the control and the polymer-coated urea are similar, falling within the range of their replicates in the no clover plot, with concentrations of 22.9 mg NO₃⁻¹-N/kg soil and 27.9 mg NO₃⁻¹-N/kg soil respectively. The peak concentration in the conventional urea treatment is quite high compared to the other treatments in the plot at 53.3 mg NO₃⁻¹/kg soil. In contrast to the analogous treatment in no clover plot, the peak concentration in the calculator side-dress treatment is very high, 52.0 mg NO₃⁻¹/kg soil. As there had not been any application of fertilizer on this plot when the cores were collected, it would be expected that the nitrate profile would be similar to the control; however, this is not the case. This anomaly can be explained only by the heterogeneous nature of field studies; there must be a high amount of residual nitrogen in the area that was cored. This result is suspect; therefore, it will not be possible to comment on

the leaching potential of the calculator side-dress treatment with red clover as a cover crop using the deep core data. The data acquired from this plot will still be used to discuss the movement of nitrate through the soil profile.

The nitrate distribution profiles changed in the fall of 2009. The shapes of the control and polymer-coated urea treatments were similar to those in the spring of 2009, with the peak concentration being the very top sampling point. In all other treatments, the peak concentrations were at a lower depth, often the second sampling point. A decrease in maximum nitrate concentration of approximately 80% was observed in all treatments in the clover plots, with the exception of the calculator side-dress treatment, which decreased by only 58%. There is no clear trend in the no clover plots. The peak concentration in the conventional urea treatment actually increased by 1%, the polymer-coated urea decreased by 54%, and the peak nitrate concentrations decreased quite substantially in both the calculator side-dress treatment and the control: by 85% and 75% respectively. In comparison to the treatments in their respective plot, the peak concentrations of the high rate side-dress treatments are quite high. The high rate side-dress in the clover plot had the highest concentration of any treatment in both plots at 88.6 mg NO₃⁻¹-N/kg soil.

In the spring of 2010, no additional fertilizer was applied before the deep cores were collected. At this time, the peak in nitrate concentration in the near surface decreased in some treatments compared to the previous fall, whereas it increased in others. In treatments that had a substantial amount of residual nitrate in the fall (concentrations greater than 15 mg NO₃⁻¹-N/kg soil), the peak concentration of nitrate decreased between the fall of 2009 and the spring 2010. In all other treatments, the peak concentration increased between the fall of 2009 and the spring 2010. The treatments that experienced a decrease in peak were the no clover conventional urea treatment, the clover calculator rate side-dress treatment, and both high rate side-dress treatments. The peak in all other treatments increased during this period. This trend can be observed in Table 3.4.4 and Figure E.1 to Figure E.9 of Appendix E.

Overall the general trend between the spring and the fall of 2009, is that peak concentrations in the deeper core profiles are attenuated. This is expected as the corn crop is taking up nitrogen for vegetative growth and grain production. Between the fall of 2009 and the spring of 2010, there are two general trends with regard to behavior of peak nitrate concentrations. The first trend is that peak nitrate concentration increases within treatments that have low residual nitrate concentrations. This is most likely due to the mineralization of organic forms of nitrogen from organic matter to inorganic forms of nitrogen. The second trend is that peak nitrate decreases over the winter in treatments that have high residual nitrate; this is likely due to the migration (or leaching) of nitrate. Although mineralization of organic

nitrogen would likely occur under treatments with high residual nitrate, this trend may be masked by the decreasing trend of peak nitrate.

During the growing season the risk of nitrate leaching is lower than over the winter because the winter generally has wetter conditions and no crop is present to take up excess nitrate. With regard to leaching potential, changes in peak concentration in the control, polymer coated urea, calculator-rate side-dress (no clover) and conventional urea (clover) suggest that these treatments have a lower leaching potential compared to the other treatments under study as these all decreased in nitrate concentration during the growing season, and had residual nitrate concentrations low enough for the release to mineral nitrogen from organic matter to be observed. All other treatments have relatively high residual nitrate concentrations in the fall, and experience a decrease peak nitrate concentration between the fall of 2009 and the spring of 2010, which suggest that leaching during the winter is likely.

3.4.7.2 Deep Core Cumulative Nitrate Mass and Depth Averaged Pore-Water Concentrations

The cumulative soil nitrate mass profile for all three sampling times of the control treatment is presented in Figure 3.4.13. The control treatment is shown again in order to be consistent with the previous section. The cumulative soil nitrate mass under all five treatments are shown in Appendix F. Six depths have been highlighted on each profile. These are the 0.36 meter below the ground surface (mbgs) (the centre of mass in the fall of 2009), 0.76 mbgs (the centre of mass in the spring of 2010), 1.00 mbgs (the end of the rooting zone), 1.83 mbgs (the maximum extent of bromide migration in the fall of 2009, 3.36 mbgs (the maximum extent of bromide migration in the spring of 2010), and 3.90 mbgs (the lowest point that all cores have in common). These points were selected in order to observe the change in nitrate in segments over time. The cumulative soil nitrate mass and cumulative pore-water concentration, which is used to calculate the depth averaged pore-water nitrate concentration (see Section 3.3.3.4) at each point of reference is presented in Table F.1 and Table F.2 of Appendix F.

A depth of one meter was chosen to represent the furthest depth of the rooting zone. This depth was selected based on studies evaluating root distribution under corn (Dwyer et al., 1996; Tufekcioglu et al., 1999). The rooting zone represents a depth to which plants may still have the ability to uptake nitrogen; only nitrate migrating below the 1 m depth was considered to be lost to the environment.

In previous research work at the site, Bekeris (2007) used the centre of mass of the bromide tracer to estimate the approximate maximum depth of the effect of nutrient reduction applied on the field. In the current study the centre of mass of the bromide tracer is located within the rooting zone in the fall of 2009 and in the spring of 2010; therefore, most of the mass would be available to the subsequent crops. During

this time period, however, changes below the rooting zone were noted. For this reason, the furthest point of migration of the tracer was used as a reference to indicate the depth of influence of the different nitrogen treatments for this study.

Figure 3.4.14 to Figure 3.4.17 are visual representations of the total soil nitrate mass within and below the rooting zone, and above the anticipated maximum downward migration of nitrate below the rooting zone based on the movement of the bromide tracer for the three coring events. Figure 3.4.18 to Figure 3.4.21 are representations of the depth-averaged pore-water concentration for the same segments for the three coring events.

In the spring of 2009, the trend in the total nitrate mass in the rooting zone is generally the same as the trends in the peak concentrations which were discussed in section 3.3.2.1 and previous section. The treatments with higher nitrate mass also had higher peak values of nitrate. Nitrate concentrations are much higher within the rooting zone than below the rooting zone. With regard to average pore-water concentrations, all treatments have average concentrations above the drinking water limit both in and below the rooting zone at this time (Figure 3.4.18 and Figure 3.4.19).

Figure 3.4.14 and Figure 3.4.15 show that in the fall of 2009 every treatment in the clover and no clover fields experienced a decrease in nitrate concentration within the rooting zone compared to the spring of 2009. This trend mimics that of the peak concentrations, discussed in previous section, where concentration decreased in almost all treatments between the spring of 2009 and the fall of 2009. Below the rooting zone, the nitrate concentrations in calculator rate side-dress and the control on clover field increased, whereas all others decreased. In the fall of 2009 total nitrate concentrations for all treatments was higher in the rooting zone compared to below the rooting zone, which suggests that most of the fertilizer applied in the spring persists in the rooting zone in the fall. The treatments with the highest average pore-water nitrate concentrations in the no clover plots below the rooting zone and above the furthest point of tracer migration were the high rate side-dress treatment ($28.0 \text{ mg NO}_3^{-1}\text{-N /L}$), the polymer-coated urea treatment ($18.6 \text{ mg NO}_3^{-1}\text{-N /L}$), and the calculator rate side-dress treatment ($17.5 \text{ mg NO}_3^{-1}\text{-N /L}$). See Figure 3.4.20 and Figure 3.4.21. All other treatments in the no clover field had pore-water nitrate concentrations that were below the MAC of $10 \text{ mg NO}_3^{-1}\text{-N /L}$. In the clover plot, the treatments with the highest concentrations for the same segments were the calculator rate side-dress ($14.5 \text{ mg NO}_3^{-1}\text{-N /L}$), high rate side-dress ($11.7 \text{ mg NO}_3^{-1}\text{-N /L}$), and the control ($11.6 \text{ mg NO}_3^{-1}\text{-N /L}$), whereas all other treatments had concentrations of below $10 \text{ mg NO}_3^{-1}\text{-N /L}$.

In the spring of 2010 the high rate side-dress treatments and the conventional urea treatments have the highest concentration of nitrate in rooting zone in both the no clover and the clover fields (high rate side-dress no clover ($13.2 \text{ g NO}_3^{-1}\text{-N /m}^2$), clover ($15.9 \text{ g NO}_3^{-1}\text{-N /m}^2$); conventional urea no clover ($10.3 \text{ g NO}_3^{-1}\text{-N /m}^2$), clover ($11.6 \text{ g NO}_3^{-1}\text{-N /m}^2$); see Figure 3.4.14 and Figure 3.4.15. Many of the treatments increase in nitrate content within the rooting zone compare to the previous fall. The exceptions are the conventional urea in the no clover plot, the calculator rate in the clover plot, and high rate side-dress treatments in the clover plot. The same trend was also observed in changes in peak nitrate concentrations between the fall of 2009 and the spring of 2010, presented in section 3.4.7.1. Increases in peak nitrate are thought to be attributed to the mineralization of organic forms of nitrogen in treatments that had low residual nitrate in the fall, and decreases were attributed to loss of nitrate to due to leaching in treatments with high residual nitrate. Below the rooting zone, the only treatments that increased in soil nitrate concentration compared to the previous fall were the conventional urea treatments in both plots and the high rate side-dress treatment on clover (see Figure 3.4.14 and Figure 3.4.15).

Figure 3.4.16 and Figure 3.4.17 divide the rooting zone into two segments: the soil influenced by the application of the nitrogen fertilizers in the spring of 2009 and the soil that is not. These figures show that there is an increase in stored nitrate between the end of the rooting zone and the furthest point of vertical migration between the fall of 2009 and the spring of 2010 in all treatments other than the control in the no clover plot. The highest increases occur under the high rate side-dress treatments and the urea treatments in both plots. These are the treatments that also have the highest concentrations in these segments. Comparing treatments the no clover and clover fields, there does not seem to be a clear trend for all the treatments in either the percent increase with respect to the fall of the total nitrate mass in this segment.

The maximum allowable concentration (MAC) for nitrate is $10 \text{ mg NO}_3^{-1}\text{-N /L}$ and so it is of interest to note the treatments that have pore-water concentrations lower than $10 \text{ mg NO}_3^{-1}\text{-N /L}$ below the rooting zone where they are influenced by the different treatments. Figure 3.4.20 and Figure 3.4.21 show the average pore-water concentrations below the rooting zone, dividing it into two segments: the soil influence by the application of the nitrogen fertilizers in the spring of 2009 and the soil that is not. In the spring of 2009, the background average pore-water nitrate concentrations below the rooting zone are all higher or equal to the MAC of $10.0 \text{ mg NO}_3^{-1}\text{-N /L}$. In the spring of 2010, treatments that had concentrations below the MAC in this segment of interest are: both polymer-coated urea treatments, both calculator rate side-dress treatments and the control in the no clover plot. Of the remaining treatments, the high rate side-dress treatments in both plots had pore-water concentrations twice as high as the MAC, whereas all other treatments had concentrations near the MAC.

Despite the small sample size, the results seem to indicate both the rate and the timing of the nitrogen fertilizer application affect the amount of nitrate lost to that environment after one year. The general trends from the deep core analysis show that treatments that received higher rates of nitrogen fertilizer had much higher cumulative nitrate below and within the rooting zone after one year. This is an example of how the rate of fertilizer application affects the amount of nitrate lost to the environment. The exception being the polymer-coated urea which behaved similarly to the calculator rate side-dress and the control treatments, despite having been applied at the same time and receiving the same application rate of nitrogen fertilizer as the conventional urea. The fact that the calculator-rate side dress and the polymer-coated urea applications had similar amounts of residual nitrate in the segment of soil below the rooting zone and above the point of furthest tracer migration as the control, are examples of how the timing of the fertilizer applications affects the amount of nitrate lost to the environment.

Table 3.4.1 Long term average daily temperatures and total precipitation for each month collected from Environment Canada's Meteorological Station at Woodstock (Environment Canada, 2011), and average daily temperature and total precipitation for between May 2009 and May 2010 collected from the meteorological station onsite.

	May	Jun	Jul	Aug	Sep	Oct	Nov	Dec	Jan	Feb	Mar	Apr	May
Woodstock Meteorological Station Long Term Averages*													
Temperature:													
Daily Average (°C)	13.2	18.2	20.4	19.6	15.4	9.1	3.1	-3	-6.3	-5.4	-0.3	6.4	6.4
Standard Deviation	2.1	1.3	1	1.2	1.1	1.7	1.6	2.7	2.8	2.8	2.3	1.7	1.7
Precipitation (mm)	80.5	84.3	95.5	91.5	93.9	73.9	85.6	78.6	64.3	53.7	71.9	80.3	80.3
Oxford County 2009-2010 Averages													
	May-09	Jun-09	Jul-09	Aug-09	Sep-09	Oct-09	Nov-09	Dec-09	Jan-10	Feb-10	Mar-10	Apr-10	May-10
Temperature:													
Daily Average (°C)	12.9	17.1	17.8	19.3	15.5	7.6	5.2	-3.2	-6.0	-4.8	2.8	10.0	14.8
Precipitation (mm)	108.0	110.2	71.4	137.9	47.7	98.6	50.5	84.1	26.2	26.9	44.5	64.8	85.9

* Environment Canada's Meteorological Station at Woodstock (Latitude: 43°08'10.044" N, Longitude: 80°46'14.040" W, Elevation: 281.90 m)

Table 3.4.2 Cost estimates of all treatment inputs.

Imperial

Costs

Polymer Coated Urea	:	\$0.94/LbN ²
Urea and Side-Dress	:	\$0.83/LbN
Price of Applying Clover	:	\$25.00/ac. ³
Side-Dress Labour Costs	:	\$30.00/ac. ²

Return

Price of Corn	:	\$4.00/bu
---------------	---	-----------

Metric

Costs

Polymer Coated Urea	:	\$2.32/kgN
Urea and Side-Dress	:	\$2.05/kgN
Price of Applying Clover	:	\$61.75/ha.
Side-Dress Labour Costs	:	\$74.10/ha.

Return

Price of Corn	:	\$0.16/kg
---------------	---	-----------

² Prices provided Cargill for the spring of 2009

³ Price of applying red clover estimated by David Start, the farmer.

Table 3.4.3 Return per treatment from the most lucrative to the least for the year of 2009.

Profit per Treatment (\$/ac.) and (\$/ha)		
C - Conventional Urea	635.07	1549.49
C - Calculator Rate Side Dress	625.33	1527.21
C - Control	610.09	1505.67
NC - Conventional Urea	593.72	1431.76
C - Polymer Coated Urea	586.67	1427.42
NC - Polymer Coated Urea	582.23	1398.80
NC - Calculator Rate Side Dress	580.39	1402.12
NC - High Rate Side Dress	559.32	1337.99
C - High Rate Side Dress	537.71	1284.61
NC - Control	473.74	1168.87

NC - No Clover

C - Clover

Table 3.4.4 Peak concentrations (mg NO₃⁻¹-N/kg soil) of each treatment the different sampling times, and percent change in peak concentration.

No Clover Block (NC)				Clover Block (C)			
	Spring 2009 (S09)	Fall 2009 (F09)	Spring 2010 (S10)		Spring 2009 (S09)	Fall 2009 (F09)	Spring 2010 (S10)
1NC	16.1	7.4	14.2	1C	27.9	5.4	9.0
2NC	41.2	41.8	11.4	2C	53.3	10.7	16.0
3NC	17.7	2.7	6.3	3C	52.0	21.9	7.1
4NC	na	18.1	13.3	4C	na	88.6	11.7
5NC	31.7	7.9	12.1	5C	22.9	4.4	5.9
	(F09 /S09) - 1	(S10 /F09) - 1	(S10 /S09) - 1		(F09 /S09) - 1	(S10 /F09) - 1	(S10 /S09) - 1
1NC	-54%	92%	-12%	1C	-81%	67%	-68%
2NC	1%	-73%	-72%	2C	-80%	50%	-70%
3NC	-85%	133%	-64%	3C	-58%	-68%	-86%
4NC		-27%		4C		-87%	
5NC	-75%	53%	-62%	5C	-81%	34%	-74%

- 1 - Polymer Coated Urea
- 2 - Conventional Urea
- 3 - Calculator Rate Side-Dress
- 4 - High Rate Side-Dress
- 5 - Control

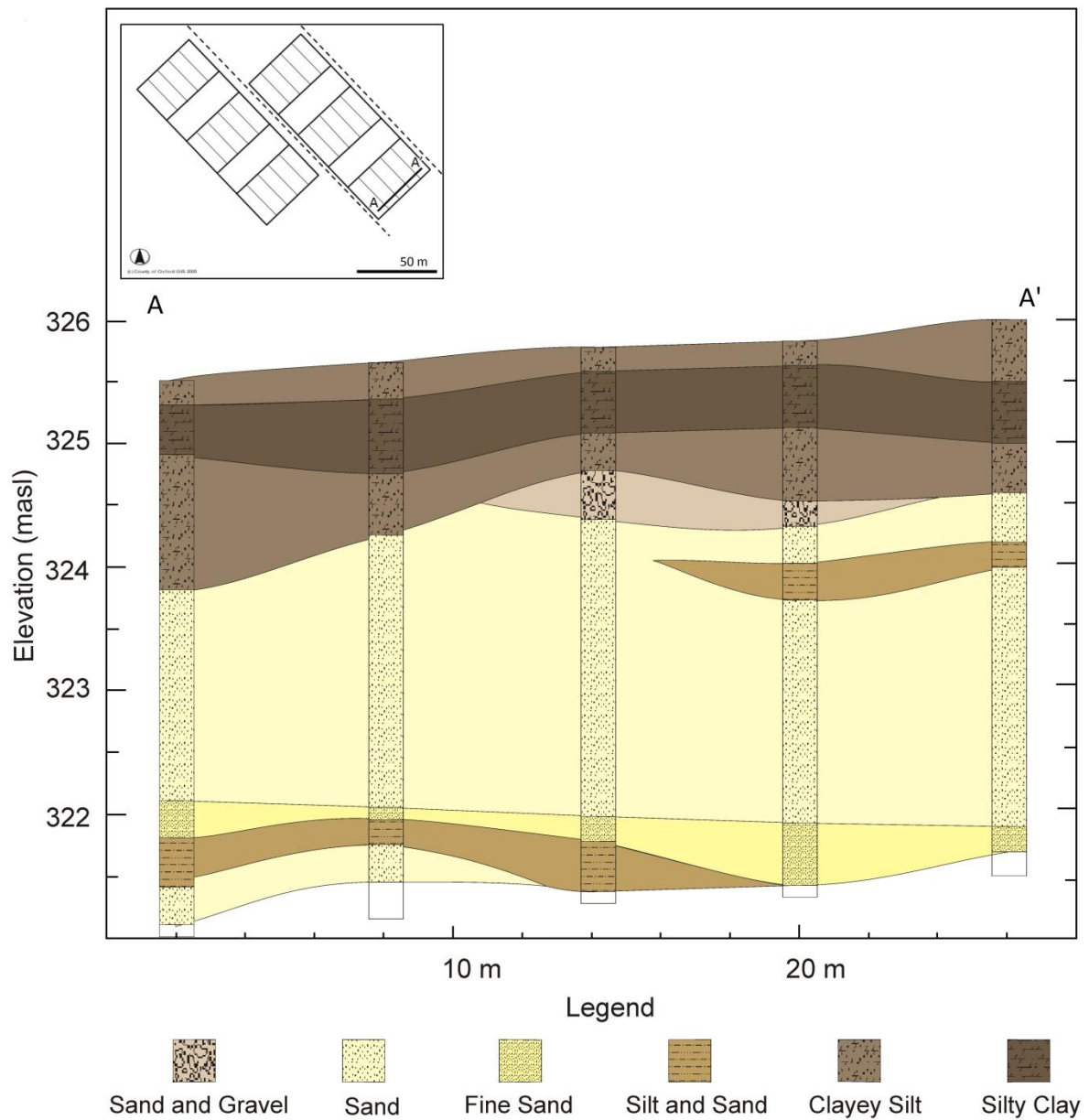


Figure 3.4.1 Stratigraphic cross-section of the no clover block. Constructed from composite cores.

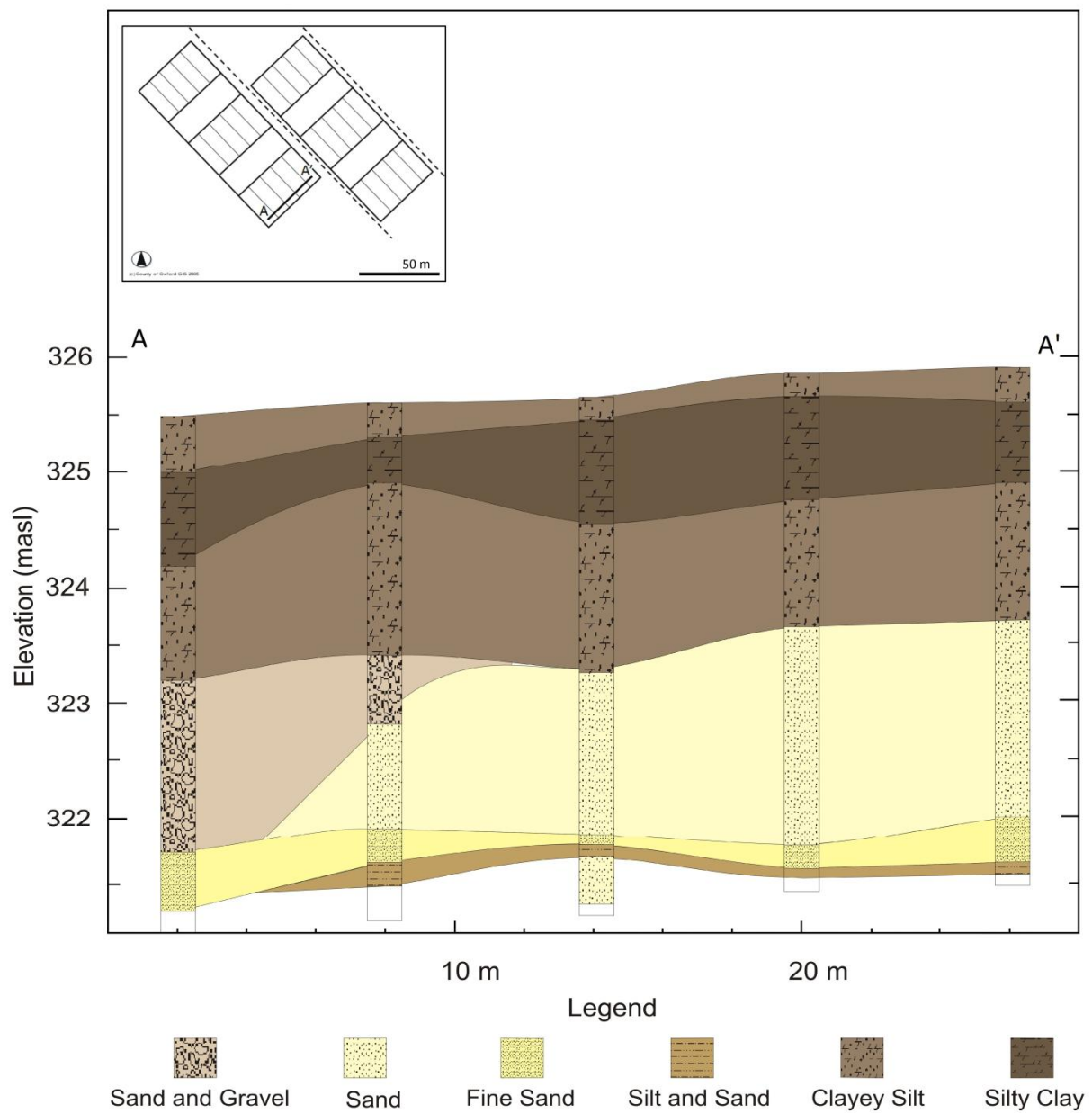


Figure 3.4.2 Stratigraphic cross-section of the clover block. Constructed from composite cores.

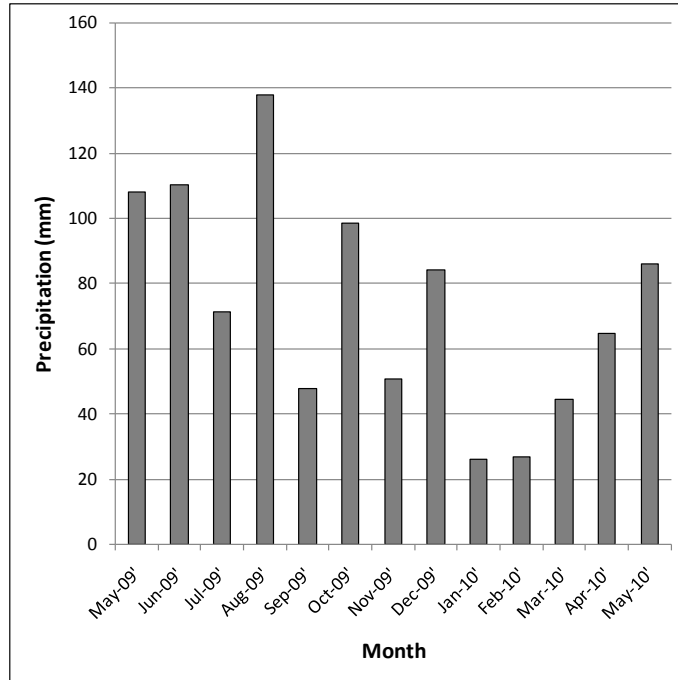


Figure 3.4.3 Total monthly precipitation for the period between May 2009 and May 2010.

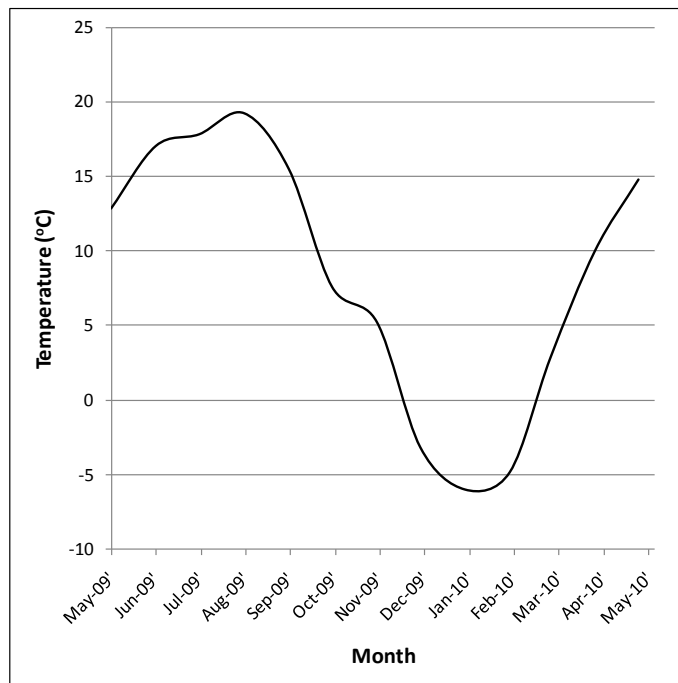


Figure 3.4.4 Average monthly temperature for the period between May 2009 and May 2010.

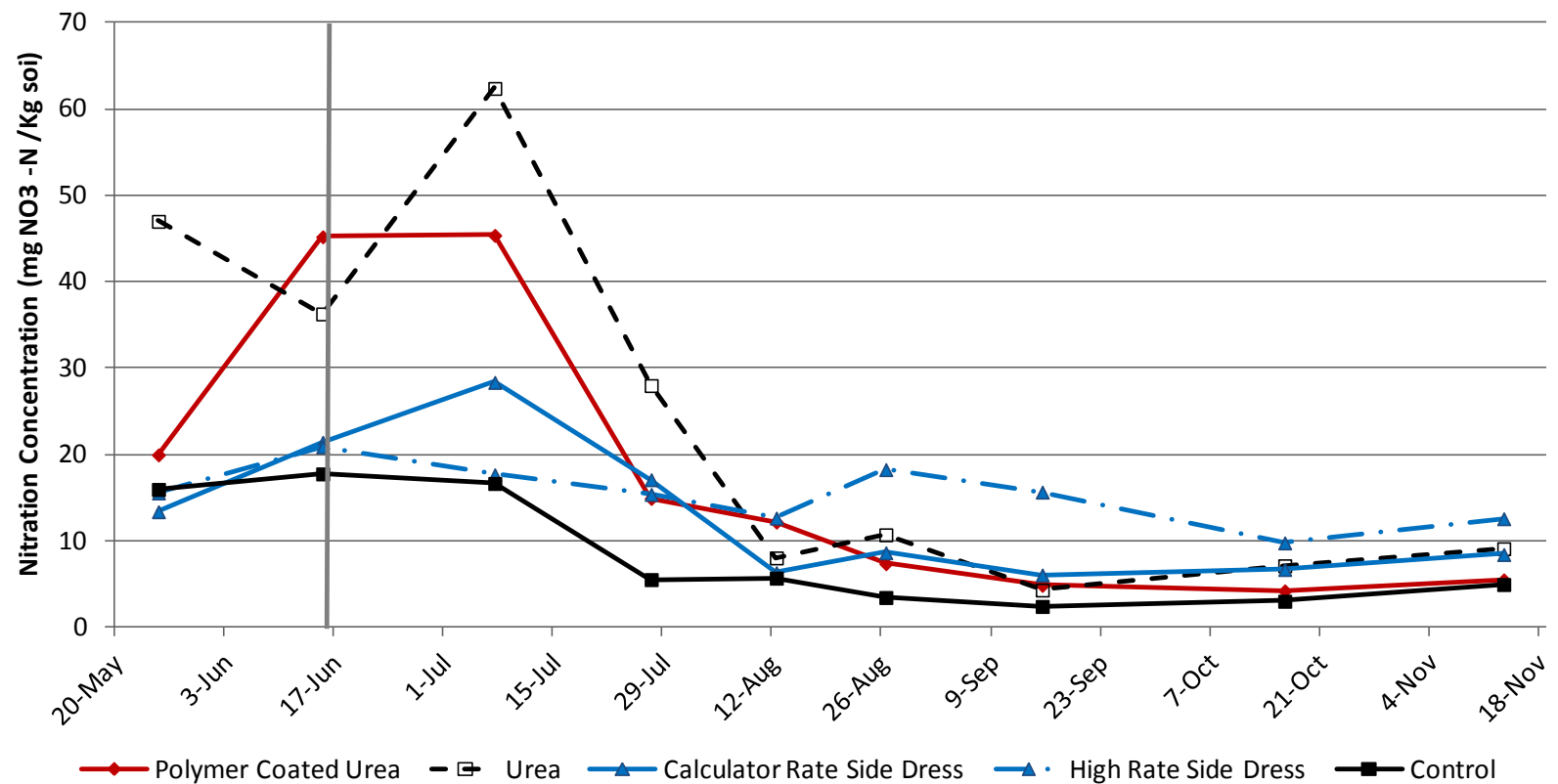


Figure 3.4.5 Soil nitrate concentration in the shallow cores taken during the growing season of 2009 in the no clover plots. Grey line indicates the timint of the application of the side-dress fertilizer.

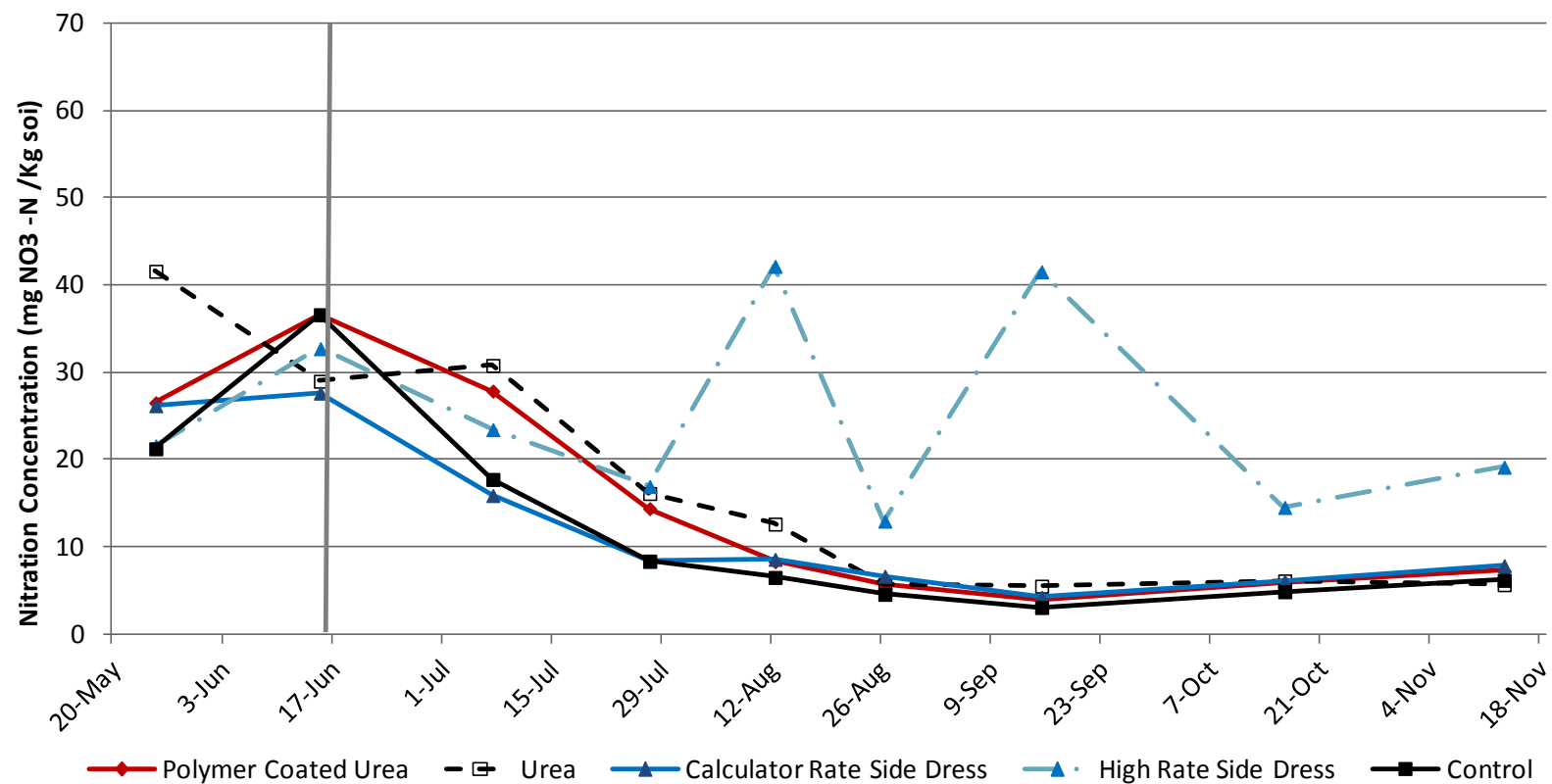


Figure 3.4.6 Soil nitrate concentration in the shallow cores taken during the growing season of 2009 in the clover block. Grey line indicates the timint of the application of the side-dress fertilizer.

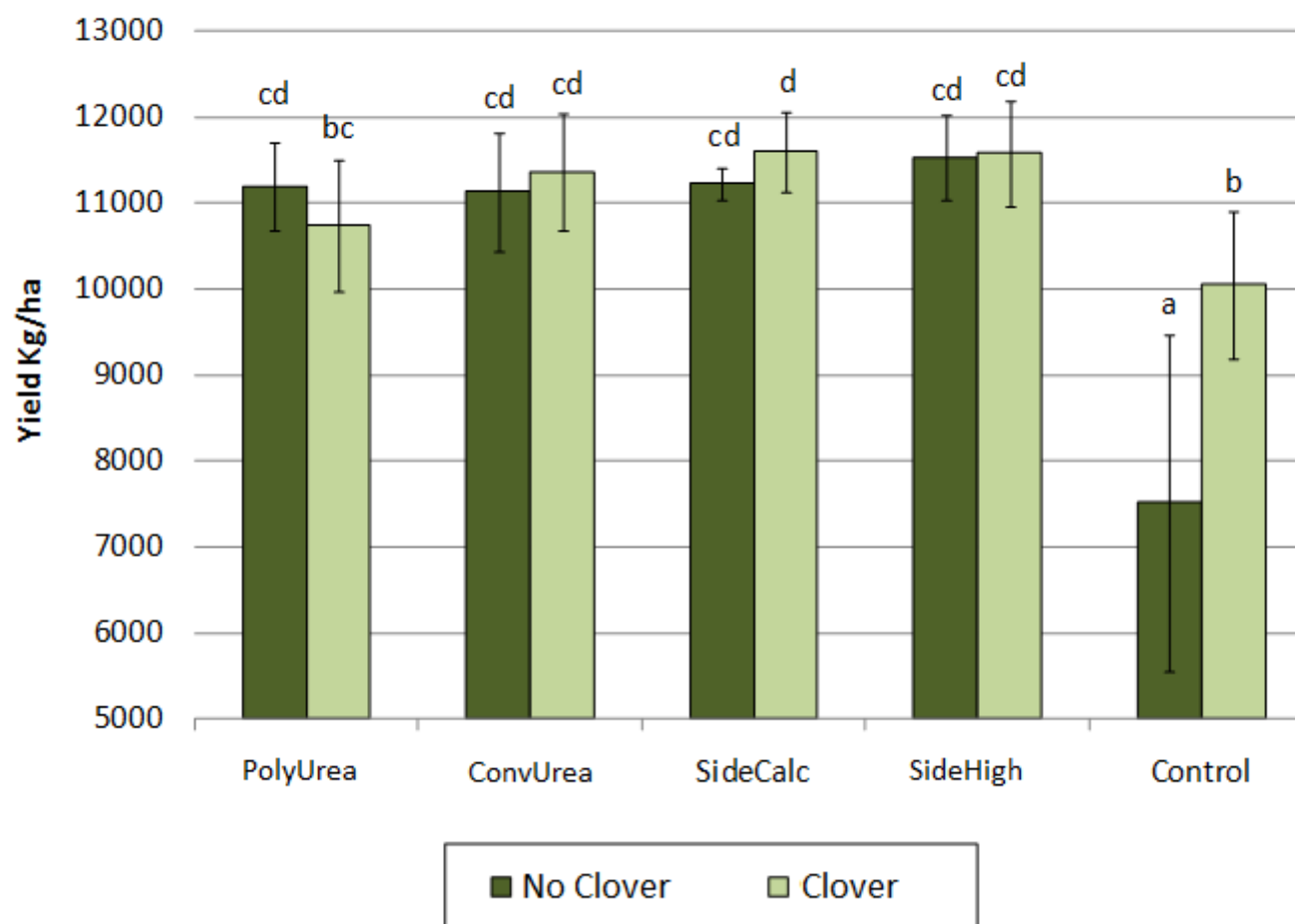


Figure 3.4.7 Corn yields (kg/ha) from the 2009 growing season in the no clover and the clover plots. Lettering scheme used denotes treatments with significantly different yields as determined by a series of paired t-tests; treatments with the same letter are similar, treatments with different letters are not. The error bars indicate the standard deviation between samples.

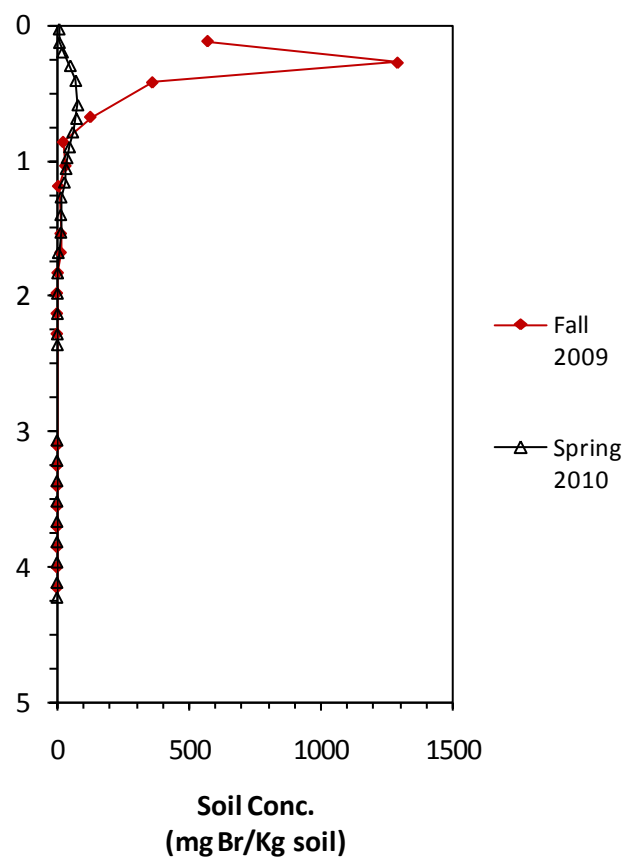
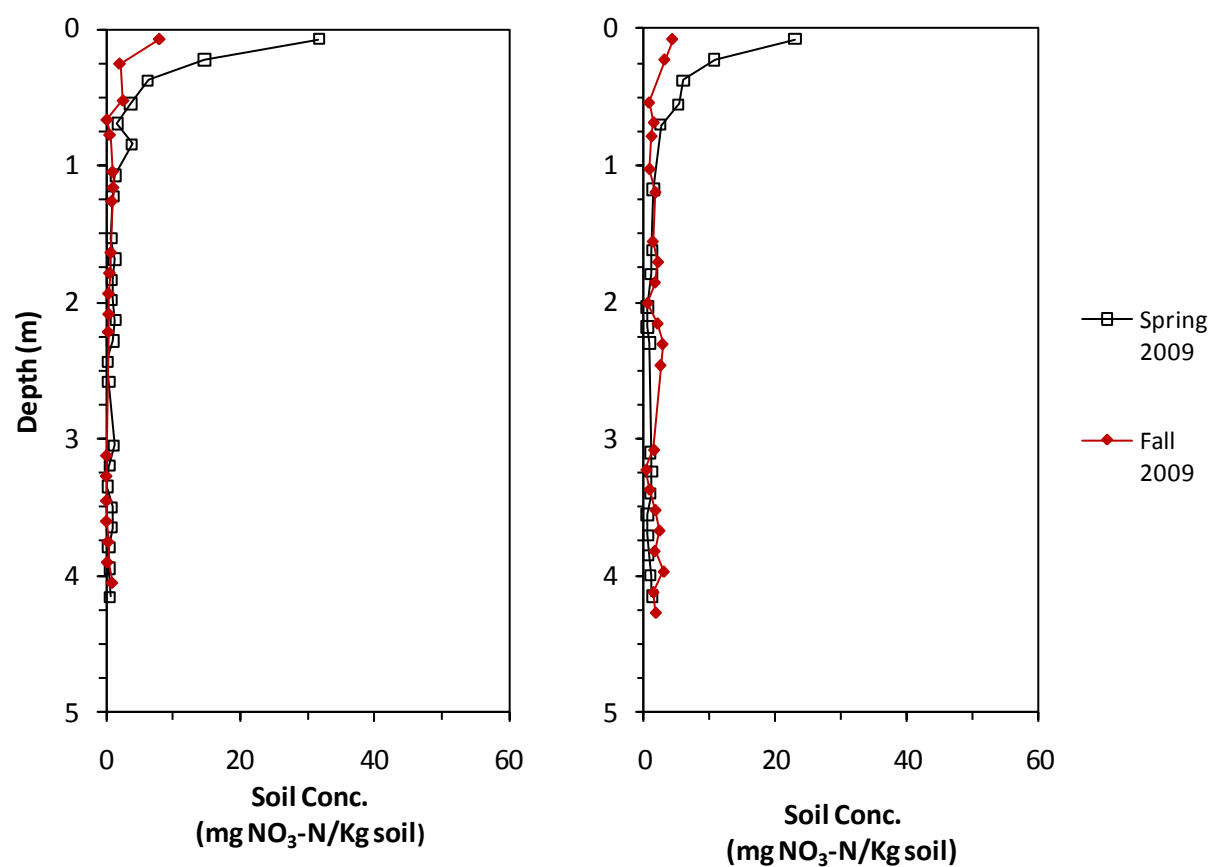


Figure 3.4.8 Soil bromide concentration profiles the fall of 2009 and the spring 2010.



(a) (b)

Figure 3.4.9 Soil nitrate concentration profiles for the control (a) no clover and (b) clover treatments in the spring of 2009 and the fall of 2009.

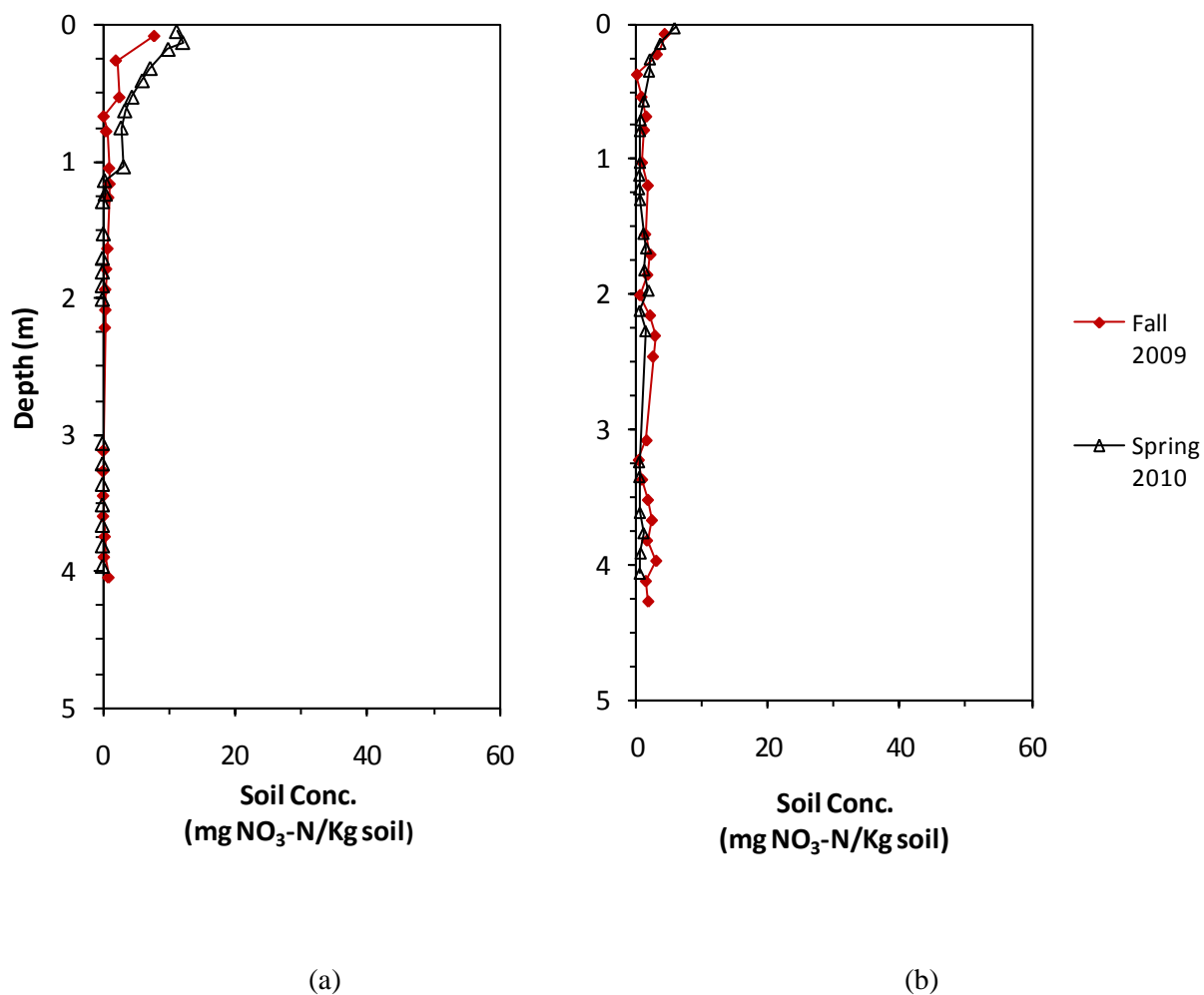


Figure 3.4.10 Soil nitrate concentration profiles for the control (a) no clover and (b) clover treatments in the fall 2009 and spring of 2010.

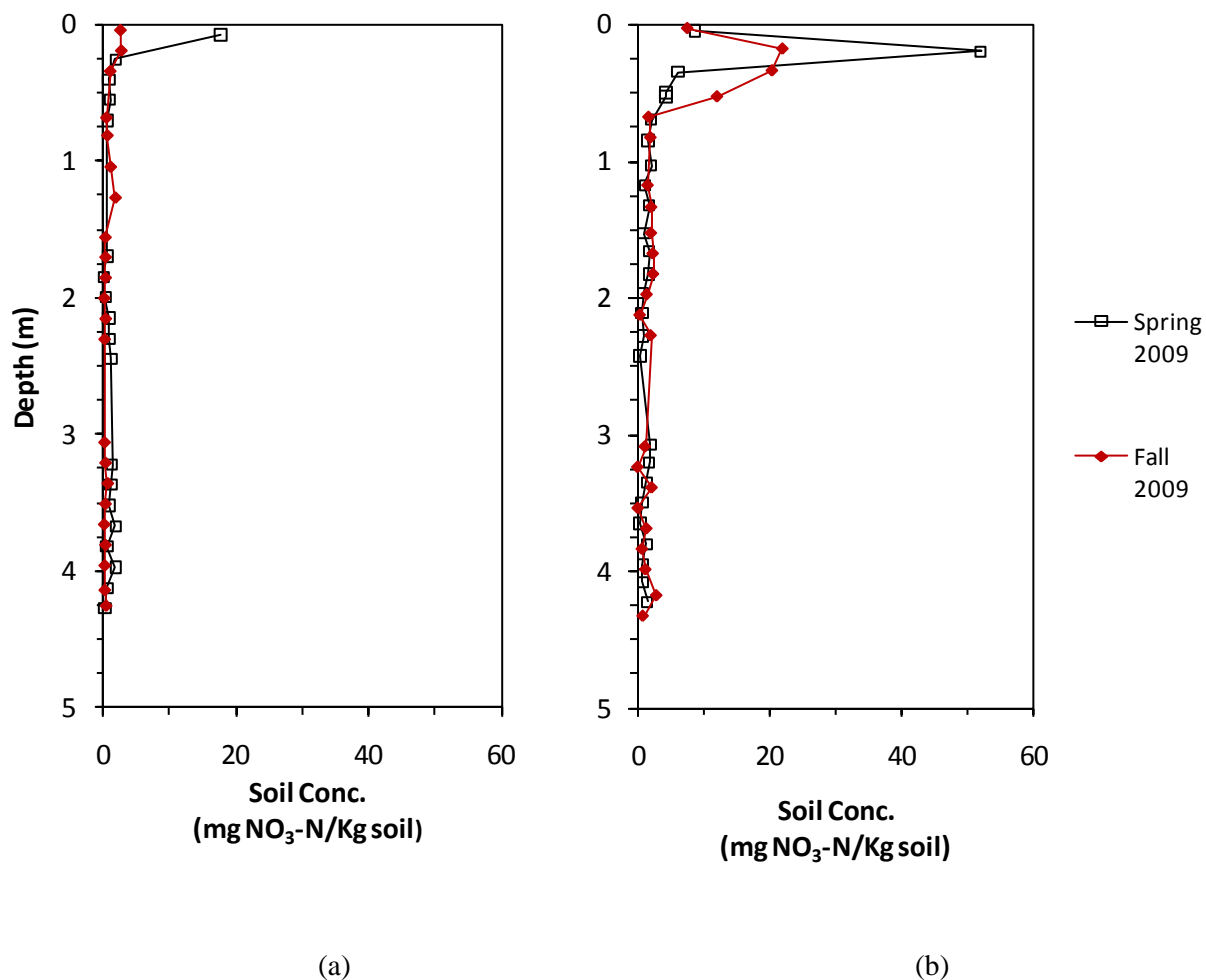
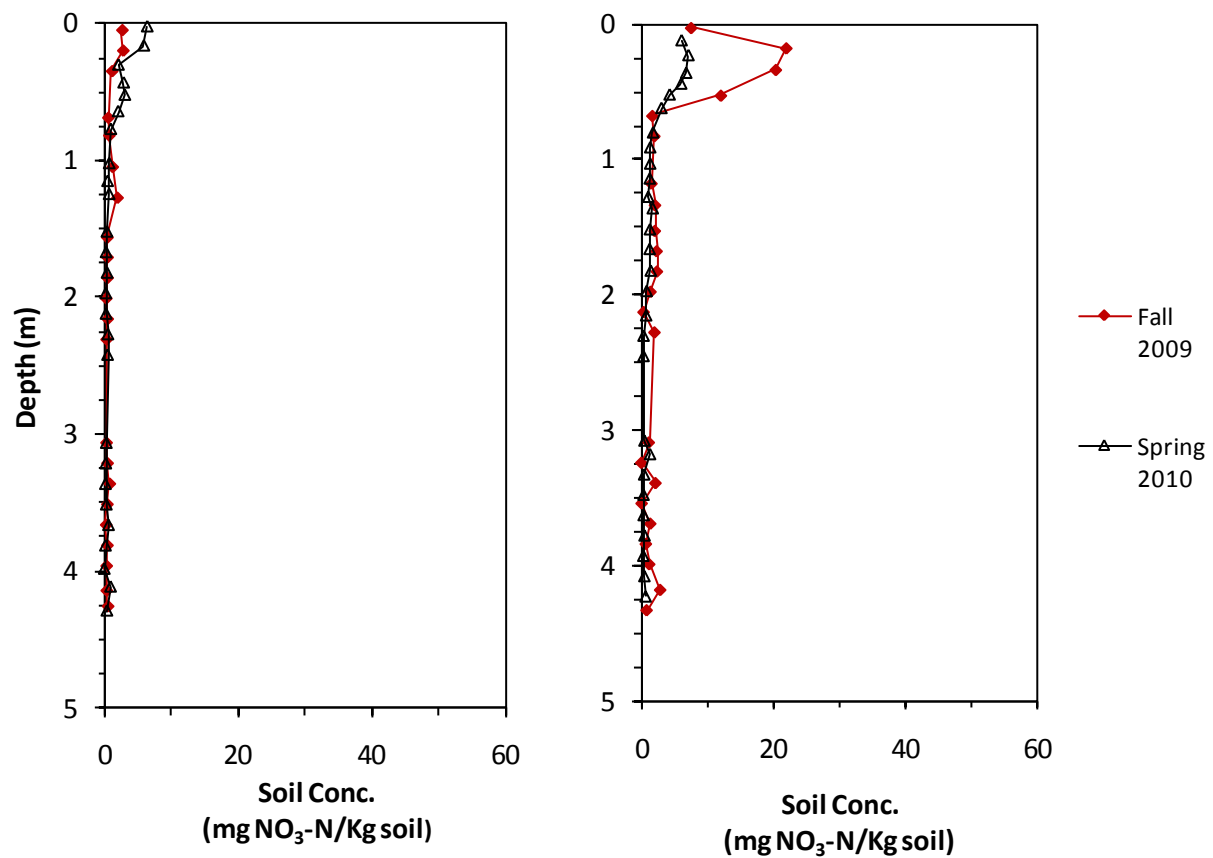


Figure 3.4.11 Soil nitrate concentration profiles for the calculator rate side-dress (a) no clover and (b) clover treatments in the spring of 2009 and the fall of 2009.



(a) (b)

Figure 3.4.12 Soil nitrate concentration profiles for the calculator rate sidedress (a) no clover and (b) clover treatments in the fall 2009 and spring of 2010.

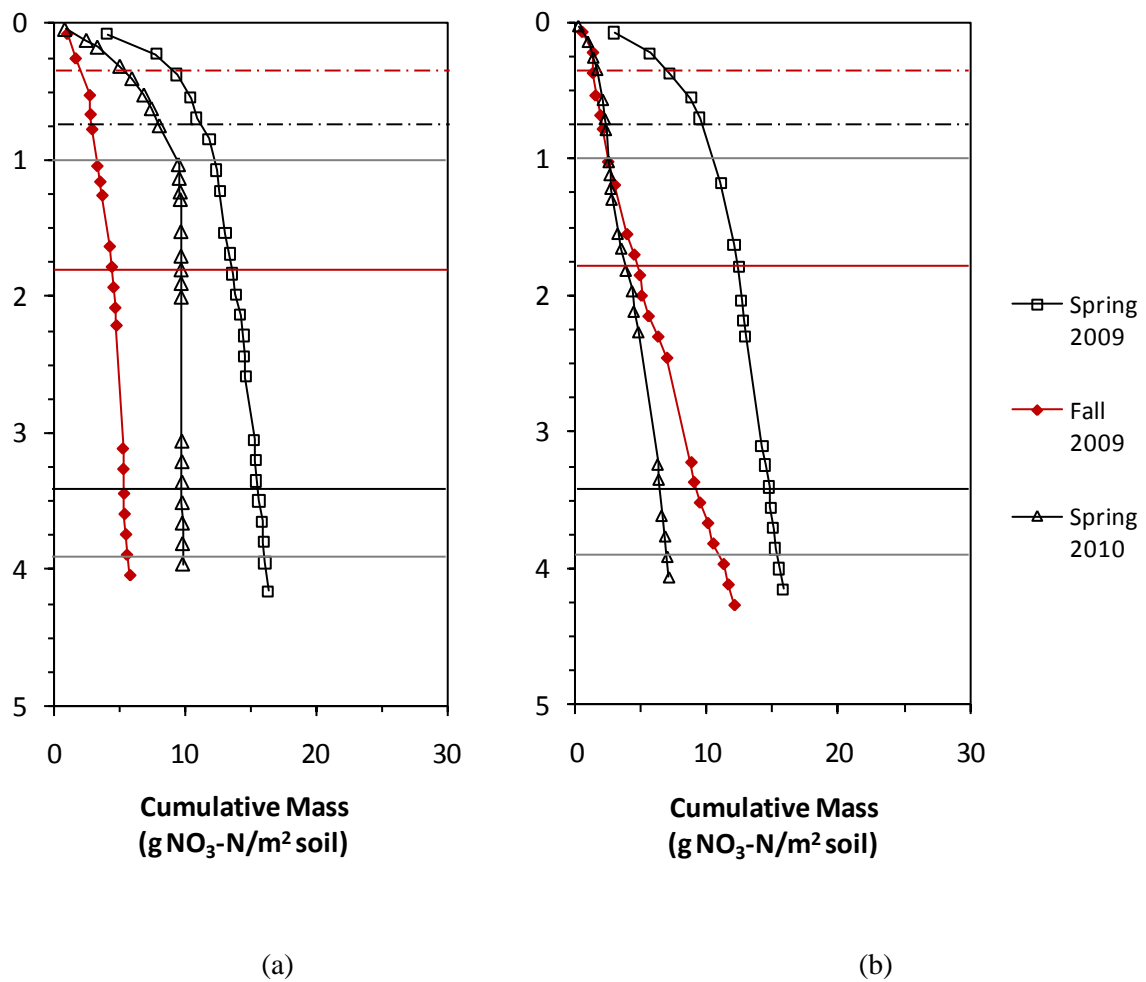


Figure 3.4.13 Cumulative nitrate mass profiles for the control (a) no clover and (b) clover treatments in the spring 2009, fall 2009 and spring 2010.

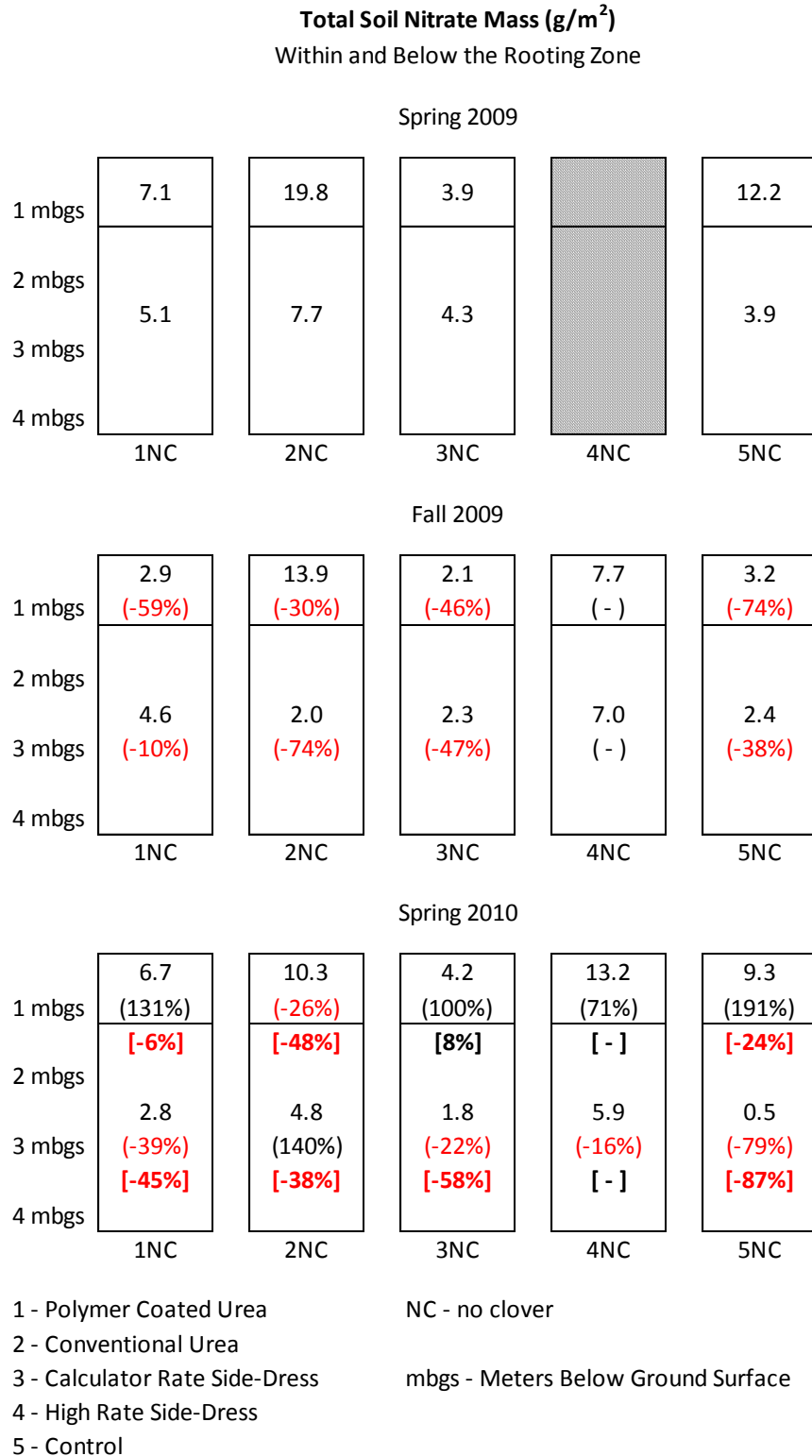


Figure 3.4.14 Representative cores of the total soil nitrate mass of each treatment and sample time in the no clover plots within and below the rooting zone. Percent change compared to the (previous core), as well as the [spring of 2009].

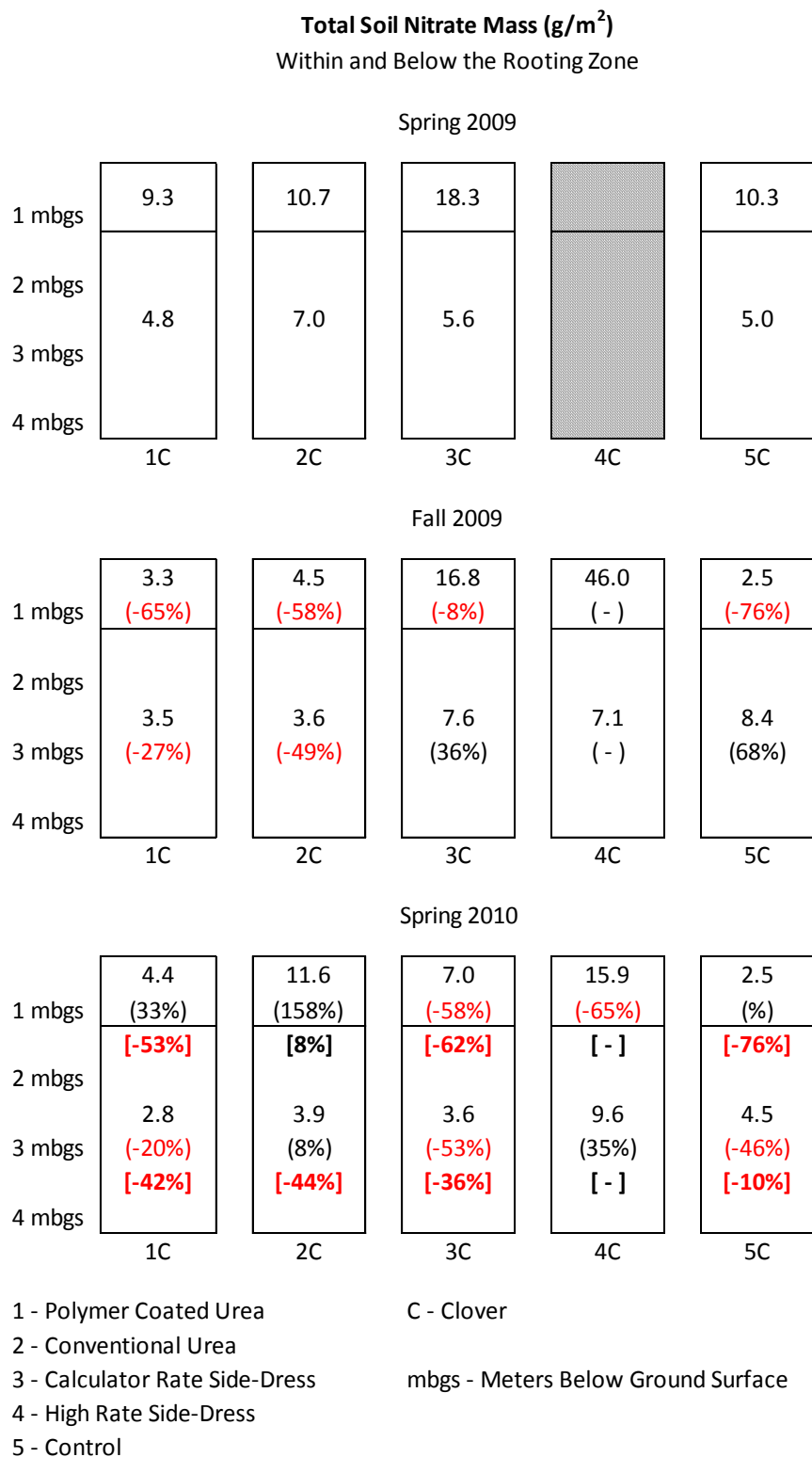


Figure 3.4.15 Representative cores of the total soil nitrate mass of each treatment and sample time in the clover plots within and below the rooting zone. Percent change compared to the (previous core), as well as the [spring of 2009].

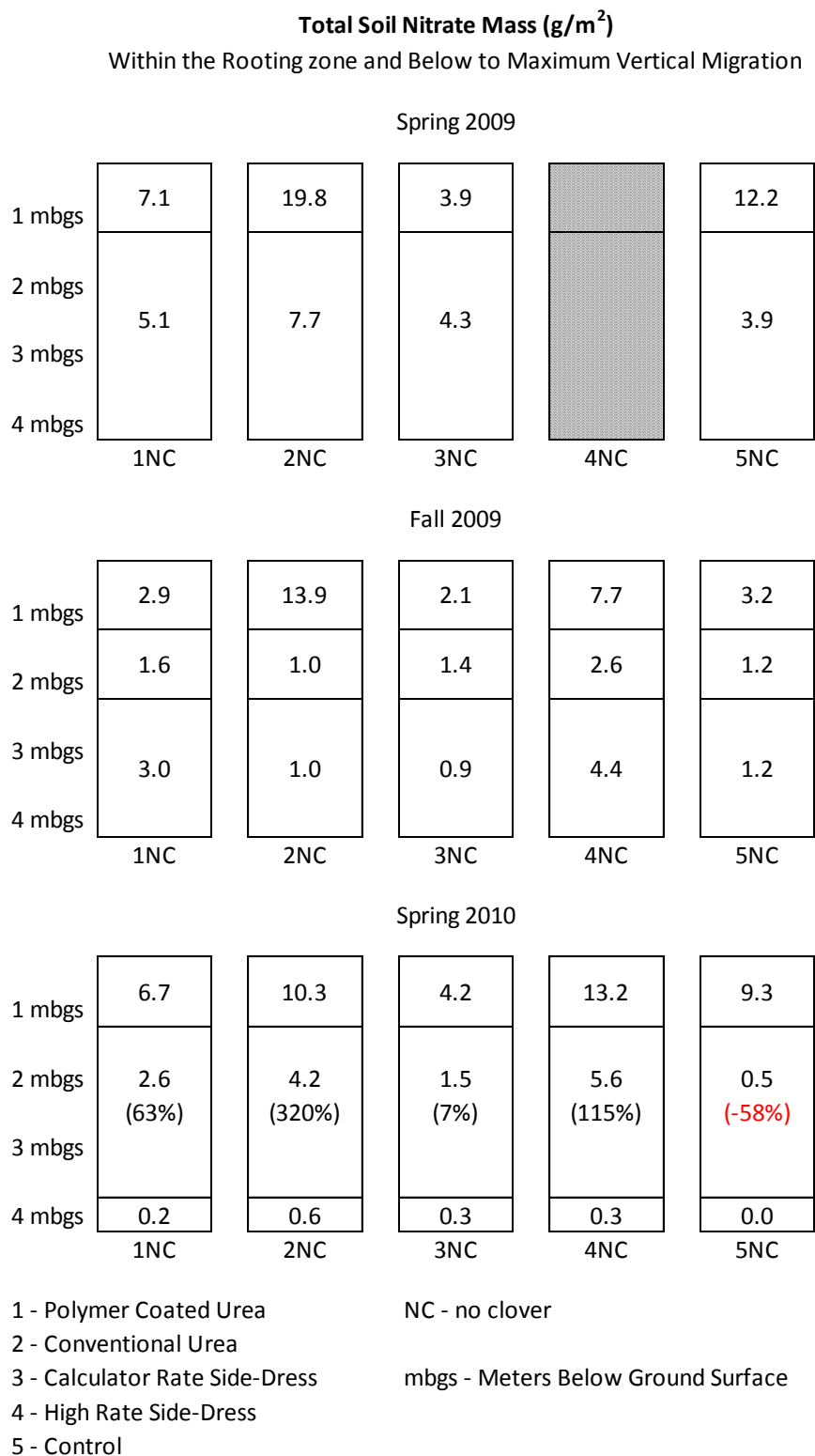


Figure 3.4.16 Representative cores of the total soil nitrate mass of each treatment and sample time in the no clover plots within and below the rooting zone to the maximum point of vertical migration. Percent change compared to the (previous core).

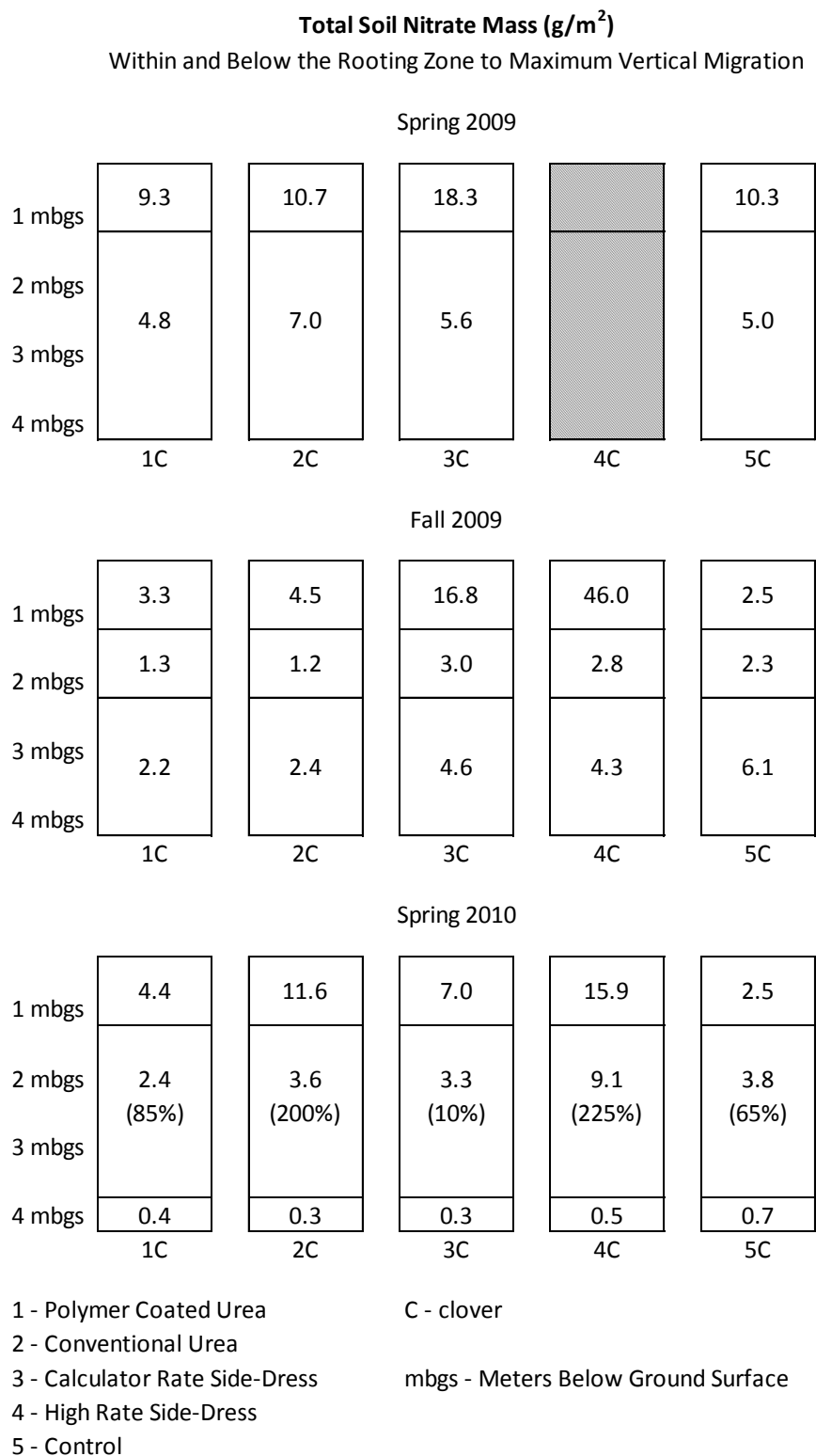


Figure 3.4.17 Representative cores of the total soil nitrate mass of each treatment and sample time in the clover plots within and below the rooting zone to the maximum point of vertical migration. Percent change compared to the (previous core).

Distance-averaged Pore-water Concentrations (mg/L)

Within and Below the Rooting Zone

Spring 2009

1 mbgs	21.6	74.2	15.8		42.9
2 mbgs	15.1	18.8	14.6		11.9
3 mbgs					
4 mbgs					
	1NC	2NC	3NC	4NC	5NC

Fall 2009

1 mbgs	11.6 (-45%)	48.4 (-36%)	7.2 (-55%)	47.3 (-)	9.8 (-78%)
2 mbgs	16.5 (9%)	5.9 (-69%)	8.9 (-39%)	30.3 (-)	5.3 (-55%)
3 mbgs					
4 mbgs					
	1NC	2NC	3NC	4NC	5NC

Spring 2010

1 mbgs	20.7 (76%) [-3%]	39.6 (-17%) [-46%]	14.8 (108%) [-6%]	55.0 (17%) [-]	30.3 (216%) [-30%]
2 mbgs	3.8 (-77%) [-75%]	10.0 (69%) [-47%]	5.5 (-39%) [-63%]	17.8 (-41%) [-]	0.8 (-86%) [-94%]
3 mbgs					
4 mbgs					
	1NC	2NC	3NC	4NC	5NC

1 - Polymer Coated Urea

NC - no clover

2 - Conventional Urea

mbgs - Meters Below Ground Surface

3 - Calculator Rate Side-Dress

4 - High Rate Side-Dress

5 - Control

Figure 3.4.18 Representative cores of the depth-averaged pore-water concentration of each treatment and sample time in the no clover block within and below the rooting zone. Percent change compared to the (previous core), as well as the [spring of 2009].

Distance-averaged Pore-water Concentrations (mg/L)

Above and Below the Rooting Zone

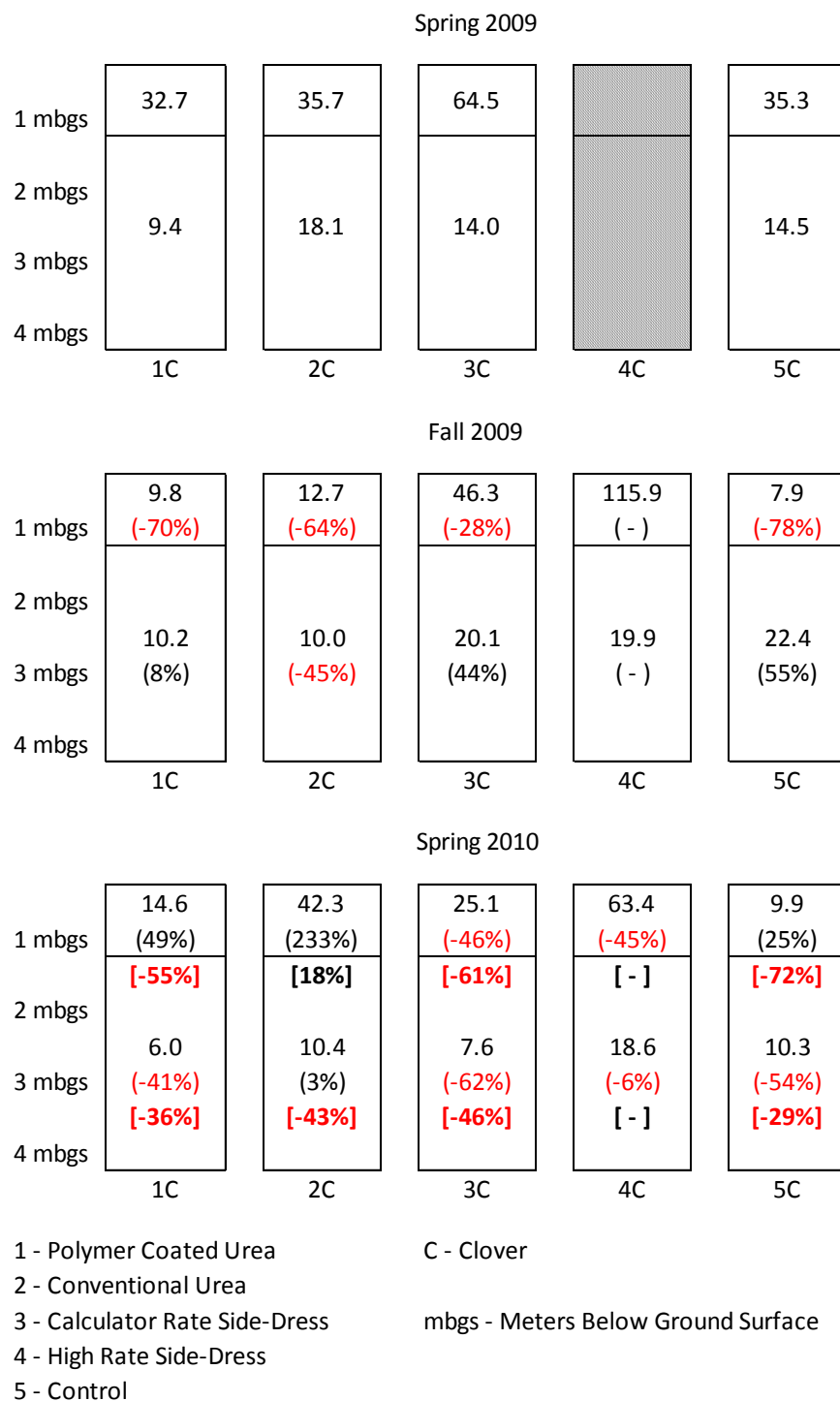


Figure 3.4.19 Representative cores of the depth-averaged pore-water concentration of each treatment and sample time in the clover block within and below the rooting zone. Percent change compared to the (previous core), as well as the [spring of 2009].

Distance-averaged Pore-water Concentrations (mg/L)
Within and Below the Rooting Zone to Maximum Vertical

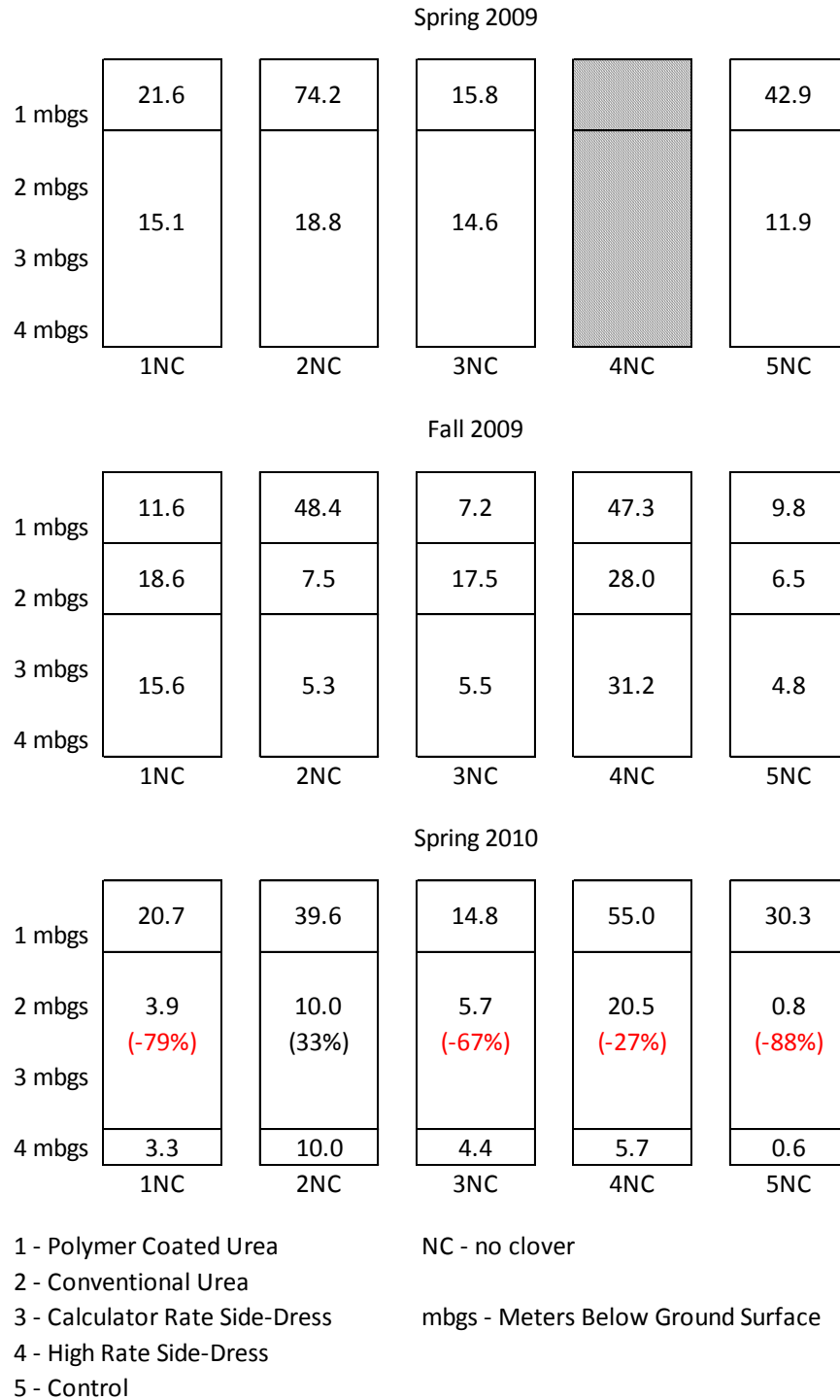


Figure 3.4.20 Representative cores of the depth-averaged pore-water concentration of each treatment and sample time in the no clover plots within the rooting zone and below the rooting zone to the maximum point of vertical migration. Percent change compared to the (previous core).

Distance-averaged Pore-water Concentrations (mg/L)
Within and Below the Rooting Zone to Maximum Vertical

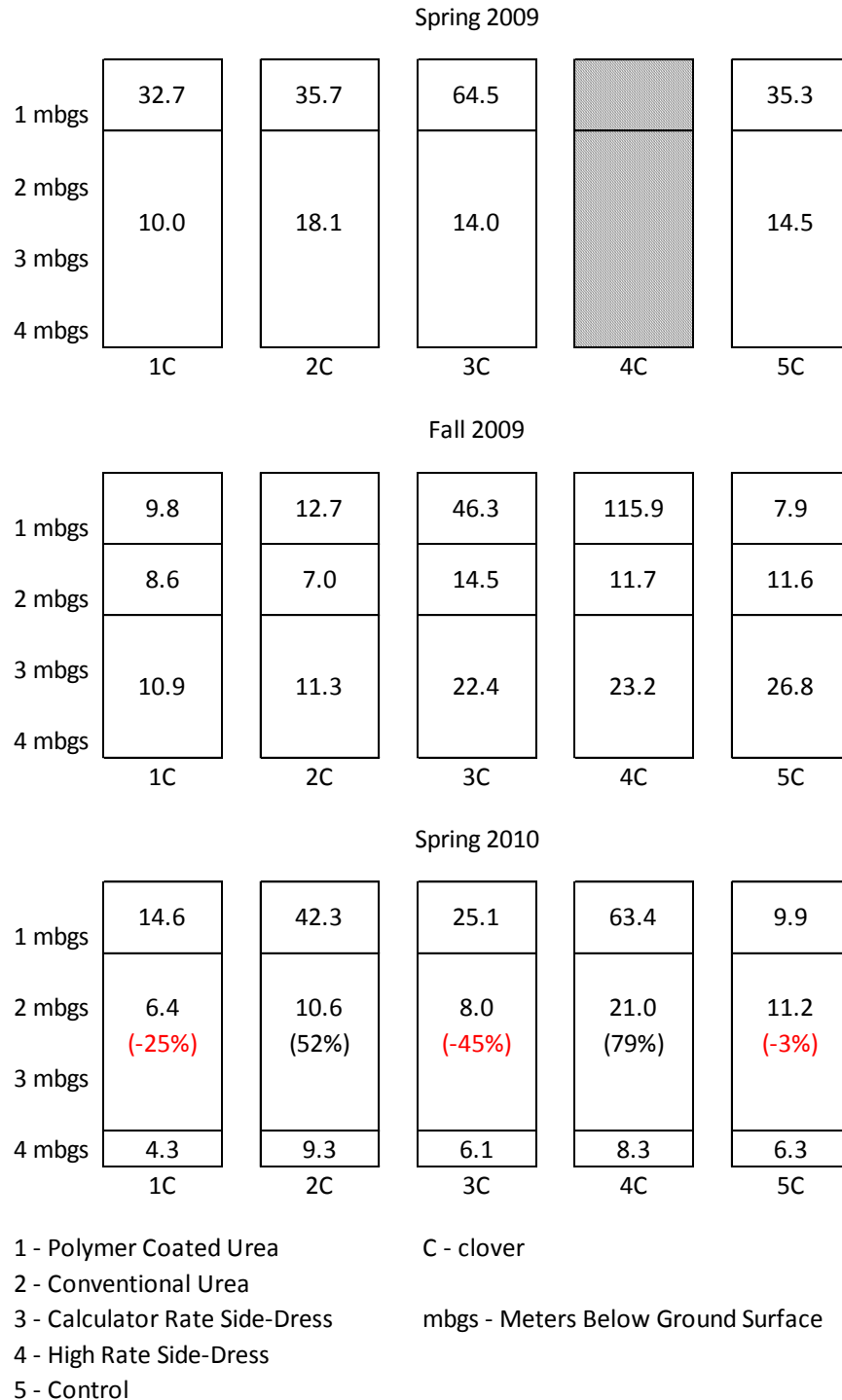


Figure 3.4.21 Representative cores of the depth-averaged pore-water concentration of each treatment and sample time in the clover block within the rooting zone and below the rooting zone to the maximum point of vertical migration. Percent change compared to the (previous core).

3.5 Discussion

This section evaluates the results relative to the study objective stated in Section 3.1.3. These were: (1) evaluate the leaching potential of combining synthetic fertilizers with a green manure to treatments with only synthetic fertilizers; (2) comparing the leaching potential of the different fertilizer treatments under study (i.e., the side-dress and polymer-coated urea fertilizers to the conventional spring applied urea); (3) evaluate the economic implications of the alternative nutrient management practices; (4) recommend treatments that reduce nitrate while maintaining crop yields. Nitrogen treatments options will be discussed with regard to their leaching potential and economic benefit. These will be presented in a similar manner as introduced in section 3.2.1, which was, comparing biologically fixed nitrogen to synthetic fertilizers (section 3.5.1), comparing control-release to conventional spring applied nitrogen fertilizers (section 3.5.2) and lastly comparing side-dressed to conventional spring applied nitrogen fertilizers (section 3.5.3).

3.5.1 Comparing Biologically Fixed Nitrogen and Synthetic Fertilizers

The shallow soil cores showed that spring applications of polymer-coated and conventional urea treatments on clover had smaller peak concentrations of nitrate in the early growing season (late June) compared to treatments in the no clover field. Groffman et al. (1987) found similar pattern when comparing treatments using spring applied synthetic fertilizer to treatments receiving legume nitrogen exclusively. As the peak concentration is not as high, the risk of deep leaching in the clover treatments is likely lessened in the early growing season compared to the treatments which received only synthetic fertilizers.

Data from the shallow sections of the deep cores do not present trends of nitrate storage which differentiates treatments with and without a clover in the rooting zone in the spring of 2009. These were collected in late May prior to the peak nitrate concentration that was observed in data derived from the shallow cores. There was also no discernible trend in the rooting zone in the fall of 2009 and the spring of 2010. After one year, no trend was discerned between treatments in the no clover and clover fields when comparing total mass in the deep cores below the rooting zone and above the furthest point of vertical migration. This result is consistent with other authors that also did not find a discernible difference in leaching under treatments with synthetic fertilizers and treatments with legumes over long periods of time (Ladd and Amato, 1986; Groffman et al., 1987 ; Harris et al., 1994; Kramer, 2002b; Stopes et al., 2002).

With the exemption of the control treatments, the average yields of the treatments in the clover field were not significantly different compared to their counterparts in the no clover field. This result is similar to Kramer et al (2002a), which did not find a significant difference in corn yields when comparing a synthetic fertilizer treatment to a treatment combining synthetic fertilizer and a legume over one growing

season. In contrast, Clark et al. (1999) found (on the same study site as Kramer et al. (2002a)) over several rotations spanning a total of 8 years, that a system combining synthetic fertilizer and legumes had higher average yields and net returns compared to a system using only synthetic fertilizer. Similar to Clark et al. (1999), with the exception of the high rate side-dress, the current study found that treatments that incorporated red clover as part of the nitrogen supply had higher economic returns than their counterparts receiving only synthetic fertilizers. This was due to the comparable yields and reduced cost associated applying clover compared to synthetic fertilizer.

3.5.2 Comparing Control-Release to Conventional Spring Applied Nitrogen Fertilizers

Data derived from the shallow cores suggested that there was a delay in the release of nitrate in the polymer-coated urea treatments compared to the conventional urea treatments indicating a reduced risk of early season leaching with this product over urea.

In the spring of 2009, the deep cores show that the total mass of nitrate in the rooting zone is lower under the polymer-coated urea treatments compared to the conventional urea treatments despite having received the same rate of nitrogen fertilizer at the same time. The total mass of nitrate in the rooting zone under the polymer coated urea is less than under the control in both plots, suggesting that there is very little release of nitrate from this treatment at this time, an observation supported by the results of the shallow cores. In the fall of 2009, the total mass of nitrate in the rooting zone decreased in all treatments, however, decreases are larger in the control treatments than in the polymer-coated urea treatments, but smaller in the conventional urea treatments compared to the polymer-coated urea treatments. Le Monte et al. (2009) also found that polymer-coated urea fertilizer had lower concentrations of residual nitrate in surface soils compared to urea at the end of the growing season. Lower residual nitrate in the fall is expected to result in a reduced risk of nitrate leaching over the winter. In the spring of 2010, the soil nitrate mass below the rooting zone and above the furthest point of migration is higher below the conventional urea treatments than under the polymer-coated urea treatments. In this segment the depth averaged pore-water concentration is near the MAC below the conventional urea treatments, however the concentrations below the polymer coated urea treatments are less than the MAC. The percent increases of nitrate in these segments compared to the previous fall are also much higher under the conventional urea than the polymer-coated urea treatments. This suggests that although there is evidence of leaching during the winter in both treatments, the loss of nitrate to the subsurface is much less under the polymer-coated urea than the conventional urea.

Overall, the polymer-coated urea treatments seem to reduce deep leaching of nitrate compared to the conventional urea treatment. The beneficial effect of this treatment seems to be the most prominent during

the winter, possibly due to lower residual nitrate in the rooting zone after harvest. As both treatments were applied at the same rate, this suggests better nitrogen use efficiency of the polymer-coated urea treatment compared to the conventional urea treatments. In addition, the polymer-coated urea treatment had similar yields to the conventional urea treatments both with and without the addition of clover nitrogen. However, due to its relatively elevated price (13% more than conventional urea), there was no economic advantage of using polymer-coated urea over conventional urea.

3.5.3 Comparing Side-Dressed to Spring Applied Nitrogen Fertilizers

The shallow core data indicates that calculator rate side-dress treatments may have lower leaching potential during the early growing season compared to the conventional urea and polymer-coated urea treatments as nitrate concentrations were lower during this period. The high rate side-dress treatment acted much like the calculator rate side-dress treatment in the early growing season, but in the later growing season (August) the concentrations of nitrate in the high rate side-dress treatments persisted at concentrations much higher than the other treatments.

The deep cores support the trend seen in the shallow cores which suggests that the calculator rate side-dress treatments may have a lower nitrate leaching potential compared to the conventional and polymer coated urea treatments, while the high rate side-dress treatment may have leached more nitrate. Note that the deep cores were taken in the spring of 2009 prior to the application of the side-dress fertilizer, and that the plot sampled for the calculator rate side-dress treatment on clover had very high residual nitrate in the spring of 2009; therefore, it is difficult to make a conclusive assessment of the benefits of this particular treatment.

In the fall of 2009, considering only the no clover plots, the total nitrate mass in the rooting zone under the conventional urea treatment is much higher than under the calculator-rate side-dress treatment, and only slightly higher under the polymer-coated urea treatment. Examining the section below the rooting zone and above the furthest point of nitrate migration, the spring applied treatments have similar total nitrogen mass to the calculator rate side-dress treatment; the polymer coated urea is slightly higher and the conventional urea is slightly lower. The high rate side-dress treatment, however, has a higher total nitrate mass in this segment compared to all other treatments.

In the spring of 2010 the total nitrate mass under the no clover calculator rate side-dress both in and below the rooting zone is low compared to both spring applied treatments. Between the fall 2009 and the spring of 2010, the calculator rate side-dress treatment in both the no clover and clover fields had smaller increases in nitrate mass below the rooting zone and above the furthest point of nitrate migration

compared to the spring applied treatments. In contrast the high rate side-dress treatments had higher total nitrate masses than any other treatments in these sections. It also had high percent increases below the rooting zone and above the furthest point of nitrate migration between the spring and previous fall, suggesting that nitrates migrated below the rooting zone during the winter. The depth averaged pore-water nitrate concentration below the rooting zone and above the furthest point of migration is less than the MAC in the calculator rate side-dress treatments, however, the average concentration in this segment under the high rate side-dress treatments are both more than double the MAC.

Overall, the calculator rate side-dress treatment seems to reduce deep leaching compared to the conventional urea treatments as well as the polymer-coated urea treatment, as low residual nitrate remain in soil above and below the rooting zone in the fall and following spring in the no clover field (Remembering that the calculator rate side-dress treatment on clover had unexplained high residual nitrate at the beginning of the study). The high rate side-dress treatments showed evidence of nitrate leaching both during the growing season and during the winter, which suggest that this treatment was applied at an inappropriately high rate. This is supported by many studies which have shown that nitrogen use efficiency of corn decrease as nitrogen fertilizer rates increase (Pumphrey and Harris, 1956; Reddy and Reddy, 1993; Ruselle et al., 1983). This inefficiency of use is an economic loss as the additional cost of nitrogen fertilizer is not made up by a proportional increase in yields.

The side-dress treatments had similar yields to the conventional urea treatments both with and without a clover cover crop. Side-dress treatments were also similar to polymer-coated urea treatments with one exception: in the clover plots the calculator rate side-dress treatment has statistically significant higher yields than the polymer-coated urea. High-rate side-dress treatments were found to not be economically advantageous; yields did not compensate for the increased cost of fertilizer. The calculator rate side-dress treatment in the clover field was found to be economically advantageous; although conventional urea treatment on clover had better economics. The no clover calculator rate side-dress treatment was found to have similar economic returns to the no clover polymer coated urea treatment.

3.6 Conclusions

This study was unique in that it compared several different combined nitrogen BMPs simultaneously from both agronomic and environmental perspectives.

The addition of a red clover produced equal or higher yields to treatments receiving only synthetic fertilizers. From an economic perspective, the integration of red clover as a supply of nitrogen is deemed advantageous over the use of synthetic fertilizers only, assuming that the clover crop takes after the seed

is broadcast, because the costs associated to the application of clover seed is less than the cost of additional fertilizer. The study did not find that the addition of clover had higher risk of nitrate leaching; however, high variability of shallow core data within each treatment, as well small sample size of the deep core data (only one core per treatment at each sampling data) due to budgetary constraints did not allow a comparison to which statistical analysis could be applied.

The treatment with the highest economic return was the conventional urea treatment on clover. The calculator rate side-dress treatment was estimated to have the second best economic return with a slight economic disadvantage over the conventional urea in the no clover plot due to the increase in required passes over fields. The delay in fertilizer application from the side-dress treatments seemed to increase the nitrogen use efficiency of crops in the calculator rate side-dress treatments as yields were comparable to spring applications of fertilizer but the application rates were lower. This finding as well as smaller peak soil nitrate concentrations in the shallow cores in the early spring, and the changes in nitrate storage in the deep cores suggests that the proper timing of the application of nitrogen fertilizer, as can be achieved with a side-dress approach, can reduce deep leaching of nitrate.

The results of high-rate side-dress treatment show that not only applying at the right time, but applying fertilizer at the right rate is essential to maximizing economics returns and reducing nitrogen losses to the environment. Where the calculator rate showed environmental advantages over the spring application of urea, the high rate side-dress treatments does not. As theses two treatments only differ in the rate of application of fertilizer, it is fair to assess that the rate of fertilizer application was excessive, which was observed to cause notable losses to the subsurface. What's more, there was an economic disadvantage of applying an excessive rate of nitrogen fertilizer due to the increased cost.

The polymer-coated urea fertilizer appeared to provide a delay in nitrate release compared to the conventional urea, a feature which has been suggested would lead to less leaching from crops during a period of low nitrogen uptake by plants. After one year, the polymer-coated urea showed a decrease in nitrate below the rooting zone compared to the conventional urea treatment. This suggests that this product has lower leaching potential than conventional spring applied urea which is likely due to increased nitrogen use efficiency by plants because of better synchrony between demand by plant and supply of nitrogen from the slow release fertilizer. Because the release of nutrient from this product is dependent on moisture, there is less control of the supply of nitrogen to crops compared to a side-dress treatment, which can be applied at a key point in the corn crop's life cycle. Compared to the polymer-coated urea treatments, the calculator rate side-dress treatment in both the no clover and clover fields had smaller increases in nitrate mass below the rooting zone and above the furthest point of nitrate migration

during the winter. The advantage of using a spring applied slow release fertilizer over a side-dress treatment is that it decreases the number of passes needed over a field in the spring, which is typically a busy time for farmers. The polymer-coated urea treatments provided similar yields to the conventional urea and the no clover calculator rate side-dress treatments; however, there were statistically significant higher yields in the calculator rate side-dress treatment compared to the polymer-coated urea treatment in the clover field. More study would be needed to assess if this would consistently be the case. An economic disadvantage was observed for the polymer coated-urea compared to the conventional urea treatments, as well as between the polymer-coated urea and the calculator rate side-dress treatment in the clover field. This is due to the higher cost of the polymer-coated urea fertilizer; the difference between the calculator side-dress and the polymer-coated urea in the clover field also likely due to the difference in yields. Similar returns were observed for the polymer-coated urea and the calculator rate side-dress treatments in the no clover field. As yields were similar, this indicates that at current prices the increased costs of the polymer-coated urea may be more or less equivalent to the increased costs associated the number of passes over the field required for the side-dress treatment.

Of the fertilizer applications under study, the side-dress treatments applied at an appropriate rate seems to be the best at providing strong economics while reducing nitrate leaching. Although the calculator rate side-dress on clover initially had high residual nitrate before the application of nitrogen fertilizer, a relatively small increase in nitrate was observed under this plot below the rooting zone between the fall of 2009 and spring of 2010. Moreover, very low concentration of nitrate within and below the rooting zone in the no clover plot, suggests that side-dressing may reduce leaching risk more than the other treatments studied.

The year in which this study was conducted was a very good year for corn; the early spring was not very wet which allowed for a early May planting date (May 5th), there were no climatic constraints to corn growth during the growing season (above average total precipitation and average daily temperatures), site conditions did not impede the application of the side-dress fertilizer treatments, and the previous clover cover crop had cover the field evenly prior to being incorporated. Environmental conditions and time management factors into the decisions that farmers make with regard to choosing a nitrogen management plan. There are limitations to some of the BMPs discussed above: clover crops may not take, site conditions may not allow a farmer to apply side-dressing within the optimum window for corn growth, or there may be time demands that make treatments requiring extra passes on a field less desirable. Such limitation need to be considered; therefore, it is important to consider that farmers need to have choices available to them so they make the best decisions with regards to the environmental conditions of a particular year while maintaining crop yields and reducing environmental risk.

3.7 Recommendations

Although the second year of the study may be able to confirm some of the conclusions that have been made, some changes to the methodology used may allow for a stronger assessment of the different treatments. The inherent difficulty in assessing the differences between treatments with the current methodology is that there were: a variety of factors that should be considered, the data available was limited, and there were some results which were deemed to be anomalies. Factors that may affect nitrogen leaching in this study include: the addition of legume nitrogen to the nitrogen supply, application rates of synthetic fertilizers, and different types of synthetic fertilizers applications.

An assessment of how the addition of clover affects nitrate leaching when paired with a synthetic fertilizer is difficult to make with the current methodology as synthetic fertilizers were applied at different rates with the clover than without. As a result, it is not possible to determine whether the total nitrogen was supplied at equivalent rates. Although the application rates for the conventional and polymer-coated urea treatments as well as the calculator rate side-dress treatment were determined using the corn calculator developed by OMAFRA (a tool which was developed from years of study) it is not fair to dismiss the application rates of the different treatments as a potential source for the differences in their performance. In future studies, to make a better assessment of the different treatments, more than one application rate could be applied in order to determine its effects on yield, leaching potential and nitrogen use efficiency. This approach could be implemented through a split-plot design. It should be mentioned that this study was completed within the context of a larger study by Don King, which did conduct a split plot study to compare different rates of polymer-coated and conventional urea, as well as different hybrids of corn; however, it was not sampled with deep cores. A better understanding of the effect of rates on the leaching potential of these treatments could have been obtained if these had been sampled.

The inclusion of other forms of data collection may help make stronger conclusions with regard to treatments that increase yields and decrease losses of nitrate to the subsurface. Nitrogen use efficiency by crops has been used by other studies as a proxy to determine potential losses from different agricultural practices (Pumphrey and Harris, 1956; Welch et al., 1971; Jung et al., 1972). It is generally determined using either of two methods: the difference method and the isotope dilution method. The latter is more involved, the former could be incorporated in the current framework of this study by simply sampling plants for nitrogen at harvest. Including analysis of total soil nitrogen at key sampling times would also help determine the risk of different treatments, especially with regard to treatments that incorporate legumes as part of the nitrogen supply because much of the nitrogen may be in organic forms. Including an analysis of all forms of mineral nitrogen for the shallow cores may be beneficial at the beginning of the growing season, since laboratory studies of polymer-coated urea have indicated that early leachate

typically contains ammonium and urea, and may not contain nitrate (Wang and Alva, 1996; Paramasivam and Alva, 1997). Limited data has made it difficult to make a strong assessment of the different treatments. Although there were three replicates of each treatment only one treatment was sampled with deep cores. The problem with the limited sampling effort from the deep cores is that the results cannot be submitted to statistical analysis in a rigorous way. A study by Campbell et al (1994) uses a methodology very similar to that used for the collection of the deep cores in order to assess the deep-leaching of soil nitrate. With respect to the collection of deep cores, their methodology differed from the current study's in the sampling effort as well as the way the cores were sampled. Deep cores were taken to a depth similar to this study; however, two cores were collected from each replicate in their study, where in this study only one core was collected from one replicate. A larger sampling effort allowed Campbell et al. (1994) to calculate values for the least square difference to determine significant difference between treatment averages. A similar approach could be used in the context of the objectives of this study, which may provide more support to the study findings. Cores were also sampled differently, where the methodology of this study sampled 0.05 m segments between 0.1 m intervals, Campbell et al. (1994) divided soil into 0.3 m segments from which subsamples were taken to determine bulk density and soil moisture, and the remaining soil from both cores were combined per depth interval and analyzed for nitrate. Their approach allowed for a good estimate of total nitrate in the soil with depth, whereas the methodology used in this study required interpolation of nitrate concentration between points of measurement to estimate cumulative nitrate. As total nitrate is of interest to the objectives of this study, the sampling method used by Campbell et al. (1994) would better suit the purposes of this study.

Lastly a problem with the sample protocol for the shallow core soil samples has been identified. Although it is not known why, the shallow core data seemed to have high variability at times within the same treatment. Typically, soil samples would be kept cool after collection to prevent changes to nitrate concentrations after samples are collected; however, samples were not immediately chilled after they were extracted. Adopting such a practice in future studies may aid in reducing possible sources of error.

Chapter 4

Estimating Recharge from an Ephemeral Stream during a Spring Melt

4.1 Introduction

During winter and spring melt events, the rapid release of stored water from the snow pack may result in the formation of ephemeral streams over relatively short time periods. The local recharge rates beneath these features are not well understood but may be of interest relative the local vulnerability of the underlying groundwater resources. The current study focuses on quantifying recharge under an ephemeral stream using temperature as a tracer and estimating infiltration rates through numerical analysis of the field data with a one-dimensional numerical model.

An ephemeral stream develops in a lowing lying area on the north-east corner of the County of Oxford lands most years during the spring melt and occasionally during winter melt events. The stream originates to the north of the study site and flows in a southeasterly direction, towards the well field as illustrated in Figure 4.3.1. The ephemeral stream passes over a section of land surface where the shallow and deeper regional aquifer units (the latter within which the municipal wells are completed) appear to be hydraulically interconnected (Haslauer, 2005). The water table is also relatively close to the ground surface in this low lying area at the site and varies annually between 2-3 m below the ground surface. Water recharging from the ephemeral stream travels only a short distance through the unsaturated zone before reaching the water table and may potentially be captured by the municipal wells. Previous studies at the site have provided evidence that rapid infiltration occurs in the area surrounding the ephemeral stream during melt events, as indicated by changes in hydraulic head and temperature in local monitoring wells (Haslauer, 2005; Koch, 2009). However, these short lived recharge events have not been quantified at the site. Quantifying the amount of recharge that occurs during spring melt is important as this represents a potential source of rapid and substantial infiltration into the underlying aquifers. This recharge could pose a risk to water quality in down gradient supply wells if this water were to transport undesirable substances.

The study presented herein is unique in its setting with regard to previous work completed using temperature as a means of estimating recharge numerically. Much of the ground breaking work using temperature to estimate fluxes beneath streams has been complete in arid environments; the current study attempts to quantify recharge in a cold weather environment, where frozen soils act as a barrier infiltration. In this study, changes in temperature in the vadose zone and in the shallow groundwater, as

well as changes in hydraulic head in the shallow groundwater were only observed once the soil began to thaw. The agricultural setting, the complex underlying hydrostratigraphy and the proximity to a large well field are also interesting aspects of the study setting.

4.1.1 Objectives and Approach

The primary goals of this study are to quantify recharge beneath an ephemeral stream at the Oxford County field site and to assess whether temperature variations above the water table can be used as a tracer to reasonably estimate recharge during a short lived spring melt recharge event. The work involves field instrumentation and monitoring linked with the use of numerical modeling tools to assist in interpretation of the field data. Secondary objectives included assessing recharge spatially and temporally at the site, and designing a method to deploy temperature probes so that they can be retrieved at a later date while still making good contact with porous media in gravelly materials.

Central to the study was the monitoring of heat transport through the variably saturated subsurface. These data were used to estimate recharge beneath the ephemeral stream during the winter melt event. This technique was selected because abrupt changes in groundwater temperature at the site during ephemeral stream events had previously been documented and used as evidence of rapid infiltration (Haslauer, 2005; Koch, 2009).

The investigation approach included monitoring subsurface temperatures at one location under the ephemeral stream using an array of thermistors inserted into the soil at different depths within the vadose zone. Stream depth, groundwater levels, water temperature, and soil moisture were measured. The resulting data was used to provide initial and time variable boundary conditions for a one-dimensional model.

Independent methods of evaluating and estimating recharge were also employed. A bromide tracer was applied to the soil surface near the installation of the soil thermistors and the temporal tracking of the infiltration of bromide tracer generated recharge estimates which were compared to the model estimates. The results were compared to previous estimates of annual recharge at the same locations. Qualitative means of assessing recharge from the ephemeral stream were also used. Hydraulic head, temperature and water chemistry were monitored in nearby observation wells which were used to characterize spatial variations in recharge.

Section 4.2 provides an overview of the mechanisms of heat transfer in porous media and previous applications of using heat as a tracer to estimate recharge. Section 4.3 describes the field data collection completed as well as the pertinent mathematical assumptions used by the model to quantify recharge.

Section 4.4 presents the results and Section 4.5 discusses the results. Section 4.6 presents the conclusions of this study and Section 4.7 makes recommendations relative to the study objectives.

4.2 Background

4.2.1 Applications of Heat Transport for Recharge Estimation

The concept that heat could be used as a groundwater tracer was recognized in the early 1900's (e.g., Schlichter 1905). Seminal theoretical work in the 1960's (Suzuki, 1960; Stallman, 1965; Bredehoeft and Papadopoulos, 1965) developed analytical solutions for heat transport as a means of quantifying groundwater movement. After the 1960's, interest in the subject waned until the later 1980's (Anderson, 2005). The advent of numerical models, improvements in automated temperature monitoring, and computational improvements resulted in more robust data acquisition and made the use of temperature as a tracer relatively inexpensive from which reliable estimates of groundwater movement could be made (Anderson, 2005; Constantz, 2008). Recently there has been an expansion in the body of literature on the subject, especially with regard to the analysis of the interexchange of water between streams and groundwater (Anderson, 2005).

In recent years, analytical (Hatch et al., 2006) and numerical models (Healy and Ronan, 1996; Šimůnek et al., 1999) have been developed to quantify the movement of water and heat between surface water bodies and the subsurface. The use of temperature as a tracer has been applied to determine recharge and discharge into continually flowing (e.g., Constantz et al. 2003b) as well as ephemeral streams (e.g., Constantz et al., 1994; Constantz and Thomas, 1996; Constantz et al., 2003b; Hoffman et al., 2005), and has been applied to characterize hyporheic exchange adjacent to in-stream geomorphic features (e.g., Lautz et al., 2010). Many of these studies were completed in the American south-west in desert environments. Heat transport has also been compared to conservative chemical tracers to determine flow through stream-sediments, and has been found to produce similar results (Constantz et al., 2003a).

Using numerical models, recharge may be estimated by matching simulated temperatures to observed temperature data by varying the thermal and hydrological properties of the soil, and flow boundary conditions (Niswonger and Prudic, 2005). Though many different numerical models exist, for this study the HYDRUS-1D model (Šimůnek et al., 1999) was employed. The mathematical development of the model is presented in Section 4.3.2.3.

4.2.2 Heat Transport through Porous Media

Heat flow through the shallow subsurface occurs mainly through two processes: advection and conduction. Heat advection is the process by which heat is transferred by traveling along with the mass of a moving fluid. In a shallow soil this fluid is usually water. Heat conduction is the process by which heat is transferred through matter by kinetic energy from particle to particle without the displacement of mass. The transfer of heat through conduction is ubiquitous in media; however, advection of heat only occurs

where flowing pore-water is present. When advection dominates heat flow, temperature variations can be used to approximate the rate of water movement into the subsurface.

Temperature variations at the ground surface are attenuated with depth due to the absorption of heat. In porous media the attenuation of heat is determined by the bulk volumetric heat capacity of the porous medium. Temperature variations at the ground surface are also delayed in time with respect to depth. This delay is a function of the temperature gradient, thermal conductivity of the sediments, and the rate of pore-water movement. Thermal properties of the porous medium can be measured in situ, or estimated using literature values if the type of porous medium is known.

In comparison to analogous hydraulic parameters, thermal parameters have a much smaller range of values; because of this there is more uncertainty related to selecting hydraulic parameters than there is in selecting thermal properties (Constantz and Stonestrom, 2005). Heat transport is sensitive to saturated hydraulic conductivity when transport occurs predominantly through advection. When conduction is the dominant means of heat transport the model is more sensitive to moisture retention parameters, like the van Genuchten empirical parameters α and n (Niswonger and Prudic, 2005). In unsaturated soils when there is no flowing water, the model is less sensitive to saturated hydraulic conductivity, although saturated hydraulic conductivity is used to determine unsaturated hydraulic conductivity (Niswonger and Prudic, 2005).

4.3 Methodology

The field, laboratory and computational methods used to assess recharge during the spring melt and to satisfy the thesis objectives stated in Section 4.1.1 are summarized in this section. Field data collection included: designing and deploying temperature probes for installation in the subsurface; measurements of transient soil temperature in the vadose zone; the collection of moisture content profiles with a neutron probe; the application of a surface applied chemical tracer and subsequent soil coring to track the tracer; and monitoring of hydraulic head, groundwater temperature, and chemistry in monitoring wells. In addition, the depth of the ephemeral stream was recorded during the course of the spring melt event. Flow of water and heat transport through the subsurface was simulated using a one-dimensional saturated and unsaturated numerical model (HYDRUS 1-D). This section is divided into two main subsections that cover the field data collection activities and describe the HYDRUS-1D model and its application to this research.

4.3.1 Field Data collection

Instrumentation and data collection was focused near and within the path of the ephemeral stream. The location of the instrumentation is presented in Figure 4.3.1 and Figure 4.3.2. Details of the field activities are provided in the subsequent sections.

4.3.1.1 Bromide Tracer

A solution of 6 kg of potassium bromide (KBr) and 18 L of deionized water was applied in December 2009 to a 3 m by 3 m area of ground near the field instrumentation within the path of the ephemeral stream (Figure 4.3.1). The area was divided equally in four sections, and the solution was applied to one quadrant at a time using watering cans. The resulting aqueous solution concentration was 2.24×10^5 ppm bromide and the surface concentration was 0.45 kg Br/m^2 . The plot was subsequently cored, and the movement of the bromide tracer was used in conjunction with nearby moisture content measurements to estimate recharge. The equations used to calculate recharge are presented in section 4.3.1.3.

4.3.1.2 Deep Core Collection

Soil was cored from the surface to a depth of 15 ft (4.5 m) and collected within 1.5 m of the neutron probe in a bromide plot previously utilized by Bekeris (2007) and Koch (2009) in May of 2009. This core was used to determine the stratigraphy at the site, which was used in the creation of the numerical model domain (Station 1_58 see Appendix H). Stratigraphy was logged using the Unified Soil Classification System (ASTM, 2006). Core extraction was accomplished using the Geoprobe® direct push method, equipped with a DT22 Sampling System [2.25 inch (5.7 cm) outer diameter (OD) core barrels]. The top 5 ft (1.50 m) was collected in two 2.5 ft (0.75 m) sections in order to maximize the amount of soil recovered in the soft top soil. The subsequent two cores were taken in 5 ft (1.50 m) long sections. The borehole was immediately filled with bentonite chips following core extraction.

The bromide plot established in December of 2009 was cored on March 5th, 2010 (just before the spring melt) by manually hammering a 2 inch (5.1 cm) ID steel core barrel into the ground in two sections to a total depth of 1 m below the ground. The same area was cored again on May 6th, 2010 using the Geoprobe® direct push method in the same manner as in May of 2009. This core is presented in Appendix H (Station 1_64), and the logged stratigraphy was also used in the creation of the model. The main purpose of these cores was to determine the vertical movement of the bromide tracer between March 5th and May 6th, 2010, which was used to approximate recharge over this period. The cores extracted on March 5th and May 6th of 2010 were also analyzed for water content and bromide concentration. Each core was cut in half lengthwise, and one half of the core was used for making water content measurements, and the mirroring half was used to analyze for nitrate, bromide and chloride

concentrations. The core taken on March 5th was sampled in 2.5 cm segments, and the core on May 7th was sampled in 5 cm segments at approximately 10 cm intervals.

4.3.1.3 Calculating Recharge Using Surface applied Bromide Tracer

Bekeris (2007) concluded that a bromide tracer test was the most appropriate method to estimate recharge in this kind of localized experiment. The recharge rate is calculated by multiplying the vertical velocity by the average volumetric water content (Bekeris, 2007; Scanlon, 2002). The average volumetric water content was obtained using monthly neutron probe data as well as volumetric water content data from the cores.

$$R_{\text{rate}} = \frac{\Delta z}{\Delta t} \theta_{v,\text{avg}} = v \cdot \theta_{v,\text{avg}} \quad (4.4.1)$$

where

- R_{rate} is the recharge rate (m/day)
- Δz is the depth traveled by the peak concentration or the depth of the centre of mass of the tracer (m)
- Δt is the time lapse between coring campaigns(days)
- $\theta_{v,\text{avg}}$ is the average volumetric water content (dimensionless ratio)
- v is the vertical velocity of the tracer (m/day)

Total recharge over a period of interest can be calculated by multiplying the recharge rate by the amount of time that passed in days.

$$R = R_{\text{rate}} \cdot \Delta t \quad (4.4.2)$$

where

- R is total recharge (m)

The depth of the centre of mass of the tracer may be calculated using the following equation (Bekeris, 2007).

$$z_{\text{centre}} = \frac{\sum_{i=1}^n C_{\text{soil},i} \cdot l_i \cdot z_i}{\sum_{i=1}^n C_{\text{soil},i} \cdot l_i} \quad (4.4.3)$$

where

- z_{centre} is the depth of the centre of mass of the tracer (m)
- z_i is the depth of the core sample (m)
- l_i is the length of the interval represented by the sample (m)

$C_{\text{soil},i}$ is the soil concentration of a given soil sample (mg/kg_{soil})

A mass balance of the bromide tracer was estimated by expanding the mass of the bromide from the deep cores collected to the entire area over which the bromide tracer was applied. Total bromide at the time the core was collected was calculated using the following equation (Bekeris, 2007).

$$M_{\text{Br}} = \left(\sum_{i=1}^n C_{\text{soil},i} \cdot l_i \right) \rho_{\text{b,ave}} \cdot A_{\text{Br}} \quad (4.4.4)$$

where

M_{Br} is the total mass of bromide in the area of application during a given coring event (kg_{Br})

$\rho_{\text{b,ave}}$ is the average bulk density of the core (g/cm³)

A_{Br} is the area of bromide application (m)

This mass can then be compared to the total mass applied to the site to calculate a mass balance. This approach assumes a uniform bromide distribution over the area of application and no lateral transport beyond the area of application.

4.3.1.4 Moisture Content

Volumetric soil moisture content was measured monthly between March and August of 2010, and four times during the month of March to coincide with the spring melt event. This information was used to set the initial conditions of the HYDRUS-1D model and to monitor changes in water content over time. Figure 4.3.2 shows the location of the neutron access tube in relation to other instruments. It should be noted that, although the neutron access tube is near the other instruments, it is not situated within the path of the ephemeral stream and does not directly represent the conditions beneath the stream during the course of the study. The implications of this are discussed in subsequent sections.

Water content measurements were collected in 0.15 m intervals along the length of each access tube using a model 503 DR Hydroprobe Neutron Moisture Probe (CPN International Inc.), hereafter referred to as the neutron probe. This instrument measures water content by correlating the proportion of fast neutrons that are redirected to the probe by water molecules to the number of emitted neutrons. Water content measurements are made within a sphere of soil surrounding the probe whose radius is inversely proportional to the soil moisture content, thus in drier soils the sphere of influence is larger (Ward and Wittman, 2009). The mechanisms of this instrument and site specific calibration used at the field site to convert readings to moisture content are detailed in Bekeris (2007).

4.3.1.5 Monitoring Wells and Groundwater Sampling

A network of monitoring wells exist in the vicinity of the ephemeral stream, these are shown in Figure 4.3.1. Information concerning the dimensions, screen depth, and location of these wells are presented in Appendix J. Hydraulic head and temperature were recorded in one hour intervals using Levellogger Gold (Model 3001 LT, Solinst Canada Ltd., Georgetown, Ontario, Canada) pressure and temperature recording device, hereafter referred to as transducers. These were installed in 18 of the 21 monitoring wells at the site. These transducers were non-vented; therefore, an adjustment was made for barometric pressure changes. Barometric pressure was obtained from hourly readings from the meteorological station located on site.

Using hydraulic head data from the spring of 2008, Koch (2009) classified wells in the vicinity of the ephemeral stream in terms of their response in hydraulic head and groundwater temperature during a spring melt event. Wells that are classified as having a fast response were either in or near the general flow path of the stream. Koch (2009) suggested that some wells may have well casings that leaked (specifically WO37), and therefore, to prevent this from occurring the well casings were examined and WO37 and WO63 were repaired as part of this current study.

Koch (2009) found that there was a notable decrease in groundwater nitrate concentrations in some wells near the stream following the spring melt. This observation raised the question of whether the fast infiltration of melt water with a relatively low concentration of nitrate was able to quickly infiltrate into the groundwater, and dilute or displace ambient groundwater nitrate concentrations. In order to assess the impact of the ephemeral stream on groundwater ionic concentration, 21 wells were sampled monthly between October 2009 and June 2010 for nitrate and chloride (i.e., before and after the spring melt).

Wells were sampled using a pump and high density polyethylene tubing (HDPE) that was cleaned with deionized water prior to and after sampling in the field. Equipment blanks were taken in order to confirm the tubing was clean. Wells with diameters smaller than 2 inch Schedule 40 PVC pipe (2.07 in; 5.26 cm ID) were sampled using a Geopump Series II peristaltic pump (Geotech Environmental Equipment Inc., Denver, Colorado, USA) with ¼ inch HDPE tubing (0.17 In; 0.43 cm ID). Wells constructed with 2 inch Schedule 40 PVC pipe (2.07 in; 5.26 cm ID) were sampled with a Grundfos Rediflow 2 submersible pump (Grundfos Canada Inc., Oakville, Ontario, Canada) with ¾ inch HDPE tubing (0.63 In; 1.59 cm ID), with the exception of WO63. WO63 was sampled with the peristaltic pump because a piece of hardware in the side wall of the casing impeded the submersible pump from being inserted. Wells were purged of three well volumes before sampling, duplicate samples were randomly taken in approximately one out of every ten samples. All samples were placed in a cooler with an ice pack in the field, and stored

in a freezer until they could be analyzed at the University of Waterloo using a Dionex ICS 3000 ion chromatograph (Dionex Corp., Bannockburn, Illinois, United States of America) equipped with a Dionex Ionpac AS 4 x 250 mm analytical column and a KOH eluent.

4.3.1.6 Temperature Probes

Seven temperature probes were installed in the unsaturated zone at various depths at the instrumented field site within the course of the ephemeral stream (Figure 4.3.2). The probes were 107B thermistors (Campbell Scientific Inc., Edmonton, Alberta, Canada), connected to a CR1000 data logger (Campbell Scientific Inc.). These probes measured soil temperatures at 15 minutes intervals. These data were used to provide evidence of infiltration and were also used in the modeling exercise to estimate recharge rates.

The probes were inserted into the ground via a casing, which allows for the easy retrieval of the probes from the soil at a later date. The details of the casing construction are shown in Figure 4.3.3. It consists of two PVC pipes; a smaller pipe ($\frac{3}{4}$ inch Schedule 40 PVC pipe (0.82 in; 2.09 cm ID)) inserted into a larger pipe (1 $\frac{1}{4}$ inch Schedule 40 PVC pipe (1.38 in; 3.51 cm ID)). The smaller pipe extends past the larger pipe and the thermistor is contained within this extension, which is perforated, capped, and covered with a fine mesh. In order to allow the thermistor to better relay the temperature of the ambient conditions, a small sand pack was fashioned around the thermistor and inserted with it into the small pipe. To isolate the thermistor from the conduction of heat within the air columns of the small pipe, a plug was inserted into the extension around the cable. To seal the gap between the large and small pipe, rubber washers were placed between the two pipes near the top and the bottom of the large pipe. A cap was placed on the top of the large tube, the cap had a hole large enough to accommodate the smaller tube. The top of the small tube and the gap between the small tube and the large tube were sealed using black electrical tape.

The casings were installed in the ground at angles of approximately 60 degrees from the ground surface at the following distances along the individual boreholes: 15 cm, 30 cm, 45 cm, 60 cm, 100 cm, 140 cm, 180 cm (see Table 4.3.1). The casings were inserted at an angle in order to minimize the potential for vertical preferential flow of infiltrating water along the casing. The calculated vertical depths below the ground surface to the tip of each probe were: 13 cm, 26 cm, 39 cm, 53 cm, 87 cm, 1.21 m and 1.56 m. The first three shallow probes were installed on December 4th, 2009. Because the surface soils were relatively soft, a larger hole was made to accommodate the large tube using a hand auger (6.7 cm; 2 $\frac{5}{8}$ inches OD), and a smaller hole was made using a soil sampling tube (2.5 cm; 1 in OD) to insert the small pipe allowing for good contact with the formation. The annuli around the casings were back filled with formation material. The four deeper probes were installed on December 8th, 2009. The holes for these

probes were made using a solid stem auger (10.2 cm; 4 in OD) attachment on the Geoprobe ®. Because the porous medium was quite stony, the annuli around the casings were backfilled around the probe to approximately 30 cm above it with native material and then the remainder was backfilled with a cement and bentonite slurry. The temperature probes were retrieved intact without injury to the instruments in the spring of 2012.

4.3.1.7 Surface Instrumentation

On March 6th, a staff gauge and a water level, temperature, and electrical conductance recording device (model 3001 LTC Levelogger Junior, Solinst Canada Ltd.) was installed at ground surface within the path of the stream near the instrumented site, hereafter referred to as the surface transducer (see Figure 4.3.2). The data collected with this device was used to determine the depth and temperature of the surface water during the melt event, and was collected at 15 minutes intervals. The height of the water column at the ground surface was used in the construction of the model for the surface boundary condition. Manual measurements were also taken in order to properly equate transducer readings to the true hydraulic head and serve as a check for the transducer measurements. As with the transducers used in the monitoring wells, the hydraulic heads recorded by the loggers needed to be barometrically corrected using data from the meteorological station located on site.

4.3.2 The HYDRUS-1D Model

HYDRUS-1D, version 4.14 (Šimůnek et al. 2008) was used to model heat and water flux through the unsaturated zone. It is a one dimensional finite element model which can simulate the movement of water, heat and solutes under variably saturated conditions. Amongst a broad range of capabilities, the model accommodates time-variant boundary conditions and transient flow conditions (Šimůnek et al. 2008). For the current application, the water flow and heat transport equations are solved in an integrated fashion for transient simulations. The equations are solved sequentially following the approach of Yeh and Cheng (1999) with the flow equation solved first followed by the heat transport equation. Below is presented a description of the unsaturated flow equation used by the model and required soil properties, heat flow equations, a description of the model domain, boundary conditions and initial conditions, and the model calibration approach.

4.3.2.1 Water Flow

One-dimensional flow in a partially saturated porous medium is described by a modified form of the Richards equation (Šimůnek et al. 2008):

$$\frac{\partial \theta}{\partial t} = \frac{\partial}{\partial x} \left[K \left(\frac{\partial h}{\partial x} + \cos \alpha \right) \right] - S \quad (4.4.4)$$

where

θ	is volumetric water content [L^3L^{-3}]
t	is time [T]
x	is a spatial coordinate [L]
h	is water pressure head [L]
K	is the unsaturated hydraulic conductivity [LT^{-1}]
α	is the angle between flow direction and the vertical axis
S	is a sink term [$L^3L^{-3}T^{-1}$]

This equation assumes that the air phase does not significantly affect the flow of liquid water and neglects the flow of water caused by thermal gradients. Unsaturated hydraulic conductivity is a function given by (Šimůnek et al. 2008):

$$K(h, x) = K_x(x)K_r(h, x) \quad (4.4.5)$$

where

K_s	is the saturated Hydraulic Conductivity [LT^{-1}]
K_r	is the relative Hydraulic Conductivity [T]

4.3.2.2 Soil Hydraulic Properties for Unsaturated Flow

Both water content and hydraulic conductivity are non-linear functions of pressure head, these may be approximated by HYDRUS by five different analytical models. The method used in this study was described in van Genuchten (1980):

$$\theta(h) = \begin{cases} \theta_r + \frac{\theta_s - \theta_r}{[1 + (\alpha|h|)^n]^m} & h < 0 \\ \theta_s & h \geq 0 \end{cases} \quad (4.4.6)$$

$$m = 1 - \frac{1}{n}, \quad n > 1$$

$$S_e = \frac{\theta - \theta_r}{\theta_s - \theta_r} \quad (4.4.7)$$

$$K(h) = K_s S_e^l \left[1 - \left(1 - S_e^{\frac{1}{m}} \right)^m \right]^2 \quad (4.4.8)$$

where

$\theta(h)$	is pressure dependent moisture content [L^3L^{-3}]
θ_r	is residual moisture content [L^3L^{-3}]

θ_s	is saturated moisture content [L^3L^{-3}]
α & n	are empirical coefficients that control the shape of the hydraulic function
h	is pressure head [L]
l	is pore-connectivity [-]
S_e	is the effective saturation [-]
θ	is moisture content [L^3L^{-3}]
$K(h)$	is pressure dependant unsaturated hydraulic conductivity [LT^{-1}]
K_s	is the Saturated hydraulic conductivity [LT^{-1}]

The pore-connectivity parameter l was estimated by Mualem (1976) to generally have a value of approximately 0.5 for most soils. Values for θ_r , θ_s , α , n , and K_s must be estimated for every soil layer simulated. These values may be specified manually, chosen from the soil catalogue produced by the model for eleven different textural classes, or estimated from basic soil information using Rosetta Lite version 1.1 (Schaap, 2003) which is accessible through HYDRUS 1-D.

4.3.2.3 Heat Transport

Neglecting the effect of water vapor diffusion on heat transport, the one-dimensional transfer of heat is

$$\frac{\partial C_p(\theta)T}{\partial t} = \frac{\partial}{\partial x} \left[\lambda(\theta) \frac{\partial T}{\partial x} \right] - C_w q \frac{\partial T}{\partial x} - C_w S T \quad (4.4.9)$$

estimated with the following Šimůnek et al. (2008):

where

$C_p(\theta)$	is the volumetric heat capacity of the porous medium [$ML^{-1}T^{-2}K^{-1}$]
C_w	is the volumetric heat capacity of liquid water [$ML^{-1}T^{-2}K^{-1}$]
T	is temperature [K]
$\lambda(\theta)$	is the apparent thermal conductivity of the soil [$MLT^{-3}K^{-1}$]
q	is darcy's flux [$L T^{-1}$]

In equation 4.4.8 the first term on the right hand side represents movement of heat by conduction through the porous medium and the second term represents the transport of heat by flowing water (advection). The volumetric heat capacity is the product of specific heat capacity and density.

$$C = c\rho \quad (4.4.10)$$

where

- C is the volumetric heat capacity of a given material [$\text{ML}^{-1}\text{T}^{-2}\text{K}^{-1}$]
- c is the specific heat capacity of a given material [$\text{L}^2\text{T}^{-2}\text{K}^{-1}$]
- ρ is the density of a given material [ML^{-3}]

The volumetric heat capacity of the porous medium is estimated by the model using the following equation, developed by de Vries (1963):

$$C_p(\theta) = C_n\theta_n + C_o\theta_o + C_w\theta_w + C_a a_v \approx (1.92\theta_n + 2.51\theta_o + 4.18\theta_w) \times 10^6 \text{ [Jm}^{-3}\text{°C}^{-1}] \quad (4.4.11)$$

where

- θ is the volumetric fraction [L^3L^{-3}]
- n indicates solid phase
- o indicates organic phase
- w indicates liquid phase
- a indicates gas phase

The apparent thermal conductivity is described as a combination the thermal conductivity of the porous medium in the absence of flow and macrodispersivity, which is a linear function of the velocity. This is described by the following equation (de Marsily, 1986):

$$\lambda(\theta) = \lambda_0(\theta) + \beta_t C_w |q| \quad (4.4.12)$$

where

- $\lambda_0(\theta)$ is the thermal conductivity of the porous medium [$\text{MLT}^{-3}\text{K}^{-1}$]
- β_t is thermal dispersivity [L]

The thermal conductivity of the porous medium includes both the solid and the liquid phase. This parameter can be estimated through one of two relationships in HYDRUS. The Chung and Horton (1987) relationship was used in this study to determine thermal conductivity. It is calculated using the following equation:

$$\lambda_0(\theta) = b_1 + b_2\theta + b_3\theta^{0.5} \quad (4.4.13)$$

where

b_1, b_2 & b_3 are empirical parameters [$\text{MLT}^{-3}\text{K}^{-1}$]

These parameters are provided by the model for three textural classes: sand, loam and clay soils. The relationships between thermal conductivity and moisture content for these three textural classes are provided in Figure 4.3.4.

4.3.2.4 Model Domain

Referring to Figure 4.3.5 the model domain for the HYDRUS simulation extends from the first temperature sensor T1 used to approximate the ground surface, which is in reality 13 cm below the surface of the ground, to the depth of the transducer in WO37, which is below the water table. The domain is 3.49 m in depth, representing the space between T1 and the depth of the transducer in WO37, and it is discretized in 350 equally spaced nodes, and 11 different soil layers. The details regarding the layering strategy will be discussed in Section 4.4.6.1.1. Note that the elevation of the ground surface at WO37 is 15 cm lower than at the neutron access tube used to define the initial moisture conditions of the soil. This difference is rectified by placing the depth the transducer 15 cm lower in order for the depth of the water table to better match the soil moisture profile.

4.3.2.5 Boundary Conditions

A visual representation of the boundary conditions is presented in Figure 4.3.5. Every simulation used a surface temperature boundary where the specified temperature was equal to the temperatures recorded at T1. This approach was used because, although temperature measurements were made using the surface transducer, these measurements were unsatisfactory because peak temperatures were much higher than air temperature recorded at the meteorological station as a result of heating of the logger by solar radiation. Each simulation prescribed a lower temperature boundary equal to the temperature recorded by the transducer in well WO37.

The surface flow boundary used in unsaturated conditions under steady state no flow conditions was a constant flux boundary equal to zero. The surface flow boundary for the case of transient, partially saturated flow (when the ephemeral stream was present) was a variable head and flux surface boundary. Because the first temperature probe was placed 13 cm below the ground surface, two different scenarios were used to approximate surface conditions. In the first scenario (scenario 1), during periods where there

was ponded water at the surface, a hydraulic head equivalent to the water column measured at the surface was used, this ignores the 13 cm of soil between the surface and the first temperature probe on hydraulic head. In the second scenario (scenario 2), a hydraulic head equivalent to the water column measured at the surface plus an additional 13 cm of head was used, this assumes that the top 13 cm soil is saturated and pressure is hydrostatic. This assumption was made as it was thought to reasonably represent the highest amount of pressure that may be imposed by the 13 cm of soil above the first temperature probe. In both scenarios, a no flow was prescribed when water was not ponded at the surface. As neither of these scenarios perfectly represents the true conditions in the field, and the true conditions would probably lie between the two, it is of interest to see how these will affect the cumulative recharge estimates. The lower boundary of every simulation was modeled as using a variable head boundary, which was set to the corrected head measured by transducer in WO37.

4.3.2.6 Initial Conditions

The initial temperature profile was determined based on data from the soil temperature probes, installed in the field at different depths. Initial temperatures for the nodes between points of measurement were linearly interpolated using the model. Initial moisture content was provided by contemporaneous neutron probe measurements, and nodes between the points of measurement were linearly interpolated by the model. Three different periods were simulated. Two were associated with time periods where the ephemeral stream was not present (April 12th to June 1st, 2010 and August 24th to October 31st, 2010). For these simulation periods, the moisture content measurements used for these simulations were taken on April 12th and August 24th, respectively. The third period was during the melt period, and was simulated between March 9th and 22nd and the initial moisture content measurements used for this simulation were taken on March 9th, 2010.

It is important to note that the level of the water table according to transducer in WO37 is higher than would be suggested by the neutron probe measurements; however, as the level reported by the transducer in WO37 is the best estimation of the changes in height of the water table, the initial moisture content of the nodes at or below the water table as reported by the transducer were set to be equal the porosity of the soil layer. The data specified for all simulations are presented graphically in Appendix T to Appendix V.

4.3.2.7 Model Calibration

Calibration entailed adjusting model parameters in order to fit simulated results to observed data. Calibrating for heat flow in variably saturated sediments can be difficult because either conduction or advection can be the dominant means of heat transport depending on the amount of flow. As discussed in Section 4.2.1, the model output will be more sensitive to different parameters depending on the degree of

saturation as moisture content is indirectly related to the amount of flow. In order to develop a complete parameter set, the model was calibrated first for gravity drained soils with steady state no flow conditions, and then further refined for partially saturated soil with variable flow conditions during the spring thaw.

Due to the large number of parameters that may be adjusted for several soil layers, it is acknowledged there may be an issue of non-uniqueness in the model results. Final parameters are selected to best represent both the soils under variable flow conditions and gravity drained conditions. The successful simulation of the field data sets under the different flow scenarios increases confidence in the uniqueness of the model results.

4.3.2.7.1 Calibrating – Gravity Drained Case

The flow of water and heat is complicated during the spring melt due to the presence of surface water mounding and thawing of frozen soils. In order to approximate soil hydraulic and heat properties, periods other than the spring melt were simulated first. During these periods, flow in the unsaturated zone is assumed to be negligible and conduction is the dominant means of heat transport. The domain is assumed to be at hydrostatic conditions, fully gravity drained and there is no standing water at the surface. There are two types of parameters that need to be calibrated when heat transport is dominated by conduction; these are soil heat parameters and soil moisture retention parameters. The soil heat parameters that need to be estimated are volumetric heat capacity and thermal conductivity. The former is approximated by the model using the moisture content, and the latter is a function of moisture content and estimated empirical parameters which alter the shape of the thermal conductivity versus moisture content curve (see Section 4.3.2.3). Because moisture content determines the values of both volumetric heat capacity and thermal conductivity, determining proper moisture retention properties is important to the simulation of heat transport in the unsaturated zone. Soil moisture parameters that need to be estimated are residual moisture content, saturated moisture content (porosity), van Genuchten α and n coefficients, pore-connectivity and saturated hydraulic conductivity. These parameters need to be adjusted in order to maintain soil moisture profiles that are consistent with the range of soil moisture profiles measured over long simulation periods. Because the moisture content profile changes very little over time at the site when the soil is gravity drained (see Section 4.4.2 and Figure L.1 of Appendix L), hydraulic parameters were selected so that the simulated moisture content profile over long simulation times had a similar shape to the measured moisture content profile used as the initial conditions. In order to simulate a moisture content profile that resembled the observed moisture content profile, the lowest soil layer was subdivided into several layers and the moisture retention parameters of these layers were varied until the simulated results resembled the observed profile more closely. Parameters for each layer were initially based on literature values and altered through a trial and error process in order to obtain the best fit with observed temperatures. The

porosity of the lower layers (8-11) was based on deep moisture content measurements where saturation is assumed to have been reached (see Figure L.1 of Appendix L). The resulting domain is described in Section 4.4.6.1.1.

4.3.2.7.2 Calibrating – Ephemeral Stream Present

During the spring melt, water was ponded at the surface and if infiltration was initiated, advective flow conditions would develop. Although saturated hydraulic conductivity values had been selected previously as part of the soil moisture parameters, values for each layer needed to be further refined because heat transport is much more sensitive to this parameter when advective flow is present. Using all the other previously calibrated moisture retention parameter values, saturated hydraulic conductivity was varied for each layer through trial and error, and the overall best fit to the observed temperature profiles was chosen.

4.3.2.7.3 Sensitivity Analysis of Saturated Hydraulic Conductivity

A sensitivity analysis of the saturated hydraulic conductivity was conducted on the period simulating the spring melt in March. The model output is highly sensitive to this parameter when advective flow is present and the range of reasonable values for a given soil can be quite varied. The soil profile could essentially be divided into two sections: the top three soil layers with lower hydraulic conductivities, and the bottom eight soil layers with higher hydraulic conductivities.

To evaluate the effect of saturated hydraulic conductivity on the temperature profiles, the final calibrated saturated hydraulic conductivity values for all the soil layers within a grouping were varied by factors of 2, 5 and 10 while the values of the other grouping remain unchanged. The values of the entire profile (i.e., all soil layers), were also be varied by factors of 2, 5 and 10. The simulated temperatures were then compared to the observed temperature profile as well as an original unvaried simulation, and the recharge estimates of each variation compared. A final set of moisture retention parameters was selected from the scenario deemed to best simulate the observed temperature profiles. The periods used to calibrate soil parameters when the ephemeral stream is not present were then re-simulated as a check for the final set of moisture retention parameters. These values are compared to field measurements made on the Oxford property by Wendt (2005) and literature values in Table 4.4.4 and Table 4.4.5.

Table 4.3.1 Temperature probe depths.

Probe	Depth of probe tip (m along borehole)	Probe length (m)	Angle from horizontal (degrees)	Actual depth the probe tip (mbgs)
T1	0.15	0.10	62	0.13
T2	0.30	0.10	62	0.26
T3	0.45	0.10	60	0.39
T4	0.60	0.10	63	0.53
T5	1.00	0.10	60	0.87
T6	1.40	0.10	60	1.21
T7	1.80	0.10	60	1.56

mbgs - meters below ground surface

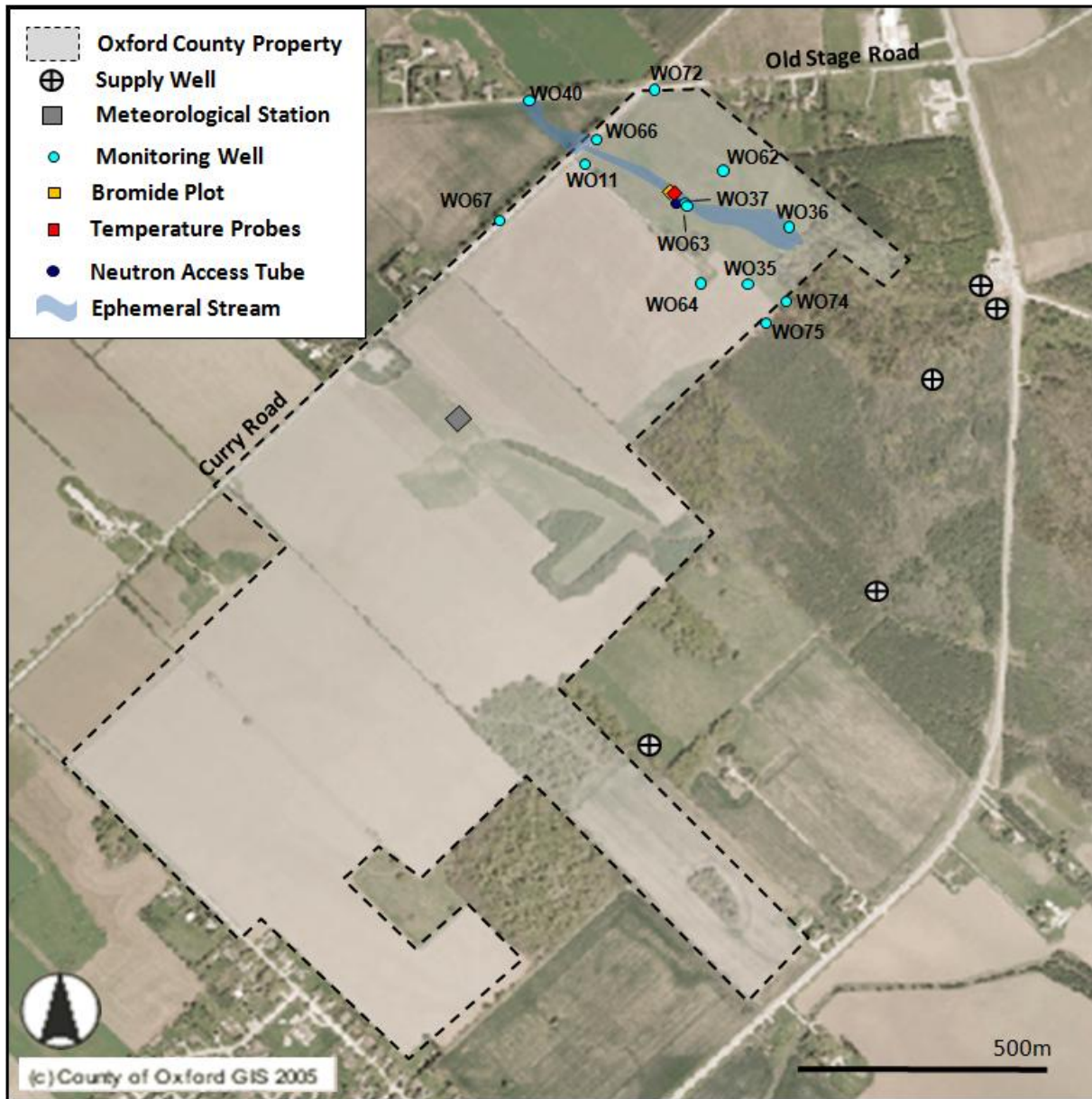
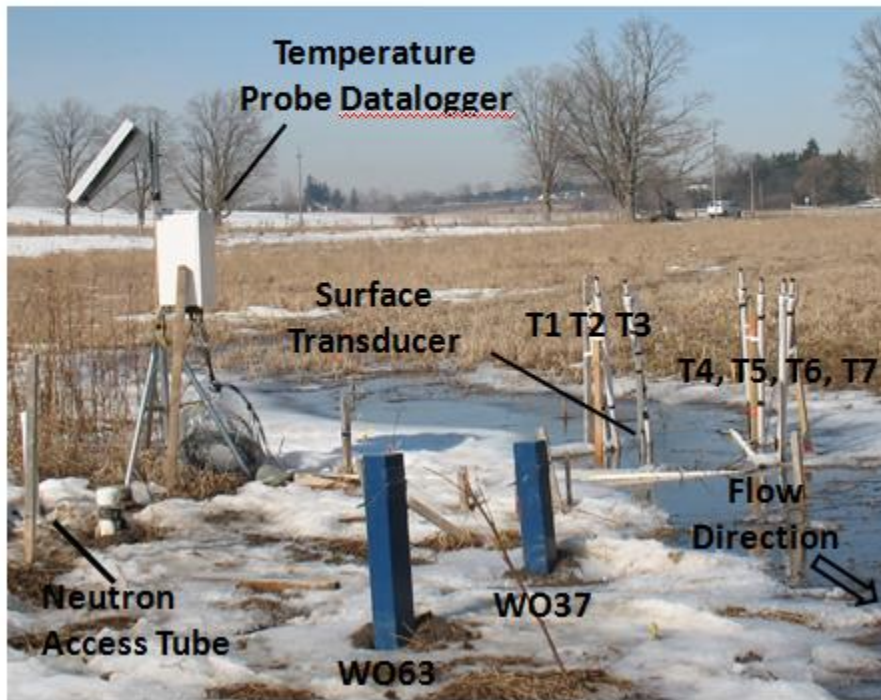


Figure 4.3.1 Map of monitoring wells sampled in the vicinity of the ephemeral stream, meteorological station, location of temperature probes, the bromide plot and neutron access tube.

Field instruments



View from Above

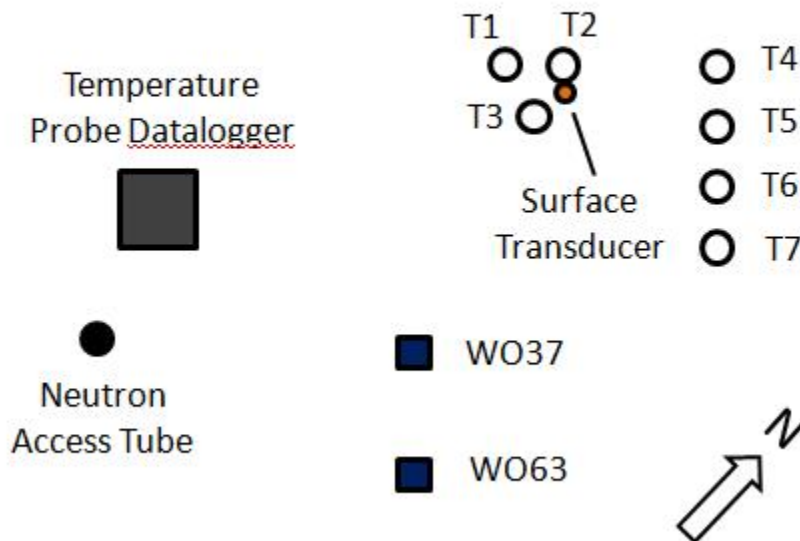


Figure 4.3.2 Field instrument installations in and near the ephemeral stream. WO37 and WO63 are monitoring wells. Soil temperature probes depths are: T1 (13 cm), T2 (26 cm), T3 (39 cm), T4 (53 cm), T5 (87 cm), T6 (121 cm) and T7 (156 cm).

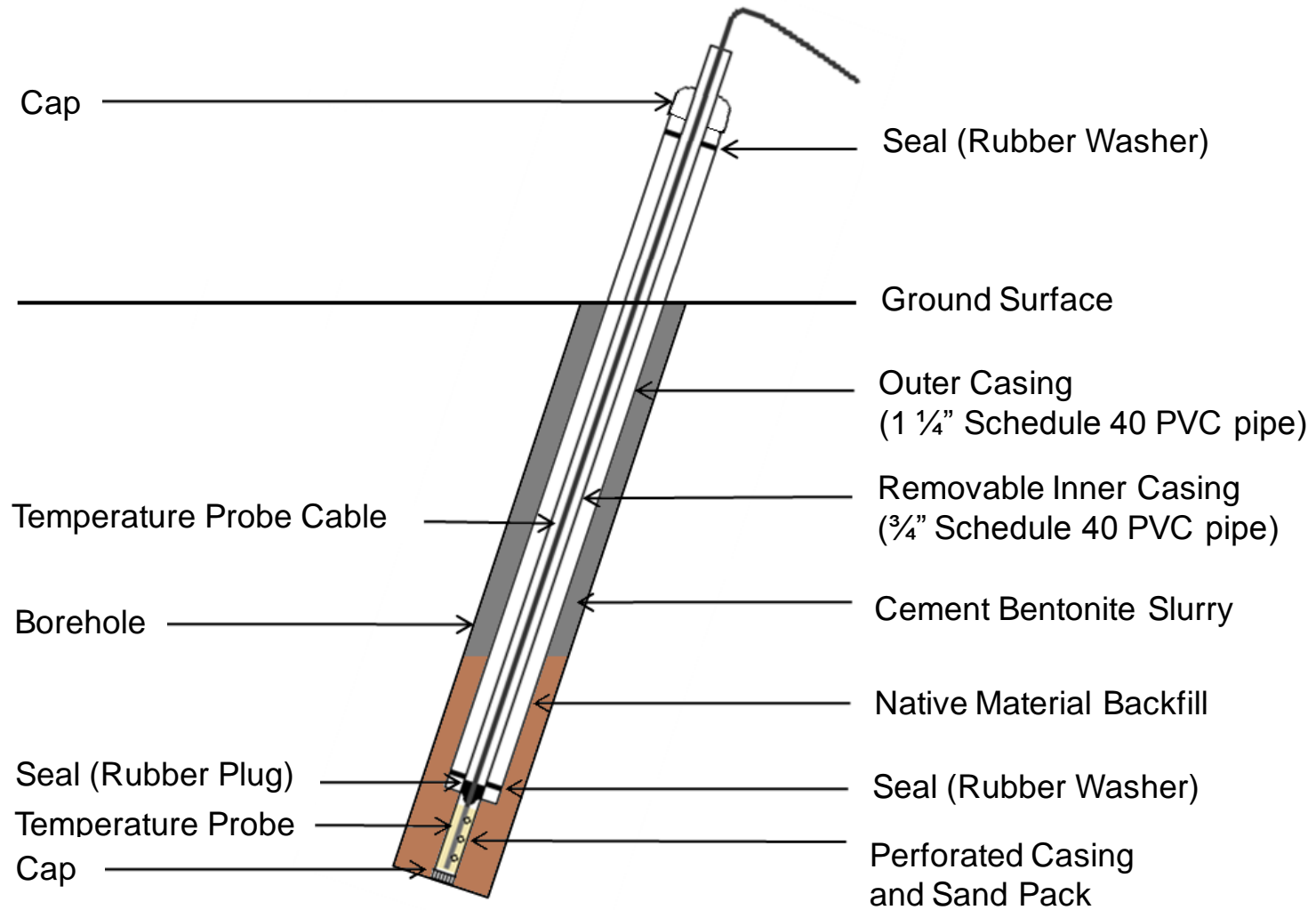


Figure 4.3.3 Schematic of a temperature probe installation showing the protective casing and borehole construction.

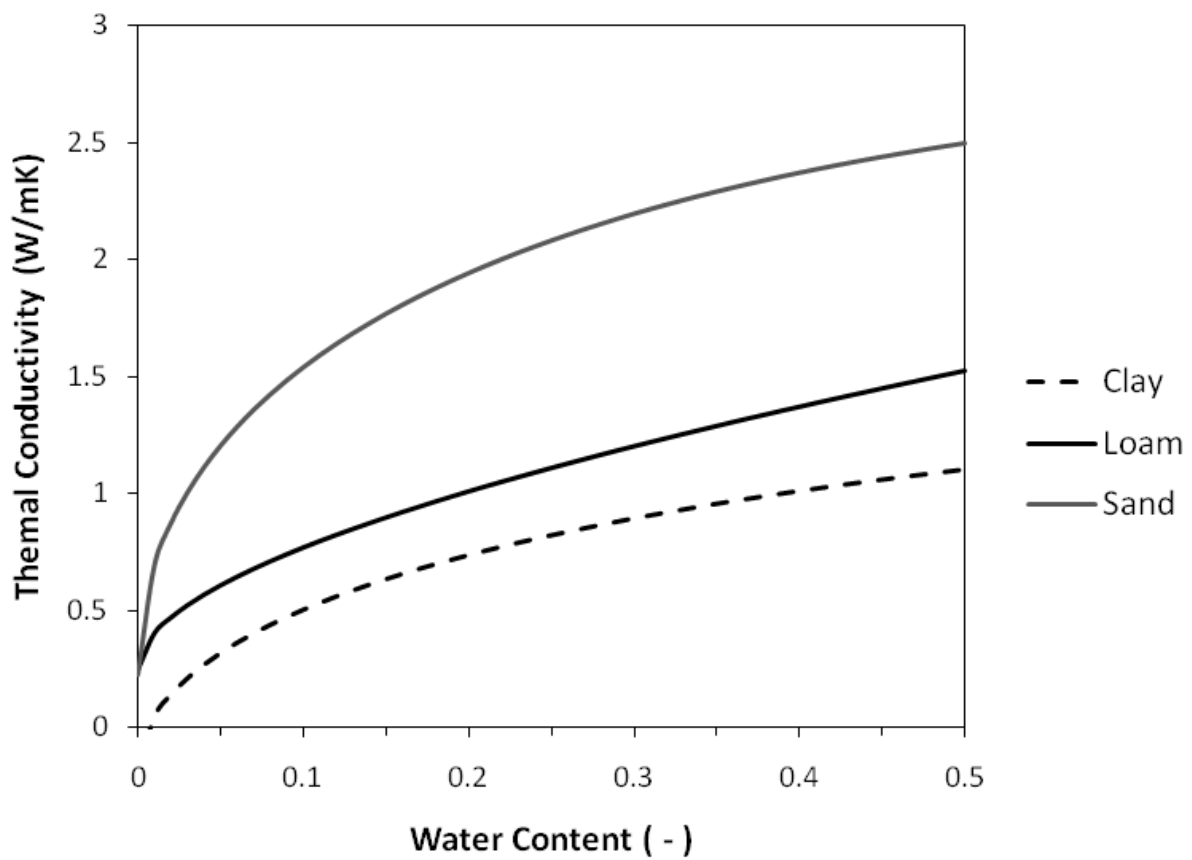


Figure 4.3.4 The Chung and Horton (1987) relationships between thermal conductivity and moisture content for Sand, Loam and Clay.

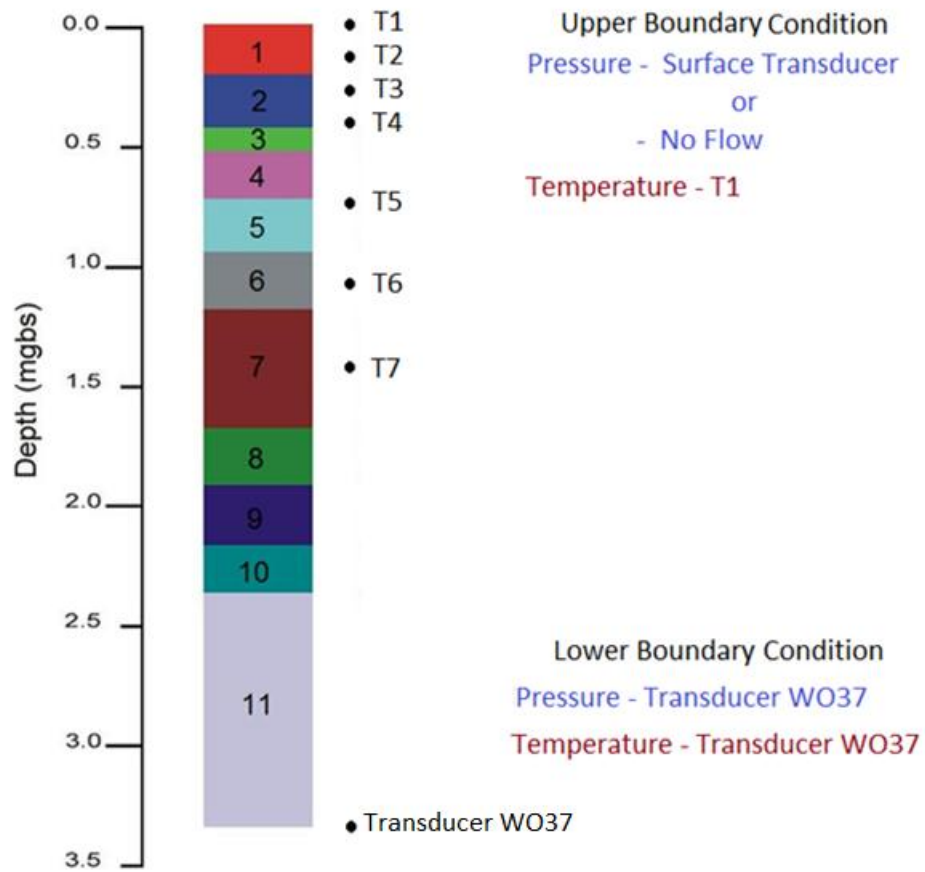


Figure 4.3.5 Visual representation of the pressure and temperature boundary conditions. WO37 is a monitoring well. T1 is a soil temperature probe placed at a depth of 13 cm below the ground surface.

4.4 Results

This section summarizes the results of the field and modeling activities used to estimate recharge beneath an ephemeral stream during the spring melt using subsurface temperature monitoring.

4.4.1 Soil Stratigraphy

A conceptual representation of the soil stratigraphy at the site, as well as the layers used by the model is presented in Figure 4.4.1. The core logs (Station 1_58 and Station 1_64) on which this composite core is based are presented in Appendix H. Even though these cores were taken at various locations in the vicinity of the instrumented site, they are very similar stratigraphically. Three distinct shallow layers were differentiated: the top soil, consisting of a clayey silt, a silty clay layer and an underlying thin layer of more clay-rich sediment denoted as clay in Figure 4.4.1. The bottom layer, forming the remainder of the domain is composed of silty sand and gravel which becomes coarser with depth. This lower layer was subdivided into eight layers within the model domain based on soil moisture distribution and will be discussed in further detail in Section 4.4.6.1.1. The final thicknesses used by the model for each layer were in part determined by soil moisture content profiles in order to better simulate soil moisture conditions.

4.4.2 Moisture Content

Figure 4.4.2 shows moisture content variation with depth during the month of March, 2010. In past years the neutron access tube would probably have been located within the stream; however, in 2010 lower flow resulted in it being located on the banks of the stream. Table L.1 in Appendix L presents values of moisture content with depth. Figure L.1 shows moisture content variations throughout 2009 and 2010. Soil moisture content is higher in the upper layers; high moisture content is maintained in the vicinity of the clay layer, and the water content gradually decreases in the silty gravel layer until the water table is approached. This pattern persists temporally as moisture content values change relatively little throughout the year. As the neutron access tube is not directly in the path of the stream, as noted earlier, measurements of soil moisture content taken during the course of the study do not reflect the influence of the melt event directly under the stream. Moisture content measurements were used specifically to set the initial conditions for the model simulations, and were also used where appropriate to estimate the soil properties through model calibration.

4.4.3 Ephemeral Stream Development

In 2010, the first evidence of the melt event was observed on March 3rd, when a pool of water was observed in a low lying area near the instrumented field in the mid afternoon. Ponded water was then observed every day over the temperature sensors from March 5th to March 10th. Typically there would be

a relatively thick layer of ice over the surface of the stream early in the morning, which would melt by mid afternoon exposing the ground and vegetation on the stream bottom. The stream flowed in a northwest to southeast direction; it passed through culverts under Old Stage Road near WO40, and at Curry Road near W011 and then flowed past the monitoring location and toward the Thornton well field (Figure 4.3.1). The stream passed over three monitoring wells, these are WO40, located at the side of Old Stage Road, as well as WO37 and WO63, which are both located near the subsurface temperature probes. WO40 is located at the terminus of a tile drain. As a result, when the tile is flowing, a large volume of water accumulated at the surface near WO40. Pictures of the ephemeral stream and melt water in the vicinity of the field site presented in Figure 4.4.3. Compared to previous years, the width and volume of water transported by the stream in 2010 seems to have been much less (see Figure 4.4.4). Pondered water was last observed at the field site on March 10th; however, the surface transducer indicates that water was also temporarily ponded over the field instruments on March 14th (Figure 4.4.16).

4.4.4 Monitoring Wells and Groundwater Sampling

4.4.4.1 Regional Hydraulic Head Fluctuations

The hydraulic heads observed during the month of March vary from well to well. Table J.1 in Appendix J indicates the aquifer in which each well is screened. The wells that are screened in Aquifer 2 and are equipped with a transducer are: WO35, WO36, WO37, WO66, WO74-S, WO75-S. The change in head over time recorded in each well relative to midnight on March 1st is presented in Figure 4.4.5. This figure shows that some wells record larger and faster changes in head, such as WO40 and WO11-18. A spatial correlation exists between the range of hydraulic head measured in individual monitoring wells during the month of March and the northing Universal Transverse Mercator (UTM) coordinate of each well. Figure 4.4.6 shows that monitoring wells further south, have a smaller range of hydraulic head, than those located further north. In particular WO40 and WO11-18 have much larger ranges in hydraulic head relative to other wells in the same vicinity. The monitoring well WO40 is the most northerly located, as mentioned previously (Section 4.4.3) it is located at the terminus of a tile drain. The change in hydraulic head recorded at this well over the month of March in response to the beginning of the spring melt was much larger (~1.1 m of head change) than at every other well monitored (~0.7 m of head change; the next largest). This is likely due to the presence of the tile drain which results in large amounts of ponded water over this well. In this case, the trend correlating higher changes in hydraulic head to wells located in the northern portion of the site could be a result of their proximity to the influence of the infiltration effects associated with the ponded water originating from the tile discharge near WO40.

Fluctuations in hydraulic head were plotted spatially in a series of maps during the month of March, 2010 (Figure 4.4.7). Change in each well is relative to the head at midnight on March 1st, 2010. These

maps incorporate all wells in which there is a transducer, regardless of screened depth and as such is regional in nature. The maps presented in Figure 4.4.7 show that changes in hydraulic head are first recorded at WO40, and that these are greatest in wells screened in Aquifer 3 in close proximity to WO40; even wells that are relatively far from the stream and located on topographical highs (e.g., WO72-M and WO72-D) record large changes in hydraulic head.

The largest change in hydraulic head (~ 0.7 m) occurs at WO40 between March 13th and March 14th, 2010 when the ephemeral stream is present. (see Figure 4.4.8). Delayed changes in hydraulic head exhibiting a similar shape, but smaller magnitude, are observed in many of the deep wells screened in the Aquifer 3 nearby (i.e., WO11-18, WO72S, WO72D). At the nested well site located near the culvert under Curry Road, WO11, an earlier and larger change in hydraulic head (~ 0.3 m) was observed in the deeper well, WO11-18, than in the shallower well, WO11-13 (~ 0.2 m). As in the case of other deep wells around it, the change in hydraulic head at WO11-18 seems to be a response to a large hydraulic head perturbation trending to the north of the field site as discussed above. These results suggest that it is likely that recharge associated with the spring melt in the vicinity of WO40 is substantial compared to other location, resulting in changes in hydraulic head being observed in deep wells down gradient.

4.4.4.2 Regional Groundwater Temperature Fluctuations

Change in groundwater temperature is a stronger indication of localized recharge than changes in head, because perturbations in this parameter are not dispersed as quickly as changes in hydraulic head from the area that was initially perturbed. As in the case of hydraulic head fluctuations, temperature fluctuations also vary from well to well across the field site. The change in temperature over time recorded in each well relative to midnight on March 1st is presented in Figure 4.4.8⁴. The three wells that exhibit the largest changes in temperature (ranging between 1 to 6.5°C) over the month of March are WO37, WO40 and WO63. A spatial correlation exists between the range of temperature in individual monitoring wells during the month of March and the ground elevation of each well casing. Figure 4.4.9 presents the range of temperatures versus the ground elevation at the casing for each well except WO40, which had a very large range (~ 6 °C) and is not shown. This figure shows that temperature variation is greater in monitoring wells at lower elevations; areas where the depth to the water table is generally the smallest. This suggests that colder water originating at ground surface is being rapidly infiltrated to the water table in the low lying areas.

⁴ Note that temperature variations recorded in each well are representative of the depth at which the level datalogger is placed and not the screen interval of the well.

As was done with regional hydraulic head data, the spatial variation in groundwater temperature relative the midnight on March 1st, 2010 was plotted in a series of maps shown in Figure 4.4.10. WO40 and WO37 were not included because the temperature fluctuations in these wells differ greatly from the wells around them, and when they were included the maps were not comprehensible. These maps show that temperature changes in wells near and in the path of the ephemeral stream are greater than at locations further away from the stream. Figure 4.4.11 presents a map of the actual groundwater temperature at midnight on March 15th, 2010, and shows that groundwater temperatures recorded in monitoring well are colder in the vicinity of the stream.

The largest change in temperature occurs at WO40, and is initiated on March 13th, 2010. As discussed in the previous section, this change occurs at the same time as a large perturbation in hydraulic head recorded at WO40. Concurrent changes in hydraulic head and temperature suggest that recharge is occurring locally at this well. Many wells screened in Aquifer 3 down gradient of WO40 had exhibited delayed changes in hydraulic head of a similar shape but smaller magnitude (i.e., WO11-18, WO72S, WO72D). However, these wells do not also have notable coinciding changes in temperature, indicating that these wells were likely responding to perturbation in head that is not local to these wells.

4.4.4.3 Groundwater Geochemistry

The wells in which there was a noticeable decrease in nitrate and chloride concentration following the spring melt are: WO11-6, WO36, WO37, WO40, WO63, WO66, and WO74S. Note that WO11-6, WO37 and WO63 also show a steep decrease in nitrate and chloride concentration in January. This is most likely in response to an earlier melt event in January that has not been discussed. The locations of these wells are presented in Figure 4.3.1. Figure 4.4.12 presents the results of monthly monitoring for these wells over the course of the monitoring period between November 2009 and June of 2010. Graphical presentations of the concentrations in the remaining wells and the entire geochemical data set are presented in Appendix K. Each of the wells where significant fluctuations in nitrate and chloride were observed is located in topographic lows. As in the case of groundwater temperature, changes in geochemistry are potential indicators of localized groundwater recharge. Notable changes in ionic concentration were generally only observed in wells near the ephemeral stream which are screened in Aquifer 2 or in section of Aquifer 3 where the two aquifer units appear to be in direct hydraulic connection. These observations, as well as previous observations concerning changes in hydraulic head and groundwater temperature, provide evidence to suggest that rapid, yet episodic groundwater infiltration may be occurring in and around the path of the ephemeral stream.

4.4.4.4 Well WO37

Figure 4.4.13 presents the long term hydraulic head and temperatures between the spring of 2005 and the fall of 2010 in well WO37. The well casing was repaired on January 16th, 2010 and is indicated on the figure by a vertical grey line. Prior to this repair, melt events recorded at this well in the late winter and early spring in 2006 to 2009 demonstrated sharp and notable responses in hydraulic head and temperature in response to melt events (Haslauer, 2005; Koch, 2009). During the late winter spring melt of 2010, such variable responses were not observed, indicating that the fast responses previously observed at this well were most likely an artifact of the well's condition.

Figure 4.4.14 shows the hydraulic head and temperature changes for WO37 during the month of March in 2010. The temperature in WO37 decreases gradually except for brief periods of time where there are fast drops in temperature. These steep declines in temperature coincide with steep increases in hydraulic head at WO37, and are highlighted in yellow on Figure 4.4.14. The first drop occurs between March 9th and 10th, and the second between March 14th and 15th. These variations in temperature and hydraulic head coincide with the period of time during which ponded water was observed at the surface over the instrumented site. The rapid response at WO37 to surface water at the site, especially the temperature response, indicates that rapid groundwater recharge is occurring locally at the instrumented site.

4.4.4.5 Soil Temperature

Figure 4.4.15 shows the air temperature, soil temperature and groundwater temperature fluctuations between January and December of 2010 at the instrumented (for relative locations see Figure 4.3.1 and Figure 4.3.2). Temperature variations in the short-term (daily and weekly) are dampened with depth; however, some longer term trends associated with the changing seasons are preserved at depth. By examining the curves from January to early March, it is evident that during the winter months frozen soil and snow cover insulate the subsurface from temperature fluctuations in the air. During this time period, temperatures in the upper 40 cm are close to or below the freezing point. At progressively greater depths, subsurface temperatures increase significantly and approach the groundwater temperature in the deepest of the soil temperature probes (Figure 4.4.15). The annual trends in subsurface temperature follow the air temperature trends remarkably well after the onset of the spring melt in March. The overall magnitude of the annual temperature variation tends to decrease slightly with depth (15°C at 13 cm and 8°C in the groundwater) and there is a notable time lag in reaching the peak temperature that increases with depth.

As stated in Section 4.3.1.7, a transducer which recorded water level and temperature was installed at the ground surface on March 6th, for relative location see Figure 4.3.2. Figure 4.4.16 presents air temperature, soil probe temperature, surface water level, surface water temperature, depth to the water

table in WO37, and groundwater temperature from March 1st to March 22nd, 2010. Standing water was observed at the instrumented field site from March 5th to March 10th. Surface water ponding was also recorded between March 14th and 15th by the surface transducer.

Because the surface transducer is positioned at the ground's surface, there are occasions when it emerges as the surface water drains, and during these times temperature spikes are noted as it is exposed to sunlight, which warms it. Note that at night the temperature recorded by the surface transducer is not the same as the air temperature; in the evening the stream froze and the recorded temperature is reflective of that. The stream would slowly thaw everyday as the air temperature increased. Between March 5th and March 10th, the two probes closest to the surface, T1 and T2, record temperatures near or below freezing, which are similar to the temperature of the surface water in the ephemeral stream when the spikes in temperature are excluded. As there is no significant contrast in temperature between the surface water and the shallow subsurface, data from these shallow probes does not provide evidence of infiltrating surface water based on temperature alone. During this period most of the other probes record very little variation in temperature; however there are exceptions. The temperature record from the T4 probe located at a depth of 53 cm contains a series of fluctuations that are not recorded by the probes above and below this depth between March 5th and March 9th. The temperature record at T3 (39 cm) shows a small dip in temperature on March 3rd, and another small decline on March 6th concurrent with the first fluctuation at T4. Other than these two anomalies, the temperature record at T3 is aligned with those from temperature probes above and below it. However, the record at T4 during the spring melt is not. These anomalies are possibly the result of water traveling through preferential pathways. This may be due to leakages of surface water along the inclined probe casing as a result of poor backfilling around the casing, or may reflect the influence of macropore flow. It is also interesting to note that the T4 data set indicates a much more rapid increase in temperature with time as the ground begins to warm up. This may be an indication that the sensor is exposed to variations in the air temperature permitting it to warm up faster. Due to this uncertainty, data from the T4 probe will not be considered further.

As surface water ponding begins to decrease, the ground water table starts to rise. This increase begins on March 9th and peaks on March 18th. During this period the water table increases by 27 cm and groundwater temperature decreases by one degree Celsius, indicating that cold water is recharging the aquifer. In early March, the lowest soil temperatures are recorded at the surface and the highest temperatures are recorded at depth. The surface (T1) begins to warm starting March 12th, and as the soil thaws, daily variations in temperature are observed and the soil profile inverts; now the highest temperatures are recorded near the surface and the lowest temperature are recorded at depth.

Prior to the surface warming on March 12th, decreases in temperature are observed at depth, most notably in T5, T6, T7, starting on March 9th which occur concurrently with the rise in the water table and the drop in the groundwater temperature discussed Section 4.4.4.4. The coincidence of these occurrences suggests that cold water is recharging the aquifer at this location from the surface downward. When cold water infiltrates at the surface, no change in temperature is observed in the surface probes because the water infiltrating has a similar temperature signature to the surrounding porous medium (e.g., frozen soil) at the surface; however, in the warmer subsurface, a temperature drop is observed as the cold water comes into contact with the warmer porous medium. A similar, albeit smaller scale temperature oscillation was observed at T6, T7, and at the groundwater transducer between March 14th and March 15th, which occurs concurrently with a brief period of standing water at the surface (Figure 4.4.16).

4.4.5 Recharge Estimate Using Bromide Tracer

The bromide solute tracer was applied to the ground surface along the anticipated path of the ephemeral stream in December 2009 near the instrumented site (Figure 4.3.2). Figure 4.4.17 and Figure 4.4.18 show the soil bromide concentration and volumetric water content profiles on March 5th, 2010 and May 6th, 2010. In March high concentrations of the bromide tracer are present in the soil with a well defined peak concentration of 4793.80 mg Br/kg soil at 0.19 m below the ground surface and the centre of mass at 0.23 m below the ground surface. The total percent mass recovery in the core recovered in March is 285%, as this is an unrealistic recovery assuming that the bromide tracer was spread out evenly over the area of application, a plausible explanation for this is that the application of the tracer must not have been evenly applied or that it pooled in some areas after application. It is also possible that there was a mistake in the preparation of the concentration of the applied tracer solution. Despite such a high recovery in March, in May only very low concentrations of bromide tracer are observed in the soil, suggesting that much of the tracer has been washed away. The total recovered mass at this time was 3%, which is very similar to the recovered bromide mass by others at this site after the melt events (Bekeris, 2007; Koch, 2009). The highest measured concentration of bromide occurs near the ground surface, as so much of the tracer mass was lost, this is interpreted to be a spurious data point as it is likely that more infiltration occurred than would be suggested by using this point to calculate recharge. Because of this, this point was not used in the interpretation of the recharge phenomena. Below this point, the next highest peak was located at 2.30 m below the ground surface.

For the sake of this analysis, different estimates for recharge are developed as described below. Table 4.4.1 presents values of recharge rates and total recharge between March 5th and May 6th, 2010, using centre of mass depth with the average, maximum and minimum volumetric water contents measured by the neutron probe, and maximum and minimum volumetric water contents from the soil cores. The range

of the recharge estimates is 0.08 to 0.19 m. Because most of the mass present in March is not present in May, the depth of the centre of mass calculated may not be representative of the true centre of mass; it is possible in this case that the depth of the peak concentration of bromide may be more representative of recharge at the site. Table 4.4.1 also shows total recharge values between March 5th and May 6th, 2010 using the depth of the peak concentration. The range of recharge estimates using this method is much higher than the range using the centre of mass (0.33 to 1.17 m). Although the tracer profiles are problematic to interpret, these ranges of recharge values will be used to compare to the results of the numerical analysis.

4.4.6 Modeling Results

A one-dimensional model as employed to simulate water and heat transport through the vadose zone of the instrumented site, in order to further quantify the groundwater recharge processes beneath the ephemeral stream. An extensive set of physical and thermal properties are required to define the subsurface, as presented earlier in Section 4.3.2, in order to represent the variably saturated porous medium. Little site specific information is available regarding the magnitude of these parameters; therefore, values representative of the sediment types encountered at the site were derived from literature sources and from those provided from the Hydrus 1-D software. In order to evaluate how representative these selected parameters were and to provide an approach to modify them to better fit the actual field conditions, a two-stage calibration process was adopted. This process is described in Section 4.3.2.7.

This section presents the results of model calibration to data collected in the early summer and early fall (gravity drained conditions), and the results of the model calibration to data collected during the spring melt (ephemeral stream present). Graphs of the inputs of the initial and variable conditions for each simulation are presented in Appendix T to Appendix V. Time and iteration criteria are presented in Appendix W. The iteration criteria selected were the suggested values from the Hydrus 1-D help function, except for the water content tolerance, which was increased slightly in order for the most computationally intensive simulations to converge.

4.4.6.1 Model Calibration – Gravity Drained Soil Conditions

The period between April 12th and May 31st, 2010 was used to develop calibrated model parameters (see Section 4.3.2.7.1). In order to test whether acceptable model results could be produced during periods other than the one used to calibrate the model, the period between to August 24th and October 31st, 2010 was simulated using the same derived parameter set and the model domain. This period was selected as antecedent moisture conditions could be estimated from a concurrent neutron probe data from the site. Simulated results that closely matched observed temperature and moisture conditions for more than one

period of time are thought to indicate that the parameters selected are satisfactory for gravity drained soil conditions where it was anticipated that there was negligible flow in the unsaturated zone. As described in Section 4.4.2, the observed moisture content profile showed little variation during the course of the monitoring period. For the first stage of calibration, initial moisture content values were assigned to be equivalent to the soil moisture values measured by the neutron probe either April 12th or August 24th for the respective depths in the profile. Initial temperature values were assigned to be equivalent to the temperature profile values measured at midnight by the temperature probes and the transducer in WO37 at the beginning of the simulation for the respective depths. The boundary condition for flow was a constant flux boundary equal to zero at the surface and the variable head boundary equal the head variation in WO37 at the bottom. Temperature boundary conditions were equal to the transient temperature measurements at T1 at the surface and to measurements at WO37 at the bottom. The model was then run forward in time.

4.4.6.1.1 Hydraulic Parameters

Hydraulic properties of the different soil layers present at the site were chosen from a selection of different soil textures provided by the HYDRUS-1D model. These properties were then adjusted in order to fit simulated to observed moisture content profiles from the neutron probe; that is, properties were chosen to maximize the concurrence between the simulated and measured moisture content with depth over long simulation periods. As it became clear that it would be difficult to maintain the moisture content profile in the lower layer due to the gradation of texture with depth, the domain was separated into 11 layers with distinct properties. Moisture content profiles for domains where the lower layer is treated as one homogeneous layer are presented in Appendix L. The top three layers represent the topsoil and two shallow clay and silt units discussed in Section 4.4.1, the lower eight represent gradations of the lower silty sand and gravel layer as it become increasingly coarser with depth (see Figure 4.4.1). This layering approach was selected as it allowed for a better fit of the simulated moisture content profile to the gradual change in moisture content of the observed profile. A previous study completed very close to the current monitoring site (~100 m to the south) also subdivided the shallow aquifer into several layers in order to better describe variable groundwater velocities with depth as opposed to assuming that the substrate was homogeneous (Critchley, 2010).

Figure 4.4.19 presents the simulated soil moisture curves every 5 days of simulation between midnight on April 12th and midnight on June 1st, 2010. As the moisture content profile closely resembles the measured soil moisture profile throughout the course of the simulation, the hydraulic parameters selected appear to represent the field soil conditions. The hydraulic parameters selected for calibrating unsaturated soil conditions are presented in Table N.1 of Appendix N. Figure 4.4.20 presents the simulated soil

moisture curves every 5 days of simulation between midnight on August 24th and midnight on October 31st, 2010. Under this second set of field conditions, the simulated soil moisture profile again matches the field data well. Based on these results, the final set of calibrated hydraulic parameters (Table N.1) was then adopted as the initial parametric values for the transient simulations during the spring melt event. Note that the simulated moisture content profiles are not as smooth as those collected by the neutron probe; there are sudden increases in water content at the boundary of different soil layers. This is presumably due the simulation of changes in capillarity between the different soils, as coarser soils lay beneath finer soils the model seems to be simulating capillary breaks between layers. It is likely that in field conditions the changes in parameters would be more gradual. Even so, such distinct changes in moisture content are difficult to detect with the neutron probe approach to measuring soil moisture content because of the depth averaging that is intrinsic to the method.

4.4.6.1.2 Heat Parameters

Because both volumetric heat capacity and thermal conductivity are estimated by the model based on the moisture content, calibration for moisture content is important for the calibration of heat transport in variably saturated soil. Once the hydraulic parameters are fixed, it is important to calibrate the model for heat parameters. As discussed in Section 4.3.2.3 volumetric heat capacity is a function of the volumetric fraction of the solid phase (soil), liquid phase (moisture content), and air phase, as such it is calculated based on the porosity of the soil and the moisture content. Thermal conductivity is calculated using empirical parameters developed by Chung and Horton (1987), which relates thermal conductivity to moisture content for three textural classes: sand, loam and clay soils. The relationships between moisture content and thermal conductivity are presented in Figure 4.3.4. The textural class selected for layer 1 was sand, loam was selected for layer 2, clay was selected for layer 3 and sand was selected for layers 5 to 11. The values used for these different soil types are shown in Table N.2 of Appendix N. These were selected in order to simulate the best fit between observed and modeled temperatures.

Figure 4.4.21 presents the fit of the simulated temperatures to observed temperatures for the period between April 12th and May 31st, 2010. Note that the depth with the simulation domain that most closely matched with the data from T3 (39 cm) temperature sensor was actually 5 cm lower than the anticipated depth of the monitoring device. Based on the goodness of model fit at each of the other monitoring depths, it was assumed that the probe depth was incorrectly measured in the field and the T3 data were assumed to be representative of a simulation depth of 44 cm, as indicated in Figure 4.4.21. This represented a minor adjustment overall. Figure 4.4.22 presents the fit of the simulated temperatures to the observed temperatures for the period between August 24th and October 31st, 2010. The simulated temperatures in both Figure 4.4.21 and Figure 4.4.22 fit the observed temperatures slightly better at

shallow depths, and diverge somewhat from the observed temperatures at deeper depths. One explanation could be that estimation errors become greater with depth as deeper simulated temperatures depend on those above them. All things considered, the model fits the observed data well in both periods simulated.

4.4.6.2 Model Calibration – Ephemeral Stream Present

As discussed in Section 4.3.2.7.2, heat transport is much more sensitive to saturated hydraulic conductivity values for each layer when advective flow is present. As such, it may require some modification from the initial values of this parameter derived from the gravity drained soil scenarios during the first stage of calibration.

The only difference in the simulation of heat transport when the ephemeral stream is present compared to gravity drained soil conditions is the transient surface flow boundary condition. Two different surface flow boundary conditions were tested. The first (scenario 1) uses a hydraulic head equivalent to the water column measured at the surface when ponded water is present, and the second (scenario 2) uses a hydraulic head equivalent to the water column measured at the surface plus an additional 13 cm, which is meant to represent the soil between the point of measurement of the head at the surface and the temperature 13 cm below the surface assuming saturated and hydrostatic conditions. For both scenarios, a no flow boundary is prescribed when no ponded water is present. Although true conditions likely reside between these two extremes, this comparison was done in order to evaluate the effect of not having temperature and hydraulic head measured at the same point.

Although ponded water over the instrumented site was first observed on March 5th, a starting date of March 9th was used for the simulation because at this time the near surface top soil has thawed enough to allow the passage of water, as indicated by the abrupt changes in temperature at depth on this day, most notably at sensors T5, T6 and T7. The initial moisture conditions used were those recorded by the neutron probe on March 3rd, as it assumed very little infiltration had occurred prior to the soil thawing. Simulations using earlier starting dates had been attempted; these did not provide a good fit to the observed data prior to March 9th. This is most likely because the heat conduction and the hydraulic parameters of the soil are different than the previously calibrated model due to the presence of ice in the soil. The results of a simulation starting on March 3rd using the parameters from the calibration for gravity drained soils are presented in Appendix O.

Hydraulic conductivity was altered in an iterative way in order to obtain the best fit for both scenarios, and only one set of final parameters was developed. The hydraulic and heat parameters used for the final calibration of the model are presented in Table 4.4.2. The result of the best fit of simulated temperatures

by the model to observed temperatures between March 9th and 22nd for scenarios 1 and 2 are presented in Figure 4.4.23 and Figure 4.4.24 respectively. The fit of the simulated temperatures for both scenarios are similar, the most noticeable difference between the two simulations can be observed at T5 and T6 where the temperature profiles drop slightly more with depth in scenario 2 than scenario 1, which results in a better fit of T6 and a worse fit of T5⁵. Nevertheless, both simulations fit the observed temperatures quite well; however, neither fits the observed data as well as the simulations developed for periods when no flow conditions prevail.

Cumulative recharge during the period of simulation was 0.13 m for scenario 1 and 0.15 m for scenario 2. Even though there was a head difference at the surface of the simulation of 0.13 m between scenario 1 and 2 during periods of flowing water, the difference in cumulative recharge is small. The difference between these two scenarios, with regard to both the fit and the resulting recharge estimations, was not very large, indicating that although the first temperature probe was placed 0.13 m below the ground surface, the effect of the 0.13 m of soil between the two sensors is not very large. The cumulative recharge overtime for scenarios 1 and 2, as well as the specified height of the water column at the surface are presented in Figure 4.4.25. The two scenarios were further compared below as part of the sensitivity analysis of saturated hydraulic conductivity.

4.4.6.3 Sensitivity Analysis of Saturated Hydraulic Conductivity

As an additional evaluation of the role of saturated hydraulic conductivity, a sensitivity analysis was conducted on this parameter. The hydraulic conductivity values obtained from calibration are presented in Table P.1 of Appendix P. As part of the sensitivity analysis, the hydraulic conductivity of the top three layers, the bottom eight layers and the whole profile were increased and decreased by factors of two, five and ten independently. This was conducted to assess the effect of hydraulic conductivity on the cumulative recharge estimation and the overall fit of simulated temperatures to observed temperatures. The assessment was done for both scenario 1 and scenario 2 simulations, which are surface boundary condition scenarios (see Section 4.3.2.5). The sensitivity analysis was also used to make a final assessment of the best fit scenario and refine the final saturate hydraulic conductivity values.

Appendix Q presents the simulated temperatures at each temperature probe resulting from the sensitivity analysis. Figure 4.4.26 presents the sensitivity analysis at T6 (121 cm below the ground surface) for scenario 2 where the hydraulic conductivity of the bottom eight layers of soil were increased

⁵ Note that there is a small fluctuation the simulated temperature at the start of the simulation a T5, this seems to be due to numerical error.

by a factor of two. It is presented as an example to illustrate the range of simulated temperatures resulting from varying the hydraulic conductivity.

In examining the results from the sensitivity analysis, some overall trends are apparent. Decreasing the hydraulic conductivity of soil layers dampened the magnitude of the temperature pulse at points of observation below the changed soil layer. This resulted in higher temperature than the original simulation. Increasing the hydraulic conductivity had the reverse effect; decreasing the simulated temperature compared to the original simulation. Adjustments made in the top three layers resulted in much larger changes to simulated temperatures profiles than did changes in the bottom eight layers. The influence of changing the saturated hydraulic conductivity of the whole soil profile was very similar to those made to the top three soil layers. This indicates that the top three layers, which have lower hydraulic conductivities, have more of an effect on advection compared to the lower layers with higher hydraulic conductivities.

The proportional change in saturated hydraulic conductivity is plotted against the simulated cumulative recharge in Figure 4.4.27. Although changes to the hydraulic conductivity in the bottom eight layers resulted in a very different simulated temperature profiles, the estimated recharge values changed very little when the hydraulic conductivity in these layers were changed. This is not the case for the top three layers where changes in hydraulic conductivity result in both changes to the simulated temperature profile and the estimated recharge. Surficial soils in this case have more control over the total recharge estimated by the model; however, changes to hydraulic conductivity in the lower soils impact the fit of the simulated temperatures to the observed temperature. Therefore, a better fit obtained by varying the hydraulic conductivity in the lower eight layers will have little effect of the total recharge estimate.

The results of the sensitivity analysis suggested that improvements of the fit of simulated temperatures to the field observations could be made through modification of the assigned values for saturated hydraulic conductivity. Based on cumulative modeling results, improvements in the model fit were achieved through minor increases in saturated hydraulic conductivity, specifically, increases in hydraulic conductivity by a factor of 2. The greatest improvements were made in the lower three temperature probes: T5, T6, T7. In general, good fits obtained at T5 and T6 resulted in a poor fit at T7, and good fits at T6 and T7 resulted in a poor fit at T5.

Table 4.4.3 presents the recharge estimate results of the sensitivity analysis. The simulations which provided a similar or improved fit to the observed temperatures profile over the original simulations are

indicated. Simulations where the hydraulic conductivity was altered in the top three soil layers as well as all the soil layers simultaneously, did not improve the overall fit to the observed temperatures. Although, for both scenario 1 and 2, increasing the hydraulic conductivity in these layers by a factor of two did improve the fit to the observed data compared to the original simulation using parameters obtained from the calibration process. Improvements to the fit of the simulated temperatures at T6 and T7 were noted when the hydraulic conductivity was increased by a factor of two in the bottom eight layers.

To assess which set of parameters best represents the field soils, the set moisture retention parameters resulting from the calibration process and the set resulting from increasing the hydraulic conductivity of the latter in the lower eight layers were used to re-simulate temperature and water content profiles for the periods between April 12th to May 31st, 2010 and August 24th to October 31st, 2010. Appendix R presents the simulated temperature profiles, and Appendix S shows the simulated moisture content profiles.

Temperature profiles for the period between August 24th and October 31st, 2010 using these two sets of parameters can be compared in Figure 4.4.28 and Figure 4.4.29. The simulated temperatures match the observed temperatures much better using the set of parameters derived from calibration. This is also the case for the period between April 12th to May 31st, 2010 (Figure R.1 and Figure R.2). Although some improvements were obtained by increasing the hydraulic conductivity in the lower eight layers when the ephemeral stream was present, the set of parameters produced from the calibration process was deemed to best represent field soils as simulated temperatures more closely resembled the observed temperatures in gravity drained soils. This set of parameters was selected as the final set of parameters (Table 4.4.2). The simulated temperature and moisture profiles presented in Appendix R and Appendix S closely resemble those presented in Figure 4.4.19 to Figure 4.4.22. The model is able to simulate different periods of time and different flow scenarios using the final set of parameters, suggesting that the conceptual model and final model domain are representative of the actual field conditions. The successful simulation of the field data sets under the different flow scenarios also increases confidence in the uniqueness of the model results.

As noted in the previous section, the difference in total recharge was small. The difference between the two scenarios was only notable when the hydraulic conductivity of surficial soils was increased substantially. Although imperfect, the scenario 2 simulations were deemed to better represent the field soil conditions as they took into account the 13 cm of soil between the surface and the first point of temperature measurement. The cumulative recharge estimate for scenario 2 using the parameters obtained from calibration was selected as the best fit scenario for the period between March 9th and March 22nd, 2010, which had a cumulative recharge estimate of 0.15 m. The final soil moisture retention values are

compared to field measurements made on the Oxford property by Wendt (2005) and literature values in Table 4.4.4 and Table 4.4.5, which compare values for silt and clay soils, and silty gravel and sand soils respectively. The final selected values are quite similar to the values from other sources.

Table 4.4.1 Recharge rate and total recharge estimations for the period between March 3rd and May 6th, 2010.
Estimations made using volumetric water contents measured with the neutron probe and measured from soil cores, and the depth to (a) the centre of mass on each soil core (0.23 m in March and 0.57 in May) (b) the peak concentration of each core (0.19 m in March and 2.3 m in May).

	Volumetric water content				
	Neutron Probe			Soil Core	
	Average	Maximum	Minimum	Maximum	Minimum
Water Content	0.322	0.360	0.237	0.55	0.15
Recharge Rate (m/day)	1.767E-03	1.972E-03	1.300E-03	3.034E-03	8.376E-04
Total Recharge (m)	0.11	0.12	0.08	0.19	0.05

(a)

	Volumetric water content				
	Neutron Probe			Soil Core	
	Average	Maximum	Minimum	Maximum	Minimum
Water Content	0.23	0.36	0.16	0.55	0.22
Recharge Rate (m/day)	7.667E-03	1.185E-02	5.174E-03	1.824E-02	7.127E-03
Total Recharge (m)	0.49	0.76	0.33	1.17	0.46

(b)

Table 4.4.2 Final moisture retention parameters.

θ_r residual soil water content; θ_s saturated soil water content; α and n empirical coefficients of the van Genuchten (1980) equation; K_s saturated hydraulic conductivity; l pore-connectivity.

Soil layer	Soil texture	θ_r (-)	θ_s (-)	α (1/m)	n (-)	K_s (m/min)	l (-)
1	Clayey Silt	0.034	0.46	1.6	1.37	4.17E-05	0.5
2	Silty Clay	0.095	0.41	1.9	1.31	4.33E-05	0.5
3	Clay	0.070	0.36	0.5	1.09	3.33E-05	0.5
4	Silty Gravel	0.068	0.37	2.0	1.24	3.07E-02	0.5
5	Silty Gravel	0.067	0.38	3.5	1.39	6.10E-02	0.5
6	Silty Gravel	0.065	0.39	5.0	1.54	9.14E-02	0.5
7	Silty Gravel	0.064	0.40	6.5	1.69	1.22E-01	0.5
8	Silty Gravel	0.062	0.43	7.9	1.83	1.22E-01	0.5
9	Silty Gravel	0.060	0.43	9.4	1.98	1.22E-01	0.5
10	Silty Gravel	0.059	0.43	10.0	2.09	1.22E-01	0.5
11	Silty Gravel	0.058	0.43	10.9	2.13	1.22E-01	0.5

Table 4.4.3 Recharge estimates from the sensitivity analysis and annotations of the fit of the temperature simulations the observed data.

Factor Adjustment of Hydraulic Conductivity	Recharge Estimate (m)	
	Scenario 1	Scenario 2
Original Simulation		
1	0.13	0.15
Top Three Layers		
2	0.23 ³	0.28 ³
5	0.50	0.66
10	0.96	1.32
0.5	0.07	0.09
0.2	0.04	0.05
0.1	0.02	0.03
Bottom Eight Layers		
2	0.13 ^{2,3}	0.16 ^{2,3}
5	0.13 ³	0.16 ³
10	0.13	0.17
0.5	0.13	0.15
0.2	0.12 ^{NC}	0.20
0.1	0.12	0.17
Whole Profile		
2	0.24 ³	0.27 ³
5	0.55	0.63
10	1.07	1.21
0.5	0.09	0.09
0.2	0.04	0.05
0.1	0.02	0.03

No footnote indicates that the fit of all the simulated temperature probes to the observed temperature profiles was not improved or was not as good as the original simulation.

¹ The fit to the observed temperature profiles at T5 is better or similar than the original simulation

² The fit to the observed temperature profiles at T6 is better or similar than the original simulation

³ The fit to the observed temperature profiles at T7 is better or similar than the original simulation

^{NC} No Comment

Table 4.4.4 Moisture retention parameters for silt and clay soils.
 θ_r residual soil water content; θ_s saturated soil water content; α and n empirical coefficients of the van Genuchten (1980) equation; K_s saturated hydraulic conductivity. Comparing (a) values determined through calibration to (b) field values measured from the County of Oxford Property soils (Wendt, 2005) and literature values (Schaap et al., 1999; Šimůnek et al., 1999).

Soil texture	θ_r (-)	θ_s (-)	α (1/m)	n (-)	K_s (m/min)	Layer
Clayey Silt	0.034	0.46	1.60	1.37	4.17E-05	Layer 1
Silty Clay	0.095	0.41	1.90	1.31	4.33E-05	Layer 2
Clay	0.070	0.36	0.50	1.09	3.33E-05	Layer 3

(a)

Soil texture	θ_r (-)	θ_s (-)	α (1/m)	n (-)	K_s (m/min)	Source
Silt / Clay	0.000 - 0.001	0.16 - 0.28	2.900 - 31.950	1.139 - 1.236	-	Wendt, 2005
Silt / Clay	0.200 - 0.239	0.40 - 0.50	2.260 - 2.430	2.144 - 2.395	-	Wentz, 2005
Clay	0.098	0.470	1.490	1.250	6.00E-10	Schaap et al., 1999
Silty Clay	0.111	0.450	1.620	1.320	6.00E-09	Schaap et al., 1999
Clayey Silt	0.079	0.450	1.581	1.416	6.00E-08	Schaap et al., 1999
Silt	0.050	0.430	0.658	1.68	4.80E-06	Schaap et al., 1999
Clay	0.068	0.38	0.80	1.09	3.33E-05	Šimůnek et al., 2009
Silty Clay	0.070	0.36	0.50	1.09	3.33E-06	Šimůnek et al., 2009
Silty Clay Loam	0.089	0.43	1.00	1.23	1.17E-05	Šimůnek et al., 2009
Clay Loam	0.095	0.41	1.90	1.31	4.33E-05	Šimůnek et al., 2009
Silty Loam	0.067	0.45	2.00	1.41	7.50E-05	Šimůnek et al., 2009
Silt	0.034	0.46	1.60	1.37	4.17E-05	Šimůnek et al., 2009
Loam	0.078	0.43	3.60	1.56	1.73E-04	Šimůnek et al., 2009

(b)

Table 4.4.5 Moisture retention parameters for silty gravel and sand soils.
 θ_r residual soil water content; θ_s saturated soil water content; α and n empirical coefficients of the van Genuchten (1980) equation; K_s saturated hydraulic conductivity. Comparing (a) values determined through calibration for silty gravel to field values measured from the County of Oxford Property (Wendt, 2005) and literature values (Schaap et al., 1999; Šimůnek et al., 1999) for (b) silty sand, (c) sand and (d) silty gravel and gravel.

Soil texture	θ_r (-)	θ_s (-)	α (1/m)	n (-)	K_s (m/min)	Layer
Silty Gravel	0.068	0.370	2.0	1.24	3.07E-02	Layer 4
Silty Gravel	0.067	0.380	3.5	1.39	6.10E-02	Layer 5
Silty Gravel	0.065	0.390	5.0	1.54	9.14E-02	Layer 6
Silty Gravel	0.064	0.400	6.5	1.69	1.22E-01	Layer 7
Silty Gravel	0.062	0.430	7.9	1.83	1.22E-01	Layer 8
Silty Gravel	0.060	0.430	9.4	1.98	1.22E-01	Layer 9
Silty Gravel	0.059	0.430	10.0	2.09	1.22E-01	Layer 10
Silty Gravel	0.058	0.430	10.9	2.13	1.22E-01	Layer 11

(a)

Soil texture	θ_r (-)	θ_s (-)	α (1/m)	n (-)	K_s (m/min)	Source
Silty Sand	0.030 - 0.061	0.230 - 0.370	1.72 - 3.67	1.592 - 4.977	2.51E-03 - 2.29E-01	Wentz, 2005
Silty Sand	0.049	0.370	3.475	1.746	3.00E-02	Schaap et al., 1999
Loamy Sand	0.057	0.410	12.400	2.280	2.43E-03	Šimůnek et al., 2009
Sandy Loam	0.065	0.410	7.500	1.890	7.37E-04	Šimůnek et al., 2009

(b)

Soil texture	θ_r (-)	θ_s (-)	α (1/m)	n (-)	K_s (m/min)	Source
Well Graded Sand	0.000 - 0.074	0.282 - 0.386	2.98 - 7.97	1.676 - 2.093	1.10E-02 - 3.26E-01	Wentz, 2005
Fine Sand	0.036	0.380	2.51	3.550	6.00E-02	Schaap et al., 1999
Medium Sand	0.053	0.360	3.524	3.177	3.00E-01	Schaap et al., 1999
Coarse Sand	0.030	0.375	29.40	3.281	6.00E-01	Schaap et al., 1999
Sand	0.045	0.430	14.50	2.680	4.95E-03	Šimůnek et al., 2009

(c)

Soil texture	θ_r (-)	θ_s (-)	α (1/m)	n (-)	K_s (m/min)	Source
Gravelly Silt	0.018 - 0.067	0.314 - 0.401	6.52 - 11.31	1.711 - 2.117	1.63E-02 - 4.67E-01	Wentz, 2005
Gravelly Silt	0.039	0.410	2.667	1.449	6.00E-05	Schaap et al., 1999
Gravel	0.005	0.280	493.0	2.190	3.00E+00	Schaap et al., 1999

(d)

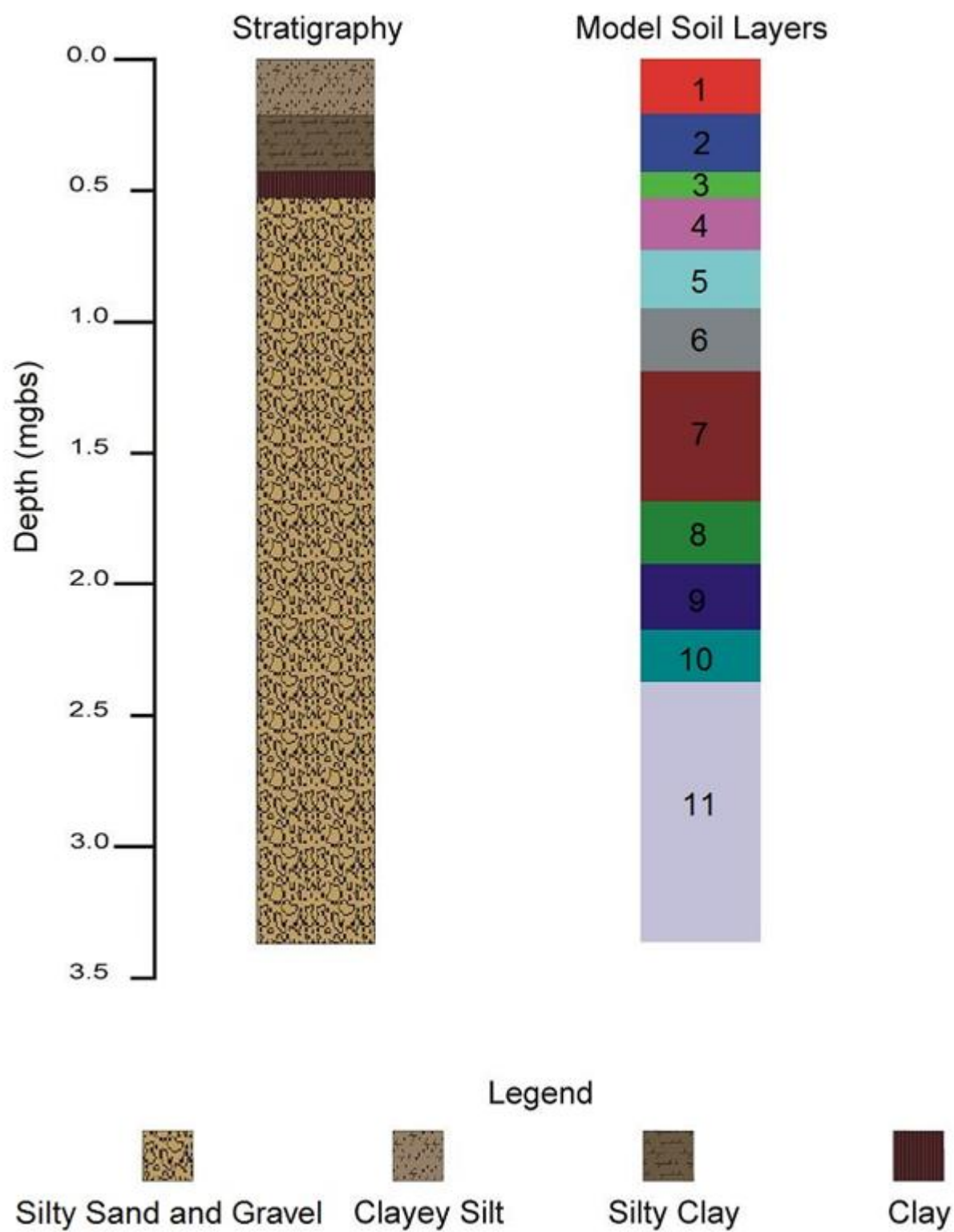


Figure 4.4.1 A conceptual representation of the soil stratigraphy used for the model, and the soil layers used by the model.

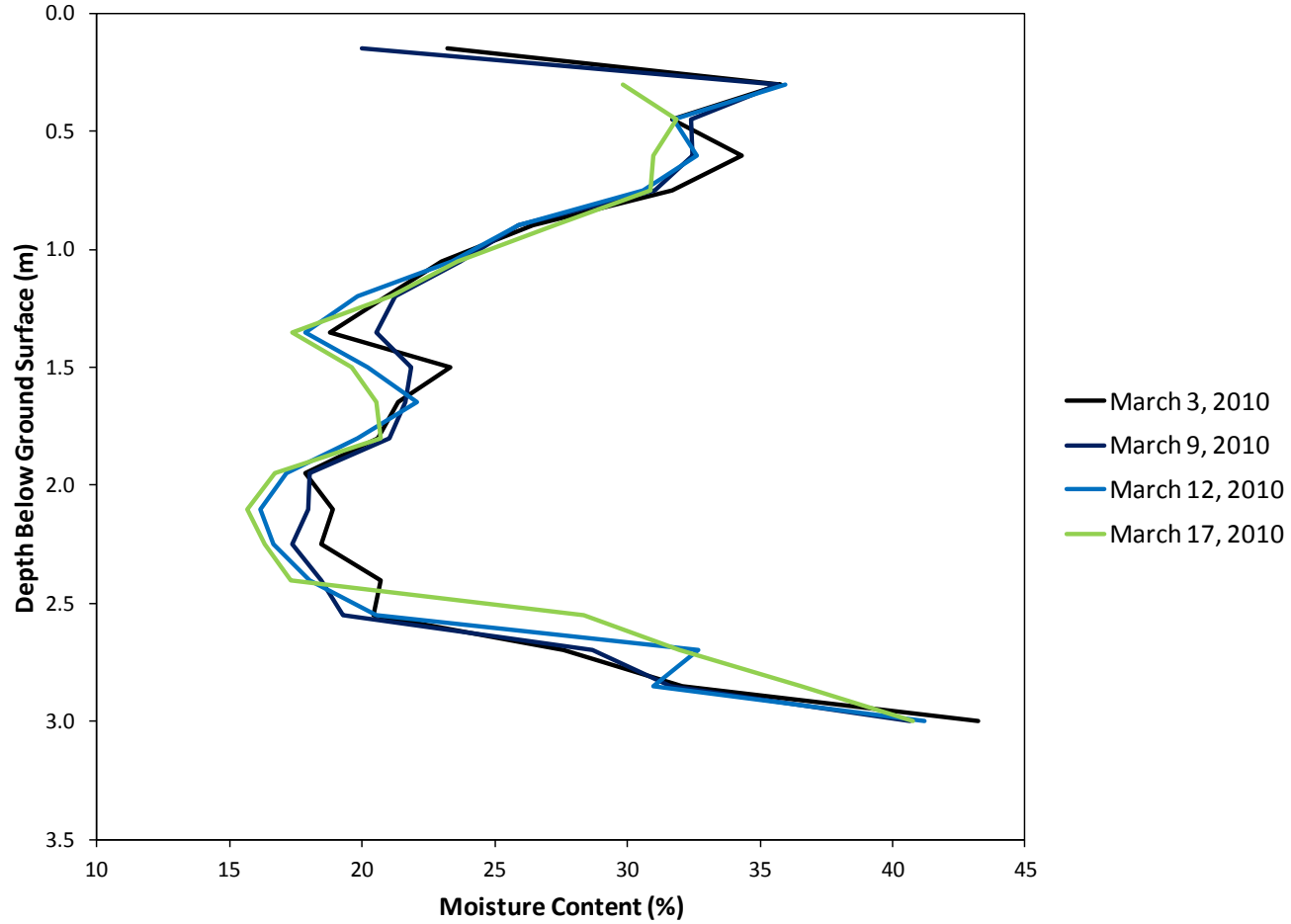


Figure 4.4.2 Moisture content profiles for the month of March measured with neutron probe.

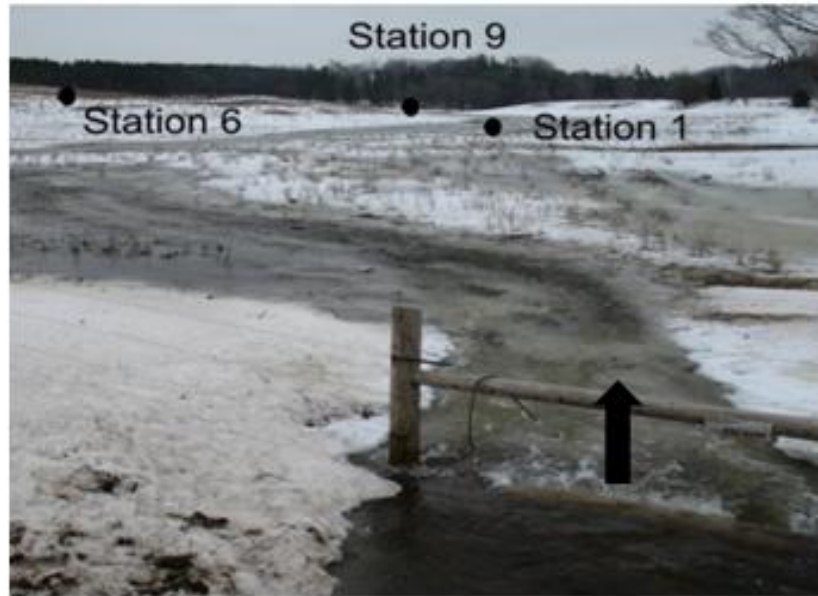


(a)



(b)

Figure 4.4.3 Pictures of Station 1 during the spring melt. (a) Picture of temperature probes from Station 1 facing toward Curry Road March 6th 2010. (b) Picture of Station 1 and temperature probes from between Station 1 and WO62 on March 9th 2010. Arrows indicate flow direction.



(a)



(b)

Figure 4.4.4 Pictures of stream flowing from Curry Road looking south over the culvert during the spring melt. (a) Picture of stream taken in by Mike Christie on March 18th, 2010 (Koch, 2009). (b) Picture of stream taken on March 9th, 2010, the day when wells and temperature probes start to record changes in temperature. Arrows indicate flow direction.

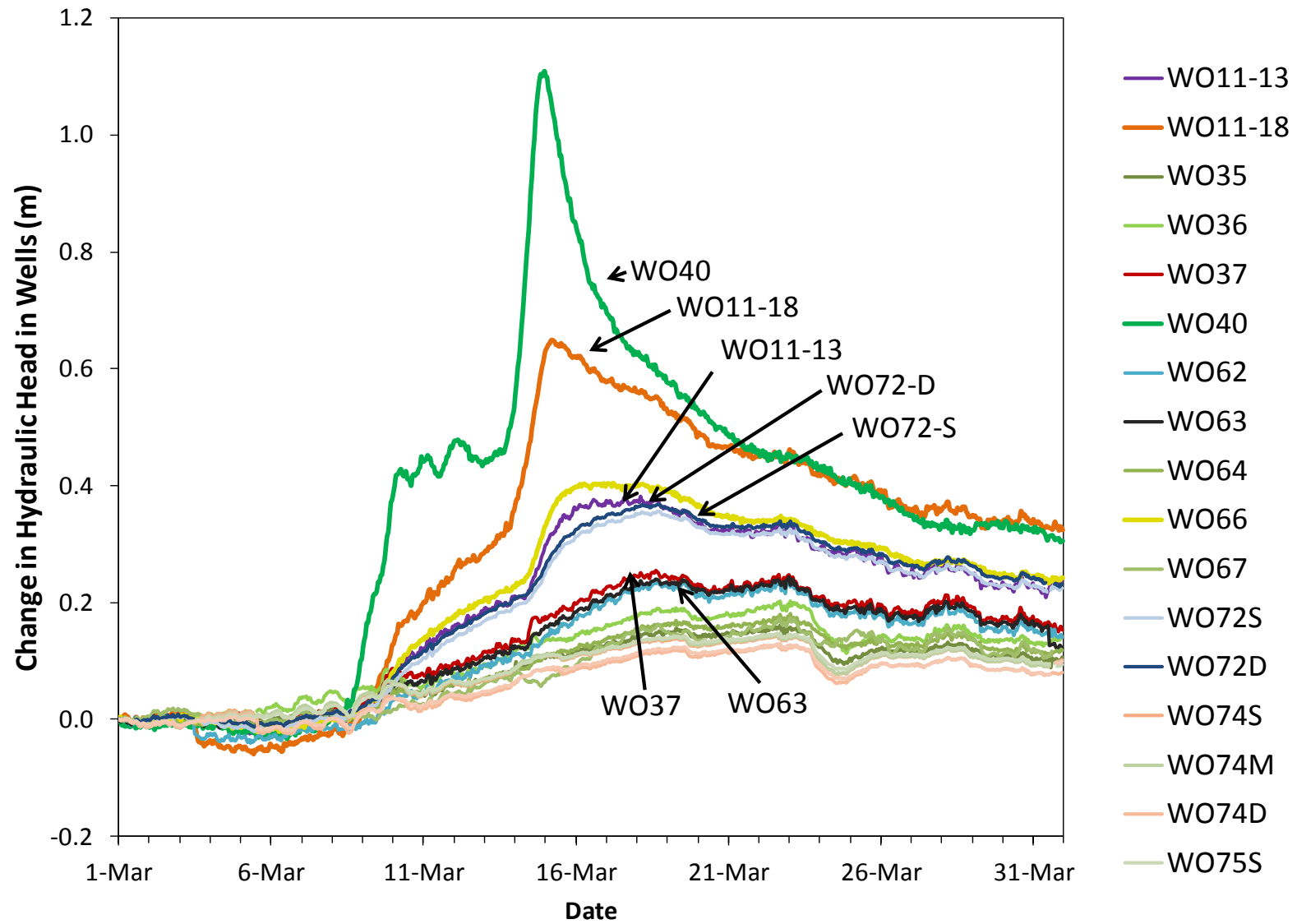


Figure 4.4.5 Change in hydraulic head over time in each monitoring well relative to March 1st, 2010 at midnight.

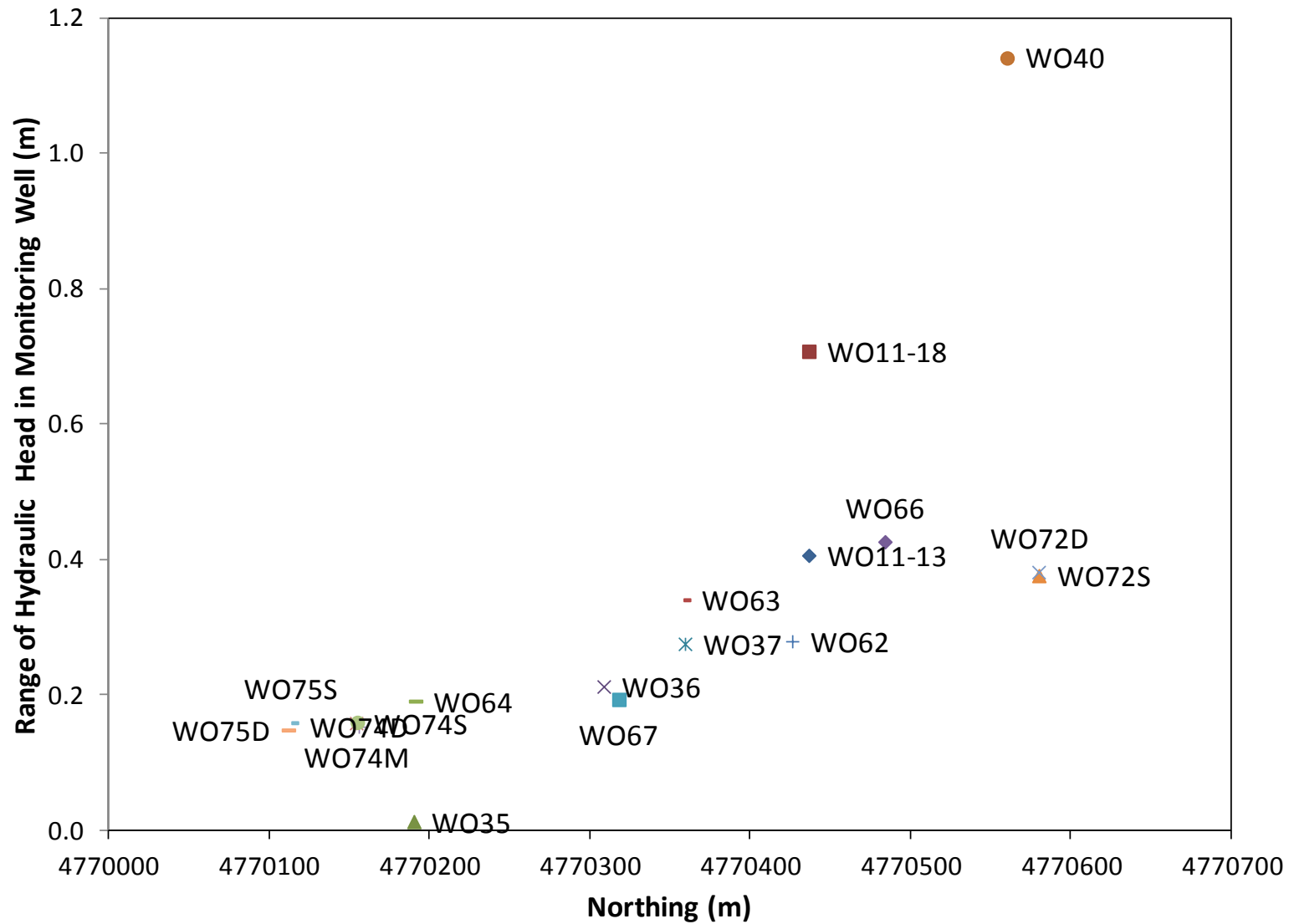


Figure 4.4.6 Range (maximum minus minimum) of changes in hydraulic head recorded in monitoring wells over the month of March plotted against the northing of the well casing.

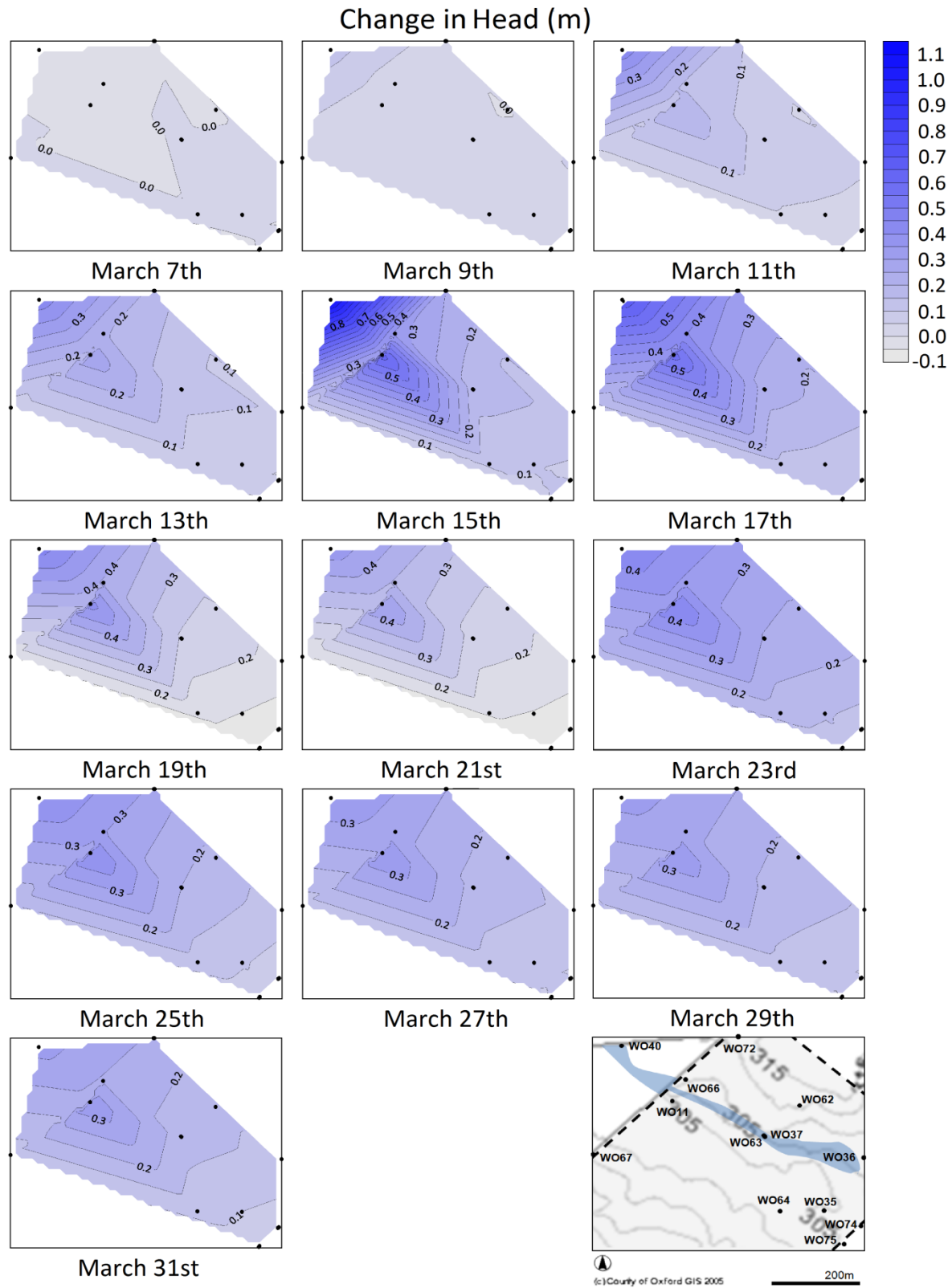


Figure 4.4.7 Maps of the change in groundwater head relative to midnight on the 1st of March, in the vicinity of the ephemeral stream during the month of March, 2010.

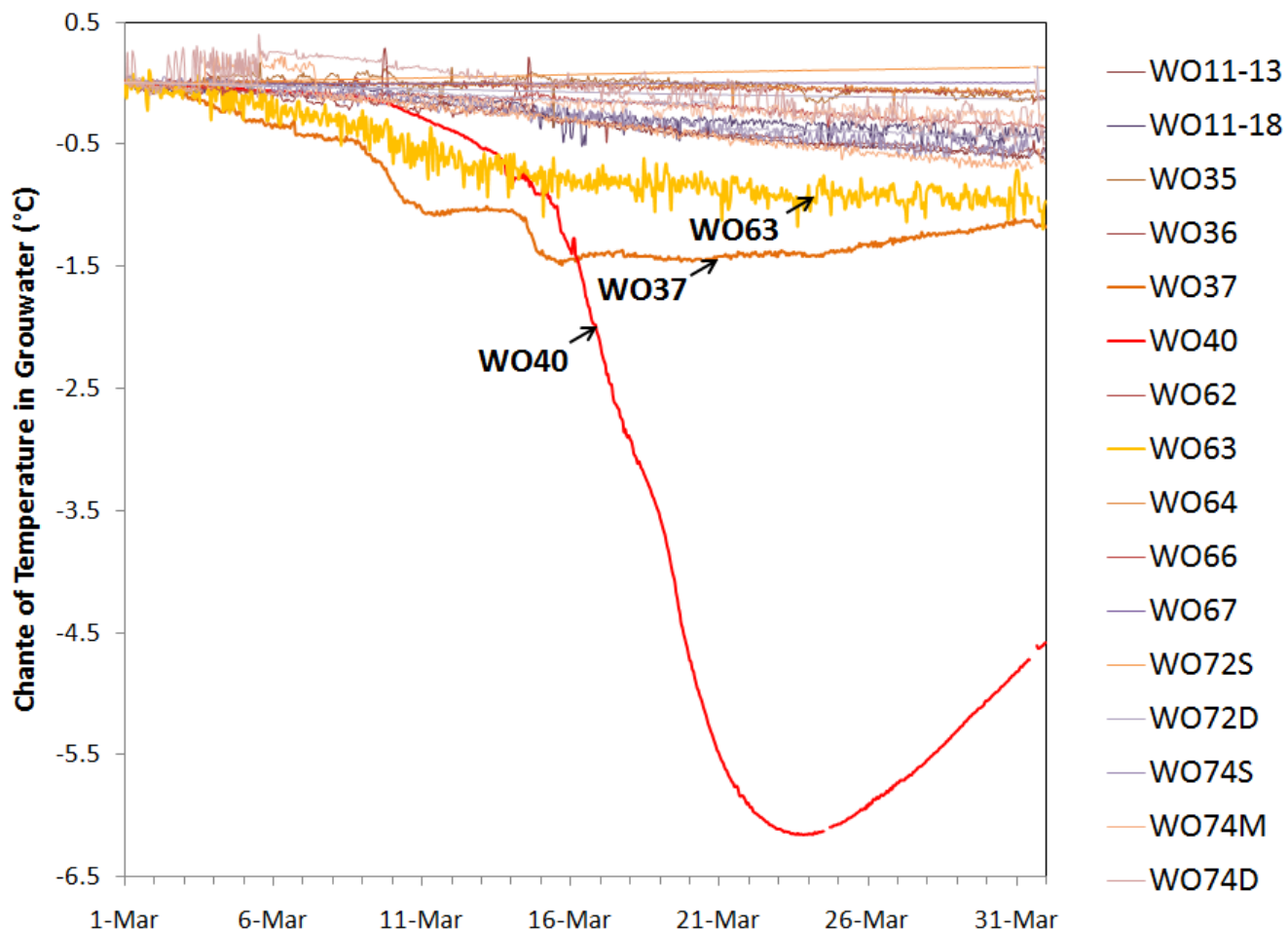


Figure 4.4.8 Change in temperature over time in each monitoring well relative to March 1st, 2010 at midnight.

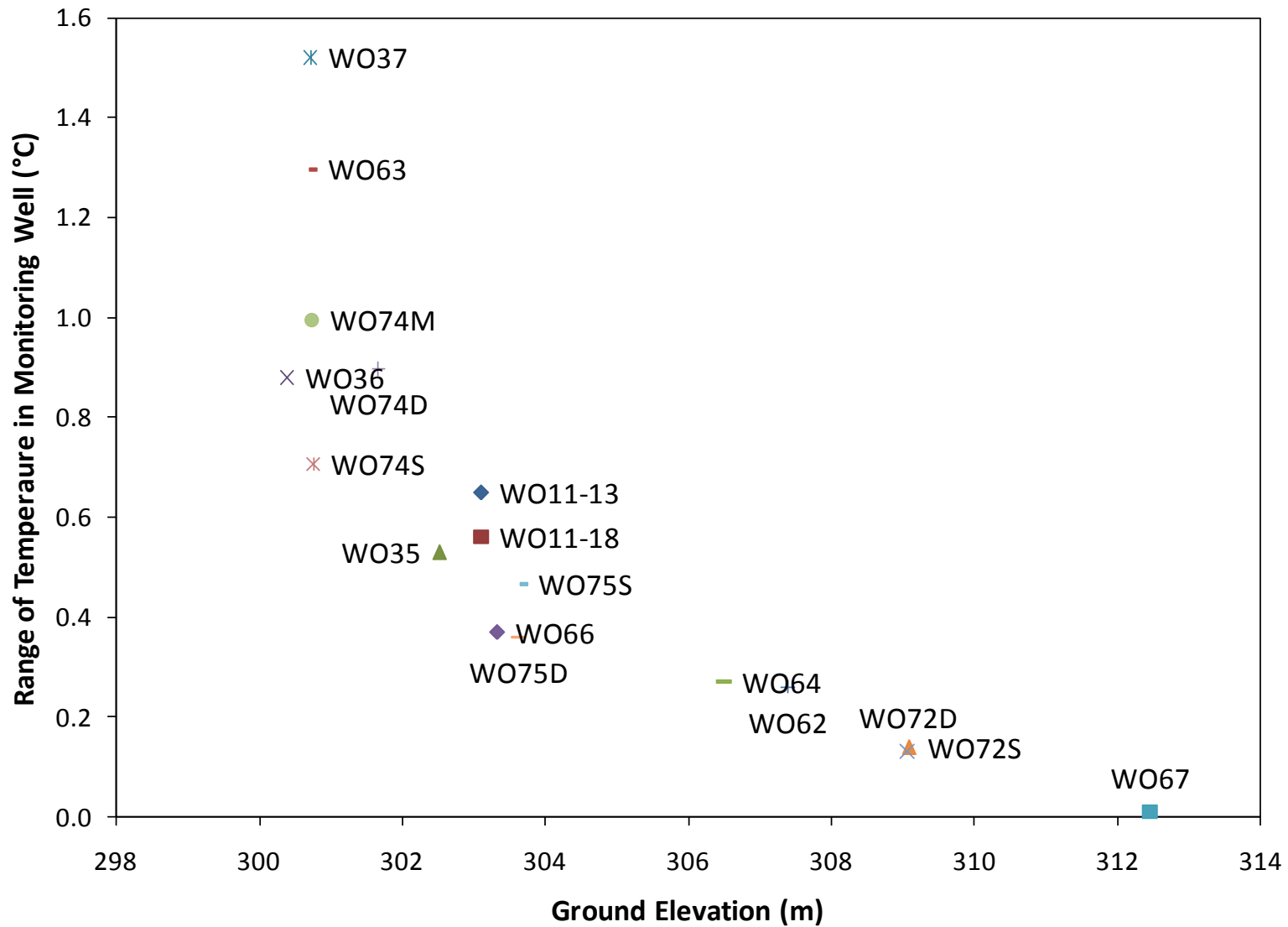


Figure 4.4.9 Range (maximum minus minimum) of temperature change recorded in monitoring wells (excluding WO40) over the month of March plotted against the elevation of the ground at the casing.

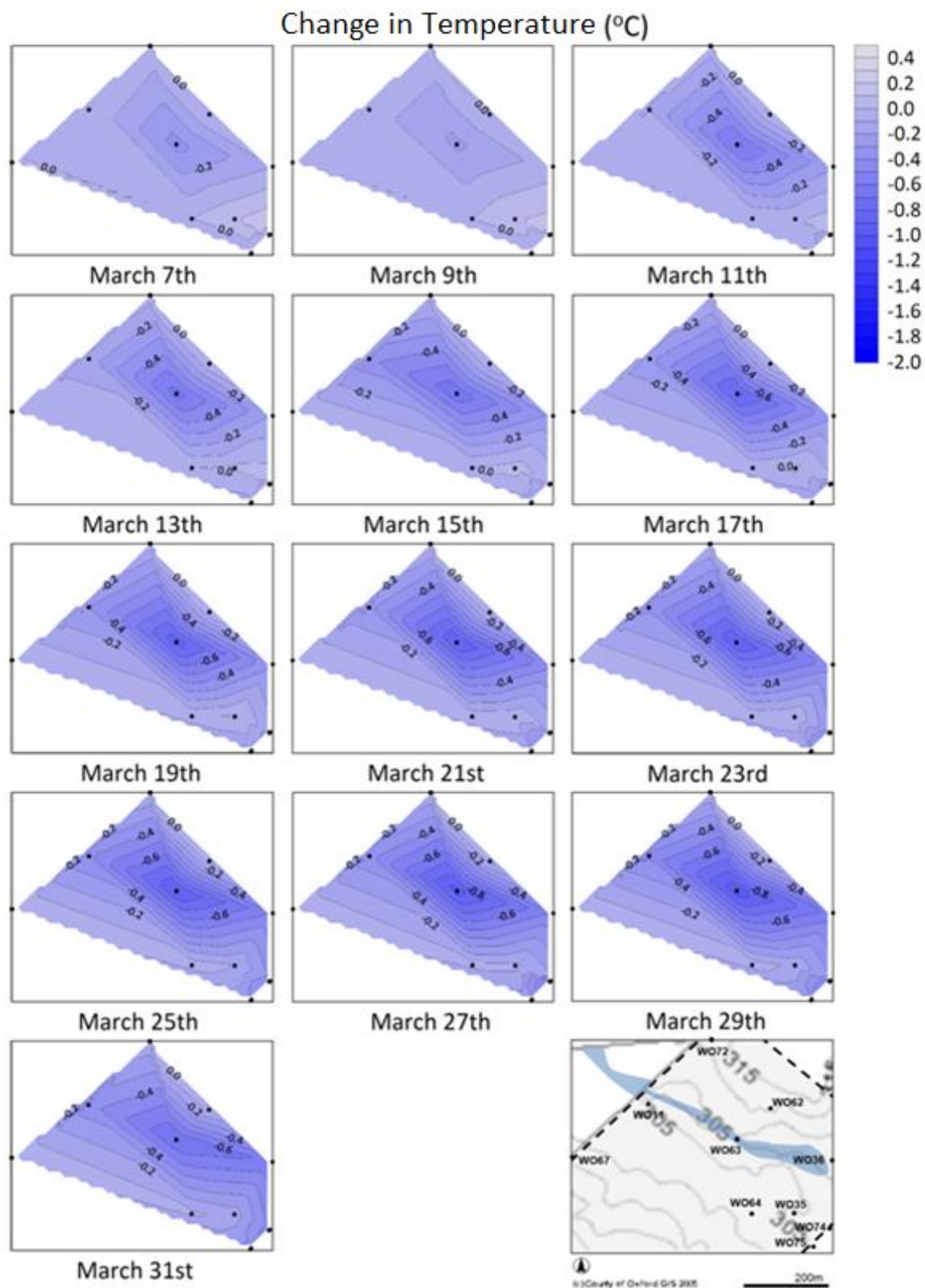


Figure 4.4.10 Maps of change in groundwater temperature in Aquifer 3 relative to midnight on the 1st of March, in the vicinity of the ephemeral stream during the month of March, 2010.

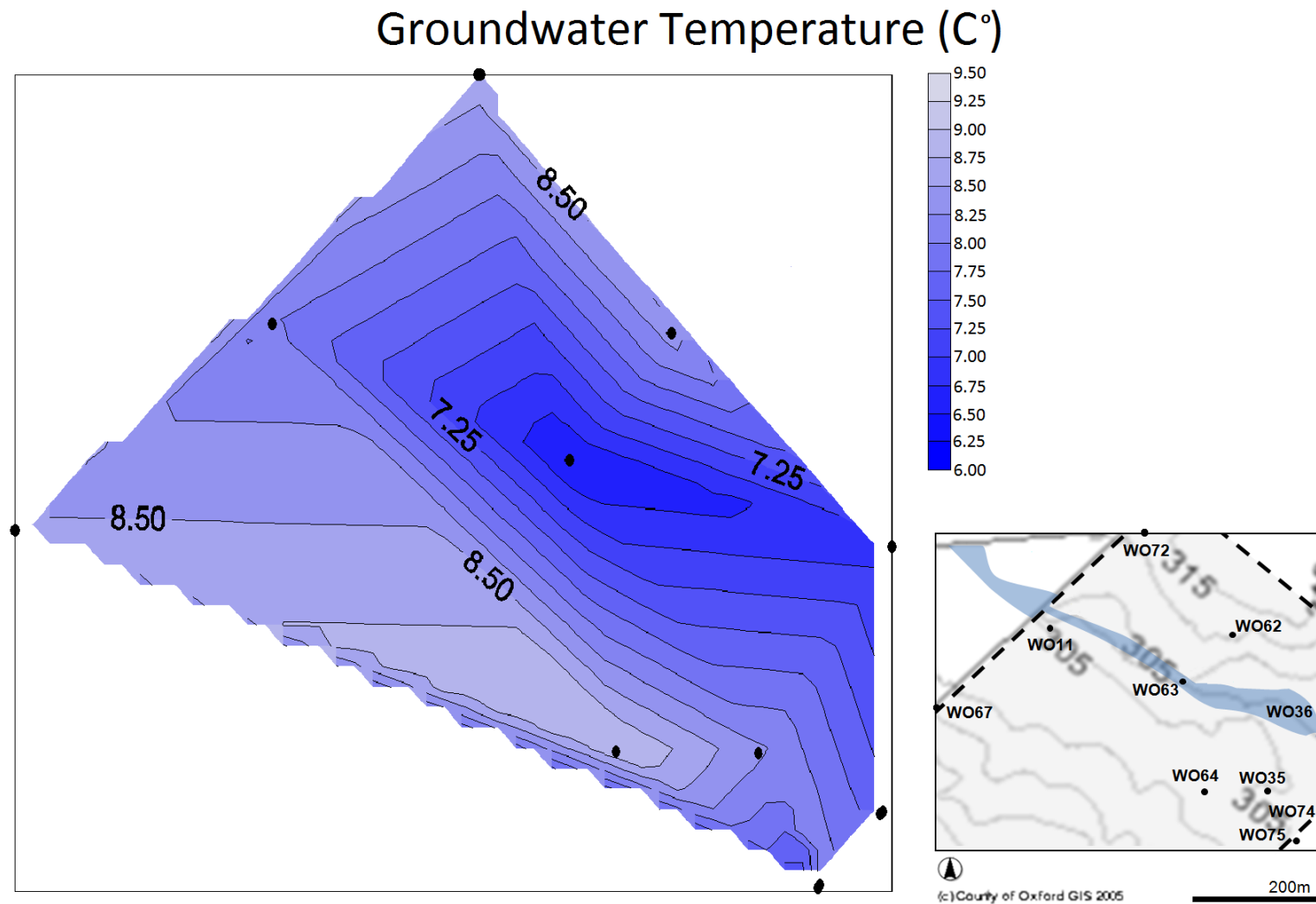


Figure 4.4.11 Maps of change in groundwater temperature in Aquifer 3 on March 15th, 2010 in the vicinity of the ephemeral stream.

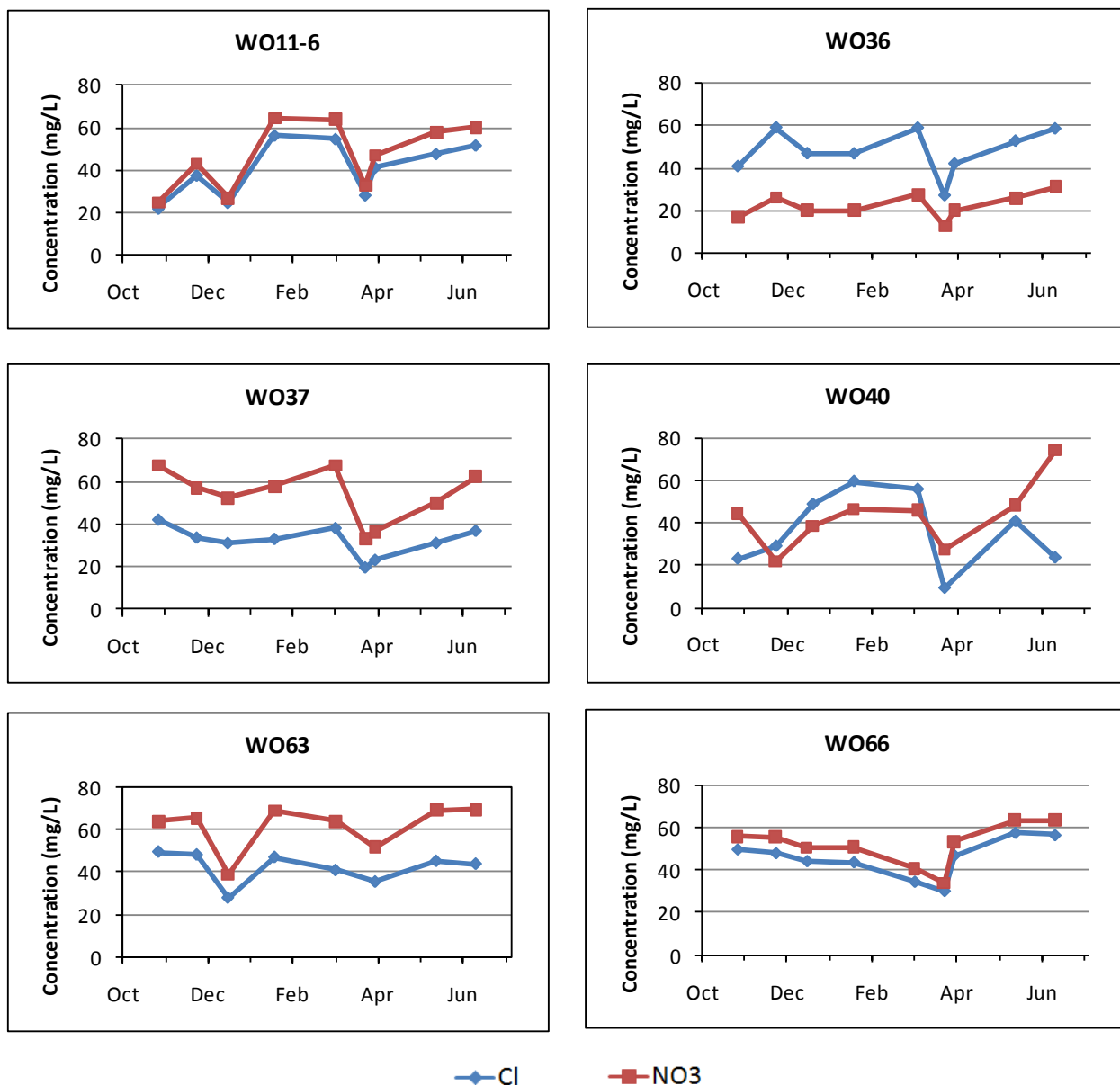


Figure 4.4.12 Monthly monitoring in wells where a notable decreases in both nitrate and chloride concentration occurred after the melt event.

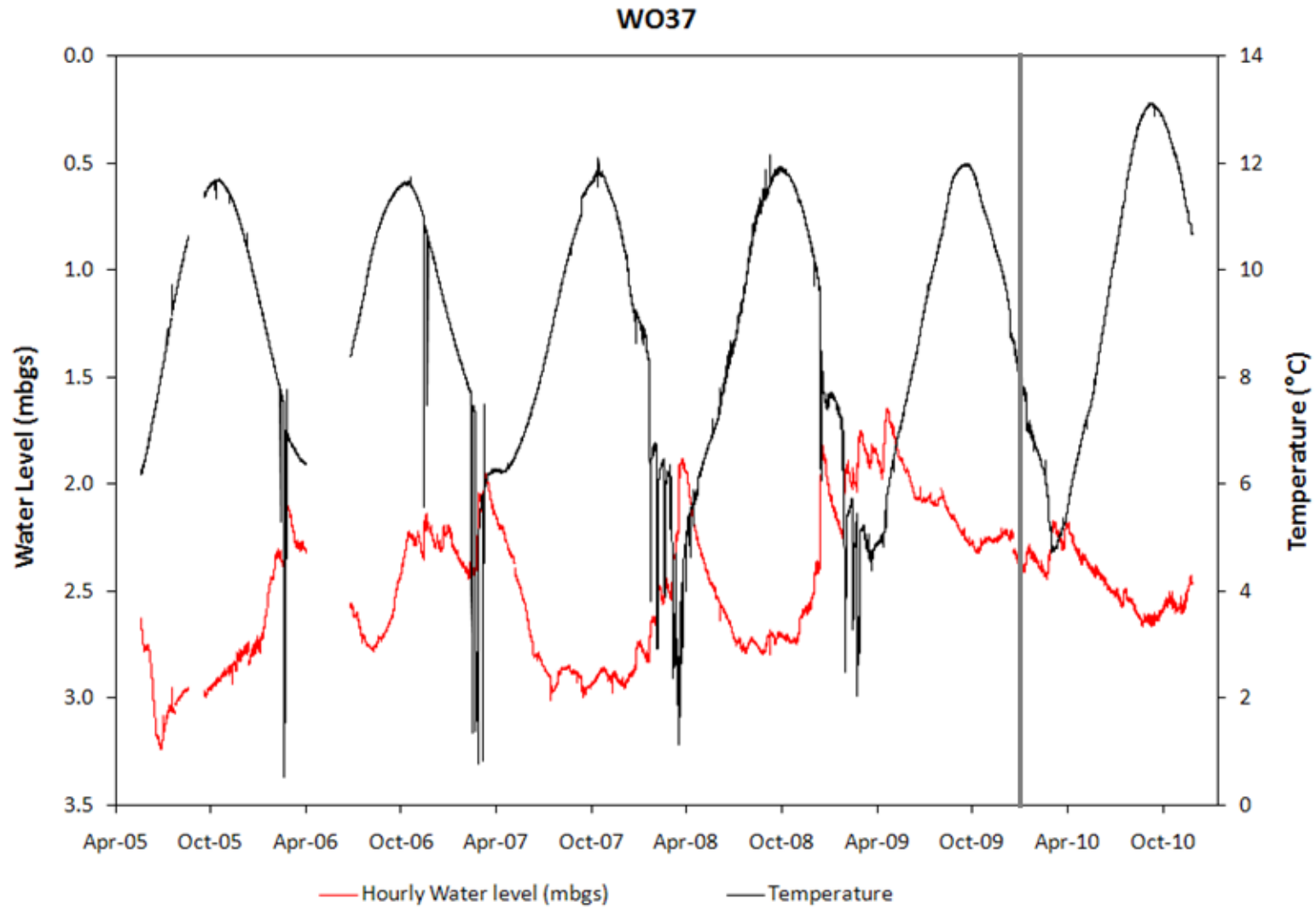


Figure 4.4.13 Water level (meters below ground surface) and temperature (°C) recorded between 2005 and 2010 in W037. The date when the well was repaired (January 16th, 2010) is marked by a vertical grey line.

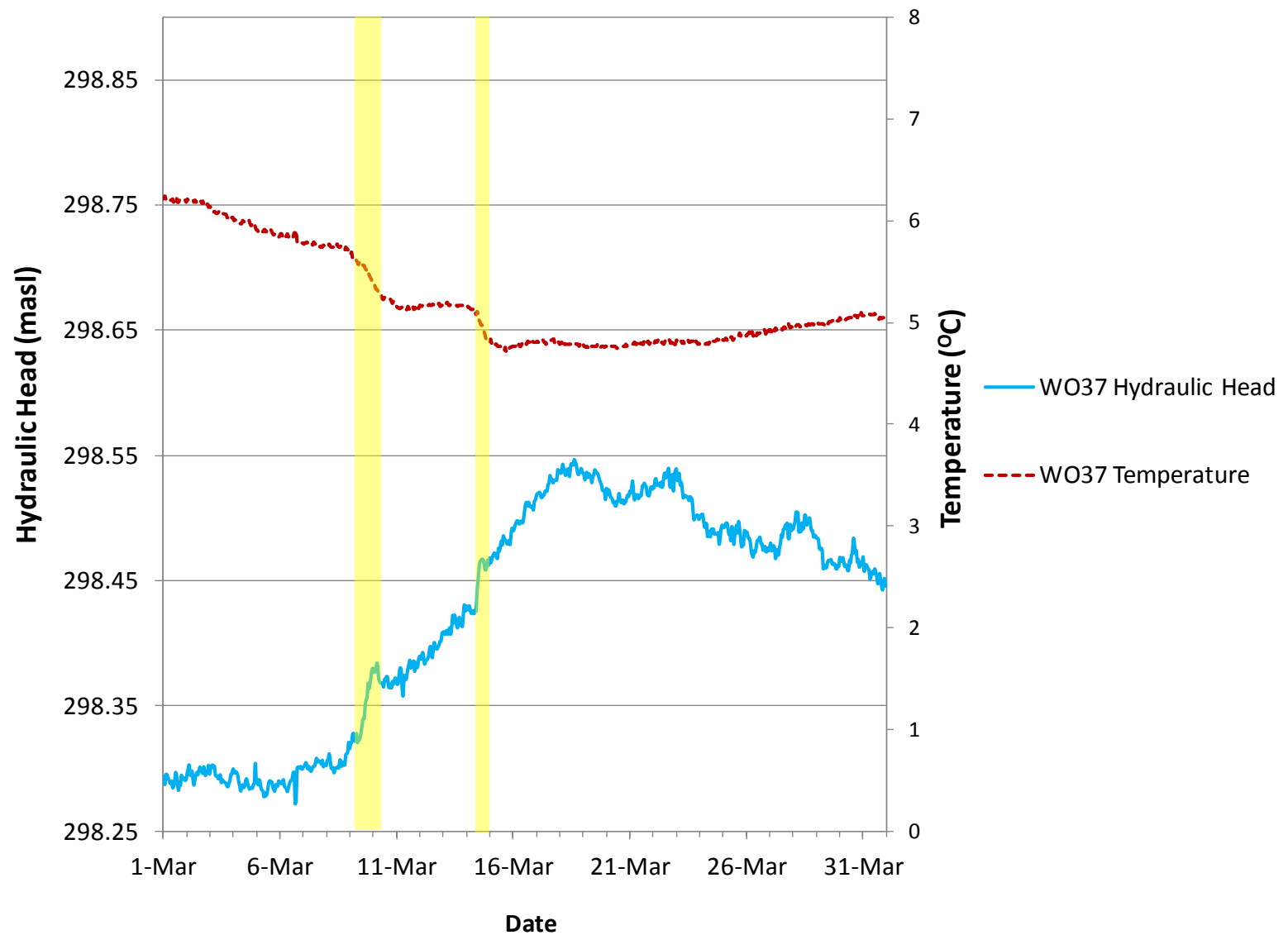


Figure 4.4.14 Pressure and temperature changes in WO37 in March, 2010. The periods highlighted in yellow are those where there is a steep decrease in groundwater temperature coinciding with a steep increase in water level.

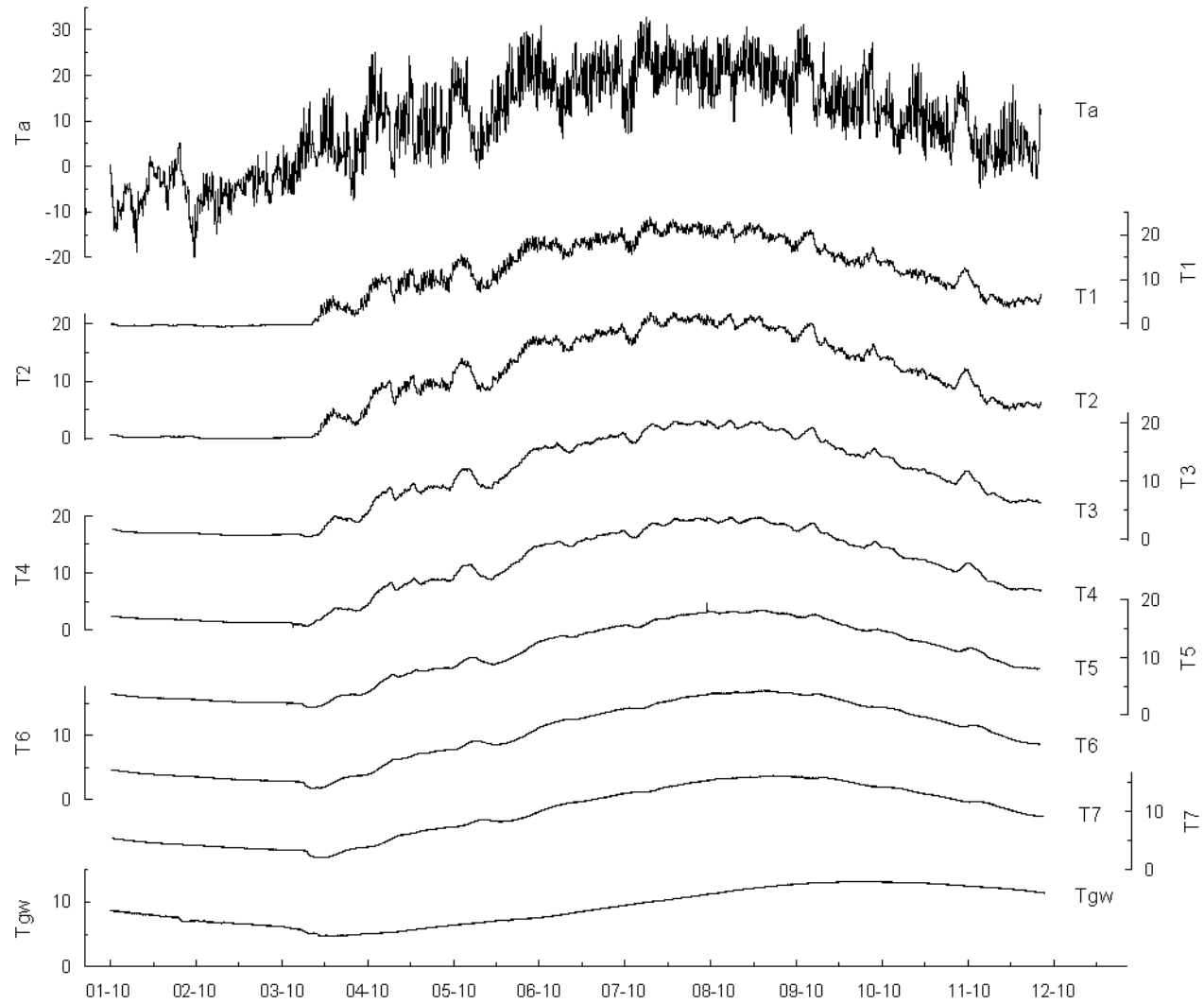


Figure 4.4.15 Air, soil and groundwater temperature (°C) between January and December of 2010. Soil temperature probes depths are: T1 (13 cm), T2 (26 cm), T3 (39 cm), T4 (53 cm), T5 (87 cm), T6 (121 cm) and T7 (156 cm).

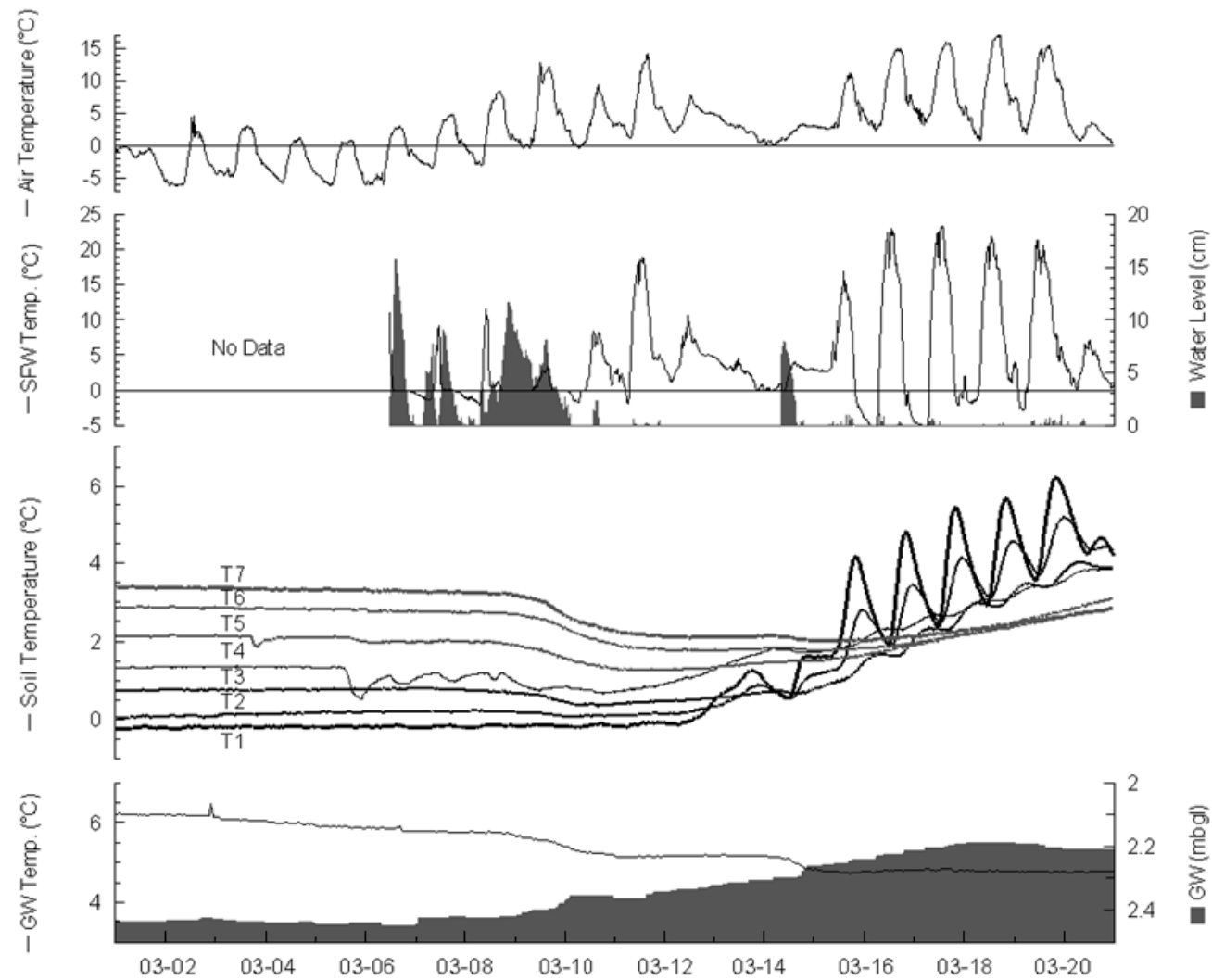


Figure 4.4.16 Air, surface water, soil and groundwater temperature (°C), surface water height (cm) and groundwater depth (mbgs) between March 1st and 22nd, 2010. Soil temperature probes depths are: T1 (13 cm), T2 (26 cm), T3 (39 cm), T4 (53 cm), T5 (87 cm), T6 (121 cm) and T7 (156 cm).

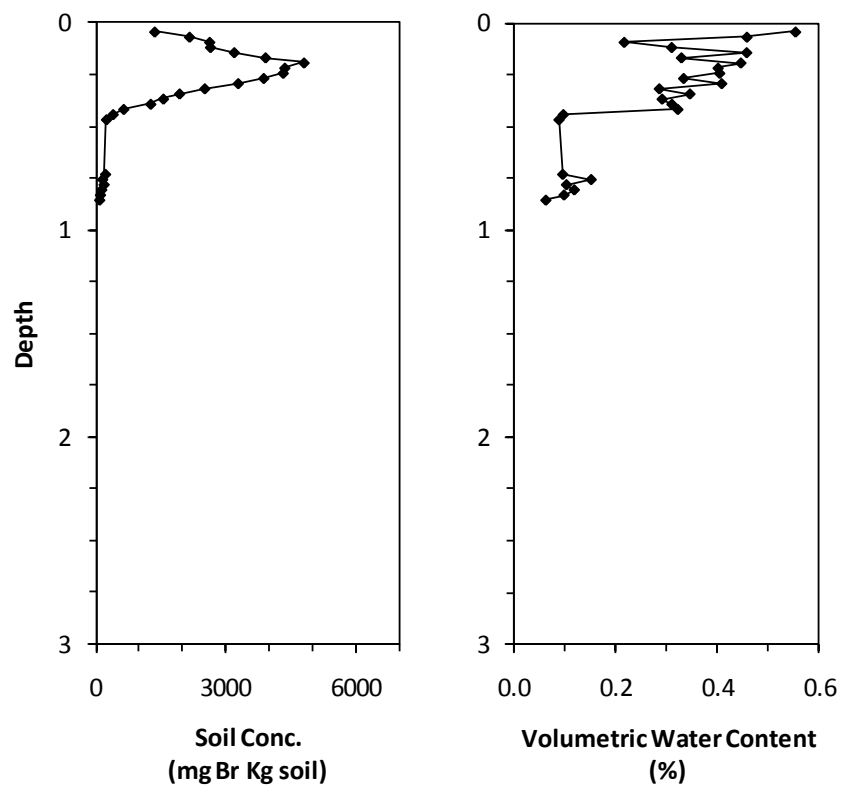


Figure 4.4.17 Soil bromide concentration and volumetric water content profiles in March 5th, 2010.

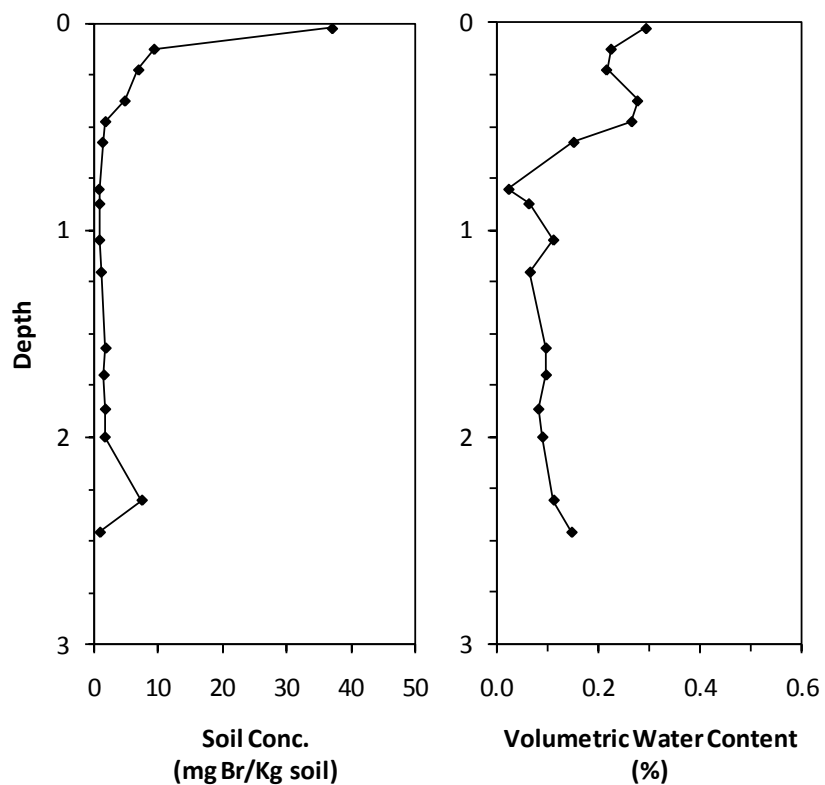


Figure 4.4.18 Soil bromide concentration and volumetric water content profiles in May 6th, 2010.

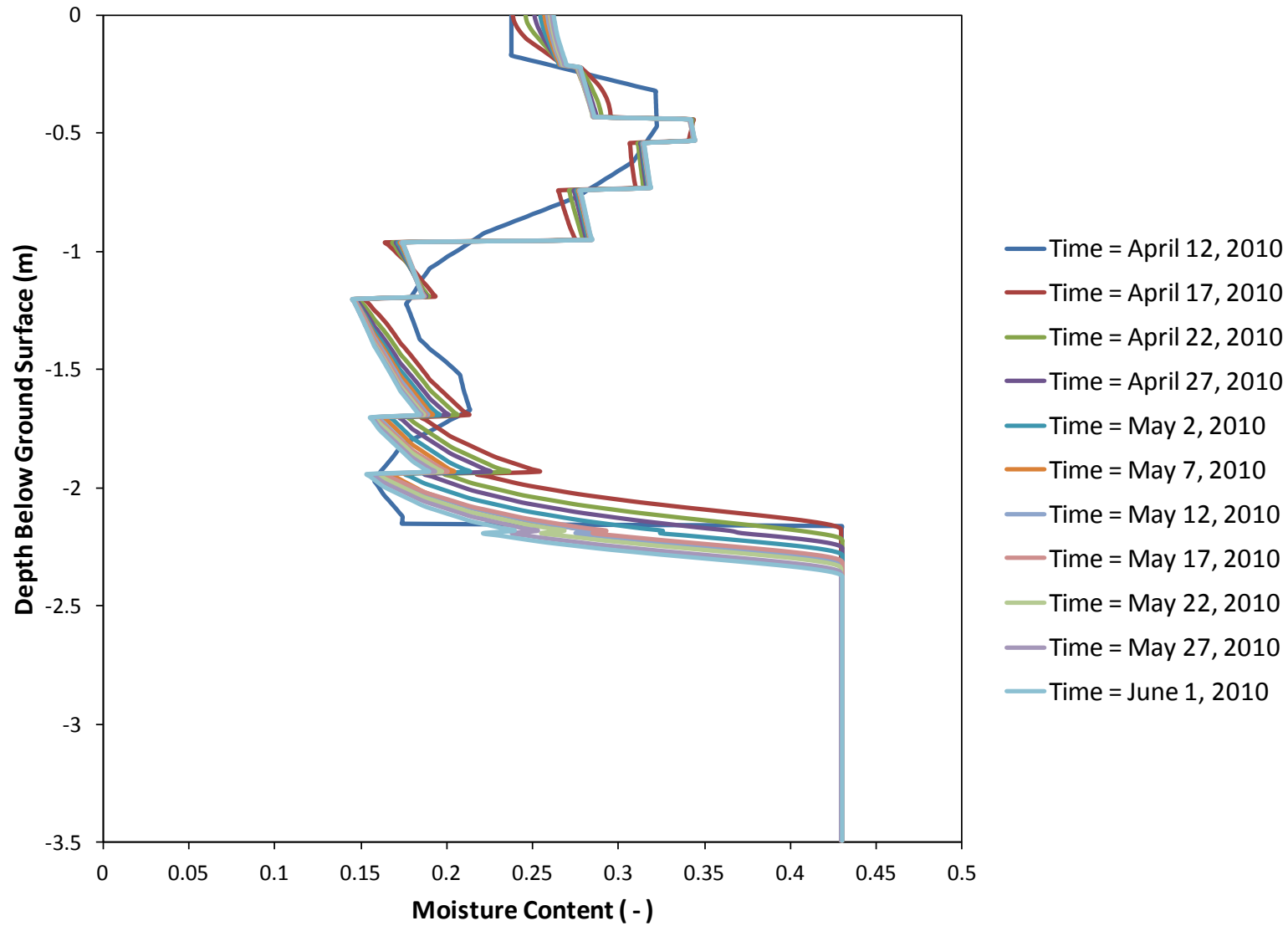


Figure 4.4.19 Simulated moisture content profiles every five days of simulation between midnight on April 12th and June 1st, 2010. The initial moisture content inputted into the model is shown on April 12th, 2010.

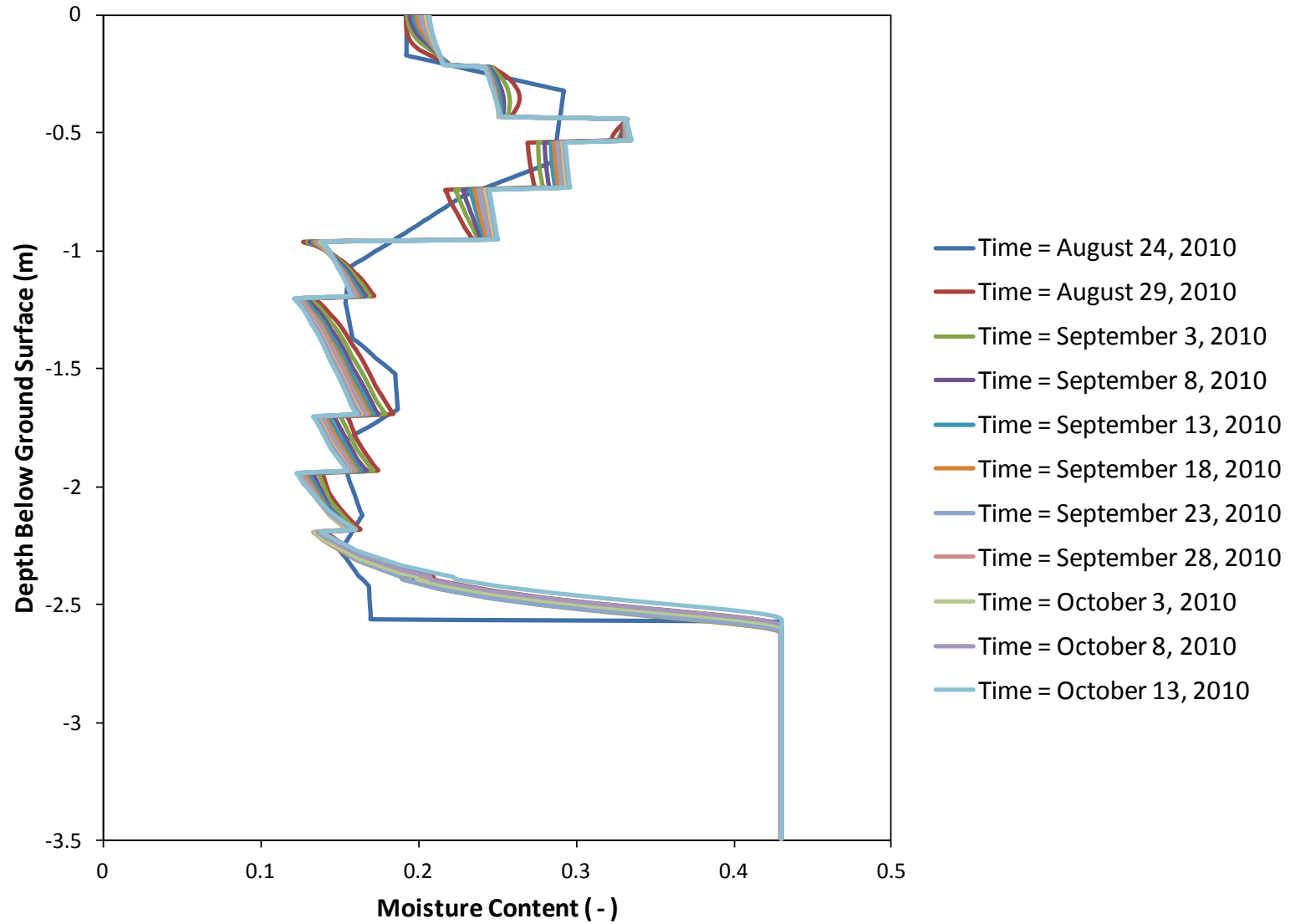


Figure 4.4.20 Simulated moisture content profiles every five days of simulation between midnight on August 24th and on October 31st, 2010. The initial moisture content inputted into the model is shown on August 24th.

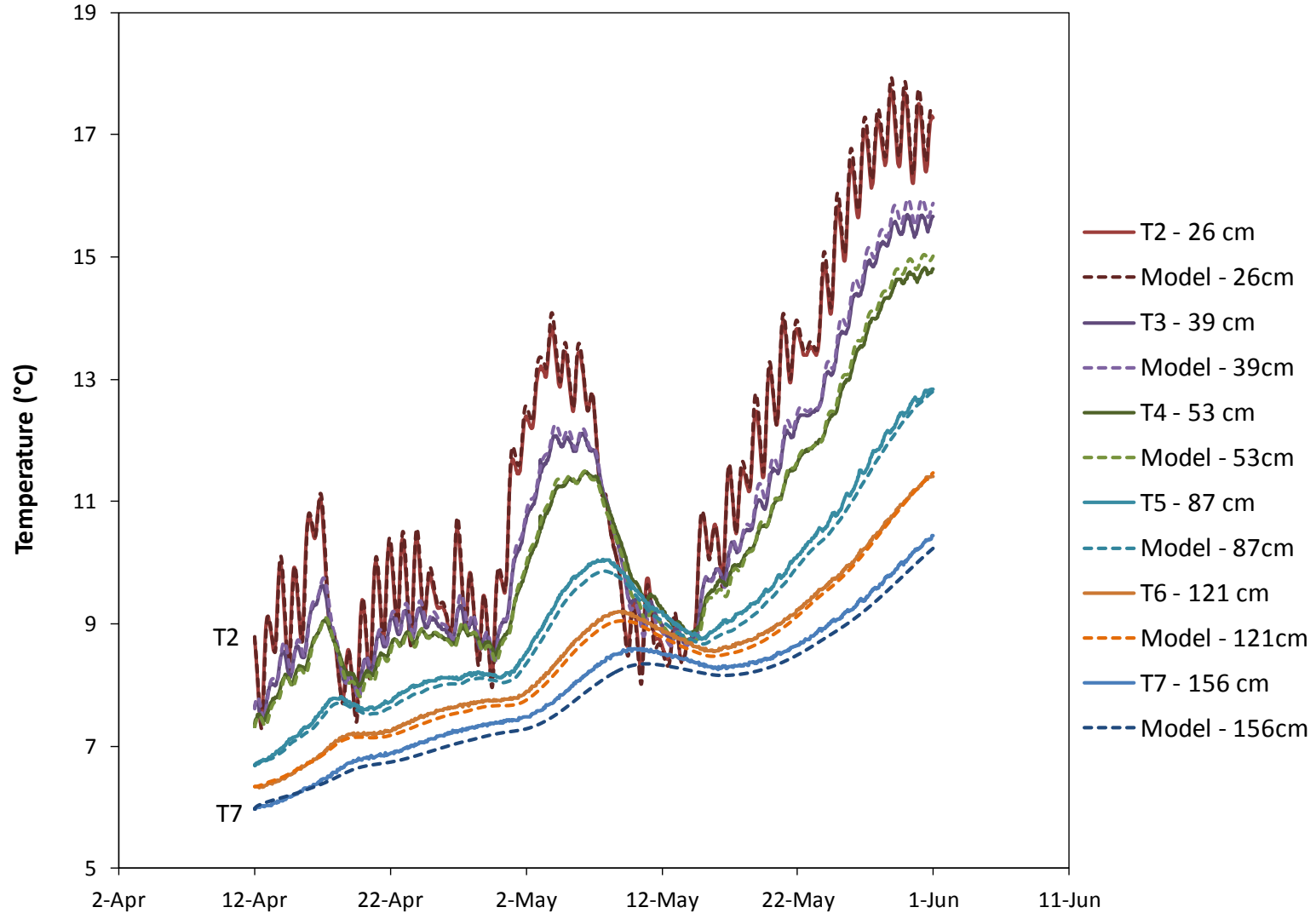


Figure 4.4.21 Simulated and observed temperature at different depths between April 12th and June 1st, 2010 for calibration in unsaturated conditions. Note that the observation node for T3 was placed 5 cm lower than indicated from field measurements.

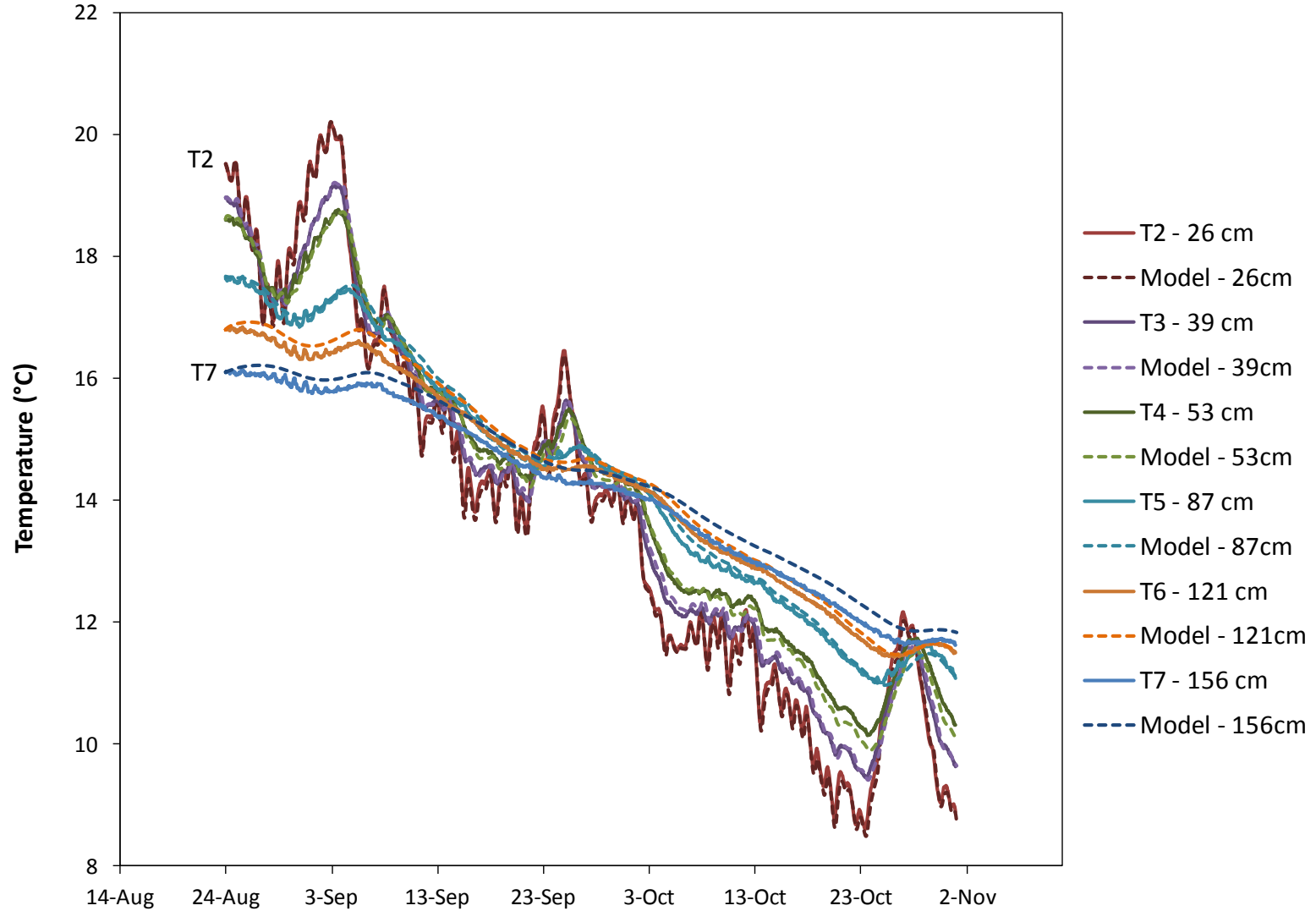


Figure 4.4.22 Simulated and observed temperature at different depths between August 24th and October 31st, 2010 for calibration in unsaturated conditions. Note that the observation node for T3 was placed 5 cm lower than indicated from field measurements.

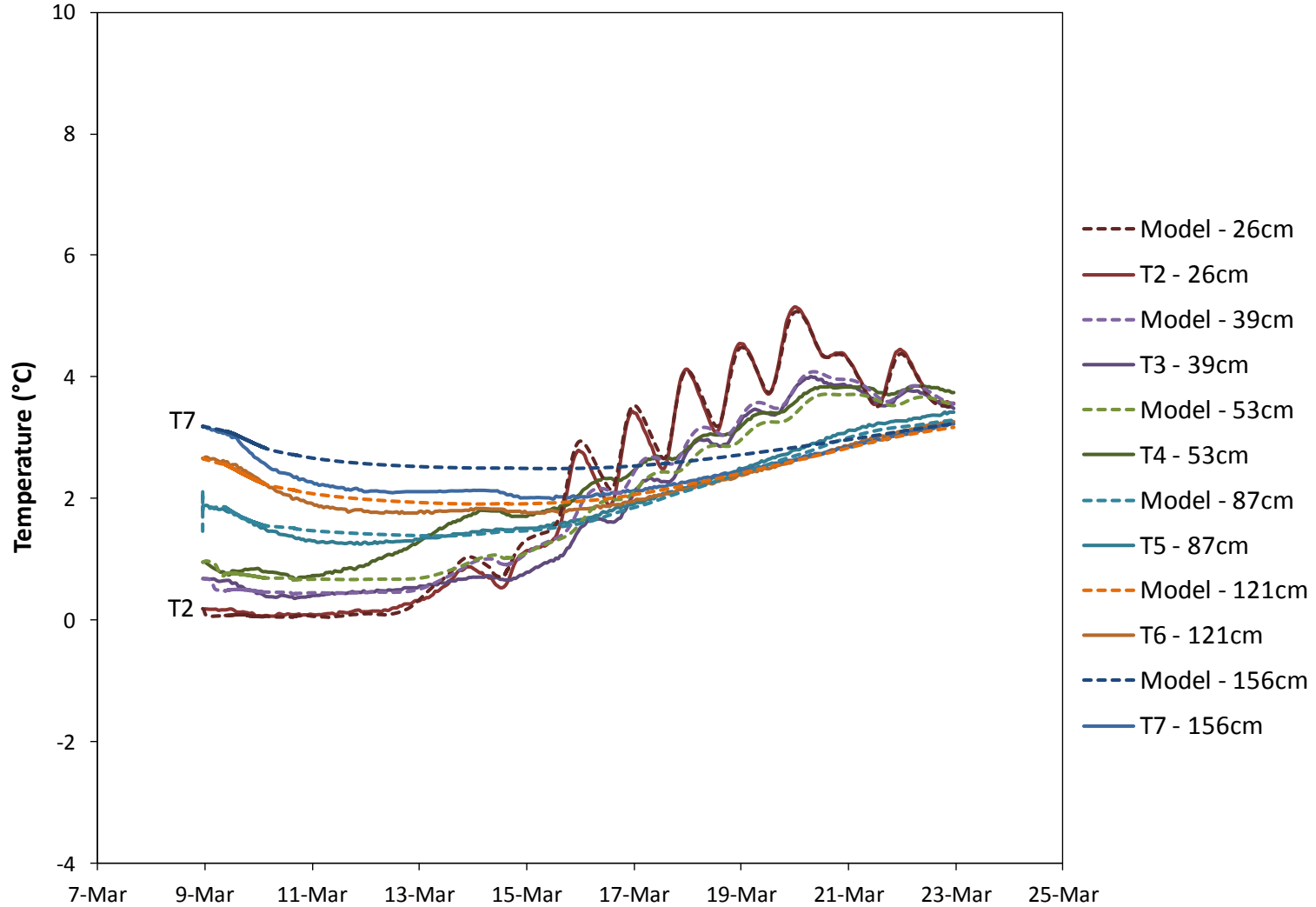


Figure 4.4.23 Scenario 1 - Simulated and observed temperature at different depths between March 9th and March 22nd, 2010, for calibration during partially saturated conditions. Note that the observation node for T3 was placed 5 cm lower than indicated from field measurements.

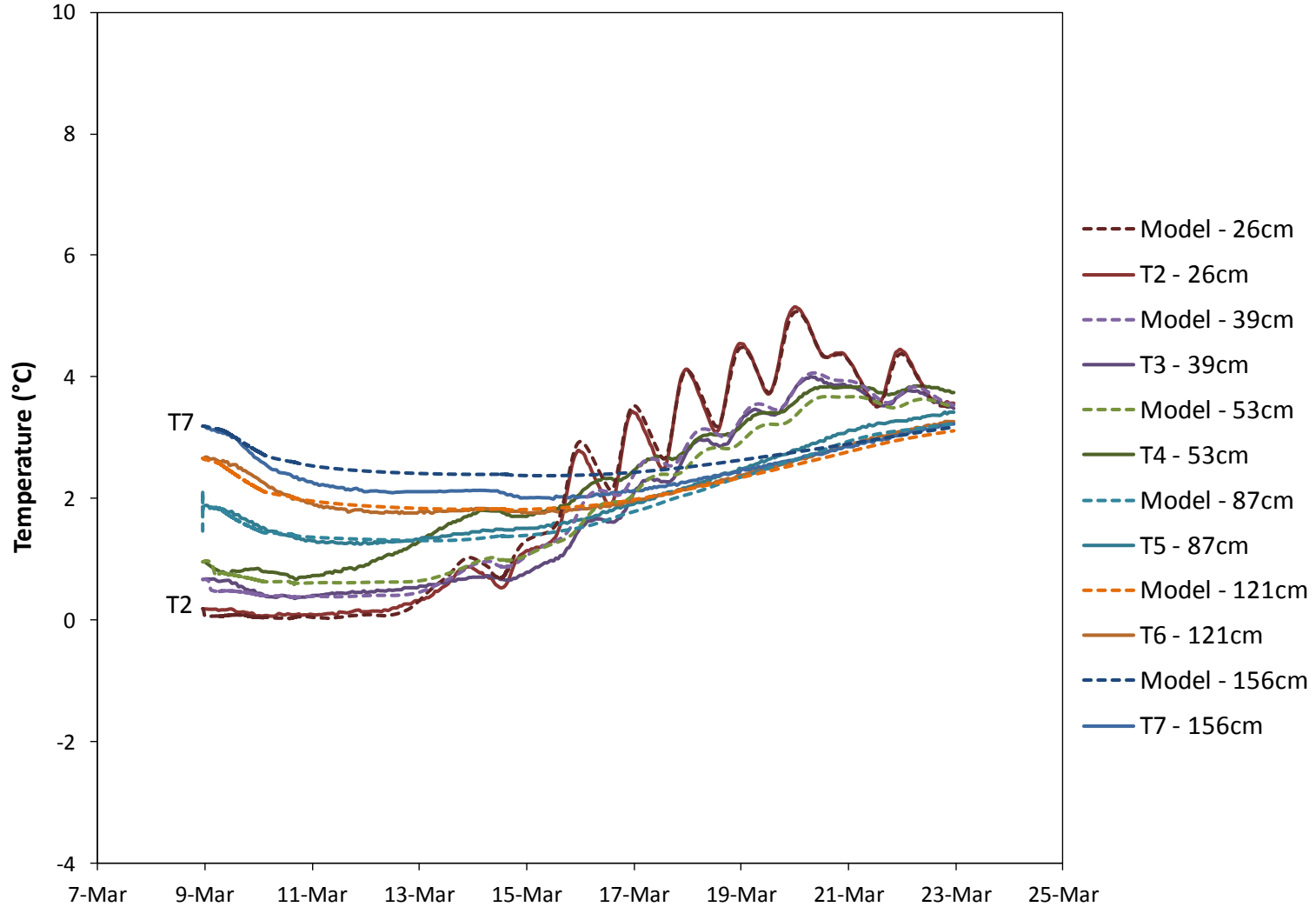


Figure 4.4.24 Scenario 2 - Simulated and observed temperature at different depths between March 9th and March 22nd, 2010, for calibration during partially saturated conditions. Note that the observation node for T3 was placed 5 cm lower than indicated from field measurements.

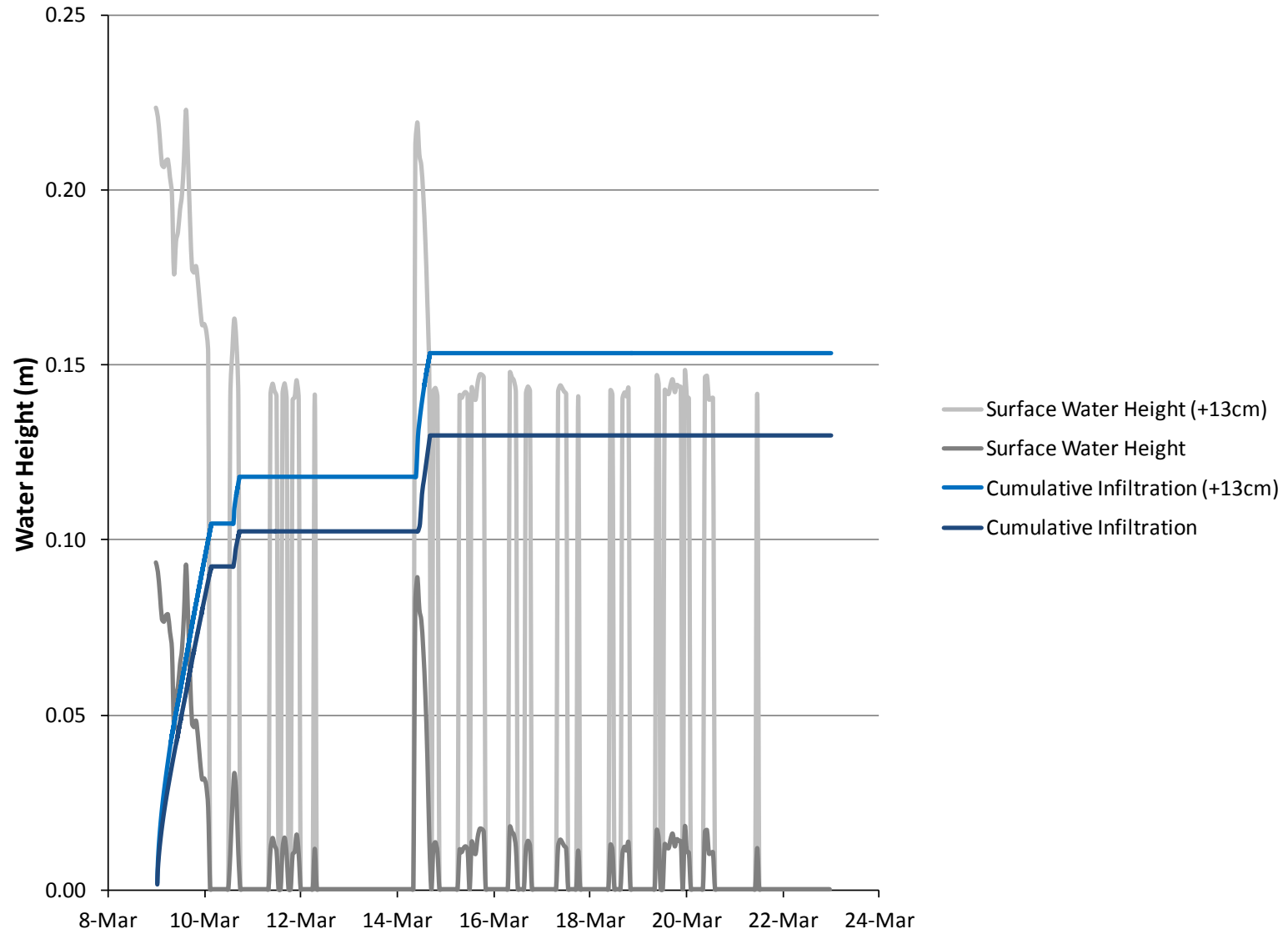


Figure 4.4.25 Cumulative infiltration (m) and the height of the water column at the surface for scenarios 1 and 2.

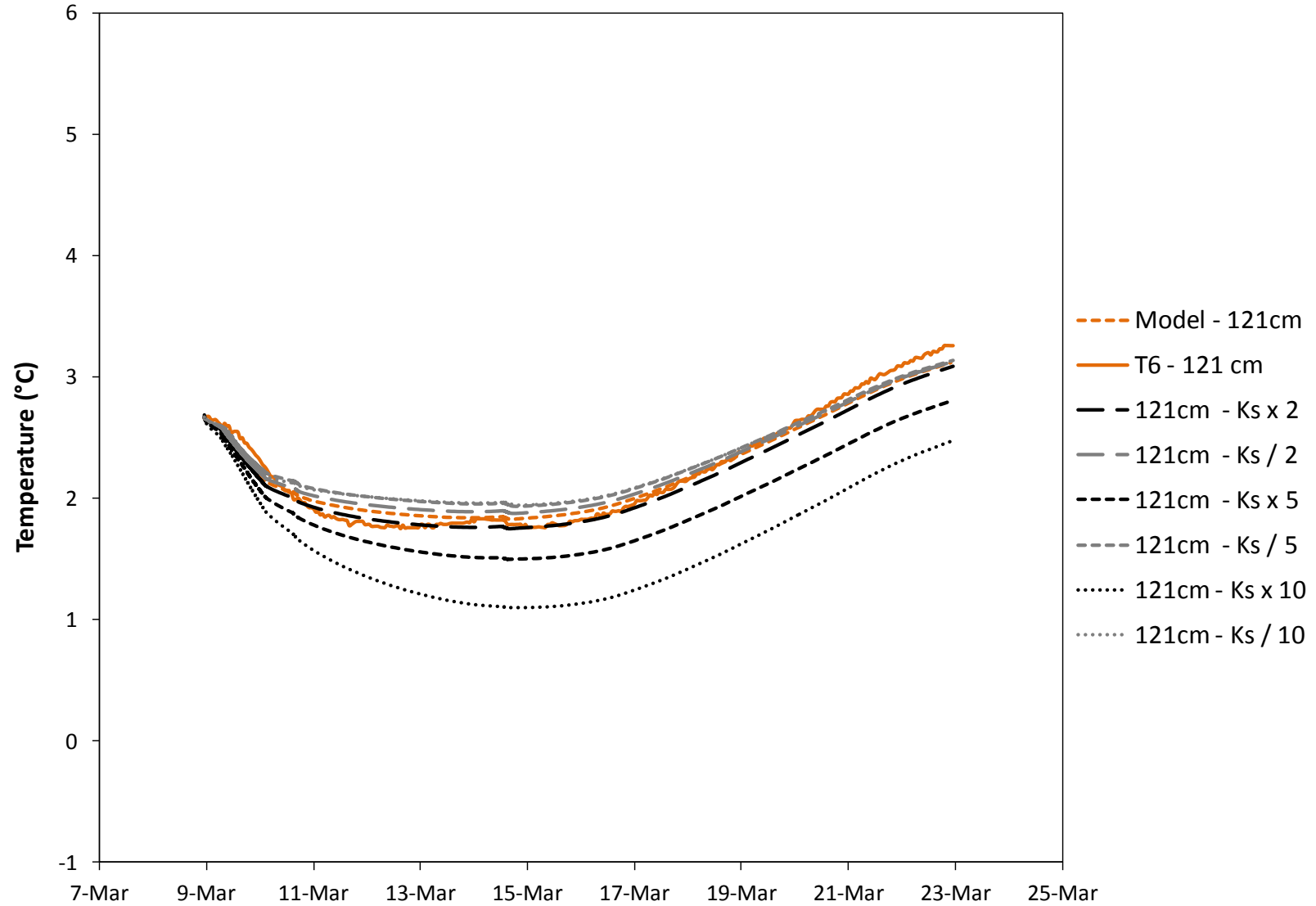


Figure 4.4.26 Example of Sensitivity Analysis Results on Simulated Soil Temperature (see Figure Q.29).

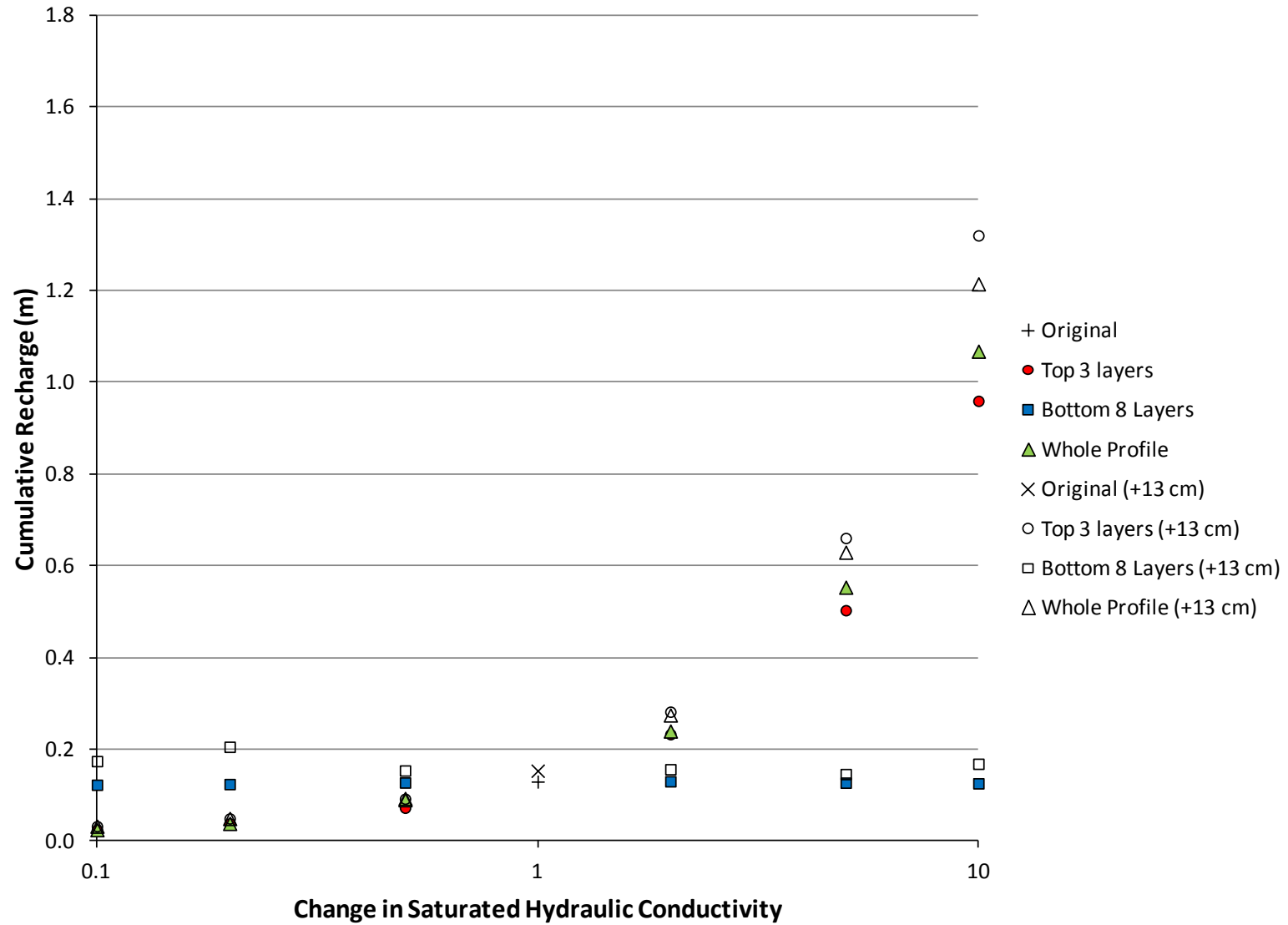


Figure 4.4.27 Change of saturated hydraulic conductivity vs. simulated cumulative infiltration for scenarios 1 and 2.

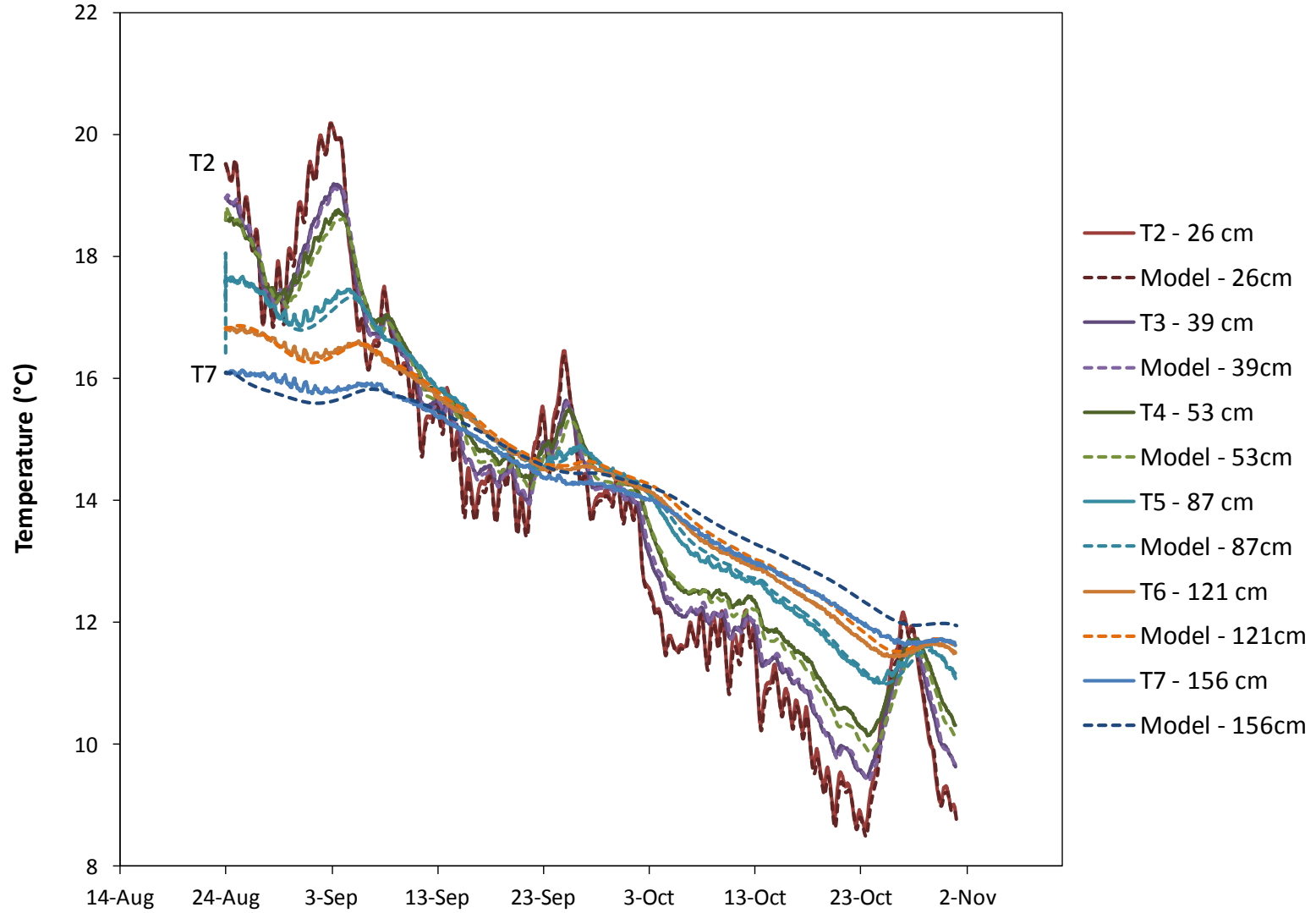


Figure 4.4.28 Simulated and observed temperature profiles between August 24th to October 31st, 2010 using the moisture retention parameters obtained from calibration when the ephemeral stream was present.

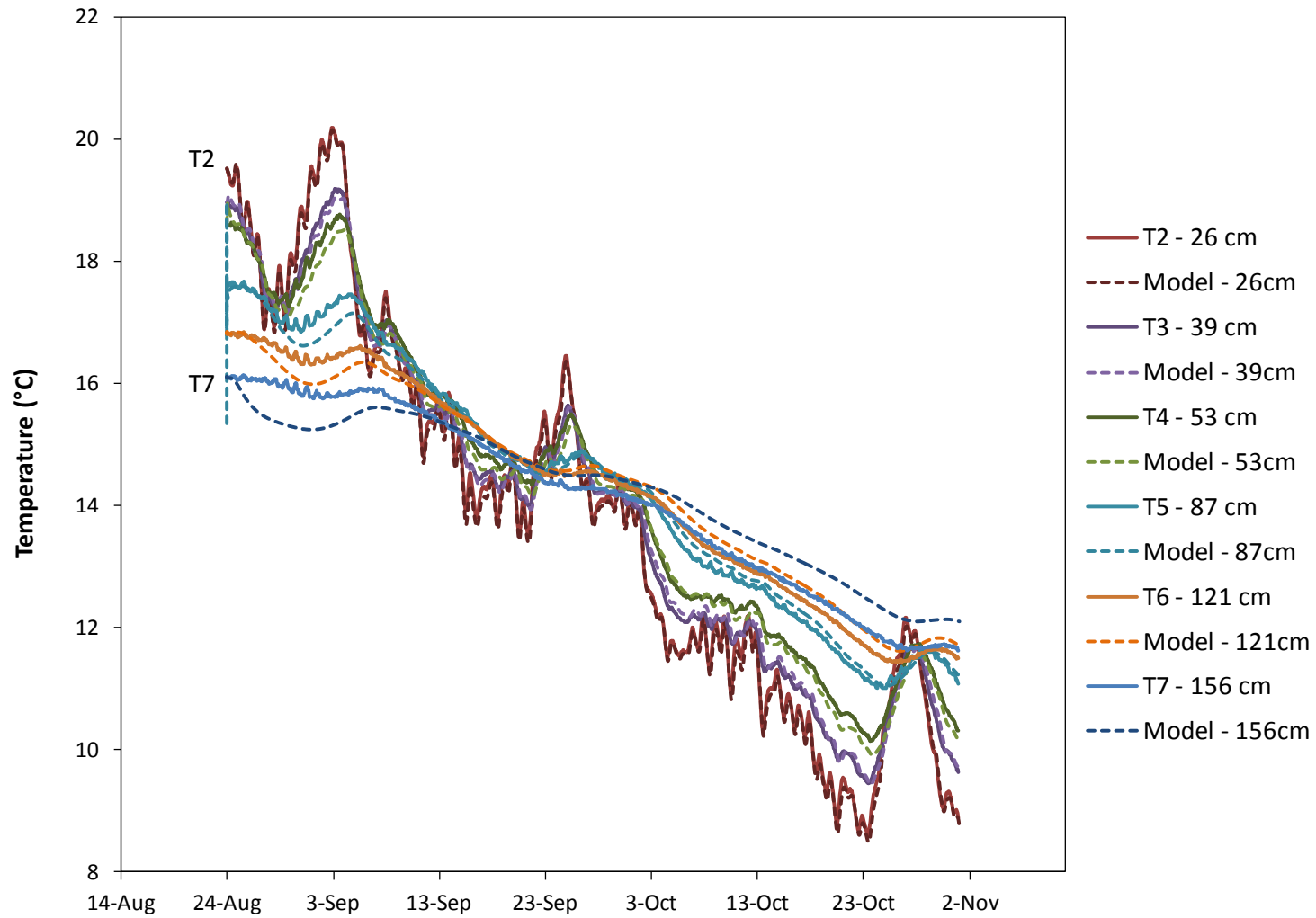


Figure 4.4.29 Simulated and observed temperature profiles between August 24th to October 31st, 2010 using altered moisture retention parameters obtained from calibration when the ephemeral stream was present by increasing the hydraulic conductivity of the lower eight layers by two.

4.5 Discussion

4.5.1 Field Monitoring

The field data collected yielded important information with regard to the nature of transient groundwater recharge during the spring melt period. Geochemical analyses of groundwater samples suggested that relatively rapid recharge occurred near and under the ephemeral stream, as dilution or displacement of the groundwater was observed in wells positioned in low lying areas where the near surface materials were relatively permeable. The regional hydraulic head and ground water temperature data aided in delineating general areas where higher rates of recharge were occurring, and helped pin point a time frame (March 9th and 10th and March 14th and 15th) during which recharge was expected to be the highest in vicinity of the soil temperature probes. This information assisted in the interpretation of transient temperature data collected from the vadose zone. The combined data suggested that higher rates of recharge were occurring in the northern portions of the field site near WO40.

During the spring melt period, changes in pressure and temperature were recorded beneath the ephemeral stream at WO37 after water had been ponded at the surface for a several days. Concurrent decreases in groundwater temperature, dilution of groundwater ionic concentrations and increases in water table levels at the site indicate that recharge of cold and relatively fresh water was occurring locally. This is supported by synchronous changes in temperature recorded by deep soil probes within the vadose zone at the same location. The evidence for localized recharge in the vicinity of the temperature probes presented promising conditions for simulating vertical advection of water from the surface downward during the spring melt.

4.5.2 Model Estimates

The model fit to the observed temperature profiles collected within the vadose zone was quite good at most depths for simulation periods considered in this study when the ephemeral stream was not present (April 12th to May 31st, 2010 and August 24th to October 31st, 2010). The fit was not as good at deeper points of observation, in particular T7 (152 cm below the ground surface), as the simulated temperatures diverged slightly from the observed temperature profiles. This is due to the difficulty in representing true soil conditions with the model, for in the field, soils are much less homogeneous and changes in soil properties are much more gradual than conditions used in the model. Overall, however, the model represented the field observed temperature data under conditions of gravity drainage very well.

The modeling of the highly transient temperature profiles collected in spring when the ephemeral stream was present was somewhat more challenging than for the periods discussed above. Although in general, the final simulations represented the transient temperature data collected throughout the vadose zone quite well, the goodness of fit reduced somewhat with depth in the profile.

Two scenarios were attempted to represent the upper pressure and flow boundary of the model as temperature and pressure measurements were not made at the same location. The pressure measurements of the stream depth were made at the surface where as temperature measurements used by the model were made 13 cm below the ground surface. Cumulative recharge estimated by the model between March 9th and 22nd for scenario 1 and 2 were 0.13 m and 0.15 m respectively, with the majority of the recharge occurring on March 9th, 10th and 14th (Figure 4.4.25). The difference between these two estimates is small, indicating that difference in placement between the surface instruments is unlikely to have had a substantial effect on the model results. The simulation produced from the unaltered set of parameters obtained from the calibration process for scenario 2 was selected as the most realistic and best fitting simulation. The final set of parameters was used to re-simulate the periods with gravity drained soils, and the simulated temperatures were found to fit the observed temperatures for these periods well. The ability of the model to simulate conditions of gravity drainage during different periods of time and different transient flow scenarios using a common set of parameters, suggests that the conceptual model and final model domain are representative of the actual field conditions and increase confidence in the uniqueness of the modeling results.

The recharge estimation of this simulation was 0.15 m. Compared to the recharge estimates by the bromide tracer, the model estimate matches recharge values calculated using the centre of mass of the bromide tracer more closely than those made using the peak concentration of bromide in the lower substrate. Total recharge estimated using the movement of the centre of mass between March 5th and May 6th, 2010 was 0.05 to 0.19 m and the estimate using the average water content measured by the neutron probe was 0.11 m (see Table 4.4.1). Given that the largest recharge event to occur between March 5th and May 6th is likely the spring melt, it is reasonable to assume that most of the recharge captured by the bromide tracer method occurred during the spring melt. It is worth noting, however, that the recovery of the tracer mass was quite low in May (only 3% of the applied tracer) and as such it is difficult to have a high degree of confidence in the recharge estimates based on the bromide data.

At a bromide site a few meters away, Koch (2009) estimated 0.34 m of recharge between January 8th and May 7th, 2008, using the centre of mass of the bromide tracer and average water content. Although this estimate is larger than the estimate made in this study for 2010, it is for a longer time period and the

author indicates that melt events occurred in January, February, March and April of that year and water levels in the stream had been higher in March of 2008 (see Figure 4.4.4). This suggests that the 2010 estimate may have a reasonable magnitude. Bekeris (2007) estimated a monthly recharge rate of 0.042 m/month between November 17th (or 18th), 2005 and May 8th, 2006 in the same area. This is equivalent to 0.24 m over that period assuming 30 days for a month. Bekeris' (2007) estimate also seems to indicate that the magnitude of the 2010 estimate during the melt event may be reasonable, assuming that it represented the largest recharge event during the test period. However, as was the case in the current study, Koch (2009) had very low recovery of the tracer in the May 2008 soil core (only 2.5%), and Bekeris (2007) also had a low recovery of the tracer in the May 2006 core (only 11%). Both these authors attributed the low recovery to lateral flushing of the soil (Koch, 2009; Bekeris; 2007), and despite the low recovery rates deemed that the resulting recharge estimates were not only reasonable but also the use of the bromide tracer was the best method they tested as it was based on physical data. Their assessment of their data lends support to the estimates made in this study. However, as there is no way to determine whether lateral flushing was the true cause of the low recovery rates, or whether the bulk of the bromide tracer was flushed through the soil vertically it is difficult to assess the accuracy of the results of bromide tracer tests.

Annual recharge was estimated by Koch (2009) and Bekeris (2007) based on bromide tracers as well as water balance models. Annual recharge was estimated to be 0.42 m by Koch (2009) between 2007 and 2008. Annual recharge was estimated to be 0.43 m by Bekeris (2007) between 2005 and 2006. Assuming that total annual recharge for the year 2010 was similar to previous years, the recharge estimated by the model of 0.15 m represents about a third of the total expected recharge for the year at this location. This illustrates that a large portion of the annual recharge in the vicinity of the ephemeral stream may occur during of short period of time. Further study is needed to assess the risk that this phenomenon may pose to the water supply at the Thornton Well Field. The spatial variability of recharge may be an important consideration in the assessment of the risk posed by this short lived event, as some locations (notably north of the instrumented site) demonstrate much higher rates of recharge. Work by Christie (n.d.) suggests that the impact may be worth investigating further as the stream was found to be a potential pathway for the transport of pathogens from the surface to groundwater, and correlated this with later occurrences of bacteria in the production wells.

4.5.3 Sources of Errors

It is difficult to perfectly represent field soil conditions in a model. Potential sources of error include both field measurements and errors associated with to the development of the conceptual model and the numerical model. With regard to the estimation of recharge using the bromide tracer, the low recovery of

the tracer represents a large source of error, as it is not possible to assess the accuracy of the measurements. Other field installations may have contributed to errors made in the course of this study; although all the field instruments are installed within several meters of each other, horizontal heterogeneity may have influenced the distribution of the assumed stratigraphic sequence that was adopted for the conceptual model of the subsurface conditions. Field measurements of moisture content may also have provided a source of error in places, particularly in the vicinity of the water table. The neutron probe provides the average water content of the soil in the vicinity in which the measurement is made, hence this type of measurement cannot precisely resolve sudden increases or decreases in water content as a result of changes in stratigraphy. Near surface measurements (above 0.3 m) made by the neutron probe were deemed to be unreliable, and are biased low because they incorporate the atmosphere, which reduces the water content estimate. As noted in Section 4.3.2.6, the level of the water table indicated by the transducer in WO37 was higher than would be suggested by the neutron probe measurements. This discrepancy could have been caused by a variety of factors including: errors in relative elevations between groundwater and moisture content measurements, inconsistencies in the measurement of moisture content by the neutron probe due to leaking into or condensation occurring in the casing, or differences in local stratigraphy. It could also be a combination of these sources of error. Despite this discrepancy, it was recognized that the height of the water table measured at WO37 was the best information available to approximate the height of the water table for the model.

One of the limitations within the numerical model was related to the simulation of moisture content profile in the numerical model. The lower layer had been subdivided in order to simulate the moisture content curve by slightly varying moisture retention parameters. Abrupt changes in moisture retention parameters at each unit interface influenced the shape of the simulated moisture content causing breaks in the curve. These changes would likely be more gradual in field soil conditions. These sharp parameter transitions likely affected the temperature profiles, subsequently impacting the ability to fit the simulation results with the field data. All these things considered, however, the simulation of temperature and cumulative recharge estimates is deemed to have produced reasonable results.

4.5.4 Temperature Probe Installations

One of the objectives of the study was to design a method of deploying the temperature probes which would allow them to make good contact with gravelly substrate without causing preferential pathways, and can allow for the retrieval of the instruments at a later date. The gravelly subsurface was of particular concern because it was thought that it would be more difficult to ensure that the probe would make good contact with soil (i.e., no air pockets around the temperature sensor) than in finer grained soils. Casing designed allowed the probes to be retrieved with relative ease without causing damage to the sensors. The

ability to match temperature variations over time with a physically consistent model (Hydrus 1-D) was one way of testing if the installation was successful. As this was accomplished, the casing design appears to be satisfactory. Another issue of concern is whether the installation of the casings resulted in preferential pathways. The temperatures observed at T4 between March 3rd and March 9th, as well as at T3 on March 3rd suggest preferential pathways exist; however, with the data at hand it is not possible to discern whether the preferential pathways are a product of poor installation of the casings or if there were simply macropores present in the soil where a probe happened to be installed.

4.6 Conclusions

This study examined recharge under an ephemeral stream. Recharge was estimated at one location within the path of the stream using temperature as a tracer. The use of temperature as a tracer for the movement of water is not, as of yet, a commonly used tool. The work presented here is unique in the setting and the season in which this tool was applied. To author's knowledge similar work has not been conducted on an ephemeral stream produced from melt events on soils that are initially frozen. The setting in which this study took place is also interesting because the site's proximity to drinking water supply wells and the nature of the hydrostratigraphy below the site.

The issue of rapid recharge was posed within the context of source water protection. Recharge was first assessed semi-quantitatively by monitoring changes in hydraulic head, temperature and water chemistry in a network of monitoring wells in the vicinity of the ephemeral stream. Large concurrent changes in hydraulic head and groundwater temperatures were noted in one well in the northern portion of the site, delayed perturbations in hydraulic head of similar shape but smaller magnitude in deep wells down gradient, suggest substantial recharge is occurring in the northern portion of the field site. Within the context of groundwater contamination, such a large recharge event may present a risk to supply wells as it is likely that water from the surface is able to reach the ground table, and then be pulled into the supply wells.

Concurrent change in temperature and head, albeit of a smaller magnitude, were also noted between March 9th and 10th as well as March 14th and 15th at the instrumented site where variations in recorded temperature were used to estimate recharge. The changes in groundwater temperature had the same shape and occurred concurrently with variation in temperature observed in the vadose zone. An indication that recharge was occurring locally at this site during this period.

The model was able to simulate changes in temperature that matched observed temperature for different periods of time and under different flow scenarios, suggesting that the model is representative of the actual field conditions and increasing confidence in the uniqueness of the model results. A recharge estimate of 0.15 m was generated by the model for the instrumented site between March 9th and 22nd, 2019. Most of the recharge occurred between March 9th and 10th and between March 14th and 15th. This estimate was compared to a recharge estimate made using a bromide tracer applied within the path of the stream as well as estimated made in previous studies for the same location. The bromide estimate was found to be similar to the estimate made by the model; however, the consistently low recovery of the tracer made it difficult to assess the accuracy of these estimates.

Although it is difficult to assess the precision of the recharge estimate made by the model, the estimate attained is deemed to be reasonable. Within the context of annual recharge at the site, this amount of recharge during such a short period of time may represent approximately one third of the total annual recharge at this location compared to previous estimates of annual recharge estimates made by others.

Overall the goals and objectives set out at the beginning of the study were met. Field monitoring yielded insight into spatial and temporal variability of groundwater recharge at the site. Temperature was simulated with success, and produced reasonable estimates of groundwater recharge indicating that detailed tracking of transient temperature in the vadose zone beneath an ephemeral stream can be used to illustrate recharge dynamics and also to permit quantitative estimates of transient groundwater recharge phenomena. The use of an advanced modeling tool is a key aspect of this result.

4.7 Recommendations

Some modifications to the current methodology could be adopted in future studies at this site in order to obtain more accurate and representative estimates of recharge under an ephemeral stream. Three aspects of the current methodology which improvement could be made include: matching the field soil conditions, errors associated with the bromide tracer, and recharge only being assessed at one location even though there is evidence of spatial variability.

With regard to matching the field soil conditions, some improvement to the data collection could be made. All the monitoring equipment could be placed closer together. In this study for example, the moisture content measurements were taken at a location that was not directly in the path of the stream in 2010, which meant that measurements taken during the spring melt were not necessarily representative of the moisture conditions under the stream. As a result, the moisture content measurements were not compared to simulated results. More precise and frequent measurements of moisture content could be made using time domain reflectometers plugged into data loggers. These could be placed strategically, for example at the boundary between visually distinct soil layers.

The difficulty in choosing appropriate soil parameters could be lessened with a more thorough site investigation. Soil moisture parameters could be measured for soil at different depths using intact soil cores to determine van Genuchten parameters and porosity. Grain size analyzes could also be conducted.

With regard to the use of the bromide tracer, adaptations to the current methodology could improve the field based estimates to which the model is compared. This could include re-coring the bromide plot immediately after standing water is no longer present at the site, which would allow the model to be compared to the tracer over the same time period. Another adaption could be to include solution samplers

or instruments that measure pore-water conductivity in conjunction with a chemical tracer, this information could be valuable in assessing whether the low recovery of the tracer is due to lateral flushing, or whether the bulk of the tracer was flushed vertically.

Lastly, expanding the study to assess recharge at several locations in and around the ephemeral stream would allow for a better understanding of the total recharge at the site during the spring melt. As mentioned previously, recharge may be spatially variable over the site.

Chapter 5

Overall Conclusions

This thesis presents two interrelated studies completed at the same field site which consider issues related to source water protection on agricultural lands. The first study focuses on the source of potential ground water contaminants, nitrate; the second considers recharge dynamics which allow surface contaminants to migrate into groundwater sources. The combined results provide insight into several of the key factors influencing the protection of groundwater sources within the agricultural landscape.

A one year experiment that compares three different fertilizer applications (conventional spring applied urea, spring applied polymer-coated urea, and early summer applied side-dressing) either with or without a clover cover crop was completed in a part of the field site with gently sloping topography. The experiment found that both the timing and the rate of nitrogen fertilizer application impacted the amount of nitrate detected below the rooting zone after one year. Synthetic fertilizers which delay the release of nitrogen to plants (polymer-coated urea and side-dress) were found to lose less nitrate to the subsurface compared to treatments that did not (conventional urea). The rate of fertilizer application was also found to affect the amount of the nitrate lost to the subsurface; a high-rate side-dress treatment was found to have much higher concentrations (more than double that of some treatments) of nitrate below the rooting zone compared to treatments which had received a nitrogen application recommended by the OMAFRAs corn calculator. The study did not find that the addition of clover had higher risk of nitrate leaching.

With the exception of the control treatments, corn yield were similar between treatments. As these were similar, the two main factors that differentiated treatments regarding their economic output in this study were the cost of the fertilizer (synthetic fertilizer or clover seed) and the cost of increased passes over the fields. The treatments that received a combination synthetic fertilizer and clover residue were found to have a better economic return compared to treatments that had only received synthetic fertilizers. This is because of the reduced cost of seed compared to synthetic fertilizer for equivalent nitrogen application rates. Fields that received clover economized between \$67.40/ha and \$100.65/ha of nitrogen fertilizer, depending on the treatment, using the OMAFRA corn calculator as a guide. The polymer-coated urea treatments were found to have relatively lower economic returns due to the higher cost of this fertilizer (13% higher compared conventional urea). The conventional spring applied urea had higher returns compared to the side-dress treatments because of the reduced cost associated with fewer passes over the

field despite a reduced fertilizer application rate with side-dressing (a difference of \$22.28/ha in the clover field and \$29.64/ha in the no clover field).

Environmental conditions and time management factors into the decisions that farmers make with regard to choosing a nitrogen management plan that maximizes their economic output. There are limitations to some of the BMPs discussed above: clover crops may not take, site conditions may not allow a farmer to apply side-dressing within the optimum window for corn growth, or there may be time demands that make treatments requiring extra passes on a field less desirable. Such limitation need to be considered; therefore, it is important to consider that farmers need to have choices available to them so they make the best decisions with regards to the environmental conditions of a particular year while maintaining crop yields and reducing environmental risk.

Groundwater monitoring at the site over the years has identified interesting recharge dynamics, particularly in the vicinity of an ephemeral stream which develops annually during spring and winter melt events in a low lying area of the study site. The ephemeral stream was observed at the site between March 5th and March 10th of 2010. Recharge was assessed semi-quantitatively by monitoring changes in hydraulic head, temperature and water chemistry in a network of monitoring wells in the vicinity of the ephemeral stream. Large concurrent changes in hydraulic head and groundwater temperatures were noted in one well in the northern portion of the site. Delayed perturbations in hydraulic head of similar shape but smaller magnitude in deep wells down gradient, suggest substantial recharge is occurring in the northern portion of the field site. Freshening of the groundwater was noted in wells located near the ephemeral stream. These observations suggest that recharge is spatially variable along the length of the stream, and that a potentially significant volume of water recharge north of the instrumented site.

The computer model Hydrus 1-D (Šimůnek et al., 1999) was used to numerically analyze spatially and temporally transient groundwater temperature data beneath the ephemeral stream during the spring melt event and during conditions when the ephemeral stream was absent. Model parameters were first calibrated by simulating periods when it was expected that soils would be gravity drained with minimal soil water flow, and then further refined by simulating the period when the ephemeral stream was present. A final set of parameters was determined, and periods with gravity drained soils were re-simulated. The model was able to simulate different periods of time and different flow scenarios using the final set of parameters, suggesting that the conceptual model and final model domain representative of the actual field conditions. The successful simulation under the different flow scenarios also increases confidence in the uniqueness of the model results. A recharge estimate of 0.15 m was generated by the model for the instrumented site between March 9th and 22nd, 2019. Most of the recharge occurred between March 9th

and 10th and between March 14th and 15th. Although it is difficult to assess the precision of the recharge estimate made by the model, the estimate attained is deemed to be reasonable. Within the context of annual recharge at the site, this amount of recharge during such a short period of time may represent approximately one third of the total annual recharge at this location compared to previous estimates of annual recharge estimates made by others. The study found that the use of temperatures as a tracer provided useful and quantifiable insight into recharge phenomena. The results of this study suggest that high rates of rapid recharge occur beneath the ephemeral stream, and are spatially variable. This type of focused infiltration that occurs during the spring melt may represent a risk to municipal water quality if the infiltrating waters are carrying contaminants.

References

- Addiscott, T.M., A.P. Whitmore and D.S. Powlson. 1991. *Farming, Fertilizers and the Nitrogen Problem*. Harpenden, UK: CAB International
- Alva, A.V. 1992. Differential leaching of nutrients from soluble vs. controlled-release fertilizers. *Environmental Management* 16, 769-776
- American Society for Testing and Materials (ASTM). 2006. *D2487-06, Standard Practice for Classification of Soils for Engineering Purposes (Unified Soil Classification System)*.
- Anderson, M.J. 2005. Heat as a Ground Water Tracer. *Groundwater*, 43, 6:951-967
- Azam, F., K.A. Malik and M.I. Sajjad. 1985. Transformations in soil and available to plants of ¹⁵N applied as inorganic fertilizer and legume residues. *Plant and Soil* 86,1-13
- Bekeris, L. 2007. Field-scale Evaluation of Enhanced Agricultural Management Practices using a Novel Unsaturated Zone Nitrate Mass Load Approach. Master's Thesis, Waterloo, Ontario: Department of Earth Sciences, University of Waterloo.
- Blaylock, A.D., J. Kaufmann, and R.D. Dowbenko. 2005. *Nitrogen fertilizer technologies*. In: Proceedings, Western Nutrient Management Conference. Salt Lake City, UT. 6: 8-13.
- Burkart, M.R. and J.D. Stoner. 2002. Nitrate in aquifers beneath agricultural systems. *Water Science and Technology* 45, 19-29
- Cassman, K.G., A. Dobermann and D.T. Walters. 2002. Agroecosystems, Nitrogen-use Efficiency, and Nitrogen Management. *Ambio* 31, 132-140
- Campbell, C.A., G.P. Lafond, R.P. Zentner and Y.W. Jame. 1994. Nitrate leaching in a Udic Haploboroll as influenced by fertilization and legumes. *Journal of environmental quality* 23, 1:195-201
- Christie, M., n.d. *Monitoring the Occurrence of Microbes Within a Well Head Protection Area in an*

- Agricultural Setting*, Unpublished M. Sc. Thesis, Waterloo, Ontario: Department of Earth Sciences, University of Waterloo.
- Clark, M.S., W.R. Horwath, C. Shennan, and K.M. Scow. 1998. Changes in soil chemical properties resulting from organic and low-input farming practices. *Agronomy Journal* 90, 662-671
- Clark, S., K. Klonsky, P. Livingston, and S. Temple. 1999. Crop-yield and economic comparisons of organic, low-input, and conventional farming systems in California's Sacramento Valley. *American Journal of Alternative Agriculture* 14, 109-121
- Cole, J. 2008. Quantification of the long-term effects from nutrient reductions on groundwater nitrate concentrations in an agricultural setting. Master's Thesis, Waterloo, Ontario: Department of Earth Sciences, University of Waterloo.
- Constantz J. and C. L. Thomas. 1996. The use of streambed temperature profiles to estimate the depth, duration, and rate of percolation beneath arroyos. *Water Resources Research* 32, 12:3597-3602
- Constantz, J., M.J. Cox, and G.W Su. 2003a. Comparison of heat and bromide as groundwater tracers near streams. *Groundwater*. 41, 5:647-656
- Constantz. J., S.W. Tyler, and E. Kwicklis. 2003b. Temperature-profile methods for estimating rates in arid environments. *Vadose Zone Journal*. 2:12-24
- Constantz, J. 2008. Heat as a tracer to determine streambed water exchanges. *Water Resources Research* 44, W00D10, doi:10.1029/2008WR006996
- Cowan, W.R. 1975. Quaternary geology of the Woodstock area, Southern Ontario. Geological Report 119, Ontario Division of Mines, Ministry of Natural Resources.
- County of Oxford GIS. 2005. County of Oxford Map Your Farm. Retrieved from: <http://maps.county.oxford.on.ca/mapyourfarm>
- Crews, T.C. and M.B. Peoples. 2004. Legume versus fertilizer sources of nitrogen: ecological tradeoffs and human needs. *Agriculture, Ecosystems and Environment* 102, 279-297

- Crews, T.C. and M.B. Peoples. 2005. Can the synchrony of nitrogen supply and crop demand be improved in legume and fertilizer-based agroecosystems? A review. *Nutrient Cycling in Agroecosystems* 72, 101-120
- Critchley, C.E. 2010. *Stimulating In Situ Denitrification in an Aerobic Highly Conductive Municipal Drinking Water Aquifer*. Master's Thesis, Waterloo, Ontario: Department of Earth Sciences, University of Waterloo
- de Marsily, G. 1986. *Quantitative Hydrogeology*, London: Academic Press.
- de Vries, D. A. 1963. The thermal properties of soils, In *Physics of Plant Environment*, ed. R. W. van Wijk, 210-235. Amsterdam: North-Holland
- Dinnes, D.L., D.L. Karlen, D.B. Jaynes, T.C. Kaspar, J.L. Hatfield, T.S. Colvin and C.A. Cambardella. 2002. Nitrogen management strategies to reduce nitrate leaching in tile-drained Midwestern soils. *Agronomy Journal* 94, 1:153–171.
- Drinkwater, L.E., P. Wagoner and M. Sarrantonio. 1998. Legume-based cropping systems have reduced carbon and nitrogen losses. *Nature* 396, 262-265.
- Du, C., J. Zhou and A. Shaviv. 2006. Release characteristics of nutrients from polymer-coated compound controlled release fertilizers. *Journal of Polymer Environment* 14, 223-230
- Dwyer, L.M., B.L. Ma, D.W. Stewart, H. N. Hayhoe, D. Balchin, J. L. B. Culley, and M. McGovern. 1996. Root mass distribution under conventional and conservation tillage. *Canadian Journal of Soil Science* 76, 23–28
- Environment Canada. 2011. National Climate data and Information Archive. Canadian Climate Normals 1971-2000. Woodstock, Ontario. Retrieved from http://www.climate.weatheroffice.gc.ca/climate_normals/results_e.html?stnID=4835&lang=e&dCode=1&StationName=WOODSTOCK&SearchType=Contains&province=ALL&provBut=&month1=0&month2=12

- Fetter, C.W. 2001. *Applied Hydrogeology*, 4th Edition. Upper Saddle River, New Jersey: Prentice Hall.
- Freeze, R.A. and J.A. Cherry. 1979. *Groundwater*. Englewood Cliffs, New Jersey: Prentice Hall.
- Gentile, R., B. Vanlauwe, P. Chivenge, J. Six. 2008. Interactive effects from combining fertilizer and organic residue inputs on nitrogen transformations. *Soil Biology and Biochemistry* 40, 2375-2384
- Groffman, P.M., P.F. Hendrix and D.A. Crossley JR. 1987. Nitrogen dynamics in conventional and no-tillage agroecosystems with inorganic fertilizer of legume nitrogen inputs. *Plant and Soil* 97, 315-332
- GOCorn.net. n.d. GOCorn.net Growing Ontario's Corn. Retrieved from <http://www.gocorn.net/>
- Goss, M.J., D.A.J. Barry, and D.L. Rudolph. 1998. Contamination in Ontario farmstead domestic wells and its association with agriculture: 1. Results from drinking water wells. *Journal of Contaminant Hydrology* 32,3-4: 267-293
- Haderlein, L., T.L. Jensen, R.E. Dowbenko and A.D. Blaylock. 2001. Controlled release urea as a nitrogen source for spring wheat in western Canada: Yield, Grain N Content, and N use efficiency. *The Scientific World* 1, 114-121
- Hanway, J.J. 1962. Corn growth and composition in relation to soil fertility: II. Uptake of N, P, and K and their distribution in different plant parts during the growing season. *Agronomy Journal* 54,217-222
- Hanway, J.J. 1963. Growth Stages of Corn (zea mays, L.). *Agronomy Journal* 55, 487-492
- Harris, G.H. and O.B. Hesterman. 1990. Quantifying and nitrogen contribution from alfalfa to soil and two succeeding crops using nitrogen-15. *Agronomy Journal* 82, 129-134
- Harris, G.H., O.B. Hesterman, E.A. Paul, S.E. Peters and R.R. Janke. 1994. Fate of legume and fertilizer nitrogen-15 in a long-term cropping systems experiment. *Agronomy Journal* 86, 910-915
- Haslauer, C.P. 2005. *Hydrogeologic Analysis of a Complex Aquifer System and Impacts of Changes in*

- Agricultural Practices on Nitrate Concentrations in a Municipal Well Field: Woodstock, Ontario.* Master's Thesis, Waterloo, Ontario: Department of Earth Sciences , University of Waterloo.
- Hauck, R.D. 1985. Slow-Release and Bioinhibitor-Amended Nitrogen Fertilizer. In *Fertilizer Technology and Use*, 3rd Edition. Ed R.C. Dinauer, S. Ernst and J.J. Mortvedt. Madison, Wisconsin: Soil Science of America, Inc.
- Hay, R.E., E.B. Earley and E.E. DeTurk. 1953. Concentration and translocation of nitrogen compounds in the corn plant (zea mays) during grain development. *Plant Physiology* 28, 606-621
- Hyatt, C.R., R.T. Venterea, C.J. Rosen, M. McNearney, M.L. Wilson and M.S. Dolan. 2010. Polymer-coated urea maintains potato yields and reduces nitrous oxide emissions in a Minnesota loamy sand. *Soil Science Society of America Journal* 74, 419-428
- Janzen, H.H., J.B. Bole, V.O. Biederbeck and A.E. Slinkard. 1990. Fate of N applied as green manure or ammonium fertilizer to soil subsequently cropped with spring wheat at three sites in western Canada. *Canadian Journal of Soil Science* 70, 313-323
- Jung P.E., L.A. Peterson and L.E. Schrader. 1972. Response of Irrigated Corn to time, rate, and source of applied N on sandy soils. *Agronomy Journal* 64, 5:668-670
- Koch, J.T. 2009. *Evaluating Regional Aquifer Vulnerability and BMP Performance in an Agricultural Environment Using A Multi-Scale Data Integration Approach.* Master's Thesis, Waterloo, Ontario: Department of Earth Sciences , University of Waterloo.
- Kramer, A.W., T.A. Doane, W.R. Horwarth, and C. van Kessel. 2002a. Combining fertilizer and organic inputs to synchronize N supply in alternative cropping systems in California. *Agriculture, Ecosystems and Environment* 91, 233-243
- Kramer, A.W., T.A. Doane, W.R. Horwarth, and C. van Kessel. 2002b. Short-term nitrogen-15 recovery vs. long-term total soil N gains in conventional and alternative cropping systems. *Soil Biology and Biochemistry* 34, 43-50
- Ladd, J.N. and M. Amato. 1986. The fate of nitrogen from legume and fertilizer sources in sils

- successively cropped with wheat under field conditions. *Soil Biology and Biochemistry* 18, 417-425.
- Lautz, L. K., Kranes N.T. and Siegel D.I. 2010. Heat tracing of heterogeneous hyporheic exchange adjacent to in-stream geomorphic features. *Hydrological Processes*. 24: 3074-3086
- LeMonte, J.L., T.W. Taysom, B.G. Hopkins, V.D. Jolley and B.L. Webb. 2009. *Residual soil nitrate and potato yield with polymer coated urea*. In: Proceedings, Western Nutrient Management Conference. Salt Lake City, Utah. 8:77-78
- Mikkelsen, R.L., H.M. Willams and A.D. Behel Jr. 1994. Nitrogen leaching and plant uptake from controlled-release fertilizers. *Fertilizer Research* 37, 43-50
- Moore, J.A. 2008. *Comparison of ESN, urea, and aqua ammonia as sources of nitrogen for corn production in Iowa*. Master's Thesis. Ames, Iowa: Iowa State University
- Mualem, Y. 1976. A new model for predicting the hydraulic conductivity of unsaturated porous Media. *Water Resource Research* 12, 3:513-522
- Muriuki, A.W., L.D. King and R.J. Volk. 2007. Nitrogen-15 recovery in cropped soil cores fertilizers with potassium nitrate and clover residues. In *Advances in Intergrated Soil Fertility Management in Sub-Saharan Africa: Challenge Opportunities*. ed Bationo, A., B. Waswa, J. Kihara and J. Kimetu. 379-388. Springer
- Nelson, L.B. 1956. The mineral nutrition of corn as related to its growth and culture. *Advances in Agronomy* 8, 321-375
- Nelson, K.A., S.M. Paniagua and P.P. Motavalli. 2009. Effect of polymer coated urea, irrigation, and drainage of nitrogen utilization and yield of corn in a claypan soil. *Agronomy Journal* 101, 681-687
- Niswonger, R. G. and Prudic, D. E. 2005. Modeling heat as a tracer to estimate streambed seepage and

- hydraulic conductivity. In *Heat as a tool for studying the movement of ground water near streams*. Ed. D.A. Stonestrom and J. Constantz, 81-89. USGS Circular 1260. Reston, Virginia: USGA
- Noellsch, A.J., P.P. Motavalli, K.A. Nelson, and N.R. Kitchen. 2009. Corn response to conventional and slow-release nitrogen fertilizers accross a claypan landscape. *Agronomy Journal* 101, 607-614
- Ontario Ministry of Agriculture, Food and Rural Affairs (OMAFRA). 2011. Corn: Fertility Management. In *Agronomy Guide*. Retreived from <http://www.omafra.gov.on.ca/english/crops/pub811/1fertility.htm#nitrate>
- Ontario Ministry of Agriculture, Food and Rural Affairs (OMAFRA). 2011. Guide Corn: Leaf Stages. In *Guide to Weed Control*. Retrieved from <http://www.omafra.gov.on.ca/english/crops/pub75/9stages.htm#introduction>
- Owens, L.B., W.M. Edwards and R.W. Van Keuren. 1994. Groundwater nitrate levels under fertilized grass and grass-legume pastures. *Journal of Environmental Quality* 23, 752-758
- Padusenko, G. 2001. Regional Hydrogeologic Evaluation of a Complex Glacial Aquifer System in an Agricultural Landscape: Implications for Nitrate Distribution. Master's Thesis, Waterloo, Ontario: Department of Earth Sciences , University of Waterloo.
- Paramasivam, S. and A. Alva. 1997. Nitrogen Recovery from Controlled-Release Fertilizers under intermittent leaching and dry cyles. *Soil Science* 162, 6: 447-453
- Power, J.F. and J.S. Schepers. 1989. Nitrate contamination of groundwater in North America. *Agriculture, Ecosystems and Environment* 26,165-187
- Pumphrey, F.V. and L. Harris. 1956. Nitrogen fertilizer for corn production on an irrigated Chestnut soil. *Agronomy Journal* 48, 207-212
- Reddy, G.B. and K.R. Reddy. 1993. Fate of nitrogen-15 enriched ammonium nitrate applied to corn. *Soil Science Society of America Journal* 57, 111-115

- Ruselle, M.P., R.D. Hauck and R.A. Olson. 1983. Nitrogen accumulation rates of irrigated maize. *Agronomy Journal* 75,4:593-595
- Sayre, J.D. 1948. Mineral accumulation in corn. *Plant Physiology* 23, 267-281
- Scanlon, B. R., R.W. Healy, and P.G. Cook. 2002. Choosing appropriate techniques for quantifying groundwater recharge. *Hydrogeology Journal* 10, 18-39.
- Schaap, M. 2003. Rosetta help file: Predicting soil hydraulic parameter from basic soil data. Rosetta Lite Version 1.1. George E. Brown Jr. Salinity Laboratory and UC Riverside, Department of Environmental Sciences
- Shaviv, A. 2005. Environmental friendly nitrogen fertilization. *Science in China Series C: Life Sciences* 48, 937-947
- Slichter, C.S. 1905. Field measurements of the rate of movement of underground waters. Water-Supply and Irrigation Paper No. 140. Washington, DC: USGS
- Šimůnek, J., M. Šejna, H. Saito, M. Sakai, and M. Th. van Genuchten. 2008. The HYDRUS-1D Software Package for Simulating the Movement of Water, Heat, and Multiple Solutes in Variably Saturated Media, Version 4.08, *HYDRUS Software Series 3*, Riverside, California: Department of Environmental Sciences, University of California Riverside
- Sinclair, T.R. and K.G. Cassman. 1999. Green revolution still too green. *Nature* 398, 556
- Smil, V. 1999. Nitrogen in crop production: An account of global flows. *Global Biogeochemical Cycles* 13, 647-662
- Smil, V. 2001. Enriching the Earth, Fritz Haber, Carl Bosch, and the Transformation of World Food Production. Cambridge, Massachusetts: The MIT Press
- Sophocleous, M. 1979. Analysis of water and heat flow in unsaturated-saturated porous media, *Water Resource Research* 15, 5:1195-1206.

- Spalding, R.F. and M.E. Exner. 1993. Occurrence of nitrate in groundwater - a review. *Journal of Environmental Quality* 22, 392-402
- Stonestrom, D.A. and J. Constantz. 2005. Heat as a tracer of water movement near streams. In *Heat as a tool for studying the movement of ground water near streams*. Ed. D.A. Stonestrom and J. Constantz, 81-89. USGS Circular 1260. Reston, Virginia: USGA
- Stopes, C., E.I. Lord, L. Philipps and L. Woodward. 2002. Nitrate leaching from organic farms and conventional farms following best practice. *Soil Use and Management* 18, 256-263
- Stute, J.K., J.L. Posner. 1995. Synchrony between legume nitrogen release and corn demand in the upper Midwest. *American Society of Agronomy* 87, 6:1063-1069
- Tilman, D. 1998. The greening of the green revolution. *Nature* 396, 211-212
- Trenkel, M.E. 1997. *Improving fertilizer use efficiency: controlled-release and stabilizer fertilizer in agriculture*. Paris, France: International Fertilizer Industry Association
- Tufekcioglu, A., J. W. Raich, T. M. Isenhardt and R. C. Schultz. 1999. Fine root dynamics, coarse root biomass, root distribution, and soil respiration in a multispecies riparian buffer in Central Iowa, USA. *Agroforestry Systems* 44, 163-174
- van Genuchten, M. Th., 1980. A closed-form equation for predicting the hydraulic conductivity of unsaturated soils. *Soil Science Society of America Journal* 44, 892-898
- Varco, J.J., W.W. Frye, M.S. Smith and C.T. MacKown. 1989. Tillage effects on nitrogen recovery by corn from a N15-labelled legume cover crop. *Soil Science Society of America Journal* 53, 822-827
- Vitousek, P.M., J.D. Aber, R.W. Howarth, G.E. Likens, P.A. Matson, D.W. Schindler, W.H. Schlesinger and D.G. Tilman. 1997. Human alteration of the global nitrogen cycle: sources and consequences. *Ecological Applications* 7, 737-750
- Ward, A. L and R.S. Wittman. 2009. *Calibration of a neutron hydroprobe for moisture measurements in*

- Waddell, J.T. S.C. Gupta, J.F. Moncrief, C.J. Rosen, and D.D. Steele. 1999. Irrigation and nitrogen management effects on potato yield, tuber quality, and nitrogen uptake. *Agronomy Journal* 91,6:991-997
- Wang, F.L., A.K. Alva. 1996. Leaching of nitrogen from slow-release urea sources in sandy soils. *Soil Science Society of America Journal* 60, 1454-1458
- Welch, L.F., D. L. Mulvaney, M.G. Oldham, L.V. Boone and J.W. Pendleton. 1971. Corn yields with fall, spring, and sidedress nitrogen. *Agronomy Journal* 63, 119-123
- Wendt, S. 2005. Hydraulic parameter investigation and ID-modelling of water flow and solute transport in the vadose zone of the Thornton well field in Woodstock, Ontario, Canada. Student Project in Hydrogeology, Waterloo, Ontario: Department of Earth Sciences , University of Waterloo.
- Wilson, M.L., C.J. Rosen and J.F. Moncrief. 2010. Effects of polymer-coated urea on nitrate leaching and nitrogen uptake by potato. *Journal of Environmental Quality* 39, 492-499
- Yeh, G.T. and H.-P. Cheng, 1999. 3DHYDGEORGEOCHEM: A 3-dimensional model of density-dependent subsurface flow and thermal multispecies-multicomponent HYDROGEOCHEMical transport. EPA/6000/R-98/159, 150p.
- Zvomuya, F., C.J. Rosen, M.P. Ruselle and S.C. Gupta. 2003. Leaching and nitrogen recovery following application of polyolefin-coated urea to potato. *Journal of Environmental Quality* 32, 480-489

Appendix A

Time Line of Field Sampling Efforts and Equipment Installation

May 5th, 2009 - Starter Nitrogen

May 5th, 2009 - Corn planted

May 5th, 2009 – Application of conventional and polymer-coated urea

May 25th and 26th, 2009 - Deep cores collected

May 25th, 2009 - Installation of the neutron access tube

June 16th, 2009 - Bromide application

June 19th, 2009 - Sidedress fertilizer application

November 11th, 2009 - Corn Harvest

November 13th, 2009 - Neutron Access tube buried

December 1st, 2009 - Deep cores collected

May 3rd and May 4th, 2010 - Deep cores collected

May 7th, 2010 - Neutron Access tube unburied

Appendix B

Shallow Core Nitrate Data

No Clover Plot

Clover Plot

Table B.1 Shallow core nitrate concentration (mg NO₃-N/kg soil) data from the no clover plot.

		25-May-09	15-Jun-09	7-Jul-09	27-Jul-09	12-Aug-09	26-Aug-09	15-Sep-09	16-Oct-09	13-Nov-09
1NC	Plot 1	17.31	65.30	66.90	20.96	11.13	5.32	6.52	4.81	6.62
	Plot 2	19.46	44.33	24.17	15.05	20.06	9.73	4.31	4.41	4.91
	Plot 3	23.20	26.08	45.14	8.83	5.42	7.12	3.81	3.51	5.02
	avg	19.99	45.24	45.40	14.95	12.20	7.39	4.88	4.24	5.52
	std	2.98	19.63	21.37	6.07	7.38	2.22	1.44	0.67	0.96
2NC	Plot 1	22.72	23.57	42.63	23.27	8.53	5.72	0.90	3.11	4.11
	Plot 2	61.37	26.88	41.02	7.22	6.72	5.02	3.81	3.71	5.42
	Plot 3	57.00	58.48	103.61	53.56	8.93	21.46	8.32	14.64	17.85
	avg	47.03	36.31	62.42	28.02	8.06	10.73	4.34	7.15	9.13
	std	21.17	19.27	35.68	23.53	1.18	9.30	3.74	6.49	7.58
3NC	Plot 1	6.37	20.20	7.42	4.01	7.42	4.91	2.31	3.11	4.61
	Plot 2	22.01	29.33	67.20	37.51	7.22	13.04	11.23	14.64	16.95
	Plot 3	11.85	14.82	10.53	9.83	4.41	8.02	4.71	2.41	3.81
	avg	13.41	21.45	28.38	17.12	6.35	8.66	6.08	6.72	8.46
	std	7.94	7.34	33.65	17.90	1.68	4.10	4.62	6.87	7.37
4NC	Plot 1	13.35	25.78	25.78	6.62	7.02	21.66	7.82	16.15	12.24
	Plot 2	24.56	24.75	15.05	7.62	23.57	11.43	10.43	5.32	10.83
	Plot 3	8.84	12.23	12.24	32.00	7.42	21.77	28.79	7.92	14.74
	avg	15.58	20.92	17.69	15.41	12.67	18.29	15.68	9.80	12.60
	std	8.09	7.54	7.15	14.37	9.44	5.94	11.43	5.65	1.98
5NC	Plot 1	7.91	13.94	10.93	6.32	4.81	3.21	0.70	2.01	4.21
	Plot 2	14.61	16.15	11.13	3.81	6.22	2.91	3.01	2.41	3.71
	Plot 3	25.44	23.27	27.98	6.52	6.12	4.31	3.61	4.71	7.02
	avg	15.99	17.79	16.68	5.55	5.72	3.48	2.44	3.04	4.98
	std	8.85	4.88	9.79	1.51	0.79	0.74	1.54	1.46	1.78

1 - Polymer Coated Urea

2 - Conventional Urea

3 - Calculator Rate Side-Dress

4 - High Rate Side-Dress

5 - Control

NC - No Clover

C - Clover

Table B.2 Shallow core nitrate concentration (mg NO₃-N/kg soil) data from the clover plot.

		25-May-09	15-Jun-09	7-Jul-09	27-Jul-09	12-Aug-09	26-Aug-09	15-Sep-09	16-Oct-09	13-Nov-09
1C	Plot 1	26.78	44.23	38.72	19.26	5.72	5.52	6.92	5.52	8.02
	Plot 2	25.18	23.87	23.47	11.63	14.74	5.82	3.51	5.82	6.72
	Plot 3	27.68	41.73	21.46	12.34	4.51	5.62	1.10	6.52	7.02
	avg	26.55	36.61	27.88	14.41	8.32	5.65	3.84	5.95	7.25
	std	1.27	11.10	9.44	4.22	5.59	0.15	2.92	0.51	0.68
2C	Plot 1	39.63	26.28	25.18	11.03	8.12	7.42	3.01	5.12	5.32
	Plot 2	37.41	26.28	41.02	14.34	17.05	4.61	3.91	5.82	5.52
	Plot 3	47.84	34.50	26.28	23.07	12.74	5.02	9.63	7.42	6.22
	avg	41.63	29.02	30.83	16.15	12.64	5.68	5.52	6.12	5.69
	std	5.49	4.75	8.84	6.22	4.47	1.52	3.59	1.18	0.47
3C	Plot 1	14.94	27.75	10.33	5.52	5.32	10.03	3.41	4.31	9.53
	Plot 2	29.09	29.28	17.15	8.93	8.22	4.61	1.81	7.22	5.42
	Plot 3	34.60	25.94	20.26	10.63	12.24	5.32	7.52	6.52	8.63
	avg	26.21	27.66	15.91	8.36	8.59	6.65	4.25	6.02	7.86
	std	10.14	1.67	5.08	2.60	3.48	2.95	2.95	1.52	2.16
4C	Plot 1	19.36	21.69	31.49	19.06	46.54	5.02	35.41	16.85	6.92
	Plot 2	21.46	42.66	24.57	24.77	70.61	25.98	38.72	19.66	28.39
	Plot 3	23.97	33.89	14.34	7.02	9.43	7.92	50.55	7.12	22.17
	avg	21.60	32.75	23.47	16.95	42.19	12.97	41.56	14.54	19.16
	std	2.31	10.53	8.63	9.06	30.82	11.36	7.96	6.58	11.05
5C	Plot 1	17.57	27.08	20.86	8.63	4.91	7.02	4.91	4.71	6.92
	Plot 2	23.27	43.93	15.95	7.42	10.33	3.11	3.01	4.61	6.32
	Plot 3	22.97	38.92	16.45	9.13	4.31	3.61	1.30	5.32	5.32
	avg	21.27	36.64	17.75	8.39	6.52	4.58	3.07	4.88	6.19
	std	3.21	8.65	2.70	0.88	3.32	2.13	1.81	0.38	0.81

1 - Polymer Coated Urea
2 - Conventiona Urea
3 - Calculator Rate Side-Dress
4 - High Rate Side-Dress
5 - Control

NC - No Clover
C - Clover

Appendix C

Soil Core Profiles

Soil Nitrate Concentration, Gravimetric Water Content, Pore-water Concentration and Bulk Density

Polymer-Coated Urea

Spring 2009, Fall 2009, Spring 2010

Conventional Urea

Spring 2009, Fall 2009, Spring 2010

Calculator Rate Side-dress

Spring 2009, Fall 2009, Spring 2010

High Rate Side-dress

Fall 2009, Spring 2010

Control

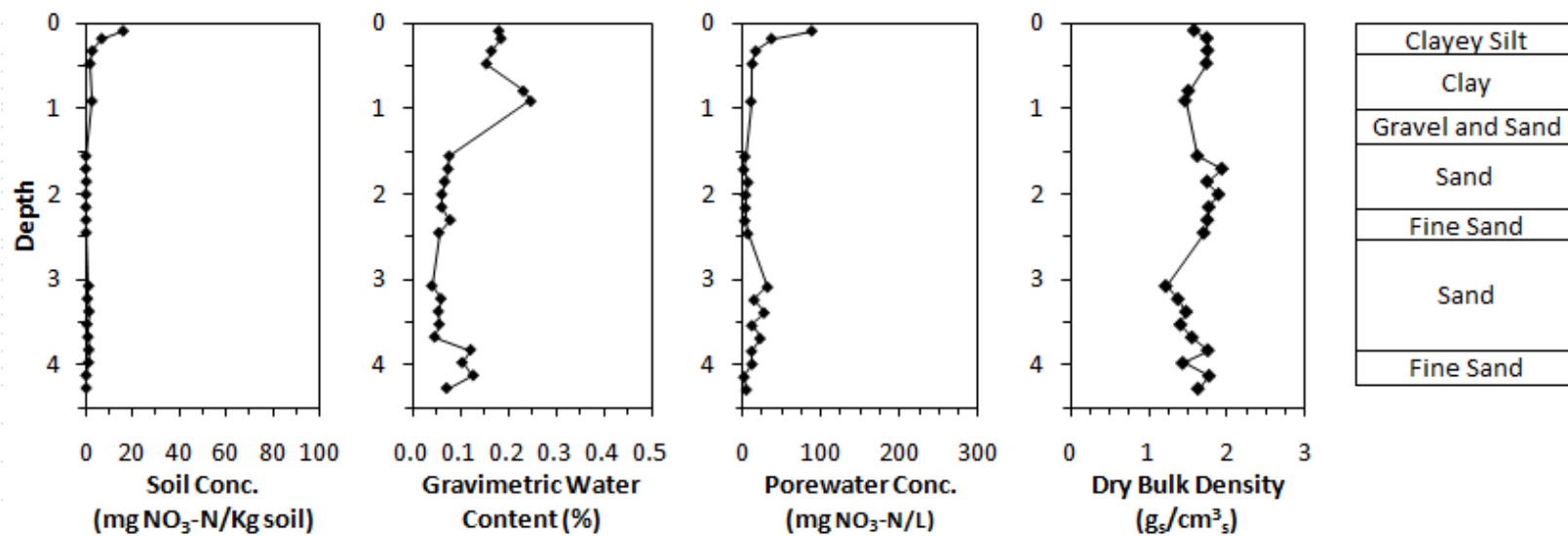
Spring 2009, Fall 2009, Spring 2010

Soil Bromide Concentration, Gravimetric Water Content and Bulk Density

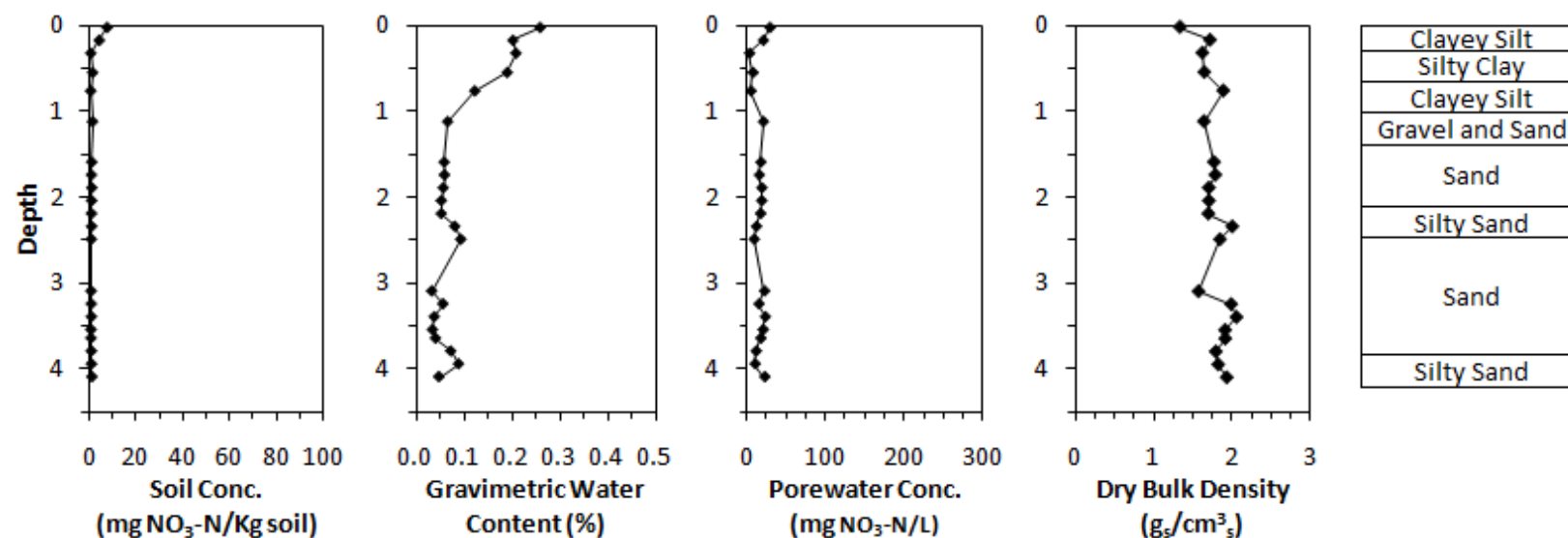
Bromide Plot

Fall 2009, Spring 2010

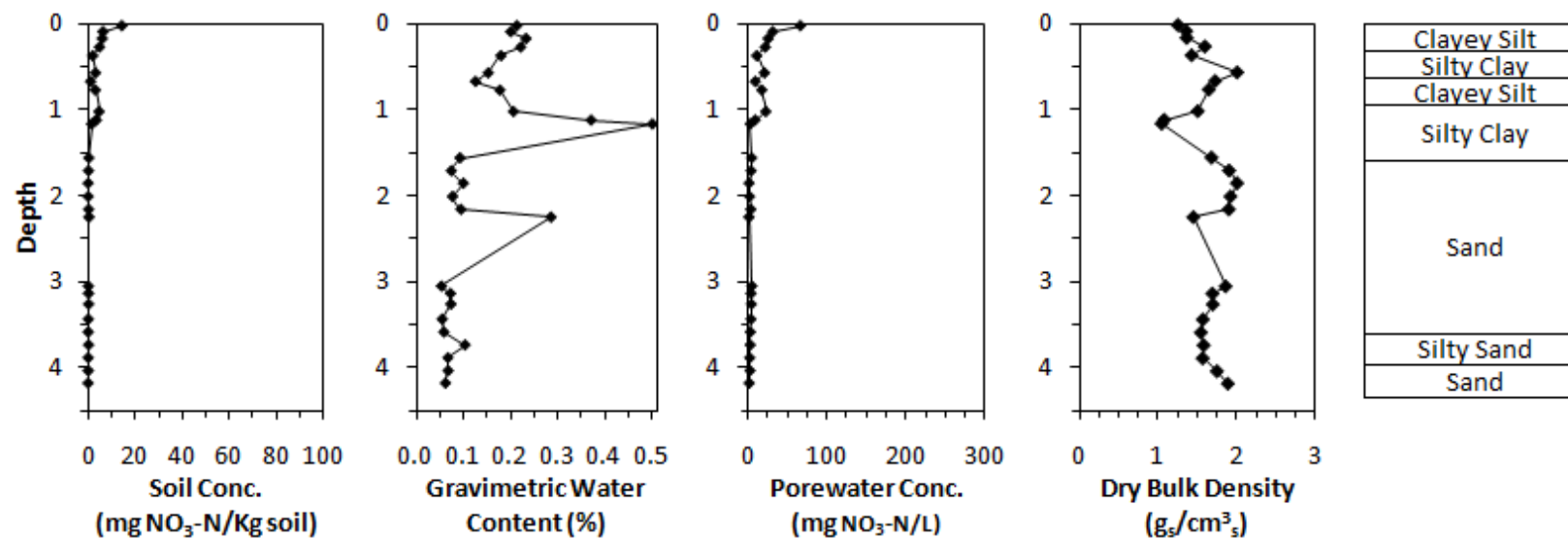
Figure C.1 Profiles of soil nitrate concentration, gravimetric soil water content, pore-water nitrate concentration and dry bulk density from cores collected from the polymer coated urea treatment in the no clover block collected in a) May 2009, b) December 2009 and c) May 2010.



(a)

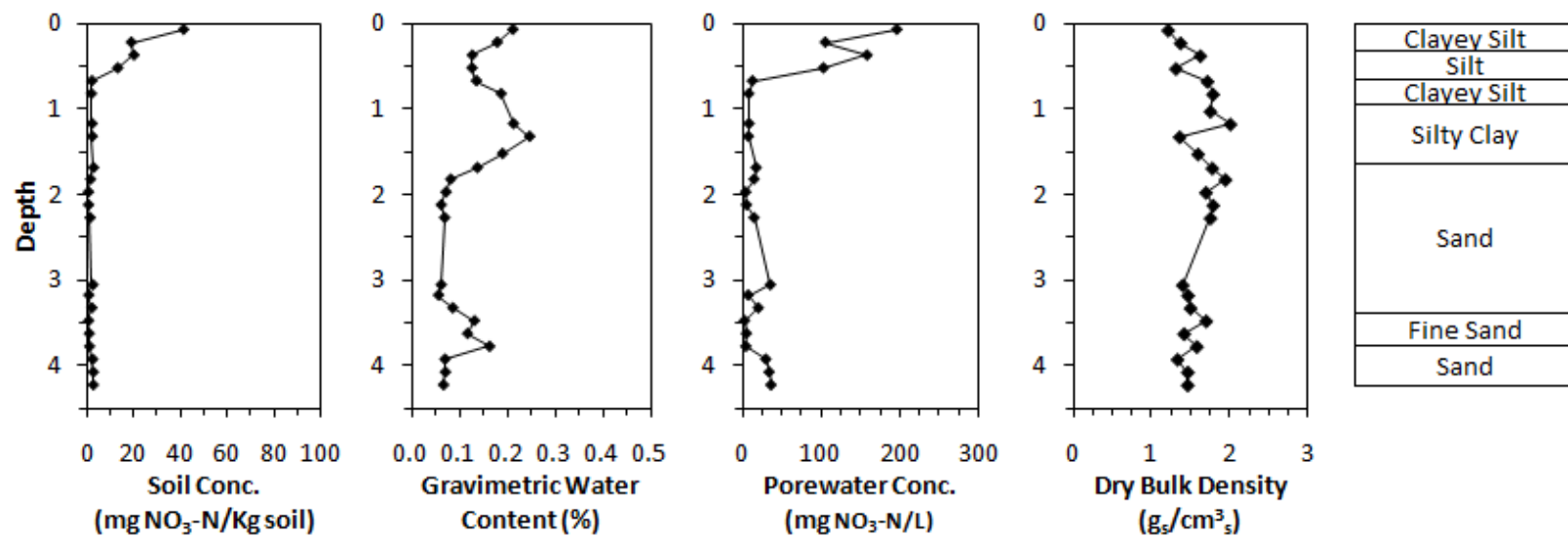


(b)

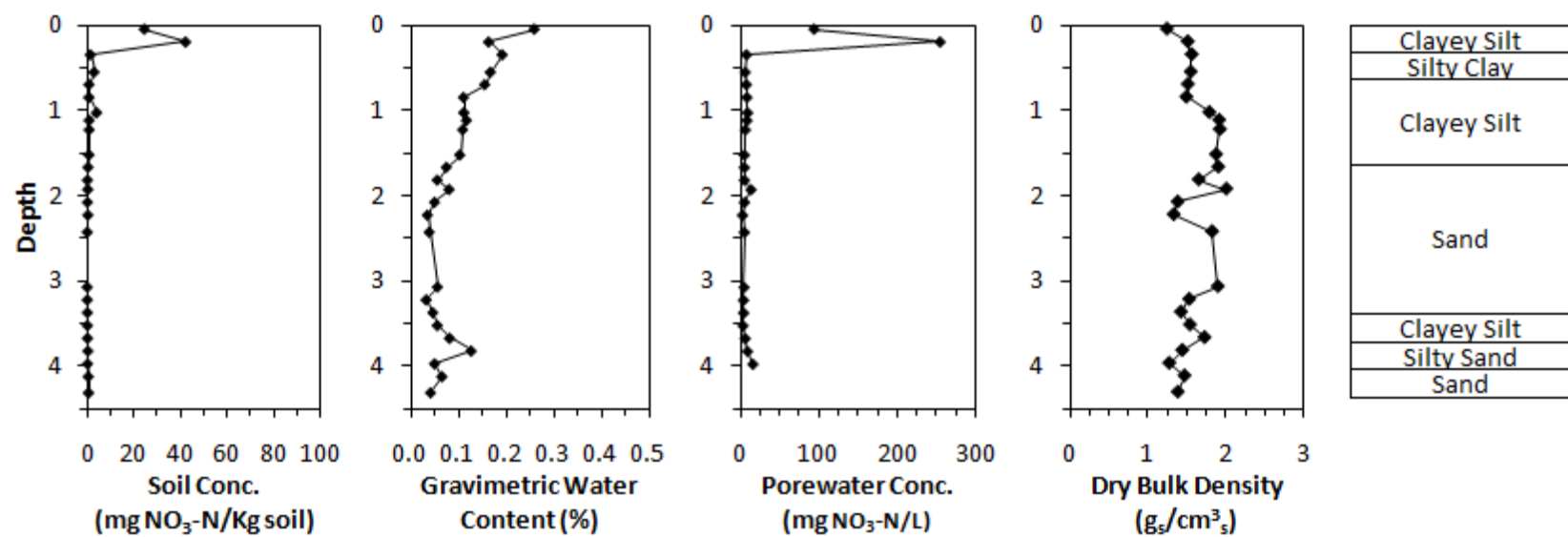


(c)

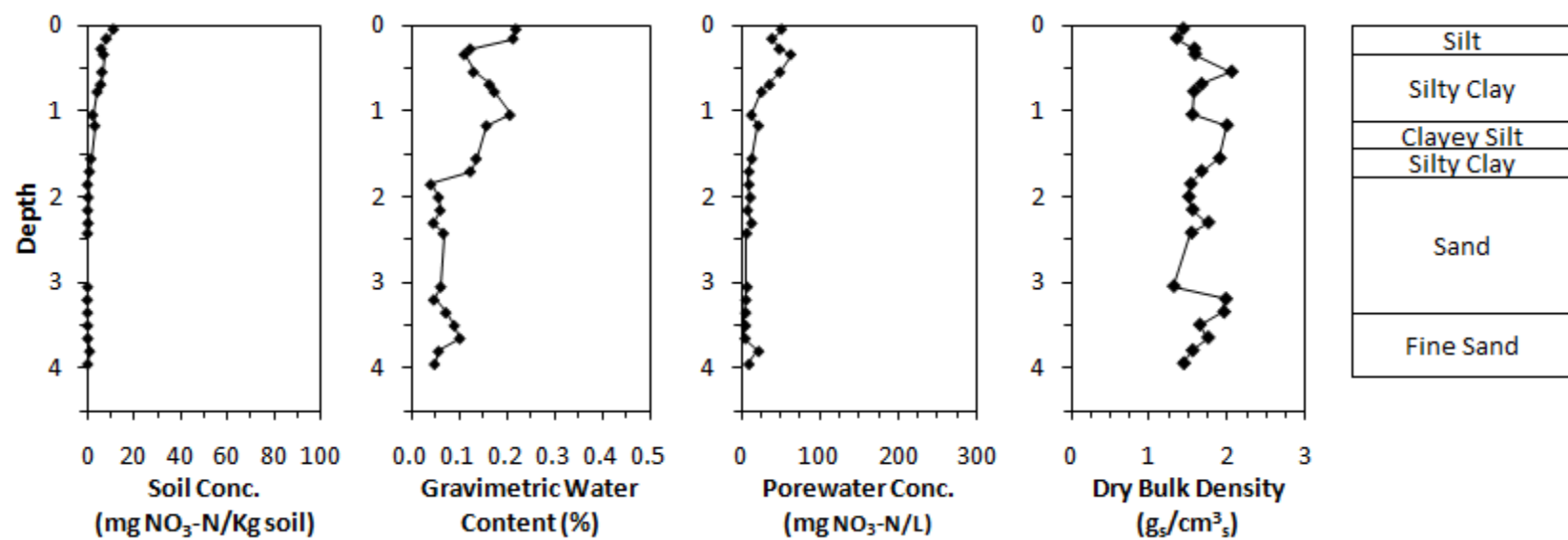
Figure C.2 Profiles of soil nitrate concentration, gravimetric soil water content, pore-water nitrate concentration and dry bulk density from cores collected from the conventional urea in the no clover block collected in a) May 2009, b) December 2009 and c) May 2010.



(a)

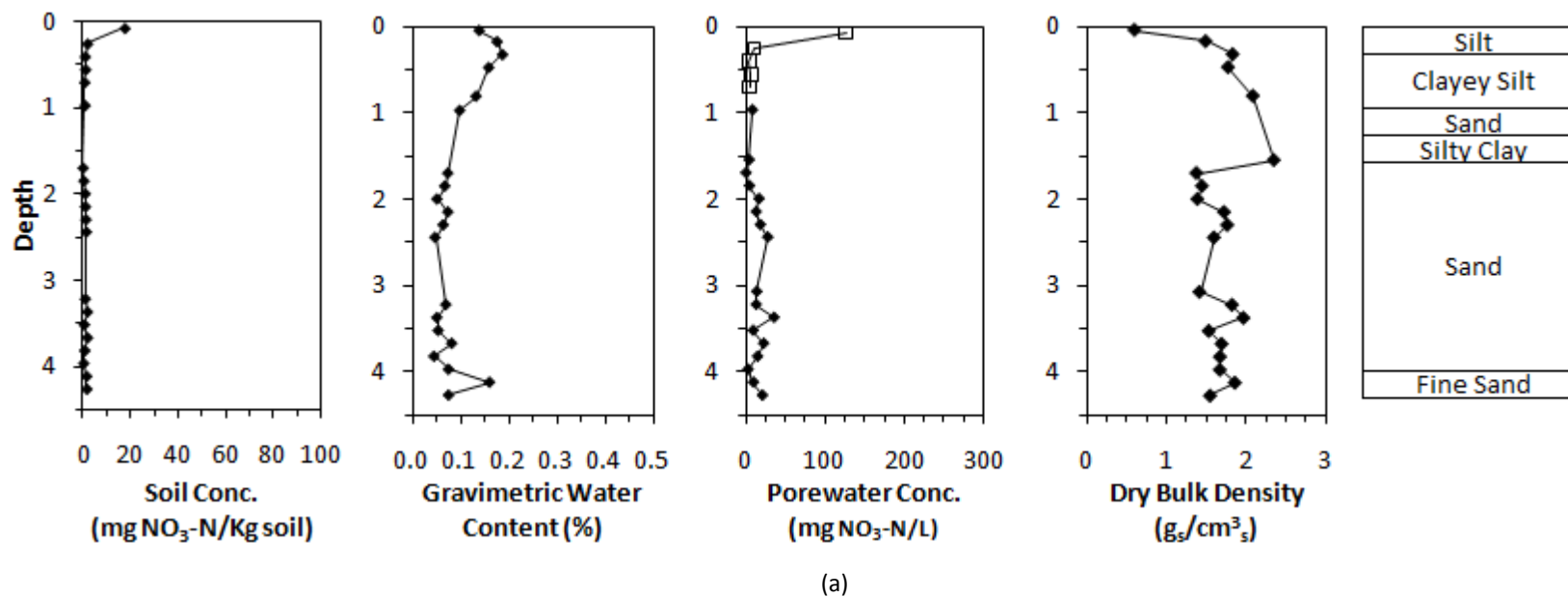


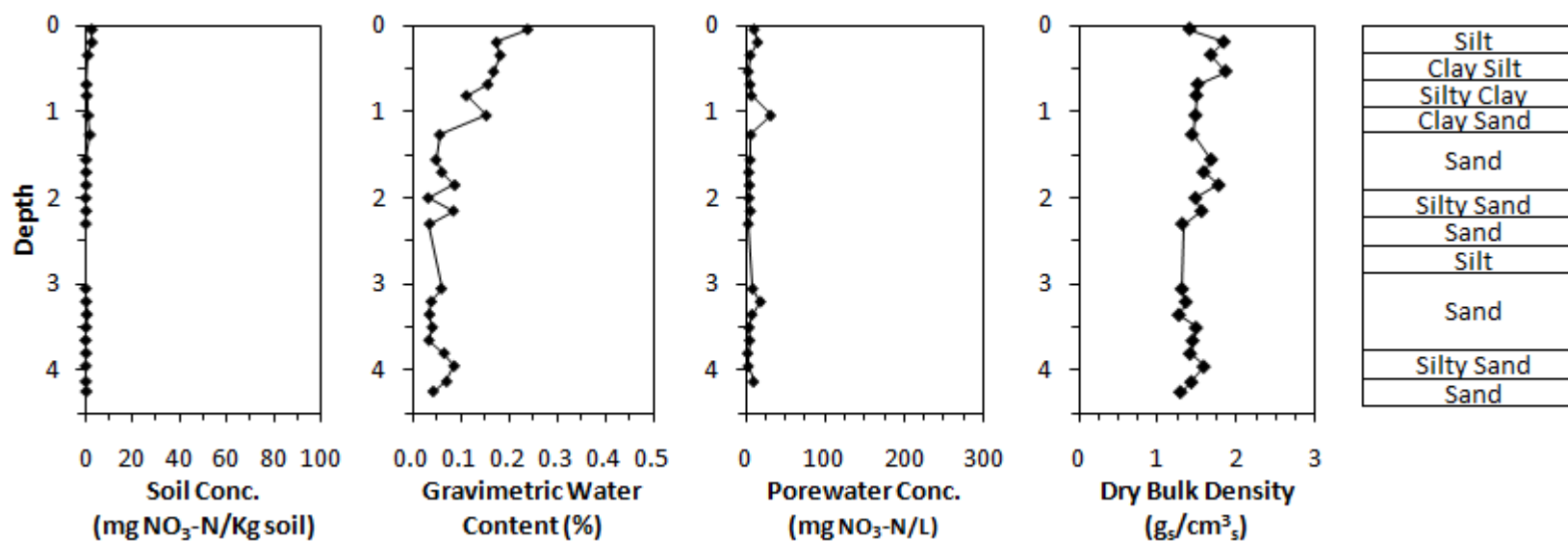
(b)



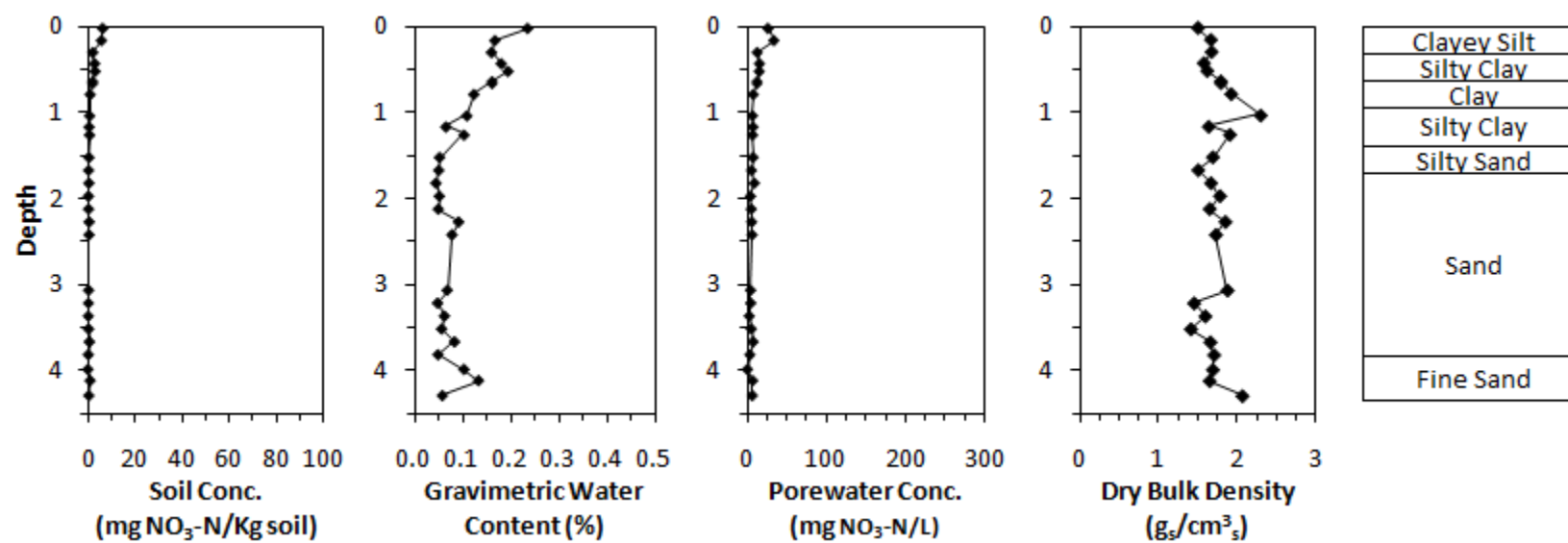
(c)

Figure C.3 Profiles of soil nitrate concentration, gravimetric soil water content, pore-water nitrate concentration and dry bulk density from cores collected from the calculator rate side-dress treatment in the no clover block collected in a) May 2009, b) December 2010.



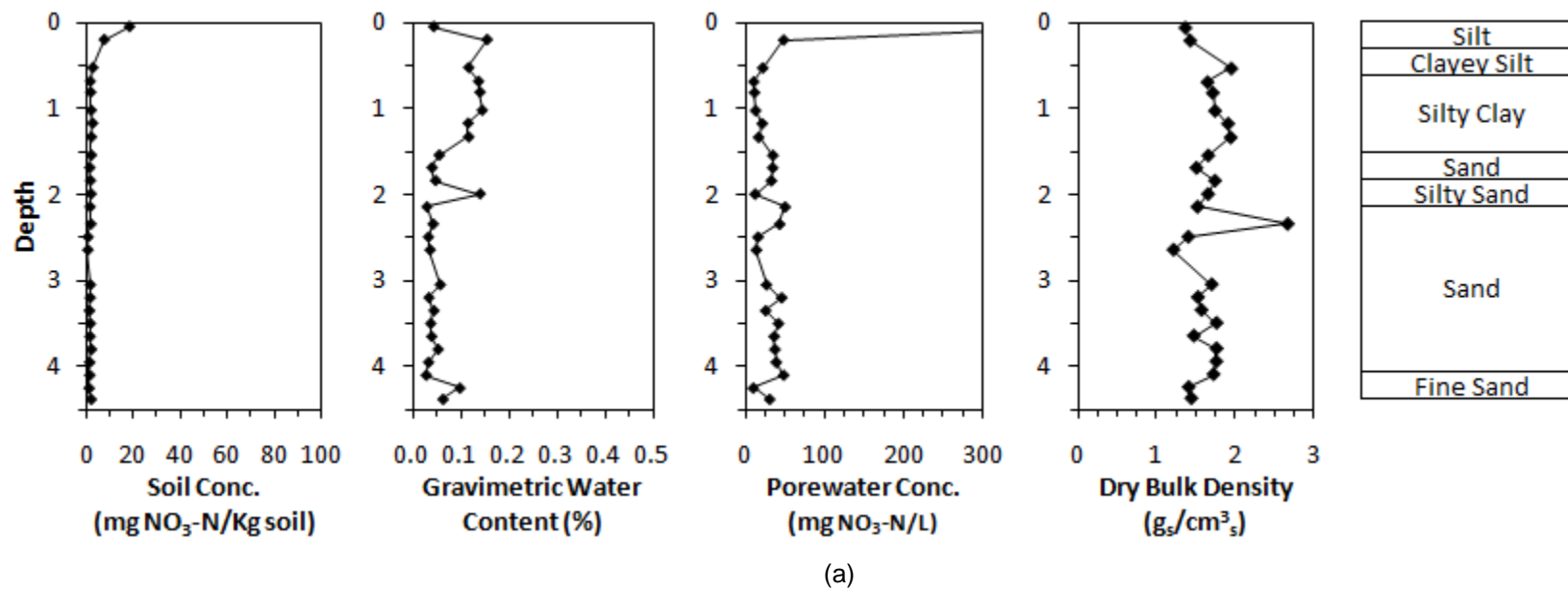


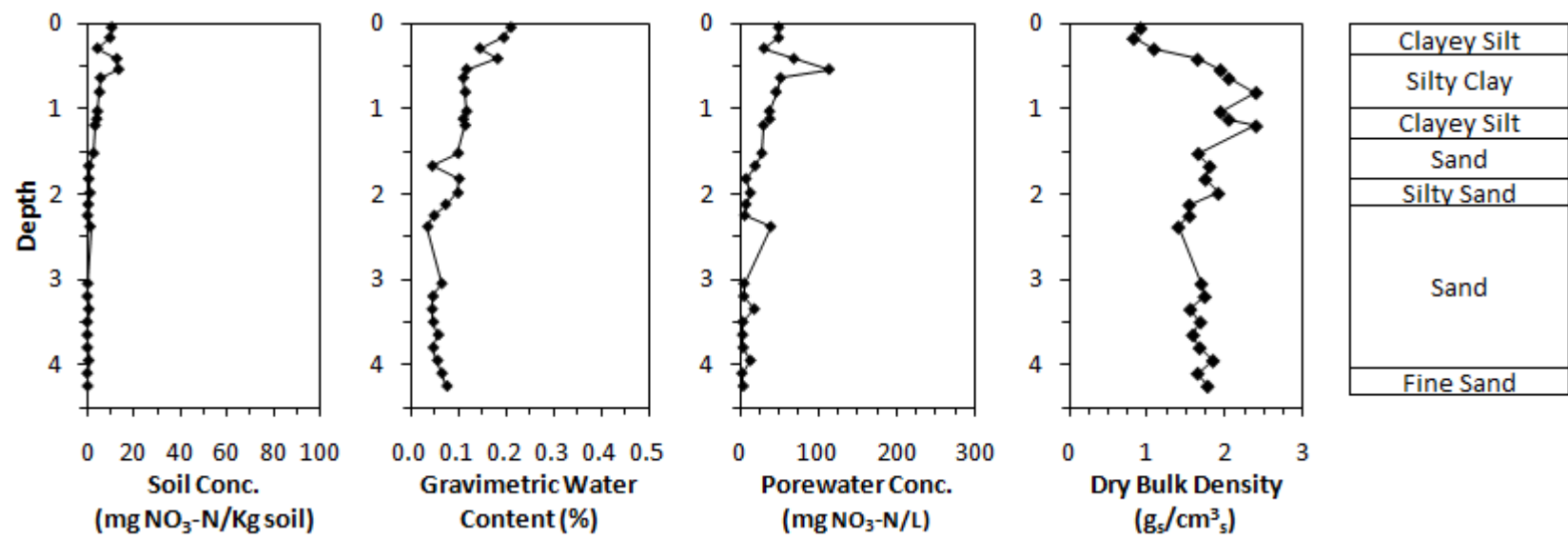
(b)



(c)

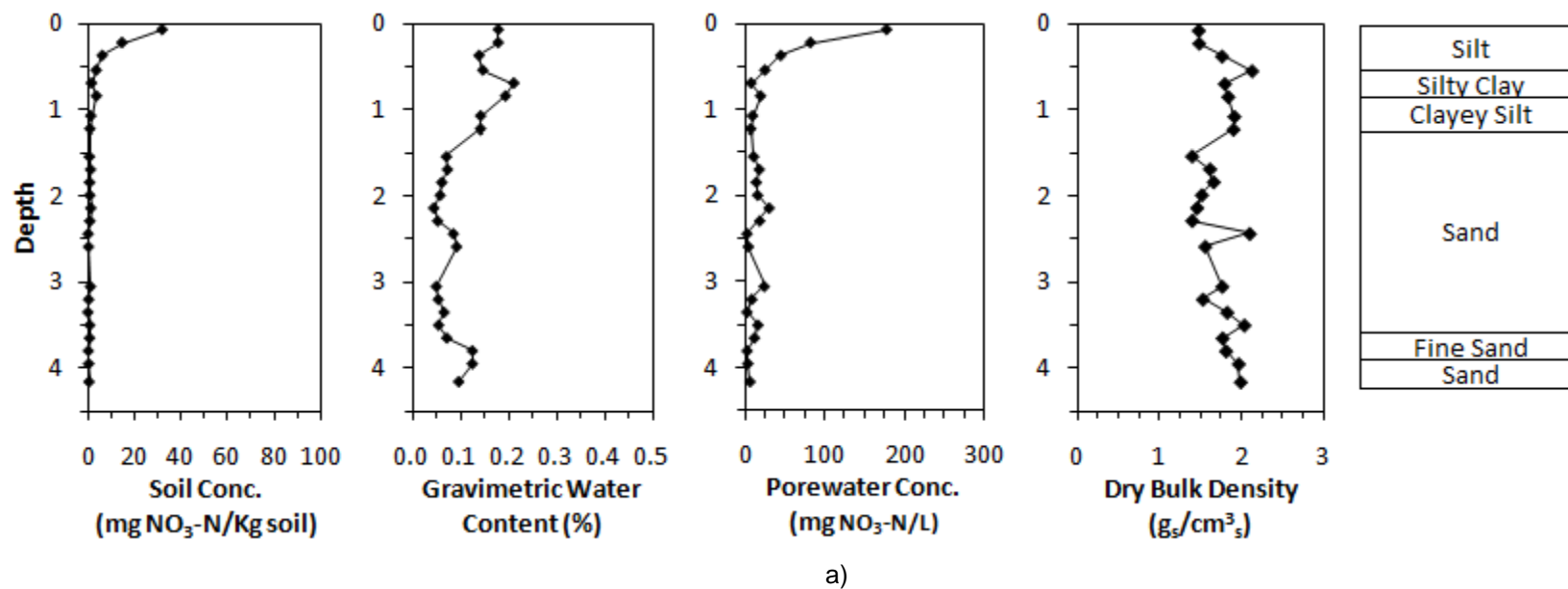
Figure C.4 Profiles of soil nitrate concentration, gravimetric soil water content, pore-water nitrate concentration and dry bulk density from cores collected from the high rate side-dress treatment in the no clover block collected in a) December 2009 and b) May 2010.

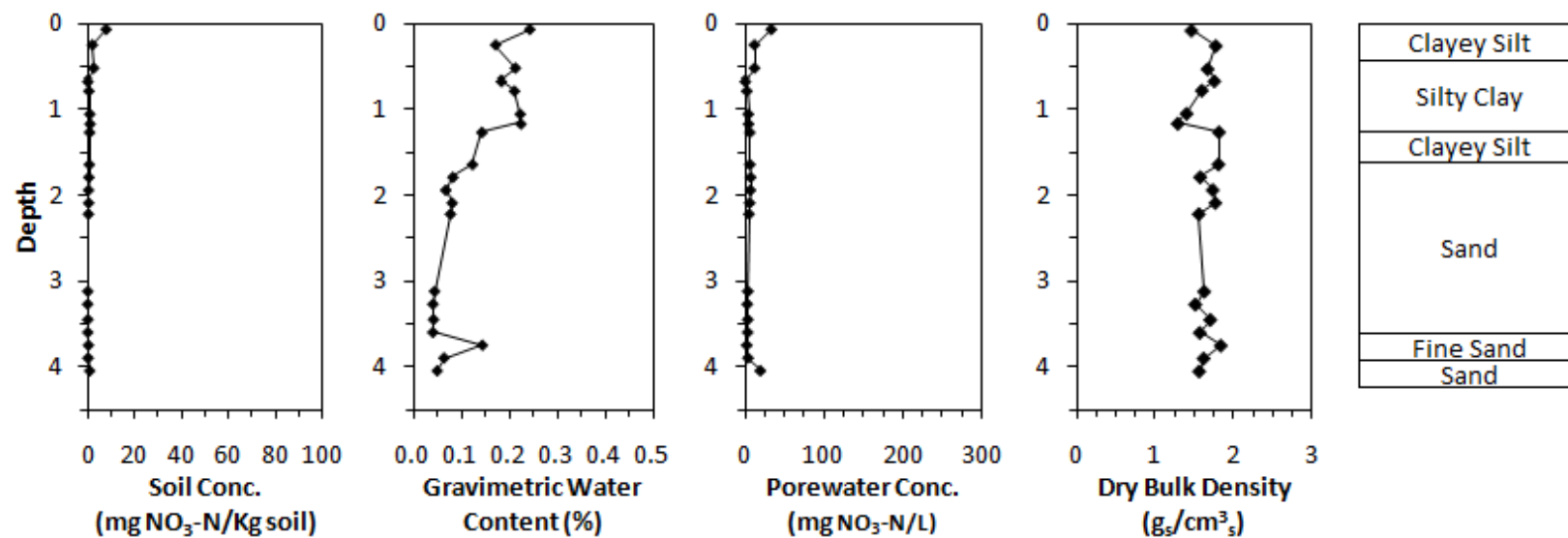




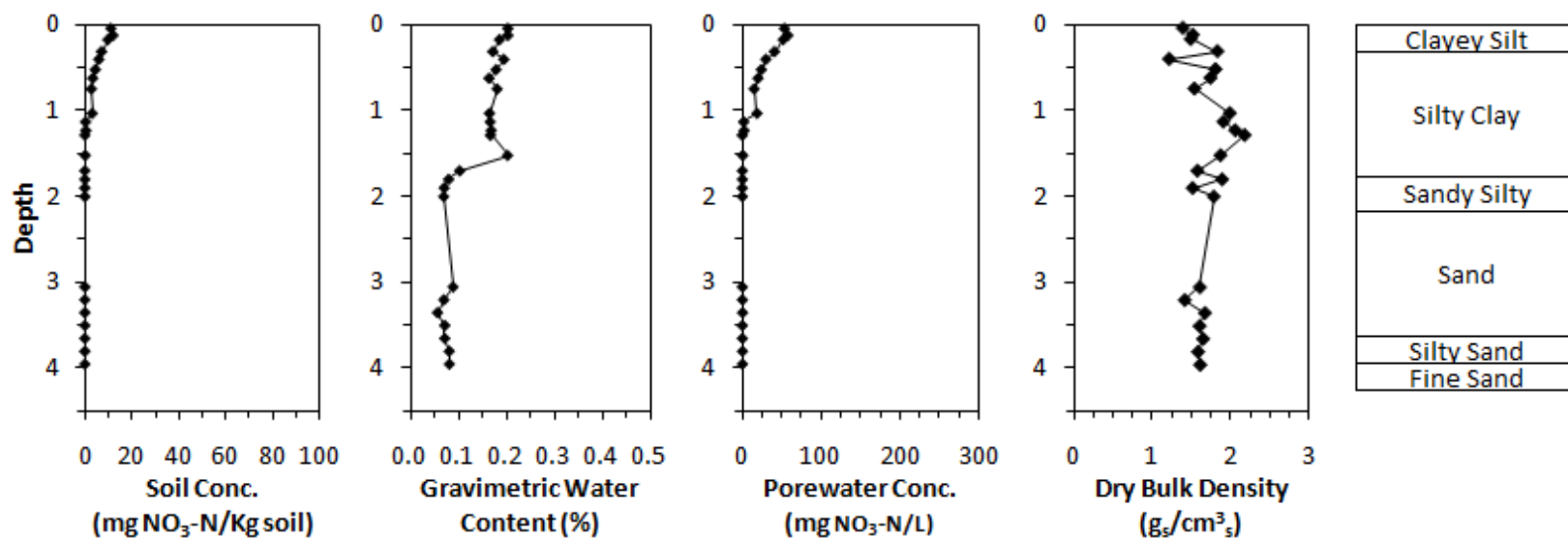
(b)

Figure C.5 Profiles of soil nitrate concentration, gravimetric soil water content, pore-water nitrate concentration and dry bulk density from cores collected from the control treatment in the no clover block collected in a) May 2009, b) December 2009 and c) May 2010.



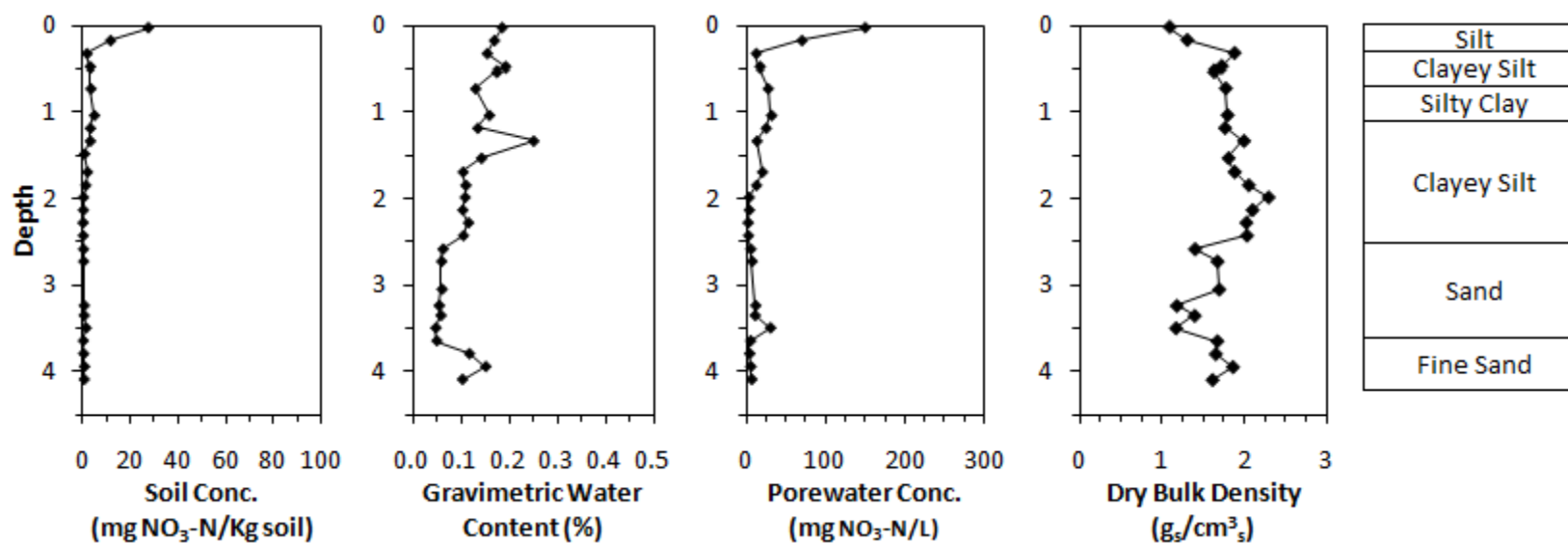


(b)

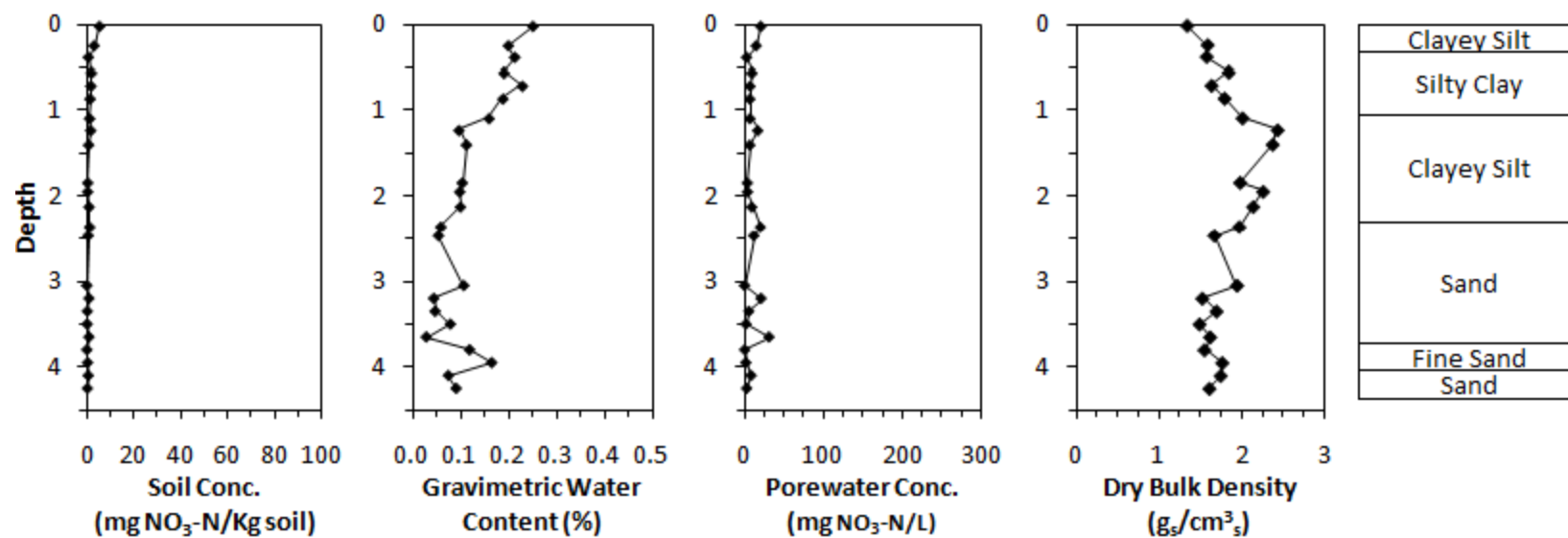


(c)

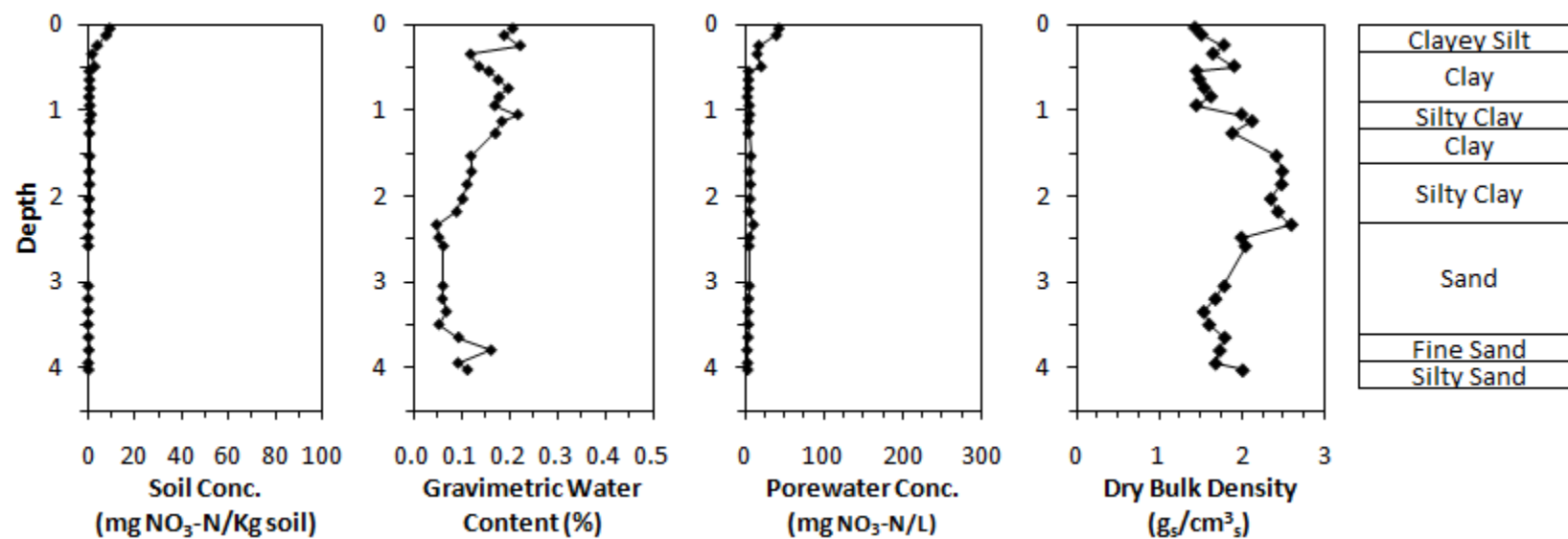
Figure C.6 Profiles of soil nitrate concentration, gravimetric soil water content, pore-water nitrate concentration and dry bulk density from cores collected from the polymer coated urea treatment in the clover block collected in a) May 2009, b) December 2009 and c) May 2010.



(a)

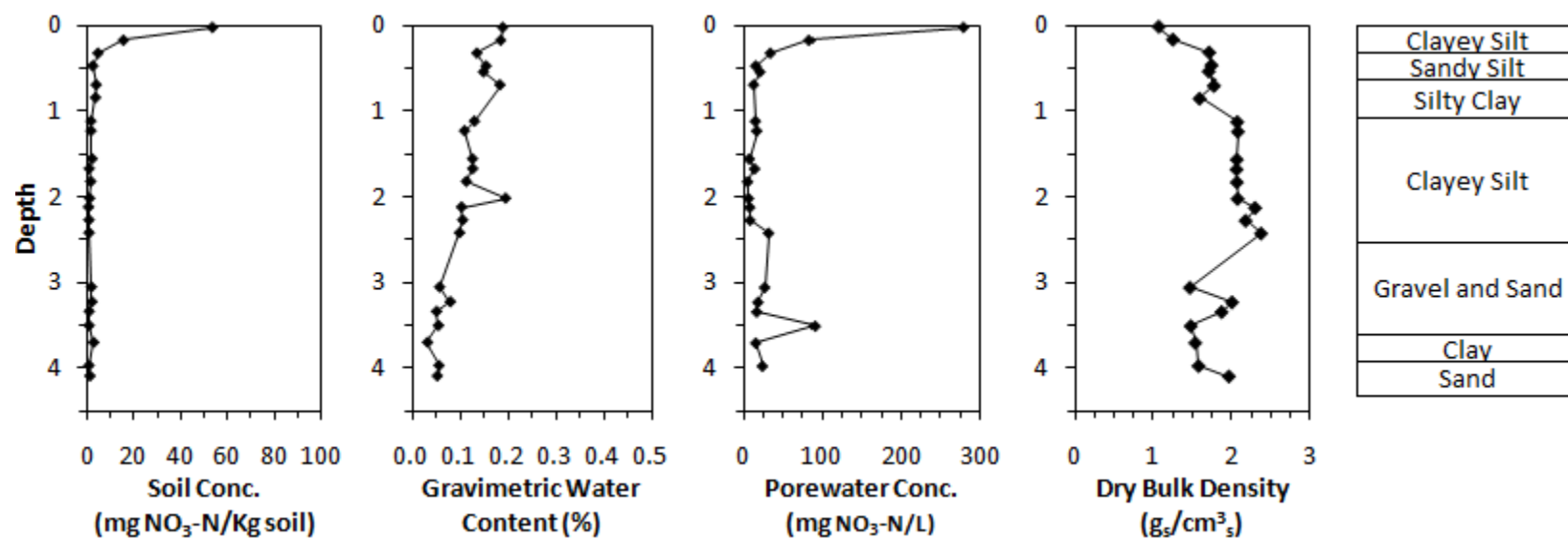


(b)

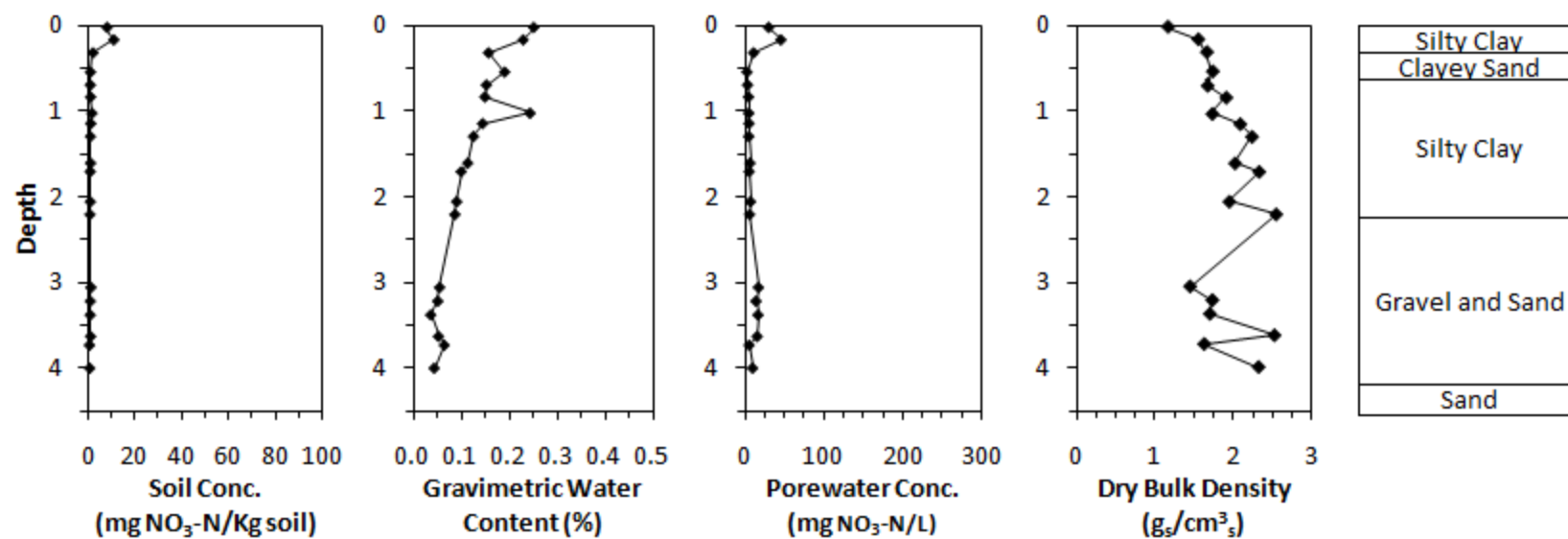


(c)

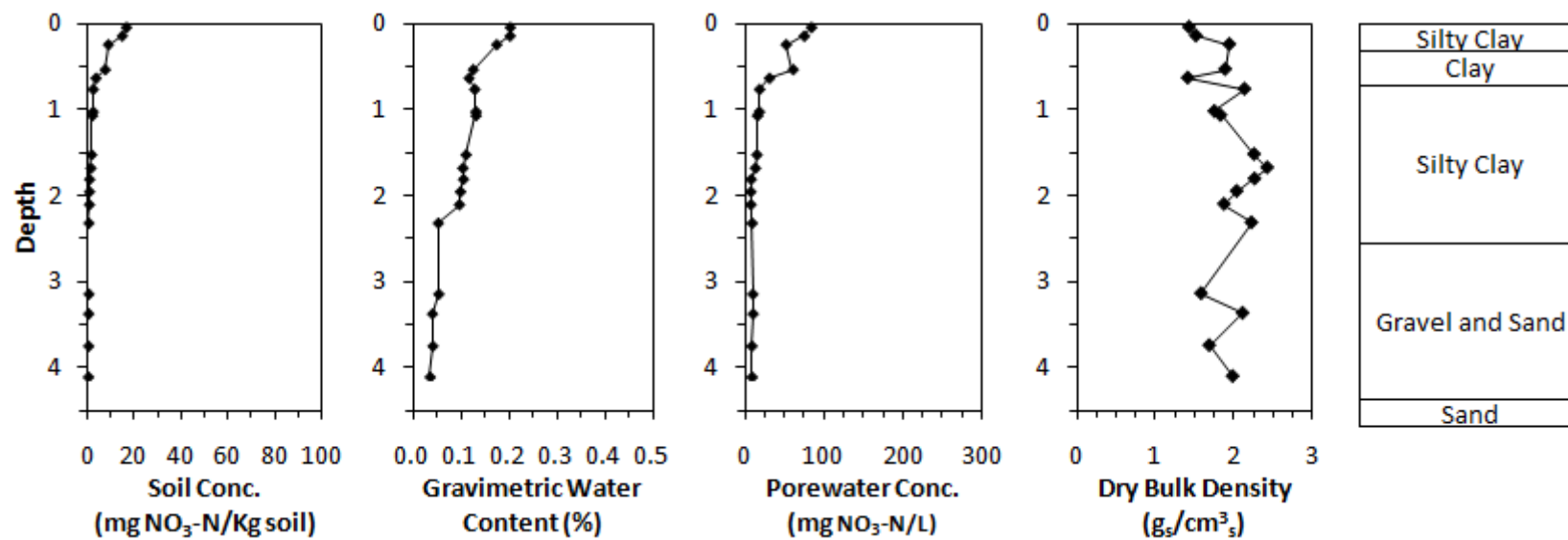
Figure C.7 Profiles of soil nitrate concentration, gravimetric soil water content, pore-water nitrate concentration and dry bulk density from cores collected from the conventional urea treatment in the clover block collected in a) May 2009, b) December 2009 and c) May 2010.



(a)

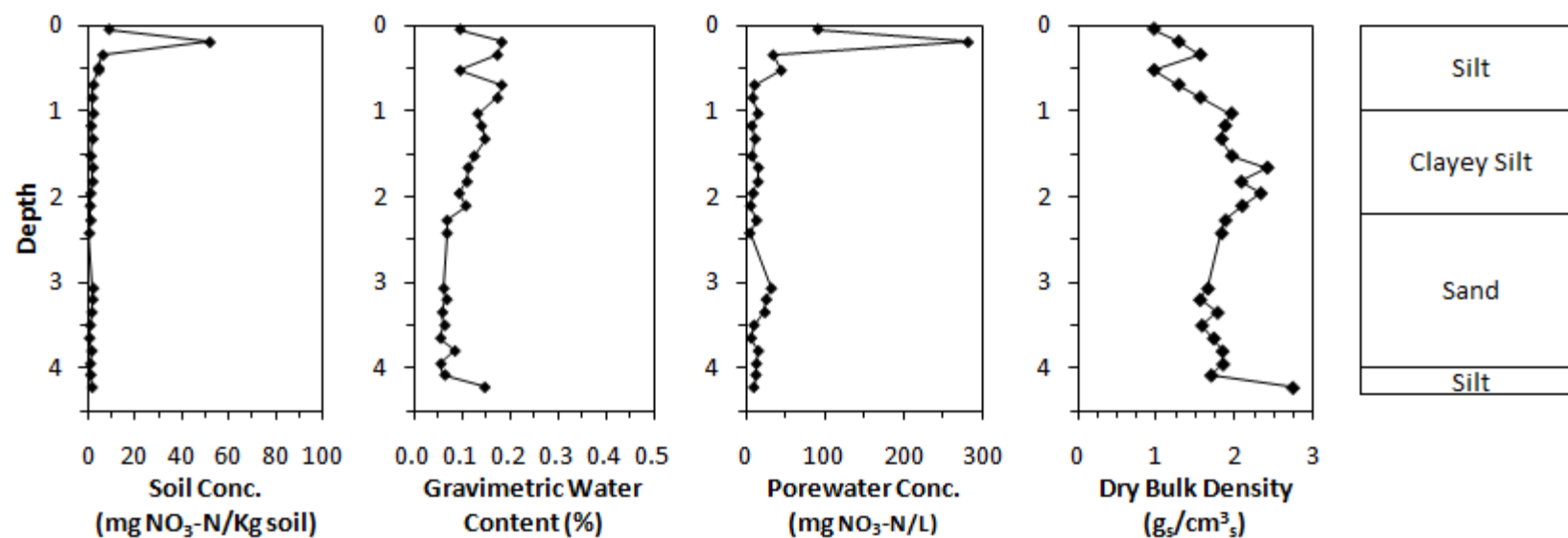


(b)

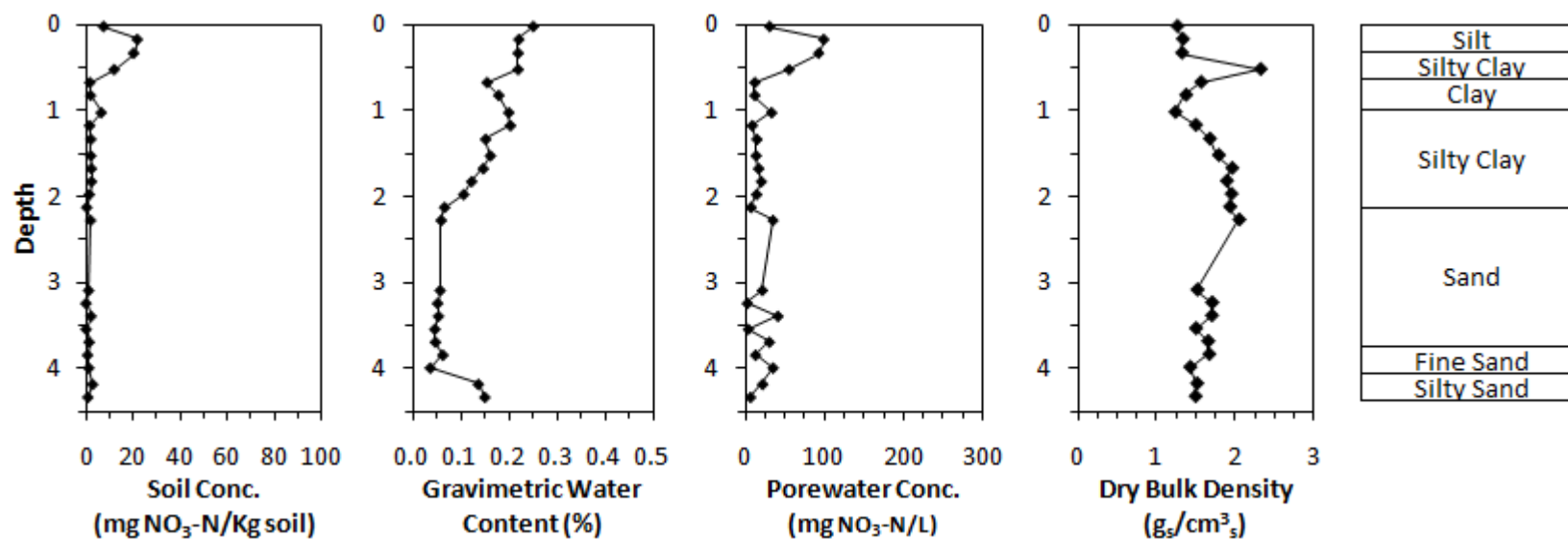


(c)

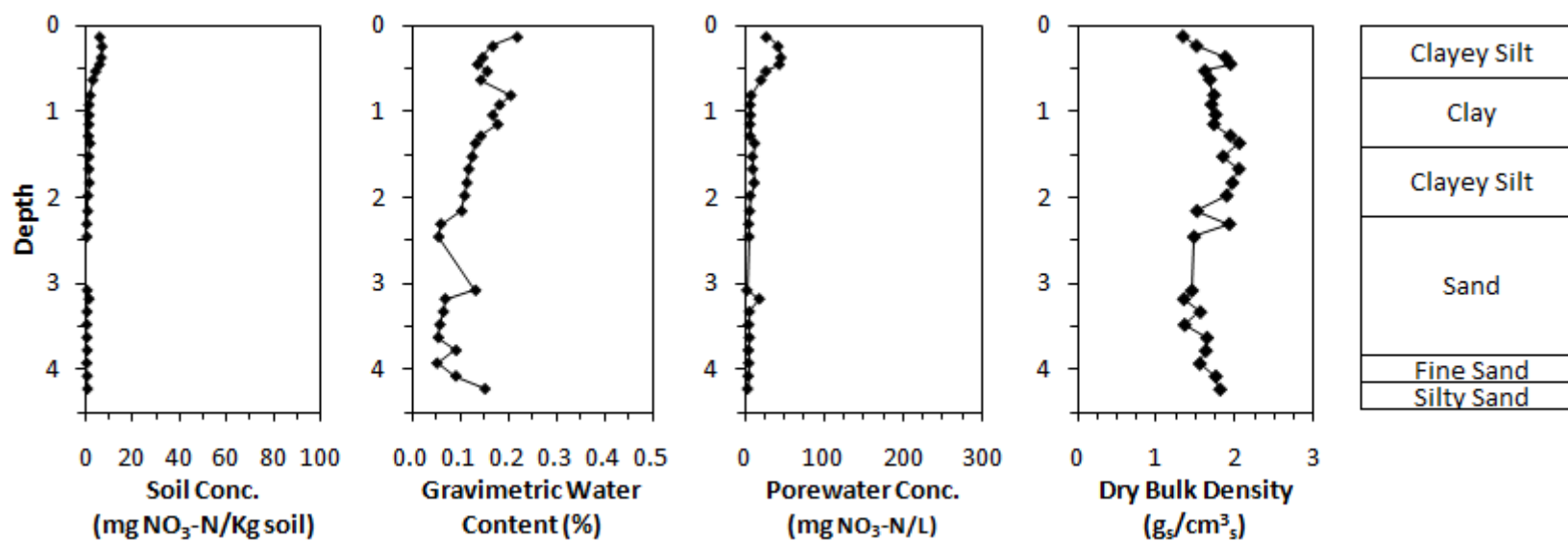
Figure C.8 Profiles of soil nitrate concentration, gravimetric soil water content, pore-water nitrate concentration and dry bulk density from cores collected from the calculator rate side-dress treatment in the clover block collected in a) May 2009, b) December 2009 and c) May 2010.



(a)

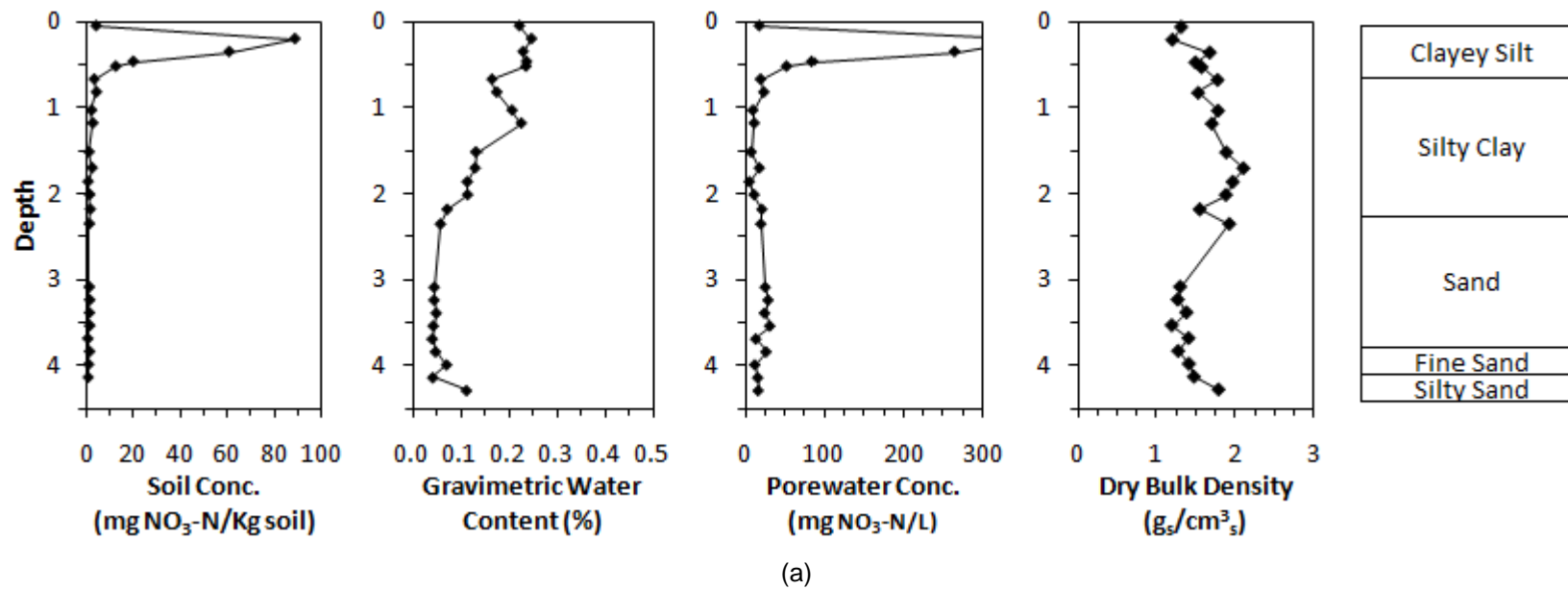


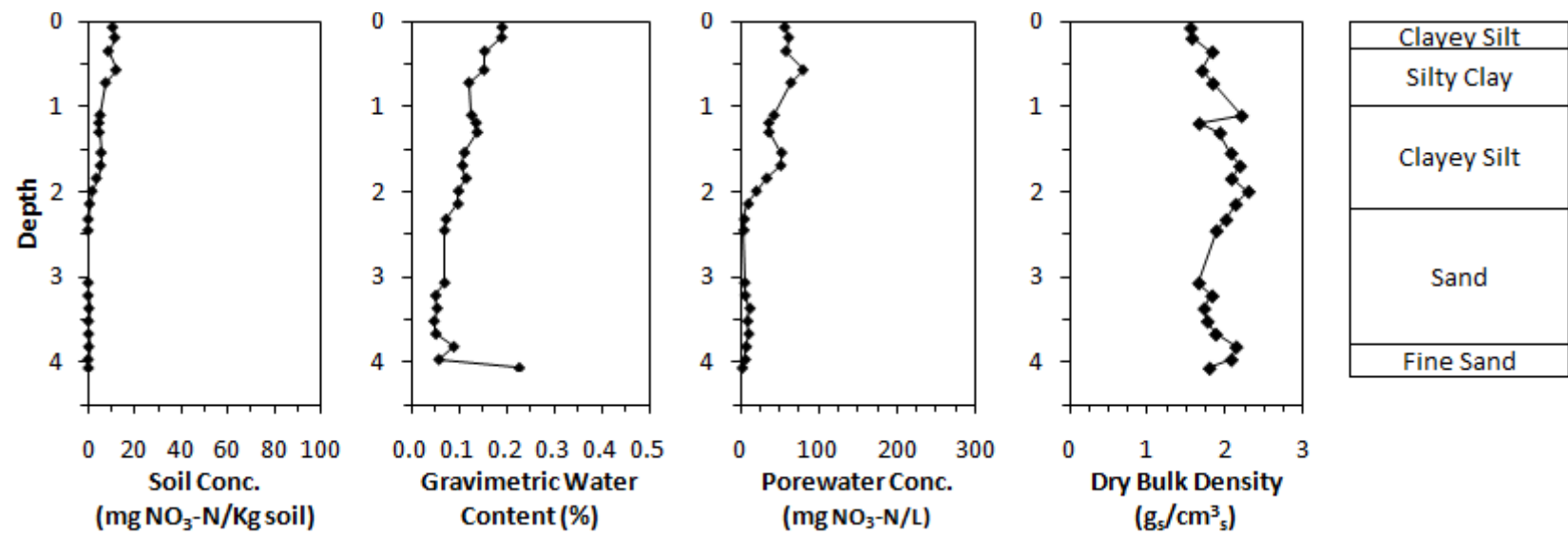
(b)



(c)

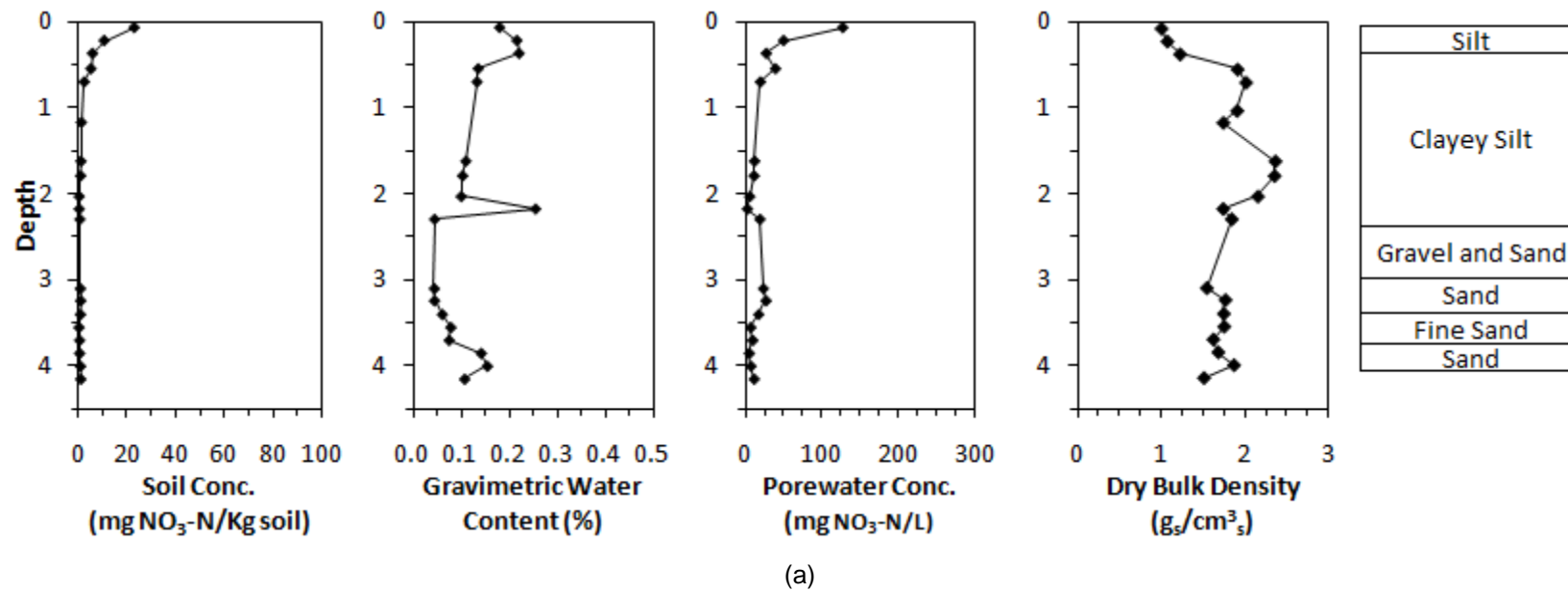
Figure C.9 Profiles of soil nitrate concentration, gravimetric soil water content, pore-water nitrate concentration and dry bulk density from cores collected from the high rate side-dress treatment in the clover block collected in a) December 2009 and b) May 2010.

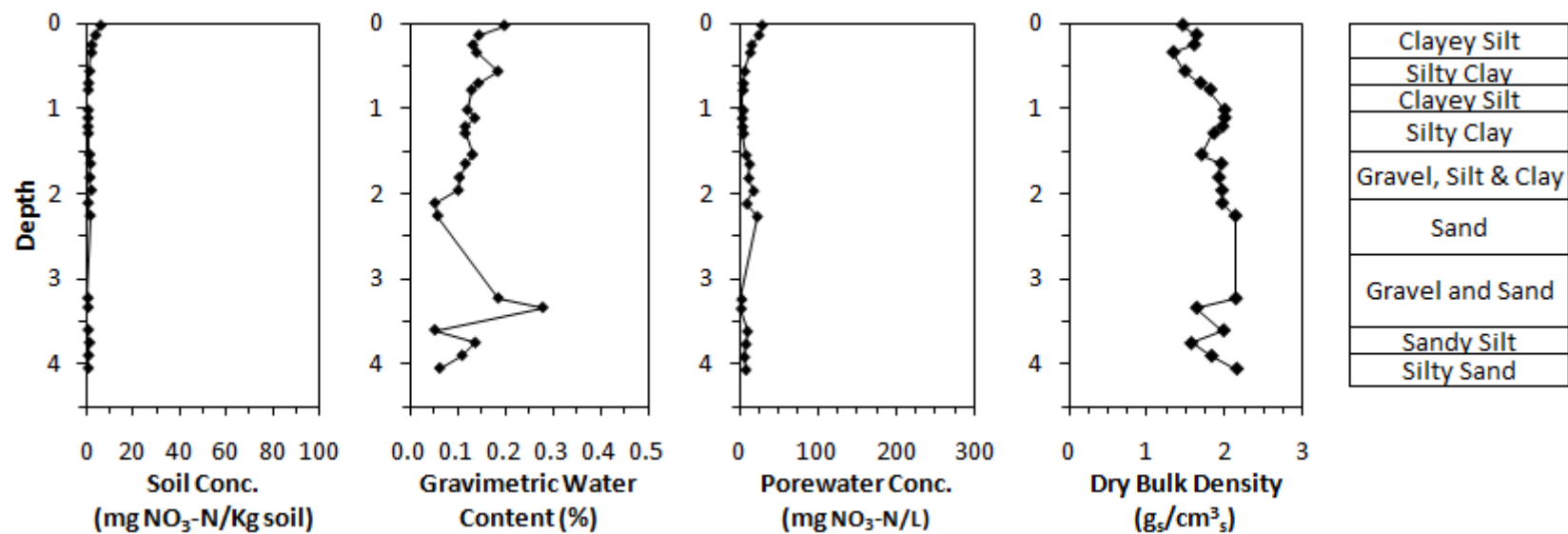




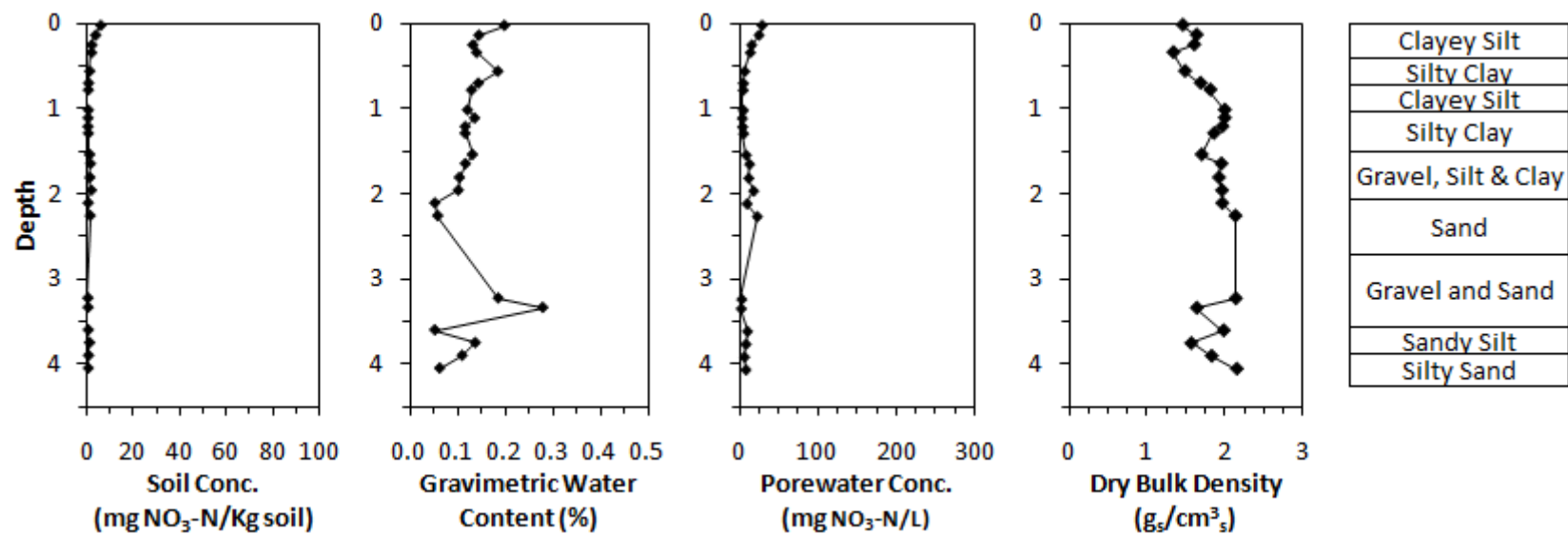
(b)

Figure C.10 Profiles of soil nitrate concentration, gravimetric soil water content, pore-water nitrate concentration and dry bulk density from cores collected from the control treatment in the clover block collected in a) May 2009, b) December 2009 and c) May 2010.



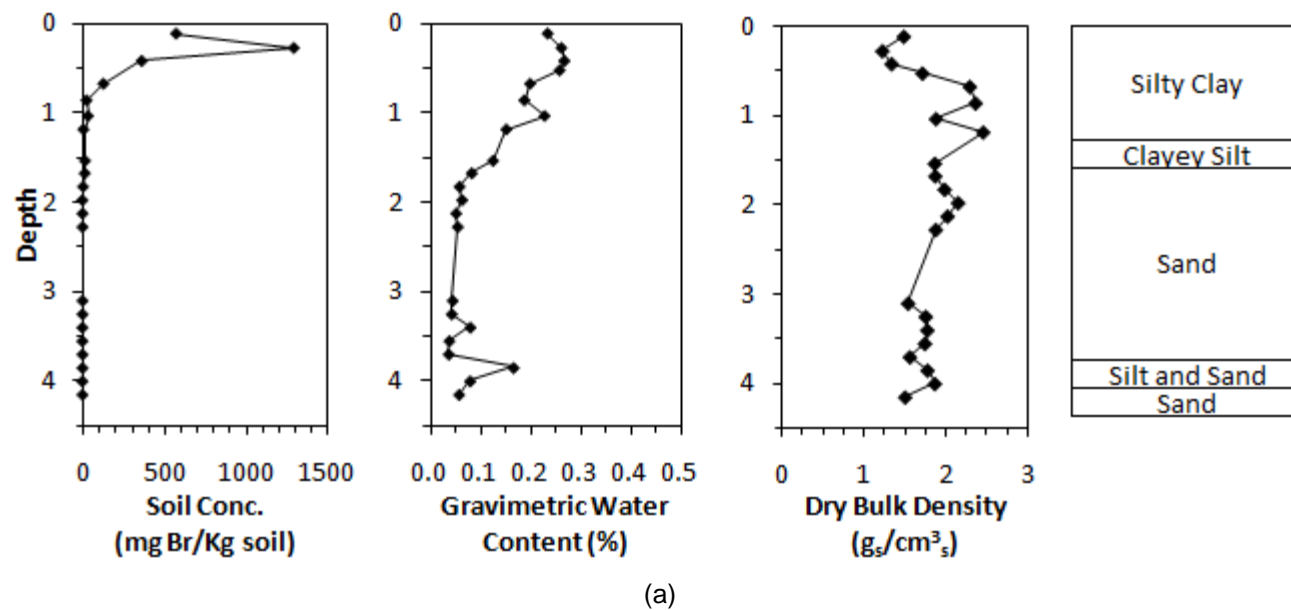


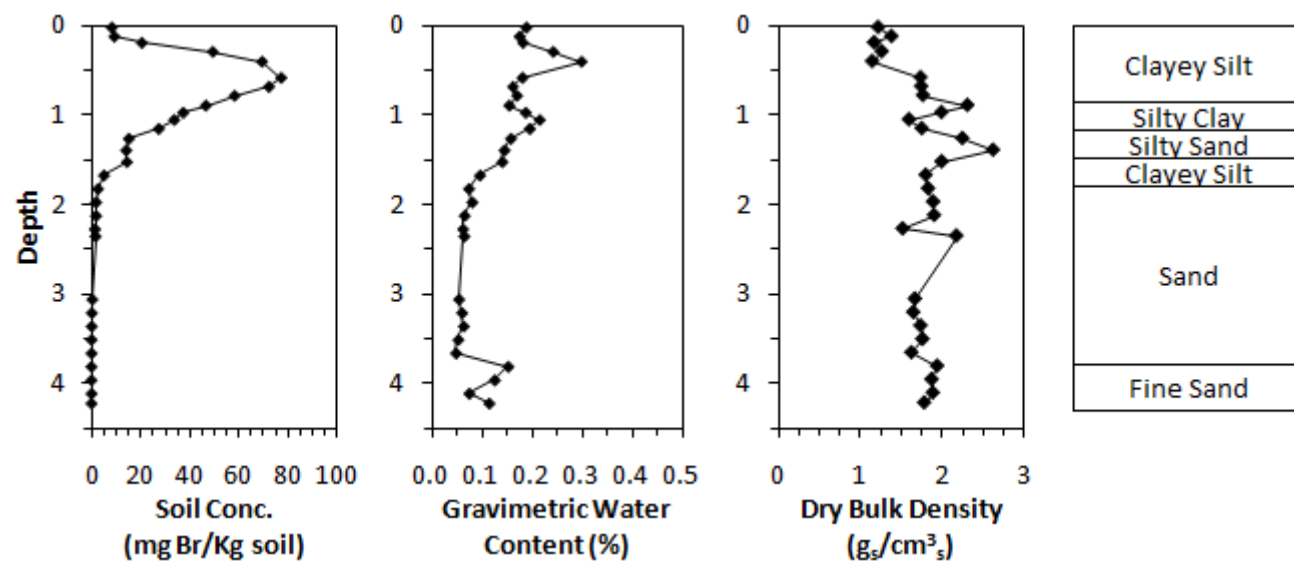
(b)



(c)

Figure C.11 Profiles of soil bromide concentration, gravimetric soil water content and dry bulk density from cores collected from the high bromide plot collected in a) December 2009 and b) May 2010.





(b)

Appendix D

Soil Core Sampling Results – Chapter 3

Table D.1 Soil nitrate, chloride, bromide, gravimetric water content (GWC), volumetric water content (VWC), and dry bulk density. Notes: (a) Non-detectable results presented as n.d.. (b) Results suspected of being pushdown are struck through.

Borehole	Depth (m)		Chloride Conc. (mg/kg soil)	Bromide Conc. (mg/kg soil)	Nitrate as N Conc. (mg/kg soil)	GWC (g _w /g _s)	VWC (cm ³ _w /cm ³ _s)	Dry Bulk Density (g _s /cm ³ _s)
	Start	Finnish						
May-09								
1ANC - a	0.07	0.11	4.33	n.d.	16.08	0.18	0.29	1.59
1ANC - b	0.16	0.20	10.56	n.d.	7.00	0.19	0.33	1.75
1ANC - c	0.30	0.35	2.96	n.d.	2.91	0.17	0.29	1.76
1ANC - d	0.45	0.50	5.99	n.d.	2.04	0.16	0.27	1.75
1BNC - a	0.77	0.82	5.27	n.d.	9.86	0.23	0.32	1.51
1BNC - b	0.89	0.94	6.22	n.d.	2.85	0.25	0.33	1.47
1CNC - a	1.53	1.58	3.17	n.d.	0.29	0.08	0.12	1.63
1CNC - b	1.68	1.73	3.46	n.d.	0.17	0.08	0.14	1.94
1CNC - c	1.83	1.88	4.16	n.d.	0.52	0.07	0.11	1.75
1CNC - d	1.98	2.03	3.23	n.d.	0.30	0.06	0.11	1.90
1CNC - e	2.13	2.18	5.31	n.d.	0.28	0.06	0.10	1.78
1CNC - f	2.28	2.33	5.47	n.d.	0.29	0.08	0.13	1.76
1CNC - g	2.43	2.48	5.64	n.d.	0.42	0.06	0.09	1.71
1DNC - a	3.06	3.11	6.69	n.d.	1.35	0.04	0.05	1.22
1DNC - b	3.21	3.26	5.32	n.d.	0.93	0.06	0.08	1.38
1DNC - c	3.36	3.41	7.18	0.35	1.55	0.06	0.08	1.48
1DNC - d	3.51	3.56	8.00	1.89	0.72	0.06	0.07	1.41
1DNC - e	3.66	3.71	6.46	n.d.	1.09	0.05	0.07	1.56
1DNC - f	3.81	3.86	6.74	n.d.	1.53	0.12	0.20	1.76
1DNC - g	3.96	4.01	6.58	n.d.	1.36	0.10	0.14	1.44
1DNC - h	4.11	4.16	4.51	n.d.	0.36	0.13	0.21	1.78
1DNC - i	4.26	4.31	7.58	n.d.	0.41	0.07	0.11	1.64
1AC - a	0.00	0.05	21.79	n.d.	27.91	0.19	0.20	1.09
1AC - b	0.15	0.20	4.34	n.d.	11.85	0.17	0.22	1.30
1AC - c	0.30	0.35	4.30	n.d.	1.84	0.15	0.29	1.87
1AC - d	0.45	0.50	2.44	n.d.	3.23	0.19	0.33	1.72
1BC - a	0.50	0.55	34.26	n.d.	26.71	0.17	0.28	1.63
1BC - b	0.69	0.74	6.06	n.d.	3.51	0.13	0.23	1.77
1CC - a	1.00	1.05	3.77	n.d.	4.98	0.16	0.29	1.79
1CC - b	1.15	1.20	5.58	n.d.	3.30	0.13	0.24	1.76
1CC - c	1.30	1.35	5.31	n.d.	3.23	0.25	0.50	1.99
1CC - d	1.45	1.50	1.69	n.d.	0.76	n.d.	n.d.	n.d.
1DC - a	1.50	1.55	11.69	n.d.	7.20	0.14	0.26	1.80
1DC - b	1.66	1.71	4.71	n.d.	2.05	0.10	0.19	1.88
1DC - c	1.82	1.86	6.28	n.d.	1.33	0.11	0.22	2.05

Borehole	Depth (m)		Chloride Conc. (mg/Kg soil)	Bromide Conc. (mg/Kg soil)	Nitrate as N Conc. (mg/Kg soil)	GWC (g _w /g _s)	VWC (cm ³ _w /cm ³ _s)	Dry Bulk Density (g _s /cm ³ _s)
	Start	Finnish						
1DC - d	1.96	2.00	1.50	n.d.	0.30	0.11	0.25	2.29
1DC - e	2.10	2.16	1.68	n.d.	0.32	0.10	0.22	2.10
1DC - f	2.25	2.30	2.11	n.d.	0.18	0.12	0.23	2.02
1DC - g	2.40	2.45	1.58	n.d.	0.20	0.10	0.21	2.03
1DC - h	2.56	2.61	3.90	n.d.	0.30	0.06	0.09	1.40
1DC - i	2.70	2.75	6.66	n.d.	0.40	0.06	0.10	1.67
1EC - a	3.02	3.07	13.37	n.d.	5.27	0.06	0.10	1.69
1EC - b	3.21	3.26	3.41	n.d.	0.60	0.05	0.06	1.17
1EC - c	3.33	3.37	3.51	n.d.	0.60	0.06	0.08	1.39
1EC - d	3.47	3.52	5.49	n.d.	1.40	0.05	0.05	1.17
1EC - e	3.62	3.67	3.79	n.d.	0.23	0.05	0.08	1.67
1EC - f	3.77	3.82	2.76	n.d.	0.41	0.12	0.19	1.65
1EC - g	3.92	3.97	2.96	n.d.	0.74	0.15	0.28	1.86
1EC - h	4.07	4.12	5.06	n.d.	0.62	0.10	0.17	1.61
2ANC - a	0.05	0.10	8.12	n.d.	41.24	0.21	0.26	1.21
2ANC - b	0.20	0.25	2.52	n.d.	18.71	0.18	0.24	1.37
2ANC - c	0.35	0.40	3.18	n.d.	19.87	0.13	0.21	1.63
2BNC - a	0.50	0.55	4.01	n.d.	12.87	0.13	0.16	1.31
2BNC - b	0.65	0.70	1.74	n.d.	1.75	0.13	0.23	1.72
2BNC - c	0.80	0.85	3.12	n.d.	1.56	0.19	0.33	1.79
2CNC - a	1.00	1.05	5.12	n.d.	5.39	n.d.	n.d.	1.76
2CNC - b	1.15	1.20	3.45	n.d.	1.85	0.21	0.43	2.02
2CNC - c	1.30	1.35	2.61	n.d.	1.95	0.25	0.33	1.36
2DNC - a	1.50	1.55	5.22	n.d.	11.39	0.19	0.30	1.60
2DNC - b	1.67	1.72	2.42	n.d.	2.42	0.14	0.24	1.78
2DNC - c	1.80	1.85	5.97	n.d.	1.22	0.08	0.16	1.95
2DNC - d	1.95	2.00	3.77	n.d.	0.32	0.07	0.12	1.70
2DNC - e	2.10	2.15	5.23	n.d.	0.33	0.06	0.11	1.79
2DNC - f	2.25	2.30	11.19	n.d.	1.03	0.07	0.12	1.76
2ENC - a	3.03	3.08	9.44	n.d.	2.19	0.06	0.09	1.40
2ENC - b	3.15	3.20	4.43	n.d.	0.43	0.06	0.08	1.47
2ENC - c	3.30	3.35	9.35	n.d.	1.74	0.09	0.13	1.50
2ENC - d	3.45	3.50	4.18	n.d.	0.40	0.13	0.22	1.70
2ENC - e	3.60	3.65	3.18	n.d.	0.62	0.12	0.16	1.41
2ENC - f	3.75	3.80	3.20	n.d.	0.76	0.16	0.26	1.58
2ENC - g	3.90	3.95	9.82	n.d.	2.07	0.07	0.09	1.33
2ENC - h	4.05	4.10	10.04	n.d.	2.38	0.07	0.10	1.46
2ENC - i	4.20	4.25	10.27	0.61	2.40	0.07	0.10	1.46
2AC - a	0.00	0.05	45.49	n.d.	53.32	0.19	0.20	1.07
2AC - b	0.15	0.20	9.13	n.d.	15.51	0.19	0.23	1.26
2AC - c	0.30	0.35	3.85	n.d.	4.67	0.14	0.23	1.72
2AC - d	0.45	0.50	2.95	n.d.	2.45	0.16	0.27	1.75
2BC - a	0.52	0.57	9.62	n.d.	8.44	0.15	0.26	1.74
2BC - b	0.67	0.72	4.52	n.d.	3.91	0.18	0.33	1.78

Borehole	Depth (m)		Chloride Conc. (mg/kg soil)	Bromide Conc. (mg/kg soil)	Nitrate as N Conc. (mg/kg soil)	GWC (g _w /g _s)	VWC (cm ³ _w /cm ³ _s)	Dry Bulk Density (g _s /cm ³ _s)
	Start	Finnish						
2BC - c	0.82	0.87	4.49	n.d.	3.64	n.d.	n.d.	1.60
2CC - a	1.10	1.14	3.72	n.d.	1.71	0.13	0.27	2.08
2CC - b	1.21	1.26	3.36	n.d.	1.68	0.11	0.23	2.09
2DC - a	1.54	1.58	3.94	n.d.	2.17	0.13	0.26	2.07
2DC - b	1.65	1.70	2.73	n.d.	0.98	0.13	0.26	2.07
2DC - c	1.80	1.85	4.82	n.d.	1.63	0.11	0.24	2.07
2DC - d	2.00	2.04	3.56	n.d.	1.07	0.20	0.41	2.08
2DC - e	2.10	2.15	2.38	n.d.	0.68	0.10	0.24	2.31
2DC - f	2.25	2.30	2.11	n.d.	0.88	0.11	0.23	2.19
2DC - g	2.40	2.45	2.92	n.d.	0.85	0.10	0.24	2.38
2EC - a	3.02	3.09	6.02	n.d.	1.83	0.06	0.08	1.47
2EC - b	3.21	3.25	22.14	0.50	2.16	0.08	0.16	2.01
2EC - c	3.32	3.36	24.38	n.d.	0.95	0.05	0.10	1.88
2EC - d	3.48	3.53	12.44	n.d.	0.93	0.05	0.08	1.48
2EC - e	3.69	3.72	24.10	n.d.	2.84	0.03	0.05	1.54
2EC - f	3.95	4.00	14.82	n.d.	0.88	0.06	0.09	1.58
2EC - g	4.07	4.12	12.05	n.d.	1.27	0.05	0.10	1.97
3ANC - a	0.05	0.10	21.74	n.d.	17.66	n.d.	n.d.	1.47
3ANC - b	0.23	0.28	6.79	n.d.	1.87	n.d.	n.d.	1.62
3ANC - c	0.38	0.43	2.34	n.d.	0.88	n.d.	n.d.	1.78
3ANC - d	0.53	0.58	4.82	n.d.	1.06	n.d.	n.d.	1.77
3ANC - e	0.68	0.73	3.31	n.d.	0.68	n.d.	n.d.	1.89
3A1NC - a	0.00	0.09	173.42	0.63	72.39	0.14	0.09	0.61
3A1NC - b	0.15	0.20	107.04	n.d.	44.52	0.18	0.27	1.50
3A1NC - c	0.30	0.35	6.11	0.31	3.46	0.19	0.35	1.84
3A1NC - d	0.45	0.50	2.34	n.d.	0.79	0.16	0.28	1.78
3A2NC - a	0.78	0.83	14.60	n.d.	4.86	0.13	0.28	2.10
3A2NC - b	0.92	1.02	7.14	2.48	0.80	0.10	0.20	2.00
3BNC - a	1.53	1.56	17.13	0.84	0.59	0.15	0.36	2.36
3BNC - b	1.67	1.72	3.63	n.d.	0.00	0.07	0.10	1.39
3BNC - c	1.82	1.87	4.80	n.d.	0.30	0.07	0.10	1.46
3BNC - d	1.97	2.02	6.36	0.00	0.85	0.05	0.07	1.40
3BNC - e	2.12	2.17	5.51	n.d.	0.96	0.07	0.13	1.73
3BNC - f	2.27	2.32	7.53	n.d.	1.17	0.07	0.12	1.77
3BNC - g	2.42	2.46	9.58	0.26	1.32	0.05	0.08	1.61
3CNC - a	3.05	3.10	34.48	0.89	1.17	0.09	0.12	1.43
3CNC - b	3.20	3.25	5.18	n.d.	0.91	0.07	0.13	1.83
3CNC - c	3.35	3.40	7.22	2.25	1.83	0.05	0.10	1.98
3CNC - d	3.50	3.55	4.14	n.d.	0.50	0.06	0.09	1.54
3CNC - e	3.65	3.70	7.22	2.21	1.83	0.08	0.14	1.70
3CNC - f	3.80	3.85	5.10	n.d.	0.67	0.05	0.08	1.68
3CNC - g	3.95	4.00	5.75	n.d.	0.21	0.08	0.13	1.68
3CNC - h	4.10	4.15	7.14	n.d.	1.50	0.16	0.30	1.87
3CNC - i	4.25	4.30	11.53	0.49	1.56	0.08	0.12	1.56

Borehole	Depth (m)		Chloride Conc. (mg/kg soil)	Bromide Conc. (mg/kg soil)	Nitrate as N Conc. (mg/kg soil)	GWC (g _w /g _s)	VWC (cm ³ _w /cm ³ _s)	Dry Bulk Density (g _s /cm ³ _s)
	Start	Finnish						
3AC - a	0.02	0.07	6.45	n.d.	8.77	0.10	0.09	0.97
3AC - b	0.17	0.22	117.05	n.d.	52.01	0.18	0.24	1.28
3AC - c	0.32	0.37	6.72	0.25	6.10	0.18	0.27	1.56
3AC - d	0.47	0.52	3.64	n.d.	4.30	n.d.	n.d.	n.d.
3BC - a	0.50	0.55	8.38	n.d.	4.31	0.10	0.09	0.97
3BC - b	0.67	0.72	2.43	n.d.	2.05	0.18	0.24	1.28
3BC - c	0.82	0.87	6.54	2.75	1.58	0.18	0.27	1.56
3CC - a	1.01	1.06	5.27	n.d.	2.06	0.13	0.26	1.95
3CC - b	1.15	1.20	2.83	n.d.	1.06	0.14	0.26	1.87
3CC - c	1.30	1.35	5.72	n.d.	1.79	0.15	0.27	1.83
3DC - a	1.50	1.55	2.39	n.d.	0.99	0.13	0.25	1.96
3DC - b	1.64	1.68	5.37	n.d.	1.81	0.11	0.27	2.41
3DC - c	1.80	1.85	6.16	n.d.	1.73	0.11	0.23	2.08
3DC - d	1.94	1.98	2.93	0.43	0.87	0.09	0.22	2.32
3DC - e	2.08	2.13	2.89	n.d.	0.66	0.11	0.23	2.09
3DC - f	2.25	2.30	8.69	n.d.	0.94	0.07	0.13	1.88
3DC - g	2.40	2.45	9.05	n.d.	0.35	0.07	0.12	1.83
3EC - a	3.04	3.09	10.47	0.20	1.98	0.06	0.10	1.65
3EC - b	3.17	3.22	5.66	n.d.	1.77	0.07	0.11	1.55
3EC - c	3.32	3.37	7.06	n.d.	1.41	0.06	0.10	1.78
3EC - d	3.47	3.52	4.68	n.d.	0.66	0.06	0.10	1.58
3EC - e	3.62	3.67	3.91	n.d.	0.38	0.05	0.09	1.73
3EC - f	3.77	3.82	7.18	n.d.	1.37	0.08	0.16	1.84
3EC - g	3.92	3.97	6.49	n.d.	0.74	0.05	0.10	1.85
3EC - h	4.05	4.10	9.72	n.d.	0.82	0.06	0.11	1.69
3EC - i	4.20	4.24	7.88	n.d.	1.49	0.15	0.41	2.73
5ANC - a	0.05	0.10	9.39	n.d.	31.72	0.18	0.27	1.48
5ANC - b	0.20	0.25	8.35	0.52	14.65	0.18	0.27	1.49
5ANC - c	0.35	0.40	5.91	n.d.	6.26	0.14	0.25	1.76
5BNC - a	0.52	0.57	3.70	n.d.	3.68	0.15	0.28	2.12
5BNC - b	0.67	0.72	3.32	n.d.	1.66	0.21	0.35	1.80
5BNC - c	0.82	0.87	5.55	n.d.	3.82	0.19	0.31	1.84
5CNC - a	1.05	1.10	5.70	0.54	1.39	0.14	0.26	1.91
5CNC - b	1.20	1.25	2.63	n.d.	1.04	0.14	0.25	1.90
5DNC - a	1.51	1.56	3.16	n.d.	0.78	0.07	0.09	1.40
5DNC - b	1.66	1.71	5.13	n.d.	1.32	0.07	0.11	1.62
5DNC - c	1.81	1.86	4.41	n.d.	0.89	0.06	0.09	1.66
5DNC - d	1.96	2.01	4.08	n.d.	0.93	0.06	0.08	1.52
5DNC - e	2.11	2.16	6.73	n.d.	1.36	0.04	0.06	1.46
5DNC - f	2.26	2.31	5.10	n.d.	0.99	0.05	0.07	1.40
5DNC - g	2.41	2.46	15.45	n.d.	0.24	0.09	0.17	2.09
5DNC - h	2.56	2.61	5.31	n.d.	0.42	0.09	0.14	1.56
5ENC - a	3.02	3.07	5.15	n.d.	1.22	0.05	0.08	1.77
5ENC - b	3.17	3.22	3.92	n.d.	0.47	0.05	0.08	1.53
5ENC - c	3.32	3.37	8.09	3.27	0.18	0.07	0.11	1.82

Borehole	Depth (m)		Chloride Conc. (mg/kg soil)	Bromide Conc. (mg/kg soil)	Nitrate as N Conc. (mg/kg soil)	GWC (g _w /g _s)	VWC (cm ³ _w /cm ³ _s)	Dry Bulk Density (g _s /cm ³ _s)
	Start	Finnish						
5ENC - d	3.47	3.52	6.56	n.d.	0.91	0.05	0.11	2.03
5ENC - e	3.62	3.67	5.67	n.d.	0.86	0.07	0.12	1.77
5ENC - f	3.77	3.82	4.49	n.d.	0.36	0.13	0.21	1.81
5ENC - g	3.92	3.97	6.77	n.d.	0.47	0.12	0.23	1.96
5ENC - h	4.13	4.18	8.39	n.d.	0.63	0.10	0.18	1.99
5AC - a	0.05	0.10	6.15	n.d.	22.92	0.18	0.18	1.00
5AC - b	0.20	0.25	3.51	n.d.	10.72	0.22	0.23	1.07
5AC - c	0.35	0.40	5.79	n.d.	5.96	0.22	0.27	1.22
5BC - a	0.53	0.58	6.00	n.d.	5.28	0.14	0.26	1.91
5BC - b	0.68	0.73	3.92	n.d.	2.55	0.13	0.27	2.01
5CC - a	1.02	1.05	9.95	n.d.	8.84	0.13	0.24	1.90
5CC - b	1.15	1.20	3.47	n.d.	1.45	n.d.	n.d.	1.74
5DC - a	1.60	1.65	6.07	n.d.	1.27	0.11	0.26	2.36
5DC - b	1.77	1.82	7.66	n.d.	1.12	0.10	0.24	2.35
5DC - c	2.01	2.06	4.07	n.d.	0.53	0.10	0.22	2.15
5DC - d	2.16	2.20	6.11	n.d.	0.57	0.26	0.45	1.74
5DC - e	2.25	2.35	14.97	n.d.	0.82	0.04	0.08	1.84
5EC - a	3.08	3.13	17.05	0.66	1.01	0.04	0.07	1.54
5EC - b	3.22	3.27	16.28	0.48	1.17	0.04	0.08	1.76
5EC - c	3.38	3.43	12.97	n.d.	1.03	0.06	0.11	1.74
5EC - d	3.53	3.58	7.45	n.d.	0.52	0.08	0.14	1.75
5EC - e	3.68	3.73	10.39	n.d.	0.68	0.07	0.12	1.62
5EC - f	3.83	3.88	7.59	n.d.	0.68	0.14	0.24	1.68
5EC - g	3.98	4.03	11.39	n.d.	1.07	0.15	0.29	1.86
5EC - h	4.13	4.18	10.92	n.d.	1.19	0.11	0.16	1.51
Dec-09								
1ANC - a	0.00	0.05	2.56	n.d.	7.42	0.26	0.34	1.33
1ANC - b	0.15	0.20	6.60	0.47	4.15	0.20	0.35	1.72
1ANC - c	0.30	0.35	2.02	n.d.	0.69	0.21	0.34	1.62
1BNC - a	0.53	0.58	2.85	n.d.	1.42	0.19	0.27	1.64
1BNC - b	0.75	0.79	1.88	n.d.	0.62	0.12	0.20	1.89
1CNC - a	1.09	1.16	8.85	n.d.	1.38	0.07	0.10	1.64
1DNC - a	1.57	1.62	0.00	5.76	1.04	0.06	0.10	1.77
1DNC - b	1.72	1.77	4.66	3.07	0.93	0.06	0.10	1.78
1DNC - c	1.87	1.92	4.71	n.d.	1.07	0.06	0.09	1.70
1DNC - d	2.02	2.07	4.63	n.d.	0.99	0.05	0.08	1.70
1DNC - e	2.17	2.22	4.95	3.84	0.91	0.05	0.08	1.70
1DNC - f	2.32	2.37	5.35	3.94	0.97	0.08	0.15	2.01
1DNC - g	2.47	2.52	4.91	4.25	0.85	0.09	0.16	1.85
1ENC - a	3.07	3.12	6.35	4.28	0.74	0.03	0.05	1.57
1ENC - b	3.22	3.27	5.34	4.12	0.86	0.06	0.11	1.99
1ENC - c	3.37	3.42	7.81	3.93	0.90	0.04	0.08	2.06
1ENC - d	3.52	3.57	6.40	n.d.	0.72	0.04	0.06	1.91
1ENC - e	3.62	3.67	6.49	n.d.	0.72	0.04	0.07	1.91
1ENC - f	3.77	3.82	6.68	n.d.	0.85	0.07	0.12	1.79

Borehole	Depth (m)		Chloride Conc. (mg/kg soil)	Bromide Conc. (mg/kg soil)	Nitrate as N Conc. (mg/kg soil)	GWC (g _w /g _s)	VWC (cm ³ _w /cm ³ _s)	Dry Bulk Density (g _s /cm ³ _s)
	Start	Finnish						
1ENC - g	3.92	3.97	6.71	2.99	0.91	0.09	0.14	1.82
1ENC - h	4.07	4.12	6.47	n.d.	1.08	0.05	0.08	1.93
1AC - a	0.00	0.05	5.38	n.d.	5.39	0.25	0.34	1.35
1AC - b	0.23	0.28	8.13	n.d.	3.14	0.20	0.32	1.60
1AC - c	0.36	0.41	3.14	n.d.	0.73	0.21	0.34	1.59
1BC - a	0.53	0.58	5.43	0.33	1.98	0.19	0.33	1.85
1BC - b	0.68	0.73	4.24	n.d.	1.80	0.23	0.35	1.64
1BC - c	0.83	0.88	2.84	n.d.	1.46	0.19	0.32	1.80
1CC - a	1.06	1.11	1.92	n.d.	1.24	0.16	0.30	2.01
1CC - b	1.20	1.25	3.53	n.d.	1.72	0.10	0.22	2.43
1CC - c	1.37	1.42	1.20	n.d.	0.85	0.11	0.24	2.37
1DC - a	1.81	1.87	1.36	n.d.	0.46	0.10	0.19	1.98
1DC - b	1.92	1.97	1.16	n.d.	0.46	0.10	0.21	2.26
1DC - c	2.10	2.15	2.38	n.d.	1.01	0.10	0.19	2.14
1DC - d	2.34	2.38	8.16	n.d.	1.28	0.06	0.10	1.97
1DC - e	2.44	2.49	7.61	n.d.	0.70	0.05	0.08	1.68
1EC - a	3.03	3.06	6.52	n.d.	0.10	0.11	0.19	1.95
1EC - b	3.17	3.22	5.77	n.d.	1.00	0.05	0.06	1.53
1EC - c	3.32	3.37	2.68	n.d.	0.31	0.05	0.08	1.70
1EC - d	3.47	3.52	2.13	n.d.	0.21	0.08	0.11	1.50
1EC - e	3.62	3.67	3.34	n.d.	0.97	0.03	0.05	1.62
1EC - f	3.77	3.82	2.64	n.d.	0.14	0.12	0.17	1.56
1EC - g	3.92	3.97	2.41	n.d.	0.41	0.16	0.27	1.77
1EC - h	4.07	4.12	2.66	n.d.	0.70	0.08	0.12	1.75
1EC - i	4.22	4.27	3.15	n.d.	0.33	0.09	0.14	1.62
2ANC - a	0.02	0.07	5.17	n.d.	24.39	0.26	0.33	1.25
2ANC - b	0.17	0.22	9.32	n.d.	41.84	0.16	0.25	1.51
2ANC - c	0.32	0.37	2.40	n.d.	1.48	0.19	0.30	1.56
2BNC - a	0.52	0.58	2.93	n.d.	3.05	0.17	0.26	1.55
2BNC - b	0.67	0.72	1.22	0.50	0.93	0.16	0.24	1.52
2BNC - c	0.82	0.87	1.94	n.d.	0.85	0.11	0.17	1.50
2CNC - a	1.04	1.04	2.09	n.d.	4.14	0.11	0.20	1.78
2CNC - b	1.09	1.14	1.06	n.d.	0.97	0.12	0.23	1.91
2CNC - c	1.20	1.25	1.20	n.d.	0.99	0.11	0.21	1.92
2DNC - a	1.50	1.54	1.80	n.d.	0.87	0.10	0.20	1.87
2DNC - b	1.64	1.69	1.89	n.d.	0.47	0.08	0.14	1.90
2DNC - c	1.79	1.84	2.82	n.d.	0.28	0.06	0.09	1.65
2DNC - d	1.90	1.95	2.19	n.d.	0.41	0.08	0.16	2.00
2DNC - e	2.05	2.10	3.24	n.d.	0.26	0.05	0.07	1.39
2DNC - f	2.20	2.25	5.95	n.d.	0.48	0.04	0.05	1.34
2DNC - g	2.40	2.45	6.36	n.d.	0.20	0.04	0.07	1.82
2ENC - a	3.04	3.09	23.75	0.36	0.15	0.06	0.11	1.89
2ENC - b	3.19	3.24	2.24	n.d.	0.16	0.03	0.05	1.53
2ENC - c	3.34	3.39	2.11	n.d.	0.22	0.05	0.07	1.43

Borehole	Depth (m)		Chloride Conc. (mg/kg soil)	Bromide Conc. (mg/kg soil)	Nitrate as N Conc. (mg/kg soil)	GWC (g _w /g _s)	VWC (cm ³ _w /cm ³ _s)	Dry Bulk Density (g _s /cm ³ _s)
	Start	Finnish						
2ENC - d	3.49	3.54	2.91	0.41	0.22	0.06	0.09	1.54
2ENC - e	3.64	3.69	1.83	0.97	0.32	0.08	0.14	1.73
2ENC - f	3.79	3.84	1.89	n.d.	0.41	0.13	0.19	1.45
2ENC - g	3.94	3.99	4.27	n.d.	0.31	0.05	0.07	1.28
2ENC - h	4.09	4.14	2.84	0.20	0.60	0.07	0.10	1.47
2ENC - i	4.28	4.33	6.20	n.d.	0.68	0.04	0.06	1.39
2AC - a	0.00	0.05	9.20	n.d.	7.82	0.25	0.29	1.16
2AC - b	0.15	0.19	35.95	n.d.	10.71	0.23	0.36	1.55
2AC - c	0.30	0.34	14.91	n.d.	1.89	0.16	0.26	1.66
2BC - a	0.52	0.57	3.59	0.53	0.76	0.19	0.33	1.73
2BC - b	0.67	0.72	2.41	n.d.	0.70	0.15	0.26	1.67
2BC - c	0.81	0.86	1.80	n.d.	0.85	0.15	0.29	1.91
2CC - a	1.00	1.05	6.99	0.97	1.47	0.24	0.42	1.73
2CC - b	1.12	1.17	2.22	n.d.	0.91	0.15	0.30	2.09
2CC - c	1.27	1.32	2.05	n.d.	0.78	0.13	0.28	2.24
2DC - a	1.58	1.63	4.43	n.d.	0.87	0.11	0.23	2.02
2DC - b	1.68	1.73	2.53	n.d.	0.67	0.10	0.23	2.33
2DC - c	2.03	2.08	3.38	n.d.	0.75	0.09	0.18	1.95
2DC - d	2.18	2.23	2.50	n.d.	0.61	0.09	0.22	2.54
2EC - a	3.02	3.08	41.24	0.85	1.04	0.06	0.08	1.44
2EC - b	3.18	3.24	14.74	0.30	0.78	0.05	0.09	1.73
2EC - c	3.35	3.39	13.78	n.d.	0.65	0.04	0.06	1.70
2EC - f	3.60	3.64	23.34	0.53	0.88	0.05	0.13	2.52
2EC - e	3.71	3.74	13.71	n.d.	0.42	0.07	0.11	1.62
2EC - d	3.96	4.02	16.08	0.40	0.47	0.04	0.10	2.32
3ANC - a	0.02	0.07	4.81	n.d.	2.53	0.24	0.34	1.41
3ANC - b	0.17	0.22	2.35	n.d.	2.67	0.17	0.32	1.84
3ANC - c	0.32	0.37	1.91	n.d.	1.03	0.18	0.31	1.68
3BNC - a	0.54	0.56	2.27	n.d.	1.28	0.17	0.31	1.86
3BNC - b	0.66	0.71	1.84	n.d.	0.47	0.16	0.24	1.52
3BNC - c	0.79	0.84	1.44	n.d.	0.61	0.11	0.17	1.50
3CNC - a	1.02	1.07	3.04	n.d.	1.11	0.15	0.23	1.49
3CNC - b	1.25	1.29	15.83	0.45	1.81	0.06	0.08	1.44
3DNC - a	1.54	1.58	3.36	n.d.	0.32	0.05	0.08	1.68
3DNC - b	1.68	1.73	2.19	n.d.	0.35	0.06	0.10	1.59
3DNC - c	1.83	1.88	1.83	n.d.	0.35	0.09	0.16	1.78
3DNC - d	1.98	2.03	3.27	n.d.	0.16	0.03	0.05	1.49
3DNC - e	2.13	2.18	2.28	n.d.	0.36	0.09	0.13	1.56
3DNC - f	2.28	2.33	5.46	n.d.	0.21	0.04	0.05	1.32
3ENC - a	3.03	3.08	9.09	n.d.	0.20	0.06	0.08	1.32
3ENC - b	3.18	3.23	2.43	n.d.	0.35	0.04	0.05	1.37
3ENC - c	3.33	3.38	3.88	n.d.	0.68	0.04	0.05	1.28
3ENC - d	3.48	3.53	3.37	n.d.	0.32	0.04	0.06	1.49
3ENC - e	3.63	3.68	3.44	n.d.	0.15	0.03	0.05	1.45

Borehole	Depth (m)		Chloride Conc. (mg/kg soil)	Bromide Conc. (mg/kg soil)	Nitrate as N Conc. (mg/kg soil)	GWC (g _w /g _s)	VWC (cm ³ _w /cm ³ _s)	Dry Bulk Density (g _s /cm ³ _s)
	Start	Finnish						
3ENC - f	3.78	3.83	2.76	n.d.	0.33	0.07	0.09	1.42
3ENC - g	3.93	3.98	2.71	n.d.	0.22	0.09	0.14	1.59
3ENC - h	4.11	4.16	3.83	n.d.	0.23	0.07	0.10	1.43
3ENC - i	4.23	4.27	9.64	n.d.	0.43	0.04	0.06	1.30
3AC - a	0.00	0.05	6.30	n.d.	7.59	0.25	0.31	1.26
3AC - b	0.15	0.20	7.68	n.d.	21.90	0.22	0.29	1.33
3AC - c	0.31	0.36	8.19	n.d.	20.32	0.22	0.29	1.32
3BC - a	0.50	0.55	6.02	n.d.	12.06	0.22	0.29	2.32
3BC - b	0.65	0.70	4.87	n.d.	1.77	0.15	0.24	1.56
3BC - c	0.80	0.85	4.96	0.11	2.05	0.18	0.24	1.37
3CC - a	1.00	1.05	5.57	n.d.	6.55	0.20	0.25	1.23
3CC - b	1.15	1.20	3.84	n.d.	1.62	0.20	0.30	1.49
3CC - c	1.31	1.36	4.49	n.d.	2.15	0.15	0.25	1.67
3DC - a	1.50	1.55	5.33	n.d.	2.12	0.16	0.29	1.78
3DC - b	1.65	1.70	6.31	n.d.	2.40	0.15	0.29	1.95
3DC - c	1.80	1.85	6.10	n.d.	2.44	0.12	0.23	1.89
3DC - d	1.95	2.00	3.94	n.d.	1.47	0.11	0.21	1.94
3DC - e	2.10	2.15	4.94	n.d.	0.43	0.07	0.13	1.93
3DC - f	2.25	2.30	10.28	n.d.	2.07	0.06	0.12	2.04
3EC - a	3.06	3.11	7.01	n.d.	1.21	0.06	0.09	1.51
3EC - b	3.21	3.26	3.25	n.d.	0.10	0.05	0.09	1.70
3EC - c	3.36	3.41	8.51	n.d.	2.22	0.05	0.09	1.70
3EC - d	3.51	3.56	4.08	n.d.	0.15	0.05	0.07	1.49
3EC - e	3.66	3.71	6.45	n.d.	1.44	0.05	0.08	1.65
3EC - f	3.81	3.86	4.65	n.d.	0.78	0.06	0.10	1.66
3EC - g	3.96	4.01	6.08	n.d.	1.28	0.04	0.05	1.42
3EC - h	4.15	4.20	10.11	n.d.	2.93	0.14	0.21	1.51
3EC - i	4.30	4.35	3.59	n.d.	0.89	0.15	0.22	1.49
4ANC - a	0.03	0.08	6.41	n.d.	18.09	0.04	0.06	1.36
4ANC - b	0.18	0.23	7.09	n.d.	7.38	0.15	0.22	1.42
4BNC - a	0.51	0.56	6.66	n.d.	2.58	0.12	0.23	1.95
4BNC - b	0.67	0.72	3.45	n.d.	1.53	0.14	0.22	1.64
4BNC - c	0.80	0.84	3.20	n.d.	1.67	0.14	0.24	1.71
4CNC - a	1.00	1.05	4.10	n.d.	1.93	0.14	0.25	1.74
4CNC - b	1.15	1.20	5.01	n.d.	2.47	0.11	0.22	1.91
4CNC - c	1.31	1.36	4.76	n.d.	1.98	0.12	0.22	1.94
4DNC - a	1.52	1.57	6.31	n.d.	1.90	0.05	0.09	1.65
4DNC - b	1.66	1.72	7.40	n.d.	1.36	0.04	0.06	1.50
4DNC - c	1.81	1.87	4.58	n.d.	1.54	0.05	0.08	1.74
4DNC - d	1.97	2.02	5.04	n.d.	1.80	0.14	0.23	1.65
4DNC - e	2.12	2.17	7.82	n.d.	1.44	0.03	0.04	1.52
4DNC - f	2.32	2.37	9.95	n.d.	1.80	0.04	0.11	2.66
4DNC - g	2.47	2.52	4.66	n.d.	0.52	0.03	0.05	1.40
4DNC - h	2.62	2.67	4.78	n.d.	0.51	0.04	0.04	1.21

Borehole	Depth (m)		Chloride Conc. (mg/kg soil)	Bromide Conc. (mg/kg soil)	Nitrate as N Conc. (mg/kg soil)	GWC (g _w /g _s)	VWC (cm ³ _w /cm ³ _s)	Dry Bulk Density (g _s /cm ³ _s)
	Start	Finnish						
4ENC - a	3.02	3.07	25.17	0.45	1.52	0.06	0.10	1.70
4ENC - b	3.17	3.22	6.21	n.d.	1.51	0.03	0.05	1.52
4ENC - c	3.32	3.37	4.63	n.d.	1.13	0.04	0.07	1.57
4ENC - d	3.47	3.52	5.90	n.d.	1.54	0.04	0.07	1.76
4ENC - e	3.62	3.67	6.50	n.d.	1.41	0.04	0.06	1.47
4ENC - f	3.77	3.82	7.47	n.d.	1.94	0.05	0.09	1.76
4ENC - g	3.92	3.97	5.77	n.d.	1.26	0.03	0.06	1.76
4ENC - h	4.07	4.12	6.11	n.d.	1.33	0.03	0.05	1.72
4ENC - i	4.22	4.27	4.86	n.d.	1.03	0.10	0.14	1.40
4ENC - j	4.36	4.39	7.28	n.d.	1.92	0.06	0.09	1.44
4AC - a	0.03	0.08	2.58	n.d.	4.06	0.22	0.29	1.32
4AC - b	0.18	0.23	15.04	4.88	88.55	0.25	0.30	1.21
4AC - c	0.33	0.38	12.85	0.22	60.56	0.23	0.38	1.68
4AC - d	0.45	0.49	8.98	n.d.	19.89	0.24	0.35	1.50
4BC - a	0.50	0.55	6.08	n.d.	12.39	0.23	0.37	1.58
4BC - b	0.65	0.70	2.44	n.d.	3.27	0.16	0.29	1.78
4BC - c	0.80	0.85	5.92	0.16	4.18	0.17	0.27	1.54
4CC - a	1.01	1.06	4.18	n.d.	2.10	0.21	0.37	1.79
4CC - b	1.16	1.21	5.71	0.12	2.70	0.22	0.38	1.71
4DC - a	1.50	1.54	2.91	n.d.	1.07	0.13	0.25	1.89
4DC - b	1.68	1.73	3.88	n.d.	2.41	0.13	0.27	2.10
4DC - c	1.84	1.89	1.02	n.d.	0.68	0.11	0.23	1.97
4DC - d	1.99	2.04	2.99	n.d.	1.36	0.11	0.22	1.88
4DC - e	2.16	2.21	8.20	n.d.	1.58	0.07	0.11	1.56
4DC - f	2.33	2.38	7.88	n.d.	1.20	0.06	0.11	1.93
4EC - a	3.06	3.11	6.30	n.d.	1.20	0.05	0.06	1.31
4EC - b	3.21	3.26	4.21	n.d.	1.36	0.05	0.06	1.28
4EC - c	3.36	3.41	4.33	n.d.	1.26	0.05	0.07	1.39
4EC - d	3.51	3.56	4.88	n.d.	1.39	0.04	0.05	1.20
4EC - e	3.66	3.71	4.67	n.d.	0.59	0.04	0.06	1.41
4EC - f	3.81	3.86	6.56	n.d.	1.32	0.05	0.06	1.28
4EC - g	3.96	4.01	3.39	n.d.	0.91	0.07	0.10	1.42
4EC - h	4.11	4.16	5.43	n.d.	0.71	0.04	0.06	1.48
4EC - i	4.26	4.31	6.45	n.d.	1.90	0.11	0.20	1.79
5ANC - a	0.05	0.10	1.64	n.d.	7.89	0.24	0.35	1.47
5ANC - b	0.23	0.28	1.68	n.d.	2.10	0.17	0.31	1.78
5BNC - a	0.50	0.55	3.03	n.d.	2.62	0.21	0.36	1.68
5BNC - b	0.64	0.69	1.10	n.d.	0.25	0.18	0.32	1.76
5BNC - c	0.75	0.80	1.10	0.75	0.64	0.21	0.34	1.60
5CNC - a	1.02	1.07	2.27	n.d.	1.07	0.22	0.31	1.40
5CNC - b	1.14	1.18	1.18	n.d.	1.15	0.22	0.29	1.29
5CNC - c	1.24	1.28	1.52	n.d.	0.94	0.14	0.26	1.82
5DNC - a	1.61	1.66	2.27	n.d.	0.82	0.12	0.22	1.82
5DNC - b	1.76	1.81	2.51	n.d.	0.63	0.08	0.13	1.58

Borehole	Depth (m)		Chloride Conc. (mg/kg soil)	Bromide Conc. (mg/kg soil)	Nitrate as N Conc. (mg/kg soil)	GWC (g _w /g _s)	VWC (cm ³ _w /cm ³ _s)	Dry Bulk Density (g _s /cm ³ _s)
	Start	Finnish						
5DNC - c	1.91	1.96	2.67	n.d.	0.49	0.07	0.12	1.74
5DNC - d	2.06	2.11	2.78	n.d.	0.52	0.08	0.14	1.78
5DNC - e	2.19	2.24	3.26	n.d.	0.44	0.08	0.12	1.56
5ENC - a	3.09	3.14	2.40	n.d.	0.19	0.04	0.07	1.63
5ENC - b	3.24	3.29	2.17	n.d.	0.15	0.04	0.06	1.52
5ENC - c	3.42	3.47	1.93	n.d.	0.18	0.04	0.07	1.71
5ENC - d	3.57	3.62	3.59	n.d.	0.17	0.04	0.07	1.58
5ENC - e	3.72	3.77	2.42	n.d.	0.41	0.14	0.27	1.85
5ENC - f	3.87	3.92	3.89	n.d.	0.29	0.06	0.10	1.62
5ENC - g	4.02	4.07	5.63	n.d.	0.98	0.05	0.08	1.57
5AC - a	0.05	0.10	4.90	n.d.	4.39	0.22	0.31	1.40
5AC - b	0.20	0.25	8.58	n.d.	3.16	0.18	0.30	1.61
5AC - c	0.35	0.40	2.15	n.d.	0.00	0.23	0.31	1.36
5BC - a	0.51	0.57	5.17	n.d.	0.72	0.23	0.27	1.18
5BC - b	0.66	0.71	5.54	n.d.	1.47	0.18	0.31	1.78
5BC - c	0.76	0.81	4.50	n.d.	1.12	0.15	0.18	1.22
5CC - a	1.00	1.05	4.58	n.d.	0.80	0.18	0.29	1.61
5CC - b	1.17	1.22	5.07	n.d.	1.73	0.18	0.28	1.56
5DC - a	1.53	1.58	4.70	n.d.	1.31	0.14	0.27	1.95
5DC - b	1.68	1.73	4.11	n.d.	2.14	0.12	0.29	2.36
5DC - c	1.83	1.88	3.98	n.d.	1.64	0.11	0.27	2.39
5DC - d	1.98	2.03	1.80	n.d.	0.49	0.11	0.24	2.24
5DC - e	2.13	2.18	5.34	n.d.	2.08	0.10	0.21	2.15
5DC - f	2.28	2.33	7.98	n.d.	2.85	0.09	0.21	2.29
5DC - g	2.43	2.49	7.23	0.35	2.54	0.05	0.09	1.84
5EC - a	3.06	3.10	41.94	0.36	4.53	0.05	0.08	4.72
5EC - b	3.20	3.24	5.93	n.d.	0.29	0.04	0.07	1.89
5EC - c	3.34	3.39	7.69	n.d.	0.82	0.05	0.09	2.03
5EC - d	3.49	3.54	9.26	n.d.	1.74	0.05	0.10	1.95
5EC - e	3.64	3.69	7.82	n.d.	2.37	0.07	0.12	1.78
5EC - f	3.79	3.84	5.43	n.d.	1.60	0.19	0.30	1.56
5EC - g	3.94	3.99	8.91	2.50	3.06	0.16	0.34	2.09
5EC - h	4.09	4.14	5.86	n.d.	1.41	0.09	0.15	1.69
5EC - i	4.24	4.29	8.33	n.d.	1.80	0.07	0.10	1.48
BrA - a	0.09	0.14	6.92	569.19	22.12	0.23	0.35	1.49
BrA - b	0.25	0.30	14.56	1286.25	41.86	0.26	0.32	1.23
BrA - c	0.40	0.44	6.07	360.57	6.39	0.27	0.36	1.34
BrB - a	0.50	0.55	41.29	4026.17	31.64	0.26	0.33	4.71
BrB - b	0.65	0.70	4.92	126.45	1.96	0.20	0.37	2.29
BrB - c	0.84	0.89	0.00	23.64	0.97	0.19	0.36	2.36
BrC - a	1.01	1.06	4.01	32.18	1.81	0.23	0.33	1.88
BrC - b	1.16	1.21	4.01	5.27	1.37	0.15	0.30	2.46
BrD - a	1.52	1.55	4.08	14.64	1.19	0.12	0.21	1.87
BrD - b	1.65	1.70	4.15	14.24	1.09	0.08	0.14	1.87

Borehole	Depth (m)		Chloride Conc. (mg/kg soil)	Bromide Conc. (mg/kg soil)	Nitrate as N Conc. (mg/kg soil)	GWC (g _w /g _s)	VWC (cm ³ _w /cm ³ _s)	Dry Bulk Density (g _s /cm ³ _s)
	Start	Finnish						
BrD - c	1.80	1.85	4.95	3.13	0.91	0.06	0.11	1.99
BrD - d	1.95	2.00	5.74	n.d.	0.94	0.06	0.13	2.15
BrD - e	2.10	2.15	6.15	n.d.	0.89	0.05	0.10	2.02
BrD - f	2.25	2.30	7.96	n.d.	0.84	0.05	0.09	1.88
BrE - a	3.07	3.12	5.02	n.d.	0.76	0.04	0.06	1.54
BrE - b	3.22	3.27	5.56	n.d.	0.73	0.04	0.07	1.76
BrE - c	3.37	3.42	5.21	n.d.	0.83	0.08	0.13	1.77
BrE - d	3.52	3.57	6.29	n.d.	0.70	0.04	0.06	1.74
BrE - e	3.67	3.72	6.59	n.d.	0.69	0.04	0.05	1.56
BrE - f	3.82	3.87	5.70	n.d.	0.99	0.17	0.27	1.78
BrE - g	3.97	4.02	5.15	n.d.	0.79	0.08	0.14	1.87
BrE - h	4.12	4.17	6.41	n.d.	0.00	0.06	0.08	1.50
May-10								
1ANC - a	0.00	0.05	21.72	1.27	14.23	0.21	0.27	1.26
1ANC - b	0.07	0.12	5.63	n.d.	6.35	0.20	0.27	1.37
1ANC - c	0.15	0.20	20.39	0.21	6.03	0.23	0.32	1.37
1ANC - d	0.25	0.30	19.21	n.d.	4.92	0.22	0.35	1.60
1ANC - e	0.35	0.40	6.04	n.d.	2.06	0.18	0.26	1.43
1BNC - a	0.55	0.60	17.54	n.d.	3.23	0.15	0.31	2.01
1BNC - b	0.65	0.70	4.82	n.d.	1.20	0.12	0.22	1.73
1BNC - c	0.75	0.80	18.37	0.17	3.16	0.18	0.29	1.65
1CNC - a	1.00	1.05	18.74	n.d.	4.71	0.21	0.29	1.51
1CNC - b	1.11	1.14	18.03	n.d.	3.50	0.37	0.35	1.09
1CNC - c	1.15	1.19	6.02	n.d.	1.64	0.50	0.45	1.05
1DNC - a	1.54	1.59	3.90	n.d.	0.46	0.09	0.11	1.69
1DNC - b	1.69	1.74	4.41	n.d.	0.32	0.07	0.11	1.91
1DNC - c	1.84	1.88	3.64	n.d.	0.17	0.10	0.14	2.01
1DNC - d	1.99	2.04	4.22	n.d.	0.19	0.08	0.11	1.93
1DNC - e	2.14	2.19	4.49	n.d.	0.37	0.09	0.14	1.91
1DNC - f	2.23	2.28	4.76	n.d.	0.48	0.29	0.42	1.46
1ENC - a	3.04	3.08	4.45	n.d.	0.27	0.05	0.09	1.86
1ENC - b	3.12	3.17	4.08	n.d.	0.30	0.07	0.11	1.70
1ENC - c	3.27	3.27	4.30	n.d.	0.34	0.07	0.11	1.70
1ENC - d	3.42	3.47	4.45	n.d.	0.22	0.05	0.08	1.58
1ENC - e	3.57	3.62	4.85	n.d.	0.19	0.06	0.08	1.55
1ENC - f	3.72	3.77	5.64	n.d.	0.34	0.10	0.15	1.59
1ENC - g	3.87	3.92	5.64	n.d.	0.17	0.07	0.10	1.57
1ENC - h	4.02	4.07	7.02	n.d.	0.19	0.07	0.11	1.76
1ENC - i	4.17	4.21	10.75	n.d.	0.11	0.06	0.10	1.89
1AC - a	0.02	0.07	16.33	n.d.	9.01	0.21	0.30	1.43
1AC - b	0.10	0.15	25.26	n.d.	7.60	0.19	0.29	1.51
1AC - c	0.22	0.27	7.07	n.d.	3.99	0.22	0.40	1.78
1AC - d	0.32	0.37	4.52	n.d.	1.91	0.12	0.20	1.65
1AC - e	0.47	0.51	20.54	n.d.	2.89	0.14	0.26	1.90
1BC - a	0.52	0.57	3.25	n.d.	0.86	0.16	0.21	1.45

Borehole	Depth (m)		Chloride Conc. (mg/kg soil)	Bromide Conc. (mg/kg soil)	Nitrate as N Conc. (mg/kg soil)	GWC (g _w /g _s)	VWC (cm ³ _w /cm ³ _s)	Dry Bulk Density (g _s /cm ³ _s)
	Start	Finnish						
1BC - b	0.62	0.67	4.17	n.d.	0.91	0.18	0.24	1.48
1BC - c	0.72	0.77	3.78	n.d.	1.02	0.20	0.28	1.54
1BC - d	0.82	0.87	3.36	n.d.	0.68	0.18	0.27	1.62
1BC - e	0.92	0.97	4.03	n.d.	1.02	0.17	0.23	1.45
1CC - a	1.08	1.02	4.22	n.d.	1.46	0.22	0.39	1.99
1CC - b	1.16	1.10	3.12	n.d.	0.91	0.18	0.35	2.12
1CC - c	1.30	1.24	2.72	n.d.	0.88	0.17	0.29	1.88
1DC - a	1.55	1.52	2.47	n.d.	0.98	0.12	0.24	2.41
1DC - b	1.73	1.70	2.07	n.d.	0.79	0.12	0.25	2.48
1DC - c	1.88	1.85	2.61	n.d.	0.85	0.11	0.24	2.48
1DC - d	2.05	2.02	2.73	n.d.	0.73	0.10	0.20	2.35
1DC - e	2.20	2.17	1.02	n.d.	0.56	0.09	0.18	2.43
1DC - f	2.35	2.32	0.98	n.d.	0.55	0.05	0.10	2.60
1DC - g	2.50	2.47	5.50	n.d.	0.33	0.05	0.08	1.99
1DC - h	2.60	2.57	6.39	0.92	0.36	0.06	0.10	2.04
1EC - a	3.06	3.03	4.07	n.d.	0.37	0.06	0.10	1.78
1EC - b	3.21	3.18	2.81	n.d.	0.31	0.06	0.09	1.68
1EC - c	3.36	3.33	3.11	n.d.	0.32	0.07	0.10	1.54
1EC - d	3.51	3.48	4.44	n.d.	0.26	0.05	0.08	1.60
1EC - e	3.66	3.63	10.25	n.d.	0.43	0.09	0.15	1.79
1EC - f	3.81	3.78	5.48	n.d.	0.55	0.16	0.25	1.73
1EC - g	3.96	3.93	12.10	n.d.	0.37	0.09	0.14	1.68
1EC - h	4.04	4.01	12.72	n.d.	0.46	0.11	0.20	2.01
2ANC - a	0.02	0.07	5.18	n.d.	11.39	0.22	0.32	1.43
2ANC - b	0.13	0.18	5.37	n.d.	8.40	0.21	0.29	1.35
2ANC - c	0.25	0.30	4.88	n.d.	6.10	0.13	0.20	1.57
2ANC - d	0.32	0.36	5.59	n.d.	7.16	0.11	0.18	1.58
2BNC - a	0.53	0.57	5.84	n.d.	6.51	0.13	0.27	2.05
2BNC - b	0.67	0.71	5.58	n.d.	5.93	0.17	0.28	1.67
2BNC - c	0.75	0.80	4.98	n.d.	4.47	0.18	0.28	1.57
2CNC - a	1.02	1.07	3.25	n.d.	2.53	0.21	0.32	1.55
2CNC - b	1.15	1.19	3.42	n.d.	3.41	0.16	0.32	1.99
2DNC - a	1.53	1.58	2.75	n.d.	1.76	0.14	0.26	1.90
2DNC - b	1.68	1.73	2.97	n.d.	1.15	0.13	0.21	1.66
2DNC - c	1.83	1.88	5.46	n.d.	0.38	0.04	0.06	1.53
2DNC - d	1.98	2.03	5.28	n.d.	0.62	0.06	0.09	1.50
2DNC - e	2.13	2.18	5.40	n.d.	0.45	0.06	0.10	1.55
2DNC - f	2.28	2.33	7.16	n.d.	0.59	0.05	0.08	1.75
2DNC - g	2.40	2.45	10.66	n.d.	0.40	0.07	0.11	1.54
2ENC - a	3.02	3.07	6.29	n.d.	0.41	0.06	0.08	1.31
2ENC - b	3.17	3.22	5.25	n.d.	0.25	0.05	0.10	1.98
2ENC - c	3.32	3.37	4.66	n.d.	0.35	0.07	0.14	1.95
2ENC - d	3.47	3.52	8.52	n.d.	0.43	0.09	0.15	1.64
2ENC - e	3.62	3.67	6.16	n.d.	0.42	0.10	0.18	1.75
2ENC - f	3.77	3.82	13.29	0.63	1.27	0.06	0.09	1.55

Borehole	Depth (m)		Chloride Conc. (mg/kg soil)	Bromide Conc. (mg/kg soil)	Nitrate as N Conc. (mg/kg soil)	GWC (g _w /g _s)	VWC (g _w /cm ³ _s)	Dry Bulk Density (g _s /cm ³ _s)
	Start	Finnish						
2ENC - g	3.92	3.97	12.61	0.42	0.45	0.05	0.07	1.44
2AC - a	0.02	0.07	23.68	n.d.	16.95	0.20	0.29	1.43
2AC - b	0.12	0.17	16.13	n.d.	15.08	0.20	0.31	1.52
2AC - c	0.22	0.27	22.17	n.d.	9.02	0.17	0.34	1.95
2BC - a	0.51	0.56	24.37	n.d.	7.60	0.13	0.24	1.89
2BC - b	0.61	0.66	7.16	n.d.	3.60	0.12	0.17	1.41
2BC - c	0.74	0.79	5.72	n.d.	2.37	0.13	0.28	2.14
2CC - a	1.00	1.05	6.83	n.d.	2.35	0.13	0.23	1.76
2CC - b	1.05	1.09	5.78	n.d.	2.07	0.13	0.24	1.83
2DC - a	1.51	1.55	6.46	n.d.	1.67	0.11	0.25	2.27
2DC - b	1.66	1.70	4.48	n.d.	1.36	0.10	0.25	2.43
2DC - c	1.79	1.83	3.42	n.d.	0.81	0.11	0.24	2.27
2DC - d	1.93	1.98	3.36	n.d.	0.73	0.10	0.20	2.04
2DC - e	2.08	2.13	3.08	n.d.	0.71	0.10	0.18	1.88
2DC - f	2.29	2.35	17.47	n.d.	0.47	0.05	0.12	2.23
2EC - a	3.11	3.17	13.68	n.d.	0.52	0.05	0.09	1.58
2EC - b	3.33	3.41	19.32	n.d.	0.41	0.04	0.09	2.12
2EC - c	3.71	3.78	14.42	n.d.	0.36	0.04	0.07	1.69
2EC - d	4.07	4.14	12.30	n.d.	0.32	0.04	0.07	1.99
3ANC - a	0.00	0.05	3.35	n.d.	6.26	0.23	0.35	1.50
3ANC - b	0.14	0.19	3.10	n.d.	5.76	0.17	0.28	1.67
3ANC - c	0.28	0.33	2.90	n.d.	2.06	0.16	0.27	1.67
3ANC - d	0.41	0.46	4.15	n.d.	2.83	0.18	0.28	1.57
3BNC - a	0.50	0.55	4.32	n.d.	3.00	0.19	0.32	1.62
3BNC - b	0.62	0.67	4.92	n.d.	2.02	0.16	0.29	1.79
3BNC - c	0.75	0.80	2.81	n.d.	0.95	0.12	0.24	1.92
3CNC - a	1.00	1.05	3.41	n.d.	0.72	0.11	0.25	2.30
3CNC - b	1.13	1.18	6.24	n.d.	0.48	0.07	0.11	1.64
3CNC - c	1.23	1.27	4.46	n.d.	0.71	0.10	0.20	1.91
3DNC - a	1.50	1.55	4.61	n.d.	0.39	0.05	0.09	1.69
3DNC - b	1.65	1.70	4.50	n.d.	0.27	0.05	0.08	1.51
3DNC - c	1.80	1.85	4.72	n.d.	0.41	0.05	0.08	1.67
3DNC - d	1.95	2.00	4.19	n.d.	0.22	0.05	0.09	1.78
3DNC - e	2.10	2.15	5.64	n.d.	0.26	0.05	0.08	1.65
3DNC - f	2.25	2.30	5.36	n.d.	0.53	0.09	0.17	1.85
3DNC - g	2.40	2.45	6.83	n.d.	0.48	0.08	0.14	1.73
3ENC - a	3.04	3.09	17.17	n.d.	0.29	0.07	0.13	1.88
3ENC - b	3.19	3.24	4.25	n.d.	0.22	0.05	0.07	1.45
3ENC - c	3.34	3.39	4.35	n.d.	0.17	0.06	0.10	1.60
3ENC - d	3.49	3.54	5.24	n.d.	0.29	0.06	0.08	1.41
3ENC - e	3.64	3.69	5.10	n.d.	0.62	0.08	0.14	1.66
3ENC - f	3.79	3.84	5.58	n.d.	0.17	0.05	0.09	1.71
3ENC - g	3.96	4.01	10.64	n.d.	0.00	0.10	0.18	1.69
3ENC - h	4.09	4.14	9.65	n.d.	0.91	0.13	0.22	1.65
3ENC - i	4.27	4.31	16.38	n.d.	0.38	0.06	0.12	2.07

Borehole	Depth (m)		Chloride Conc. (mg/kg soil)	Bromide Conc. (mg/kg soil)	Nitrate as N Conc. (mg/kg soil)	GWC (g _w /g _s)	VWC (cm ³ _w /cm ³ _s)	Dry Bulk Density (g _s /cm ³ _s)
	Start	Finnish						
3AC - a	0.10	0.15	6.41	n.d.	6.07	0.22	0.29	1.34
3AC - b	0.21	0.26	7.81	0.53	7.10	0.17	0.25	1.51
3AC - c	0.35	0.38	7.00	n.d.	6.77	0.15	0.27	1.87
3AC - d	0.43	0.46	6.72	n.d.	6.01	0.14	0.26	1.93
3BC - a	0.50	0.55	9.15	n.d.	4.27	0.16	0.25	1.61
3BC - b	0.60	0.65	6.73	n.d.	3.04	0.14	0.24	1.67
3BC - c	0.78	0.83	8.12	n.d.	1.79	0.20	0.35	1.73
3BC - d	0.89	0.94	6.11	n.d.	1.35	0.18	0.31	1.69
3CC - a	1.01	1.06	6.53	n.d.	1.34	0.17	0.29	1.75
3CC - b	1.12	1.17	8.05	n.d.	1.28	0.18	0.31	1.73
3CC - c	1.26	1.30	4.21	n.d.	1.05	0.14	0.28	1.93
3CC - d	1.35	1.38	6.02	n.d.	1.73	0.13	0.27	2.05
3DC - a	1.50	1.54	5.07	n.d.	1.30	0.12	0.23	1.84
3DC - b	1.64	1.69	4.51	n.d.	1.26	0.12	0.24	2.04
3DC - c	1.80	1.85	5.42	n.d.	1.43	0.11	0.22	1.96
3DC - d	1.95	2.00	5.81	n.d.	0.82	0.11	0.21	1.89
3DC - e	2.13	2.18	5.03	n.d.	0.74	0.10	0.16	1.51
3DC - f	2.28	2.33	7.68	n.d.	0.35	0.06	0.12	1.92
3DC - g	2.43	2.48	7.34	n.d.	0.34	0.06	0.08	1.48
3EC - a	3.05	3.10	6.96	n.d.	0.49	0.13	0.19	1.45
3EC - b	3.15	3.20	7.93	n.d.	1.32	0.07	0.09	1.35
3EC - c	3.30	3.35	2.98	n.d.	0.44	0.07	0.10	1.55
3EC - d	3.45	3.50	2.83	n.d.	0.34	0.06	0.08	1.36
3EC - e	3.60	3.65	3.76	n.d.	0.37	0.05	0.09	1.64
3EC - f	3.75	3.80	3.08	0.59	0.50	0.09	0.15	1.62
3EC - g	3.90	3.95	6.36	n.d.	0.31	0.05	0.08	1.55
3EC - h	4.05	4.10	6.56	n.d.	0.48	0.09	0.16	1.75
3EC - i	4.20	4.25	4.33	n.d.	0.65	0.15	0.27	1.80
4ANC - a	0.03	0.08	6.91	n.d.	10.43	0.21	0.19	0.92
4ANC - b	0.15	0.20	3.62	n.d.	9.68	0.19	0.16	0.83
4ANC - c	0.28	0.32	3.73	n.d.	4.45	0.14	0.16	1.09
4ANC - d	0.40	0.44	5.66	n.d.	12.56	0.18	0.30	1.65
4BNC - a	0.52	0.57	12.49	n.d.	13.32	0.12	0.23	1.94
4BNC - b	0.62	0.67	5.78	n.d.	5.73	0.11	0.22	2.04
4BNC - c	0.79	0.83	6.24	n.d.	5.28	0.11	0.27	2.39
4CNC - a	1.01	1.06	4.52	n.d.	4.43	0.12	0.23	1.94
4CNC - b	1.10	1.15	7.59	n.d.	4.21	0.11	0.22	2.04
4CNC - c	1.18	1.22	4.93	n.d.	3.43	0.11	0.27	2.39
4DNC - a	1.50	1.55	5.16	n.d.	2.79	0.10	0.16	1.66
4DNC - b	1.65	1.70	5.30	n.d.	0.87	0.04	0.08	1.80
4DNC - c	1.80	1.85	3.24	n.d.	0.80	0.10	0.18	1.75
4DNC - d	1.97	2.02	3.52	n.d.	1.32	0.10	0.19	1.91
4DNC - e	2.10	2.15	3.28	n.d.	0.57	0.07	0.11	1.54
4DNC - f	2.23	2.28	2.97	n.d.	0.30	0.05	0.07	1.54
4DNC - g	2.36	2.41	5.29	n.d.	1.40	0.04	0.05	1.40

Borehole	Depth (m)		Chloride Conc. (mg/kg soil)	Bromide Conc. (mg/kg soil)	Nitrate as N Conc. (mg/kg soil)	GWC (g _w /g _s)	VWC (cm ³ _w /cm ³ _s)	Dry Bulk Density (g _s /cm ³ _s)
	Start	Finnish						
4ENC - a	3.02	3.07	4.85	n.d.	0.35	0.06	0.11	1.69
4ENC - b	3.17	3.22	3.68	n.d.	0.23	0.05	0.08	1.74
4ENC - c	3.32	3.37	6.80	n.d.	0.82	0.04	0.07	1.55
4ENC - d	3.47	3.52	5.76	n.d.	0.18	0.05	0.08	1.68
4ENC - e	3.62	3.67	5.04	n.d.	0.21	0.06	0.09	1.59
4ENC - f	3.77	3.82	6.57	n.d.	0.20	0.05	0.08	1.67
4ENC - g	3.92	3.97	11.37	n.d.	0.75	0.06	0.10	1.84
4ENC - h	4.07	4.12	12.84	n.d.	0.18	0.06	0.11	1.65
4ENC - i	4.22	4.27	11.33	n.d.	0.33	0.08	0.13	1.77
4AC - a	0.05	0.10	5.69	n.d.	10.79	0.19	0.30	1.55
4AC - b	0.17	0.22	7.36	22.50	11.70	0.19	0.30	1.57
4AC - c	0.33	0.38	7.18	n.d.	8.96	0.15	0.28	1.83
4BC - a	0.55	0.60	8.21	n.d.	12.24	0.15	0.26	1.70
4BC - b	0.70	0.75	6.31	n.d.	7.82	0.12	0.22	1.84
4CC - a	0.00	0.00	7.11	n.d.	11.77	0.16	0.35	2.24
4CC - b	1.08	1.13	5.46	n.d.	5.42	0.13	0.28	2.21
4CC - c	1.17	1.22	4.96	n.d.	4.92	0.14	0.23	1.66
4CC - d	1.28	1.33	6.12	n.d.	5.04	0.14	0.27	1.93
4DC - a	1.52	1.57	5.02	n.d.	5.90	0.11	0.23	2.08
4DC - b	1.67	1.72	5.53	n.d.	5.56	0.11	0.23	2.19
4DC - c	1.82	1.87	4.32	n.d.	3.85	0.12	0.24	2.08
4DC - d	1.97	2.02	3.99	n.d.	1.98	0.10	0.23	2.30
4DC - e	2.12	2.17	2.52	n.d.	0.94	0.10	0.21	2.13
4DC - f	2.30	2.35	13.17	n.d.	0.32	0.07	0.15	2.01
4DC - g	2.43	2.48	15.86	n.d.	0.27	0.07	0.13	1.88
4EC - a	3.04	3.09	10.15	n.d.	0.35	0.07	0.12	1.66
4EC - b	3.19	3.24	8.87	n.d.	0.29	0.05	0.09	1.83
4EC - c	3.34	3.39	9.89	n.d.	0.64	0.05	0.09	1.73
4EC - d	3.49	3.54	10.61	n.d.	0.42	0.05	0.09	1.77
4EC - e	3.64	3.69	13.03	n.d.	0.53	0.05	0.10	1.88
4EC - f	3.79	3.84	11.34	n.d.	0.62	0.09	0.19	2.14
4EC - g	3.94	3.99	15.35	n.d.	0.33	0.06	0.12	2.08
4EC - h	4.04	4.09	21.92	n.d.	0.43	0.23	0.41	1.80
5ANC - a	0.02	0.07	9.28	n.d.	11.15	0.20	0.29	1.39
5ANC - b	0.10	0.15	14.10	n.d.	12.06	0.20	0.31	1.52
5ANC - c	0.15	0.20	16.32	n.d.	9.88	0.19	0.28	1.49
5ANC - d	0.29	0.34	18.39	n.d.	7.19	0.17	0.32	1.83
5ANC - e	0.38	0.43	18.80	n.d.	6.00	0.20	0.24	1.22
5BNC - a	0.50	0.55	18.00	n.d.	4.46	0.18	0.33	1.81
5BNC - b	0.60	0.65	18.18	n.d.	3.38	0.17	0.29	1.74
5BNC - c	0.73	0.77	16.84	n.d.	2.82	0.18	0.28	1.54
5CNC - a	1.01	1.06	18.67	0.40	3.19	0.17	0.33	1.99
5CNC - b	1.11	1.16	2.92	n.d.	0.34	0.17	0.32	1.91
5CNC - c	1.21	1.26	3.19	n.d.	0.47	0.17	0.35	2.06

Borehole	Depth (m)		Chloride Conc. (mg/kg soil)	Bromide Conc. (mg/kg soil)	Nitrate as N Conc. (mg/kg soil)	GWC (g _w /g _s)	VWC (cm ³ _w /cm ³ _s)	Dry Bulk Density (g _s /cm ³ _s)
	Start	Finnish						
5CNC - d	1.27	1.31	0.78	n.d.	0.05	0.17	0.37	2.18
5DNC - a	1.50	1.55	1.13	0.05	0.17	0.20	0.38	1.87
5DNC - b	1.68	1.73	1.05	0.03	0.04	0.10	0.16	1.58
5DNC - c	1.78	1.83	1.32	0.01	0.03	0.08	0.15	1.89
5DNC - d	1.88	1.93	1.55	0.04	0.03	0.07	0.11	1.52
5DNC - e	1.98	2.03	1.60	n.d.	0.03	0.07	0.12	1.79
5ENC - a	3.03	3.08	1.19	n.d.	0.03	0.09	0.14	1.61
5ENC - b	3.18	3.23	1.08	n.d.	0.03	0.07	0.10	1.42
5ENC - c	3.33	3.38	1.66	n.d.	0.03	0.06	0.09	1.67
5ENC - d	3.48	3.53	1.27	n.d.	0.03	0.07	0.11	1.61
5ENC - e	3.63	3.68	2.75	n.d.	0.03	0.07	0.12	1.65
5ENC - f	3.78	3.83	2.92	n.d.	0.04	0.08	0.13	1.59
5ENC - g	3.93	3.98	2.66	n.d.	0.04	0.08	0.13	1.61
5AC - a	0.00	0.05	2.50	n.d.	5.91	0.20	0.29	1.46
5AC - b	0.12	0.16	2.17	0.61	3.69	0.15	0.24	1.63
5AC - c	0.23	0.28	2.59	n.d.	2.08	0.13	0.21	1.60
5AC - d	0.32	0.37	2.52	n.d.	1.94	0.14	0.19	1.34
5BC - a	0.54	0.59	2.85	n.d.	1.15	0.19	0.28	1.49
5BC - b	0.68	0.73	3.46	n.d.	0.64	0.15	0.25	1.68
5BC - c	0.76	0.81	3.38	n.d.	0.54	0.13	0.24	1.81
5CC - a	1.00	1.04	3.26	n.d.	0.54	0.12	0.24	1.99
5CC - b	1.09	1.14	4.17	n.d.	0.42	0.14	0.27	1.99
5CC - c	1.20	1.23	2.45	n.d.	0.40	0.12	0.23	1.96
5CC - d	1.27	1.32	3.39	n.d.	0.55	0.12	0.22	1.86
5DC - a	1.52	1.57	4.52	n.d.	1.08	0.13	0.23	1.70
5DC - b	1.63	1.68	6.05	n.d.	1.50	0.12	0.23	1.95
5DC - c	1.79	1.84	5.42	2.36	1.22	0.11	0.20	1.92
5DC - d	1.94	1.99	5.16	n.d.	1.87	0.10	0.20	1.96
5DC - e	2.09	2.14	12.58	n.d.	0.50	0.05	0.11	1.96
5DC - f	2.24	2.29	17.54	n.d.	1.37	0.06	0.13	2.13
5EC - a	3.20	3.26	10.55	n.d.	0.40	0.19	0.40	2.13
5EC - b	3.32	3.37	13.16	n.d.	0.44	0.28	0.46	1.64
5EC - c	3.58	3.63	6.62	n.d.	0.53	0.05	0.11	1.98
5EC - d	3.73	3.78	6.58	n.d.	1.08	0.14	0.22	1.57
5EC - e	3.88	3.93	7.91	n.d.	0.65	0.11	0.20	1.82
5EC - f	4.03	4.08	6.67	n.d.	0.50	0.06	0.14	2.14
BrA - a	0.00	0.05	4.73	8.25	0.99	0.19	0.23	1.22
BrA - b	0.10	0.15	4.37	9.23	1.00	0.17	0.24	1.39
BrA - c	0.17	0.22	4.21	20.49	1.27	0.18	0.21	1.17
BrA - d	0.27	0.32	4.63	49.30	2.34	0.24	0.31	1.27
BrA - e	0.38	0.43	1.76	69.38	2.77	0.30	0.34	1.15
BrB - a	0.56	0.61	1.80	77.08	2.82	0.18	0.29	1.74
BrB - b	0.66	0.71	1.67	72.15	2.52	0.16	0.24	1.75
BrB - c	0.76	0.81	6.23	58.16	2.20	0.17	0.26	1.77

Borehole	Depth (m)		Chloride Conc. (mg/kg soil)	Bromide Conc. (mg/kg soil)	Nitrate as N Conc. (mg/kg soil)	GWC (g _w /g _s)	VWC (cm ³ _w /cm ³ _s)	Dry Bulk Density (g _s /cm ³ _s)
	Start	Finnish						
BrB - d	0.87	0.92	1.18	46.45	1.47	0.15	0.28	2.31
BrB - e	0.95	1.00	1.14	37.25	1.15	0.19	0.29	1.99
BrC - a	1.03	1.08	1.17	33.62	1.06	0.21	0.32	1.60
BrC - b	1.13	1.18	1.18	27.38	0.87	0.19	0.30	1.75
BrC - c	1.24	1.29	0.74	15.18	0.47	0.16	0.32	2.25
BrC - d	1.38	1.41	0.98	14.13	0.46	0.14	0.32	2.62
BrD- a	1.50	1.55	0.91	14.41	0.47	0.14	0.26	2.00
BrD- b	1.65	1.70	0.88	5.04	0.17	0.09	0.16	1.80
BrD- c	1.80	1.85	1.01	2.62	0.12	0.07	0.12	1.83
BrD- d	1.95	2.00	0.88	1.85	0.09	0.08	0.14	1.89
BrD- e	2.10	2.15	1.64	1.81	0.08	0.06	0.11	1.90
BrD- f	2.25	2.30	2.65	1.41	0.08	0.06	0.09	1.52
BrD- g	2.33	2.38	2.50	1.66	0.10	0.06	0.12	2.18
BrE- a	3.03	3.08	1.07	0.27	0.03	0.05	0.08	1.67
BrE- b	3.18	3.23	1.30	0.10	0.04	0.06	0.09	1.65
BrE- c	3.33	3.38	1.02	0.04	0.04	0.06	0.10	1.74
BrE- d	3.48	3.53	1.28	n.d.	0.04	0.05	0.08	1.76
BrE- e	3.63	3.68	1.39	n.d.	0.03	0.05	0.07	1.63
BrE- f	3.78	3.83	1.54	n.d.	0.04	0.15	0.28	1.94
BrE- g	3.93	3.98	1.74	n.d.	0.05	0.12	0.22	1.87
BrE- h	4.08	4.13	2.53	n.d.	0.03	0.07	0.13	1.89
BrE - i	4.19	4.24	2.32	n.d.	0.03	0.11	0.19	1.78

Appendix E

Soil Nitrate Concentration Profiles

Spring 2009 and Fall 2009

Polymer-Coated Urea

Conventional Urea

Calculator Rate Side-dress

High Rate Side-dress

Control

Fall 2009 and Spring 2010

Polymer-Coated Urea

Conventional Urea

Calculator Rate Side-dress

High Rate Side-dress

Control

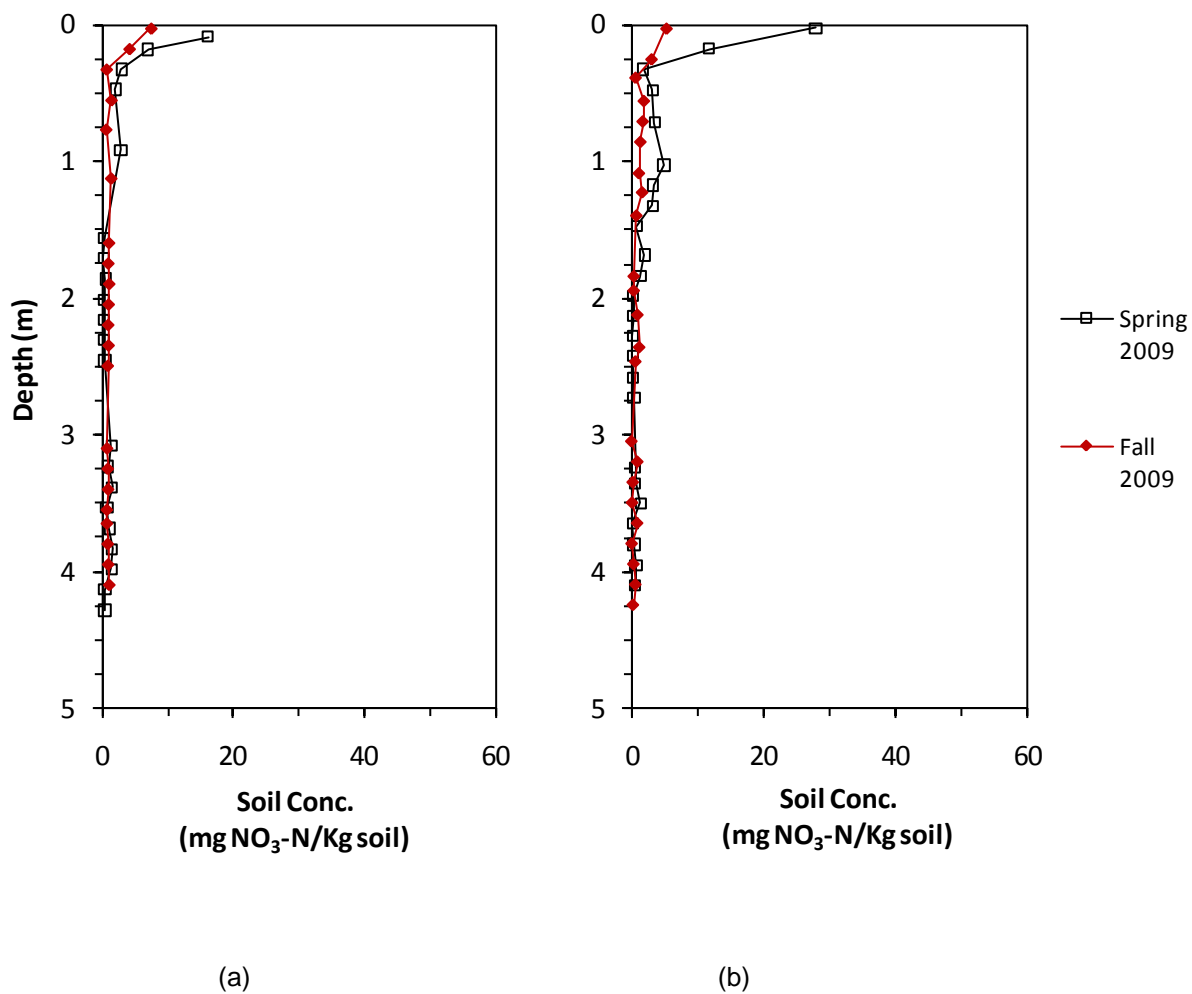


Figure E.1 Soil nitrate concentration profiles for the polymer coated urea (a) no clover and (b) clover treatments in the spring of 2009 and the fall of 2009.

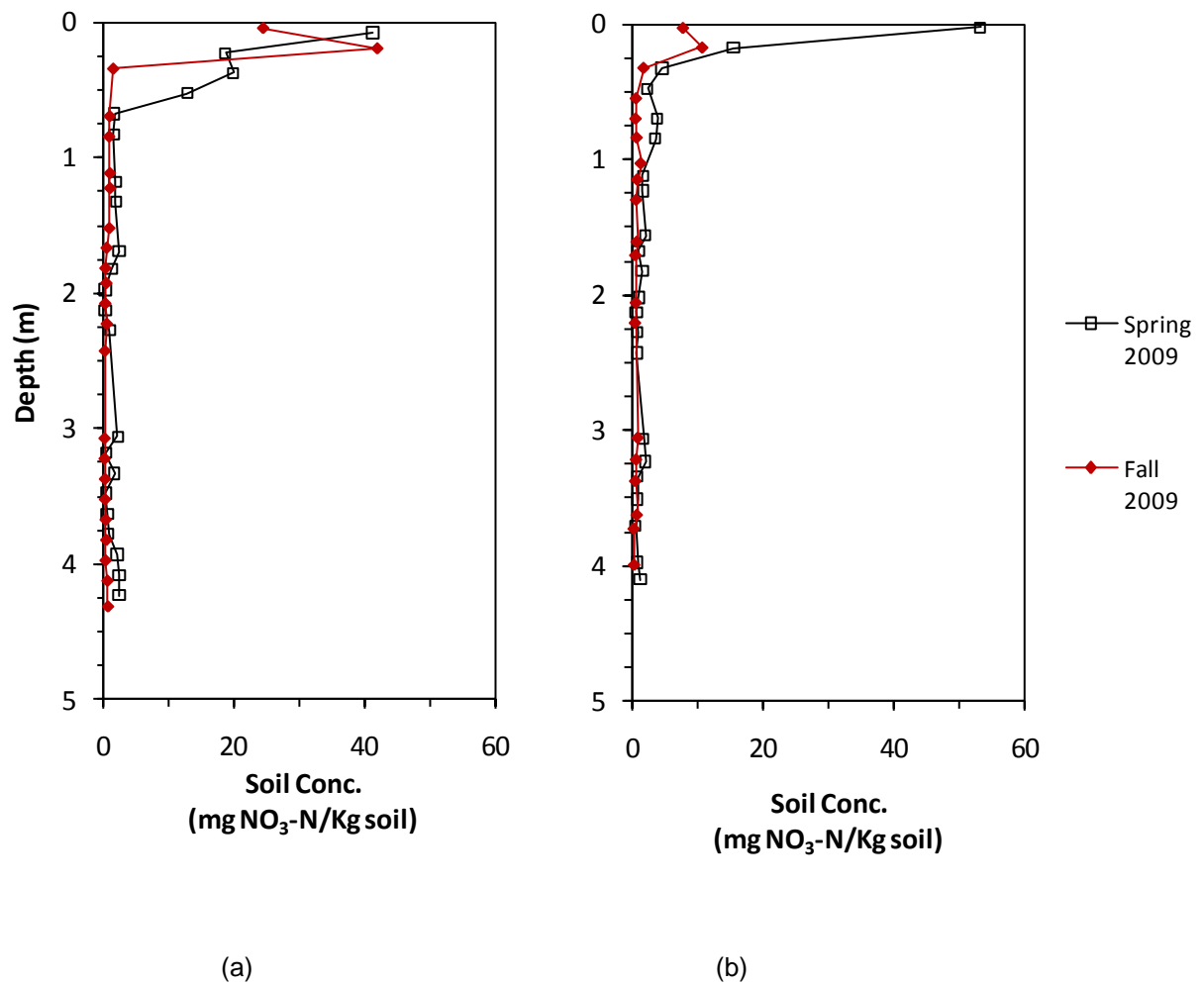


Figure E.2 Soil nitrate concentration profiles for the conventional urea (a) no clover and (b) clover treatments in the spring of 2009 and the fall of 2009.

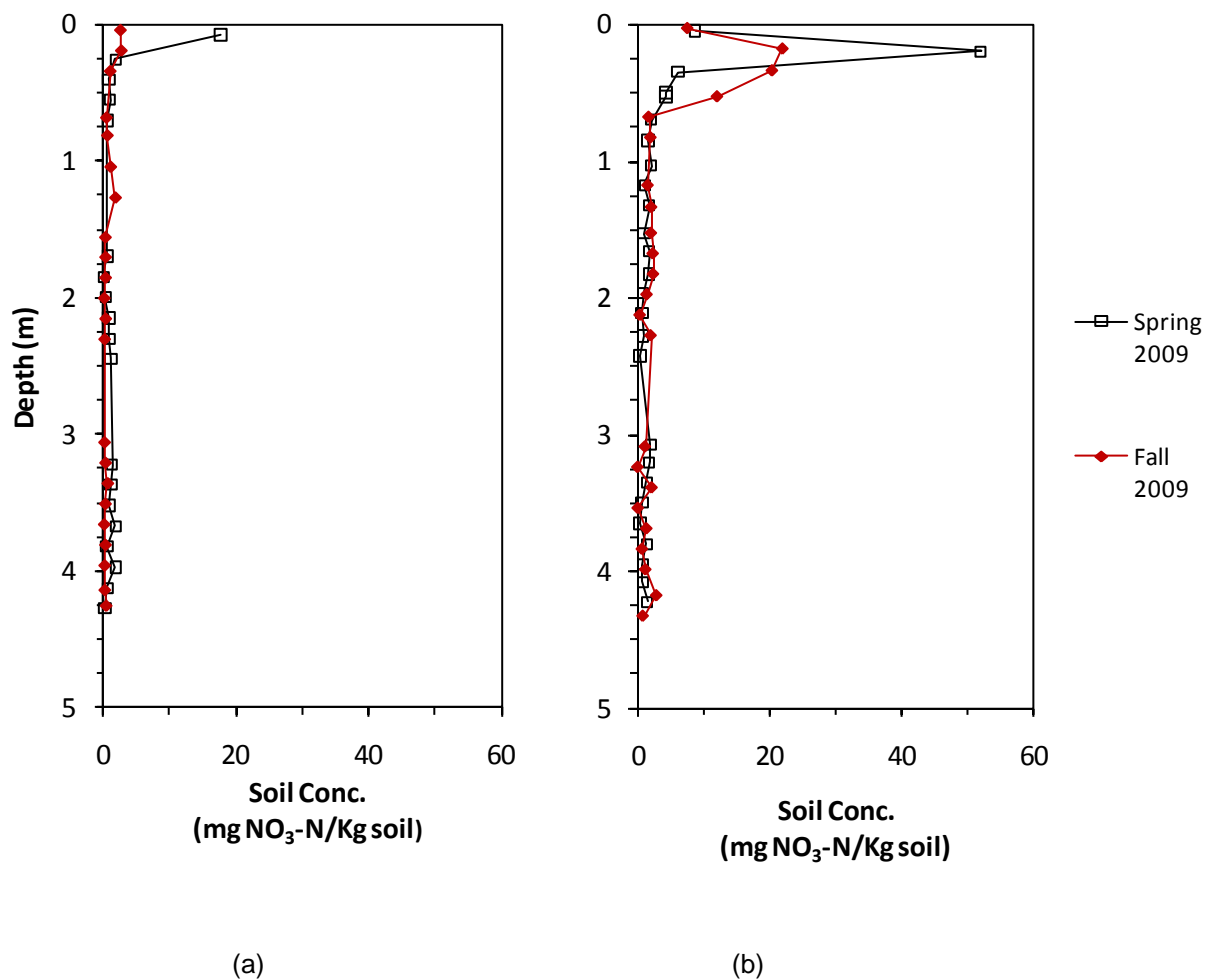


Figure E.3 Soil nitrate concentration profiles for the calculator rate side-dress (a) no clover and (b) clover treatments in the spring of 2009 and the fall of 2009.

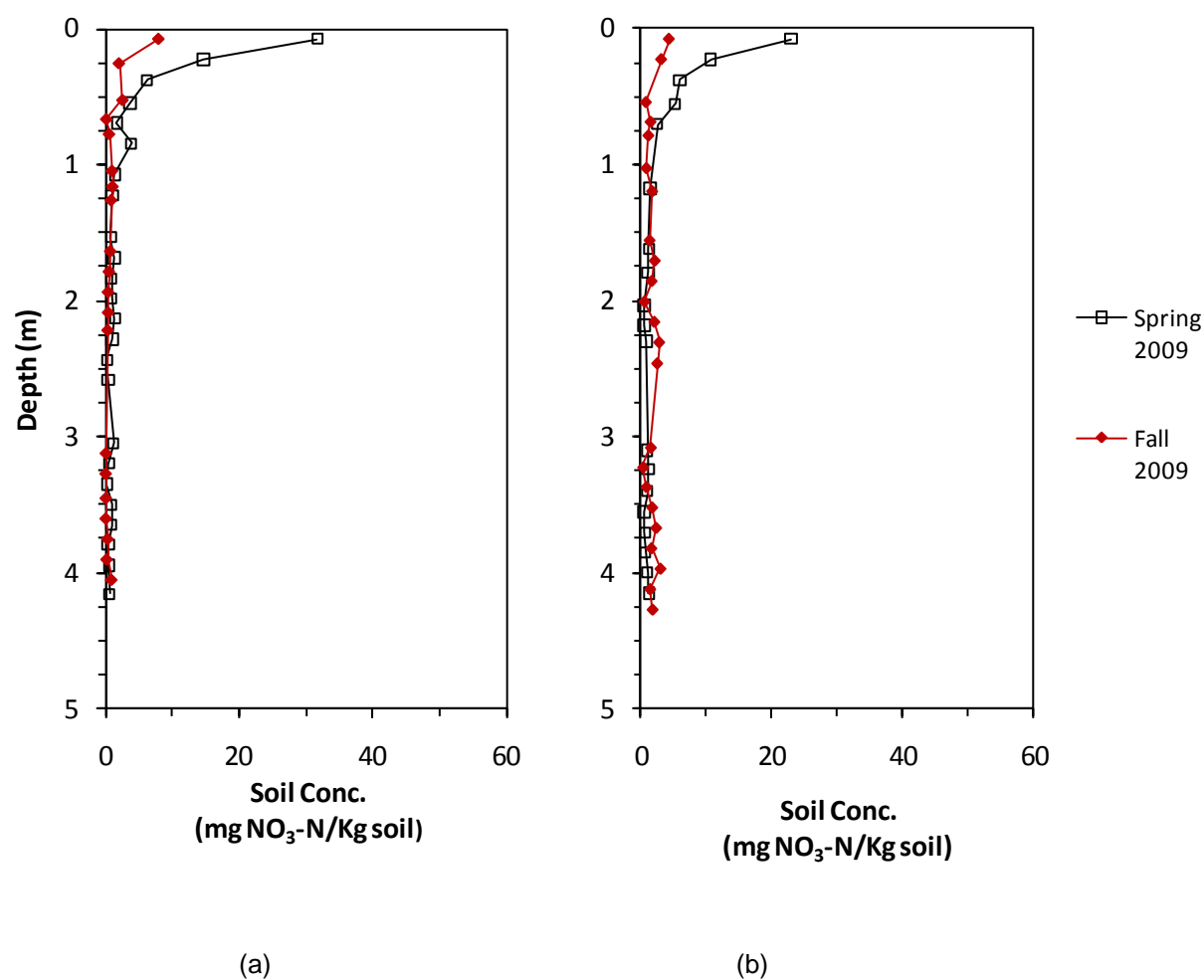
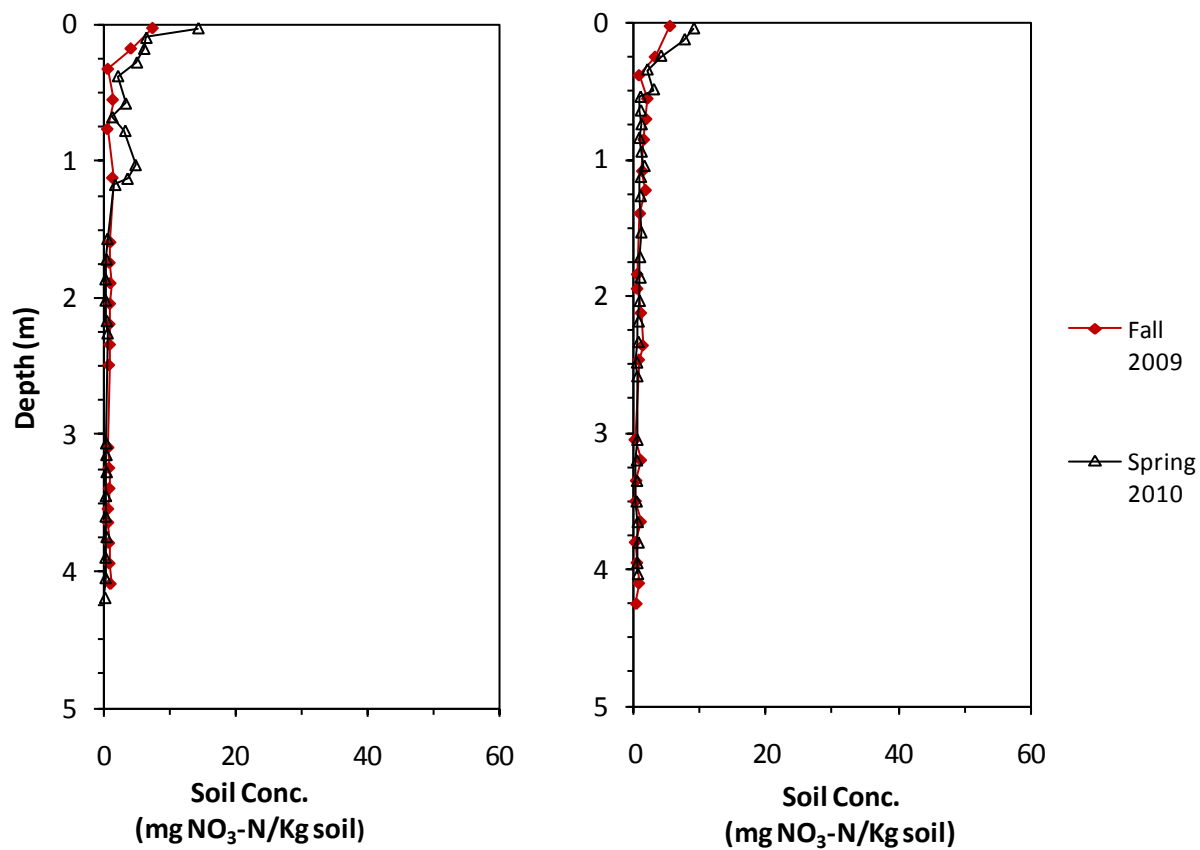
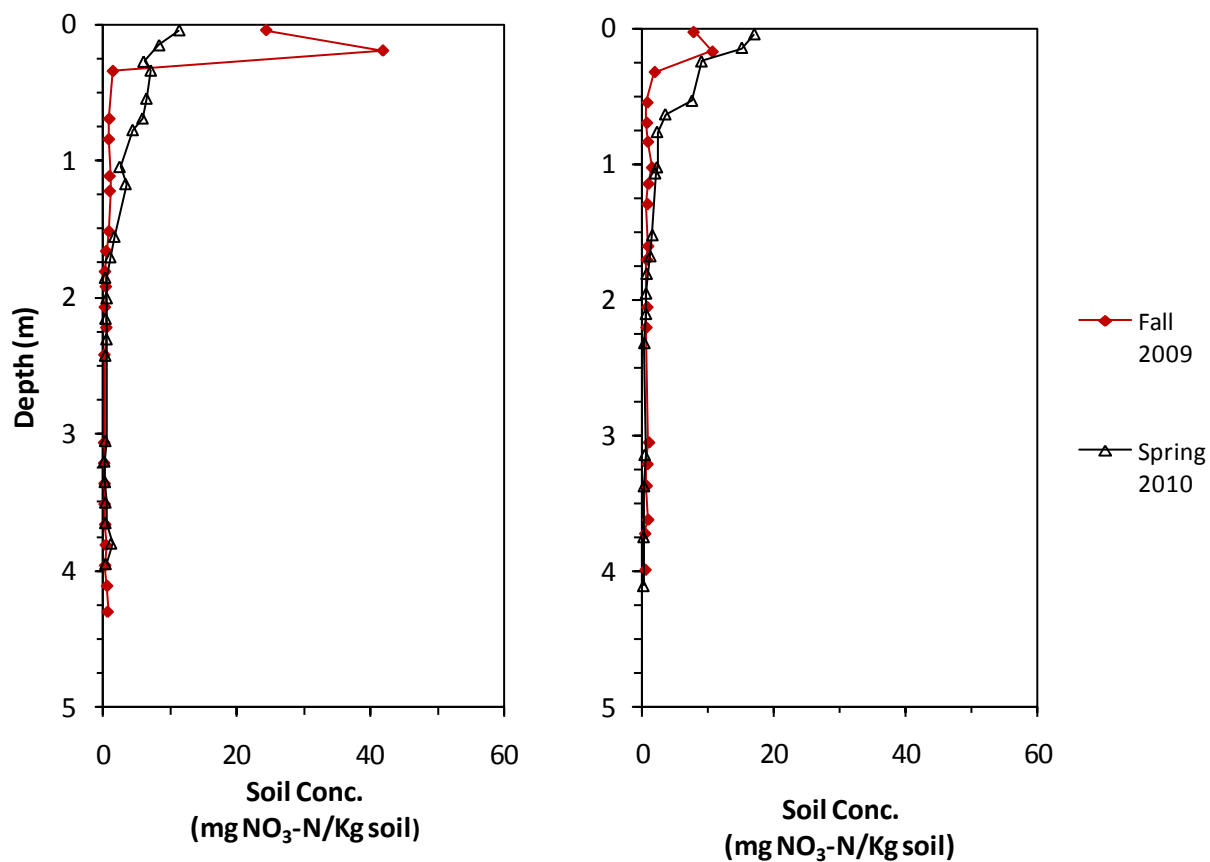


Figure E.4 Soil nitrate concentration profiles for the control (a) no clover and (b) clover treatments in the spring of 2009 and the fall of 2009.



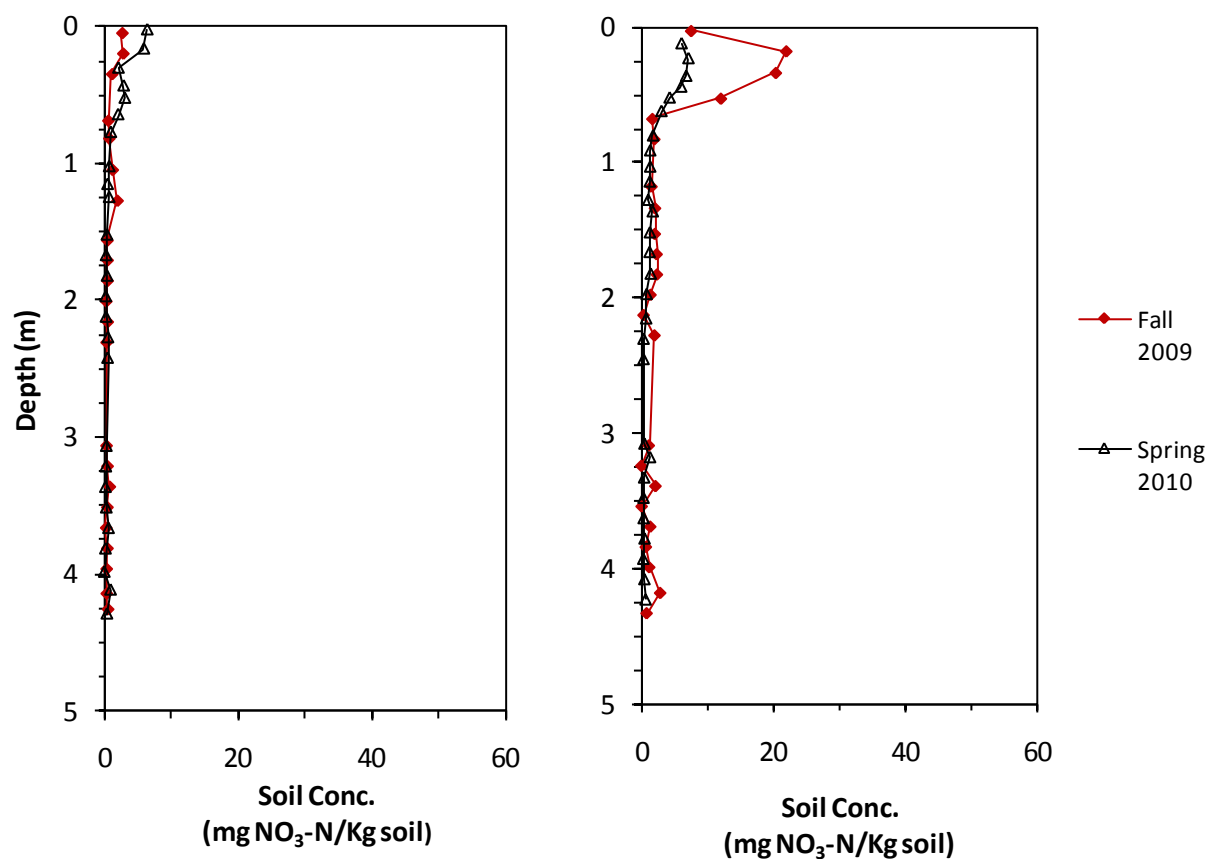
(a) (b)

Figure E.5 Soil nitrate concentration profiles for the polymer-coated urea (a) no clover and (b) clover treatments in the fall 2009 and spring of 2010.



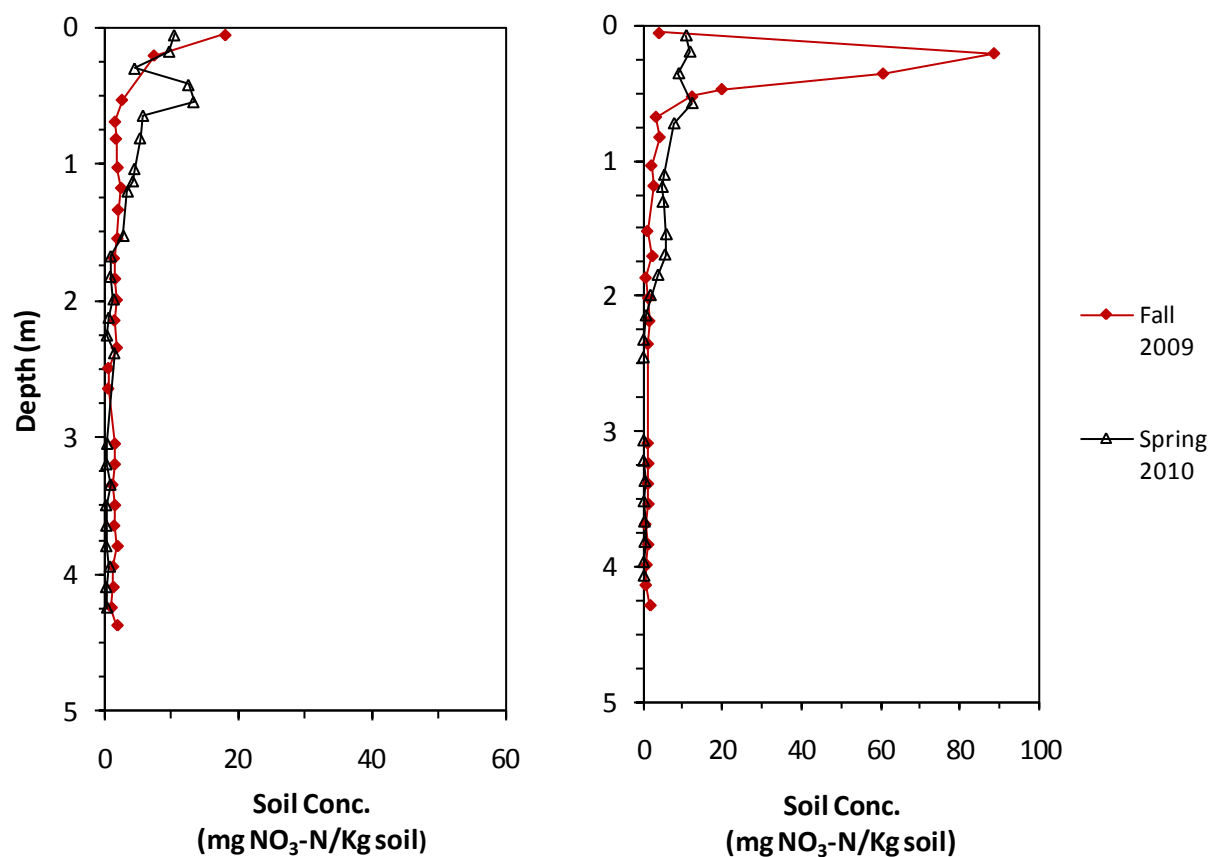
(a) (b)

Figure E.6 Soil nitrate concentration profiles for the conventional urea (a) no clover and (b) clover treatments in the fall 2009 and spring of 2010.



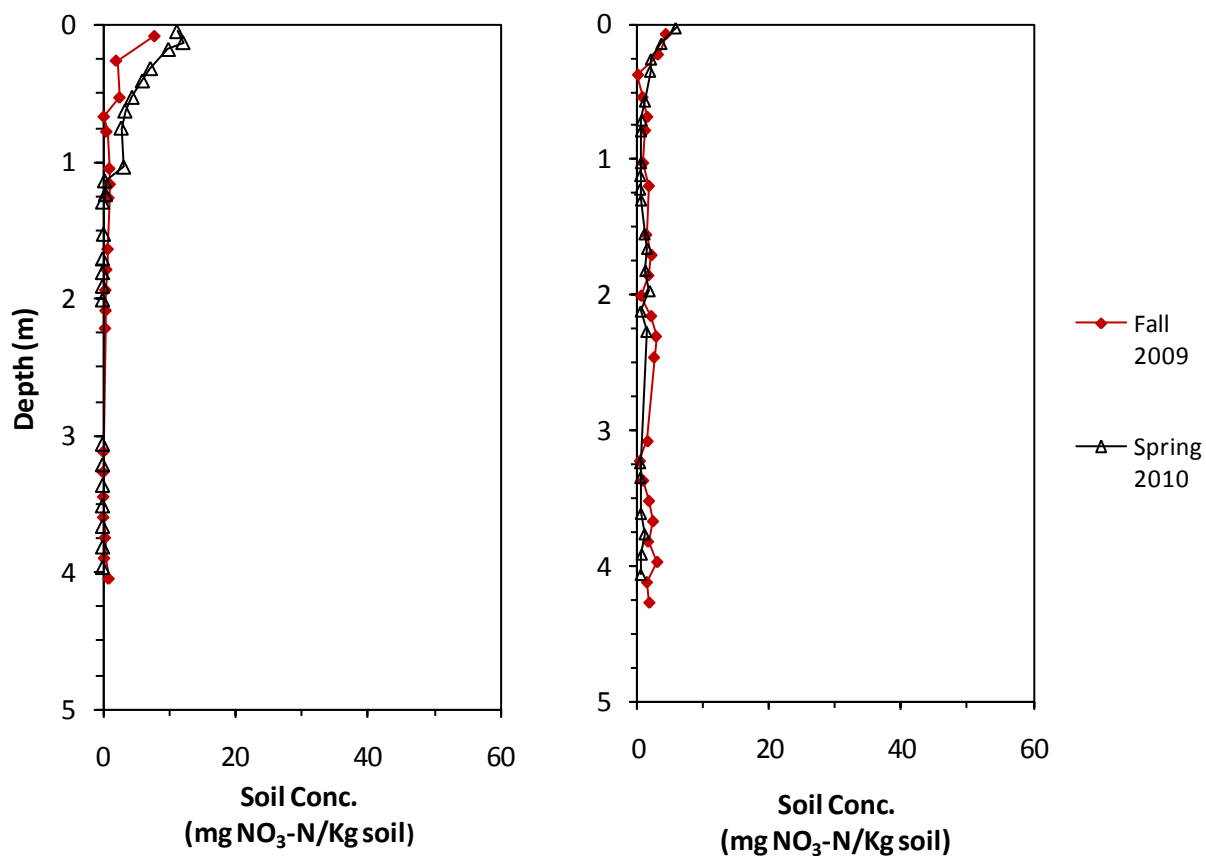
(a) (b)

Figure E.7 Soil nitrate concentration profiles for the calculator rate sidedress (a) no clover and (b) clover treatments in the fall 2009 and spring of 2010.



(a) (b)

Figure E.8 Soil nitrate concentration profiles for the high rate sidedress (a) no clover and (b) clover treatments in the fall 2009 and spring of 2010.



(a) (b)

Figure E.9 Soil nitrate concentration profiles for the control (a) no clover and (b) clover treatments in the fall 2009 and spring of 2010.

Appendix F

Cumulative Nitrate

Cumulative Nitrate Profiles

Polymer-Coated Urea
Spring 2009, Fall 2009, and Spring 2010

Conventional Urea
Spring 2009, Fall 2009, and Spring 2010

Calculator Rate Side-dress
Spring 2009, Fall 2009, and Spring 2010

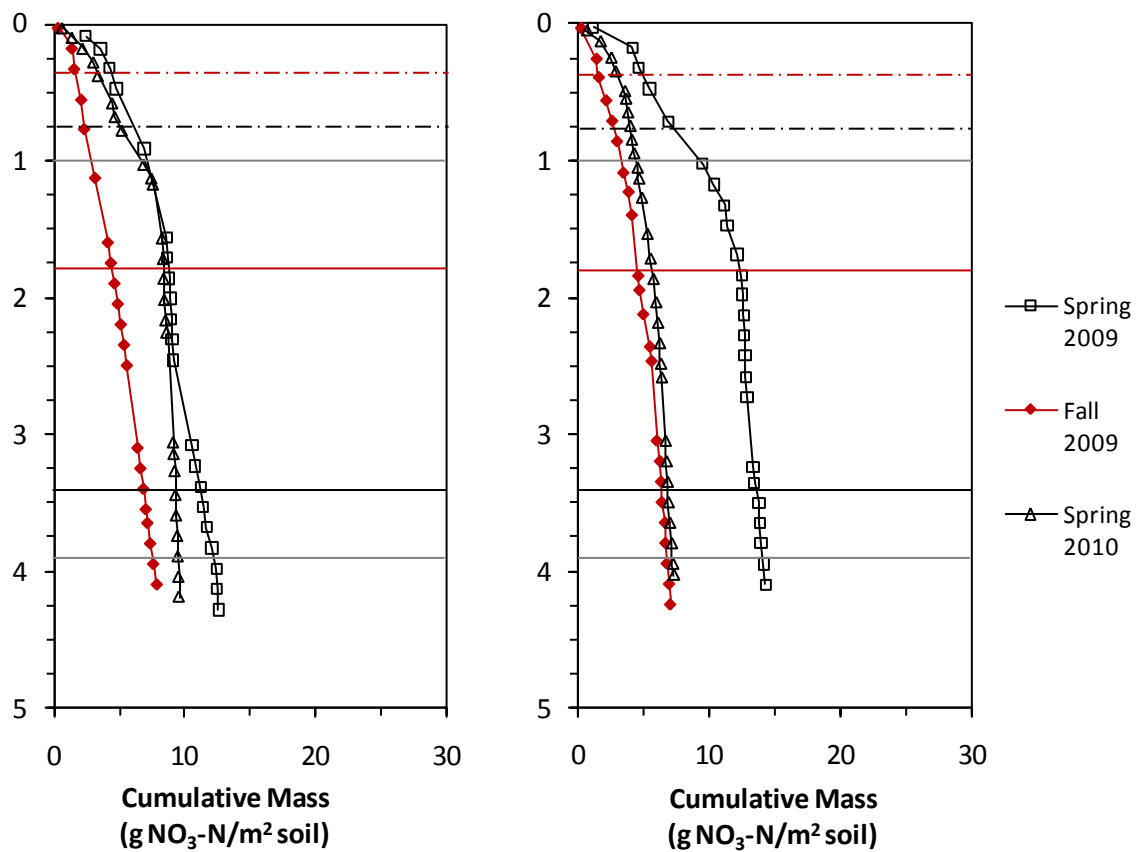
High Rate Side-dress
Fall 2009 and Spring 2010

Control
Spring 2009, Fall 2009, and Spring 2010

Cumulative Nitrate Table

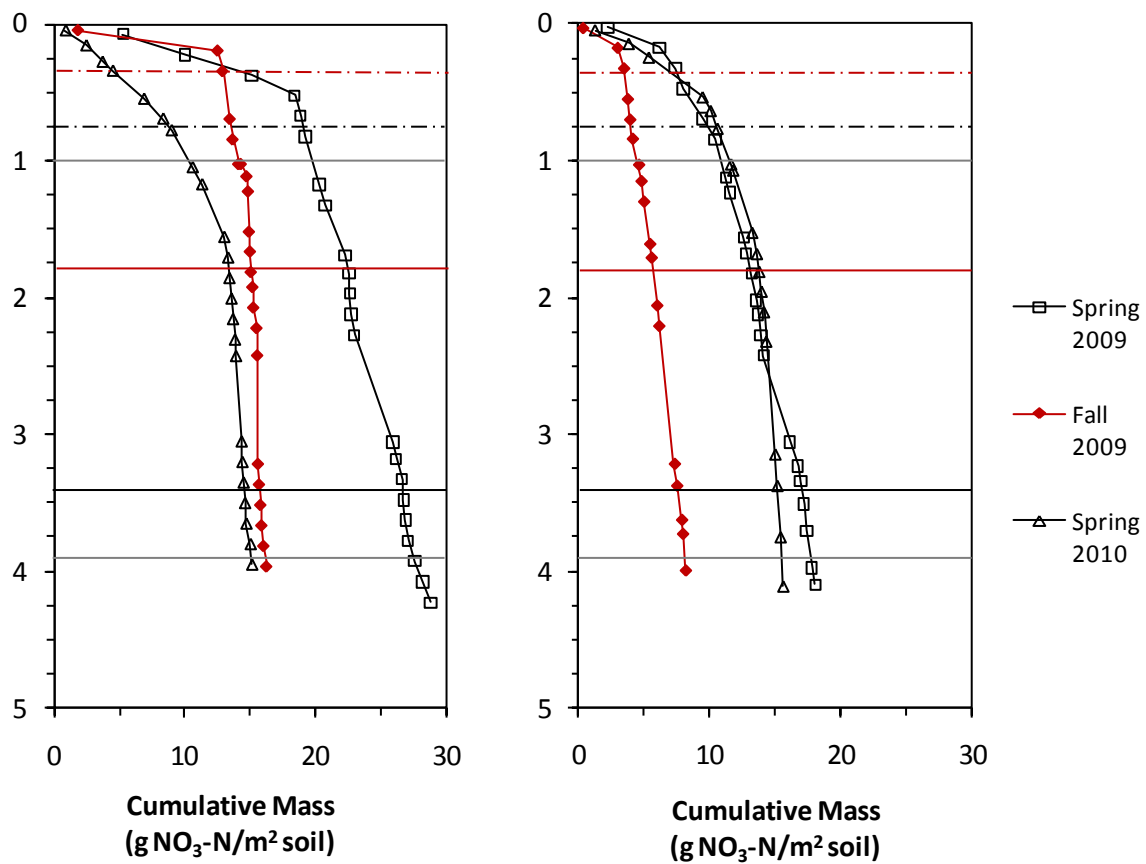
Soil Nitrate Mass

Pore-water



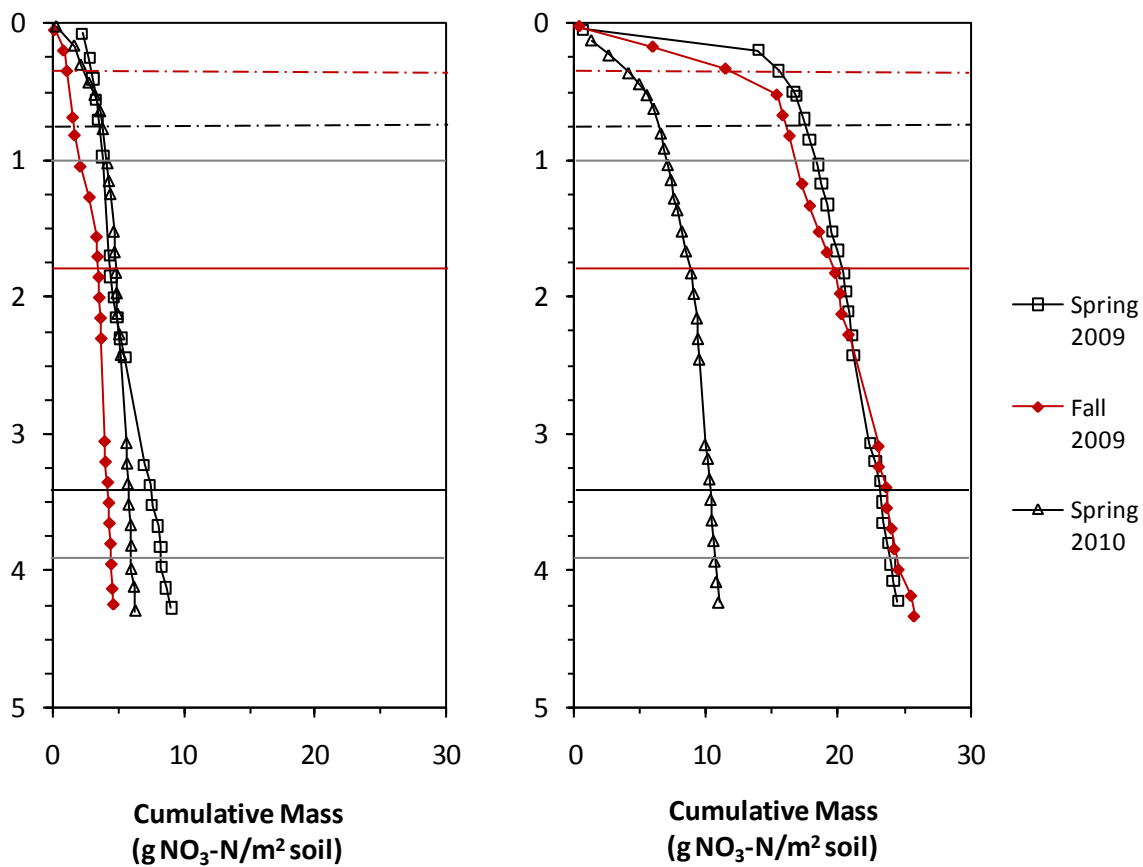
(a) (b)

Figure F.1 Cumulative nitrate mass profiles for the polymer coated urea (a) no clover and (b) clover treatments in the spring 2009, fall 2009 and spring 2010.



(a) (b)

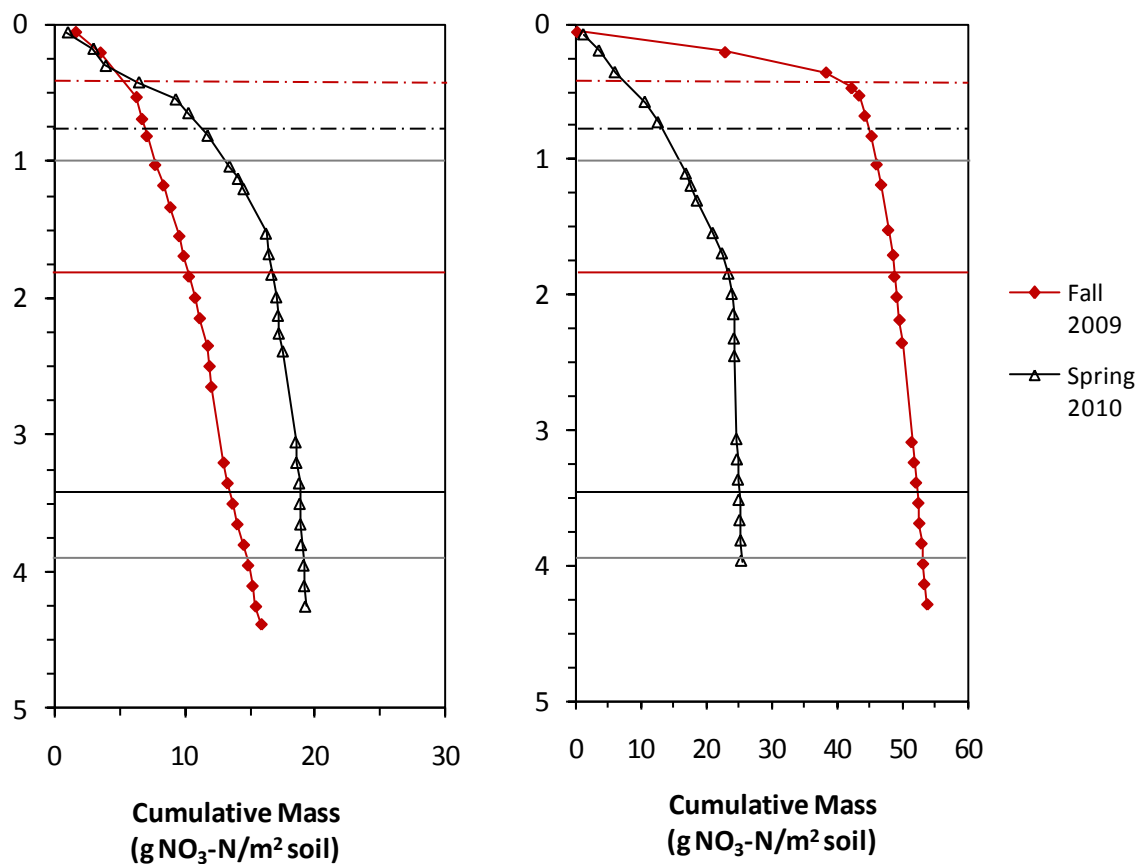
Figure F.2 Cumulative nitrate mass profiles for the conventional urea (a) no clover and (b) clover treatments in the spring 2009, fall 2009 and spring 2010.



(a)

(b)

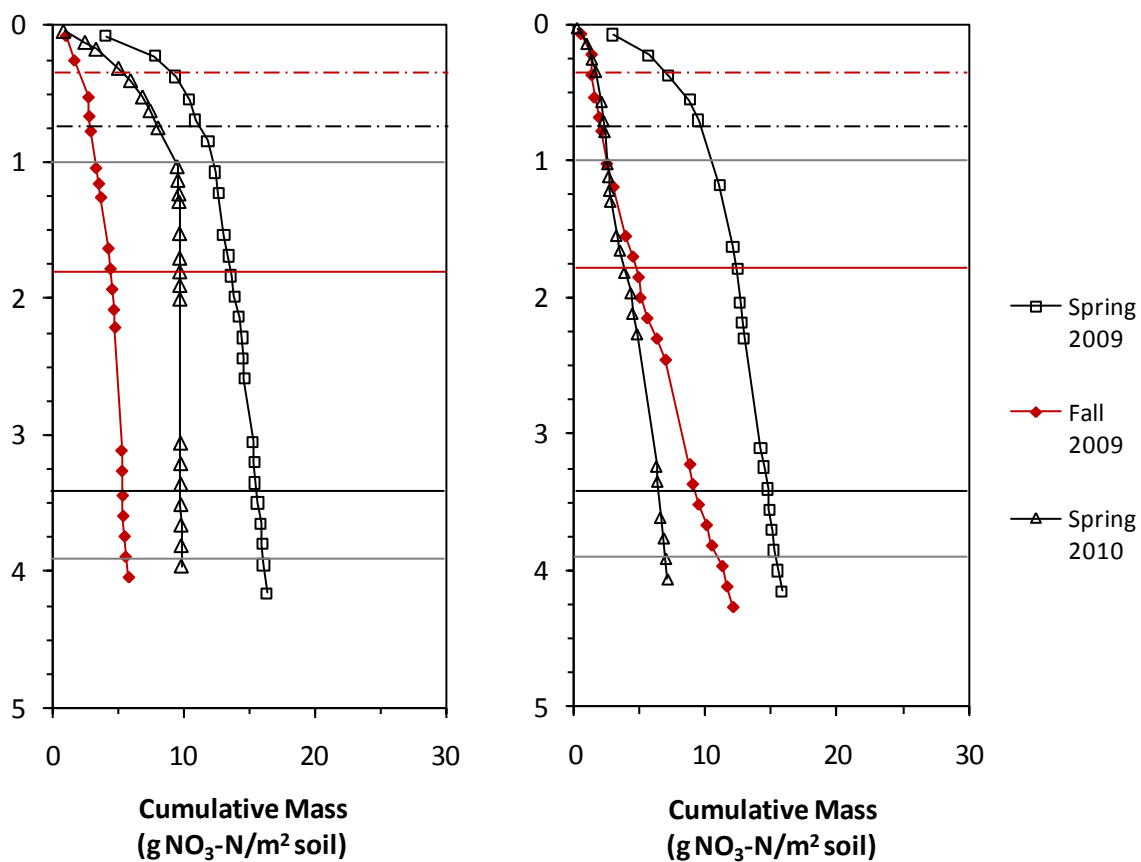
Figure F.3 Cumulative nitrate mass profiles for the calculator rate side-dress (a) no clover and (b) clover treatments in the spring 2009, fall 2009 and spring 2010.



(a)

(b)

Figure F.4 Cumulative nitrate mass profiles for the high rate side-dress (a) no clover and (b) clover treatments in the fall 2009 and spring of 2010



(a) (b)

Figure F.5 Cumulative nitrate mass profiles for the control (a) no clover and (b) clover treatments in the spring 2009, fall 2009 and spring 2010.

Table F.1 Cumulative mass (g/m²) at points of examination on the (a) no clover plots and (b) the clover plots.

	0.37	0.76	1	1.83	3.36	3.9
1NC - spring 2009	4.4	6.2	7.1	8.8	11.1	12.2
1NC - fall 2009	1.7	2.3	2.9	4.5	6.8	7.5
1NC - spring 2010	3.3	5.1	6.7	8.4	9.3	9.5
2NC - spring 2009	14.9	19	19.8	22.6	26.7	27.5
2NC - fall 2009	13	13.6	13.9	14.9	15.6	15.9
2NC - spring 2010	4.8	8.9	10.3	13.4	14.5	15.1
3NC - spring 2009	3	3.6	3.9	4.4	7.4	8.2
3NC - fall 2009	1.2	1.6	2.1	3.5	4.2	4.4
3NC - spring 2010	2.4	3.8	4.2	4.8	5.7	6
4NC - spring 2009						
4NC - fall 2009	5	6.9	7.7	10.3	13.3	14.7
4NC - spring 2010	5.4	11.3	13.2	16.7	18.8	19.1
5NC - spring 2009	9.3	11.3	12.2	13.6	15.5	16.1
5NC - fall 2009	2.1	2.9	3.2	4.4	5.3	5.6
5NC - spring 2010	5.6	8.1	9.3	9.7	9.8	9.8

	0.37	0.76	1	1.83	3.36	3.9
1C - spring 2009	4.9	7.3	9.3	12.5	13.5	14.1
1C - fall 2009	1.5	2.8	3.3	4.6	6.4	6.8
1C - spring 2010	3	4	4.4	5.7	6.8	7.2
2C - spring 2009	7.6	9.8	10.7	13.2	17	17.7
2C - fall 2009	3.5	4	4.5	5.7	7.5	8.1
2C - spring 2010	7.2	10.6	11.6	13.8	15.2	15.5
3C - spring 2009	15.7	17.6	18.3	20.4	23.2	23.9
3C - fall 2009	12.2	16.1	16.8	19.8	23.5	24.4
3C - spring 2010	4.2	6.4	7	8.9	10.3	10.6
4C - spring 2009						
4C - fall 2009	38.9	44.9	46.0	48.8	52.1	53.1
4C - spring 2010	6.5	13.2	15.9	23.4	25.0	25.5
5C - spring 2009	7.1	9.6	10.3	12.4	14.6	15.3
5C - fall 2009	1.4	2.1	2.5	4.8	9.0	10.9
5C - spring 2010	1.7	2.3	2.5	3.9	6.3	7

mbgs - meters below ground surface

(a)

(b)

Table F.2 Cumulative pore-water concentration (g m/Lpore-water) at points of examination on the (a) no clover plots and (b) the clover plots. These values are divided by the length of the segment of interest to determine the depth average pore-water nitrate concentration.

(mbgs)	0.37	0.76	1	1.83	3.36	3.9
1NC - spring 2009	14.5	19.2	21.6	27.2	56.6	65.4
1NC - fall 2009	4.6	7.0	11.9	27.3	51.2	59.6
1NC - spring 2010	9.3	16.1	21.0	25.1	30.3	32.1
2NC - spring 2009	53.3	72.2	74.3	85.5	123.2	128.7
2NC - fall 2009	43.6	46.0	47.9	54.1	62.8	65.0
2NC - spring 2010	18.3	35.2	39.8	52.4	63.3	68.7
3NC - spring 2009	12.0	14.3	15.8	19.2	50.7	58.2
3NC - fall 2009	3.7	5.5	7.1	21.6	30.2	33.0
3NC - spring 2010	8.3	13.1	14.8	20.7	28.2	30.6
4NC - spring 2009						
4NC - fall 2009	36.1	44.4	47.4	70.6	114.5	135.2
4NC - spring 2010	17.4	45.8	55.3	76.1	103.7	106.8
5NC - spring 2009	32.2	39.0	42.2	52.2	71.8	76.7
5NC - fall 2009	6.1	8.5	9.4	14.8	22.7	24.8
5NC - spring 2010	17.3	25.5	29.7	31.0	31.6	31.9

(mbgs)	0.37	0.76	1	1.83	3.36	3.9
1C - spring 2009	16.8	25.2	32.7	45.0	54.2	60.1
1C - fall 2009	4.4	8.0	9.8	16.9	33.9	39.5
1C - spring 2010	9.4	13.4	14.6	19.9	29.7	32.0
2C - spring 2009	25.4	32.6	35.7	47.4	79.1	88.3
2C - fall 2009	9.5	11.3	12.7	18.5	34.9	41.8
2C - spring 2010	23.4	38.0	42.3	53.6	67.4	72.4
3C - spring 2009	52.7	61.4	64.5	74.3	98.8	105.1
3C - fall 2009	32.6	43.9	46.3	58.3	94.5	104.7
3C - spring 2010	14.4	23.2	25.1	33.5	43.9	47.2
4C - spring 2009						
4C - fall 2009	96.1	112.5	115.9	125.6	161.2	173.6
4C - spring 2010	22.3	50.5	63.4	101.4	112.9	117.4
5C - spring 2009	20.8	27.2	35.3	47.0	73.1	77.3
5C - fall 2009	4.0	6.4	7.9	17.5	59.7	72.9
5C - spring 2010	6.8	8.9	9.9	16.6	36.3	39.7

mbgs - meters below ground surface

(a)

(b)

Appendix G

Moisture Content – Chapter 3

Moisture content measurements with depth taken with the neutron probe in 2009-2010

Table G.1 Neutron probe measurement of moisture content from June 2009 to March 2010.

Depth Below Ground Surface (m)	June 16 th , 2009	June 23 rd , 2009	July 21 st , 2009	October 13 th , 2009	Depth Below Ground Surface (m)	March 17 th , 2010
0.14	20.75	20.76	17.94	23.05	12.9	
0.29	24.57	23.30	22.21	23.98	27.9	26.54
0.44	25.76	24.19	24.00	24.26	42.9	22.82
0.59	26.32	25.14	24.98	23.35	57.9	26.01
0.74	26.29	25.30	25.48	23.25	72.9	24.88
0.89	26.47	25.47	26.33	23.87	87.9	25.33
1.04	26.77	26.16	26.12	25.14	102.9	26.91
1.19	26.72	25.45	25.83	25.45	117.9	25.54
1.34	25.48	23.69	24.12	23.65	132.9	26.80
1.49	24.41	23.19	24.01	25.54	147.9	25.66
1.64	19.87	17.37	18.80	18.41	162.9	18.91
1.79	13.32	13.05	12.29	12.20	177.9	15.39
1.94	12.13	11.53	11.20	10.06	192.9	16.04
2.09	16.66	15.57	15.52	15.02	207.9	18.60
2.24	15.17	14.24	14.43	12.76	222.9	17.17
2.39	15.78	14.14	14.25	13.52	237.9	17.39
2.54	14.58	13.64	13.27	12.60	252.9	17.48
2.69	13.39	12.81	13.09	12.47	267.9	17.19
2.84	13.88	13.52	13.51	12.39	282.9	14.22
2.99	12.33	10.83	11.86	11.61	297.9	12.22
3.14	11.46	10.02	10.14	9.76	312.9	10.11
3.29	11.77	10.36	11.41	10.73	327.9	12.16
3.44	14.77	13.71	13.13	13.20	342.9	15.12
3.59	13.68	12.44	13.26	12.50	357.9	11.81
3.74	12.60	11.47	11.50	10.11	372.9	12.24
3.89	23.05	21.74	22.22	21.53	387.9	25.60
4.04	26.26	25.39	25.64	25.39	402.9	21.22
4.19	14.82	13.64	13.75	12.74	417.9	11.61
4.34	15.35	14.34	14.34	13.05	432.9	14.92
4.49	14.31	13.31	13.65	13.06	447.9	13.36
4.64	13.70	13.01	12.86	12.06	462.9	12.46
4.79	12.02	11.02	10.53	10.08	477.9	8.48
4.94	16.26	15.04	14.27	11.30	492.9	13.28
5.09	19.53	18.25	17.88	15.84	507.9	13.65
5.24	14.76	12.57	12.69	11.30	522.9	8.39
5.39	8.76	7.06	7.12	5.83	537.9	5.96
5.54	9.93	8.11	8.51	7.45	552.9	7.72
5.69	9.91	9.71	9.13	8.57	567.9	8.21
5.84	12.27	11.24	10.90	9.67	582.9	9.38
5.99	15.55	14.66	14.16	13.12	597.9	13.16
6.14	15.70	14.86	14.69	13.09	612.9	11.40
6.29	11.10	10.45	9.93	9.06	627.9	7.47
6.44	11.63	11.00	10.94	10.11	642.9	12.22
6.59	16.81	15.85	15.46	13.99	657.9	
6.74	19.75	19.11		18.60		

Table G.2 Neutron probe measurement of moisture content from May 2010 and December 2010.

Depth Below Ground Surface (m)	May 5 th , 2010	Depth Below Ground Surface (m)	July 7 th , 2010	August 24 th , 2010	October 6 th , 2010	December 7 th , 2010
		0.21	15.63	23.59		25.12
		0.36	16.69	27.14		29.84
		0.51	17.14	27.90	25.38	29.45
0.58	19.59	0.66	25.02	27.77	27.77	30.28
0.73	26.10	0.81	26.77	26.75	26.79	26.40
0.88	26.23	0.96	27.07	27.73	26.46	26.31
1.03	26.45	1.11	27.37	27.62	27.32	26.72
1.18	27.01	1.26	25.63	25.98	26.54	26.01
1.33	25.92	1.41	26.39	25.63	26.14	25.44
1.48	25.83	1.56	24.07	22.70	23.75	23.58
1.63	18.58	1.71	16.84	16.28	15.85	17.72
1.78	12.51	1.86	10.90	11.47	12.05	16.00
1.93	13.57	2.01	15.97	16.21	16.84	17.95
2.08	16.59	2.16	16.15	16.66	15.72	19.97
2.23	16.04	2.31	16.25	15.41	15.11	18.75
2.38	14.95	2.46	16.02	15.27	14.18	17.92
2.53	14.52	2.61	14.92	14.90	12.74	16.88
2.68	14.70	2.76	15.27	14.34	13.11	16.59
2.83	15.30	2.91	14.46	14.03	12.95	15.50
2.98	12.88	3.06	12.91	11.95	10.85	13.42
3.13	11.31	3.21	12.25	11.88	10.79	13.63
3.28	12.49	3.36	14.12	14.05	11.45	15.98
3.43	16.49	3.51	18.65	17.53	15.46	16.31
3.58	14.60	3.66	14.63	14.02	10.79	10.84
3.73	13.90	3.81	17.22	18.03	15.97	14.81
3.88	25.39	3.96	28.21	28.90	27.77	27.53
4.03	24.83	4.11	19.46	18.71	17.75	16.18
4.18	14.82	4.26	14.55	14.08	13.48	12.23
4.33	17.29	4.41	16.13	16.25	15.14	13.94
4.48	14.63	4.56	14.81	14.20	14.31	12.48
4.63	14.42	4.71	12.49	12.25	12.12	10.20
4.78	11.76	4.86	12.25	11.87	17.39	9.34
4.93	15.15	5.01	17.66	17.81	18.31	15.16
5.08	17.39	5.16	16.16	15.30	15.53	13.63
5.23	9.98	5.31	8.53	8.43	9.17	7.56
5.38	6.26	5.46	7.41	7.79	7.96	7.29
5.53	8.15	5.61	9.34	9.16	9.35	8.70
5.68	8.50	5.76	9.92	10.32	9.86	9.01
5.83	10.45	5.91	11.96	12.79	13.25	12.48
5.98	13.80	6.06	15.30	15.64	15.04	15.68
6.13	11.62	6.21	10.81	11.33	10.55	10.32
6.28	7.28	6.36	8.11	9.06		8.01
6.43	10.74	6.51	13.69			14.10
6.58	13.06	6.66	16.21			16.17
6.73		6.81				

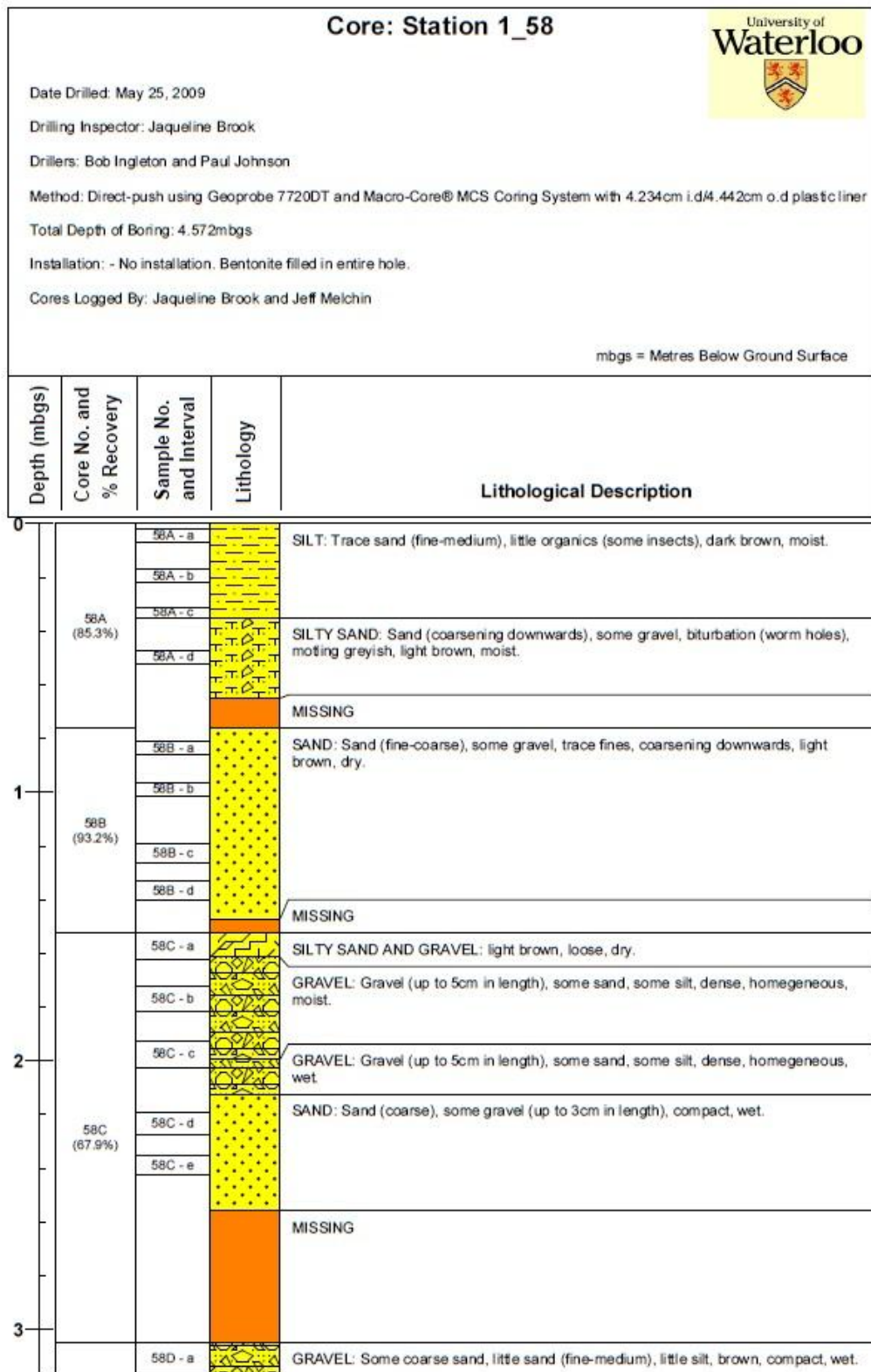
Appendix H

Stratigraphic Core Logs – Chapter 4






Core Log – Station 1 (May 25th, 2009)

Core Log – In the in stream bromide plot near Station 1 (May 6th, 2010)

Figure H.1 Stratigraphic core logs taken from Station 1 on May 25th, 2009



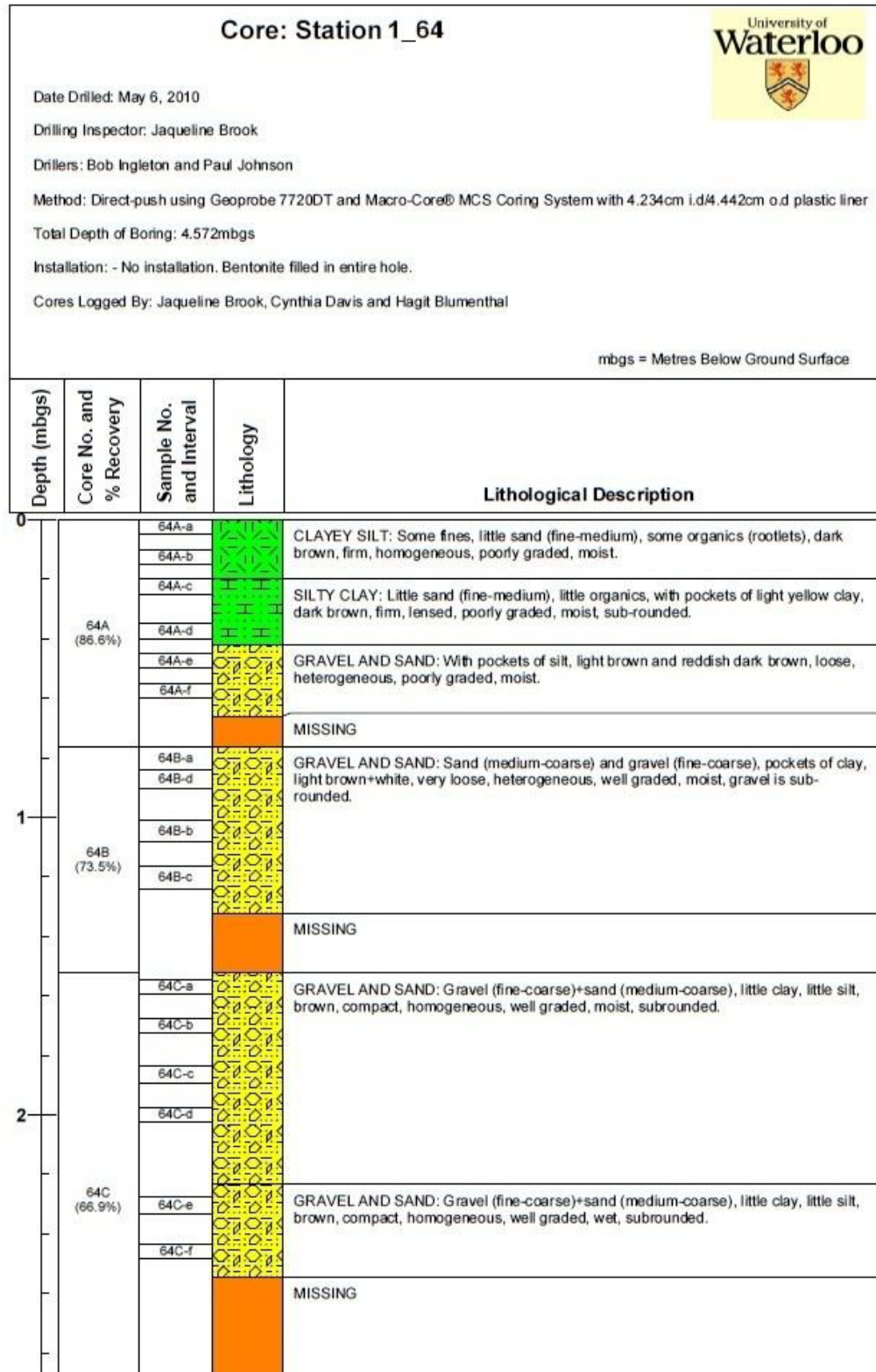
1 of 2

Core: Station 1_58				
Depth (m)	Core No. and % Recovery	Sample No. and Interval	Lithology	Lithological Description
4	58D (57.1%)			
		58D - b		SAND: Sand (coarse), some sand (fine-medium), little silt, brown, wet.
		58D - c		GRAVEL: Some sand (coarse), little sand (fine-medium), little silt, brown, compact, wet.
		58D - d		
				MISSING



Notes:

- the 'Missing' data from all cores are assumed to be from the bottom of each core interval
- surveyed using Thales MobileMapper CE

Figure H.2 Stratigraphic core logs taken at their stream bromide plot near Station 1 on May 6th, 2010



1 of 2

Core: Station 1_64				
Depth (m)	Core No. and % Recovery	Sample No. and Interval	Lithology	Lithological Description
3	64D (50.5%)	64D-a		GRAVEL AND SAND: Sand (coarse: some sand is fine-medium), and gravel (fine-coarse), trace clay, light brown, very loose, heterogeneous, well ghraded, wet, gravel is sub-rounded
		64D-b		
		64D-c		
		64D-d		
		64D-e		
4				MISSING

Notes:

- the 'Missing' data from all cores are assumed to be from the bottom of each core interval
- surveyed using Thales MobileMapper CE

Appendix I

Soil Core Sampling Results – Chapter 4

Table I.1 Soil bromide, gravimetric water content (GWC), volumetric water content (VWC), dry bulk density.

Borehole	Depth (m)		Bromide Conc. (mg/kg soil)	GWC (g _w /g _s)	VWC (cm ³ _w /cm ³ _s)	Dry Bulk Density (g _s /cm ³ _s)
	Start	Finnish				
Mar-11						
St1-C1-(1)-1	0.03	0.06	1342.03	0.55	0.55	1.00
St1-C1-(1)-2	0.06	0.08	2147.53	0.47	0.46	0.98
St1-C1-(1)-3	0.08	0.11	2612.71	0.41	0.22	0.53
St1-C1-(1)-4	0.11	0.13	2630.66	0.37	0.31	0.83
St1-C1-(1)-5	0.13	0.16	3180.94	0.34	0.46	1.34
St1-C1-(1)-6	0.16	0.18	3904.22	0.32	0.33	1.02
St1-C1-(1)-7	0.18	0.21	4793.80	0.31	0.45	1.45
St1-C1-(1)-8	0.21	0.23	4349.12	0.30	0.40	1.35
St1-C1-(1)-9	0.23	0.26	4311.65	0.31	0.40	1.32
St1-C1-(1)-10	0.26	0.28	3862.27	0.30	0.33	1.11
St1-C1-(1)-11	0.28	0.31	3272.39	0.29	0.41	1.39
St1-C1-(1)-12	0.31	0.33	2499.74	0.27	0.29	1.04
St1-C1-(1)-13	0.33	0.36	1916.89	0.27	0.35	1.28
St1-C1-(1)-14	0.36	0.38	1542.67	0.26	0.29	1.12
St1-C1-(1)-15	0.38	0.41	1250.29	0.25	0.31	1.25
St1-C1-(1)-16	0.41	0.43	625.56	0.21	0.32	1.54
St1-C1-(1)-17	0.43	0.46	380.75	0.17	0.10	0.58
St1-C1-(1)-18	0.46	0.48	226.88	0.14	0.09	0.61
St1-C1-(2)-1	0.72	0.74	204.95	0.12	0.10	0.77
St1-C1-(2)-2	0.74	0.77	137.16	0.10	0.15	1.52
St1-C1-(2)-3	0.77	0.79	171.06	0.08	0.10	1.21
St1-C1-(2)-4	0.79	0.82	116.34	0.07	0.12	1.59
St1-C1-(2)-5	0.82	0.84	87.21	0.08	0.10	1.19
St1-C1-(2)-6	0.84	0.87	69.25	0.08	0.06	0.81
May-11						
1-64A-a	0.00	0.05	37.00	0.26	0.30	1.15
1-64A-b	0.10	0.15	9.29	0.20	0.23	1.13
1-64A-c	0.20	0.25	6.87	0.19	0.22	1.14
1-64A-d	0.35	0.40	4.74	0.20	0.28	1.42
1-64A-e	0.45	0.50	1.72	0.18	0.27	1.49
1-64A-f	0.55	0.60	1.26	0.10	0.15	1.56
1-64B-a	0.76	0.84	0.70	0.02	0.02	1.58
1-64B-d	0.84	0.90	0.80	0.03	0.06	1.96

Borehole	Depth (m)		Bromide Conc. (mg/kg soil)	GWC (g _w /g _s)	VWC (cm ³ _w /cm ³ _s)	Dry Bulk Density (g _s /cm ³ _s)
	Start	Finnish				
1-64B-b	1.01	1.08	0.78	0.04	0.11	2.73
1-64B-c	1.16	1.24	1.06	0.05	0.07	1.41
1-64C-a	1.54	1.59	1.78	0.06	0.10	1.54
1-64C-b	1.67	1.72	1.49	0.05	0.10	2.10
1-64C-c	1.83	1.89	1.71	0.04	0.08	2.07
1-64C-d	1.97	2.02	1.65	0.04	0.09	2.07
1-64C-e	2.27	2.33	7.41	0.05	0.11	2.29
1-64C-f	2.43	2.48	0.89	0.07	0.15	2.12

Appendix J

Monitoring Well Dimensions and Location

Table J.1 Dimensions of monitoring wells sampled in the vicinity of the ephemeral stream, and aquifer in which the well is screened based on the hydrogeological model developed by the Oxford property by Haslauer (2005).

Well Name	Northing (m)	Easting (m)	Casing Elevation (masl)	Ground Elevation (masl)	Top of Screen (mbgs)	Bottom of Screen (mbgs)	Well Screen Aquifer
WO11-6	4770436.41	519657.02	303.48	303.10	5.788	6.550	2
WO11-8	4770436.47	519657.04	303.48	303.10	7.938	8.700	-
WO11-10	4770436.47	519656.95	303.50	303.10	9.788	10.550	-
WO11-13*	4770436.53	519656.98	303.17	303.10	11.928	12.690	-
WO11-18*	4770436.57	519657.08	303.18	303.10	17.288	18.050	3
WO35*	4770190.27	519977.77	303.00	302.52	5.180	6.700	2
WO36*	4770308.65	520061.88	300.90	300.39	3.350	4.880	2
WO37*	4770359.33	519848.92	301.22	300.72	3.350	4.880	2
WO40*	4770560.16	519548.21	305.10	304.19	6.400	7.920	3
WO62*	4770426.20	519922.21	307.59	307.39	13.720	16.760	3
WO63*	4770358.50	519849.88	301.38	300.71	10.670	13.720	3
WO64*	4770191.36	519883.68	307.46	306.50	15.850	18.900	3
WO66*	4770484.02	519684.34	304.29	303.33	5.49	8.53	2
WO67*	4770318.11	519488.23	313.23	312.46	15.240	18.290	3
WO72S*	4770580.01	519792.67	310.04	309.09	13.410	16.400	3
WO72D*	4770579.85	519790.61	310.01	309.06	17.870	20.670	3
WO74S*	4770154.26	520053.88	301.67	300.75	9.140	10.360	2
WO74M*	4770154.99	520055.01	301.67	300.74	12.5	13.75	3
WO74D*	4770155.92	520056.09	301.66	300.79	14.94	17.98	3
WO75S*	4770113.95	520015.09	303.62	302.68	8.84	10.36	2
WO75D*	4770112.02	520013.59	303.65	302.80	18.29	21.34	3

* Transducer

Appendix K

Monthly Groundwater Chemistry Monitoring Results

Table K.1 Chloride and Nitrate concentrations, and manual water level measurements relative to the top of the well casing from monthly monitoring.

Well Name	Date	Cl (mg/L)	NO ₃ (mg/L)	Manual water level (mbgl)
October				
WO11-6	29/10/2009	22.1608	24.8717	4.609
WO11-8	29/10/2009	39.3639	43.0259	4.605
WO11-10	29/10/2009	57.7716	69.2129	4.599
WO11-13	29/10/2009	48.0778	57.3338	3.969
WO11-18	29/10/2009	15.9514	0.3088	3.946
WO35	29/10/2009	30.8398	63.1639	4.524
WO36	29/10/2009	40.8336	17.1687	2.407
WO37	29/10/2009	42.0904	67.5422	2.356
WO40	29/10/2009	23.0194	44.6602	4.283
WO62	29/10/2009	58.4238	39.2818	9.657
WO63	29/10/2009	49.3205	63.8939	2.532
WO66	29/10/2009	49.7207	55.8104	4.394
WO67	29/10/2009	71.1403	66.5029	---
WO72S	29/10/2009	80.6318	27.5873	10.538
WO72D	29/10/2009	58.2402	59.3512	10.476
WO74S	29/10/2009	24.4378	45.3958	---
WO74M	29/10/2009	41.9520	62.0469	2.066
WO74D	29/10/2009	30.5607	44.4819	2.927
WO75S	29/10/2009	28.9813	60.4580	4.748
WO75D	29/10/2009	23.4152	42.9311	4.897
November				
WO11-6	25/11/2009	37.7518	43.1705	4.561
WO11-8	25/11/2009	57.7158	62.9458	4.567
WO11-10	25/11/2009	49.0475	60.6606	4.557
WO11-13	25/11/2009	52.1517	63.5217	3.967
WO11-18	25/11/2009	14.5468	0.2913	3.892
WO35	25/11/2009	22.0525	43.4530	4.464
WO36	25/11/2009	59.0973	26.1770	2.313
WO37	25/11/2009	33.5794	57.0766	2.319
WO40	25/11/2009	29.0142	22.1001	7.013
WO62	25/11/2009	45.7905	31.8536	9.623
WO63	25/11/2009	47.9494	65.3027	2.316
WO64	25/11/2009	16.7559	31.1313	8.337
WO66	25/11/2009	47.9098	55.3345	4.317

Well Name	Date	Cl (mg/L)	NO ₃ (mg/L)	Manual water level (mbgl)
WO67	26/11/2009	42.2012	39.0474	12.111
WO72S	25/11/2009	51.9674	25.6614	10.469
WO72D	25/11/2009	44.0395	48.2650	10.449
WO74S	25/11/2009	22.1650	38.7964	2.869
WO74M	25/11/2009	26.5278	41.8680	2.866
WO74D	25/11/2009	42.3383	58.0333	2.916
WO75S	26/11/2009	23.6936	47.5950	4.714
WO75D	25/11/2009	22.0706	39.1649	2.936
December				
WO11-6	17/12/2009	24.8662	26.8765	4.529
WO11-8	17/12/2009	49.7065	54.3178	4.532
WO11-10	17/12/2009	42.4597	51.5697	4.535
WO11-13	17/12/2009	36.0807	43.5806	3.944
WO11-18	17/12/2009	13.4992	0.4582	3.746
WO35	21/12/2009	21.2640	40.7878	4.344
WO36	17/12/2009	46.9208	20.0790	2.337
WO37	17/12/2009	31.0338	52.1890	2.276
WO40	21/12/2009	48.7101	38.7219	5.183
WO62	21/12/2009	37.0021	26.3914	9.553
WO63	17/12/2009	27.8724	38.5984	2.302
WO66	17/12/2009	44.0843	50.4979	4.266
WO67	21/12/2009	68.2888	65.2156	12.081
WO72S	21/12/2009	39.4812	24.2718	10.413
WO72D	21/12/2009	49.8470	55.5632	10.363
WO74S	21/12/2009	21.2552	36.1626	2.872
WO74M	21/12/2009	26.5219	41.7445	2.846
WO74D	21/12/2009	36.0450	47.5953	2.906
WO75S	21/12/2009	19.0142	38.8086	4.718
WO75D	21/12/2009	37.5208	64.3982	4.797
January				
WO11-6	19/01/2010	56.5738	64.4554	4.794
WO11-8	19/01/2010	41.1020	47.4191	4.802
WO11-10	19/01/2010	41.2469	50.1482	4.765
WO11-13	19/01/2010	42.9217	52.2441	4.189
WO11-18	19/01/2010	14.7377	0.3973	3.898
WO35	19/01/2010	26.0969	49.6980	4.474
WO36	19/01/2010	46.8278	20.2173	2.417
WO37	19/01/2010	32.9456	57.7525	2.336
WO40	19/01/2010	59.4926	46.4713	5.313
WO62	19/01/2010	52.4515	37.9606	9.637
WO63	19/01/2010	46.8075	68.7968	2.352

Well Name	Date	Cl (mg/L)	NO ₃ (mg/L)	Manual water level (mbgl)
WO64	19/01/2010	43.1078	38.7610	8.354
WO66	19/01/2010	43.5820	50.8106	4.406
WO67	19/01/2010	32.3423	61.0593	11.831
WO72S	19/01/2010	53.2203	34.6377	10.508
WO72D	19/01/2010	49.2560	55.4922	10.458
WO74S	19/01/2010	26.2112	44.5528	2.934
WO74M	19/01/2010	26.2018	41.0205	2.914
WO74D	19/01/2010	42.4049	55.7267	2.998
WO75S	19/01/2010	23.7822	47.7944	4.788
WO75D	19/01/2010	29.9317	50.6890	4.907
March				
WO11-6	03/03/2010	54.8820	64.0203	4.724
WO11-8	03/03/2010	52.9800	60.8844	5.122
WO11-10	03/03/2010	0.0000	54.4495	5.205
WO11-13	03/03/2010	41.4095	51.4565	4.419
WO11-18	03/03/2010	12.7081	0.4751	4.024
WO35	03/03/2010	28.0984	55.2452	4.594
WO36	05/03/2010	58.9578	27.6965	---
WO37	03/03/2010	38.1036	67.7524	2.376
WO40	05/03/2010	55.7620	46.1170	---
WO62	03/03/2010	51.4610	39.2279	9.702
WO63	03/03/2010	40.7157	63.9032	2.392
WO64	05/03/2010	26.8547	50.4220	8.384
WO66	03/03/2010	34.1877	40.7449	4.466
WO67	05/03/2010	52.3155	46.1410	---
WO72S	03/03/2010	32.6824	25.4410	10.558
WO72D	03/03/2010	59.1271	68.1507	10.518
WO74S	05/03/2010	35.9877	61.8693	2.952
WO74M	05/03/2010	27.0911	42.6880	2.936
WO74D	05/03/2010	22.7057	30.6552	3.037
WO75S	05/03/2010	19.0142	38.5273	4.808
WO75D	05/03/2010	14.6411	25.5039	4.907
WO11-6	24/03/2010	28.4475	32.7361	4.369
WO11-8	24/03/2010	59.0563	67.4887	4.357
WO36	24/03/2010	27.2178	12.6982	2.317
WO37	24/03/2010	19.3748	33.1974	2.156
WO40	24/03/2010	9.2954	27.4731	4.923
WO66	24/03/2010	29.7596	33.8910	4.136
WO11-6	31/03/2010	41.4655	47.0794	4.414
WO11-8	31/03/2010	60.6285	69.2187	4.425
WO11-10	31/03/2010	62.0301	69.1692	4.427
WO11-13	31/03/2010	62.4064	69.3298	3.831

Well Name	Date	Cl (mg/L)	NO ₃ (mg/L)	Manual water level (mbgl)
WO11-18	31/03/2010	15.4652	0.2066	3.624
WO36	31/03/2010	42.8779	20.4438	---
WO37	31/03/2010	22.9683	36.3492	2.196
WO62	31/03/2010	57.1529	44.2230	9.534
WO63	31/03/2010	35.3277	51.6565	2.262
WO64	31/03/2010	32.8144	62.5745	8.316
WO66	31/03/2010	46.8457	53.3892	4.196
WO67	31/03/2010	72.3768	64.3863	12.107
WO72S	31/03/2010	60.2958	54.2715	10.350
WO72D	31/03/2010	60.7746	67.3979	10.294
WO74S	31/03/2010	28.5955	48.2652	2.882
WO74M	31/03/2010	41.4408	65.9373	2.863
WO74D	31/03/2010	51.1306	66.2814	2.944
WO75S	31/03/2010	22.2331	43.7912	4.741
WO75D	31/03/2010	24.0694	40.8082	4.876
May				
WO11-6	13/05/2010	47.8855	57.9354	4.584
WO11-8	13/05/2010	56.4788	63.4302	---
WO11-10	13/05/2010	62.9639	68.9747	4.565
WO11-13	13/05/2010	62.2063	66.5149	3.989
WO11-18	13/05/2010	13.9649	0.1574	3.734
WO35	13/05/2010	29.8182	64.6487	---
WO36	13/05/2010	52.8045	26.0416	---
WO37	13/05/2010	31.0653	49.8593	2.296
WO40	13/05/2010	40.7017	48.4108	---
WO62	13/05/2010	54.5372	40.3960	9.652
WO63	13/05/2010	45.0017	69.1501	2.432
WO64	13/05/2010	30.8527	58.0413	8.374
WO66	13/05/2010	57.6610	63.4849	4.436
WO67	13/05/2010	61.1724	54.0283	11.521
WO72S	13/05/2010	47.5911	40.3085	10.498
WO72D	13/05/2010	63.8418	68.1140	10.448
WO74S	13/05/2010	30.2611	49.2614	2.952
WO74M	13/05/2010	38.2191	57.5893	2.926
WO74D	13/05/2010	49.0446	58.1782	3.007
WO75S	13/05/2010	23.7978	48.3566	4.808
WO75D	13/05/2010	40.8711	64.6412	4.927
June				
WO11-6	10/06/2010	51.9203	60.2873	---
WO11-8	10/06/2010	56.7068	63.7685	---
WO11-10	10/06/2010	61.2976	68.8307	---

Well Name	Date	Cl (mg/L)	NO ₃ (mg/L)	Manual water level (mbgl)
WO11-13	10/06/2010	62.3813	69.4267	---
WO11-18	10/06/2010	17.3394	0.0000	---
WO35	10/06/2010	30.1704	65.5839	---
WO36	10/06/2010	58.5523	31.2570	---
WO37	10/06/2010	36.8263	62.4726	---
WO40	10/06/2010	23.5674	74.2854	---
WO62	10/06/2010	51.7573	38.2226	---
WO63	10/06/2010	43.6669	69.2643	---
WO64	10/06/2010	30.5142	57.5260	---
WO66	10/06/2010	56.5610	63.2414	---
WO67	10/06/2010	64.9317	56.8527	---
WO72S	10/06/2010	49.8668	42.7626	---
WO72D	10/06/2010	49.9828	51.9159	---
WO74D	10/06/2010	27.8234	55.3547	---
WO74M	10/06/2010	41.7790	62.1514	---
WO74S	10/06/2010	33.1416	53.5630	---
WO75D	10/06/2010	38.5953	61.9765	---
WO75S	10/06/2010	26.7848	54.9640	---

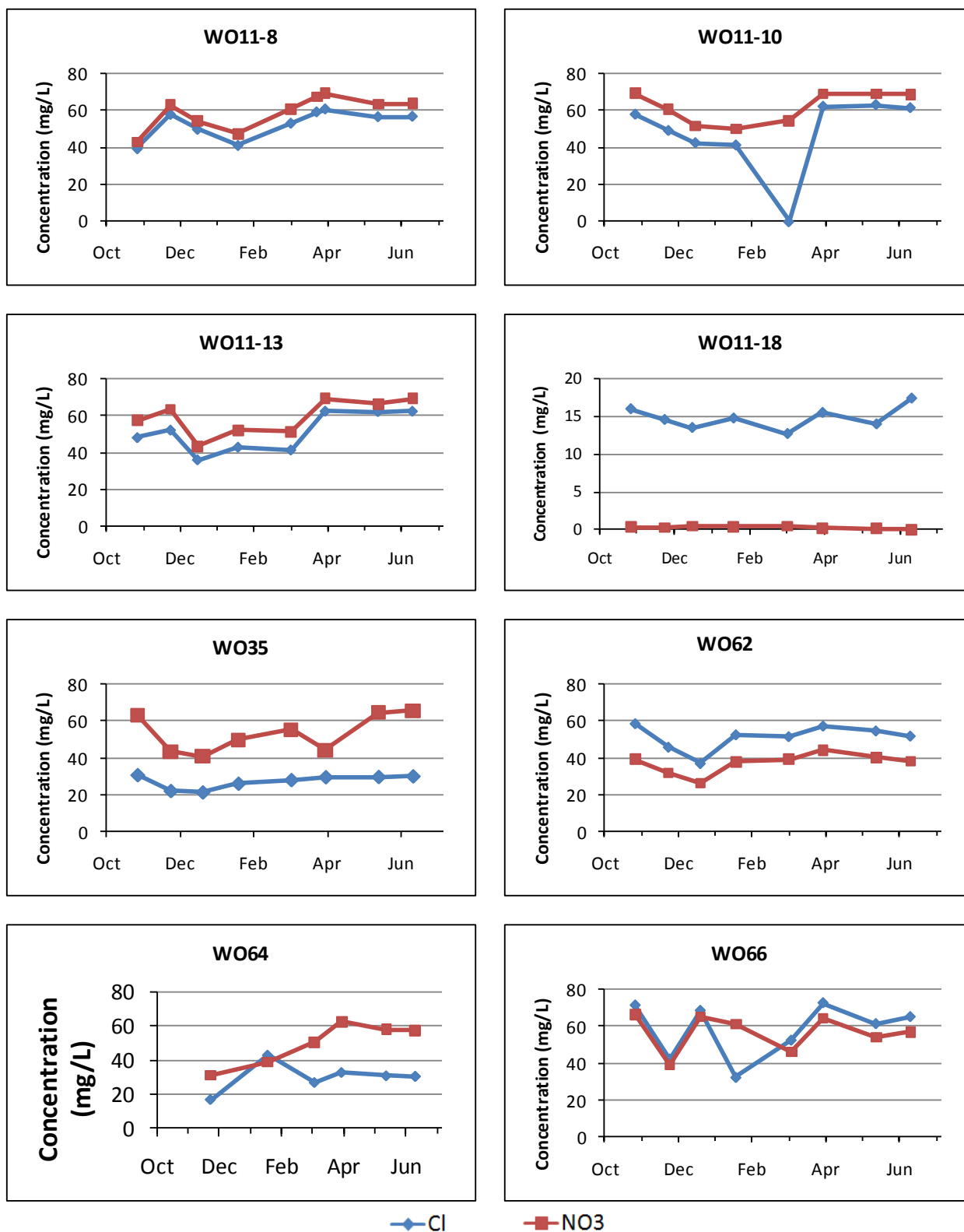


Figure K.1 Monthly monitoring in wells WO11-8, WO11-10, WO11-13, WO11-18, WO35, WO62, WO64 and WO66.

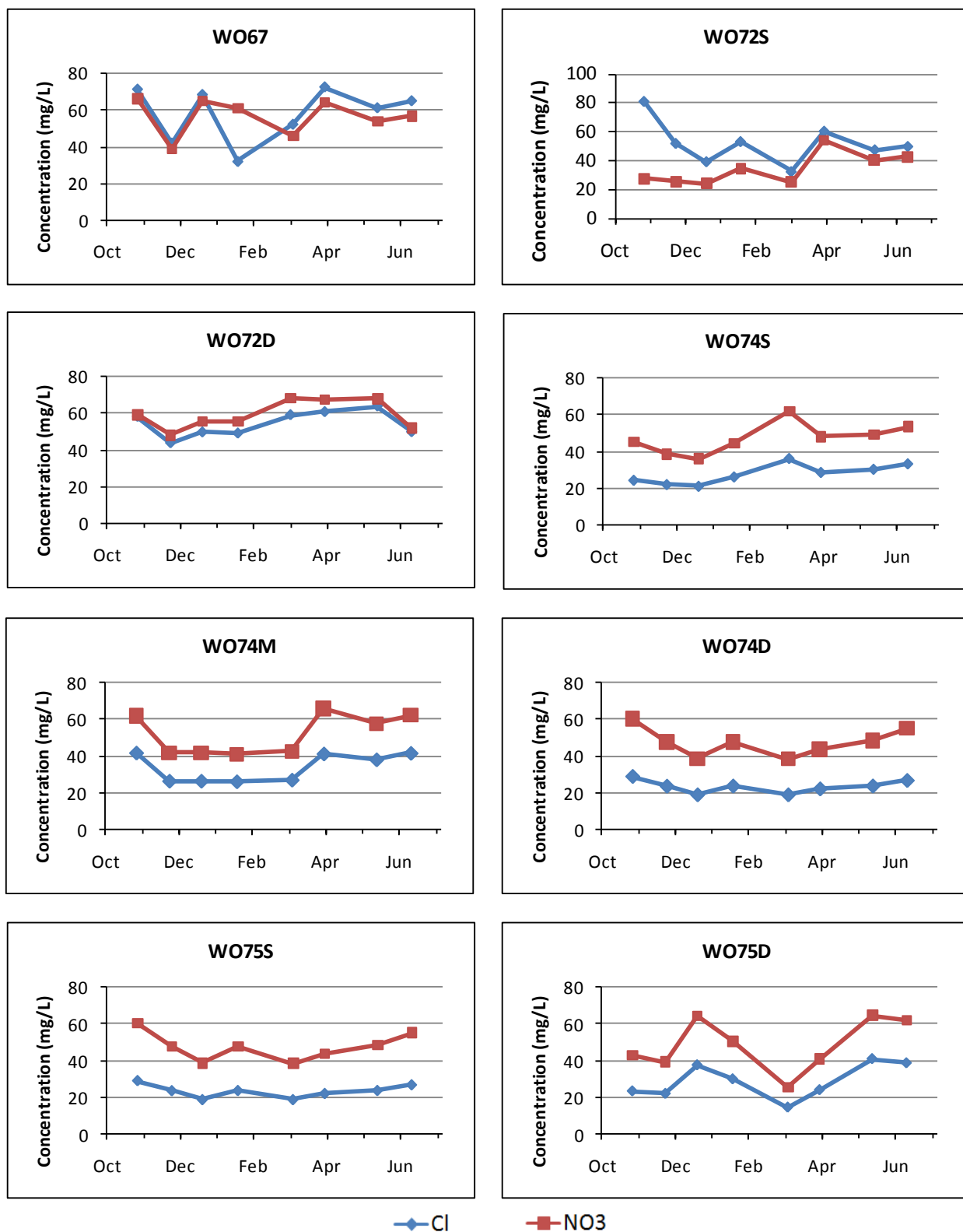


Figure K.2 Monthly monitoring in wells WO67, WO72S, WO72D, WO74S, WO74M, WO74D, WO75S and WO75D.

Appendix L

Moisture Content – Chapter 4

Table L.1 Moisture content measurements with depth taken with the neutron probe during 2010.

Depth Below Ground Surface (m)	March 3, 2010	March 9, 2010	March 12, 2010	March 17, 2010	April 12, 2010	May 28, 2010	July 8, 2010	August 24, 2010
0.15	23.21	19.98						
0.30	35.79	35.68	35.95	29.83	23.70	15.56	19.88	19.19
0.45	31.71	32.40	31.77	31.86	32.15	28.44	27.66	29.17
0.60	34.30	32.48	32.62	30.98	32.23	30.11	28.05	28.87
0.75	31.71	31.05	30.58	30.90	30.82	29.53	29.39	28.57
0.90	26.47	25.92	25.89	27.26	27.51	26.09	24.08	22.69
1.05	23.01	23.73	23.37	23.58	22.18	21.78	19.81	19.20
1.20	20.91	21.28	19.81	21.10	18.96	18.74	17.25	15.54
1.35	18.82	20.52	17.89	17.38	17.59	16.02	15.17	15.32
1.50	23.31	21.88	20.21	19.64	18.35	17.51	16.49	15.82
1.65	21.37	21.63	22.09	20.57	20.73	18.73	18.59	18.45
1.80	20.60	21.05	19.83	20.71	21.30	19.69	18.80	18.63
1.95	17.85	18.01	17.13	16.75	17.26	15.93	15.13	14.85
2.10	18.92	17.96	16.17	15.69	15.70	15.45	14.67	15.50
2.25	18.44	17.37	16.65	16.31	17.30	16.70	16.37	16.42
2.40	20.70	18.48	18.03	17.32	17.24	15.47	14.89	14.90
2.55	20.42	19.29	20.56	28.35	28.60	18.13	16.57	16.73
2.70	27.58	28.68	32.66	31.96	31.45	28.23	17.25	16.86
2.85	32.05	31.61	30.98	36.53	36.77	38.98	36.38	21.79
3.00	43.24	40.66	41.20	40.76	41.71	44.33	44.28	42.13

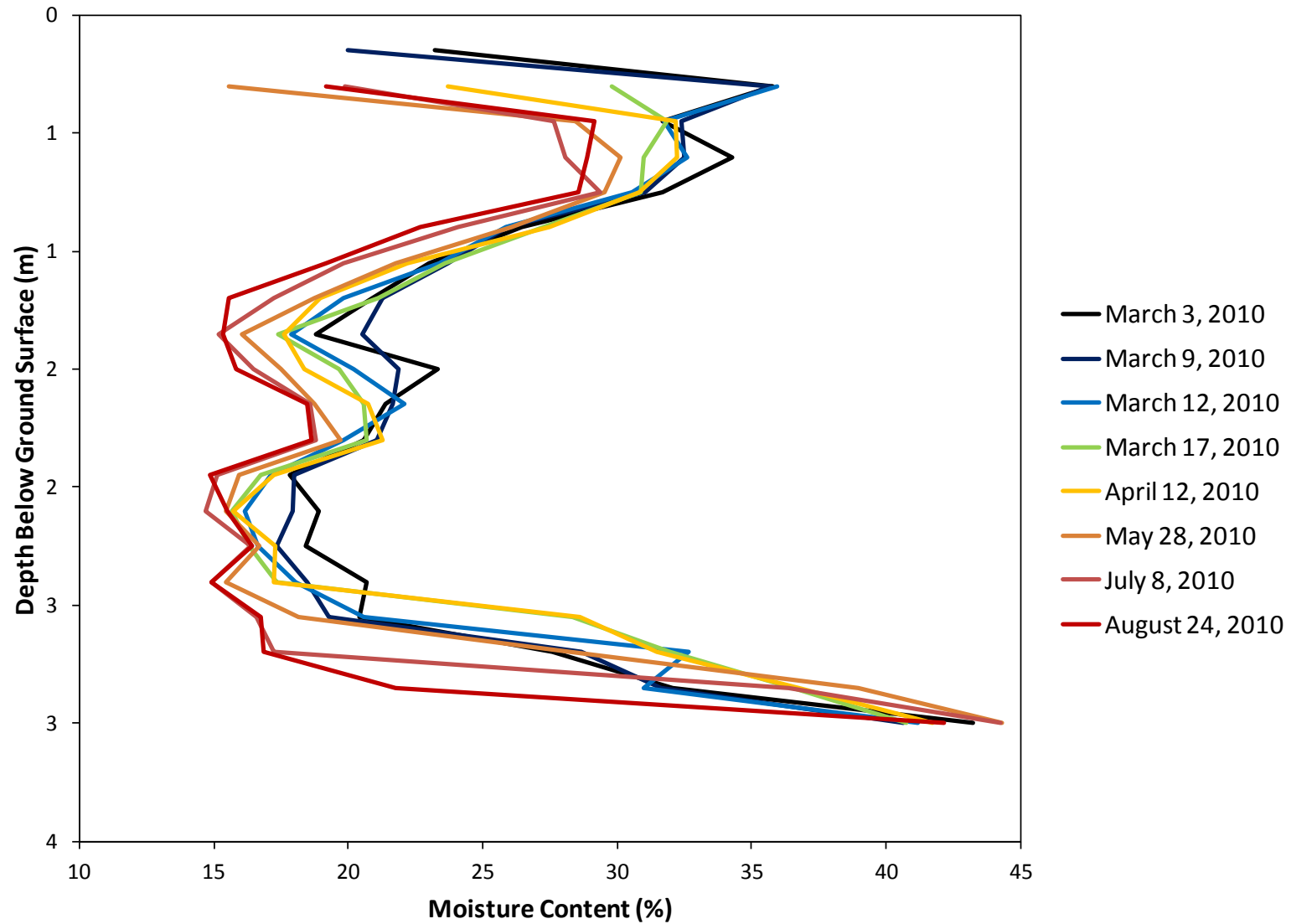


Figure L.1 Moisture content profiles between March to August, 2010 measured with neutron probe.

Appendix M

Simulated Moisture Content - Homogeneous Lower Layer

April 12th to June 1st, 2010

Simulated Moisture Content Profile Using Moisture Retention Parameters for a Siltier Soil

Moisture Retention Parameters of a Siltier Soil

Simulated Moisture Content Profile Using a Moisture Retention Parameters for a Less Silty Soil

Moisture Retention Parameters of a a Less Silty Soil

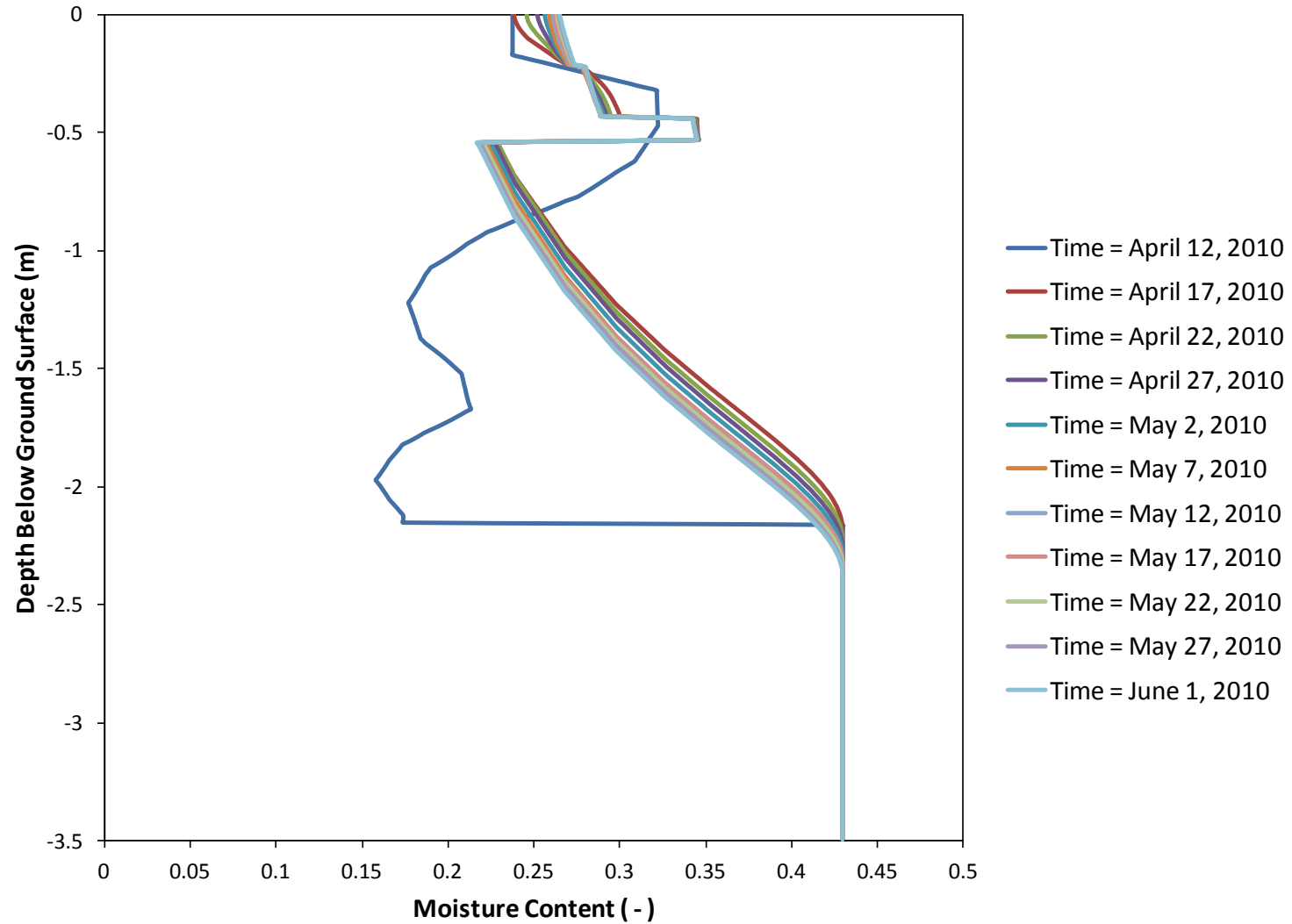


Figure M.1 Simulated moisture content profile using a homogeneous lower layer with a moisture retention parameters of siltier soil (sandy loam). (Moisture retention parameters are presented in Table M.1)

Table M.1 Moisture Retention Parameters for a siltier soil (sandy loam).

Soil layer	θ_r (-)	θ_s (-)	α (1/m)	n (-)	K_s (m/min)	I (-)
1	0.034	0.46	1.60	1.37	4.1667E-05	0.5
2	0.095	0.41	1.90	1.31	4.3333E-05	0.5
3	0.070	0.36	0.50	1.09	3.3333E-06	0.5
5	0.065	0.43	1.34	1.89	7.368E-04	0.5

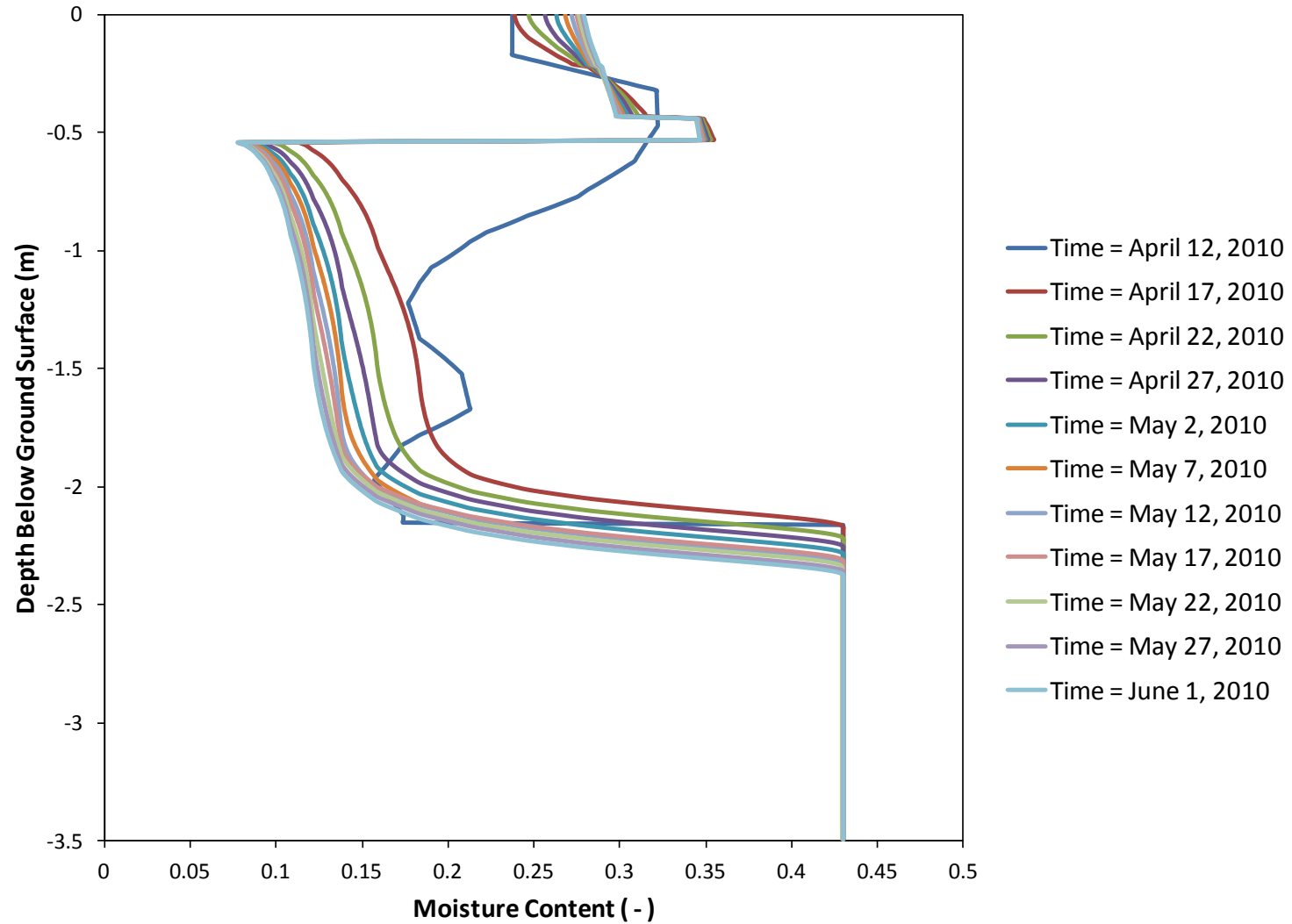


Figure M.2 Simulated moisture content profile using a homogeneous lower layer with a moisture retention parameters of a less silty soil (equal to layer 11 of the soil parameters used for the model calibration in unsaturated conditions see Table N.1). (Moisture retention parameters are presented in Table M.2)

Table M.2 Moisture Retention Parameters for a less silty soil (equal to layer 11 of the soil parameters used for the model calibration in unsaturated conditions see Table N.1)

Soil layer	θ_r (-)	θ_s (-)	α (1/m)	n (-)	K_s (m/min)	I (-)
1	0.034	0.46	1.60	1.37	4.1667E-05	0.5
2	0.095	0.41	1.90	1.31	4.3333E-05	0.5
3	0.070	0.36	0.50	1.09	3.3333E-06	0.5
4	0.061	0.43	10.90	2.09	1.5844E-03	0.5

Appendix N

Input Parameters for Gravity Drained Model Calibration

Table N.1 Moisture retention parameters: θ_r residual soil water content; θ_s saturated soil water content; α and n empirical coefficients of the van Genuchten (1980) equation; K_s saturated hydraulic conductivity; I pore-connectivity.

Soil layer	θ_r (-)	θ_s (-)	α (1/m)	n (-)	K_s (m/min)	I (-)
1	0.034	0.46	1.60	1.37	4.17E-05	0.5
2	0.095	0.41	1.90	1.31	4.33E-05	0.5
3	0.070	0.36	0.50	1.09	3.33E-06	0.5
4	0.069	0.37	1.34	1.17	1.74E-04	0.5
5	0.068	0.38	2.25	1.27	3.61E-04	0.5
6	0.065	0.39	5.00	1.54	9.14E-04	0.5
7	0.064	0.40	6.50	1.69	1.22E-03	0.5
8	0.062	0.43	7.90	1.83	1.52E-03	0.5
9	0.060	0.43	9.40	1.98	1.82E-03	0.5
10	0.059	0.43	10.00	2.13	2.13E-03	0.5
11	0.061	0.43	10.90	2.09	1.58E-03	0.5

Table N.2 Heat parameters (b₁, b₂ and b₃ are Chung and Horton (1987) empirical parameters; C_n is the volumetric heat capacity of the porous medium; C_o is the volumetric heat capacity of organic matter; C_w is the volumetric heat capacity of water; $\lambda_0(\theta)_s$ is the thermal conductivity of the saturated porous medium.

Soil Layer	Soil texture	β_t (m)	b ₁ (kg m/min ³ °C)	b ₂ (kg m/min ³ °C)	b ₃ (kg m/min ³ °C)	C _n (kg / m min ² °C)	C _o (kg / m min ² °C)	C _w (kg / m min ² °C)	$\lambda_0(\theta)_s$ (kg m/min ³ °C)
1	Sand	0.05	49248	-519696	1060340	6.91200E+09	9.03596E+09	1.50480E+10	2.45
2	Loam	0.05	52488	84888	331344	6.91200E+09	9.03596E+09	1.50480E+10	1.38
3	Clay	0.05	-42552	-207792	544536	6.91200E+09	9.03596E+09	1.50480E+10	0.65
4	Sand	0.05	49248	-519696	1060340	6.91200E+09	9.03596E+09	1.50480E+10	2.32
5	Sand	0.05	49248	-519696	1060340	6.91200E+09	9.03596E+09	1.50480E+10	2.34
6	Sand	0.05	49248	-519696	1060340	6.91200E+09	9.03596E+09	1.50480E+10	2.36
7	Sand	0.05	49248	-519696	1060340	6.91200E+09	9.03596E+09	1.50480E+10	2.37
8	Sand	0.05	49248	-519696	1060340	6.91200E+09	9.03596E+09	1.50480E+10	2.41
9	Sand	0.05	49248	-519696	1060340	6.91200E+09	9.03596E+09	1.50480E+10	2.41
10	Sand	0.05	49248	-519696	1060340	6.91200E+09	9.03596E+09	1.50480E+10	2.41
11	Sand	0.05	49248	-519696	1060340	6.91200E+09	9.03596E+09	1.50480E+10	2.41

Appendix O

Simulated and Observed Temperature Beginning on March 3rd, 2010

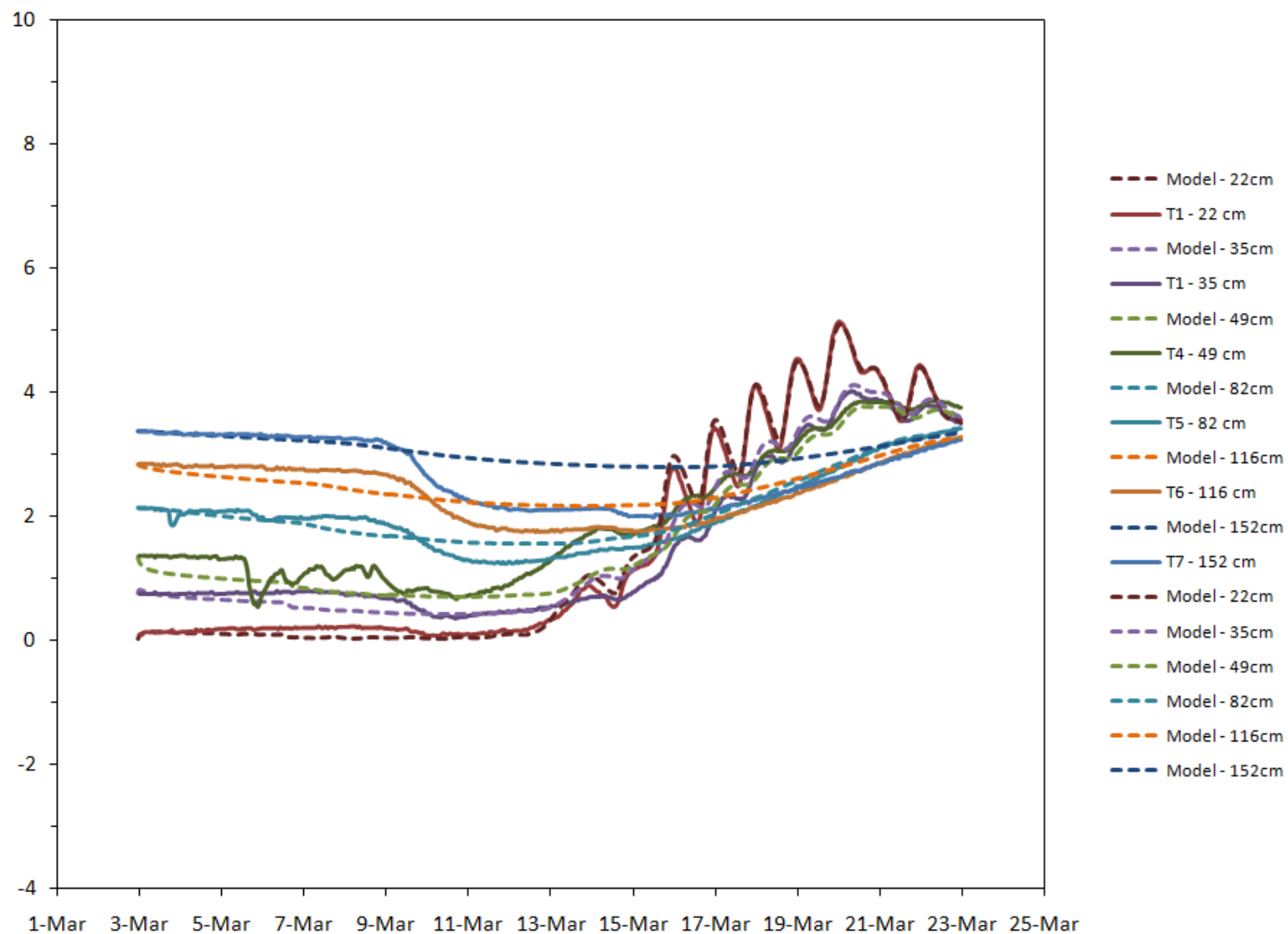


Figure 0.1 Simulated and observed temperature at different depths between March 3rd and March 22nd, 2010. Note that the observation node for T3 was placed 5cm lower than indicated from field measurements.

Appendix P

Inputted Moisture Retention Parameters - Ephemeral Stream Present

Table P.1 Moisture retention parameters: θ_r residual soil water content; θ_s saturated soil water content; α and n empirical coefficients of the van Genuchten (1980) equation; K_s saturated hydraulic conductivity; I pore-connectivity.

Soil layer	θ_r (-)	θ_s (-)	α (1/m)	n (-)	K_s (m/min)	I (-)
1	0.034	0.46	1.60	1.37	4.17E-05	0.5
2	0.095	0.41	1.90	1.31	4.33E-05	0.5
3	0.070	0.36	0.50	1.09	3.33E-05	0.5
4	0.069	0.37	1.34	1.17	3.07E-02	0.5
5	0.068	0.38	2.25	1.27	6.10E-02	0.5
6	0.065	0.39	5.00	1.54	9.14E-02	0.5
7	0.064	0.40	6.50	1.69	1.22E-01	0.5
8	0.062	0.43	7.90	1.83	1.22E-01	0.5
9	0.060	0.43	9.40	1.98	1.22E-01	0.5
10	0.059	0.43	10.00	2.13	1.22E-01	0.5
11	0.061	0.43	10.90	2.09	1.22E-01	0.5

Appendix Q

Sensitivity Analysis

Scenario 1 – Surface Pressure Boundary Equals the Water Column at the Surface

Hydraulic Conductivity of the Top Three Soil Layers Adjusted by Factors of 2 and 10

Hydraulic Conductivity of the Bottom Eight Soil Layers Adjusted by Factors of 2 and 10

Hydraulic Conductivity of the Whole Soil Profile Adjusted by Factors of 2 and 10

Scenario 2 – Surface Pressure Boundary Equals the Water Column at the Surface Plus 13 cm

Hydraulic Conductivity of the Top Three Soil Layers Adjusted by Factors of 2 and 10

Hydraulic Conductivity of the Bottom Eight Soil Layers Adjusted by Factors of 2 and 10

Hydraulic Conductivity of the Whole Soil Profile Adjusted by Factors of 2 and 10

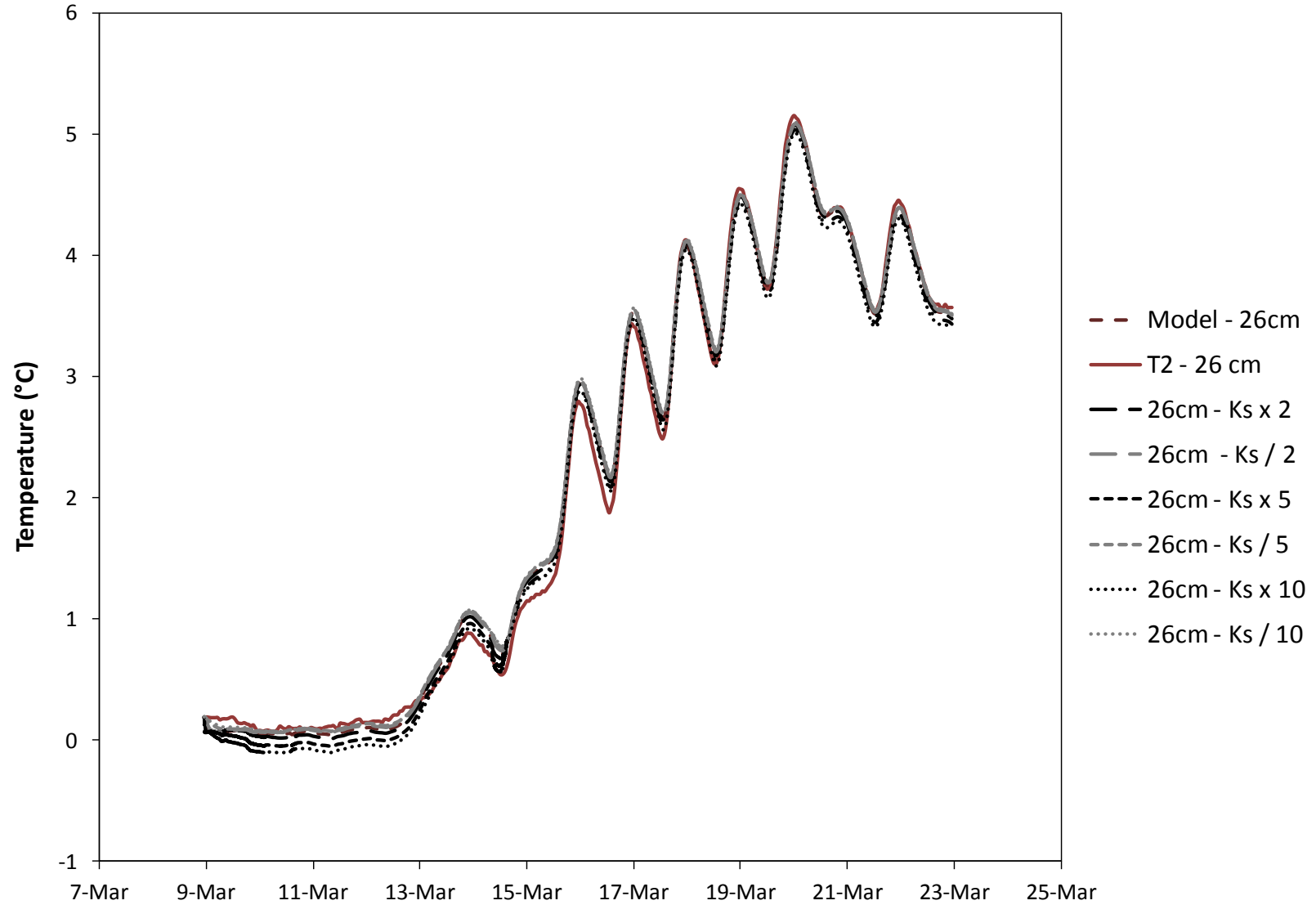


Figure Q.1 Scenario 1 – Hydraulic Conductivity of the Top Three Soil Layers Adjusted by Factors of 2, 5 and 10 – T2

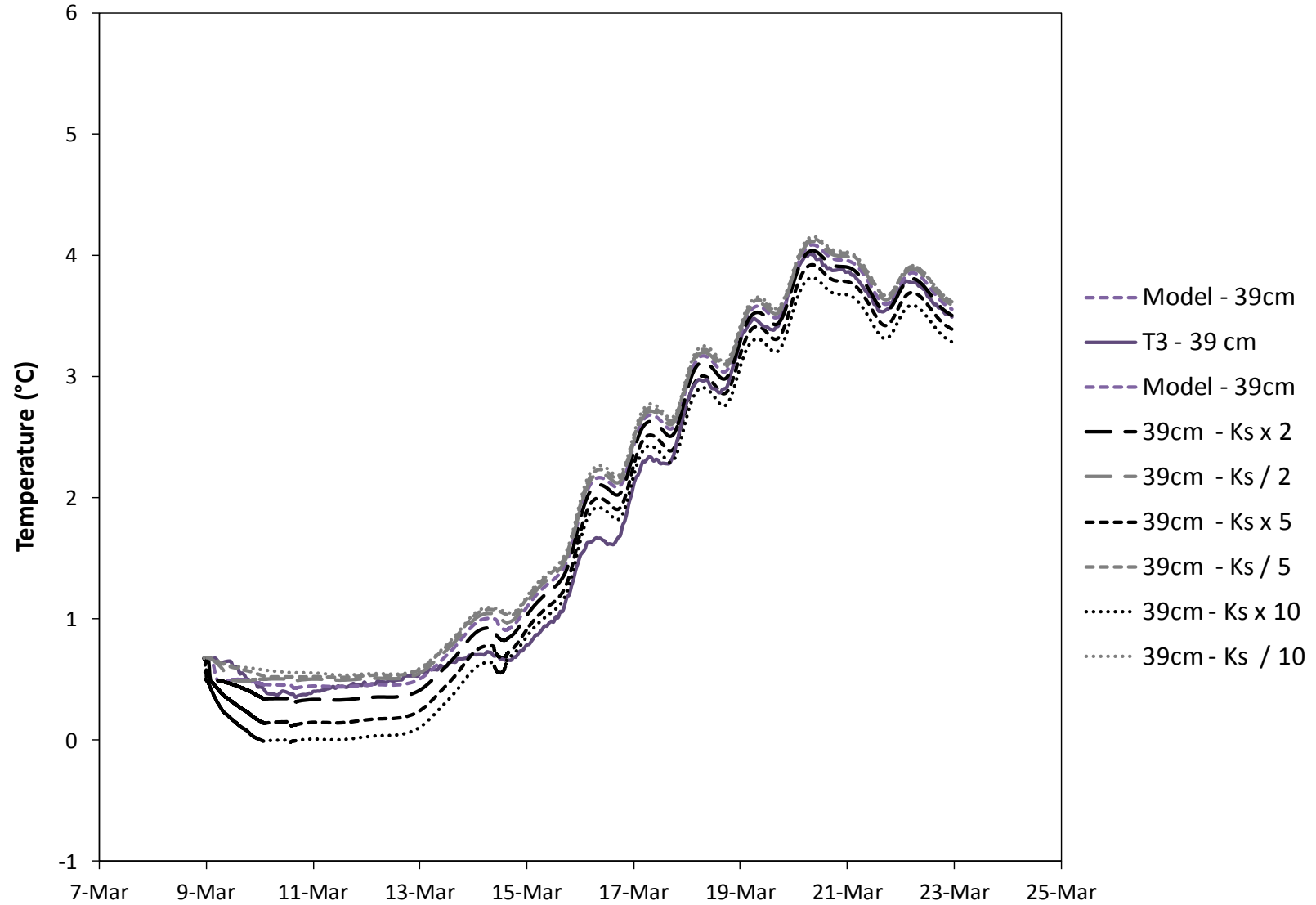


Figure Q.2 Scenario 1 – Hydraulic Conductivity of the Top Three Soil Layers Adjusted by Factors of 2, 5, and 10 – T3

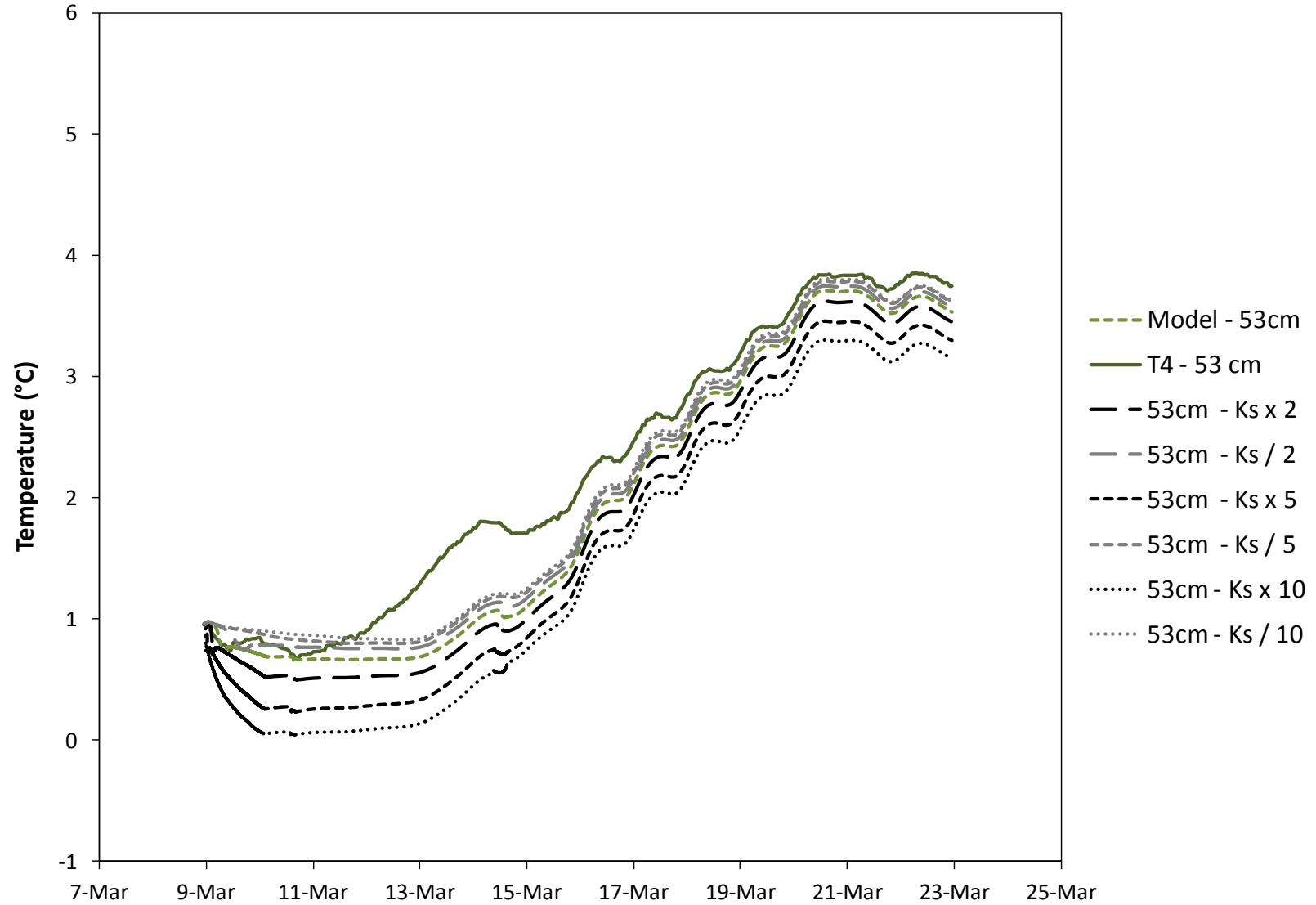


Figure Q.3 Scenario 1 – Hydraulic Conductivity of the Top Three Soil Layers Adjusted by Factors of 2, 5, and 10 – T4

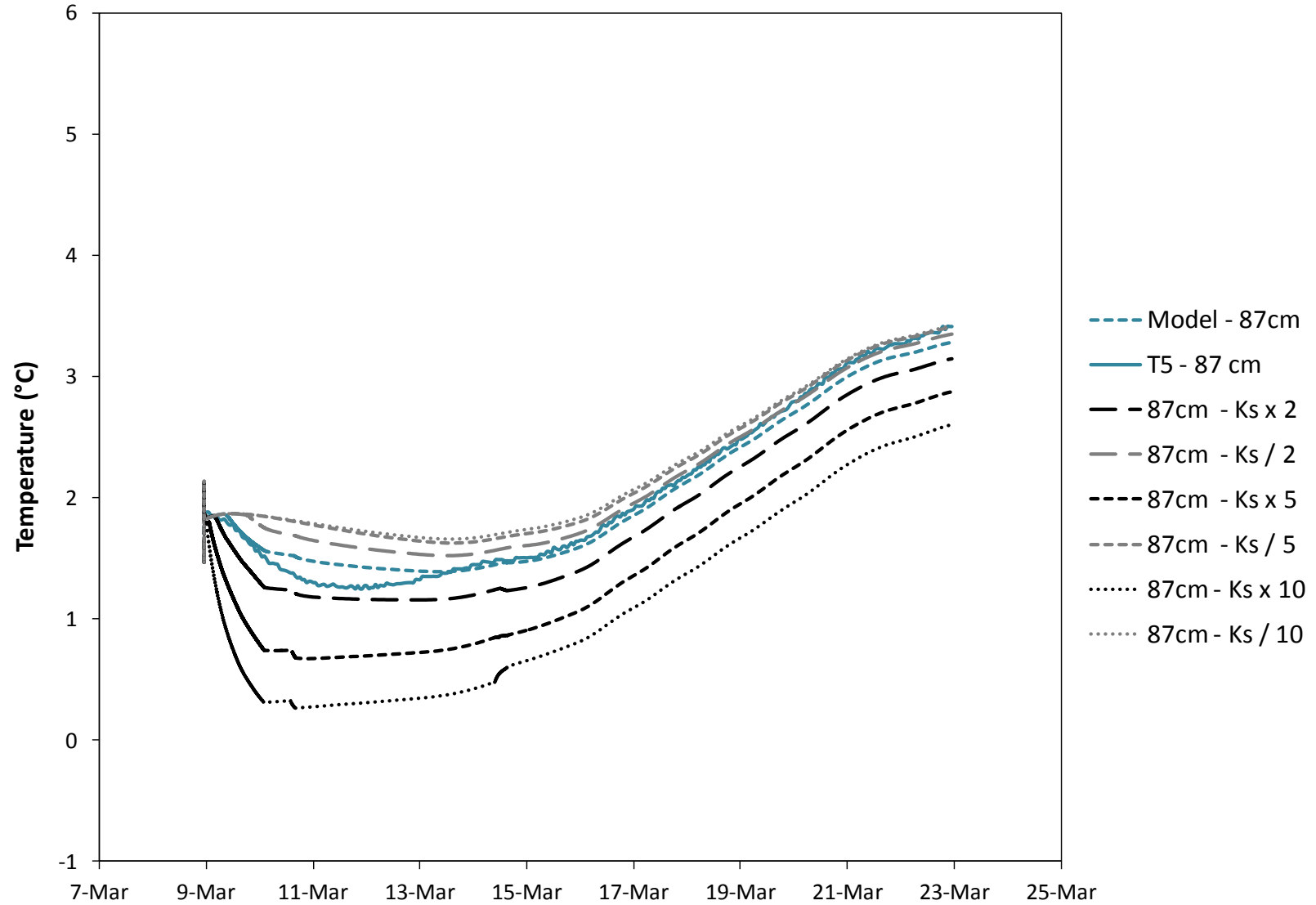


Figure Q.4 Scenario 1 – Hydraulic Conductivity of the Top Three Soil Layers Adjusted by Factors of 2, 5, and 10 – T5

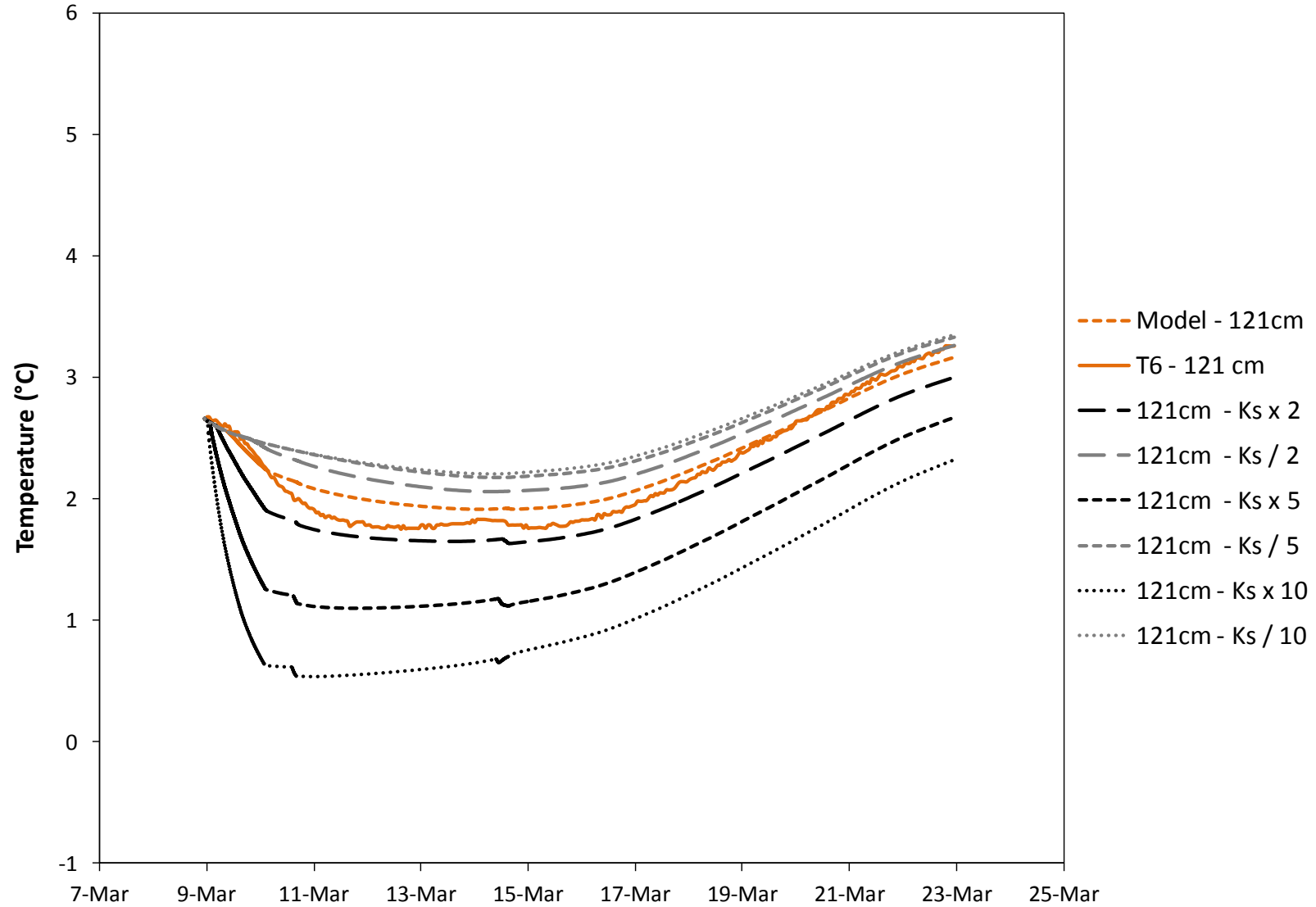


Figure Q.5 Scenario 1 – Hydraulic Conductivity of the Top Three Soil Layers Adjusted by Factors of 2, 5, and 10 – T6

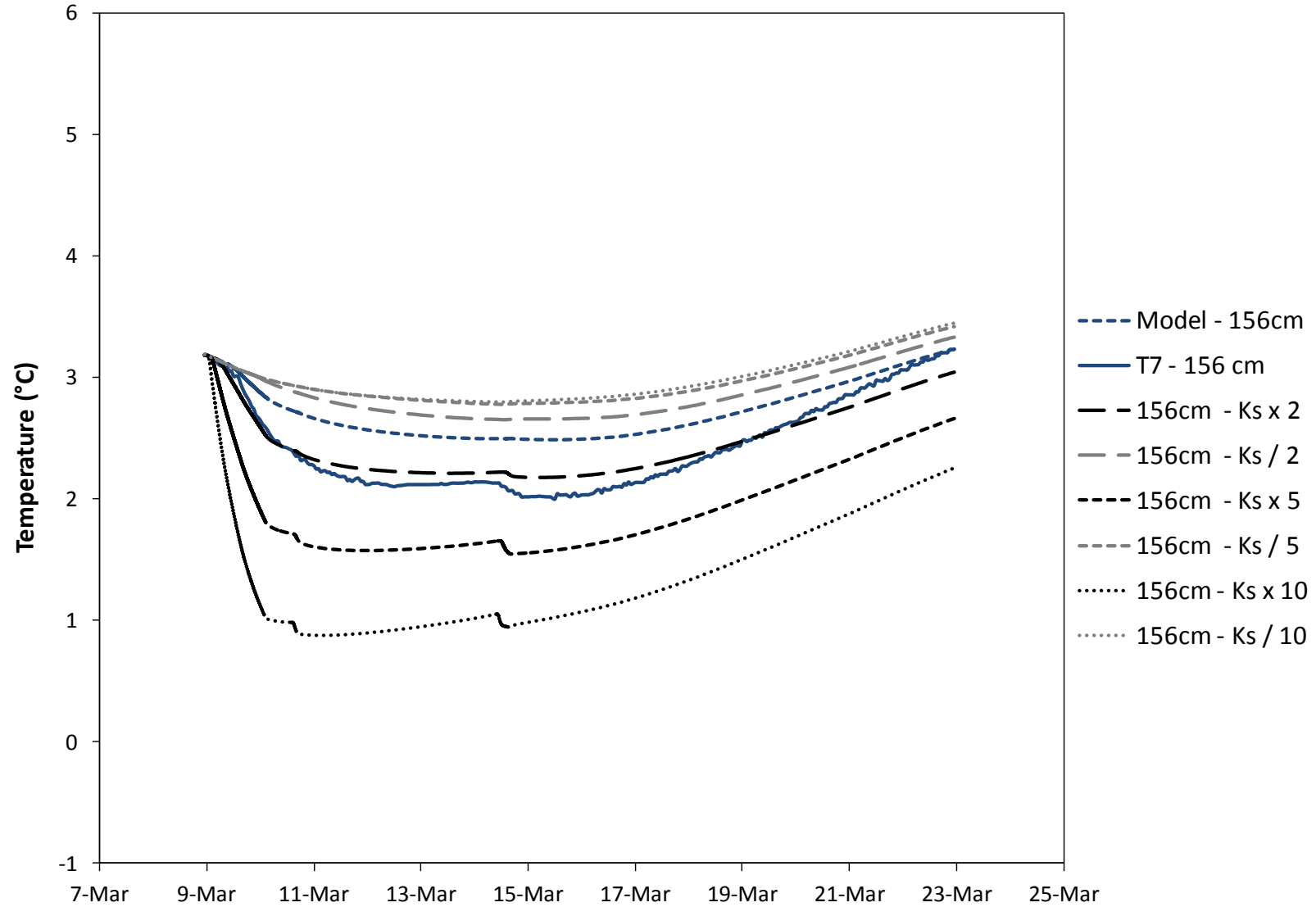


Figure Q.6 Scenario 1 – Hydraulic Conductivity of the Top Three Soil Layers Adjusted by Factors of 2, 5, and 10 – T7

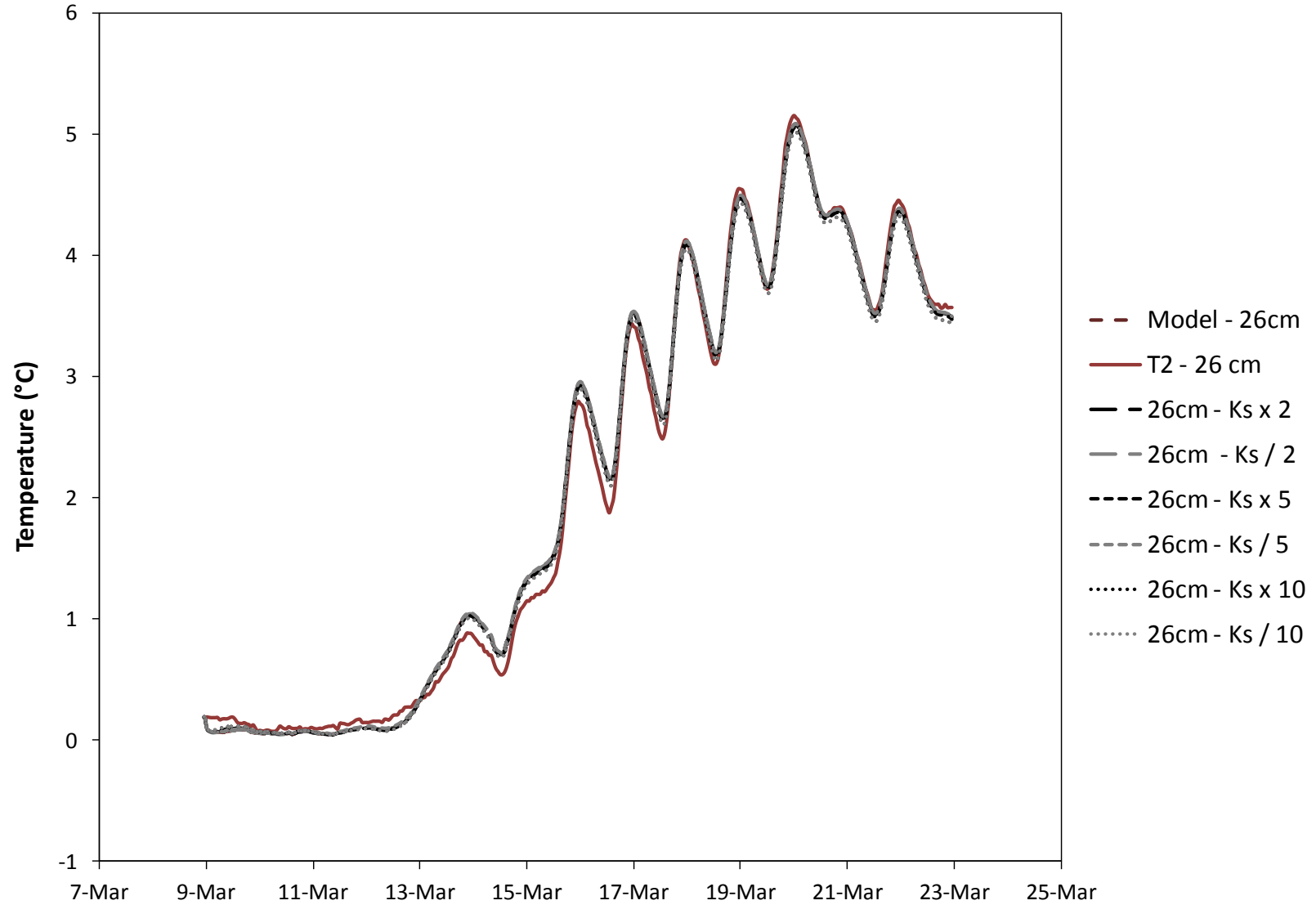


Figure Q.7 Scenario 1 – Hydraulic Conductivity of the Bottom Eight Soil Layers Adjusted by Factors of 2, 5, and 10 – T2

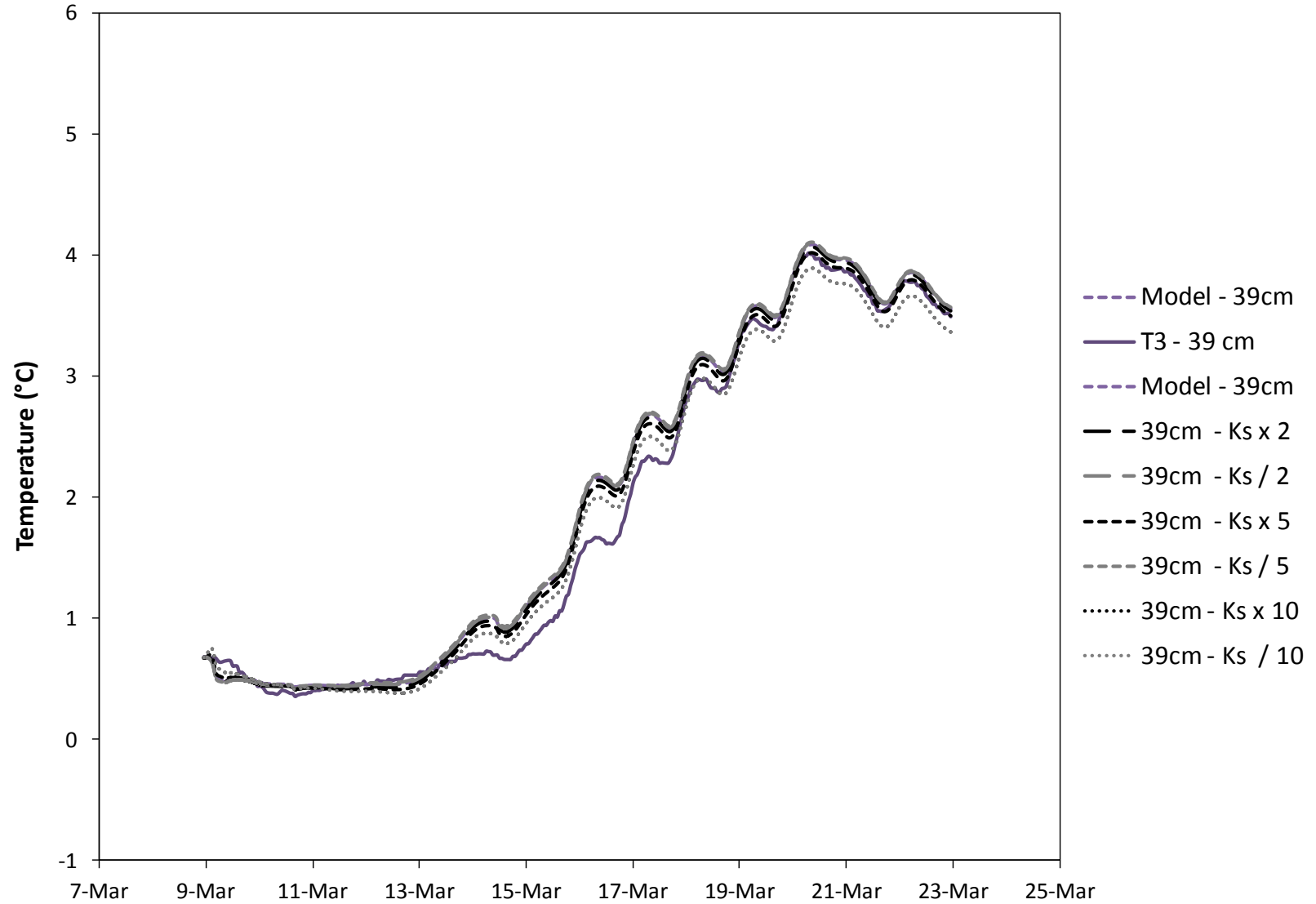


Figure Q.8 Scenario 1 – Hydraulic Conductivity of the Bottom Eight Soil Layers Adjusted by Factors of 2, 5, and 10 – T3

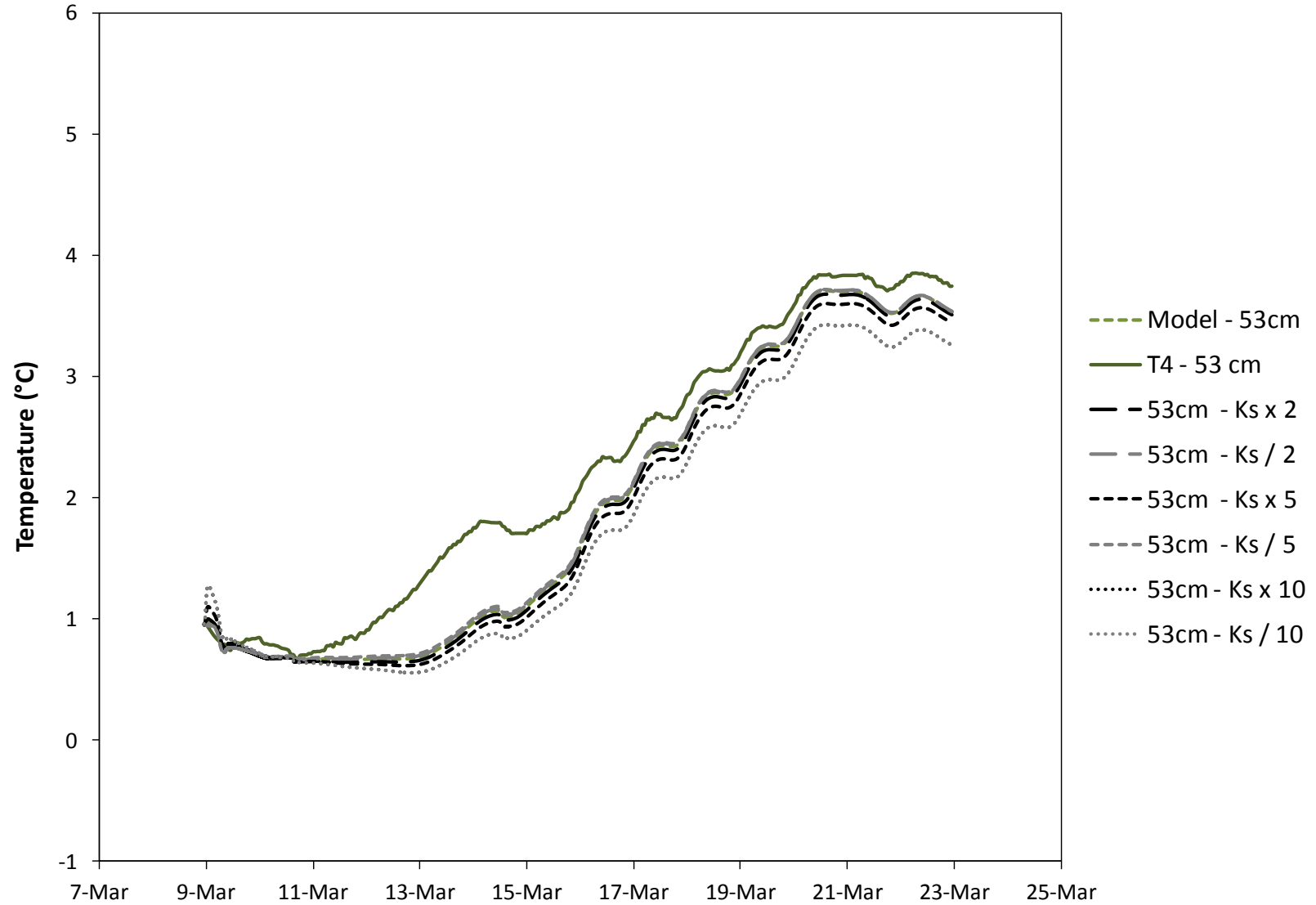


Figure Q.9 Scenario 1 – Hydraulic Conductivity of the Bottom Eight Soil Layers Adjusted by Factors of 2, 5, and 10 – T4

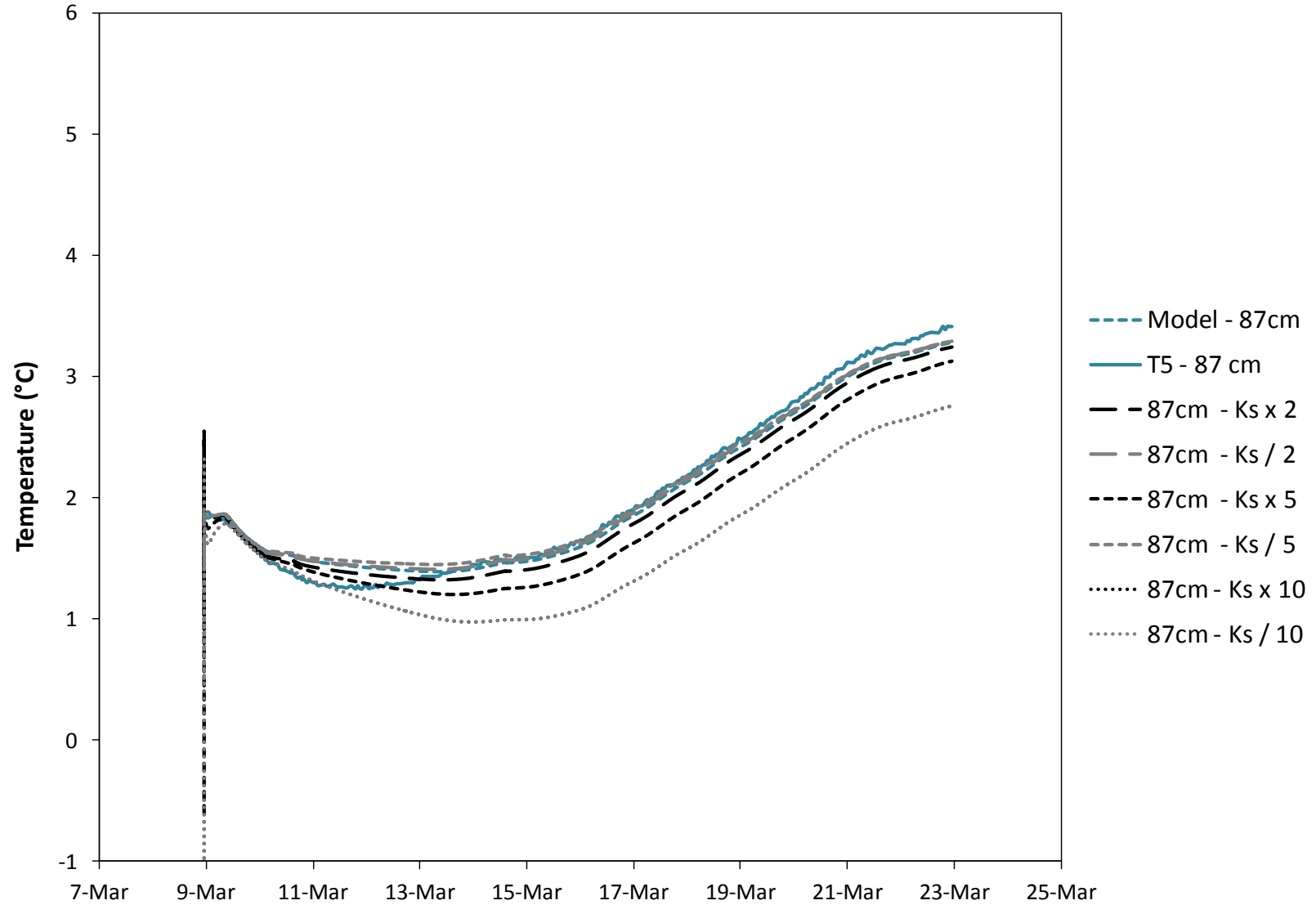


Figure Q.10 Scenario 1 – Hydraulic Conductivity of the Bottom Eight Soil Layers Adjusted by Factors of 2, 5, and 10 – T5

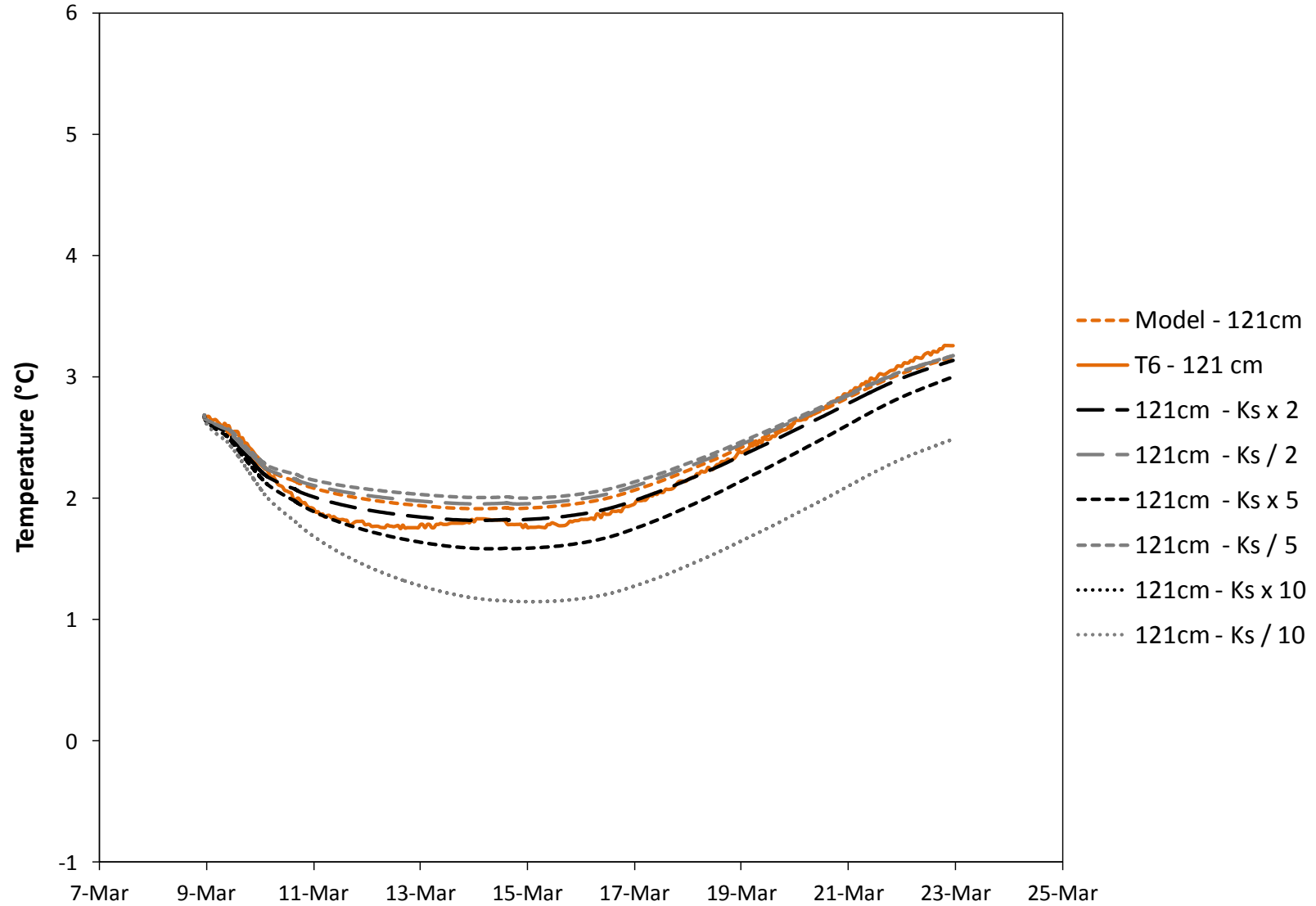


Figure Q.11 Scenario 1 – Hydraulic Conductivity of the Bottom Eight Soil Layers Adjusted by Factors of 2, 5, and 10 – T6

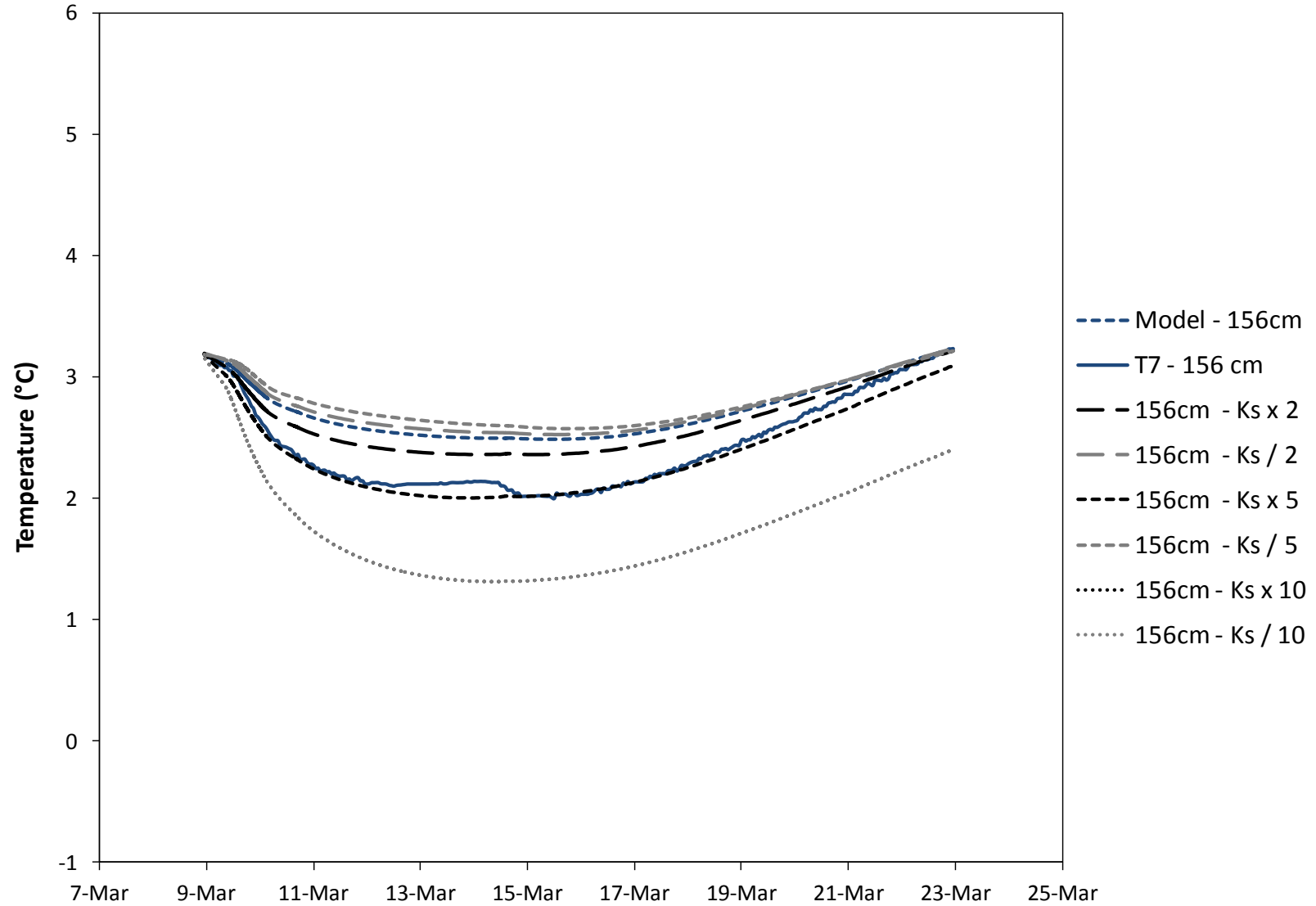


Figure Q.12 Scenario 1 – Hydraulic Conductivity of the Bottom Eight Soil Layers Adjusted by Factors of 2, 5, and 10 – T7

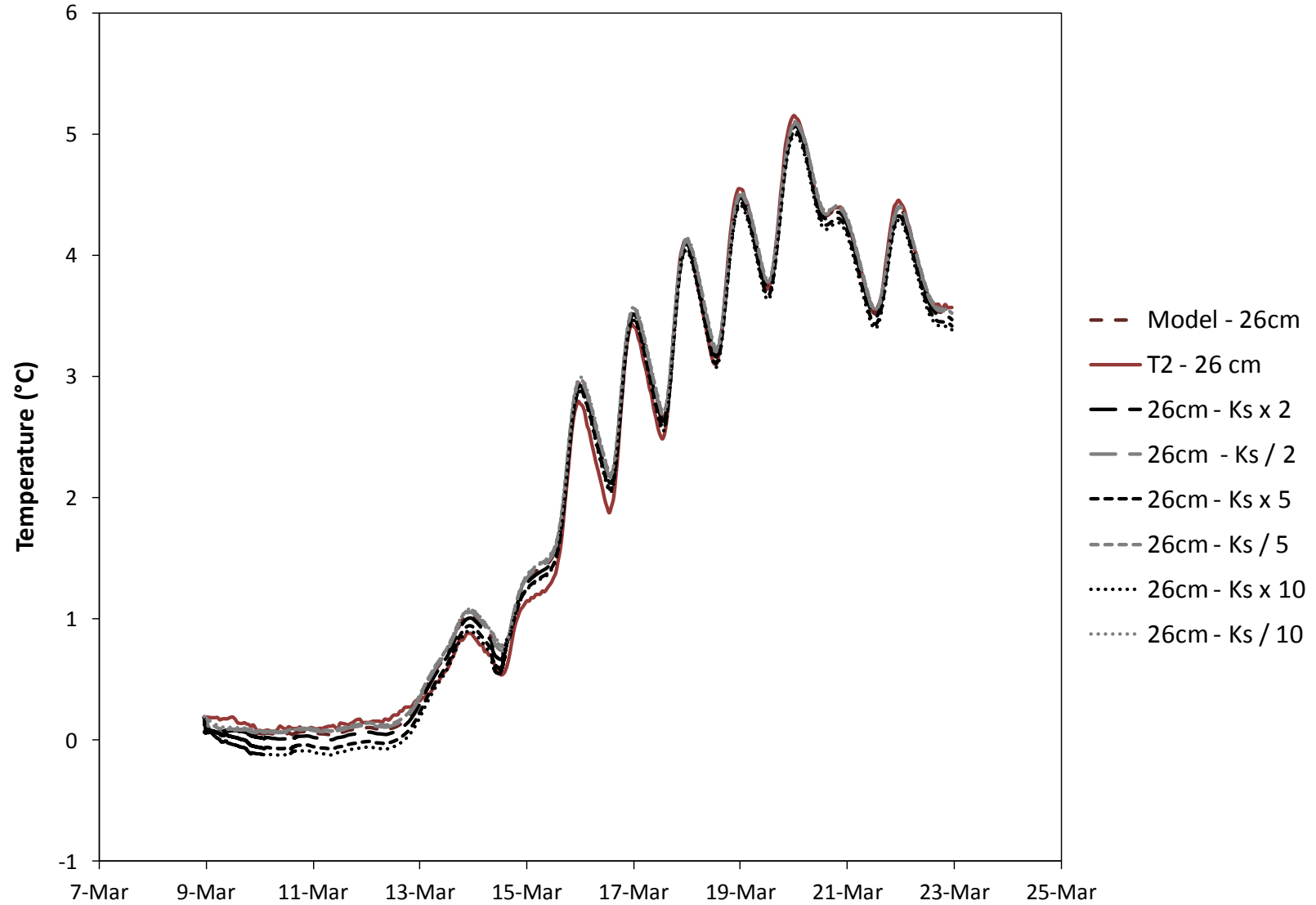


Figure Q.13 Scenario 1 – Hydraulic Conductivity of the Whole Soil Profile Adjusted by Factors of 2, 5, and 10 – T2

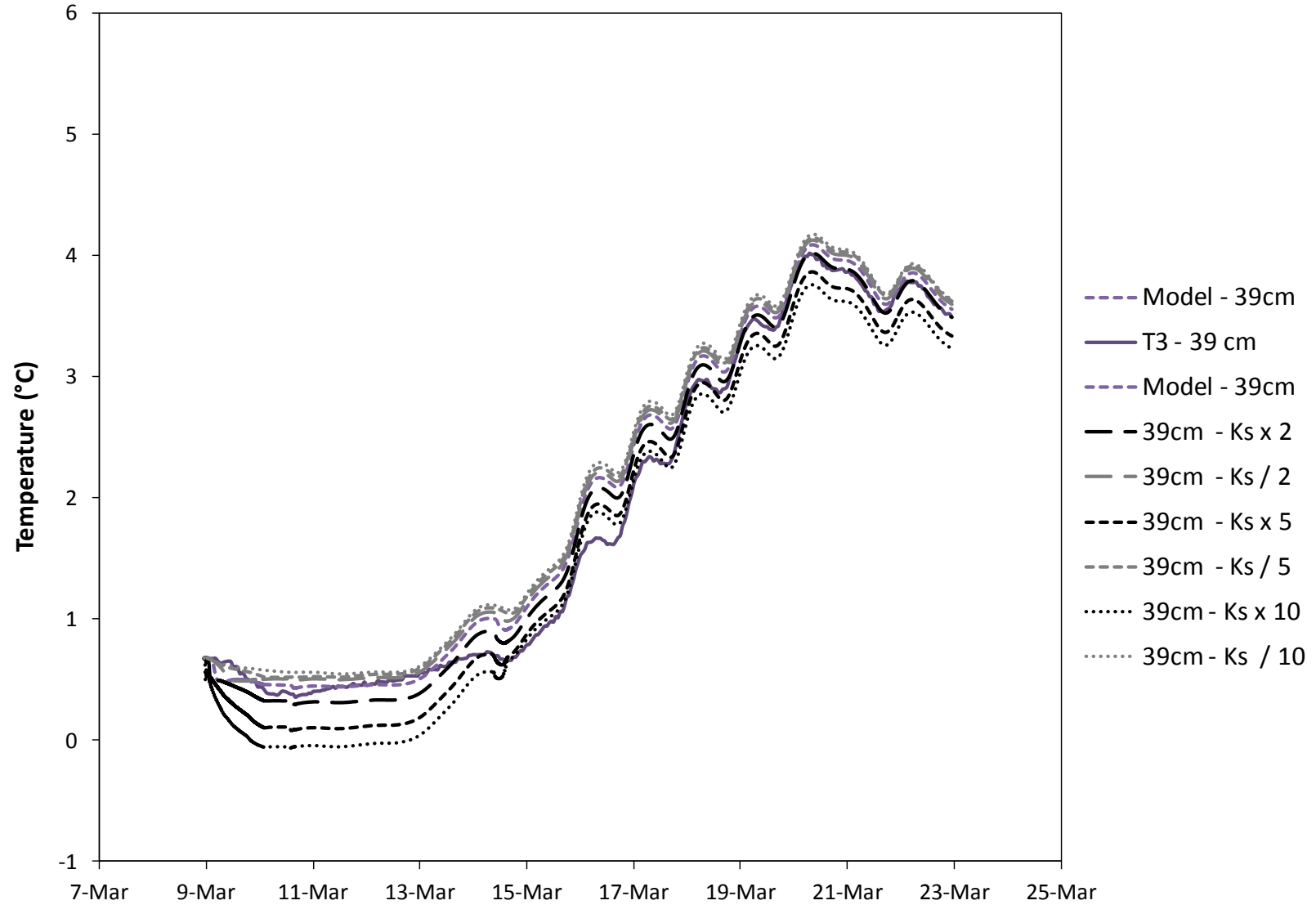


Figure Q.14 Scenario 1 – Hydraulic Conductivity of the Whole Soil Profile Adjusted by Factors of 2, 5, and 10 – T3

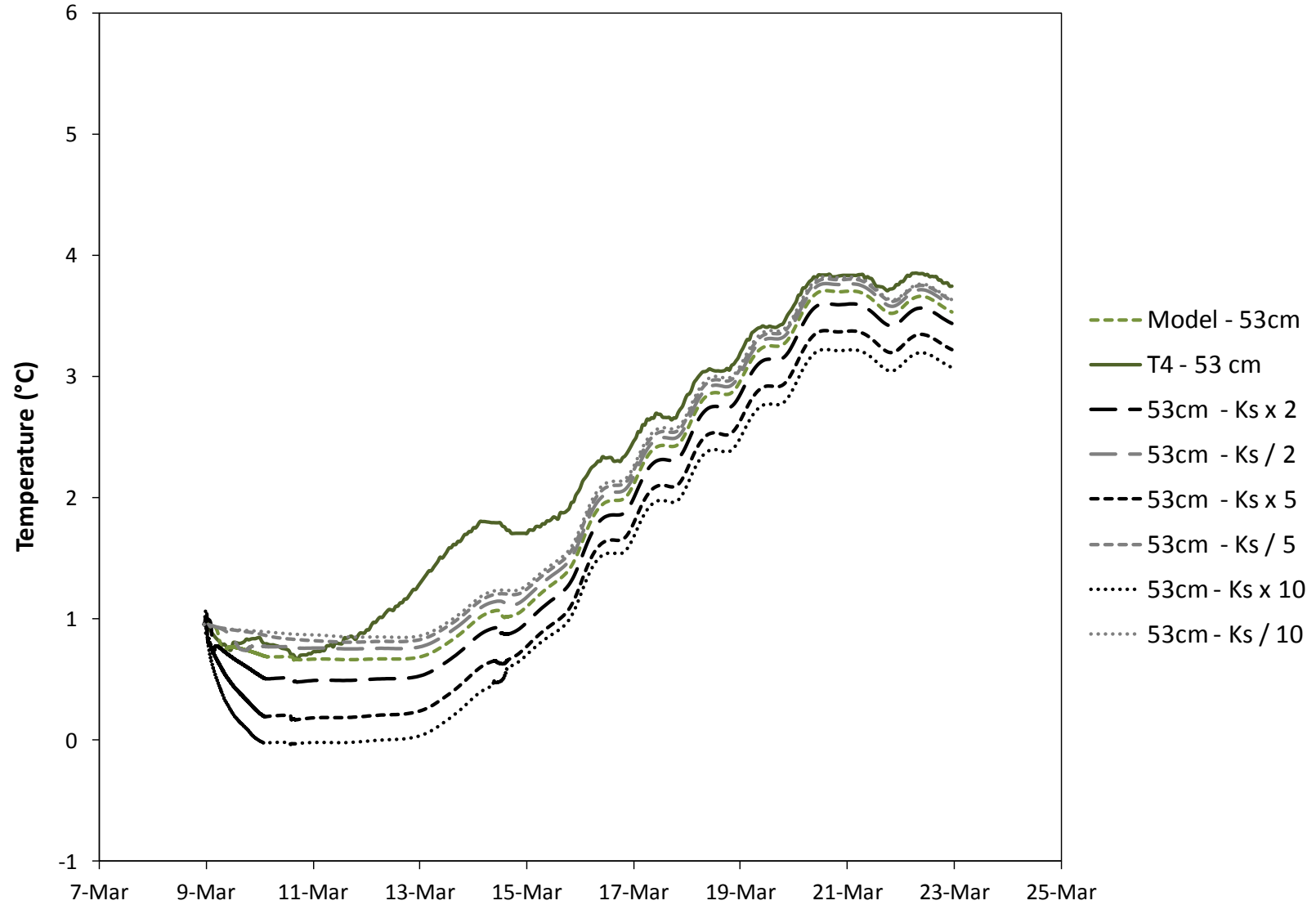


Figure Q.15 Scenario 1 – Hydraulic Conductivity of the Whole Soil Profile Adjusted by Factors of 2, 5, and 10 – T4

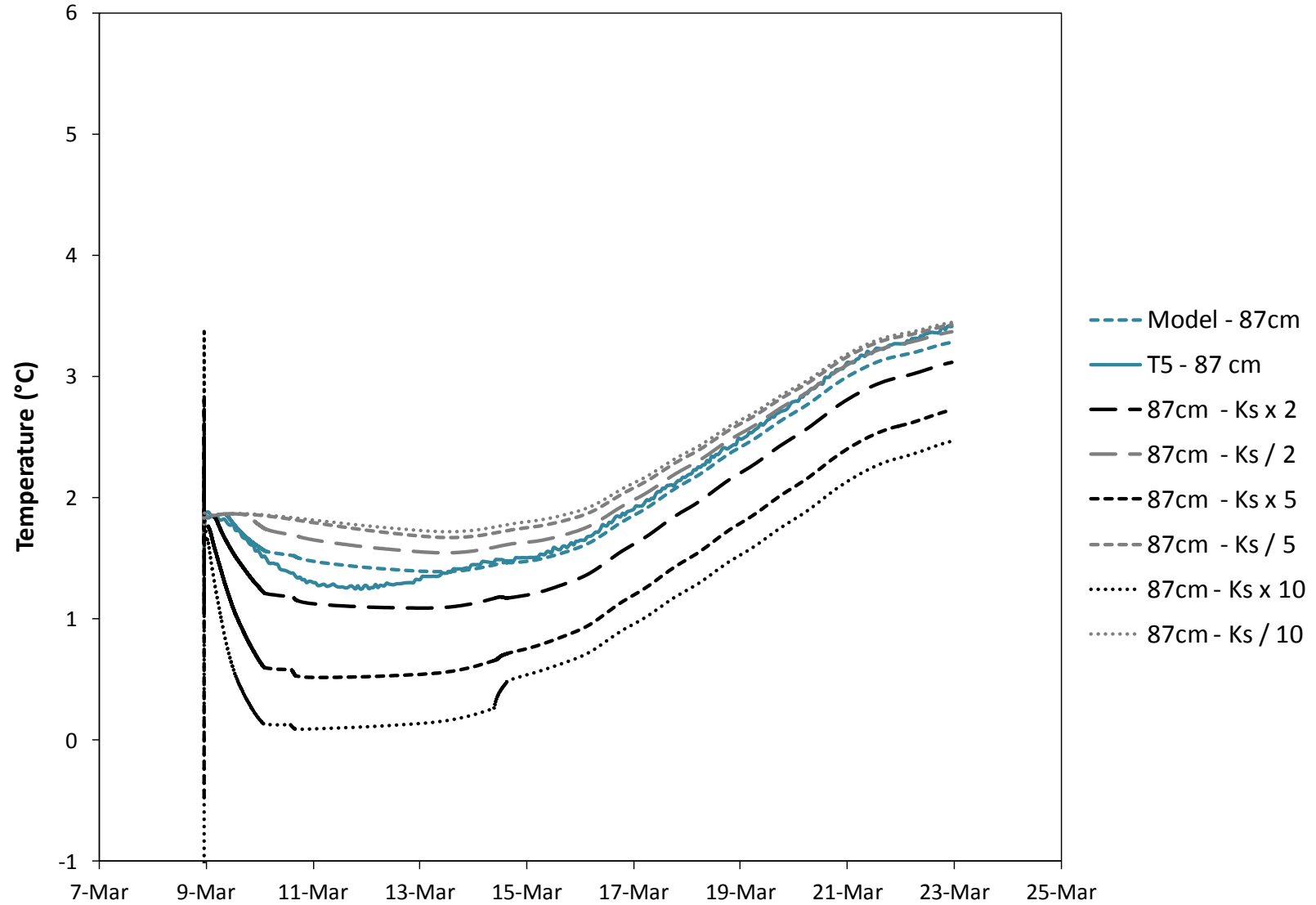


Figure Q.16 Scenario 1 – Hydraulic Conductivity of the Whole Soil Profile Adjusted by Factors of 2, 5, and 10 – T5

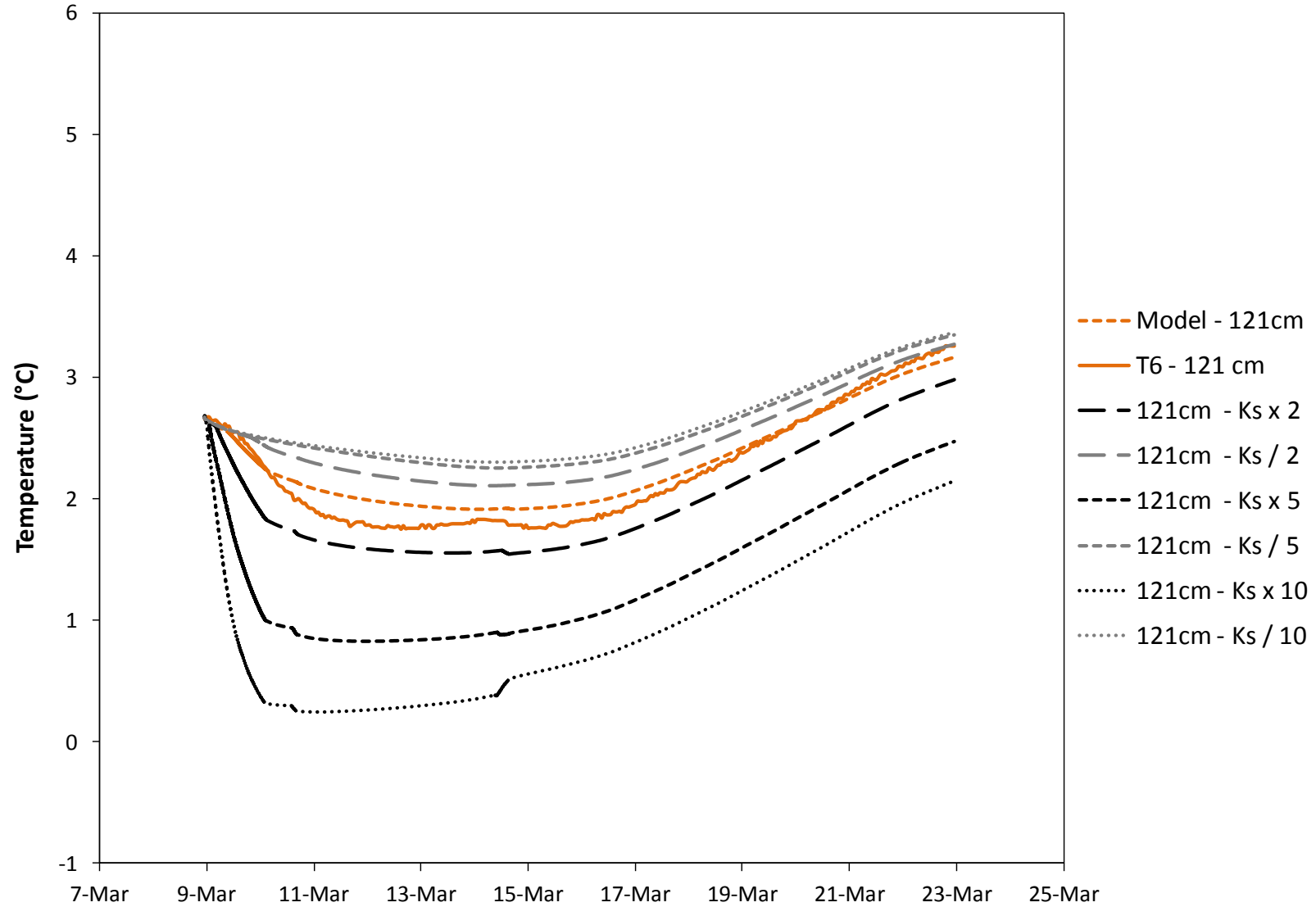


Figure Q.17 Scenario 1 – Hydraulic Conductivity of the Whole Soil Profile Adjusted by Factors of 2, 5, and 10 – T6

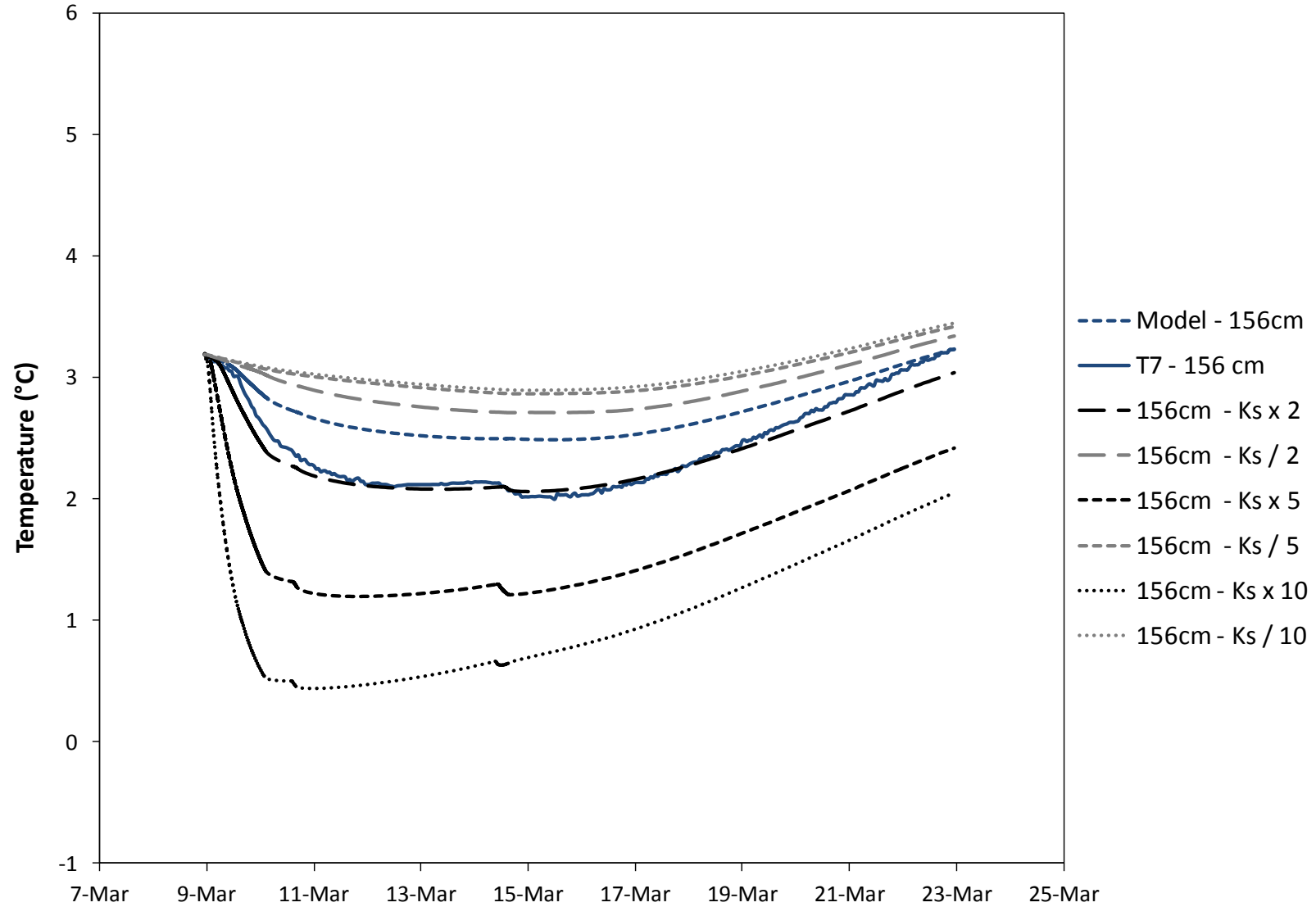


Figure Q.18 Scenario 1 – Hydraulic Conductivity of the Whole Soil Profile Adjusted by Factors of 2, 5, and 10 – T7

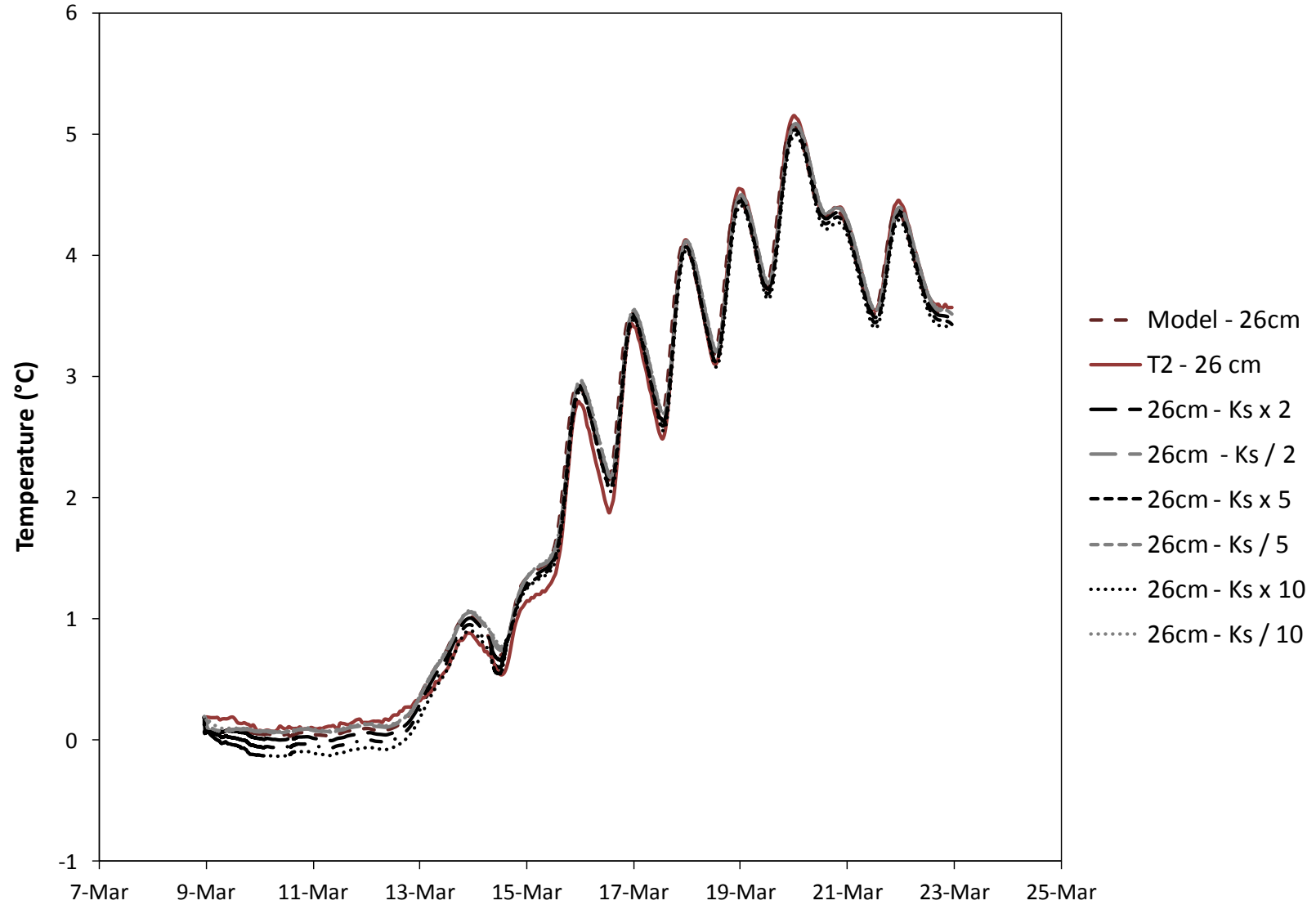


Figure Q.19 Scenario 2 – Hydraulic Conductivity of the Top Three Soil Layers Adjusted by Factors of 2, 5, and 10 – T2

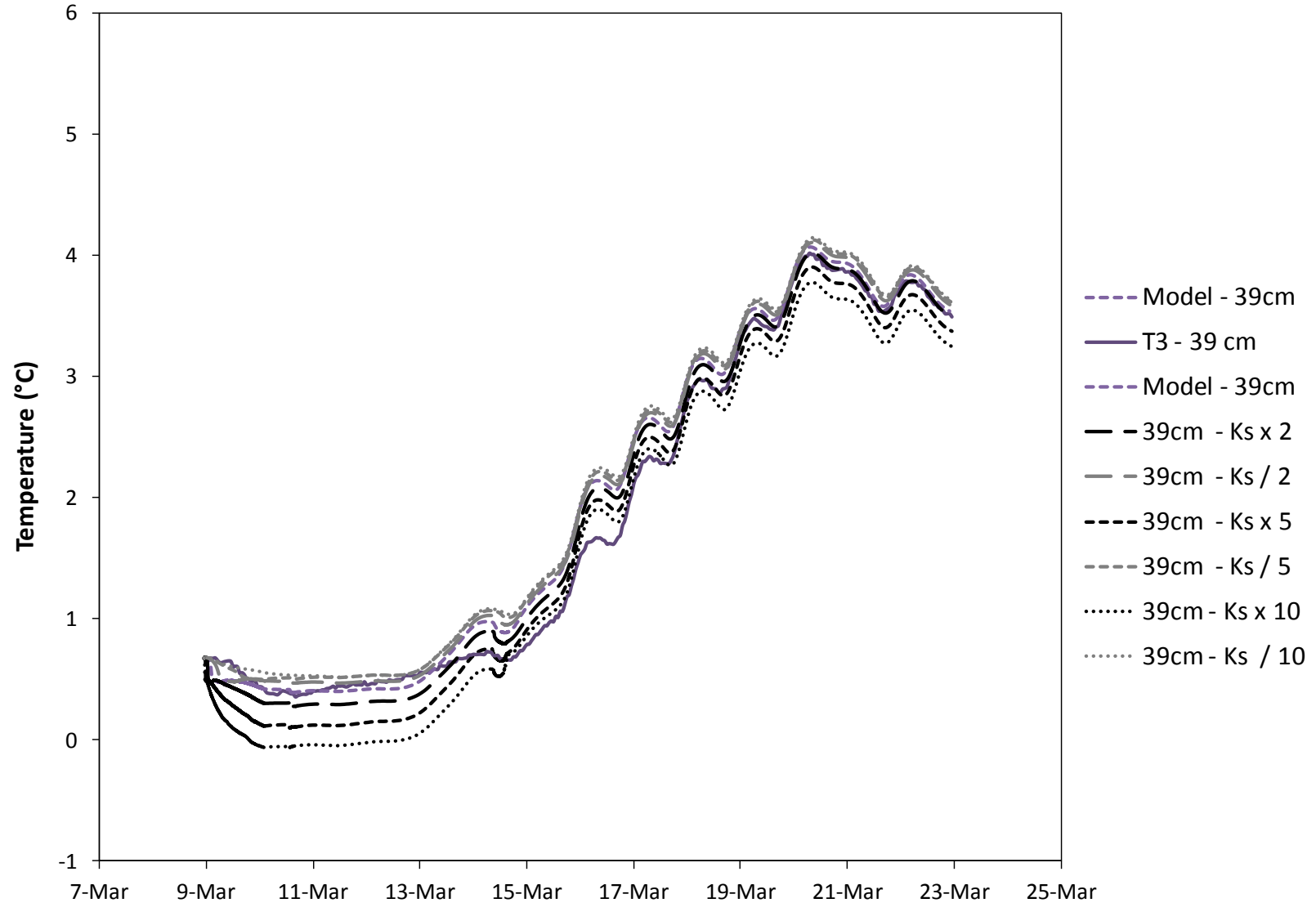


Figure Q.20 Scenario 2 – Hydraulic Conductivity of the Top Three Soil Layers Adjusted by Factors of 2, 5, and 10 – T3

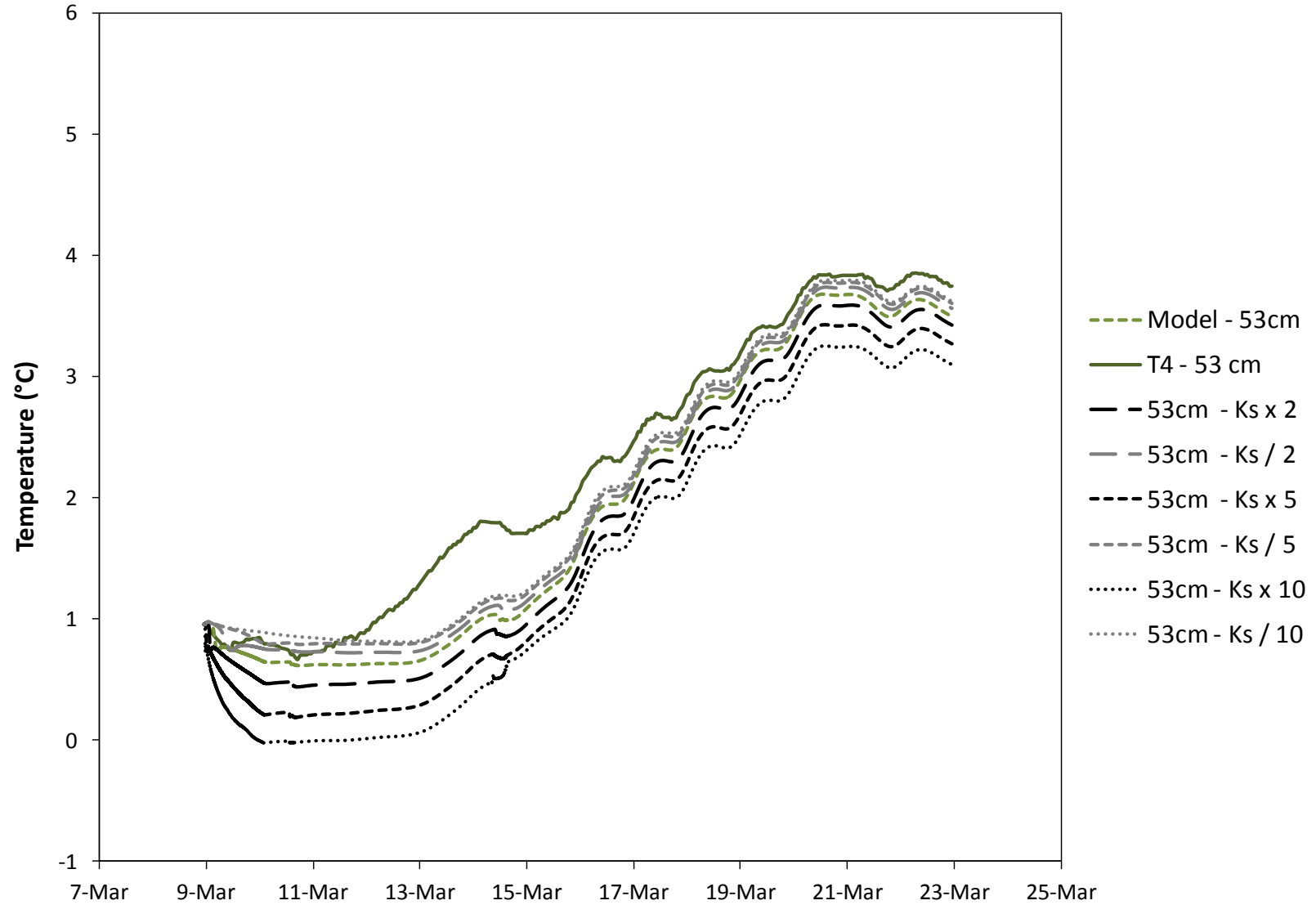


Figure Q.21 Scenario 2 – Hydraulic Conductivity of the Top Three Soil Layers Adjusted by Factors of 2, 5, and 10 – T4

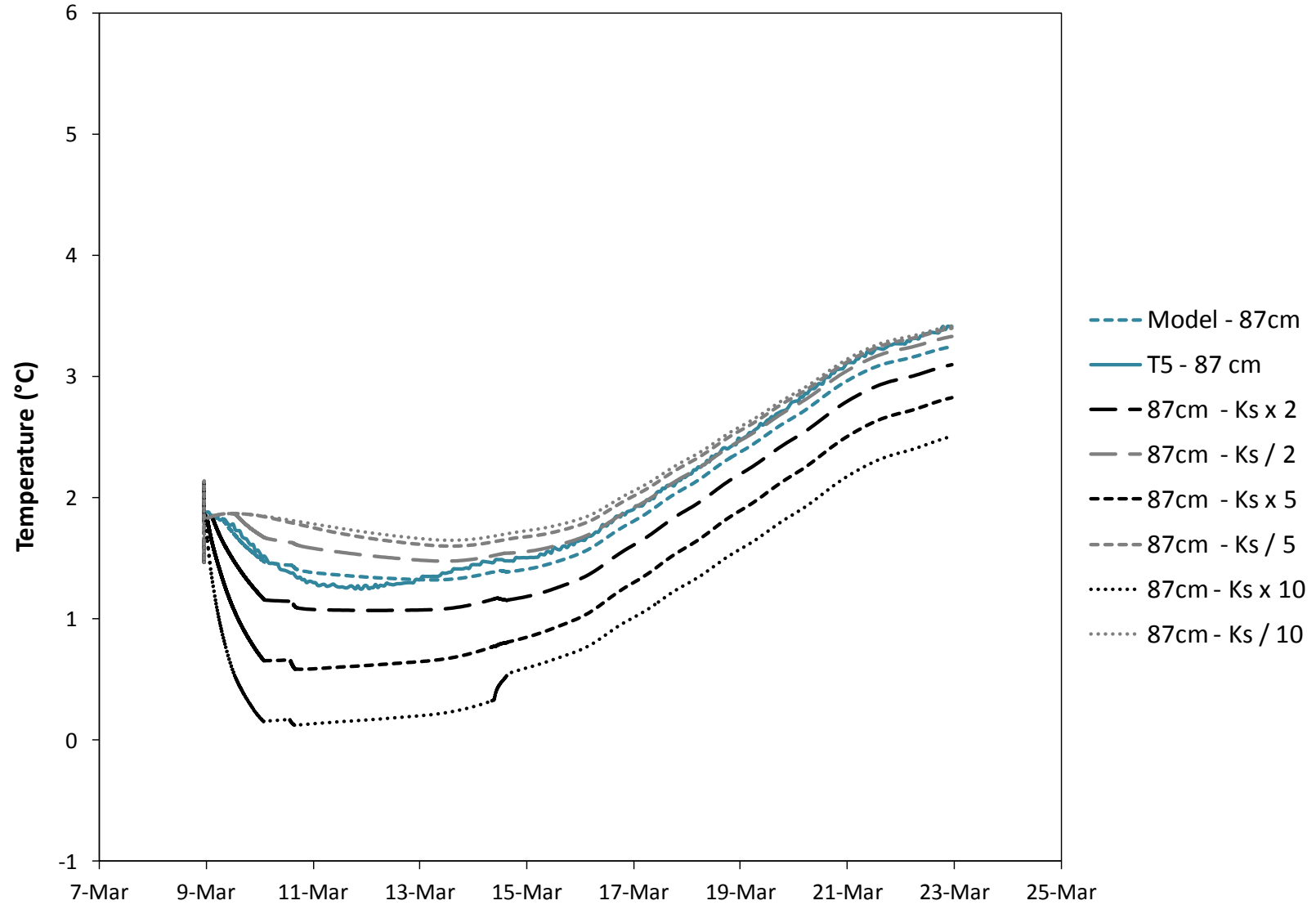


Figure Q.22 Scenario 2 – Hydraulic Conductivity of the Top Three Soil Layers Adjusted by Factors of 2, 5, and 10 – T5

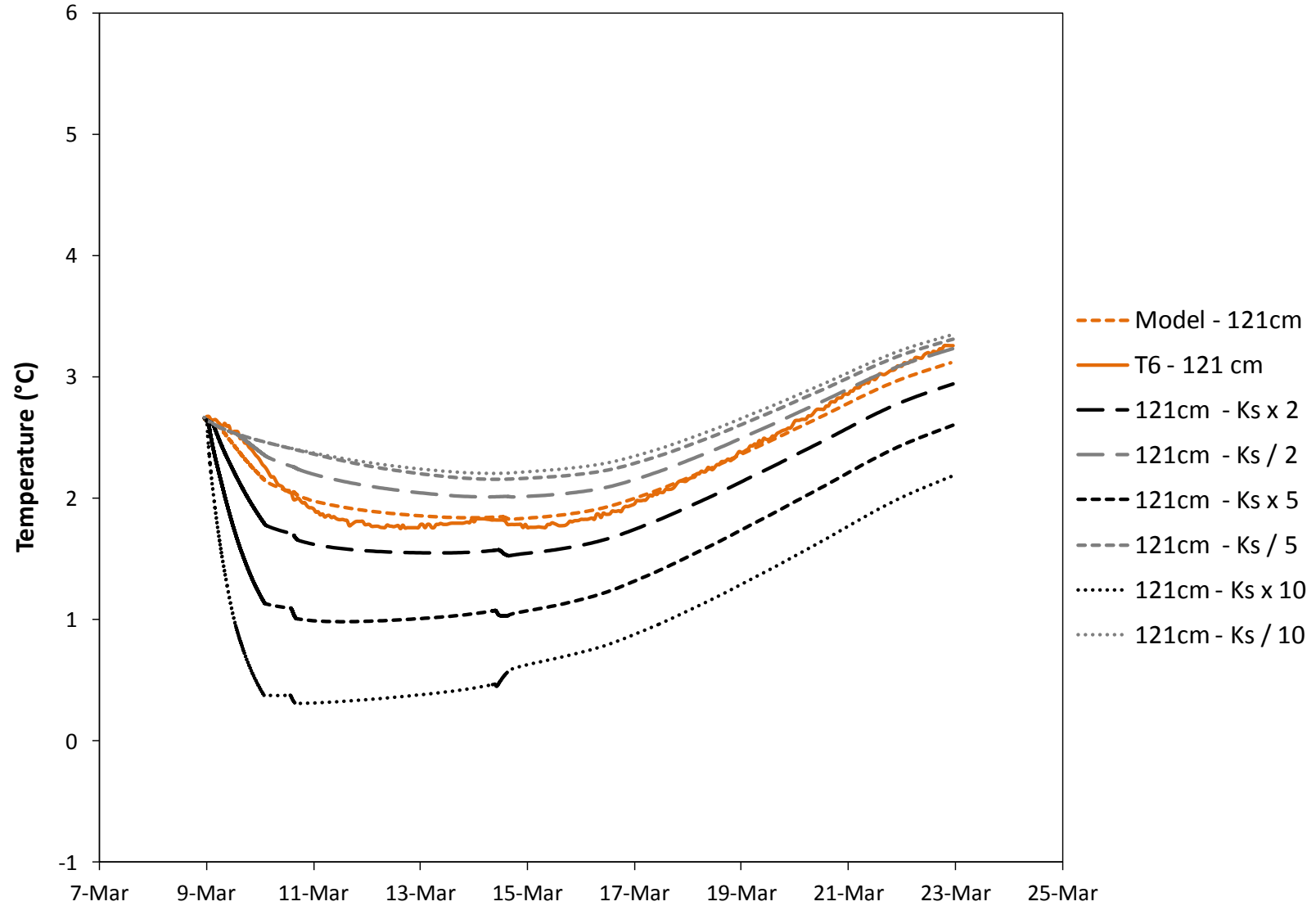


Figure Q.23 Scenario 2 – Hydraulic Conductivity of the Top Three Soil Layers Adjusted by Factors of 2, 5, and 10 – T6

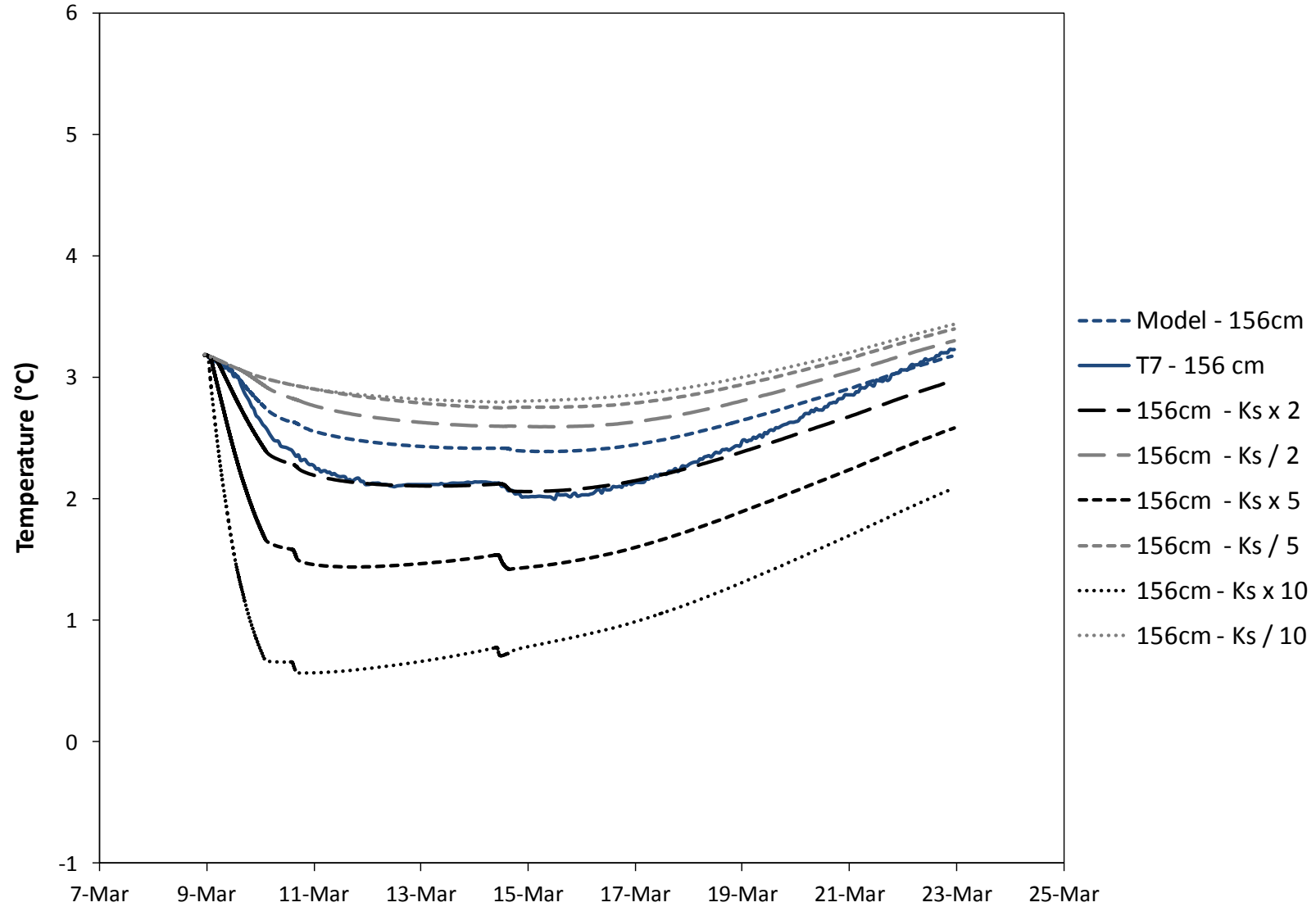


Figure Q.24 Scenario 2 – Hydraulic Conductivity of the Top Three Soil Layers Adjusted by Factors of 2, 5, and 10 – T7

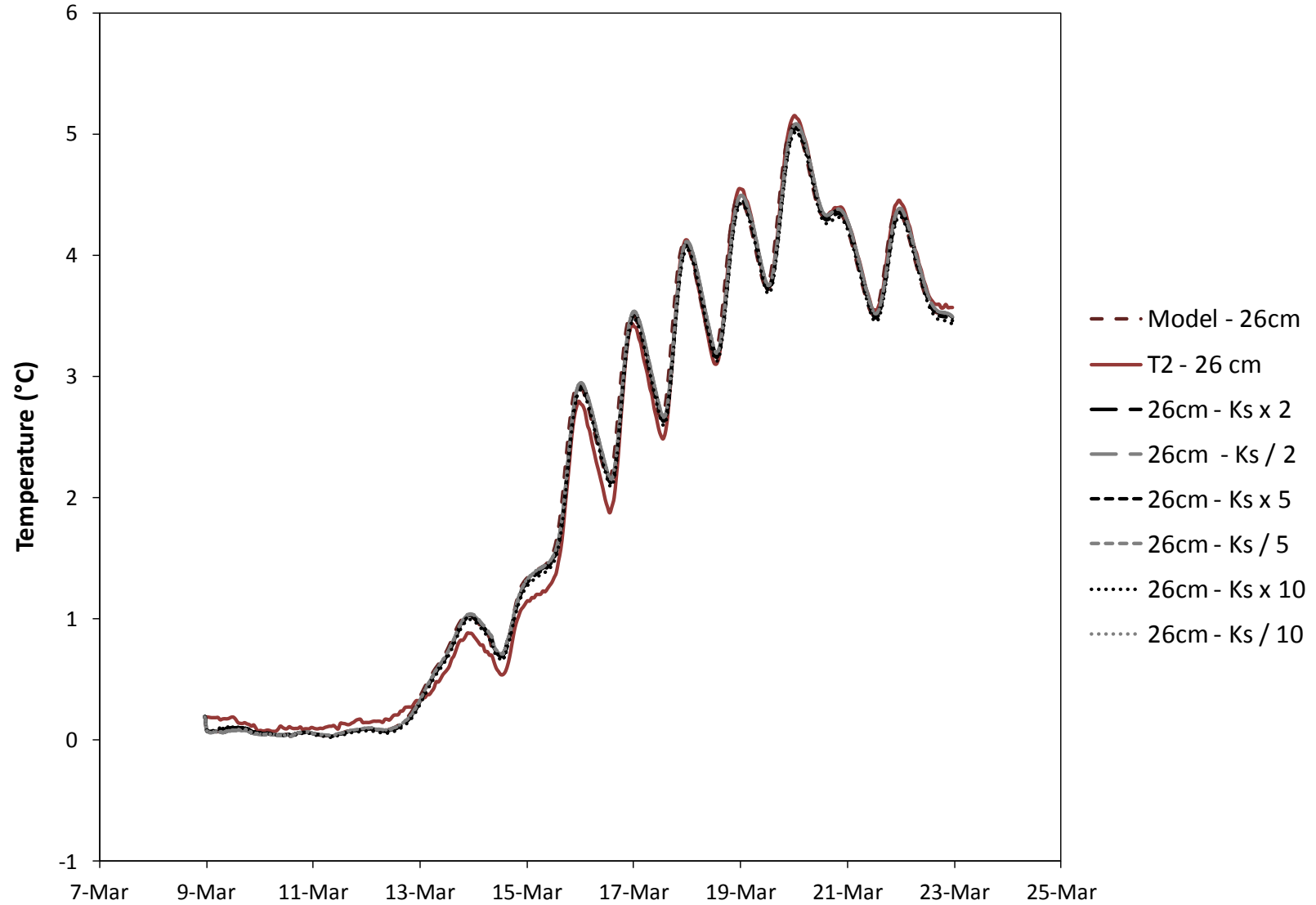


Figure Q.25 Scenario 2 – Hydraulic Conductivity of the Bottom Eight Soil Layers Adjusted by Factors of 2, 5, and 10 - T2

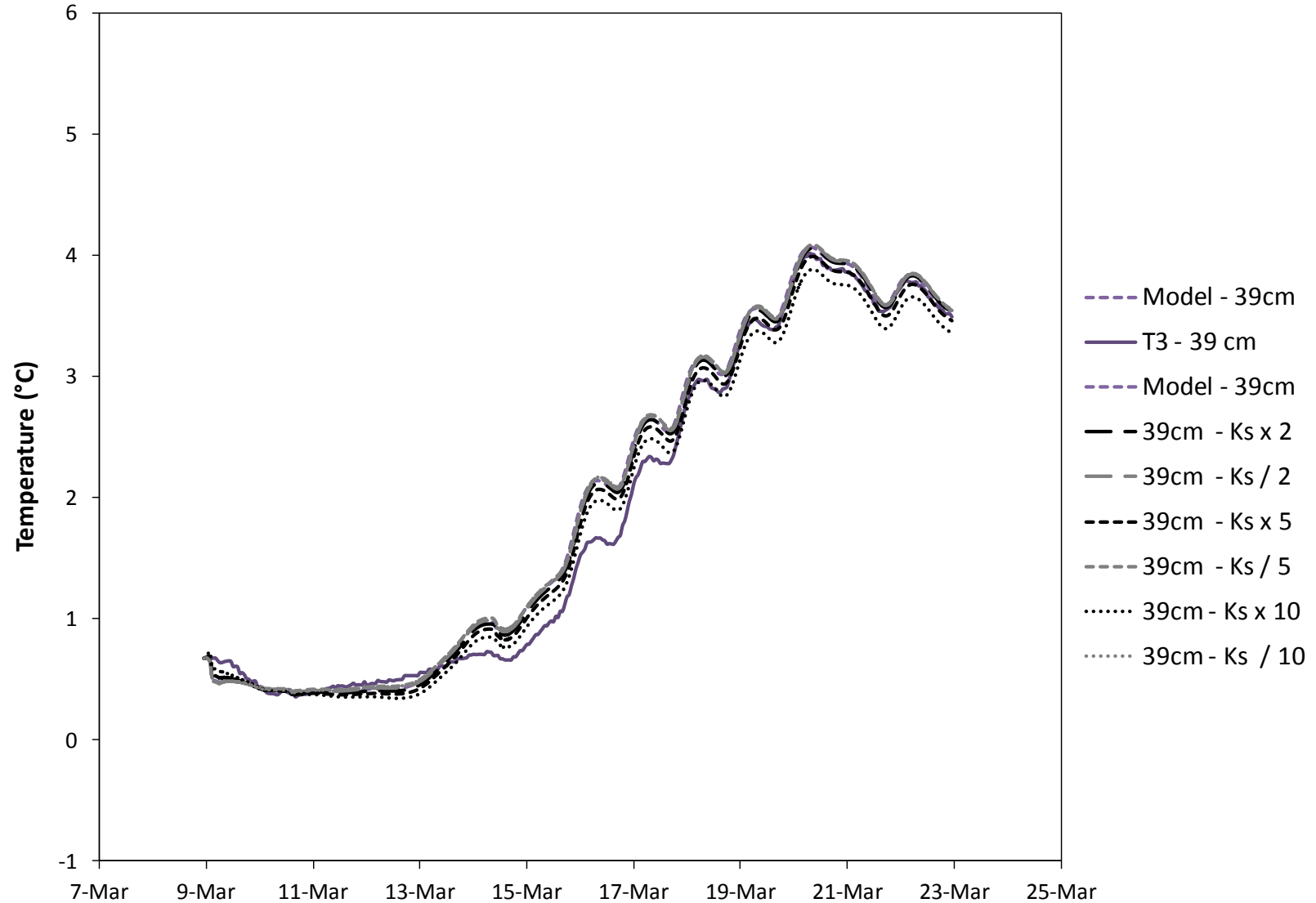


Figure Q.26 Scenario 2 – Hydraulic Conductivity of the Bottom Eight Soil Layers Adjusted by Factors of 2, 5, and 10 – T3

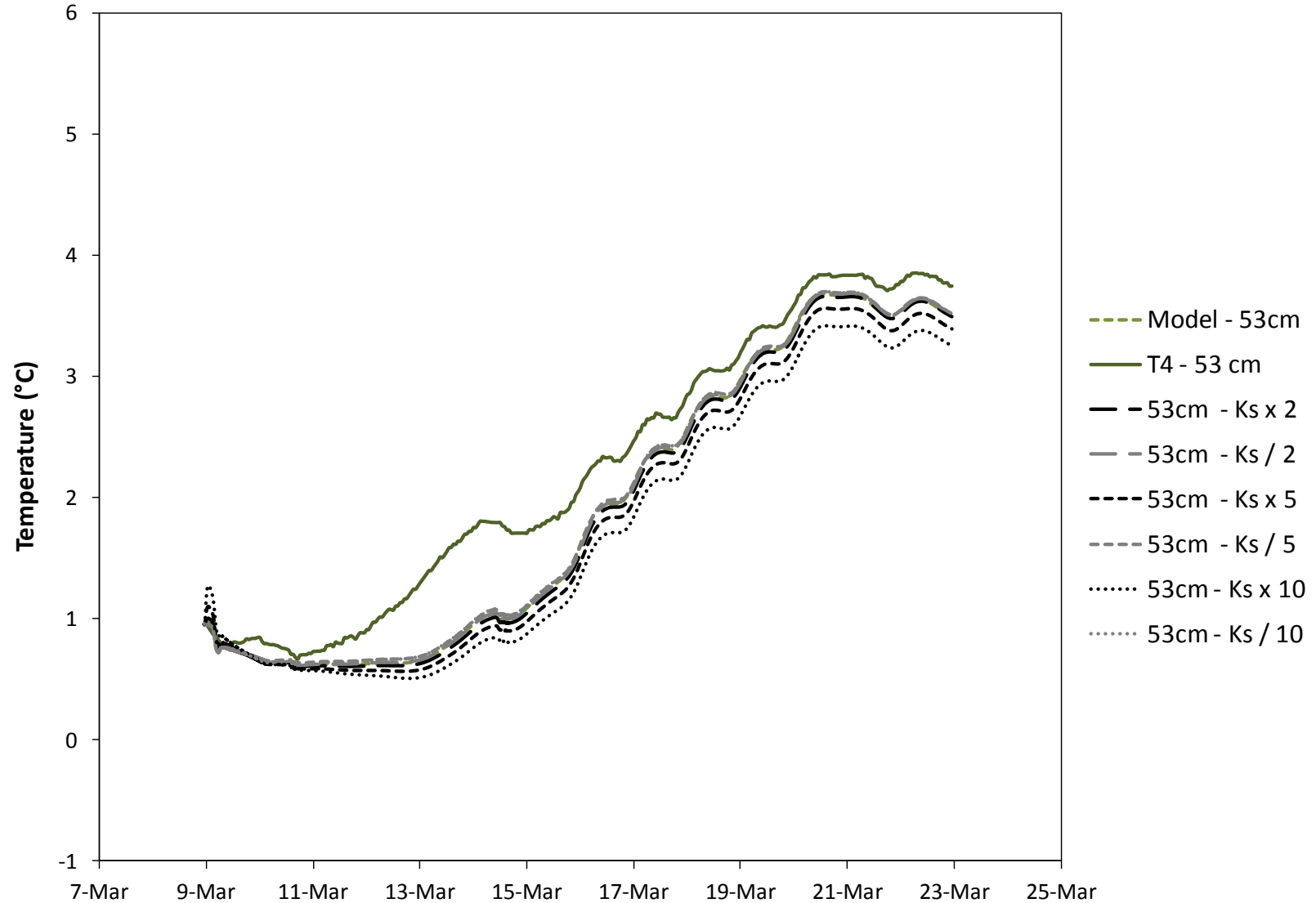


Figure Q.27 Scenario 2 – Hydraulic Conductivity of the Bottom Eight Soil Layers Adjusted by Factors of 2, 5, and 10 – T4

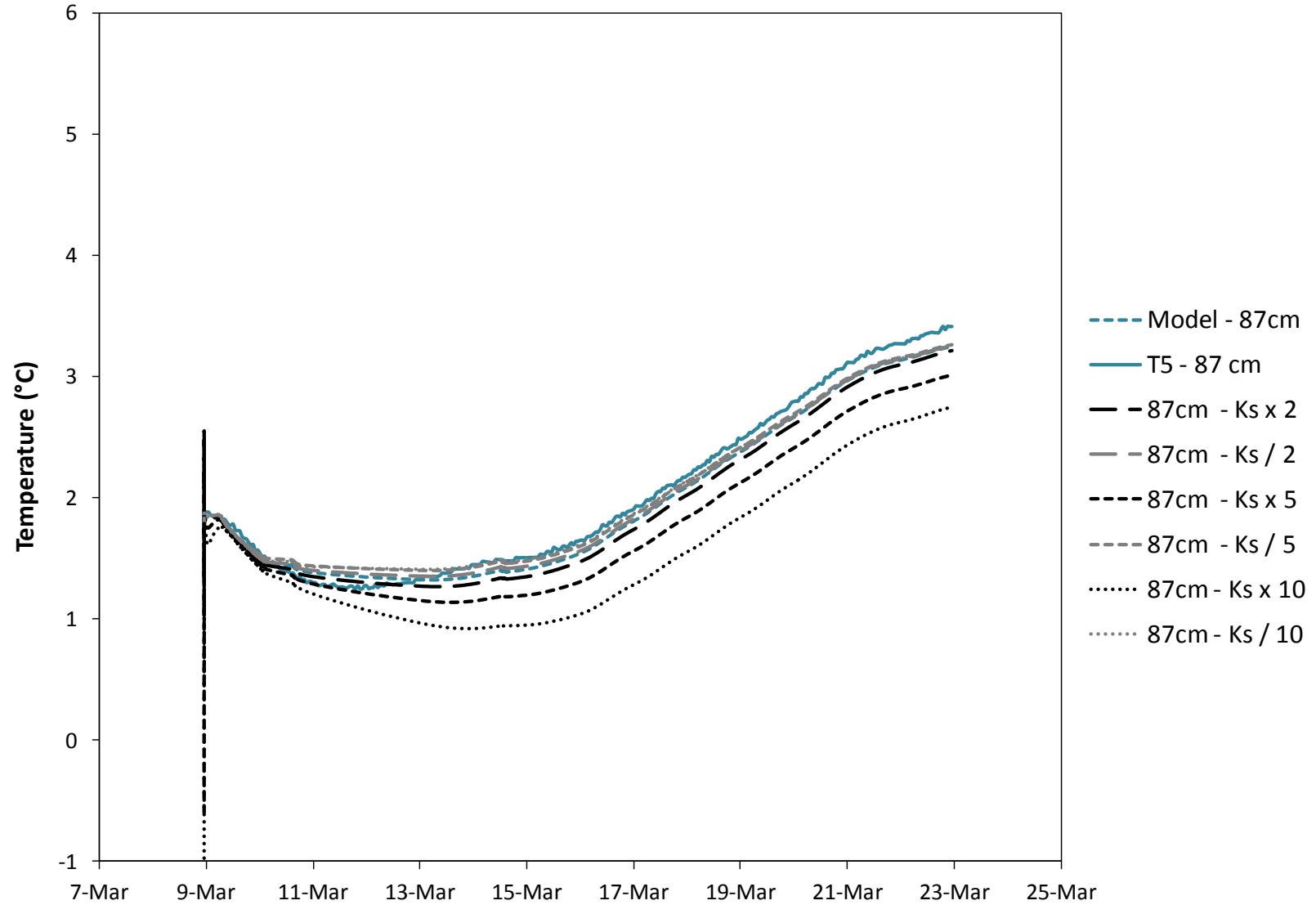


Figure Q.28 Scenario 2 – Hydraulic Conductivity of the Bottom Eight Soil Layers Adjusted by Factors of 2, 5, and 10 – T5

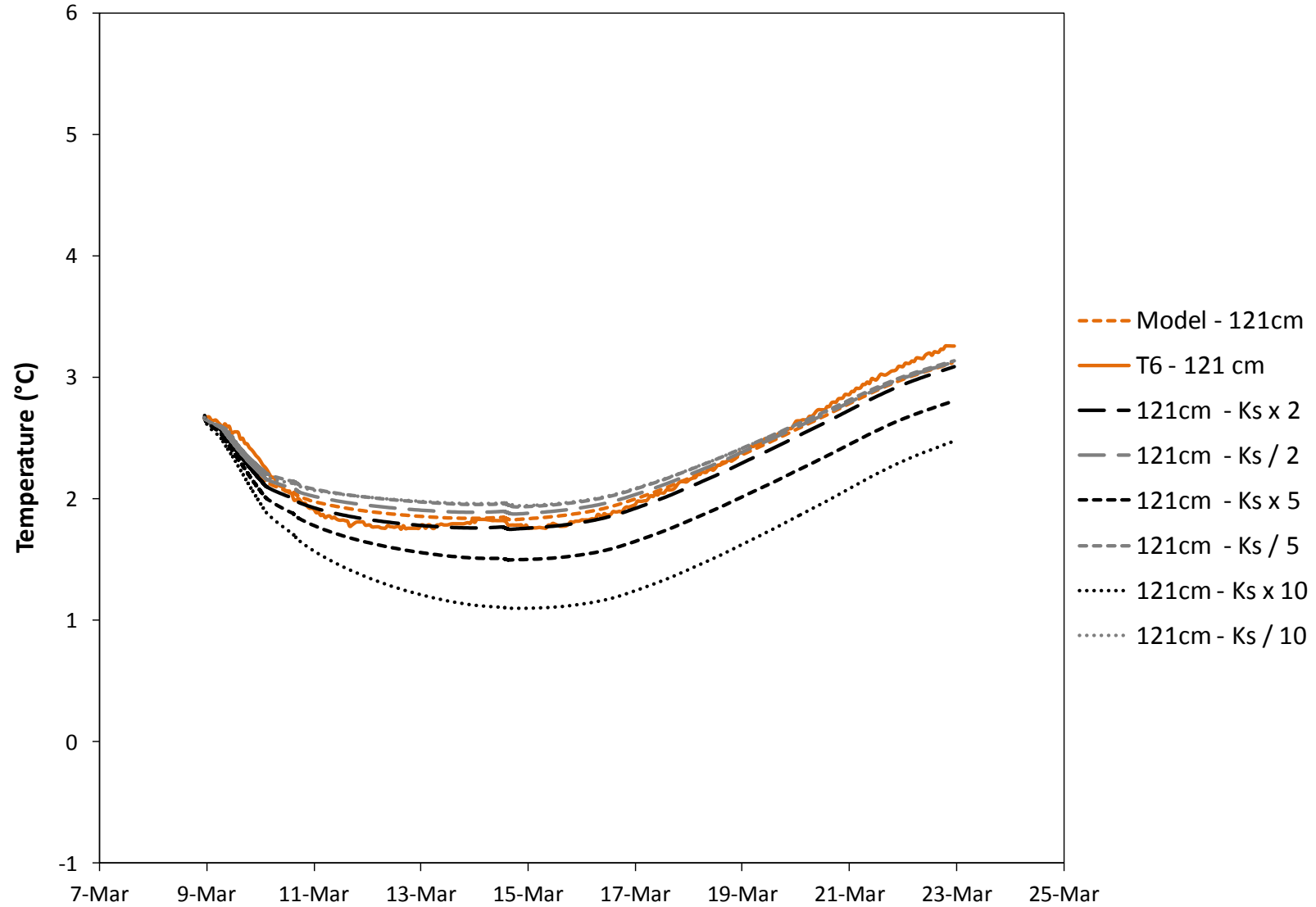


Figure Q.29 Scenario 2 – Hydraulic Conductivity of the Bottom Eight Soil Layers Adjusted by Factors of 2, 5, and 10 – T6

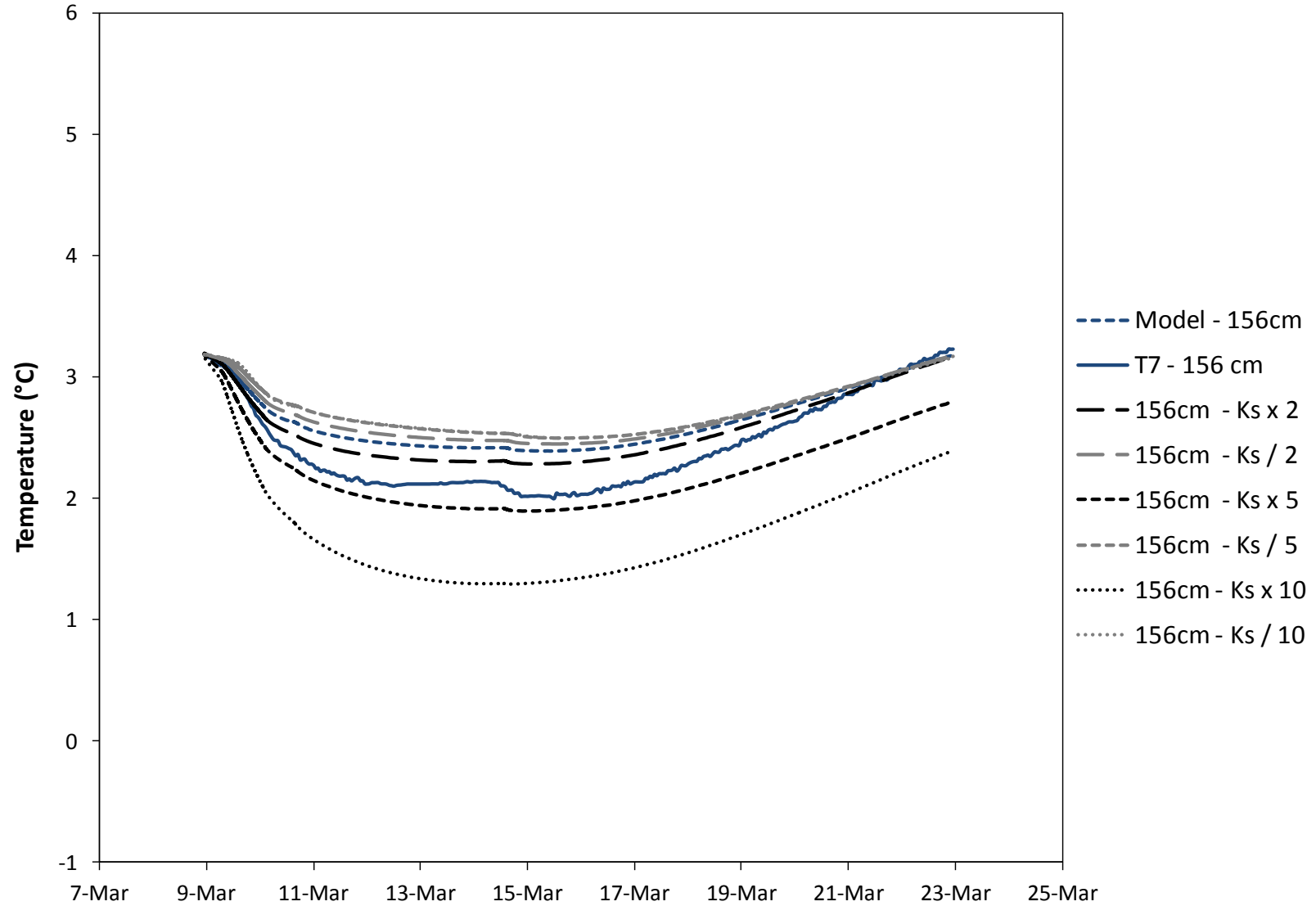


Figure Q.30 Scenario 2 – Hydraulic Conductivity of the Bottom Eight Soil Layers Adjusted by Factors of 2, 5, and 10 – T7

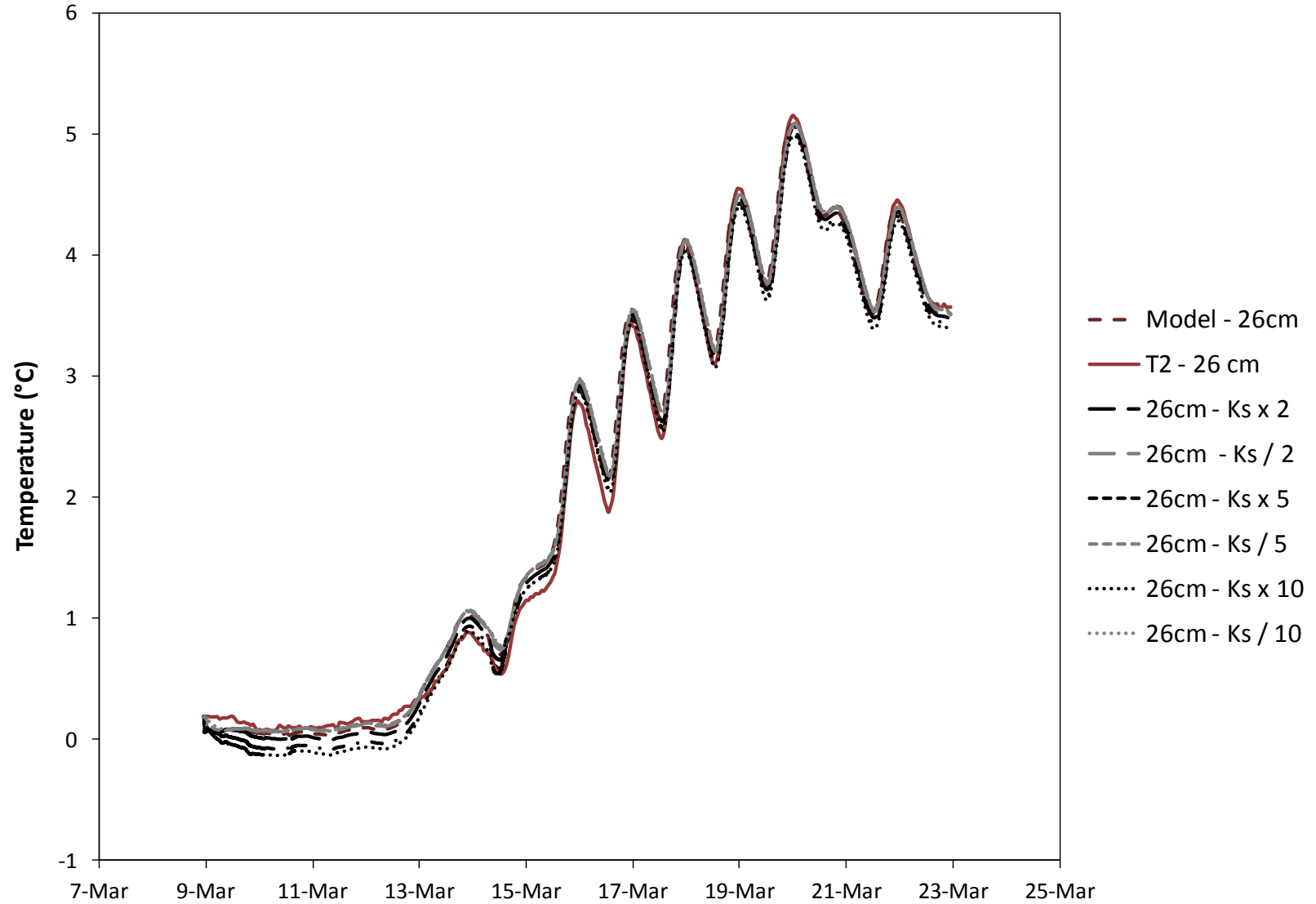


Figure Q.31 Scenario 2 – Hydraulic Conductivity of the Whole Soil Profile Adjusted by Factors of 2, 5, and 10 – T2

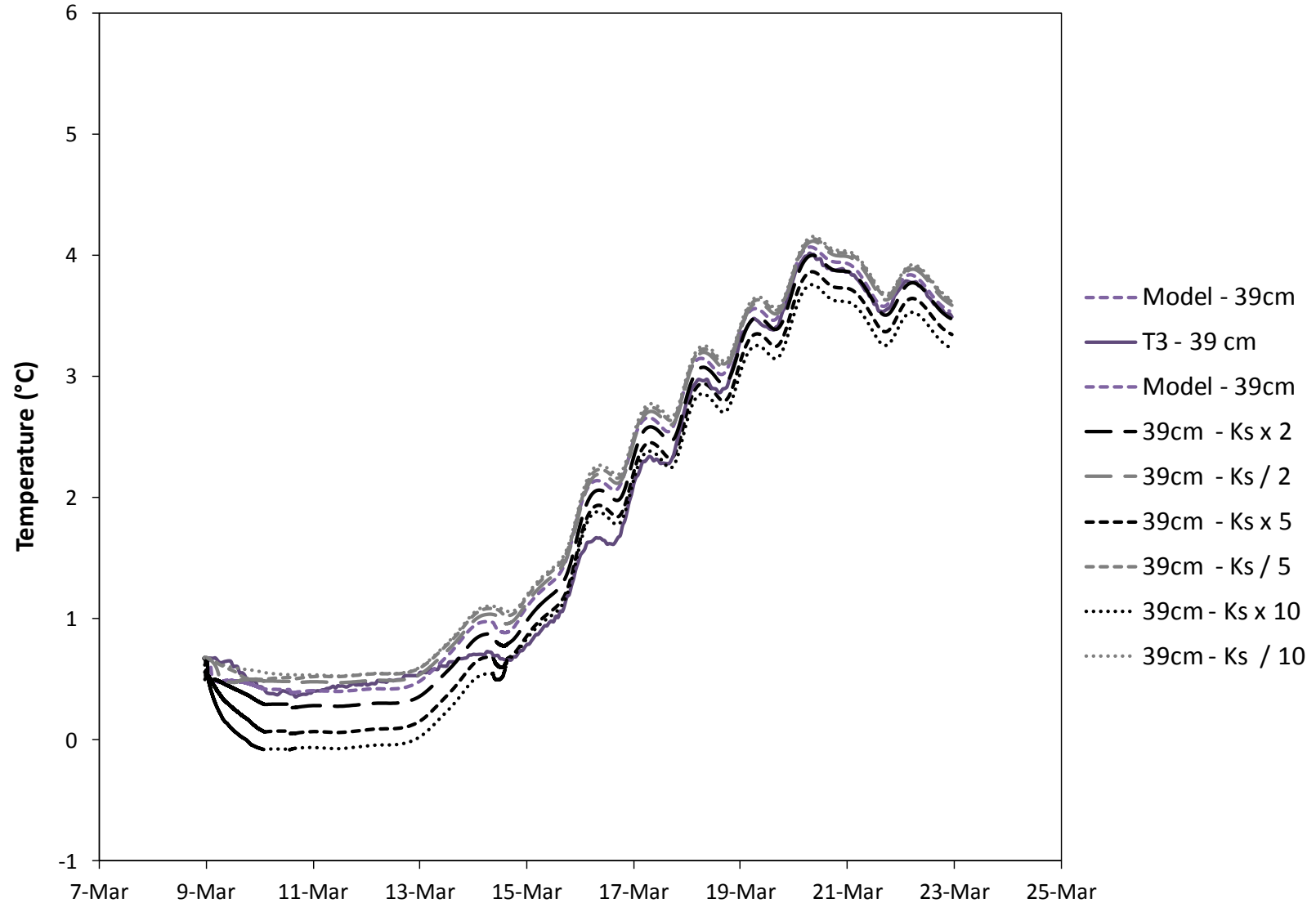


Figure Q.32 Scenario 2 – Hydraulic Conductivity of the Whole Soil Profile Adjusted by Factors of 2, 5, and 10 – T3

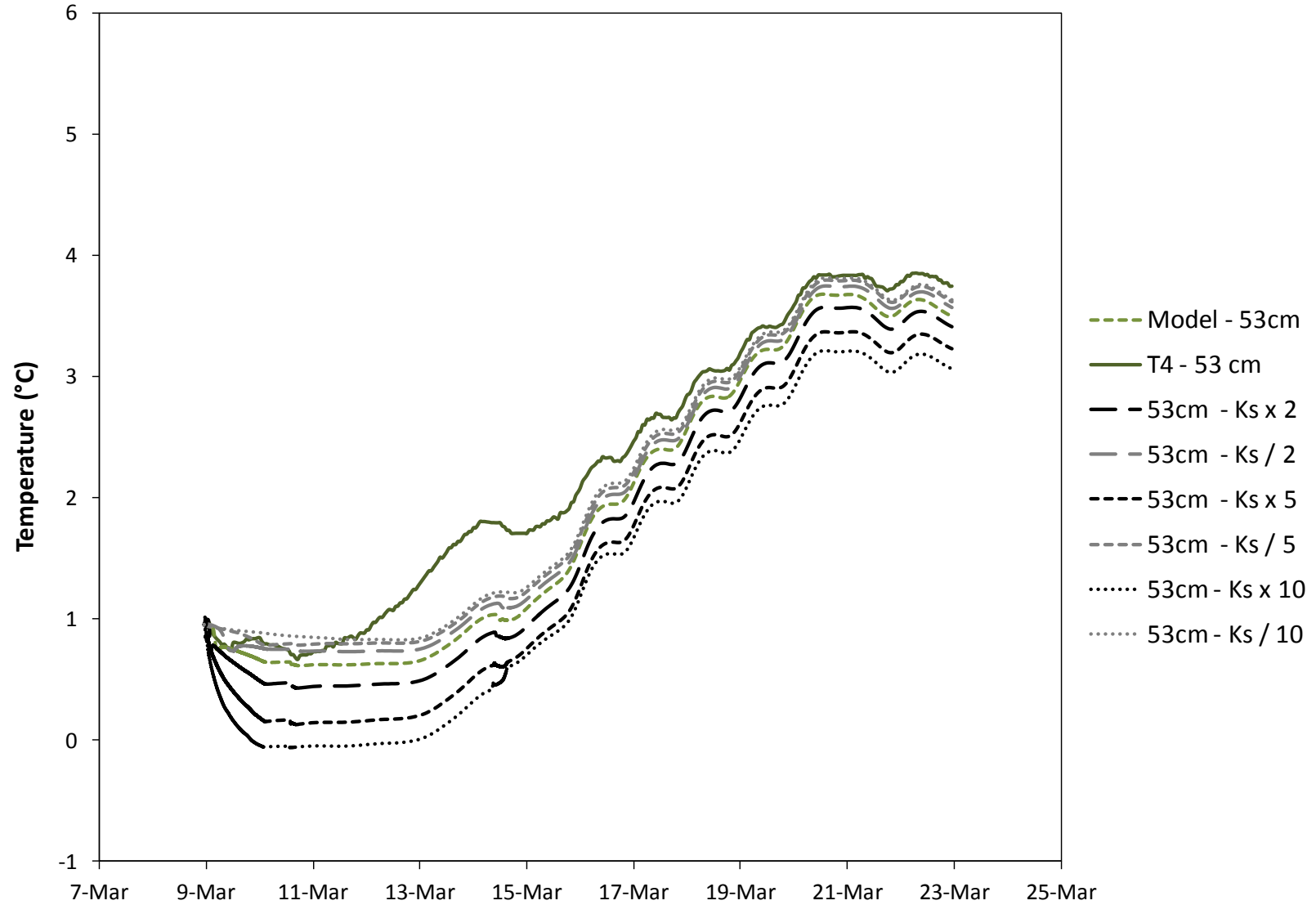


Figure Q.33 Scenario 2 – Hydraulic Conductivity of the Whole Soil Profile Adjusted by Factors of 2, 5, and 10 – T4

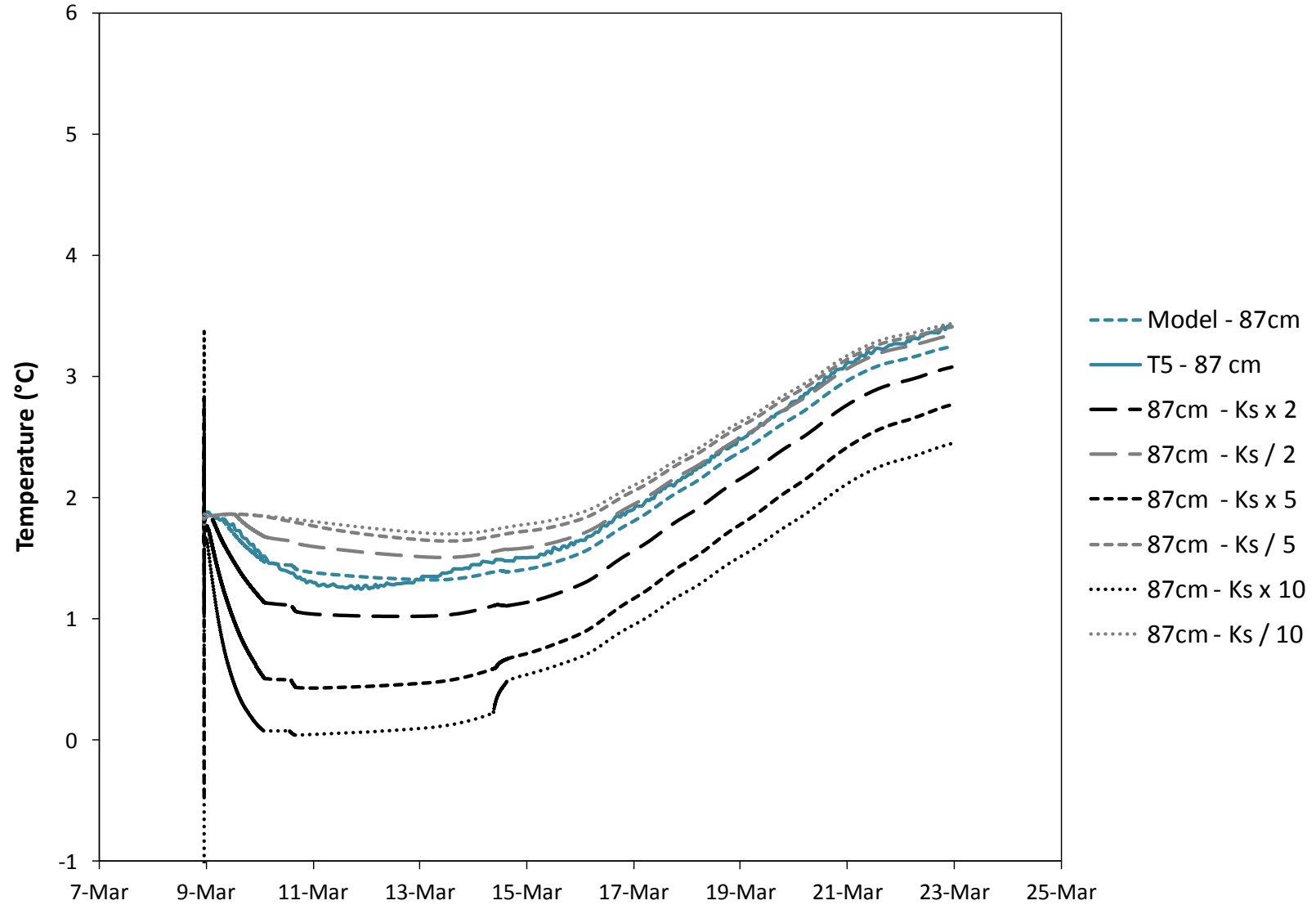


Figure Q.34 Scenario 2 – Hydraulic Conductivity of the Whole Soil Profile Adjusted by Factors of 2, 5, and 10 – T5

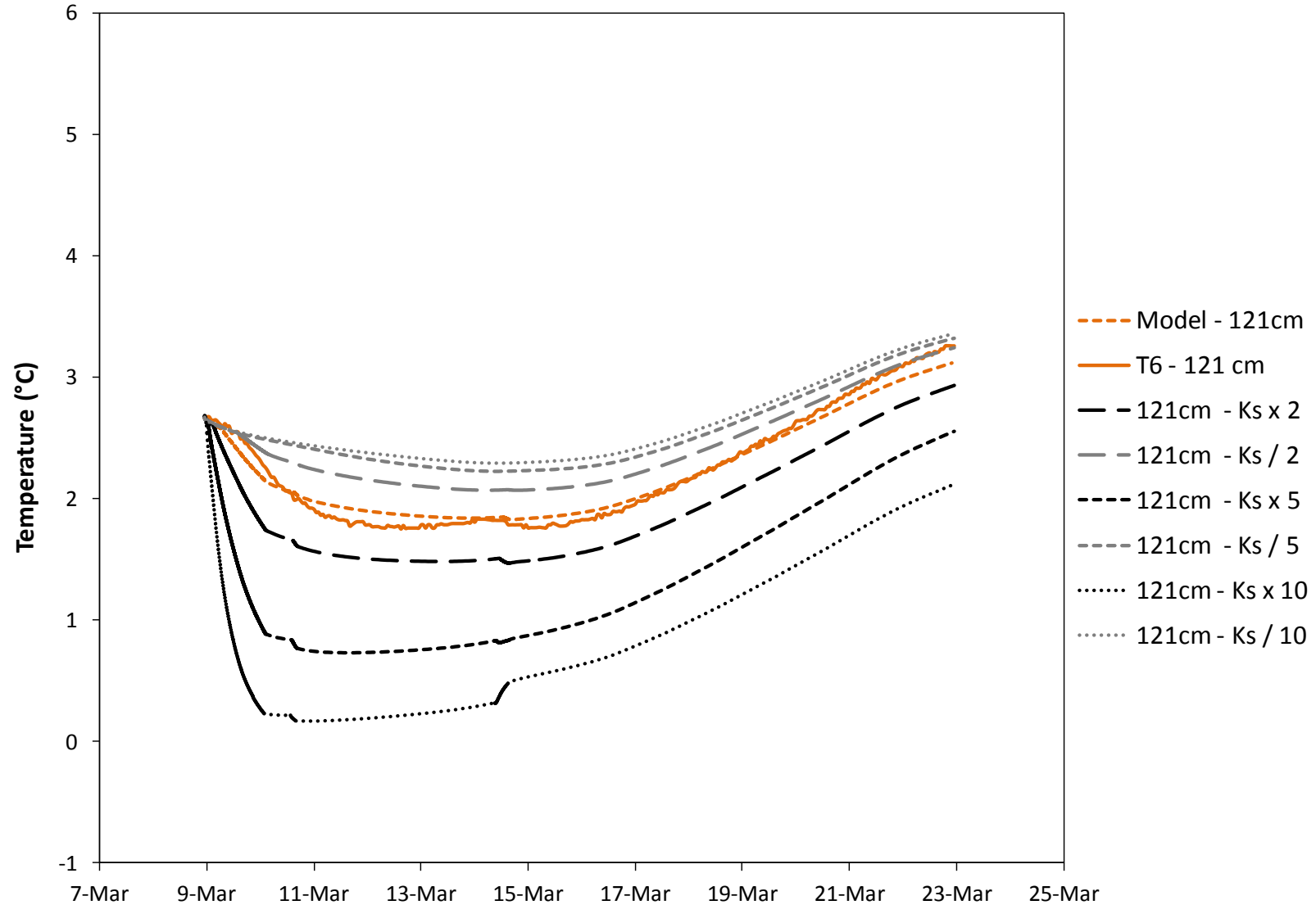


Figure Q.35 Scenario 2 – Hydraulic Conductivity of the Whole Soil Profile Adjusted by Factors of 2, 5, and 10 – T6

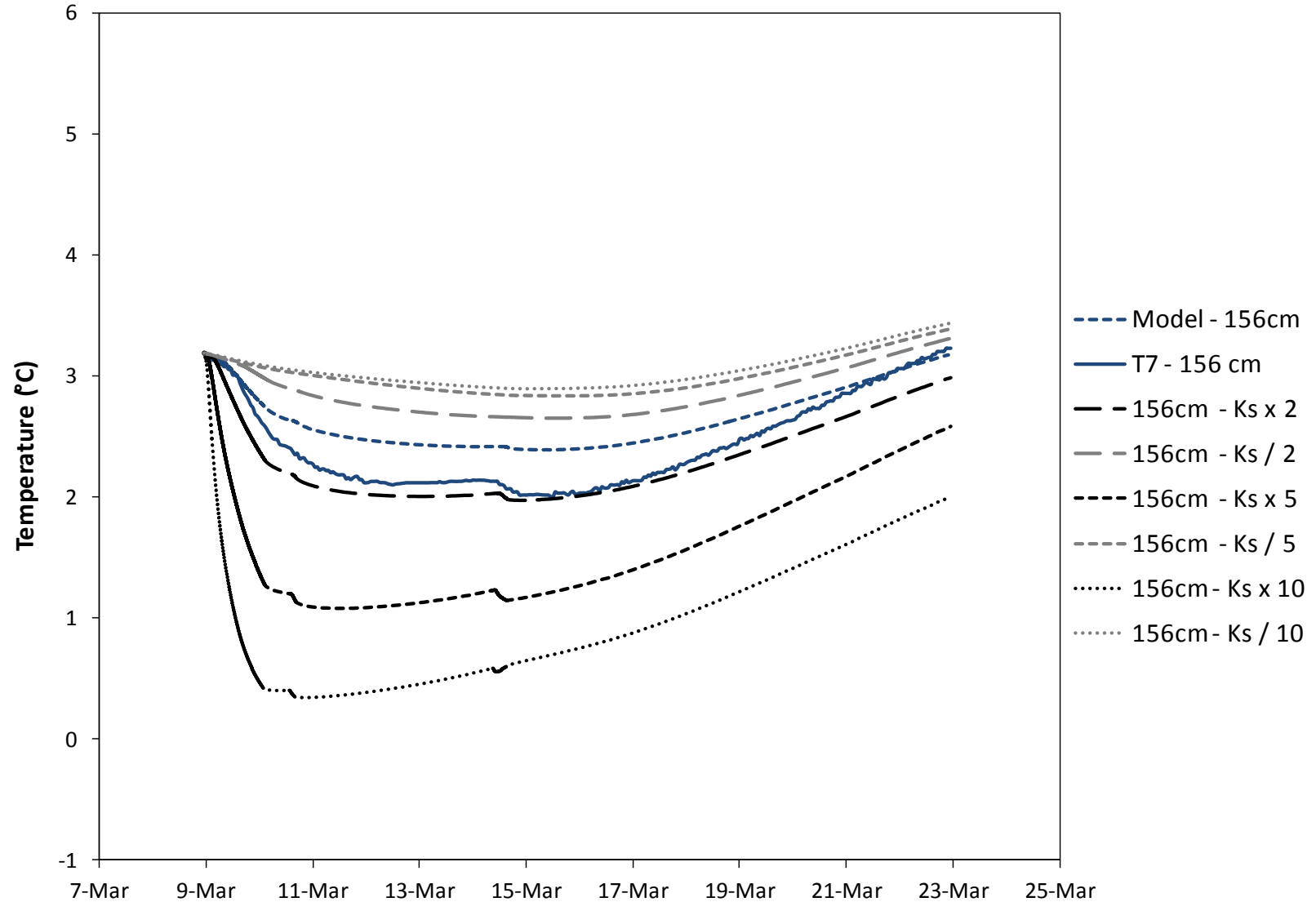


Figure Q.36 Scenario 2 – Hydraulic Conductivity of the Whole Soil Profile Adjusted by Factors of 2, 5, and 10 – T7

Appendix R

Simulated and Observed Temperatures – Gravity Drained

April 12th to June 1st, 2010

Fully Drained Conditions Using Moisture Retention Parameters from Model Calibration for Soil when the Ephemeral Stream is Present

Fully Drained Conditions Using Altered Moisture Retention Parameters from Model Calibration for Soil when the Ephemeral Stream is Present by Increasing the Hydraulic Conductivity of the Lower Eight Layers by 2

August 24th to October 31st, 2010

Fully Drained Conditions Using Moisture Retention Parameters from Model Calibration for Soil when the Ephemeral Stream is Present

Fully Drained Conditions Using Altered Moisture Retention Parameters from Model Calibration for Soil when the Ephemeral Stream is Present by Increasing the Hydraulic Conductivity of the Lower Eight Layers by 2

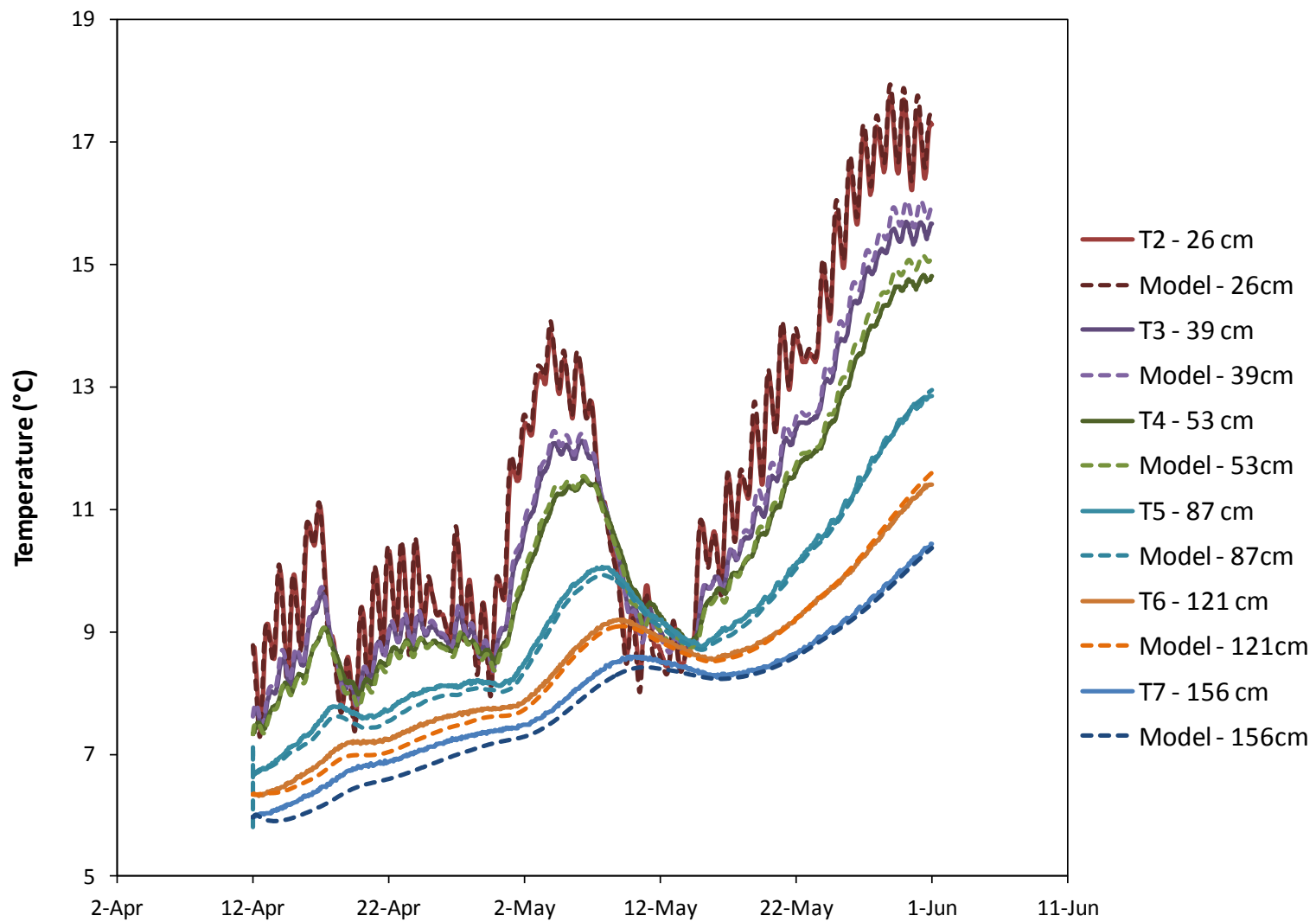


Figure R.1 Simulated and observed temperature profiles between April 12th to June 1st, 2010 using the moisture retention parameters obtained from calibration when the ephemeral stream was present.

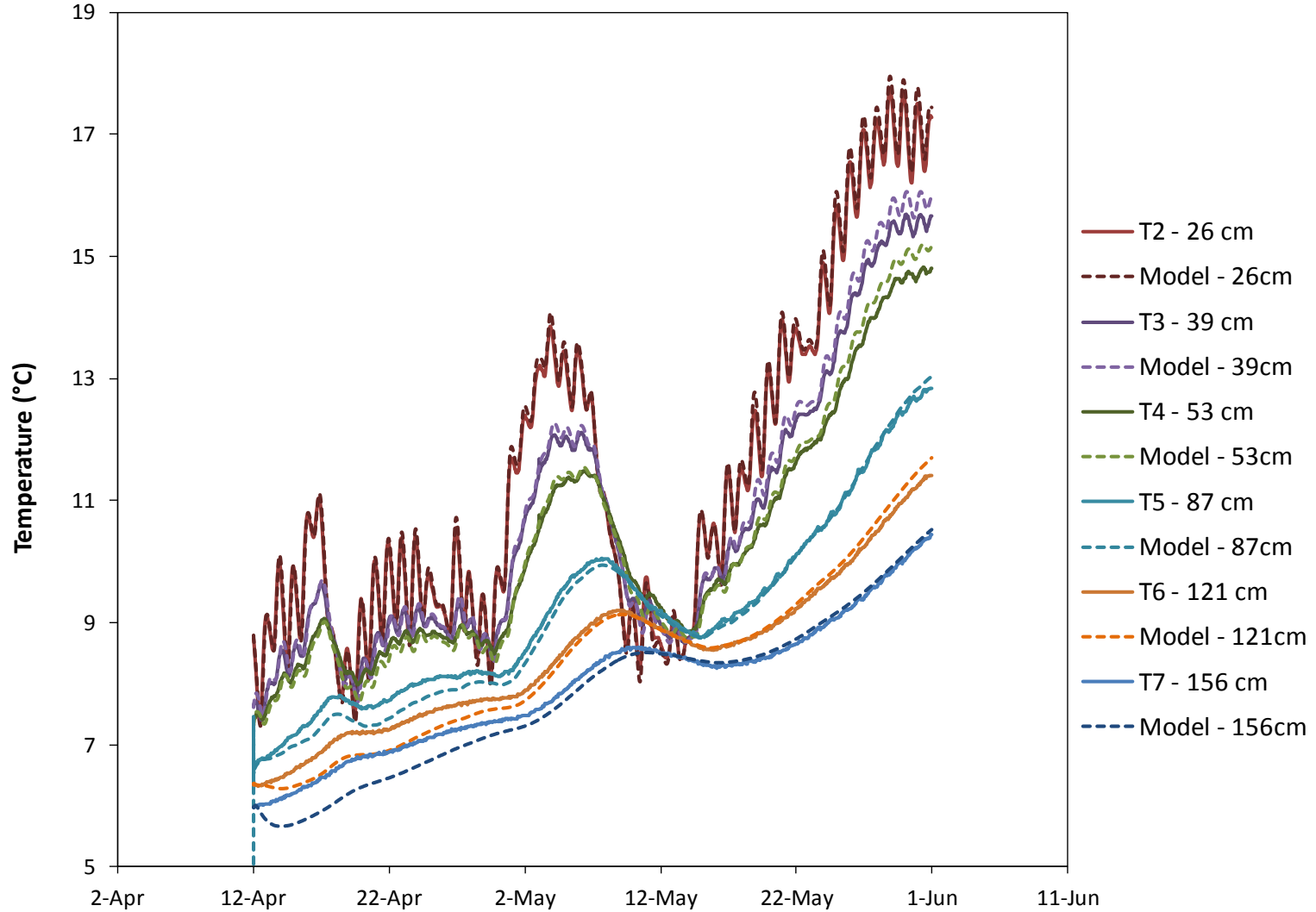


Figure R.2 Simulated and observed temperature profiles between April 12th to June 1st, 2010 using altered moisture retention parameters obtained from calibration when the ephemeral stream was present by increasing the hydraulic conductivity of the lower eight layers by two.

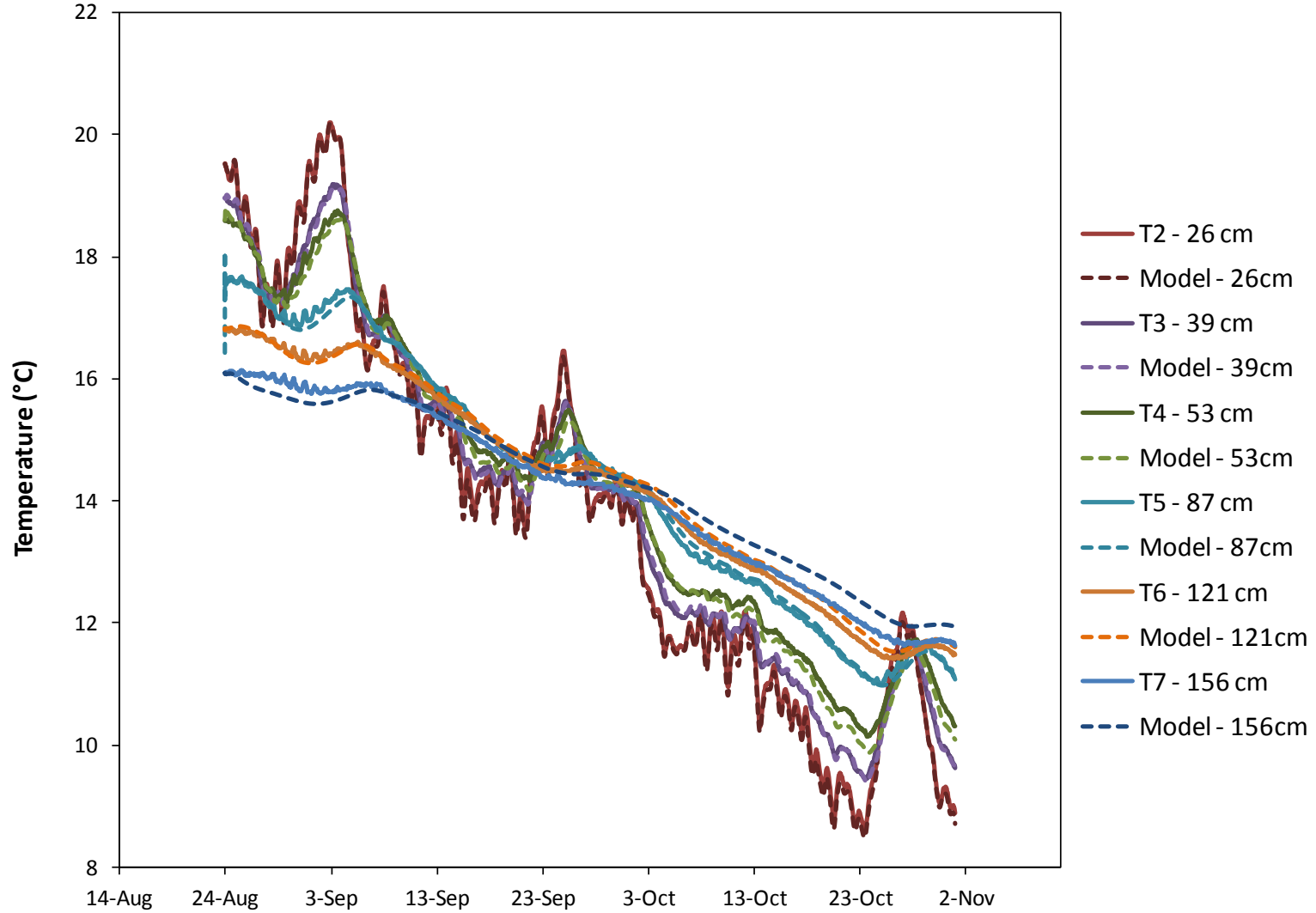


Figure R.3 Simulated and observed temperature profiles between August 24th to October 31st, 2010 using the moisture retention parameters obtained from calibration when the ephemeral stream was present.

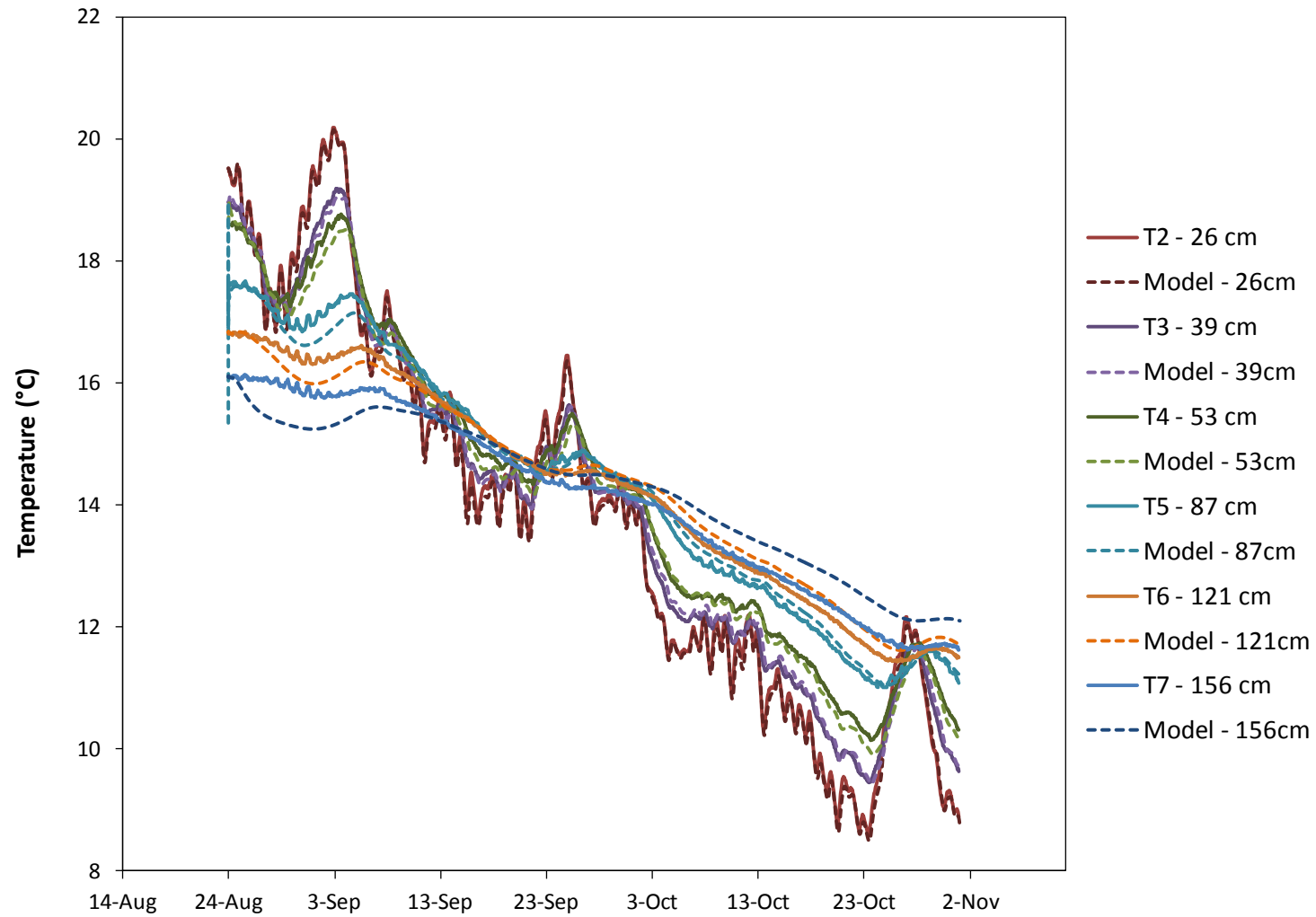


Figure R.4 Simulated and observed temperature profiles between August 24th to October 31st, 2010 using altered moisture retention parameters obtained from calibration when the ephemeral stream was present by increasing the hydraulic conductivity of the lower eight layers by two.

Appendix S

Simulated and Observed Moisture Content - Fully Drained

**Fully Drained Conditions Using Final Moisture Retention Parameters for Soil when the Ephemeral
Stream is Present**

April 12th to June 1st, 2010

August 24th to October 31st, 2010

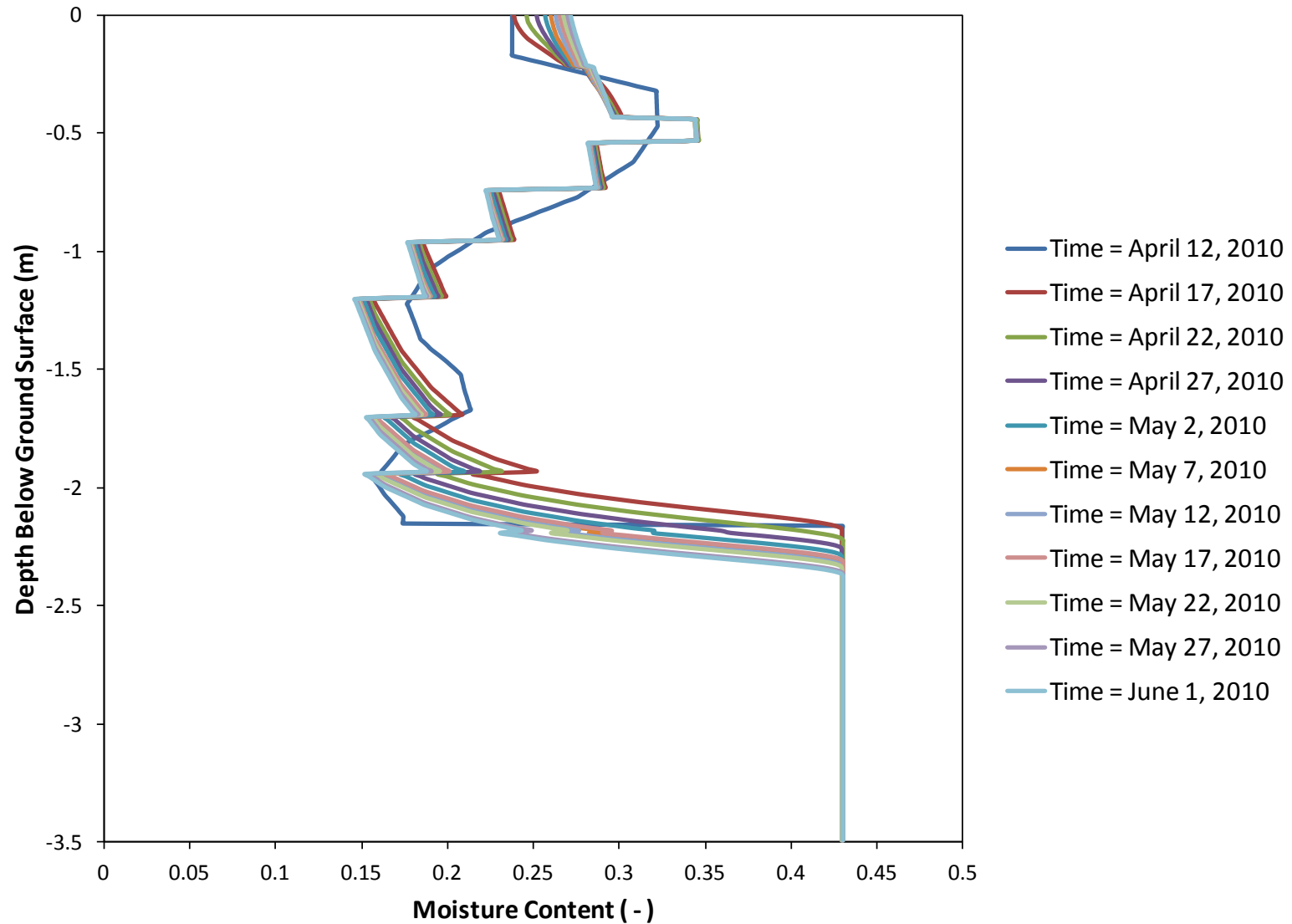


Figure S.1 Simulated moisture content profile every five days of simulation between April 12th to June 1st, 2010 using the moisture retention parameters obtained from calibration when the ephemeral stream was present.

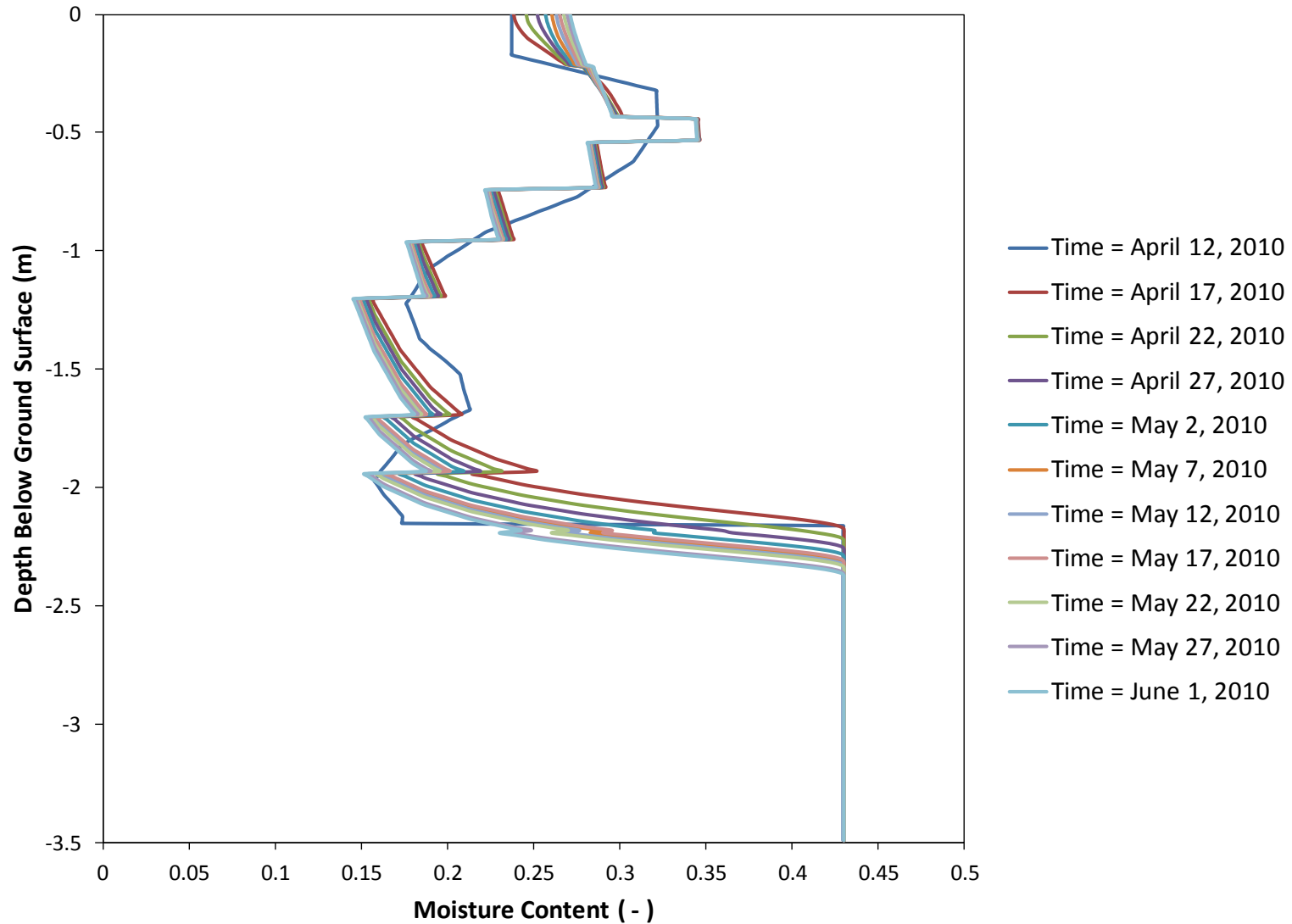


Figure S.2 Simulated moisture content profile every five days of simulation between April 12th to June 1st, 2010 using altered moisture retention parameters obtained from calibration when the ephemeral stream was present by increasing the hydraulic conductivity of the lower eight layers by two.

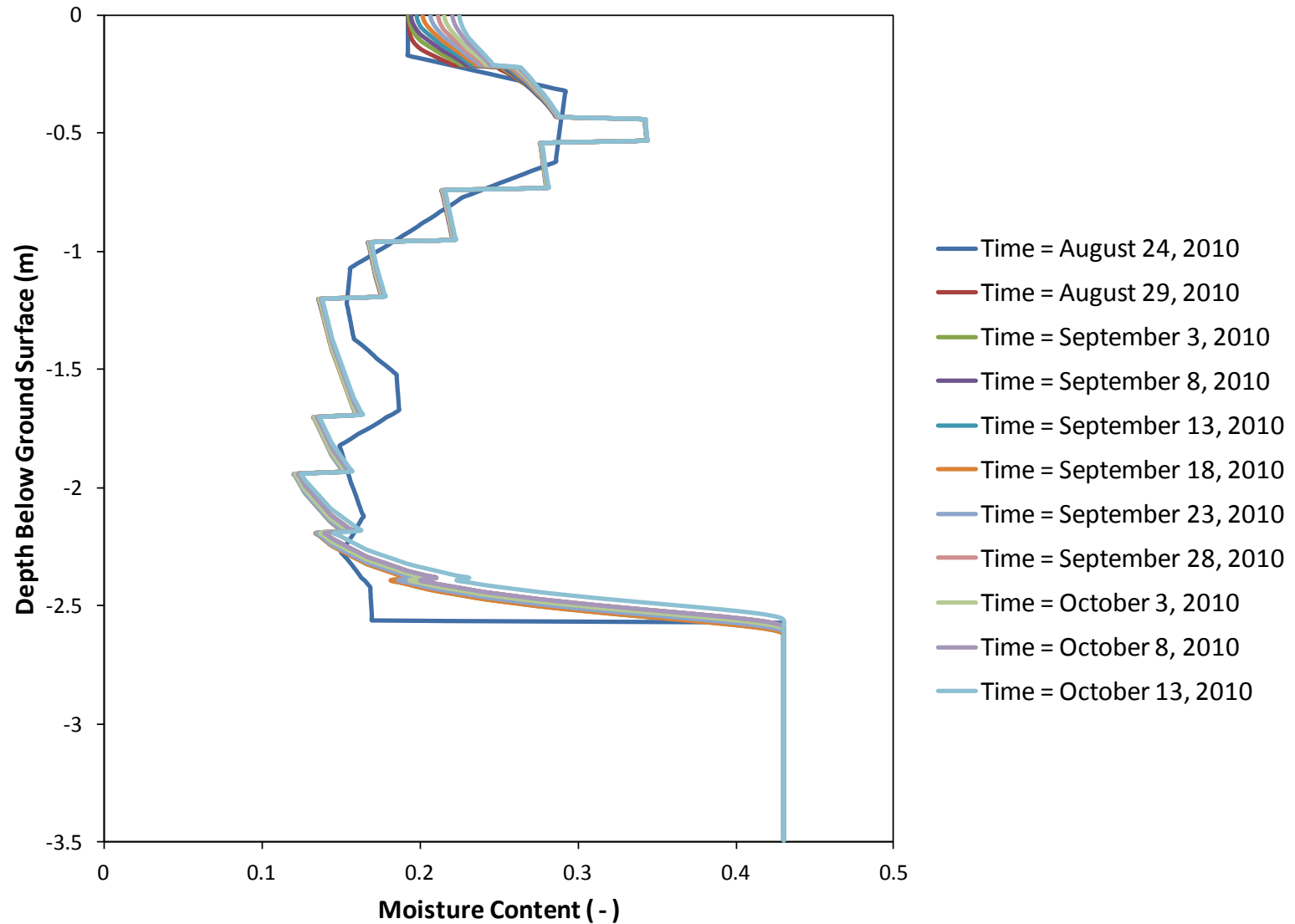


Figure S.3 Simulated moisture content profile every five days of simulation between August 24th to October 31st, 2010 using the moisture retention parameters obtained from calibration when the ephemeral stream was present.

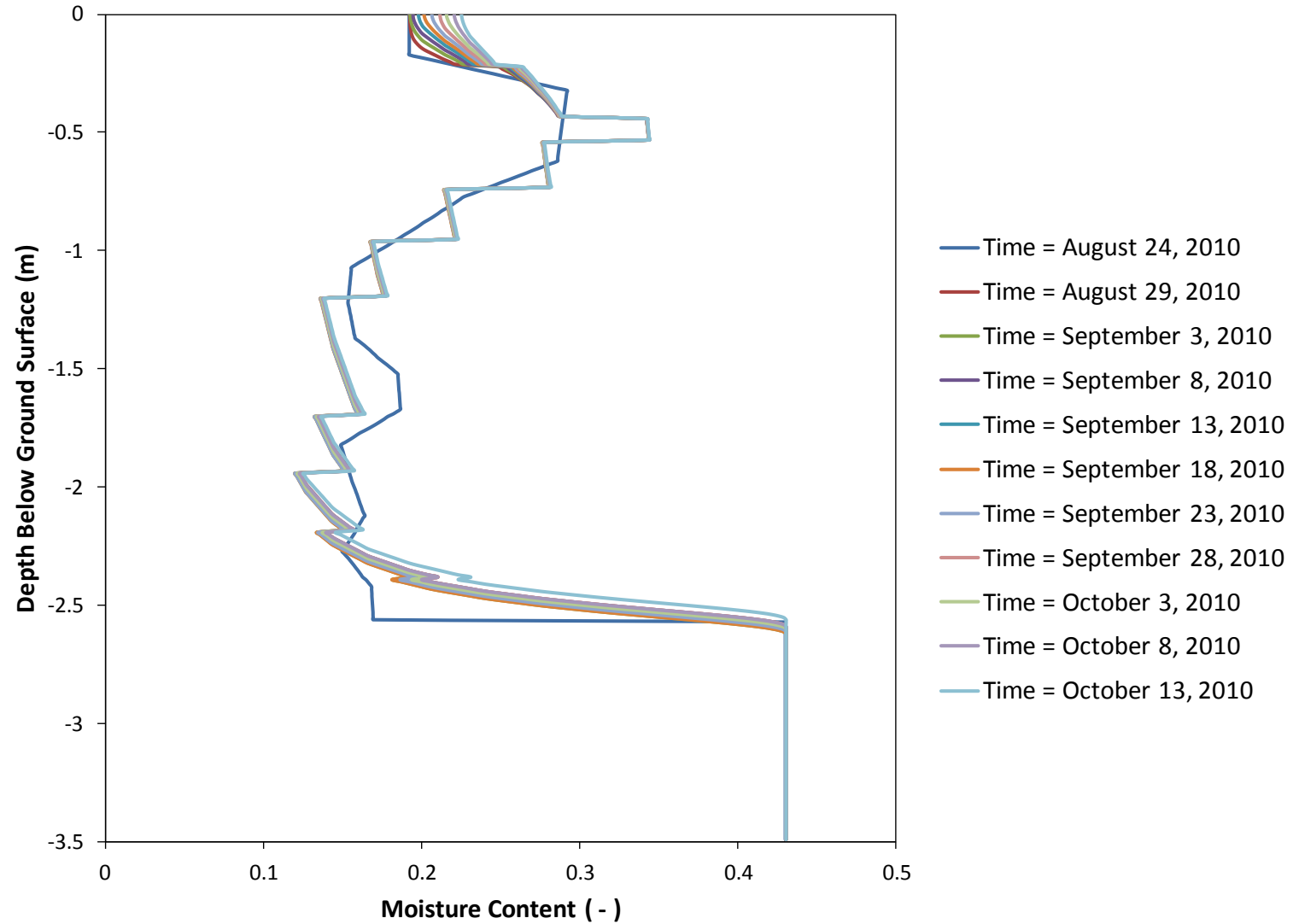


Figure S.4 Simulated moisture content profile every five days of simulation between August 24th to October 31st, 2010 using altered moisture retention parameters obtained from calibration when the ephemeral stream was present by increasing the hydraulic conductivity of the lower eight layers by two.

Appendix T
Boundary Conditions - April 12th to June 1st, 2010

Initial Boundary Conditions

Variable Boundary Conditions

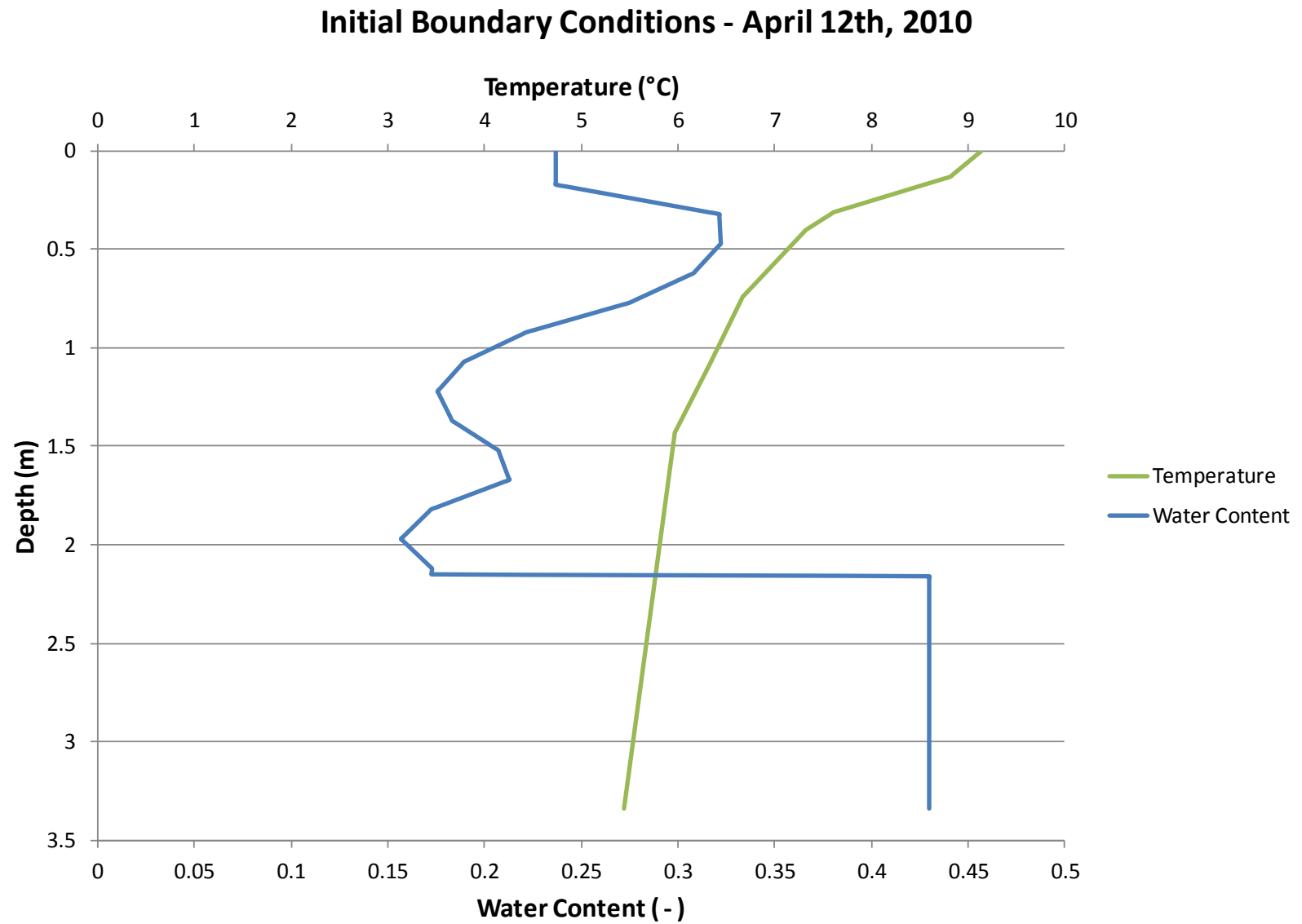


Figure T.1 Initial Boundary Conditions: Temperature and Moisture Content

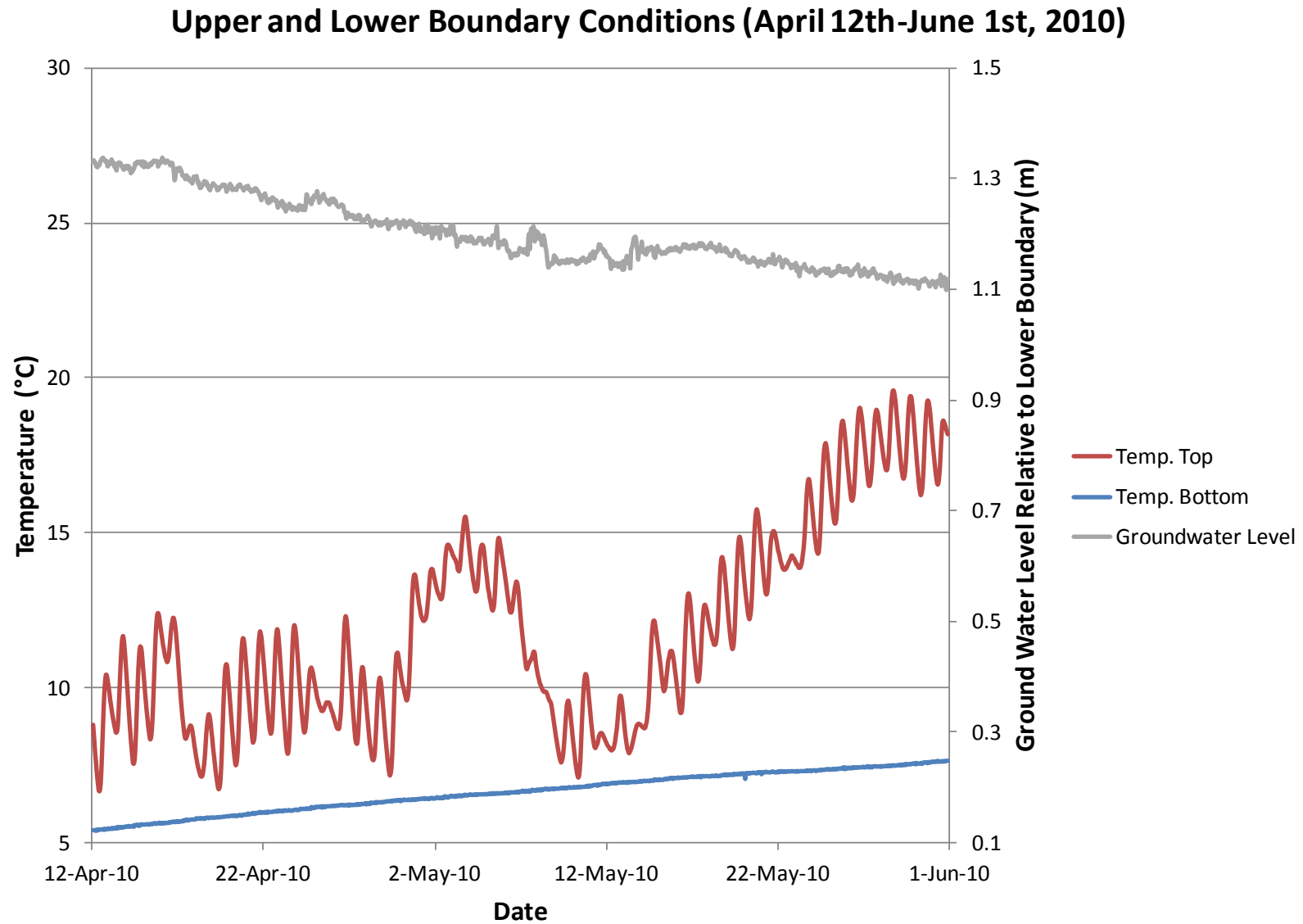


Figure T.2 Variable Boundary Conditions: Groundwater Level and Temperature

Appendix U

Boundary Conditions – August 24th to October 1st, 2010

Initial Boundary Conditions

Variable Boundary Conditions

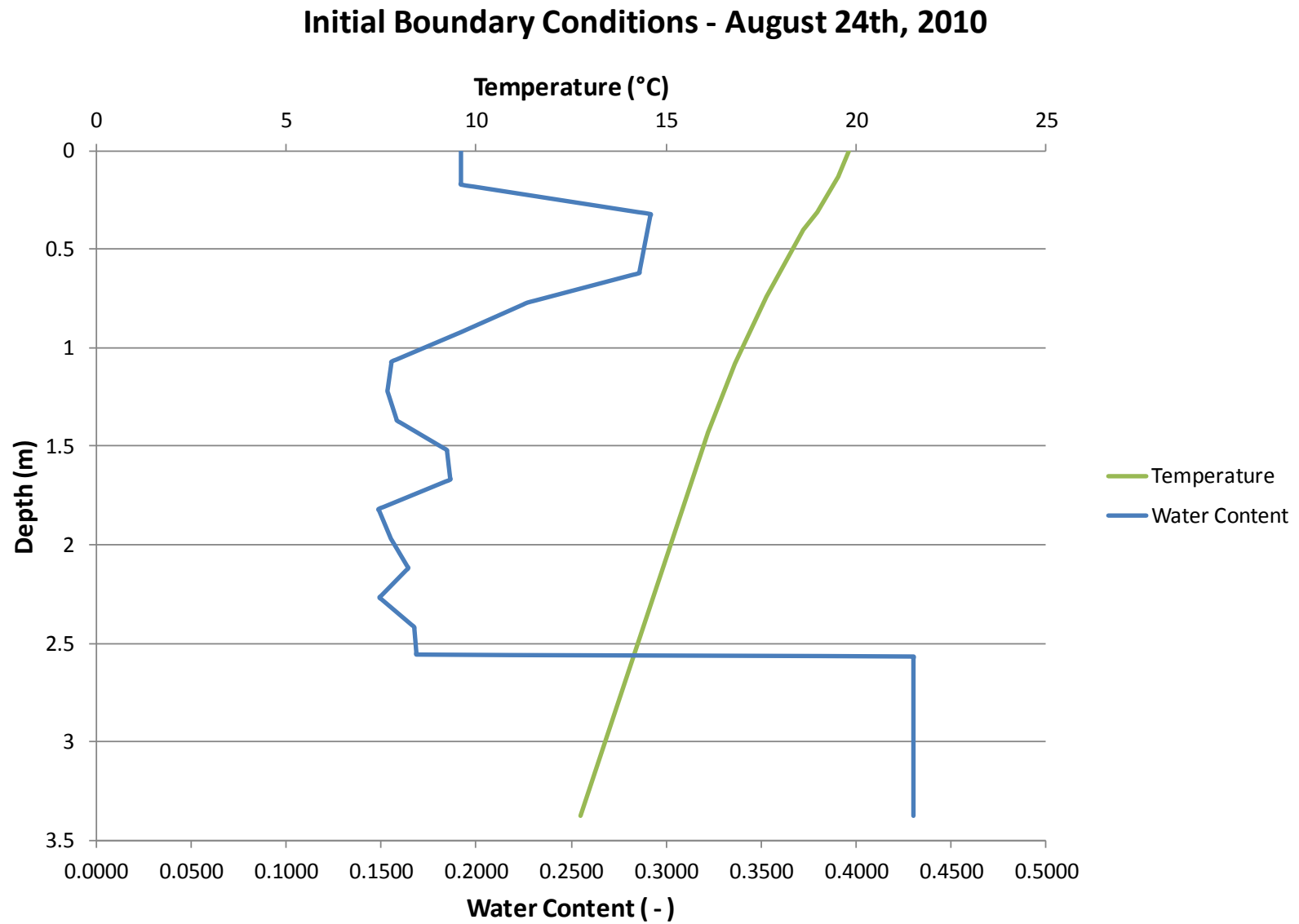


Figure U.1 Initial Boundary Conditions: Temperature and Moisture Content

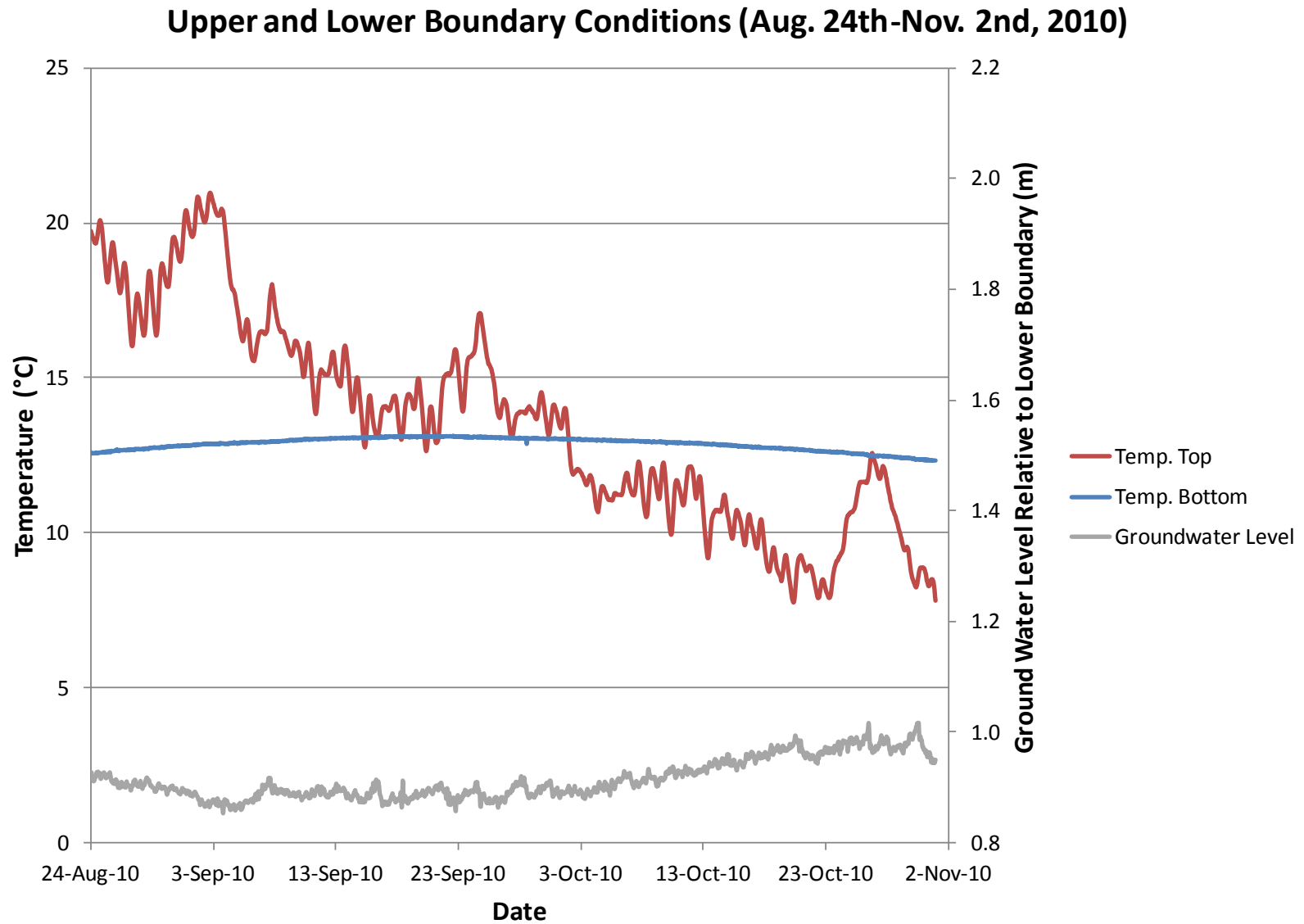


Figure U.2 Variable Boundary Conditions: Groundwater Level and Temperature

Appendix V
Boundary Conditions - March 9th to March 22nd, 2010

Initial Boundary Conditions

Variable Boundary Conditions

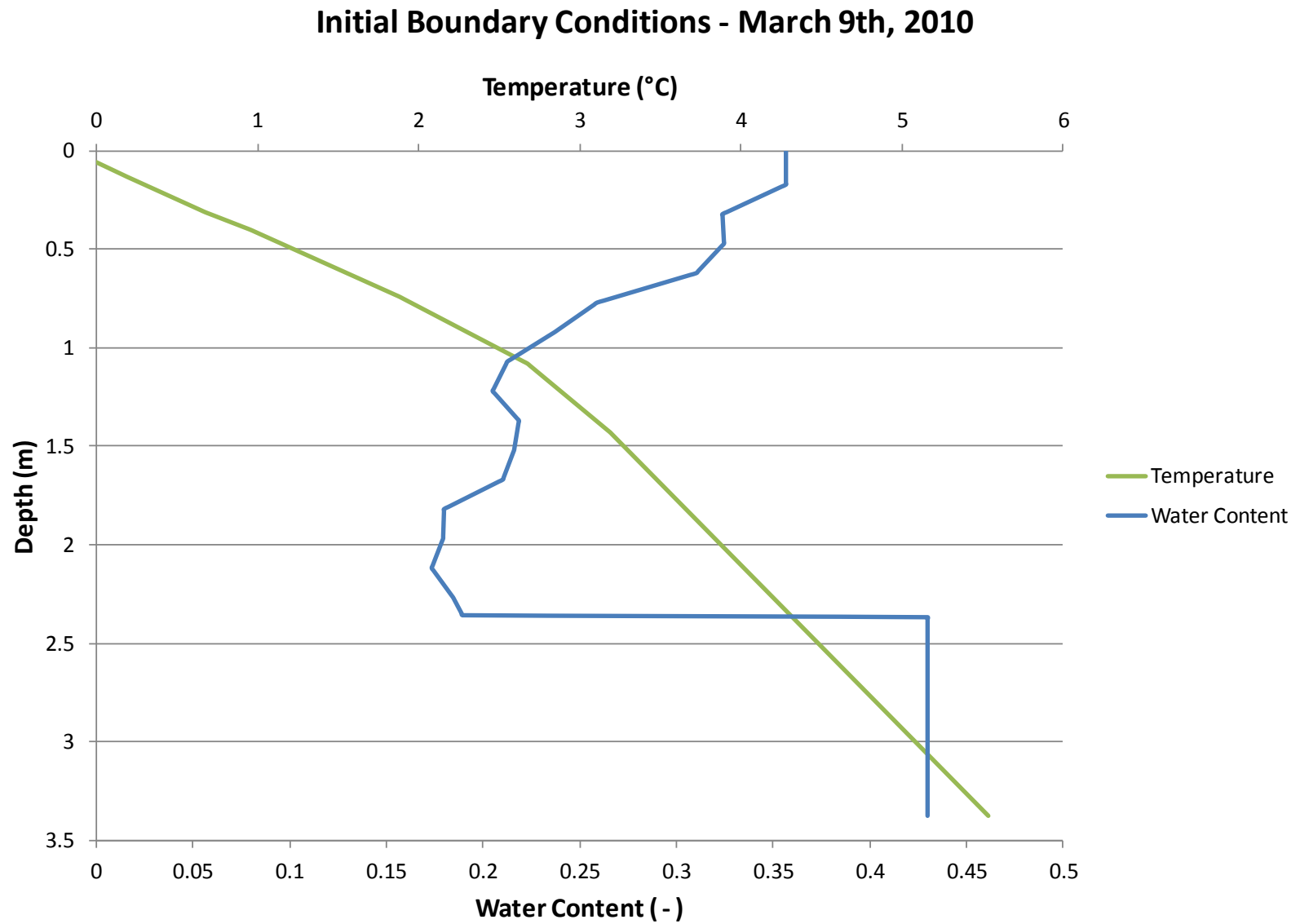


Figure V.1 Initial Boundary Conditions: Temperature and Moisture Content

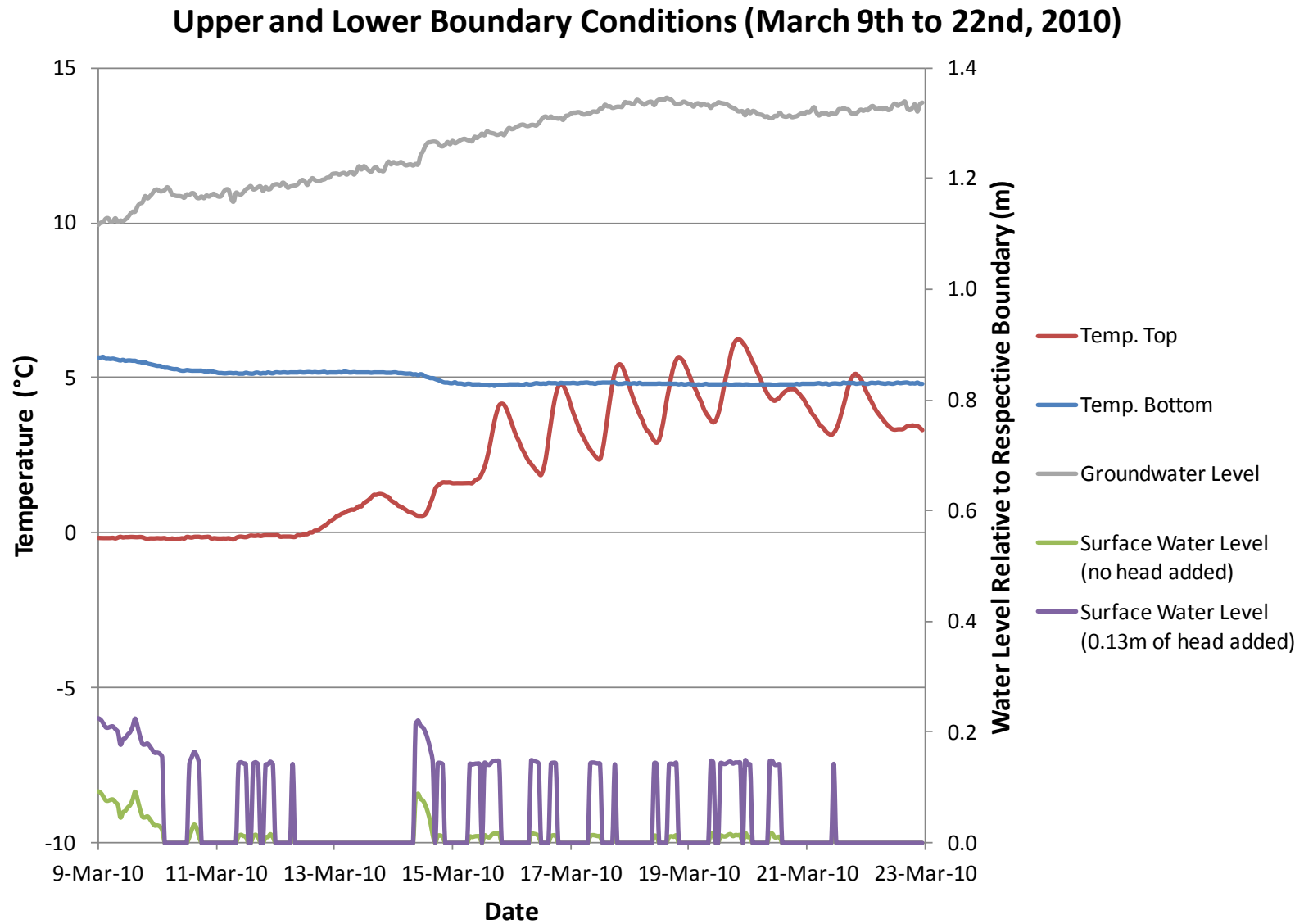


Figure V.2 Variable Boundary Conditions: Groundwater Level and Temperature

Appendix W

Iteration Criteria for All Simulations

Table W.1 Iteration criteria used to run all simulations. Definitions of all the different terms are taken from the help function of the Hydrus 1-D model (Šimůnek et al., 1999).

20	Maximum Number of Iterations: “Maximum number of iterations allowed during any time step, while solving the nonlinear Richards’ equation using a modified Picard method. Recommended and default value is 20.”
0.0007	Water Content Tolerance: “Absolute water content tolerance for nodes in the unsaturated part of the flow region [-] (its recommended value is 0.0001). This parameter represents the maximum desired absolute change in the value of the water content between two successive iterations during a particular time step.”
0.1	Pressure Head Tolerance: “Absolute pressure head tolerance for nodes in the saturated part of the flow region [L] (its recommended value is 0.1 cm). This parameter represents the maximum desired absolute change in the value of the pressure head between two successive iterations during a particular time step.”
3	Lower Optimal Iteration Range: “When the number of iterations necessary to reach convergence for water flow is less than this number, the time step is multiplied by the upper time step multiplication factor (the time step is increased). Recommended and default value is 3.”
7	Upper Optimal Iteration Range: “When the number of iterations necessary to reach convergence for water flow is higher than this number, the time step is multiplied by the lower time step multiplication factor (the time step is decreased). Recommended and default value is 7.”
1.3	Lower Time Step Multiplication Factor: “If the number of iterations necessary to reach convergence for water flow is less than the lower optimal iteration range, the time step is multiplied by this number (the time step is increased). Recommended and default value is 1.3.”
0.7	Upper Time Step Multiplication Factor: “If the number of iterations necessary to reach convergence for water flow is higher than the upper optimal iteration range, the time step is multiplied by this number (the time step is decreased). Recommended and default value is 0.7.”
1.0E-08	Lower Limit of the Tension Interval: “Absolute value of the lower limit [L] of the pressure head interval for which a table of hydraulic properties will be generated internally for each material.”
100	Upper Limit of the Tension Interval: “Upper value of the lower limit [L] of the pressure head interval for which a table of hydraulic properties will be generated internally for each material.”